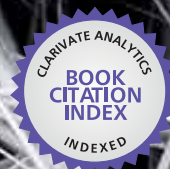




IntechOpen

Composites from Renewable and Sustainable Materials

Edited by Matheus Poletto



WEB OF SCIENCE™



COMPOSITES FROM RENEWABLE AND SUSTAINABLE MATERIALS

Edited by **Matheus Poletto**

Composites from Renewable and Sustainable Materials

<http://dx.doi.org/10.5772/62936>

Edited by Matheus Poletto

Contributors

Sherif Mehanny, Saiful Izwan Abd Razak, Izzati Fatimah Wahab, Emilio Pérez-Pacheco, Jorge Carlos Canto Pinto, Víctor Manuel Moo Huchin, Iván Alfredo Estrada Mota, Raciél Javier Estrada León, Luis Chel-Guerrero, Douglas Fox, Jeremiah Woodcock, Jeffrey Gilman, John Shields, Mauro Zammarano, Chelsea Davis, Rick Davis, Sbazolcs Matko, Noy Kaufman, Gonzalo Martínez-Barrera, Nelly González-Rivas, Enrique Viguera-Santiago, Angel Martínez-López, Jorge A. Tello-González, Carmina Menchaca-Campos, Izabella Krucinska, Eulalia Gliścińska, Marina Michalak, Michał Puchalski, Danuta Ciechańska, Janusz Kazimierzczak, Arkadiusz Bloda, Ruey Shan Chen, Sahrim Ahmad, Ester Zuza, Emilio Meaurio, Jose-Ramon Sarasua, Hyun-Joong Kim, Ranjeth Kumar Reddy T, Ji-Won Park, Adeshina Fadeyibi, Zinash Delebo Osunde, Gbabo Agidi, Evans Egwim, Peter Aba Idah, Ion N. Mihailescu, Anita-Ioana Visan, Carmen-Georgeta Ristoscu, Yang Hu, Yongjun Zhu, Xin Zhou, Denis Rodrigue, Rodolfo Rendon, Amanda Ortiz, Efrain Tovar-Sánchez, Emmanuel Flores-Huicochea, Hanna Brodowsky, Edith Mäder, Thi Thu Loan Doan, Miguel Angel Hidalgo-Salazar

© The Editor(s) and the Author(s) 2016

The moral rights of the and the author(s) have been asserted.

All rights to the book as a whole are reserved by INTECH. The book as a whole (compilation) cannot be reproduced, distributed or used for commercial or non-commercial purposes without INTECH's written permission.

Enquiries concerning the use of the book should be directed to INTECH rights and permissions department (permissions@intechopen.com).

Violations are liable to prosecution under the governing Copyright Law.



Individual chapters of this publication are distributed under the terms of the Creative Commons Attribution 3.0 Unported License which permits commercial use, distribution and reproduction of the individual chapters, provided the original author(s) and source publication are appropriately acknowledged. If so indicated, certain images may not be included under the Creative Commons license. In such cases users will need to obtain permission from the license holder to reproduce the material. More details and guidelines concerning content reuse and adaptation can be found at <http://www.intechopen.com/copyright-policy.html>.

Notice

Statements and opinions expressed in the chapters are those of the individual contributors and not necessarily those of the editors or publisher. No responsibility is accepted for the accuracy of information contained in the published chapters. The publisher assumes no responsibility for any damage or injury to persons or property arising out of the use of any materials, instructions, methods or ideas contained in the book.

First published in Croatia, 2016 by INTECH d.o.o.

eBook (PDF) Published by IN TECH d.o.o.

Place and year of publication of eBook (PDF): Rijeka, 2019.

IntechOpen is the global imprint of IN TECH d.o.o.

Printed in Croatia

Legal deposit, Croatia: National and University Library in Zagreb

Additional hard and PDF copies can be obtained from orders@intechopen.com

Composites from Renewable and Sustainable Materials

Edited by Matheus Poletto

p. cm.

Print ISBN 978-953-51-2793-2

Online ISBN 978-953-51-2794-9

eBook (PDF) ISBN 978-953-51-4145-7

We are IntechOpen, the world's leading publisher of Open Access books Built by scientists, for scientists

3,750+

Open access books available

115,000+

International authors and editors

119M+

Downloads

151

Countries delivered to

Our authors are among the
Top 1%

most cited scientists

12.2%

Contributors from top 500 universities



WEB OF SCIENCE™

Selection of our books indexed in the Book Citation Index
in Web of Science™ Core Collection (BKCI)

Interested in publishing with us?
Contact book.department@intechopen.com

Numbers displayed above are based on latest data collected.
For more information visit www.intechopen.com



Meet the editor



Matheus Poletto is a professor and researcher at the Universidade de Caxias do Sul. He is an expert in composite science, working with thermoplastic composites and cellulosic materials. He has published over 100 scientific and conference papers and several book chapters. He obtained the degree in Chemical Engineering and master's degree in Materials Science and Engineering from the Universidade de Caxias do Sul, Brazil, and his PhD in Materials Engineering from the Universidade Federal do Rio Grande do Sul, Brazil, in 2014. Professor Matheus currently works with cellulosic and lignocellulosic materials studying the effect of fiber composition on the thermal and mechanical properties of polymer composite materials. He is also a member of the Polymer Research Laboratory group from the Universidade de Caxias do Sul.

Contents

Preface XIII

- Chapter 1 **Polyolefine Composites Reinforced by Rice Husk and Saw Dust 1**
Thi Thu Loan Doan, Hanna M. Brodowsky and Edith Mäder
- Chapter 2 **Characterization of Rice Husk Biofibre-Reinforced Recycled Thermoplastic Blend Biocomposite 25**
Ruey Shan Chen and Sahrim Ahmad
- Chapter 3 **High-Content Lignocellulosic Fibers Reinforcing Starch-Based Biodegradable Composites: Properties and Applications 45**
Sherif Mehanny, Lamis Darwish, Hamdy Ibrahim, Mohamed Tarek El-Wakad and Mahmoud Farag
- Chapter 4 **Polysaccharides as Composite Biomaterials 65**
Izzati Fatimah Wahab and Saiful Izwan Abd Razak
- Chapter 5 **Thermoplastic Starch (TPS)-Cellulosic Fibers Composites: Mechanical Properties and Water Vapor Barrier: A Review 85**
Emilio Pérez-Pacheco, Jorge Carlos Canto-Pinto, Víctor Manuel Moo-Huchin, Iván Alfredo Estrada-Mota, Raciél Javier Estrada-León and Luis Chel-Guerrero
- Chapter 6 **Composite Coatings Based on Renewable Resources Synthesized by Advanced Laser Techniques 107**
Anita-Ioana Visan, Carmen-Georgeta Ristoscu and Ion N. Mihailescu
- Chapter 7 **Biodegradable Polylactide-Based Composites 133**
Ester Zuza, Emilio Meaurio and Jose-Ramon Sarasua

- Chapter 8 **The Role of Biopolymers in Obtaining Environmentally Friendly Materials 151**
Rodolfo Rendón-Villalobos, Amanda Ortíz-Sánchez, Efraín Tovar-Sánchez and Emmanuel Flores-Huicochea
- Chapter 9 **Waste and Recycled Materials and their Impact on the Mechanical Properties of Construction Composite Materials 161**
Gonzalo Martínez-Barrera, Nelly González-Rivas, Enrique Viguera-Santiago, Ángel Martínez-López, Jorge A. Tello-González and Carmina Menchaca-Campos
- Chapter 10 **Renewable Biocomposite Properties and their Applications 177**
Thimmapuram Ranjeth Kumar Reddy, Hyun-Joong Kim and Ji-Won Park
- Chapter 11 **Epoxy Composites Using Wood Pulp Components as Fillers 199**
Douglas M. Fox, Noy Kaufman, Jeremiah Woodcock, Chelsea S. Davis, Jeffrey W. Gilman, John R. Shields, Rick D. Davis, Szabolcs Matko and Mauro Zammarano
- Chapter 12 **Bio-Based Composites for Sound Absorption 217**
Eulalia Gliścińska, Izabella Krucińska, Marina Michalak, Michał Puchalski, Danuta Ciechańska, Janusz Kazimierzak and Arkadiusz Bloda
- Chapter 13 **Nano-Rheological Behaviour of Cassava Starch-Zinc Nanocomposite Film under Dynamic Loading for High Speed Transportation of Packaged Food 241**
Adeshina Fadeyibi, Zinash D. Osunde, Gbabo Agidi, Evans C. Egwim and Peter A. Idah
- Chapter 14 **Multifunctional Wound-Dressing Composites Consisting of Polyvinyl Alcohol, Aloe Extracts and Quaternary Ammonium Chitosan Salt 255**
Yang Hu, Yongjun Zhu and Xin Zhou
- Chapter 15 **Production and Characterization of Hybrid Polymer Composites Based on Natural Fibers 273**
Wendy Rodriguez-Castellanos and Denis Rodrigue

Chapter 16 **Viscoelastic Performance of Biocomposites** 303
Miguel Ángel Hidalgo Salazar

Preface

Growing interest has been devoted in the last years to materials derived from renewable and sustainable resources mainly due to the increasing concerns associated with environment, waste accumulation and disposal, and the inevitable depletion of fossil resources. It becomes clear that ecological efficiency, green chemistry, renewable resources, and sustainable manufacturing should be the cornerstones for development of new methods and materials that offset the use of fossil fuels, utilize wastes, and are biodegradables or recyclables. So, the necessity of more renewable and sustainable composite materials can lead to the development of new technologies and processes that can contribute to the environment and life quality. Renewable and sustainable materials are of great concern in scientific research and industry. These materials include biomass as industrial and agricultural residues and energy crops. The utilization of such materials as reinforcement or to improve specific properties in composite or nanocomposites materials is an excellent alternative. Among the advantages that can be cited are the strong ecological appeal, low cost, and higher specific mechanical properties. Therefore, a solid knowledge is necessary to transform renewable and sustainable materials into useful products. So, this book intends to develop a deeper understanding about the fundamental aspects and current applications of renewable and sustainable materials in engineering applications. *Composites from Renewable and Sustainable Materials* consists of sixteen chapters related to the renewable materials, biomaterials, natural fibers, biodegradable composites, starch, and recycled materials. This is a useful book for readers from diverse areas, such as physics, chemistry, biology, materials science, and engineering. It is hoped that this book will expand the reader's knowledge about this fascinating area.

Matheus Poletto

Center of Exact Science and Technology (CCET)

University of Caxias do Sul (UCS)

Brazil

Polyolefine Composites Reinforced by Rice Husk and Saw Dust

Thi Thu Loan Doan, Hanna M. Brodowsky and
Edith Mäder

Additional information is available at the end of the chapter

<http://dx.doi.org/10.5772/65264>

Abstract

Due to the global demand for fibrous light-weight materials, research on composites reinforced with plant materials has increased. Natural fiber reinforced composites offer several advantages: light weight, competitive specific mechanical properties, easy processing, large volume availability, low cost, and low environmental footprint. Especially, using agricultural wastes such as rice husk, saw dust etc. as fillers/fibres in composites provides the chance to improve material properties while improving their sustainability. In the present work, rice husk and saw dust were chosen as fillers for their differing morphology, aspect ratios, and difference of structure. As matrices, polyethylene (PE) and polypropylene (PP) were studied, either neat or modified with maleic anhydride grafted PP/PE as coupling agent or compatibilizer between hydrophobic matrices and hydrophilic bio-fillers. The bending modulus is improved due to filler addition. In presence of compatibilizer, the improved interfacial interaction leads to improved bending and tensile strength as well as toughness. Furthermore, the influence of the filler and compatibilizer on composite properties such as hardness, dynamic mechanical behaviour, thermal expansion, thermal degradation, melting and crystallisation behaviour are presented.

Keywords: natural fibers, bio-fillers, composites, interphase

1. Introduction

The global demand for light-weight materials calls for the broad use of fiber-reinforced plastic materials [1]. Developing composites using natural fibers provides the chance to improve

materials while decreasing their ecological footprint. Even using agricultural and forestry wastes such as rice husks (RHs), coconut fibers, bagasse, and saw dust (SD) can lead to significantly improved material properties [2].

Rice husk and saw dust, by-products of the rice milling and wood sawing processes respectively, are potential reinforcing fillers for thermoplastic matrix composites because of their lignocellulosic characteristics. These fillers offer advantages of easy processing, large volume availability, annual renewability, low cost, light weight, competitive specific mechanical properties, and high sustainability. The morphology differs: Rice husk is made up of rectangular platelets and saw dust of short fiber bundles.

The most common thermoplastics used as matrices for bio-fillers are polyethylene (PE) and polypropylene (PP). When a polyolefin is used as a matrix for a bio-filler composite, the incompatibility between hydrophobic matrix and hydrophilic bio-filler is an important issue. Therefore, there have been many studies on improving interfacial interactions between the polymers and bio-fillers. According to previous studies, the best solution of the problem is using an appropriate coupling agent or compatibilizer such as maleic anhydride-functionalized polyolefin, for example, maleic anhydride-grafted polypropylene (MAPP) for PP or maleic anhydride-grafted polyethylene (MAPE) for PE [3–8].

Biomaterials such as saw dust, bamboo powder, or grain husks used as fillers in polymer matrix composites are natural compounds, mainly containing cellulose, hemicellulose, and lignin. Their degradation takes place at a relatively low temperature, around 200°C [1]. Therefore, bio-fillers will be subjected to thermal degradation during composite processing with the majority of common thermoplastic polymers [2]. This leads to undesirable properties, such as odor and browning along with a reduction in mechanical properties of the bio-composite [2, 3]. Therefore, it is important to understand and predict the thermal decomposition processes of bio-filler in order to better design composite processes and estimate the influence of the thermal decomposition on composite properties [4].

In this work, the suitability of rice husk and saw dust as reinforcing agents for composites based on different polyolefine matrices was evaluated. The filler morphology is characterized. Mechanical tests of their composites were evaluated as a function of filler content and filler morphology. The effect of maleated polyolefines as compatibilizers on the mechanical properties of the composites as well as hardness of the composites was studied.

Thermal studies of biomaterial-filled polyolefine (PP, PE) composites included thermomechanical analysis (TMA) and the thermal and mechanical dynamic behavior according to the filler loading and the presence of compatibilizers. The crystallization is characterized by differential scanning calorimetry (DSC) analysis and the thermal degradation by thermogravimetric analysis (TGA).

2. Experimental

2.1. Materials

Polypropylene, Advanced PP-1100N, and high-density polyethylene, EL-Lene H5818J, were supplied by Advanced Petrochemical Co. and SCG Plastics Co., Ltd, Thailand, respectively. Two compatibilizers, maleic anhydride-grafted polypropylene Polybond 3200 and maleic anhydride-grafted polyethylene Polybond 3029, were provided by Chemtura, USA. **Table 1** shows the typical physical properties of the matrix polymers and compatibilizers.

Polymers properties	PP	PE	MAPP	MAPE
Density (g/cm ³)	0.91	0.96	0.91	0.96
Melting point (°C)	163	131	157	130
Melt flow index (g/10 min)	12*	18**	115*	
MA content (%)	–	–	1.0	1.6
Tensile strength (MPa)	35.0	28.0	–	–
Notched Izod impact strength (kJ/m ²)	3.0	4.8	–	–

*MFI at 230°C/2.16 kg
**MFI at 190°C/2.16 kg

Table 1. Properties of studied polymer materials.

Rice husk obtained from a rice mill factory in Danang, Vietnam, was ground. Saw dust from *Acacia auriculiformis* tree was collected from a Wood processing factory in Danang, Vietnam. Rice husk and saw dust were screened and dried at 80°C for 24 h before preparing the composites. Where a wood block was used for comparison, its dimensions were the same as those of the composite samples in the tests.

2.2. Methods

2.2.1. Aspect ratio of fillers

A digital microscope (Keyence VHX-100, Japan) and the corresponding imaging system were used for the aspect ratio determination. About 500-mg fillers of each filler type, classified by the sieve opening, were placed on a glass dish under the microscope. The optical light was adjusted to achieve the best focusing alignment and image resolution. The filler images taken with a digital camera were used to measure the length and diameter of individual filler particles. A minimum of 100 filler particles were measured for each sample. The aspect ratio was described as the ratio of length and width of the fibrous wood and as length and width of the rice husk platelets. Note the latter were not characterized by the length-to-plate-thickness ratio.

2.2.2. Particle size distribution of fillers

To evaluate the particle size distribution, fillers were classified after grinding (for rice husk) by screening into four mesh size ranges 20–35, 35–45, 45–80, and >80 per inch (approximately 500–850, 350–500, 180–350 μm , and <180 μm). The filler particles were then weighed in order to determine the weight of the fillers in each mesh size range.

2.2.3. Preparation of the composites

Composites were produced in a two-stage process. In the first stage, bio-fillers and polyolefine were compounded with and without compatibilizer using the twin-screw extruder Rheomex CEW100 QC, Haake, Germany. The mixing zone temperature of the extruder was 160°C for PE and 190°C for PP matrix composites. The rotation speed of the screws was 50 rpm. In the second stage, the extrudate in the form of strands was cooled to room temperature and then granulated.

The compound granules were dried at 80°C for 24 h before injection molding. The specimens were prepared using the injection molding machine MiniJet II, Haake, Germany, at cylinder temperatures of 180°C for PE and 190°C for PP matrix composites under an injection pressure of 800 bar.

2.2.4. Mechanical testing

Tensile and bending tests were conducted with the Universal Testing Machine AG-X plus, Shimadzu, Japan, according to ISO 527-3 and ISO 178, respectively. Notched Izod impact tests were conducted with HIT 50P, Zwick/Roell, Germany, according to ISO 180 at room temperature. Each value obtained represents the average of at least five samples.

2.2.5. Hardness tests

The hardness determination of the composites was carried out according to ISO 2039-1 on specimens of 80 mm \times 10 mm \times 4 mm. The specimens were loaded using the force of 132.39 N for a duration of 30 s. Each value obtained represents the average of 10 positions of measurement.

2.2.6. SEM analysis

Studies on the morphology of fillers and the tensile fracture surfaces of the composites were carried out using a FE-SEM (Ultra 55, Carl Zeiss SMT AG, Germany).

2.2.7. Thermomechanical analysis (TMA)

The thermal expansion tests of the composites and pure polyolefine samples were conducted using a thermomechanical analyzer (TMA Q400 V7.4 Build 93, TA Instruments) from -10 to 100°C at a heating rate of 2°C/min in a nitrogen atmosphere. The expansion mode with a constant compression load of 0.02 N was used on specimen of 5 mm \times 5 mm \times 4 mm.

2.2.8. Dynamic mechanical thermal analysis (DMTA)

Dynamic mechanical thermal analysis was carried out (DMA Q800 V20.24 Build 43, TA Instruments) in N₂ atmosphere. The dimensions of the test specimens were 17.5 mm × 10 mm × 4 mm. The tests were performed using a three-point bending-rectangular measuring system at 1-Hz test frequency. The heating rate was 1 K/min in the temperature range of -50 to 150°C. E' (storage modulus), E'' (loss modulus), and Tan δ (damping peak) of the samples were determined as a function of temperature.

2.2.9. Differential scanning calorimetry (DSC)

The samples used for the differential scanning calorimetric analysis were cut from extruded pellets. Approximately 10 mg of each sample was used. The equipment (DSC Q2000 V24.10 Build 122, TA Instruments) was programmed to work at the temperature range between 0 and 250°C, under a nitrogen flow of 50 mL/min. The heating and cooling rates were 10 K/min.

The values of melting temperature (T_m) and the melting enthalpy (ΔH_m) were calculated from the second heating. The crystallization temperature (T_c) was calculated from the cooling cycle.

2.2.10. Thermogravimetric analysis (TGA)

The samples used for the thermogravimetric analysis were cut from extruded pellets. Approximately 10 mg of each sample was used. The thermogravimetric analysis (TGA Q500 V6.7 Build 203) was carried out under nitrogen and air atmospheres in a temperature range of 23–700°C. The heating rate of the analysis was 10 K/min.

3. Results and discussion

3.1. Characterization of the fillers

Filler particle size and shape are important factors for reinforcement materials. **Figure 1** shows selected SEM images of RH and SD fillers. The morphologies differ strongly: SD is made up of lengthwise agglomerated fibers, whereas RH is made up of platelets with protrusions aligned in a regular pattern (**Figures 1b, d** and **2**). Detailed analysis shows a hollow cellular structure in both fillers (**Figure 1c, d**). The milling leads to different modes of fracture: In saw dust, the fibers separate, partially branch off or break, sometimes the cells collapse or the cell walls open, resulting in a highly nonuniform morphology with an irregular surface, which will allow to interact with the molten polyolefine during compounding and increase the chance of mechanical interlocking. In contrast, in RH the platelets have a highly regular pattern of 30 μm protrusions in a 90° array on the outside and a smooth inside. In the detailed image (**Figure 2a**), additional hair-like structures become visible between the protrusions. Platelet fracture occurs mainly along the lines between the protrusions, leading to platelets of angular shape and of rather uniform thickness (50 μm), and the cellular structure is contained within the platelet.

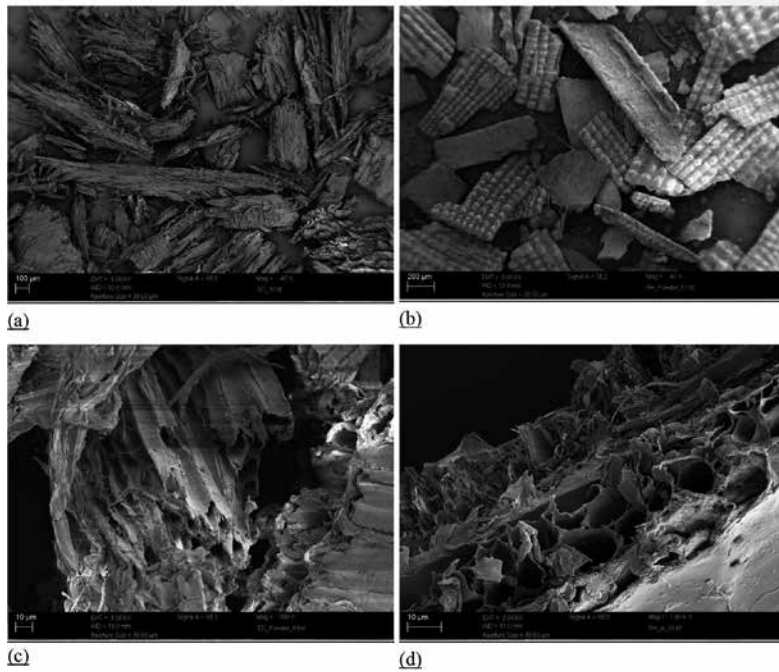


Figure 1. SEM micrographs of the fillers: surface morphology of (a, c) saw dust and (b, d) rice husk.

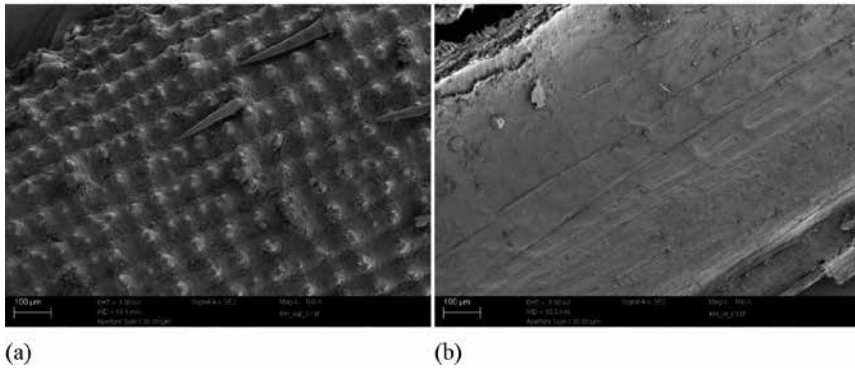


Figure 2. SEM micrographs of the morphology of rice husk (a) outer and (b) inner surface.

The filler surface layer plays an important role in surface tension and thus in wettability. It has been postulated that the inner RH surface contains lipid and proteinaceous compounds bound to the protein molecule by ester or thioester bonds [9]. The amount of lipid on the filler surface has an influence on hydrophobicity and surface tension.

Figure 3 shows particle size distribution and aspect ratio of the rice husk and saw dust fillers. About 80% of RH and SD fillers were in the range of 180–500 μm. The aspect ratio of both saw

dust and rice husk fillers is quite small. The fibrous saw dust has a higher aspect ratio in the range of 4–5 compared to rice husk filler formed of rectangular platelets with an aspect ratio of 2–3. Note that for better comparison, length-to-width ratio is used for both filler types. The commonly used aspect ratio for platelets—diameter to thickness—scales with the particle size as the thickness is around 50 μm for all platelets.

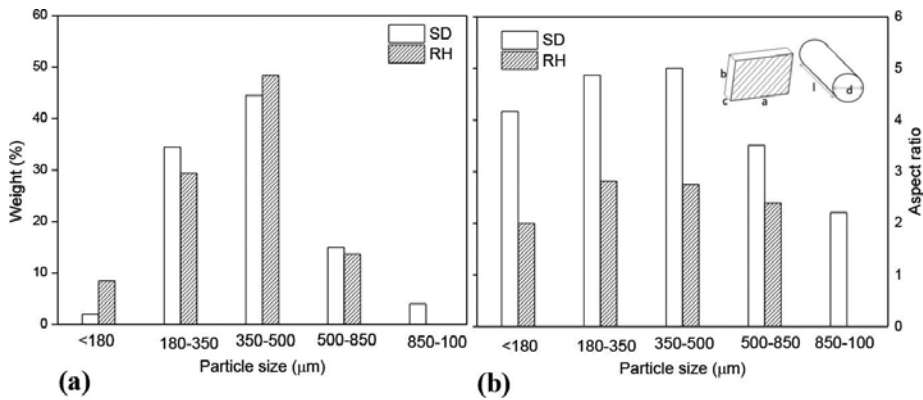


Figure 3. Size distribution (a) and aspect ratio (b) of filler particles (saw dust SD and rice husk RH). inset: Model of filler shape: platelets ($a \times b \times c$) for rice husk, circular rods (length l , diameter d) for saw dust. Note: Here calculation of aspect ratio is l/d for a rod and a/b for platelets.

A simple model is used to estimate the surface area of the particles, cf. **Figure 3b** inset: RH platelets may be modeled as rectangular blocks of 50 μm thickness and SD as spherical rods. The surface-to-volume ratio of a thin platelet is dominated by thickness (or, $2/\text{side length } a + 2/\text{side length } b + 2/\text{thickness}$), whereas that of a long circular rod is roughly proportional to the inverse of the diameter ($4/\text{diameter} + d/\text{rod length}$). A rough estimate of the surface area per volume (with a size distribution and aspect ratio as shown in **Figure 3** and considering the densities of 1.3 g/cm^3 for SD and 1.5 g/cm^3 for RH) shows that in a given weight, RH contains a factor of two higher number of particles, but the filler surface area vs. particle size distribution is only slightly shifted to smaller particle sizes in SD. The total filler surface area of the two filler types is equal according to this simple model.

3.2. Mechanical properties of the composites

The good specific mechanical properties are the prime reason for the application of filled polymer composites. The mechanical properties of the filler/polymer composites depend strongly on filler loading, interfacial adhesion, the degree of dispersion, and the filler particle size [10, 11]. **Figures 4, 5, and 6a** show the effects of filler content on the mechanical properties of bio-filler/polyolefine composites. The stated filler content is the wt.%, with a density of 1.3 g/cm^3 for SD and 1.5 g/cm^3 for RH, and the volume contents are approximately 4% lower for SD and 7% lower for RH.

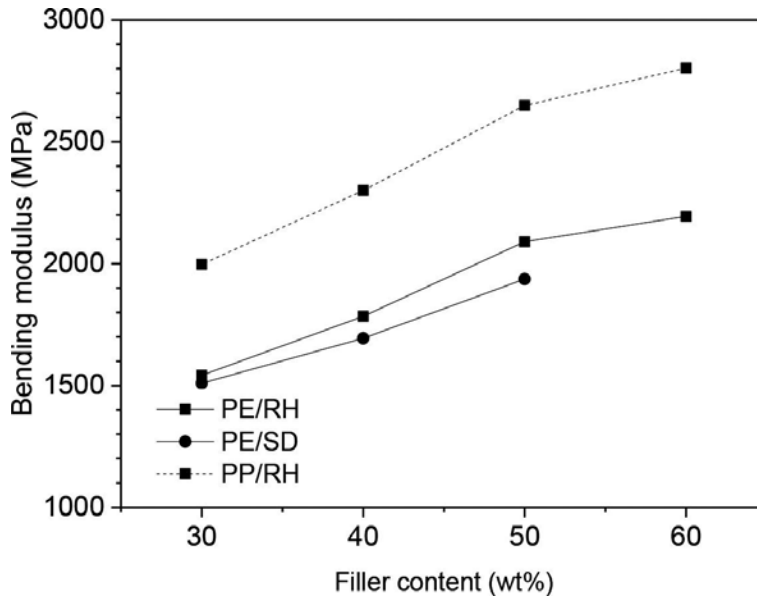


Figure 4. Influence of filler content on bending modulus of the three composites, no compatibilizer added.

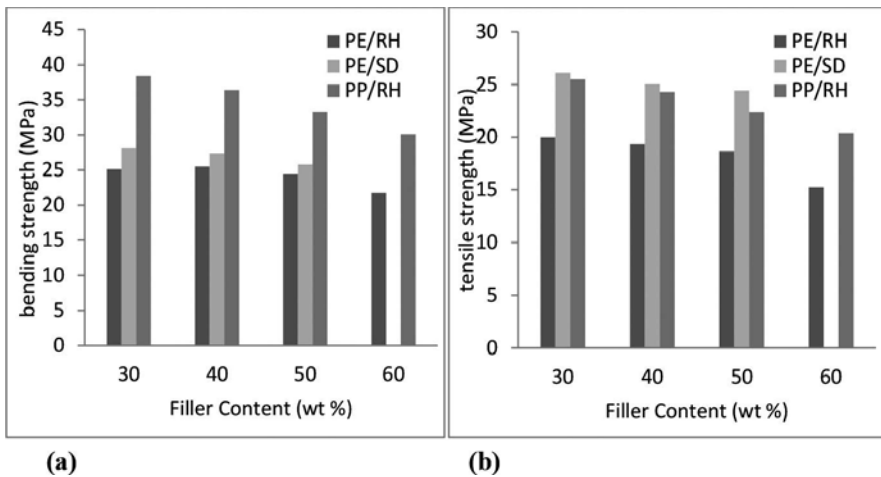


Figure 5. Effect of filler content on (a) bending strength (b) tensile strength of the composites, no compatibilizer added.

The addition of stiff fillers to the polyolefine matrices improves the stiffness of the composite, and the bending modulus increases linearly with filler content (Figure 4). The modulus reflects the capability of fiber and polymer matrix to transfer the elastic deformation in the case of small strains without interface fracture. The modulus of filled PP is 25% higher than that of both filled PEs. It is noted that at high content of saw dust (above 50 wt%), the viscosity of melt compound is very high, leading to voids and reducing the modulus.

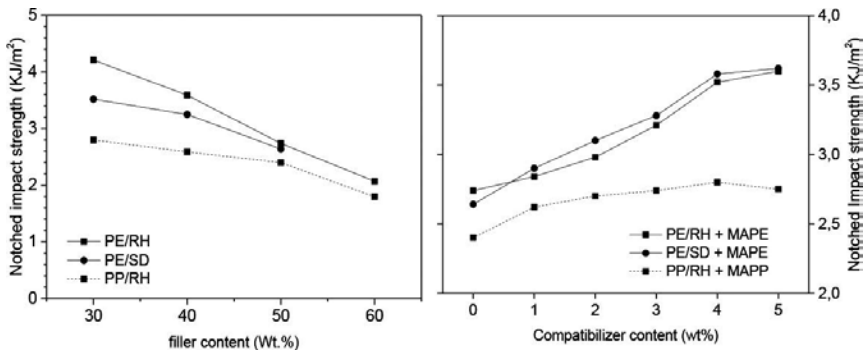


Figure 6. Left: Effect of filler content on impact strength of the composites, no compatibilizer added. Right: Influence of compatibilizer content on impact strength of the composites at 50% filler content.

The bending strengths (**Figure 5a**) are mainly influenced by the matrix type: PP/RH has 40% increased bending strength compared to the PE composites. Considering the volume filler content, the data for the bending strength of PE/RH and PE/SD coincide.

The saw dust/polyethylene composites show 20% higher tensile strengths compared to the rice husk/polyethylene composites (**Figure 5b**). This is probably caused by the higher cellulose content, better adhesion, and the higher aspect ratio of saw dust compared to the rice husk filler [12]. The tensile strength of the PP/RH composite is 20% higher than that of the PE/RH.

There is a clear decrease in tensile and bending strength in dependence on filler content throughout the investigated range. The fillers introduce a large interface area; in unmodified polymers, this is dominant due to weak interfacial interaction between the polar bio-filler and the apolar polyolefine matrix. As filler is added, this surface area increases, resulting in a slight decrease in the tensile, bending, and impact strengths of three composite systems PE/RH, PE/SD, and PP/RH in the absence of compatibilizer. The decrease is linear up to 50 wt.% (i.e., 46 vol.% of SD, 43 vol.% of RH) of filler. Specimens of 60 wt.% SD in PE could not be injection molded with the current set up, and samples of 60 wt.% RH in PE showed a stronger-than-linear decrease. At concentrations approaching the theoretical packing limit (e.g., 74 vol.% for oriented spherical rod fillers), defects and voids occur, the viscosity increases, and the weak, unbound interphase plays an increasing role.

Figure 6 presents the notched Izod impact strengths of rice husk and saw dust composites. The impact strength of a composite is influenced by many factors, especially the toughness of the filler and matrix components, and the dynamic stress transfer of the interphase, which in turn is determined by particle size, shape, and filler surface properties [13–15]. The notched impact strength of RH/PE composites, **Figure 6a**, is better than that of SD/PE composites when no compatibilizer is added. The PP/RH composites show lower impact toughness than PE composites. This trend is similar to a polypropylene composite system published by Bledzki et al. [15], where it is attributed to the brittleness and local internal deformation found more commonly in wood composites. Particle size, shape, and filler surface properties have influence

on the impact strength [14]. The nature of the interphase plays an important role, and in the case of fibrous material, the frictional work involved in pulling the fibers out of the matrix.

A matrix modification was performed by using compatibilizers (MAPE for PE matrix composites and MAPP for PP matrix composites) in order to improve the bonding strength between the bio-fillers and the matrix polyolefine. **Figures 6b** and 7 show the effect of compatibilizer content on the impact strength of the composites containing 50 wt.% filler. Tensile, bending, and impact strengths increased while adding compatibilizer and leveled off at above 2 wt.% MAPP for PP matrix composites and at above 4 wt.% MAPE for PE matrix composites. The increase in strengths of the composites is due to the improved interfacial adhesion between the fillers and polyolefine matrices. The maleic anhydride groups of compatibilizer interact with the polar filler surface (through chemical coupling or hydrogen bonding), while their polyolefine chains diffuse into the polyolefine matrices. Therefore, the interfacial strength is improved, as seen before, for example, by Marti-Ferrer et al. and Correa et al. [4, 5]. The increase in tensile, bending, and impact strengths due to the compatibilizers is higher than the losses due to the inclusion of fillers.

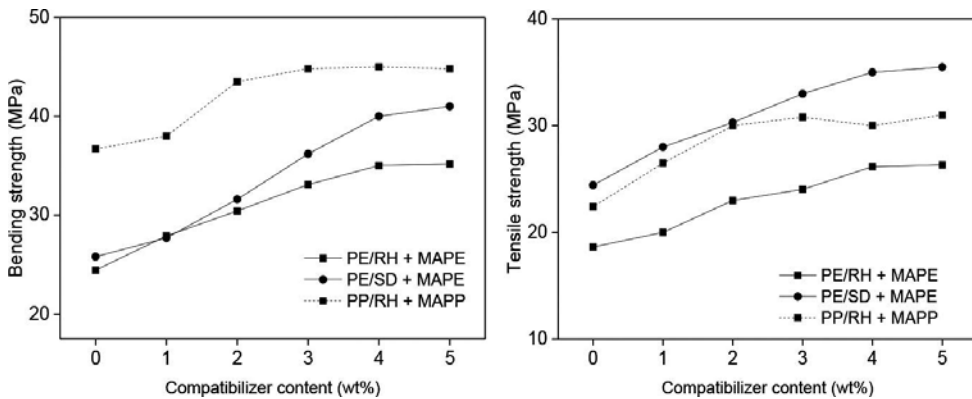


Figure 7. Influence of compatibilizer content on bending (left) and tensile strength (right) of the composites at 50% filler content.

3.3. Composite fracture surfaces and cross-sectional analysis

Figure 8 shows SEM images of the tensile fracture surfaces of the composites at 50 wt.% filler without and with compatibilizers (2 wt.% MAPP for PP matrix composites and 4 wt.% MAPE for PE matrix composites). Adding the compatibilizers changes the fracture behavior of the composites. The unmodified composites fail at the interphases of the filler particles. Voids at the interphase (especially the outside surface of RH particles) and pull-out cavities (especially in the higher aspect ratio SD particles) are visible. In the modified composite, the interfacial interaction is improved, shifting the failure into the matrix with far less pull-out cavities and polymer-coated or partially coated filler particles.

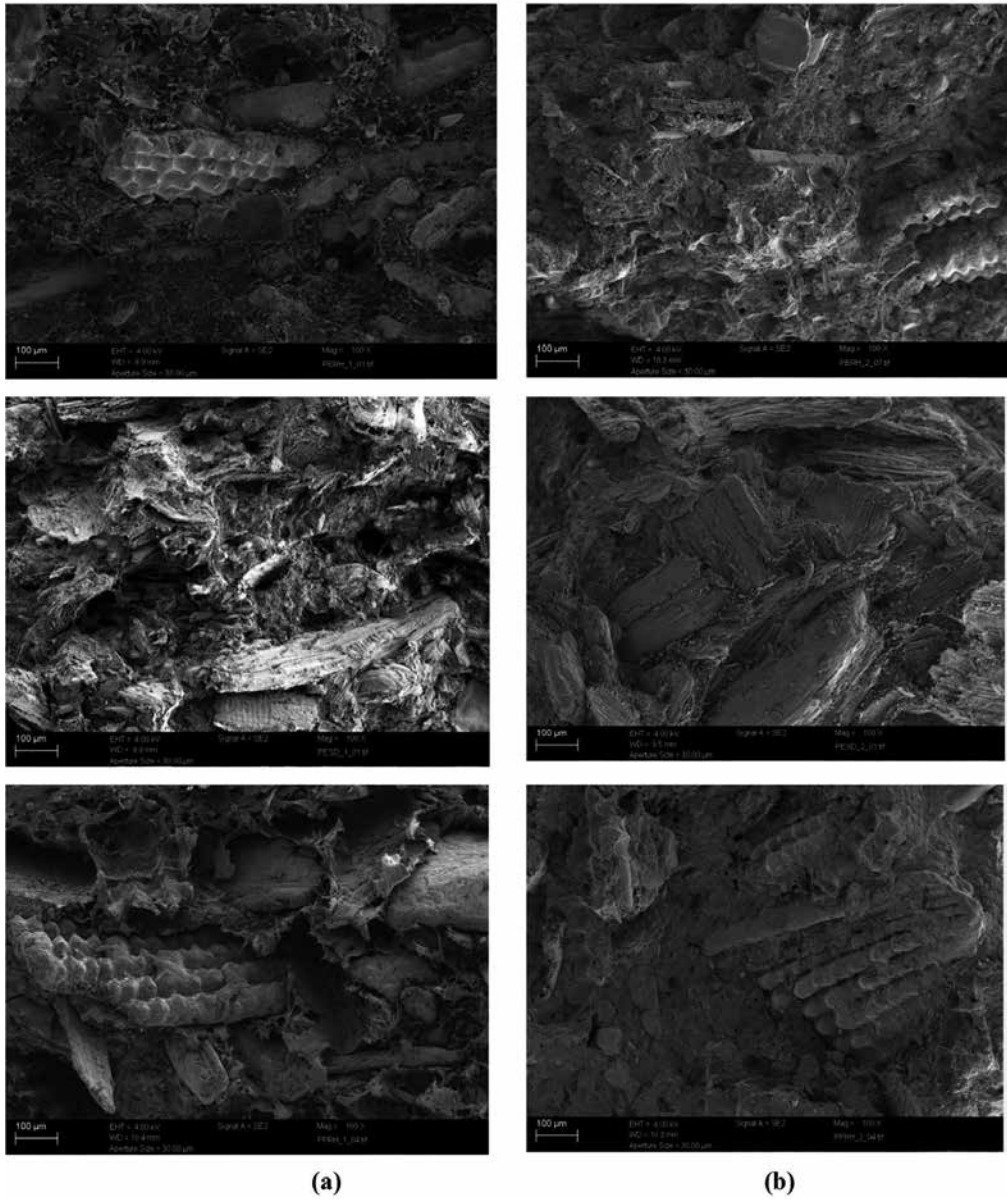


Figure 8. SEM micrographs of tensile fracture surfaces of PE/RH composites (top), PE/SD composites (middle), and PP/RH composites (bottom), (a) without and (b) with compatibilizer. Scale bar: 100 µm.

Figure 9 shows SEM micrographs of polished cross-sections for the composites in the longitudinal and transverse specimen direction. The saw dust is oriented along the specimen long axis due to the injection molding process. Here, an anisotropic mechanical behavior is expected. In rice husk, no preferred orientation of the platelets is seen for either PP/RH (as **Figure 9** bottom) or PE/RH (not shown here).

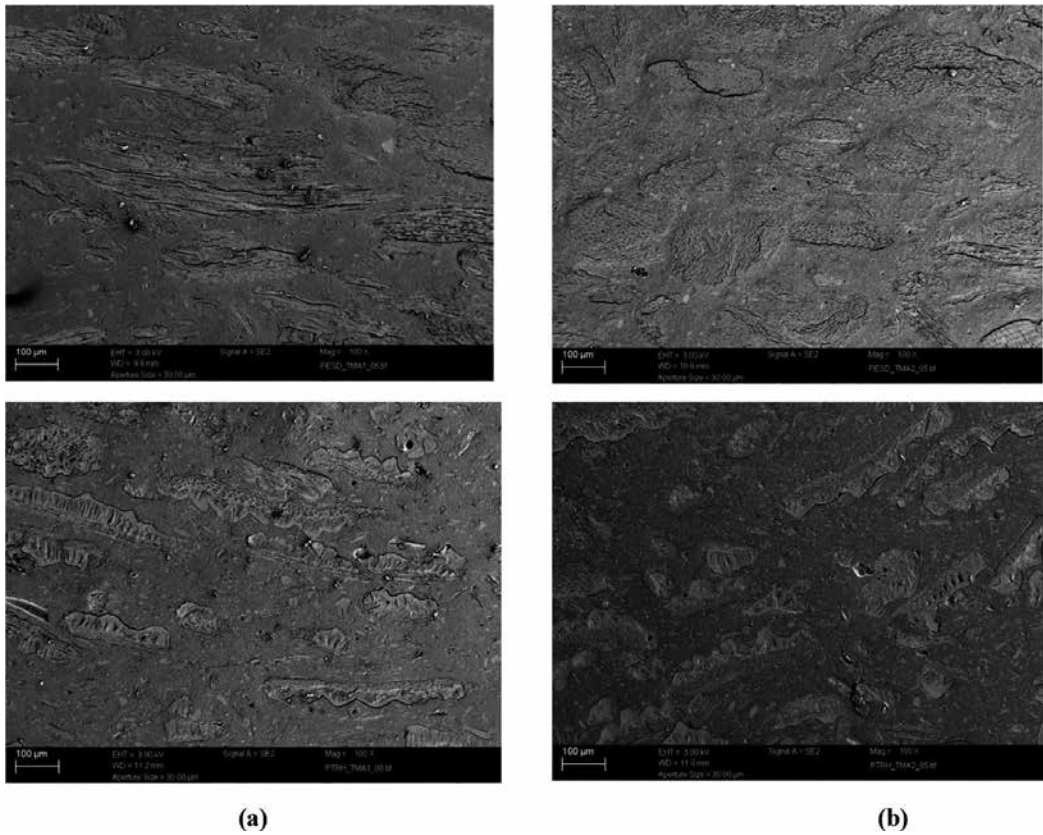


Figure 9. SEM photomicrographs of polished samples of PE/SD composites (top) and PP/RH composites (bottom), in x-direction (a) and in z-direction (b).

3.4. Hardness

Figure 10 shows the effect of the fillers on the hardness of three modified matrix composites [PE/RH (MA), PE/SD (MA), and PP/RH (MA)]. The fillers increased the hardness of polyolefines significantly. Neat and filled polypropylene had a higher hardness than neat resp. filled polyethylene. The addition of 50 wt.% fillers improved significantly the hardness of three composite systems. The hardness of PE and PP matrix composites increased about 78 and 65%, respectively. This was expected, since the chosen bio-fillers display considerably higher hardness than the soft polyolefine matrices, the hardness of RH being higher than that of SD. Thus, it was also expected that for the PE composites, the hardness of the PE/RH composites would be higher than that of the PE/SD composite. In fact, they had the same value at 50 wt.% filler content. This result could be caused by the higher volume content of SD filler (43 vol.%) compared to that of RH (39 vol.%). The hardness values can be considered as a measure of the wear resistance, since hard materials resist friction and wear better [15].

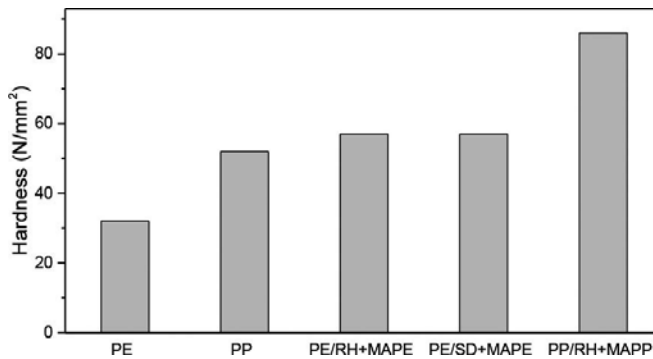


Figure 10. Hardness of polyolefine and filler/polyolefine composites at 50 wt.% filler content.

3.5. Thermomechanical analysis (TMA)

Figure 11 shows the thermal expansion as determined by TMA in x-direction and the coefficient of thermal expansion (CTE) values of the modified matrix composites [PE/RH (MA), PE/SD (MA), and PP/RH (MA)], respectively. The CTE values of pure PE and PP were determined to $134 \times 10^{-6}/^{\circ}\text{C}$ and $123 \times 10^{-6}/^{\circ}\text{C}$ for the temperature range of -10 to 50°C , respectively. Thermal expansion is higher for the range 50 – 100°C ($210 \times 10^{-6}/^{\circ}\text{C}$ for PE and $163 \times 10^{-6}/^{\circ}\text{C}$ for PP). CTE values of pure PE and PP decreased to 30–62% by adding 50 wt.% filler. While the CTE values of rice husk composites are isotropic, the difference in CTE values in longitudinal and transverse directions of the saw dust composite is quite high, especially in the high-temperature range 50 – 100°C ($94 \times 10^{-6}/^{\circ}\text{C}$ in x-direction and $187 \times 10^{-6}/^{\circ}\text{C}$ in z-directions). This reflects on the one hand the anisotropic behavior of the saw dust [16] and on the other hand the aspect ratio of the SD particles which in injection molding lead to orientation of the filler particles, confer Figure 9.

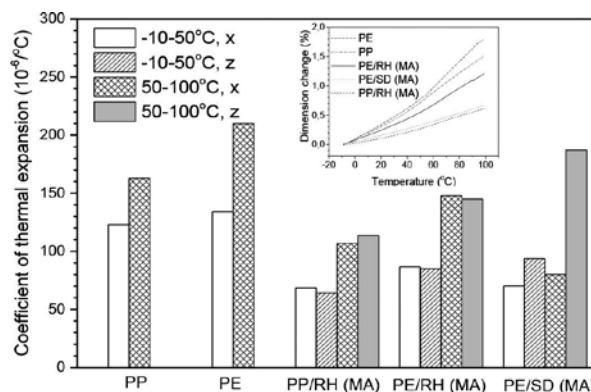


Figure 11. Coefficient of thermal expansion of polyolefine and filler/polyolefine composites, inset: Dimension change of polyolefine and filler/polyolefine composites in x-direction.

3.6. Dynamic mechanical thermal analysis (DMTA)

Dynamic mechanical thermal analysis (DMTA) is a sensitive technique that characterizes the mechanical responses of materials by monitoring property changes with respect to the temperature and/or frequency of oscillation [17]. It has been commonly used as a technique for investigating the viscoelastic behavior of the composites for determining their dynamic modulus such as storage modulus (E'), viscous behavior (loss modulus E''), and energy damping ($\tan \delta$) as a function of temperature [18–19]. The elastic component describes the energy stored in the system, while the viscous part describes the energy dissipated.

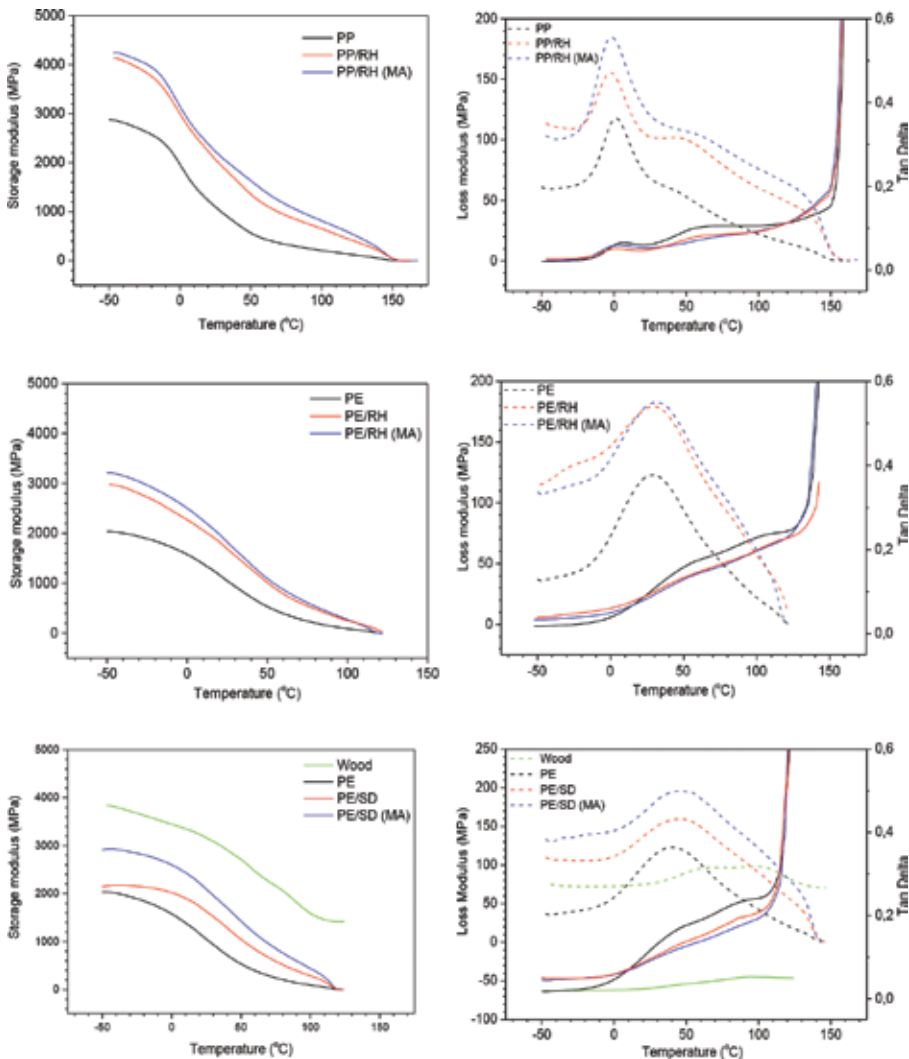


Figure 12. DMTA: storage modulus (left), loss modulus, and $\tan \delta$ (right) of PP, PE, wood, and composites with 50% filler loading, without and with compatibilizer.

Figure 12 shows the storage modulus E' , the loss modulus E'' , and $\tan \delta$ values of the composites without and with compatibilizers as well as the stock materials PP, PE, and wood. The storage modulus (E') of polypropylene and polyethylene matrix composites was higher than those of pure polypropylene and polyethylene matrices, respectively. This is the expected effect caused by the addition of high surface rigid fillers into semi-rigid polyolefine matrices. In all the systems, the storage modulus drops with increasing temperature due to the increased segmental mobility of the polymer chains. The E' value of polypropylene systems decreased rapidly at the glass transition above 0°C , whereas the E' value of wood and polyethylene systems decreased in a wider range around 30°C .

The temperature dependence of loss modulus and $\tan \delta$ for the polyolefine, wood, and three composite systems without and with compatibilizers is presented in **Figure 12**. The loss modulus (E'') is a measure of the absorbed energy due to the relaxation and is associated with viscous response of the viscoelastic materials. E'' of polyolefine and composites increased with temperature and had a peak in the transition region about 0 and 30°C for PP and PE systems, respectively.

The damping factor $\tan \delta$, defined as the ratio of the loss modulus to the storage modulus (E''/E'), is commonly used to characterize viscoelastic behavior of the materials, for example, T_g and energy dissipation of composite materials. With increasing temperature, the $\tan \delta$ values of PP and PP matrix composites increased due to the increased polymer chain mobility of the matrix and exhibited two relaxation peaks in the vicinity of 5 and 70°C . The low-temperature peak is related to the glass transition of the amorphous polymer fractions [20–21]. The high-temperature peak corresponds to the α transition related to the PP crystalline fractions. The α transition peak of the modified PP composite (81°C) was higher than that of the unmodified one (72°C) that can be a result of the existence of enhanced transcrystallinity around the fibers in the modified composites [20, 22].

For the polyethylene system, $\tan \delta$ curves of neat PE and the composites had less distinctive α transition processes compared to the loss modulus curves and there was no peak corresponding to the T_g of polyethylene (approximately -130°C) because it was not sufficiently cooled down to this temperature while carrying out the test. The α relaxation is generally attributed to segmental motions in the noncrystalline phase [23]. The α transition of the composites shifted to higher temperature compared to neat polyolefine. An addition of compatibilizer also led to shift slightly the α transition curve to the higher temperature, that is an indication of the presence of some processes, which have restricted the mobility of the chains in the crystalline phase so that more energy is required for the transition to happen. Therefore, the natural fibers somehow restricted the matrix polymer chains and increased the α transition temperature [17].

3.7. Differential scanning calorimetry (DSC) analysis

Differential scanning calorimetry (DSC) can be used to measure melting temperature (T_m), crystallization temperature (T_c), and crystalline content (X_c) of materials. **Figure 13** presents the heating and cooling thermograms for neat matrices and modified polyolefine composites which contain 50 wt.% fillers. The T_m of neat matrices and the composites was obtained from

the maximum of the endothermic melting peak (heating curves). The T_m of polyolefines was not significantly changed by the addition of bio-fillers. The peak area is reduced by 50% due to the filler, as expected.

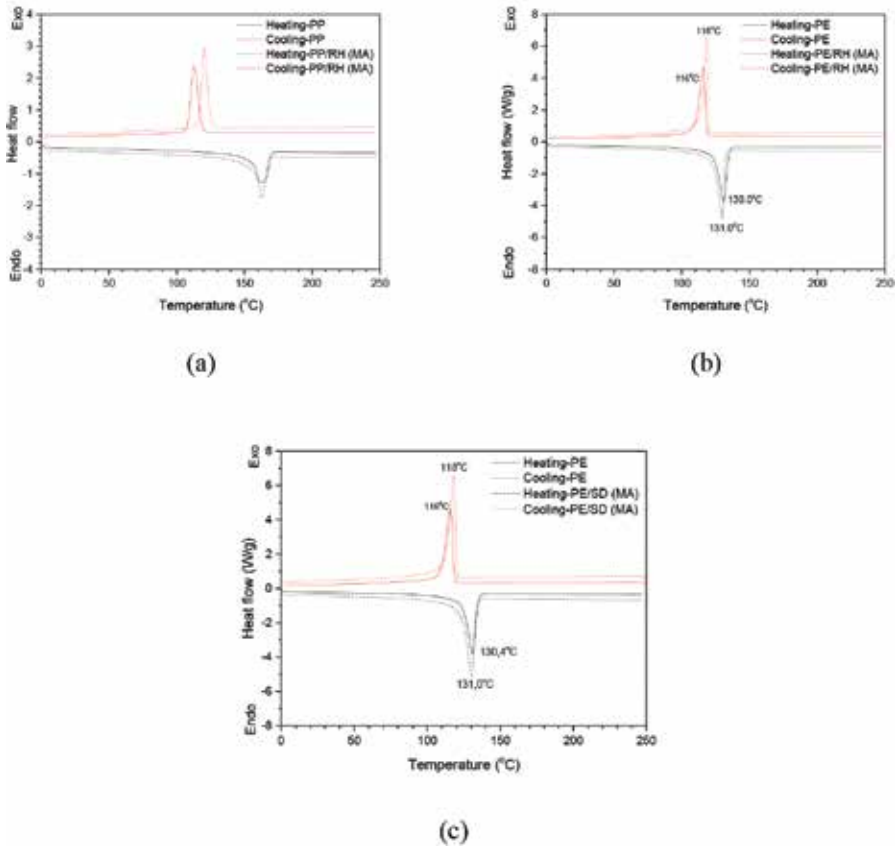


Figure 13. DSC heating (2nd run) and cooling curves of neat matrix and modified composites (50% filler) of (a) PP/RH, (b) PE/RH, and (c) PE/SD without and with compatibilizer.

To characterize the polyolefine crystallization, the crystallization peaks of the cooling run were analyzed, confer **Table 2**. T_c of neat matrices and the composites was obtained from the maximum of the exothermic crystallization peak. The crystallization is influenced by the fillers: For PP matrix without filler, the crystallization peak was observed at $T_c = 113^\circ\text{C}$, while for the PP matrix composites, these exothermic peaks shifted to higher temperatures ($T_c = 120^\circ\text{C}$).

This shift to earlier crystallization in the cooling run is due to the nucleating ability of the compatibilizer MAPP, which is enriched in the interphase, and perhaps the cellulosic filler surface, creating a transcrystalline interphase morphology, which improves the material properties [24].

The T_c of polyethylene systems ($T_c = 116^\circ\text{C}$) does not increase significantly upon addition of the fillers ($T_c = 118^\circ\text{C}$). As the neat PE crystallizes only 10°C below T_m and PE is a fast crystallizing thermoplast (i.e., the width of the crystallization peak is narrow), nucleation influences T_c less than in PP, where the difference $T_m - T_c = 30^\circ\text{C}$.

Samples	T_m ($^\circ\text{C}$)	T_c ($^\circ\text{C}$)	T_c ($^\circ\text{C}$) (onset)
PP	162.2	112.9	118.3
PP/RH (MA)	162.7	120.5	124.6
PE	131.0	115.9	118.1
PE/RH (MA)	130.0	118.5	119.6
PE/SD (MA)	130.4	118.2	119.7

Table 2. Thermal properties determined by DSC.

3.8. Thermogravimetric analysis (TGA)

Thermogravimetric analysis is becoming an increasingly useful tool for material characterization, particularly in the development of new materials. It is essential to monitor not only the final properties of the composites but also the basic raw materials through the processing procedure to the final product. Optimization of the processing temperature and time with an understanding of matrix, reinforcing element and interface between matrix and reinforcing phase, can lead to the best balance of composite properties such as modulus, thermal stability, and damping behavior [25]. Thermogravimetric analysis (TGA) can determine the moisture content, thermal cleavage, thermal degradation temperature, and thermal stability of composite materials [26, 27]. The differential thermogravimetric analysis (DTG) i.e. the slope of the TGA data curve, permits a more detailed analysis of thermal decomposition.

3.8.1. Fillers and Polyolefines

Figure 14 shows the results of the thermal analysis of the used polyolefines and fillers performed in nitrogen and air atmosphere. The TGA and DTG curves of the fillers in nitrogen as well as air atmosphere show a slight weight loss between 40 and 100°C , indicating the vaporization of water. A second weight loss from approximately 150 – 500°C is due to the decomposition of the three major constituents of bio-fillers, namely cellulose (275 – 350°C), hemicellulose (150 – 350°C), and lignin (250 – 500°C) [26, 28–30]. At 700°C , rice husk and saw dust leave a greater char content, decomposing only by about 65 and 80% in nitrogen cf. **Table 3**. The ash in the RH is mainly composed of silica (96%) [26]. In an air atmosphere, rice husk degradation shifted to lower temperature values and split into two processes (320 and 438°C). The second may be associated with thermal oxidation degradation of char. Therefore, the residues of RH filler at 700°C in the air atmosphere (20%) were lower than that in nitrogen atmosphere (36%).

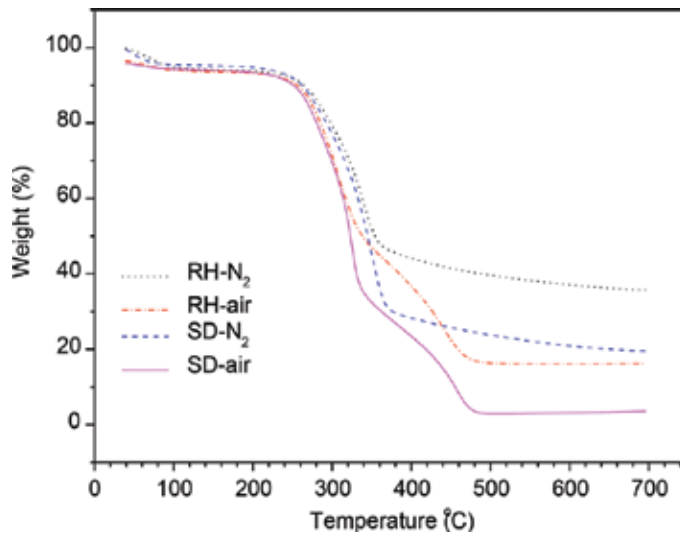


Figure 14. TGA curves of stock materials: fillers saw dust and rice husk as well as polyolefines PP and PE in nitrogen and air atmospheres.

	Residue in nitrogen atmosphere			Residue in air atmosphere		
PP	1.8			0.8		
PE	1.8			1.0		
RH	35.7			19.8		
SD	19.6			7.8		
Filler content	30%	40%	50%	30%	40%	50%
PP/RH	11.0	12.7	14.1	5.5	6.9	8.0
PE/RH	10.9	12.2	18.8	5.5	6.7	9.4
PE/SD	4.5	7.4	8.8	1.0	1.0	1.3

Table 3. Residues of polymers and fillers as well as their composites at 700°C in nitrogen and air atmosphere in %.

PE and PP decompose at temperatures above 400°C, cf. **Figure 14**. In nitrogen atmosphere, thermal degradation of PP and PE occurs very rapidly at 468 and 488°C, respectively. In air, the thermal resistance of both polyolefines (PP and PE) starts at 250°C. While PP is fully degraded at 380°C, PE decomposed more gradually and is fully degraded at 470°C. The maximum decomposition rates of PP and PE in the air occurred at 371 and 399°C, respectively. Both PP and PE decomposed almost completely. Residues of both polyolefines at 700°C were <2% in nitrogen and <1% in air atmosphere.

3.8.2. Composites

Figure 15 shows the TGA and DTG curves of the polyolefines, fillers, and the composites with filler content ranging from 30 to 50 wt.% in nitrogen and air atmosphere. The TGA or DTG

analyses performed in nitrogen atmosphere show two regions of thermal decomposition that consist of the superposition of the profiles of filler and polyolefines. As the filler is less thermally stable than the matrix polymer, when filler loading is increased, the thermal stability of the composites slightly decreases, whereas the final ash content increased (**Table 3**).

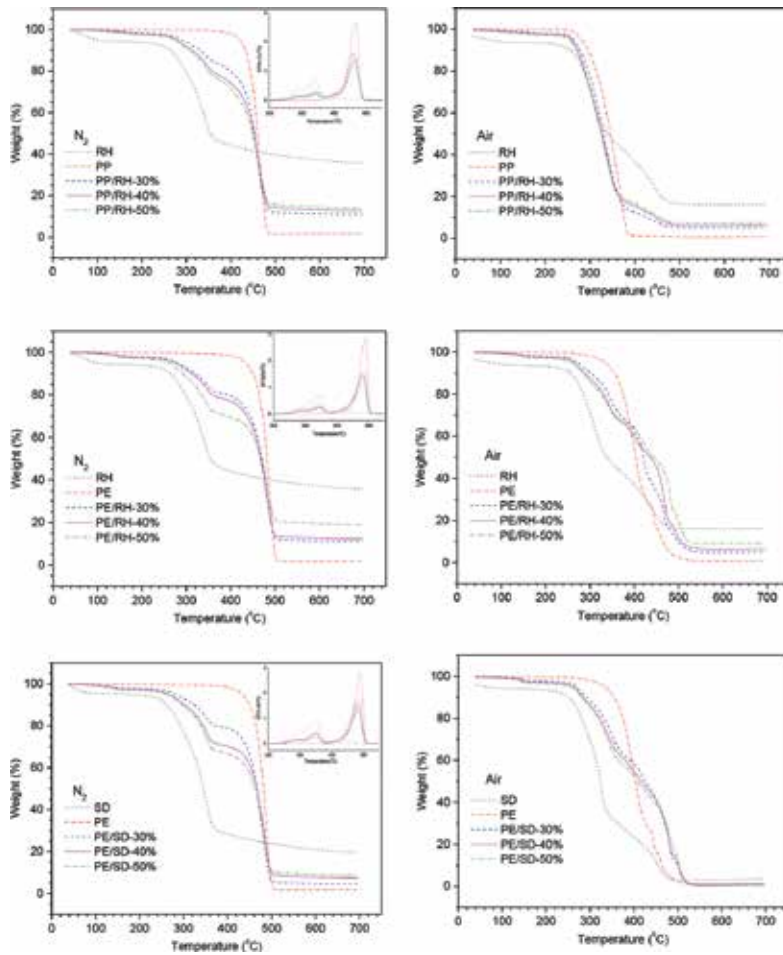


Figure 15. TGA of fillers, plastics, and the composites in nitrogen (left) and air (right) of PP/RH (top), PE/RH (middle), and PE/SD (bottom) composites, inset in left images: DTG.

In the case of the two studied PE composites decomposed in air, the TGA/DTG curves of the composites correspond to the superposition of the separate components only up to 400°C, whereas the charring behavior is different. The final reduction is only reached at 500°C, 60°C above the temperature where both PE and filler are completely degraded thermally oxidatively. That may be due to a thermally stable material (char), formed during the oxidation or thermal degradation of hemicellulose, cellulose, and lignin, providing a thermal shielding and acting as diffusion barrier on the polyethylene decomposition process. Moreover, the second

peak of decomposition of olefinic products or their oxidation degradation products containing functional groups such as C=O, O-H, and C-O-C which formed in the first stage of polyethylene degradation appears at 438°C. This second main peak of PE degradation is in superposition with the second main peak of the bio-fillers due to degradation of char (**Figure 15a**). Therefore, the second-stage degradation of both polyethylene and the bio-fillers is competitive at above 438°C, that can also lead to retard the degradation of the composite. However, there is a one-step degradation of polypropylene in air atmosphere and PP fully degraded at 380°C. Therefore, RH char did not affect the degradation of polypropylene.

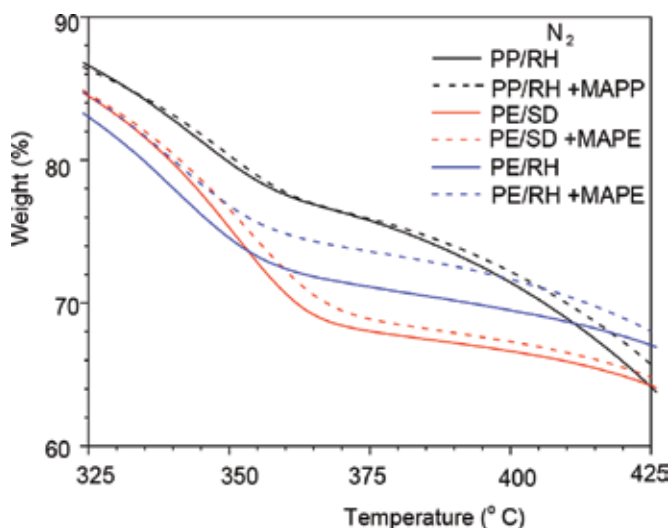


Figure 16. Effect of compatibilizers on TGA of 50% filler composites in nitrogen atmosphere.

The RH-filled PE leaves a bigger residue than the SD-filled PE, as expected from the TGA analysis of the fillers. The residues of rice husk composites (10.9–18.8% in nitrogen and 5.5–9.4% in air atmosphere) were much higher than those of saw dust composites (4.5–8.8% in nitrogen and 1.0–1.3% in air atmosphere) due to high ash content of rice husk compared to saw dust. The residue is in all cases 0–10% smaller than the value calculated from the residues of the separate components, and only in the saw dust composites in air, it is a third of the expected value. The filler/matrix interaction leads to a more profound decomposition maybe due to a wick effect.

Figure 16 shows the TGA curves of the composites at 50 wt.% filler without and with compatibilizers (2 wt.% for PP matrix composites and 4 wt.% for PE matrix composites). The thermal stability and degradation temperature of the composites with compatibilizers [PP/RH (MA), PE/RH (MA), and PE/SD (MA)] were slightly higher than those of the composites without compatibilizers (PP/RH, PE/RH, and PE/SD). The improved thermal stability of the composites with compatibilizers is due to enhanced interfacial interaction and additional intermolecular bonding (ester and hydrogen bonds) between hydroxyl groups of rice husk, saw dust and the anhydride functional groups of compatibilizers.

4. Conclusions

The performance of rice husk and saw dust fillers, used as low ecological footprint reinforcement of PE and PP, was investigated. SEM micrographs show the different morphology of rice husk platelets and fibrous saw dust fillers. Rice husk has the higher stiffness and the higher density of the two fillers considered. In a PE or PP matrix, the fillers increase the bending moduli. In composites without compatibilizer, an increase in filler load leads to decreased tensile, bending, and impact strengths.

Here, PE matrix composites with saw dust have smaller moduli but higher strengths than those with rice husk filler. The tensile, bending, and impact strengths of bio-filler/polyolefine composites increase with increasing compatibilizer content, due to the improvement in interfacial bonding strength between filler and matrix. The coefficient of thermal expansion of PP and PE decreased upon adding rice husk and saw dust fillers.

The thermal stability of the fillers or natural fibers in general is not as high as that of high-performance fibers. This limits the matrices of thermoplastic composites with bio-fillers to those materials processable below 200°C, such as PP, PE, or polylactic acid (PLA).

Rice husk and saw dust can be used as fillers in manufacturing inexpensive polyolefine composites for furniture and household articles as well as construction materials, generating economic development for rural areas and reducing environmental pollution caused by these bio-wastes if unused.

Acknowledgements

The authors are thankful to Chemtura Company for supplying the materials; Dr. Jianwen Liu, Sabine Krause, Birgit Schulze, Liane Häussler, Thanh Tran, Hang Tran, Dung Pham, Hieu Nguyen, Dat Nguyen, Xuan Vo, Linh Nguyen, Quang Le, Huan Vo, Chuong Hien, Men Tran, Truong Le, Huan Le, Nghia Tran, and Linh Pham for experimental assistance.

Author details

Thi Thu Loan Doan¹, Hanna M. Brodowsky^{2*} and Edith Mäder²

*Address all correspondence to: brodowsky@ipfdd.de

¹ Danang University of Science and Technology, Department of Chemical and Material Engineering, Danang, Vietnam

² Leibniz-Institut für Polymerforschung e.V., Department of Composite Materials, Dresden, Germany

References

- [1] Faruk O, Bledzki AK, Fink HP, Sain M. Biocomposites reinforced with natural fibres: 2000–2010. *Progr. Polym. Sci.* 2012; 37:1552-1596. doi: 10.1016/j.progpolymsci.2012.04.003
- [2] Yao F, Wu Q, Lei Y, Xu Y. Rice straw fibre-reinforced high-density polyethylene composite: effect of fiber type and loading. *Ind. Crops Prod.* 2008;28(1):63–72. doi: 10.1016/j.indcrop.2008.01.007
- [3] Panthapulakkal S, Sain M, Law S, Effect of coupling agents on rice-husk-filled HDPE extruded profiles. *Polym. Int.* 2005;54:137–142. doi: 10.1002/pi.1657
- [4] Marti-Ferrer F, Vilaplana F, Ribes-Greus A, Benedito-Borras A, Sanz-Box C. Flour rice husk as filler in block copolymer polypropylene: effect of different coupling agents. *J. Appl. Polym. Sci.* 2006; 99:1823–1831. doi: 10.1002/app.22717
- [5] Correa CA, Razzino C, Hage E. Role of maleated coupling agents on the interface adhesion of polypropylene-wood composites. *J. Thermoplast. Compos. Mater.* 2007;20:323–339. doi: 10.1177/0892705707078896
- [6] Keener TJ, Stuart RK, Brown TK. Maleated coupling agents for natural fibre composites. *Composites A.* 2004;35:357–362. doi: 10.1016/j.compositesa.2003.09.014
- [7] Doan TLL, Gao SL, Mäder E. Jute/polypropylene composites I. Effect of matrix modification. *Compos. Sci. Technol.* 2006;66:952–963. doi: 10.1016/j.compscitech.2005.08.009
- [8] Doan TTL, Brodowsky HM, Mäder E. Jute fibre/ polypropylene composites II. Thermal, hydrothermal and dynamic mechanical behaviour. *Compos. Sci. Technol.* 2007;67(13): 2707–2714. doi:10.1016/j.compscitech.2007.02.011
- [9] Negri AP, Cornell HJ, Rivett DE. A model for the surface properties of fibers. *J. Text. Res.* 1992;63:109–16.
- [10] Essabir H, Hilali E, ElGharad A, El Minor H, Imad A, Elamraoui A, Al Gaoudi O. Mechanical and thermal properties of bio-composites based on polypropylene reinforced with nut shells of Argan particles. *Mater. Des.* 2013;49:442–448. doi: 10.1016/j.matdes.2013.01.025
- [11] Fu SY, Feng XQ, Lauke B, Mai YW. Effects of particle size, particle/matrix interface adhesion and particle loading on mechanical properties of particulate–polymer composites. *Composites B* 2008;39:933–61. doi: 10.1016/j.compositesb.2008.01.002
- [12] Yao F, Wu Q, Lei Y, Xu Y. Rice straw fiber-reinforced high-density polyethylene composite: effect of fiber type and loading. *Ind. Crops Prod.* 2008;28(1):63–72. doi: 10.1016/j.indcrop.2008.01.007

- [13] Bledzki AK, Mamun AA, Volk, J. Barley husk and coconut shell reinforced polypropylene composites: the effect of fibre physical, chemical and surface properties. *Compos. Sci. Technol.* 2010;70:840–846. doi: 10.1016/j.compscitech.2010.01.022
- [14] Bledzki AK, Mamun AA, Volk J. Physical, chemical and surface properties of wheat husk, rye husk and soft wood and their polypropylene composites. *Composites A* 2010;41:480–488. doi: 10.1016/j.compositesa.2009.12.004
- [15] Bledzki AK, Mamun AA, Bonnia NN, Ahmad S. Basic properties of grain by-products and their viability in polypropylene composites. *Ind. Crops Prod.* 2012;37:427–434. doi: 10.1016/j.indcrop.2011.05.010
- [16] Lee SM, Cho D, Park WH, Lee SG, Han SO, Drzal LT. Novel silk/poly(butylene succinate) biocomposites: the effect of short fibre content on their mechanical and thermal properties. *Compos. Sci. Technol.* 2005;65:647–657. doi: 10.1016/j.compscitech.2004.09.023
- [17] Behzad M, Tajvidi M, Ehrahimi G, Falk RH. Dynamic mechanical analysis of compatibilizer effect on the mechanical properties of wood flour/high-density polyethylene composites. *IJE Trans. B* 2004;17:95–104.
- [18] Lopez-Manchado MA, Arroyo M. Thermal and dynamic mechanical properties of polypropylene and short organic fibre composites. *Polymer* 2000;41:7761–7767. doi: 10.1016/S0032-3861(00)00152-X
- [19] Ray D, Sarkar BK, Das S, Rana AK. Dynamic mechanical and thermal analysis of vinyl ester-resin-matrix composites reinforced with untreated and alkali-treated jute fibres. *Compos. Sci. Technol.* 2002;62:911–917. doi: 10.1016/S0266-3538(02)00005-2
- [20] Amash A, Zugenmaier P. Study on cellulose and xylan filled polypropylene composites. *Polym. Bull.* 1998;40: 251-258. doi: 10.1007/s002890050249
- [21] Garcia-Martinez JM, Laguna O, Areso S, Collar EP. A dynamic-mechanical study of the role of succinil-fluoresceine grafted atactic polypropylene as interfacial modifier in polypropylene/talc composites.: Effect of grafting degree. *Eur. Polym. J.* 2002; 38:1583-1589. doi: 10.1016/S0014-3057(02)00051-4
- [22] Quan H, Li ZM, Yang MB, Zhang R. On transcrystallinity in semi-crystalline polymer composites. *Compos. Sci. Technol.* 2005; 65:999-1021. doi: 10.1016/j.compscitech.2004.11.015
- [23] Sirotkin RO, Brooks NW, The dynamic mechanical relaxation behavior of polyethylene copolymers cast from solution. *Polymer* 2001;42 :9801-9808. doi: 10.1016/S0032-3861(01)00535-3
- [24] Na K, Park HS, Won HY, Lee JK, Lee KH, Nam JY, Jin BS. SALS study on transcrystallization and fiber orientation in glass fiber/polypropylene composites. *Macromol. Res.* 2006;14:499-503. doi: 10.1007/BF03218715

- [25] George J, Bhagawan SS, Thomas S. Thermogravimetric and dynamic mechanical analysis of pineapple fibre reinforced polyethylene composites. *J. Therm. Anal.* 1996;47: 1121-1140. doi: 10.1007/BF01979452
- [26] Kim HS, Yang HS, Kim HJ, Lee BJ, Hwang TS. Thermal properties of agro-flour-filled biodegradable polymer bio-composites. *J. Therm. Anal. Cal.* 2005;81:299. doi: 10.1007/s10973-005-0782-7.
- [27] Mohanty S, Verma SK, Nayak SK. Compos. Dynamic mechanical and thermal properties of MAPE treated jute/HDPE. *Composites. Sci. Technol.* 2006;3/4:538-547. doi: 10.1016/j.compscitech.2005.06.014
- [28] Marcovich NE, Villar MA. Thermal and mechanical characterization of linear low-density polyethylene/wood flour composites. *J. Appl. Polym. Sci.* 2003;90:2775-2784. doi: 10.1002/app.12934
- [29] Wielage B, Lampke T, Marx G, Nestler K, Starke D. Thermogravimetric and differential scanning calorimetric analysis of natural fibres and polypropylene. *Thermochim. Acta* 1999;337:169-177. doi:10.1016/S0040-6031(99)00161-6
- [30] Hatakeyema H, Tanamachi N, Matsumura H, Hirose S, Hatakeyama T. Bio-based polyurethane composite foams with inorganic fillers studied by thermogravimetry. *Thermochim. Acta* 2005;431:155-161. doi:10.1016/j.tca.2005.01.065

Characterization of Rice Husk Biofibre-Reinforced Recycled Thermoplastic Blend Biocomposite

Ruey Shan Chen and Sahrim Ahmad

Additional information is available at the end of the chapter

<http://dx.doi.org/10.5772/65026>

Abstract

In this century, the developing country has a high potential towards the growth of green composites, and therefore there is significant achievement in green technology especially in the field of building constructions and automotive because of the environment and sustainability issues. The market for development of advanced biocomposite materials produced from biomass and recyclable post-consumer plastics is increasing. Natural fibre-reinforced biocomposites based on rice husk biofibre (RHB), recycled high-density polyethylene (rHDPE) and recycled polyethylene terephthalate (rPET) were prepared through a two-step extrusion and hot pressing. The influence of thermoplastic blend (TPB) matrix types (uncompatibilized and compatibilized with 5 parts per hundred compound (phc) ethylene-glycidyl methacrylate (E-GMA) copolymer) and high fibre contents of 50, 60, 70 and 80 wt% RHB on the composite properties was studied. Maleic anhydride polyethylene (MAPE) was added as a coupling agent to enhance the interfacial adhesion of the fibre-matrix phases. Results showed that water absorption, thickness swelling (TS) and tensile and flexural properties enhanced tremendously with the increase of rice husk filler loadings. Biocomposites based on compatibilized blend matrix exhibited higher mechanical properties and dimensional stability than those based on uncompatibilized ones. Thermal analysis results from thermogravimetric analysis (TGA) and differential scanning calorimetry (DSC) indicated the notable improvement in thermal stability as the added rice husk (RH) fibre content increased. From these results, we can conclude that RHF can work well with rHDPE/rPET thermoplastic blend for manufacturing high loading biocomposite products.

Keywords: green composite, high fibre loading, recycled polymer blend, agro waste, melt blending, properties

1. Introduction

Nowadays, environmental friendliness is becoming one of the important criterions to be considered in material selection for the introduction of new materials and products resulting from global ecological concern and new rules and regulations [1, 2]. Waste plastic industrial and agricultural materials are currently becoming of interest worldwide in the field of composite materials, as a result of the increasing demand for environmentally friendly raw materials. The development of new biocomposites composed of recycled materials by post-consumer polymers as matrixes and agro-waste fibres as reinforcement phases and the better understanding of their fibre-matrix interactions will enhance their aggregated values and applications. Consequently, these reduce their environmental impact as waste materials and help to close the carbon cycle and manufacture greener composites [3, 4]. Natural fibre-reinforced thermoplastic composites have been used in various applications as furniture and architectural materials and, more recently, in the construction and automotive industry [5, 6].

Malaysia is well endowed with rich and renewable natural tropical forest resources which provide a variety of natural fibres. Rice husk (RH), one type of natural fibres, is an agricultural industrial residue generated during the rice-milling process in rice-producing countries, especially in the Asian, Pacific and North American regions [7]. In the paddy plants of Malaysia, with a land area of approximately 680 thousand hectares, a total of 840 thousand tons of RH is produced annually [8]. For every one million tonnes of paddy rice harvested, it is estimated that about 200 thousand tonnes of the RH was used for the purposes as fuel sources, animal beddings and landfill. The raw RH comprises several components with different percentages that are 25–35 % of cellulose, 18–21 % of hemicellulose, 26–31 % of lignin, 15–17 % of silica, 2–5 % of solubles and 7.5 % of moisture content. The use of RH in composite industry might be because of its low cost and bulk density, abundant, toughness, abrasive in nature, resistance to weathering, renewability, biodegradability and nonhazardousness [9, 10]. Compared to wood-based composites, the composites containing RH possess better water absorption and dimensional stability, as well as higher resistance to biological and termite attack. Therefore, these composites are progressively being used in automotive industry for interior parts such as car trims and door panels and in the building construction like interior panels, decks and window and door frames [7].

The worldwide fabrication and consumption of plastics have resulted in a remarkable contribution to municipal solid waste (MSW) [11]. For example, plastic wastes accounts for 24 % of the annual 7.7 million tonnes of the MSW generated in Peninsular Malaysia with the population of 28.45 million inhabitations in 2010 [12]. Majority of them consist of a significant amount of polyethylene (PE) and polyethylene terephthalate (PET) [13]. High-density polyethylene (HDPE) and PET are widely used in packaging industry, and their annual rates of consumption are kept increasing. Blends of HDPE/PET possess the intermediate characteristics and properties between both polymer components. As compared to PET, they have lower brittleness; as compared to HDPE, they have higher stiffness, flow better and are fast cooling. It has been revealed that ethylene-glycidyl methacrylate (E-GMA) copolymer serves as the most effective compatibilizer in order to enhance the miscibility between the hydrophobic

HDPE and hydrophilic PET, thus improving the blend properties [14]. The resultant blends made of recycled polymers have been used in wood-plastic composites (WPC) as matrices [15].

Both thermoplastic and thermoset polymers either in the form of virgin or recycled can be used in the manufacture of natural fibre-polymer composites (NFPCs). Because recycled polymers are produced in large amounts daily and are cheaper than virgin polymers, the waste polymers offer a promising raw material source for the composites [16]. Traditionally, a single type of polymer is used as matrix in NFPCs [16–18]. However, there are very limited studies on the NFPCs made of polymer blends [15, 19].

In this chapter, the influence of rice husk biofibre (RHB) contents (50–80 wt%) on the physical, mechanical, thermal and morphological properties of recycled thermoplastic blend (TPB) was investigated.

2. Experimental details

Thermoplastic blend (TPB) matrix used recycled high-density polyethylene (rHDPE) with a density of 923 kg/m³ and melt flow index of 0.72 g/10 min at 190 °C and recycled polyethylene terephthalate (rPET) with an intrinsic viscosity of 0.68 dL/g. Ethylene-glycidyl methacrylate (E-GMA) copolymer (trade name of Lotader AX8840), with a melt flow index of 5 g/10 min at 190 °C and a glycidyl methacrylate content of 8 %, was used as compatibilizer for immiscible TPB. Rice husk flour (RHF) with particle size of 100 mesh was used as agro-waste filler. Maleic anhydride polyethylene (MAPE), a coupling agent with a melting peak temperature of 135.2 °C, was used. All the raw materials were supplied by a local factory, namely, Bio Composite Extrusions Sdn. Bhd.

2.1. Preparation of thermoplastic blend (TPB)

The rHDPE and rPET were compounded via extrusion process by using a laboratory-scale co-rotating twin screw extruder (Thermo Prism TSE 16 PC). The screw-rotating speed was fixed at 30 rpm. The four barrel temperatures from feeding to die zones were set as 250, 270, 240 and 190 °C, respectively. For the uncompatibilized thermoplastic blend (UTPB), the weight ratio of rHDPE/rPET was fixed at 75/25 (wt%). Meanwhile, 5 parts per hundred compounds (phc) of E-GMA was added in the compatibilized thermoplastic blend (CTPB) with the same ratio of both plastics.

2.2. Preparation of RHF-reinforced biocomposites

The pre-extruded TPB pellets were compounded with RHF and 3 phc of MAPE at temperature profiles of 170, 215, 210 and 195 °C and screw speed of 30 rpm. Prior to extrusion, RHF was oven-dried at 90 °C for 24 h to remove the moisture of RHF. After extrusion, the compression moulding was performed at 200 °C using a hot/cold press machine (LP50, Labtech Engineering Company Ltd.). The preheating, venting, full pressing and cold pressing times were set at 3,

2, 5 and 5 min, respectively. In this study, the experimental variables studied were polymer blend types (UTPB and CTPB) and rice husk flour content (50, 60, 70 and 80 wt%).

2.3. Characterization

Water absorption and thickness swelling (TS) tests were performed according to the ASTM D 570-98 method. The specimen (dimension: $76.2 \times 25.4 \times 3.2$ mm) for each formulation was oven-dried for 24 h at 100 °C. Each oven-dried specimen was weighed using an analytical balance with a precision of 1 mg; the thickness of each oven-dried specimen was measured using a digital calliper with a precision of 0.01 mm. The specimens were then soaked in distilled water at 25 °C. The weight and thickness changes were determined periodically until 119 days. Specimens were removed from the water, wiped dry with tissue paper and measured. The percentages of water absorption (WA) and thickness swelling (TS) were calculated using Eqs. 1 and 2:

$$\text{WA (\%)} = \frac{W_t - W_0}{W_0} \times 100 \quad (1)$$

$$\text{TS(\%)} = \frac{T_t - T_0}{T_0} \times 100 \quad (2)$$

where W_0 and W_t represent the oven-dry weight (the initial weight) and weight after water exposure at time t , respectively, whereas T_0 and T_t represent the oven-dry thickness and thickness after water exposure at time t , respectively. Three replicates of specimens were tested for each formulation to obtain the average results.

Compression-moulded composite panels were cut according to ASTM D 638-03 (type I) for tensile testing, ASTM D 790-03 for flexural testing and ASTM D 256-05 for impact strength. Both tensile and flexural testings are carried out using a universal testing machine (model Testometric M350-10CT) at 5 mm/min. The notched Izod impact testing was performed using the Ray-Ran Universal Pendulum Impact System at 3.46 ms^{-1} and 2.765 J with a load weight of 0.452 kg. In mechanical tests, five replicates of specimens were tested for each formulation to obtain the average results.

Thermogravimetric analysis (TGA) and differential scanning calorimetry (DSC) were conducted using a Mettler Toledo TGA/SDTA851e and DSC 882e, respectively, on the samples of about 10–15 mg. Samples of TGA were tested at a heating rate of 10 °C/min over the temperature range from 25 °C to 600 °C, the temperature of complete degradation. Balance accuracy of TGA is ± 0.1 %. The DSC samples were scanned from 25 °C to 300 °C at heating rate of 10 °C/min, under atmospheric air flow condition. Burning test was carried out in accordance to ASTM D 5048-90 (procedure A—test of bar specimens) to determine the relative burning characteristics and flame-resistance properties. The burning rates of specimens are calculated using the

equation of $V = L/t$ where V is the burning rates (mm/s), L is the burned length (mm) and t is the burning time (seconds).

The morphology of the fracture surface of broken sample from tensile testing was analysed using SEM (VPSEM Philips XL-30). The samples were sputter-coated with gold before examination of SEM.

3. Results and discussion

3.1. Long-term water absorption and thickness swelling

Theoretically, the shape of the sorption curve plotted with experimental values is represented by the Fick's equation as $\log(M_t/M_m) = \log(k) + n\log(t)$, where M_t is the water absorbed at time t , M_m is the maximum water absorbed at saturation point and k and n are the diffusion kinetic parameters. The n values determined the diffusion behaviour cases: case I ($n = 0.5$) is Fickian diffusion, case II ($n \geq 1$) is relaxation controlled, and case III ($0.5 < n < 1$). The k values represent the interaction between the material and moisture. Both coefficients of n and k are determined from the slope and intercept of log plot of M_t/M_m versus t which can be drawn from experimental data, respectively [1]. As shown in **Table 1**, the value of n is close to 0.5 which confirmed that all the investigated biocomposites exhibited Fickian diffusion behaviour. The k value was found to increase with the increasing wt% of RHB in the biocomposites irrespective of the TPB matrix types, in which a higher value of k indicates that the biocomposite attained the saturation point of WA in a shorter period of time. This was due to the increased hydroxyl and carbonyl groups as the RHB content increased [2].

Composite samples	n	k (h^{-n})	M_m (%)	$D \times 10^{-13}$ ($\text{m}^2 \text{s}^{-1}$)	TS_∞ (%)	$K_{SR} \times 10^{-3}$ (h^{-1})
Biocomposite UTPB/RHB						
0 wt% RHB	–	–	0.22 ± 0.04	–	0.19 ± 0.03	–
50 wt% RHB	0.467	0.021	8.76 ± 0.32	1.84 ± 0.09	4.94 ± 0.68	3.53 ± 0.17
60 wt% RHB	0.522	0.022	13.73 ± 0.55	3.47 ± 0.13	5.49 ± 0.75	4.39 ± 0.31
70 wt% RHB	0.511	0.025	14.16 ± 0.59	5.66 ± 0.49	6.76 ± 0.58	4.50 ± 0.43
80 wt% RHB	0.489	0.800	18.97 ± 0.73	42.54 ± 1.05	9.41 ± 0.77	10.29 ± 0.82
Biocomposite CTPB/RHB						
0 wt% RHB	–	–	0.14 ± 0.02	–	0.14 ± 0.01	–
50 wt% RHB	0.504	0.019	6.92 ± 0.22	2.02 ± 0.06	4.17 ± 0.26	2.10 ± 0.14
60 wt% RHB	0.470	0.020	9.96 ± 0.43	2.04 ± 0.11	4.56 ± 0.34	2.21 ± 0.16
70 wt% RHB	0.524	0.023	13.13 ± 0.67	5.35 ± 0.37	6.08 ± 0.52	3.74 ± 0.28
80 wt% RHB	0.496	0.028	14.71 ± 0.84	6.46 ± 0.61	8.71 ± 0.79	4.66 ± 0.50

Table 1. Diffusion kinetic parameters, coefficients and permeability of biocomposites.

The diffusion coefficient D represents the ability of water molecules to penetrate inside the composites, which can be computed with Eq. 3, in the case where the M_t value is $< 60\%$ of the M_m value.

$$D = \pi \left[\frac{\theta}{4M_m} \right] \quad (3)$$

where D is the diffusion coefficient, θ is the slope of the linear portion of M_t against \sqrt{t}/h and h is the height (thickness) of composite panel [3]. In **Table 1**, the M_m and D increase with the RHB content which indicates that the biocomposites containing the higher wt% of natural fibre tended to absorb more water. This phenomenon could be explained by the components of RHB (cellulose, hemicellulose and lignin) that mostly contain polar hydroxyl groups which tend to combine with water molecules by forming hydrogen bond [4]. The difference in D between UTPB and CTPB matrixes was more predominant in the biocomposites at higher wt% of fibre. Especially at 80 wt% RHB, a remarkable decrease in M_m and D was observed for the biocomposites based on CTPB matrix as compared to UTPB ones. This confirmed the reduction of water absorption. This was probably because the free hydroxyl and carboxyl groups available in hydrophilic rPET play the role in absorbing water as there are lack of chemical interaction and bonding between polar rPET and nonpolar rHDPE chains in the case of without compatibilizer in the UTPB matrix [5]. Meanwhile, the presence of E-GMA compatibilizer tended to bind the rHDPE and rPET together, hence decreasing the hydrophilicity of CTPB matrix as well as reducing the WA.

The theoretical WA can be estimated using Fick's second law of diffusion. For the initial part of the curve where $M_t/M_m < 0.6$ [6], it can be predicted using Eq. 4. For the second half-sorption curve where $M_t/M_m > 0.6$ [6], an approximation has been proposed with Eq. 5 [7]:

$$\frac{M_t}{M_m} = \frac{4}{h} \sqrt{\frac{Dt}{\pi}} \quad (4)$$

$$\frac{M_t}{M_m} = 1 - \exp \left[-7.3 \left(\frac{Dt}{h^2} \right)^{0.75} \right] \quad (5)$$

Figures 1 and **2** depict the long-term WA of TPB/RHB biocomposites measured after a certain period of immersion in distilled water, respectively. The experimental data, as represented by the various symbols, show that the water absorbed by the biocomposites increased sharply with time and then gradually slowed until it reached an equilibrium state (M_m). The solid curves display the estimation of theoretical WA behaviour following Fick's second law of diffusion (Eqs. 4 and 5). All the curves in both **Figures 1** and **2** were found to follow the Fickian-type behaviour, as conformed to the coefficient of n which was close to 0.5 (**Table 1**). Thus, it

can be concluded that the experimental results will fit the Fickian mode of diffusion, especially in the initial stage of diffusion. This result is in agreement with the previous studies on polymer/natural fibre composites [6, 8]. **Figures 3 and 4** present the thickness swelling (TS) of immersed UTPB and CTPB biocomposites filled with RHB. It can be observed that TS was positively related to the WA where TS increased rapidly in the initial stage for all RHB contents and then remained constant. The higher the RHB loading, the more hydrogen bonding was created in the fibre cell wall by the adsorbed water, and thus, the higher TS of biocomposites was obtained.

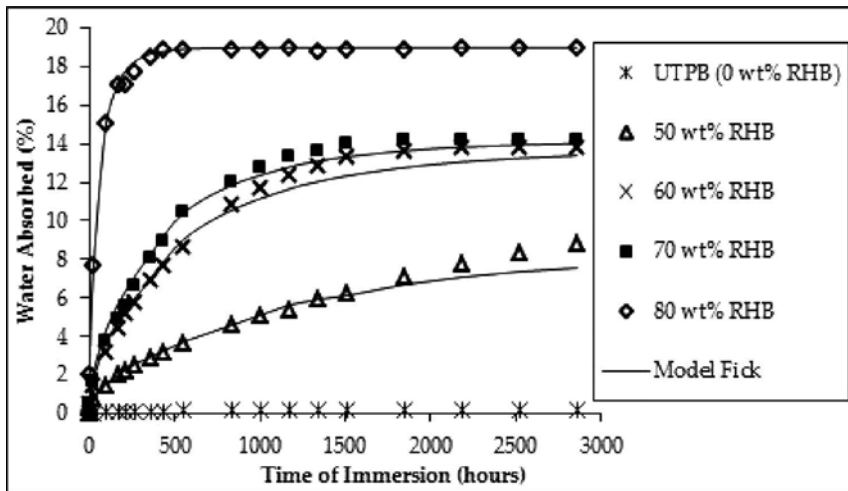


Figure 1. Water absorption of immersed UTPB/RHB biocomposites after a certain period.

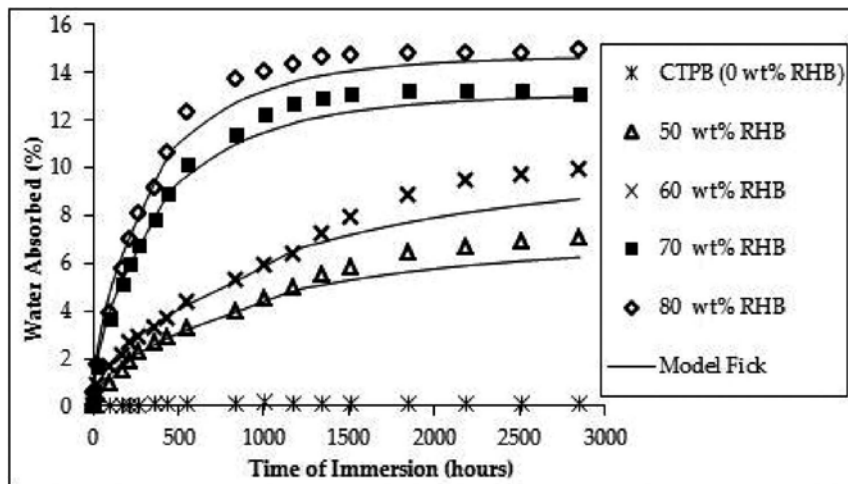


Figure 2. Water absorption of immersed CTPB/RHB biocomposites after a certain period.

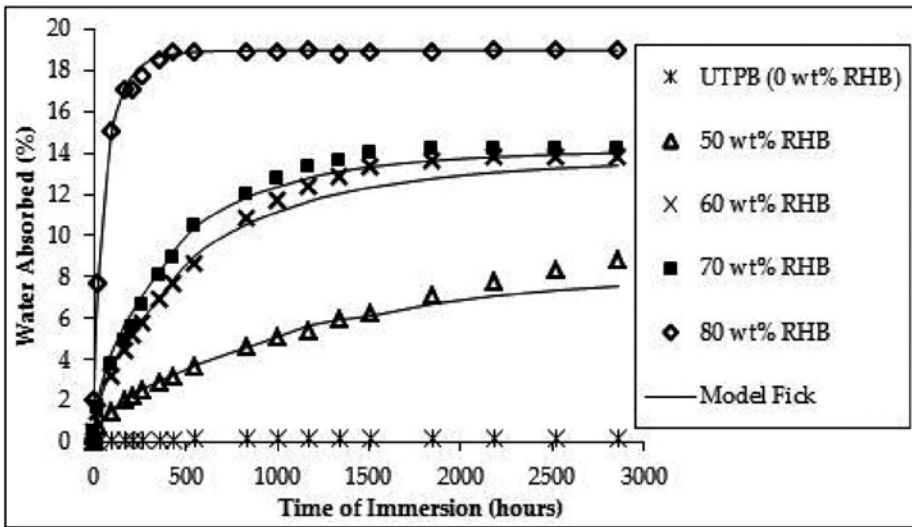


Figure 3. Thickness swelling of immersed UTPB/RHB biocomposites after a certain period.

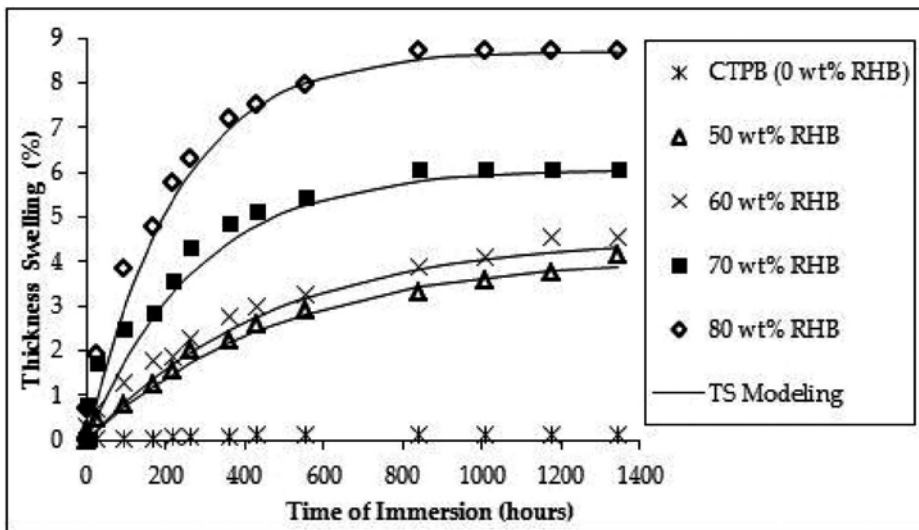


Figure 4. Thickness swelling of immersed CTPB/RHB biocomposites after a certain period.

Theoretically, the swelling behaviour can be computed by the model suggested by Shi and Gardner [9], which gives Eq. 6 after being rearranged and taking the natural logarithm:

$$\ln\left(\frac{100T_{\infty}}{TS(t)+100} - T_0\right) = \ln(T_{\infty} - T_0) - K_{SR}t \tag{6}$$

where $TS(t)$ is the TS at time t , T_∞ and T_0 are the equilibrium and initial thickness of sample, respectively, and K_{SR} is the intrinsic relative swelling rate (a constant). As shown in **Table 1**, the T_∞ and K_{SR} values increased with the RHB wt%, which indicates the higher swelling rate that the composite required a shorter time to reach the equilibrium TS [10]. The CTPB/RHB biocomposites exhibited lower K_{SR} values than that of UTPB/RHB biocomposites. This was probably attributed to better compatibility of TPB matrix which led to better fibre-matrix adhesion, and thus the water was difficult to access in the cellulose [2]. From **Figures 3** and **4**, the experimental results fitted well with the predicted TS from swelling model (solid curve).

3.2. Tensile properties

The influences of the TPB matrix types and RHB contents on the tensile strength and elastic modulus of biocomposites are presented in **Figures 5** and **6**, respectively. In general, the compatibilization of incompatible rHDPE and rPET by E-GMA was capable to improve the tensile properties of CTPB-based biocomposites with and without the presence of RHB. This was because of the E-GMA copolymer that acted as compatibilizer in order to enhance the compatibility and adhesion between rHDPE and rPET components [11]. Therefore, the CTPB blend and composites possessed higher tensile strength and elastic modulus than the UTPB ones.

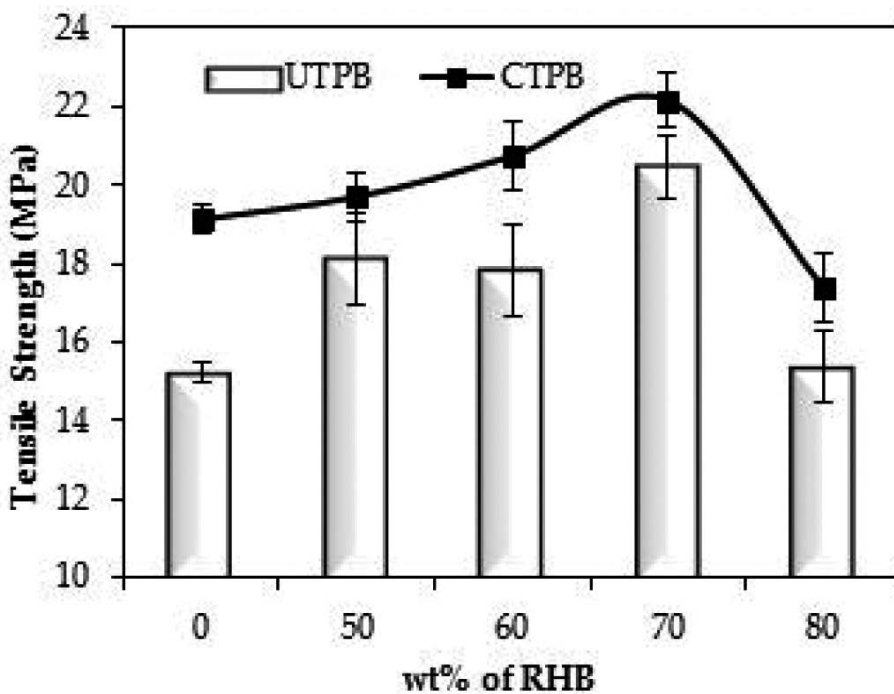


Figure 5. Tensile strength of TPB/RHB biocomposites.

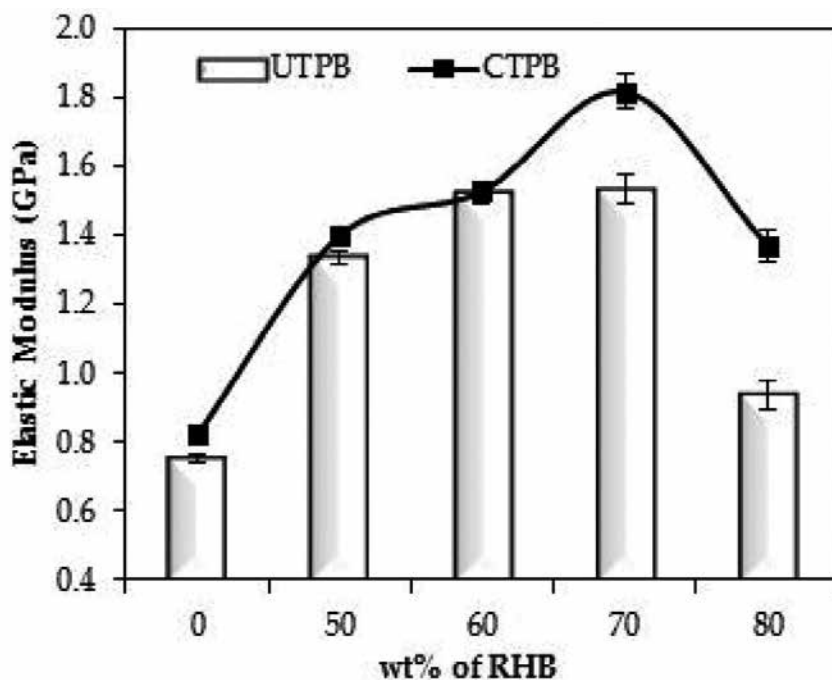


Figure 6. Elastic modulus of TPB/RHB biocomposites.

From Figure 5, both composites based on UTPB and CTPB show a similar trend. Tensile strength increased with increasing RHB up to maximum values achieved at 70 wt%, which were 20.5 and 22.2 MPa, respectively, for UTPB- and CTPB-based composites. This phenomenon suggests that the adhesion and interfacial bonding between the hydrophilic fibre and hydrophobic matrix are enhanced via the surface modification by coupling agent (MAPE) in which RHB can effectively transfer stress to each other [12]. As RHB content increased up to 80 wt%, it is found that tensile strength of composite decreased but the values were still higher than the pure blend (UTPB and CTPB). This possible reason is that the fibres acted as defects when the content of RHB exceeded the limit, which was at 70 wt% in this study. At high fibre content, fibres were not sufficiently wetted by the matrix (lower content), and this resulted in the fibre agglomerations which blocked the stress distribution. This could be further explained by the fact that the high content of RHB will need higher amount of coupling agent in order to give better interfacial adhesion and reinforcement effect with polymer matrix [13]. Somehow, CTPB-based composites exhibited higher values of tensile strength than that of UTPB-based composites. On the other hand, the increase of elastic modulus (Figure 6) with the RHB content (0–70 wt%) can be related to the enhanced stiffness which was imparted by the intrinsic characteristic of RHB. This trend is logic for biocomposite containing low stiffness polymer matrix and high stiffness filler [12]. However, elastic modulus is reduced when 80 wt% RHB is added into the composite. This may be due to the weaker interfacial interaction of RHB-polymer matrix and rHDPE-rPET in UTPB matrix.

3.3. Flexural properties

Figures 7 and 8 depict the modulus of rupture (MOR) and modulus of elasticity (MOE) of biocomposites based on two types of TPB with different contents of RHB.

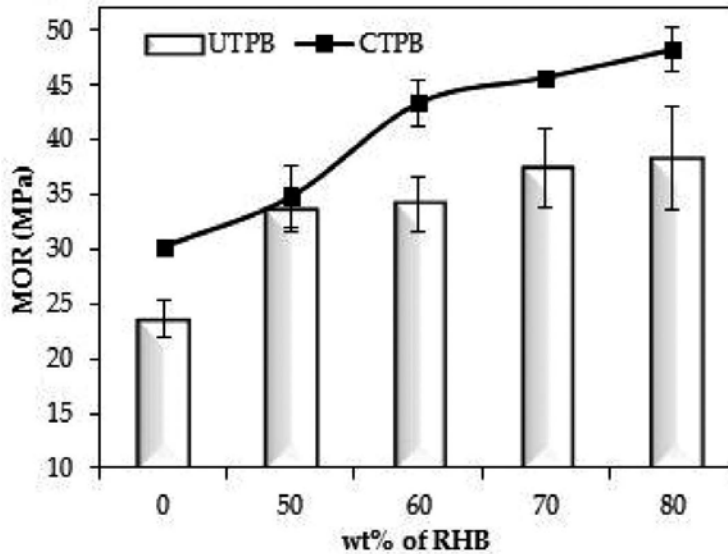


Figure 7. Modulus of rupture (MOR) of TPB/RHB biocomposites.

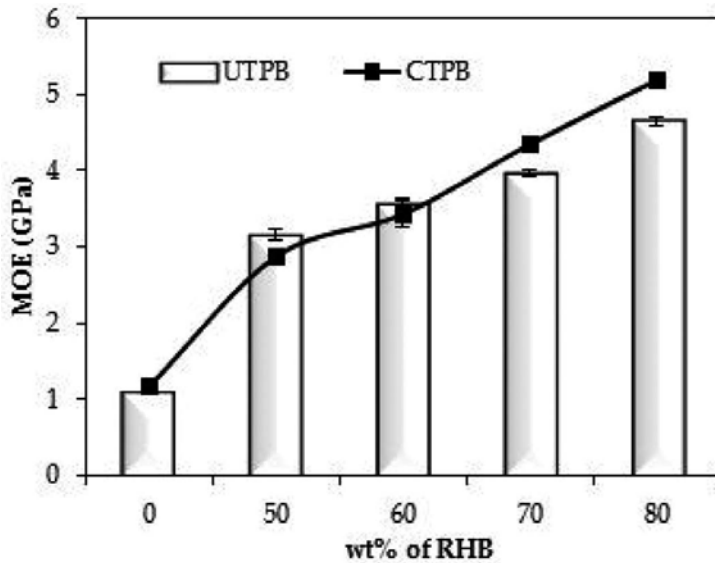


Figure 8. Modulus of elasticity (MOE) of TPB/RHB biocomposites.

The results showed that the presence of RHB improved the flexural properties of biocomposites. In **Figure 7**, CTPB-based biocomposites had higher MOR values than the UTPB-based biocomposites. This was attributed to the compatibilizing reaction for inherently immiscible TPB matrix which then improved adhesion between fibre and polymer blend matrix besides the enhanced compatibility between polymer blend components. Meanwhile, the incorporation of E-GMA into the CTPB matrix seemed not to provide a significant effect in the MOE of biocomposites (**Figure 8**). Comparing to UTPB-based composite, the MOE for CTPB-based composite reinforced with 50–60 wt% RHB was slightly lower. This phenomenon is associated to the weak intrinsic mechanical properties of E-GMA [14]. However, for the composites with higher content of RHB (70–80 wt%), this factor can be negligible due to relatively low content of the matrix (30 wt% and lower).

3.4. Impact properties

Figure 9 presents the impact strength of TPB/RHB biocomposites. For neat blends without the presence of RHB, compatibilization reaction of E-GMA provided a reinforcement effect and led to a significant increase of impact strength for CTPB matrix. However, this large improvement decreased when RHB was added to the blend matrix, which was because rice husk is one kind of stiff inorganic fillers [15]. The impact strength is reduced with RHB content. At high fibre content, there were many interactions between fillers as a result of the filler agglomerations in the composite which were more susceptible to the cracks than the fibre-matrix interface. This indicates that the cracks spread more easily in the biocomposites with high content of rice husk, thus decreasing the impact strength [16].

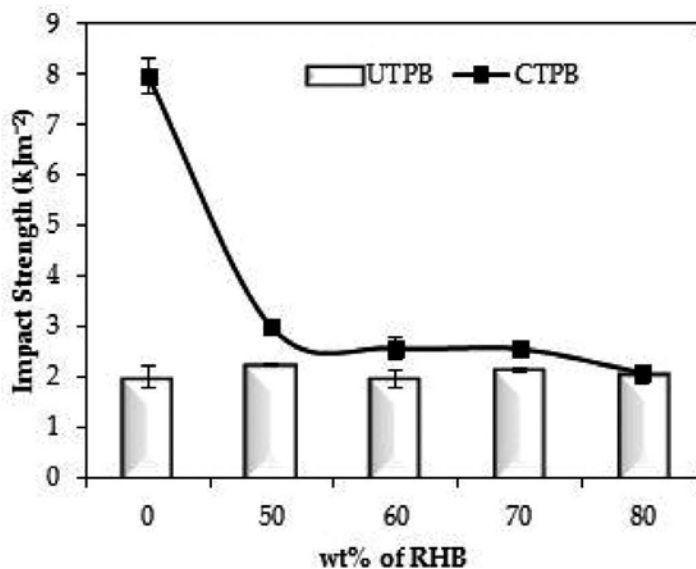


Figure 9. Impact strength of TPB/RHB biocomposites.

3.5. Differential scanning calorimetry (DSC)

Figure 10 depicts the melting temperature (T_m) of (a) rHDPE and (b) rPET components for TPB/RHB biocomposites that are measured from DSC testing. According to Kiziltas et al. (2011), the T_m of the composites plays a crucial role in determining the processing temperature and thermal properties [17]. As shown in **Figure 10**, neat UTPB showed a T_m of rHDPE component at 135.6 °C and T_m of rPET component at 252.8 °C, whereas neat CTPB possessed a lower T_m values of about 133.6 °C for rHDPE and 251.2 °C for rPET which were attributed to the improvement of compatibility between two polymer components with the use of E-GMA as compatibilizer. The reduced T_m values by the addition of E-GMA might be because E-GMA has lower molecular mass which promotes the composite degradation at lower temperature values. In overall, it can be observed that the addition of RHB into polymer blend reduced the T_m by approximately 1.2–5.2 °C. This phenomenon proved the enhancement in the processing temperature of rHDPE after reinforced with RHB [18].

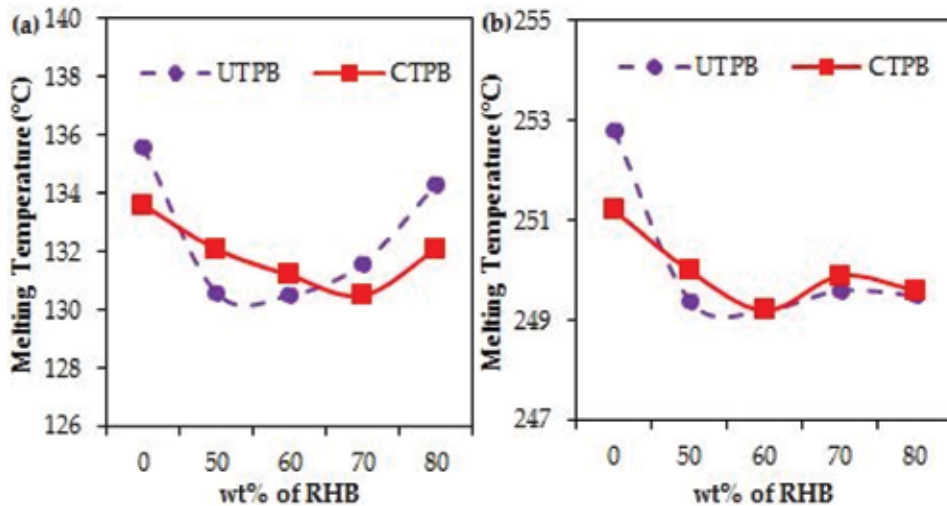


Figure 10. Melting temperature of (a) rHDPE and (b) rPET components in biocomposites.

Besides T_m , DSC testing also has provided the data of crystallinity level (χ_c) for TPB/RHB biocomposites, as presented in **Figure 11**. It was noted that the increasing RHB content from 50 to 80 wt% reduced the χ_c of TPB/RHB biocomposites. This was due to the incorporation of RHB that restricted the movement of polyethylene (PE) chain from crystallization process [19]. The CTPB/RHB biocomposites exhibited higher percentage of crystallinity than that of UTPB/RHB biocomposites. This suggests that the presence of E-GMA in the CTPB matrix improved the crystallinity by promoting the migration and diffusion of PE chains in order to form crystals in the surrounding of the rice husk surface. Several previous research results have reported that the addition of coupling agent copolymer enhanced the crystallinity of biocomposites [20, 21].

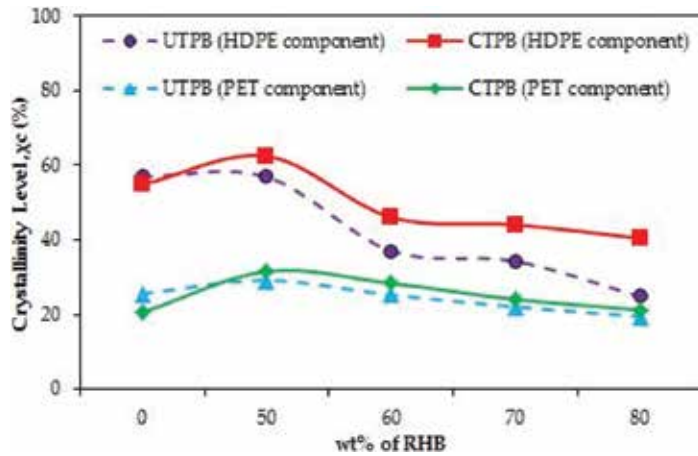


Figure 11. Crystallinity level (χ_c) of TPB/RHB biocomposites.

3.6. Thermogravimetric analysis (TGA)

Figure 12 presents (a) decomposition temperature (T_d) and (b) residues after heating at 600 °C that were obtained from TGA thermogram of TPB/RHB biocomposites. The neat UTPB and CTPB exhibited a one-step weight loss from 400 °C to 500 °C with the maximum decomposition temperature (T_d) at 471 °C and 469 °C, respectively (Figure 12(a)). This process occurred because the neat polymer blend comprised a series of interchained monomers, where an increase of temperature promoted the random chain scission through thermal degradation and depolymerization (at T_d) [22]. The lower T_d for CTPB than that of UTPB was due to an increase of rHDPE-rPET interaction because of the addition of E-GMA compatibilizer which possessed a lower decomposition temperature [23].

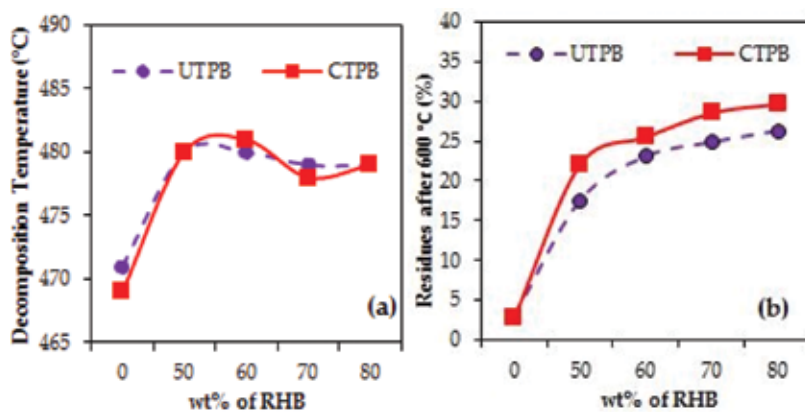


Figure 12. TGA thermogram data: (a) main decomposition temperature (T_d) of polymer component and (b) residues after 600 °C for TPB/RHB biocomposites.

In the presence of RHB in TPB matrix, the peaks of T_d have shifted to higher temperatures (478–481 °C), irrespective of matrix types and RHB contents. This behaviour suggests the improvement of thermal stability of TPB matrix by the incorporation of RHB that restricted the movement of polymer chains and thus delayed the thermal degradation process. Upon heating at temperature beyond 600 °C, both the neat UTPB and CTPB showed the relatively small amount of residues (**Figure 12(b)**). This is because the thermal degraded polymeric materials will further breakdown into gaseous products at higher heating temperature after T_d [22]. It can be observed that the residue weight of samples increased continuously with the increase of RHB content, up to 26.3 % and 29.6 % for composites containing 80 wt% RHB based on UTPB and CTPB matrix, respectively. These results were consistent with the high amount of silica present in the RHB.

3.7. Fire retardancy

Figure 13 shows the burning rate of both UTPB- and CTPB-based biocomposites filled with RHB. The neat TPB had the highest burning rate that was about 0.73 0.02 mm/s for UTPB and 0.71 ± 0.02 mm/s for CTPB. A slightly lower burning rate for CTPB than that of UTPB reflects that the CTPB sample showed better fire retardancy property than UTPB ones. This is probably ascribed to the enhanced compatibility of TPB with the aids of E-GMA copolymer.

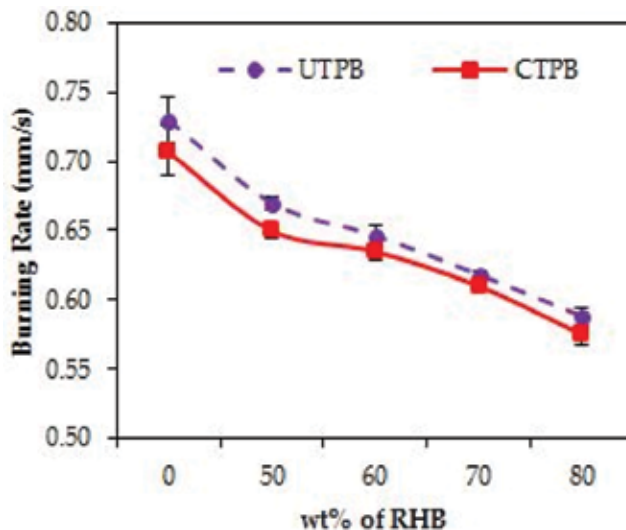


Figure 13. Burning rate of TPB/RHB biocomposites.

For biocomposites containing RHB, the fire retardancy increased by 6–24 % with increasing content of RHB from 40 wt% to 80 wt%. This enhancement might be due to the nature characteristic of silica (relatively high amount, 15–17 % in the raw rice husk) that delayed the combustion [24]. All the CTPB/RHB biocomposites gave lower burning rate (higher fire retardancy) than UTPB/RHB biocomposites. The burning test results showed that the CTPB

(miscible) seemed to improve the interaction between RHB and TPB matrix more effectively than UTPB (immiscible)- based biocomposites.

3.8. Morphological observation

The morphology of the fracture surfaces for (a) 50 wt% RHB/UTPB, (b) 50 wt% RHB/CTPB, (c) 80 wt% RHB/UTPB and (d) 80 wt% RHB/CTPB biocomposites is illustrated in **Figure 14**. Two striking observations can be seen in the surface morphology changes of biocomposites with different RHB contents and TPB matrix types. First, by comparing the effect of RHB contents, the 50 wt% RHB as in **Figure 14(a/b)** was perfectly attached and strongly adhered to the TPB matrix, in which this observation indicates the efficiency of composite material compounding and good fibres-matrix interfacial bonding.

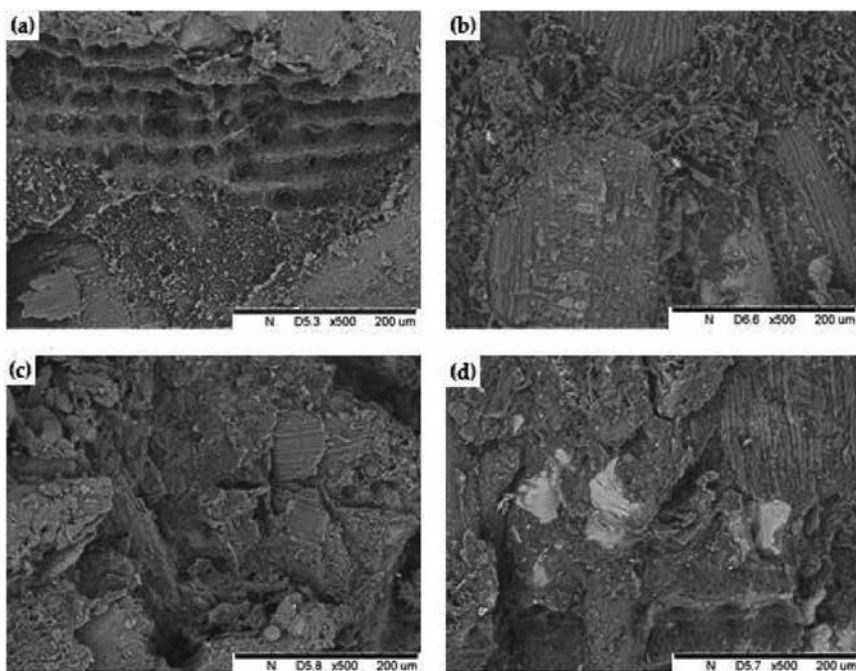


Figure 14. SEM micrograph of (a) 50 wt% RHB/UTPB, (b) 50 wt% RHB/CTPB, (c) 80 wt% RHB/UTPB and (d) 80 wt% RHB/CTPB biocomposites (magnification, 500 \times).

Meanwhile, the 80 wt% RHB as in **Figure 14(c/d)** showed poorer fibre dispersion and the existence of more clear holes or cavities in the fracture surface morphologies which resulted from insufficient adhesion between filler and matrix. This was then led to the fibre-fibre contact (fibre agglomeration) dominated in the composites. Second, by comparing the effect of TPB matrix types, the UTPB-based biocomposites (**Figure 14(a/c)**) present relatively coarse and obvious phase separation morphology with inhomogeneous filler distribution in the matrix. This can be explained by the fact of the great difference in the polymer solubility parameters

[25], in which rHDPE is nonpolar and rPET is polar. The CTPB-based biocomposites in **Figure 14(b/d)** displayed more homogenous and finer morphology structure which proved the enhanced interfacial adhesion between polymers as well as between fibres and TPB matrix via incorporation of compatibilizer in the matrix.

4. Biocomposite product developments

The authors have carried out the collaboration with Bio Composite Extrusions Sdn. Bhd. and Integral Wood Sdn. Bhd. under TechnoFund grant which produced some of the composite panels and prototypes as shown in **Figure 15** (<http://bcextrusions.com/>).



Figure 15. Photograph of biocomposite products, buildings and constructions.

5. Conclusion

Rice husk biofibre (RHB)-reinforced recycled high-density polyethylene/recycled polyethylene terephthalate (rHDPE/rPET) biocomposites were fabricated via a two-step melt-blending method. The TPB matrix types (UTPB and CTPB) and RHB contents have significantly affected

the physical properties, mechanical behaviours, thermal stability and morphological performance of biocomposites. As RHB contents increased from 40 to 80 wt%, tensile and flexural properties as well as thermal stability improved remarkably but reduced the impact strength. In the long-term water immersion test, the water absorption and thickness swelling increased with the content of RHB and immersion time regardless of the matrix types. The diffusion coefficient and swelling rate parameter that are determined from the Fickian and swelling model, respectively, increased with the RHB contents. Biocomposites based on CTPB matrix possessed higher mechanical properties and dimensional stability than those based on UTPB matrix. Based on the findings in this study, it is proven that natural fibres/recycled thermoplastic blend biocomposites are suitable for the outdoor applications such as in the field of buildings and constructions.

Acknowledgements

The authors would like to thank Integral Wood Sdn. Bhd. and Bio Composite Extrusions Sdn. Bhd. for material donations and the Universiti Kebangsaan Malaysia (UKM) for financial support under the science fund Grant UKM DPP-2015-035 and DPP-2015-FST.

Author details

Ruey Shan Chen* and Sahrim Ahmad

*Address all correspondence to: rueyshanchen@hotmail.com

School of Applied Physics, Faculty of Science and Technology, National University of Malaysia, Bangi, Selangor, Malaysia

References

- [1] Panthapulakkal S, Sain M. Studies on the water absorption properties of short hemp-glass fiber hybrid polypropylene composites. *Journal of Composite Materials*. 2007;41:1871–83. DOI:10.1177/0021998307069900
- [2] Adhikary KB, Pang S, Staiger MP. Long-term absorption and thickness swelling behaviour of recycled thermoplastics reinforced with *Pinus radiata* sawdust. *Chemical Engineering Journal*. 2008;142:190–8. DOI:10.1016/j.cej.2007.11.024
- [3] Nosbi N, Akil HM, Mohd Ishak ZA, Abu Bakar A. Degradation of compressive properties of pultruded kenaf fiber reinforced composites after immersion in various solutions. *Materials and Design*. 2010;31(10):4960–4. DOI:10.1016/j.matdes.2010.04.037

- [4] Shinoj S, Panigrahi S, Visvanathan R. Water absorption pattern and dimensional stability of oil palm fiber-linear low density polyethylene composites. *Journal of Applied Polymer Science*. 2010;117(2):1064–75. DOI:10.1002/app.31765
- [5] Ping ZH, Nguyen QT, Chen SM, Zhou JQ, Ding YD. States of water in different hydrophilic polymers—DSC and FTIR studies. *Polymer*. 2001;42:8461–7. doi:10.1016/S0032-3861(01)00358-5
- [6] Scida D, Assarar M, Poilâne C, Ayad R. Influence of hygrothermal ageing on the damage mechanisms of flax-fibre reinforced epoxy composite. *Composites Part B: Engineering*. 2013;48:51–8. DOI:10.1016/j.compositesb.2012.12.010
- [7] Shen CH, Springer GS. Moisture absorption and desorption of composite materials. *Journal of Composite Materials*. 1976;10:2–20. doi: 10.1177/002199837601000101
- [8] Fávaro SL, Lopes MS, De Carvalho Neto AGV, De Santana RR, Radovanovic E. Chemical, morphological, and mechanical analysis of rice husk post-consumer polyethylene composites. *Composites: Part A*. 2010;41:154–60. DOI:10.1016/j.compositesa.2009.09.021
- [9] Shi SQ, Gardner DJ. Hygroscopic thickness swelling rate of compression molded wood fiberboard and wood fiber/polymer composites. *Composites Part A: Applied Science and Manufacturing*. 2006;37(9):1276–85. doi:10.1016/j.compositesa.2005.08.015
- [10] Osman EA, Vakhguel A. Kenaf/recycled jute natural fibers unsaturated polyester composites: water absorption/dimensional stability and mechanical properties. *International Journal of Computational Materials Science and Engineering*. 2012;1(1): 17 pages. DOI:10.1142/S2047684112500108
- [11] Lei Y, Wu Q. Wood plastic composites based on microfibrillar blends of high density polyethylene/poly(ethylene terephthalate). *Bioresource Technology*. 2010;101:3665–71. DOI:10.1016/j.biortech.2009.12.069
- [12] El-Shekeil YA, Sapuan SM, Abdan K, Zainudin E.S. Influence of fiber content on the mechanical and thermal properties of kenaf fiber reinforced thermoplastic polyurethane composites. *Materials and Design*. 2012;40:299–303. DOI:10.1016/j.matdes.2012.04.003
- [13] Ashori A, Nourbakhsh A. Mechanical behavior of agro-residue-reinforced polypropylene composites. *Journal of Applied Polymer Science*. 2009;111:2616–20. DOI:10.1002/app.29345
- [14] Mbarek S, Jaziri M, Chalamet Y, Carrot C. Effect of the viscosity ratio on the morphology and properties of PET/HDPE blends with and without compatibilization. *Journal of Applied Polymer Science*. 2010;117:1683–94. DOI:10.1002/app.32050
- [15] Nourbakhsh A, Baghlani FF, Ashori A. Nano-SiO₂ filled rice husk/polypropylene composites: physico-mechanical properties. *Industrial Crops and Products*. 2011;33:183–7. DOI:10.1016/j.indcrop.2010.10.010

- [16] Yang W, Hu Y, Tai Q, Lu H, Song L, Yuen RKK. Fire and mechanical performance of nanoclay reinforced glass-fiber/PBT composites containing aluminium hypophosphite particles. *Manufacturing*. 2011;42(7):794–800. DOI:10.1016/j.compositesa.2011.03.009
- [17] Kiziltas A, Gardner D, Han Y, Yang, H-S. Thermal properties of microcrystalline cellulose-filled PET–PTT blend polymer composites. *Journal of Thermal Analysis and Calorimetry*. 2011;103:163–70. DOI:10.1007/s10973-010-0894-6
- [18] Yao F, Wu Q, Lei Y, Xu Y. Rice straw fiber-reinforced high-density polyethylene composite: effect of fiber type and loading. *Industrial Crops and Products*. 2008;28(1): 63–72. DOI:10.1016/j.indcrop.2008.01.007
- [19] Chun KS, Husseinsyah S, Syazwani NF. Properties of kapok husk-filled linear low-density polyethylene eco-composites: effect of polyethylene-grafted acrylic acid. *Journal of Thermoplastic Composite Materials*. 2015. DOI:10.1177/0892705715583175
- [20] Kim H-S, Lee B-H, Choi S-W, Kim S, Kim H-J. The effect of types of maleic anhydride-grafted polypropylene (MAPP) on the interfacial adhesion properties of bio-flour-filled polypropylene composites. *Composites: Part A*. 2007;38:1473–82. DOI:10.1016/j.compositesa.2007.01.004
- [21] Khalil R, Chryss A, Jollands M, Bhattacharya S. Effect of coupling agents on the crystallinity and viscoelastic properties of composites of rice hull ash-filled polypropylene. *Journal of Materials Science*. 2007;42(24):10219–27. DOI:10.1007/s10853-007-1732-5
- [22] Kim H-S, Kim S, Kim H-J, Yang H-S. Thermal properties of bio-flour-filled polyolefin composites with different compatibilizing agent type and content. *Thermochimica Acta*. 2006;451(1–2):181–8. DOI:10.1016/j.tca.2006.09.013
- [23] Deka BK, Maji TK. Study on the properties of nanocomposite based on high density polyethylene, polypropylene, polyvinyl chloride and wood. *Composites Part A: Applied Science and Manufacturing*. 2011;42(6):686–93. DOI:10.1016/j.compositesa.2011.02.009
- [24] Arora S, Kumar M, Kumar M. Flammability and thermal degradation studies of PVA/ rice husk composites. *Journal of Reinforced Plastics and Composites*. 2012;31(2):85–93. DOI:10.1177/0731684411431765
- [25] Chen RS, Ab Ghani MH, Salleh MN, Ahmad S, Gan S. Influence of blend composition and compatibilizer on mechanical and morphological properties of recycled HDPE/PET blends. *Materials Sciences and Application*. 2014;5(13):943–52. DOI: 10.4236/msa.2014.513096

High-Content Lignocellulosic Fibers Reinforcing Starch-Based Biodegradable Composites: Properties and Applications

Sherif Mehanny, Lamis Darwish, Hamdy Ibrahim,
Mohamed Tarek El-Wakad and Mahmoud Farag

Additional information is available at the end of the chapter

<http://dx.doi.org/10.5772/65262>

Abstract

Natural source-based composites became promising substitutes and synthetic petrochemical-based counterparts. So far, thermoplastic starch and lignocellulosic fibers are the most common materials for making such eco-friendly “green” materials. Low cost, abundance, and renewability are the factors that lead to deploying these two types of materials. In this chapter, we are conducting further analysis for previously published results of six types of high-content natural fiber-reinforced starch-based composites. All composites were prepared by compression molding under pressure from 5 to 20 MPa and temperature from 130 to 160°C. Composites exhibited highest tensile strength and modulus of elasticity at fiber weight content from 50 to 70%, and then mechanical properties deteriorated significantly at 80% fiber content due to the insufficient starch resin. For instance, the tensile strength was boosted up from 2-12 MPa for thermoplastic starch to reach 55, 45, 32, 28, 44, 365 MPa for flax, bagasse, date palm fiber (DPF), banana, bamboo, and hemp composites, when fiber content was increased from 0% to the optimum fiber content (50-70%). Kelly-Tyson (random 2d) was the optimum model to predict random fiber composite. Increasing the fiber content and choosing a fiber with high cellulose content significantly improve the moisture resistance of the composites. Fick’s law of diffusion predicted the water uptake property successfully. The thermal stability of composites was improved with increasing the fiber weight content as well. This is attributed to the high thermal stability of cellulose when compared to starch. Properties exhibited by starch-based high-content natural fiber composite are promising for many industrial and biomedical applications.

Keywords: natural fibers, composite, mechanical properties, water uptake, thermal properties, theoretical models

1. Introduction

In the past two decades, environmentally friendly biodegradable plastics have been receiving attention because of the need to diminish the worldwide pollution caused by petroleum-based synthetic plastics [1, 2]. Biodegradability by definition corresponds to the capacity of the material to be completely assimilated by indigenous micro-organisms in the ecosystem. Every year more than 300 million tons of plastics are produced for different applications [3]. In addition to nonrenewability of the synthetic plastics resource, disposing of those types of plastics in landfill will inevitably release toxins in the soil and underground water. Moreover, contaminants can be absorbed in food resources and eventually accumulated in the human body [4, 5].

Bioplastics from natural resources provide reliable and sustainable alternative to synthetic polymer. Starch is the most commonly studied materials as an eco-friendly polymer that is based on renewable plant material, fully biodegradable, and low cost [6, 7]. There are some challenges that oppose the development of starch-based plastics. Those challenges are mainly poor long-term stability, low water resistance, deterioration of mechanical properties due to moisture uptake, and the relatively fast biodegradability [8]. To overcome those challenges, natural lignocellulosic fibers have been widely utilized to improve the properties of the starch-based plastics [9]. Comparable to synthetic fibers, natural fibers are less dense in addition to being fully degradable. Furthermore, the reinforcement of lignocellulosic fibers significantly improves the mechanical properties of starch-based matrix [10]. Sisal, jute, kenaf, coir, wood, pulp, cellulose, bagasse, banana, orange, and flax fibers are lignocellulosic fibers that have been all studied and found to substantiate enhancement for the starch-based matrix's versatile properties [10–14]. The objective of this article is to review and conduct further analysis to understand the effect of high-fiber content (flax, palm, banana, bagasse, bamboo, and hemp) on mechanical and physical properties. Moreover, experimental results reported before will be compared with theoretical models, selecting the most appropriate model.

1.1. Preparation and characterization

For flax, bagasse, banana, and date palm fiber (DPF) preparation took place by preheating the composite, pressing at 5 MPa and 150°C for 30 min [13–16]. Bamboo-reinforced starch composite was prepared by pressing at 20 MPa and 130 C for 5 min [17]. Hemp-reinforced starch composite was prepared by pressing at 10 MPa and 130 C for 5 min [18]. All fibers except bamboo and hemp were subjected to alkaline (NaOH) treatment before composite preparation. In this chapter, we will deal with tensile, moisture, and thermal results, and further details concerning experimental procedures can be found in the cited articles.

2. Results and properties

2.1. Tensile properties

2.1.1. Strength

Role of mixture (ROM) and inverse role of mixture (IROM) are the most common theories to predict composite mechanical behavior. ROM assumes that there is a perfect bond between

fibers and matrix, also that the strain (and stress for IROM) in the fibers is equal to the strain in the matrix. This model deals with aligned continuous fiber composites [19, 20].

ROM equation predicts tensile strength in longitudinal direction:

$$\sigma_L = \sigma_F V_F + \sigma_M V_M \quad (1)$$

IROM equation predicts tensile strength in transversal direction:

$$\sigma_T = \frac{\sigma_F \sigma_M}{V_M \sigma_F + V_F \sigma_M} \quad (2)$$

where σ_F is the fiber tensile strength, σ_M is the matrix tensile strength, V_F is the fibers volume fraction, and V_M is the matrix volume fraction. In order to transform fiber weight fraction (W_F) to volume fraction (V_F), we will be in need to the following equation:

$$V_F = \frac{\rho_M W_F}{\rho_M W_F + \rho_F W_M} \quad (3)$$

where ρ_F is the fiber density, ρ_M is the matrix density, and W_M is the matrix weight fraction.

Kelly-Tyson formulates an approach to deal with discontinuous (random and unidirectional) fiber, overcoming the problem of unequal strain in the fibers and the matrix by assuming perfect bonding between fibers and matrix. If the fiber is shorter than the critical length (L_c), it cannot be loaded to its failure stress, and the strength of the composite is then determined by the strength of the fiber/matrix bond, in addition to fiber strength. So for fibers' length greater than L_c , the composite tensile strength can be calculated as follows [19]:

$$L_C = \frac{\sigma_F d}{2\tau} \quad (4)$$

$$\sigma_C = \varepsilon \left(1 - \frac{L_C}{2L} \right) \sigma_F V_F + \sigma_M V_M \quad (5)$$

where L_c is the critical length, d is the fibers' average diameter, τ is the shear strength of fiber/matrix bond (about 0.5 of matrix strength), ε equals 1 in case of unidirectional distribution and three-eighth in random distribution. L is the fibers' average length, σ_F is the fibers' tensile strength, σ_M is the matrix tensile strength, V_F is the fibers' volume fraction, and V_M is the matrix volume fraction. Different properties have been investigated from low to high fiber weight content (50–80%; **Figure 1**). For all types of fibers, mechanical properties improved as the fiber content increased from 0 to 50–70%. Strength of 0% (starch matrix) was around 4 MPa for the flax, bagasse, and DPF. Starch matrix recorded lower strength in the case of banana composite (2 MPa), whereas starch-based resin strength used in bamboo and hemp composites was 12 MPa. Among the first four types of composites, 50–60% fibers' composite was 8–15 times higher than 0%, depending on the fiber type. Flax composite exhibited the highest mechanical properties with tensile strength surpassing 60 MPa, banana composite was the lowest in strength (27 MPa). About 80% composite was flimsy with

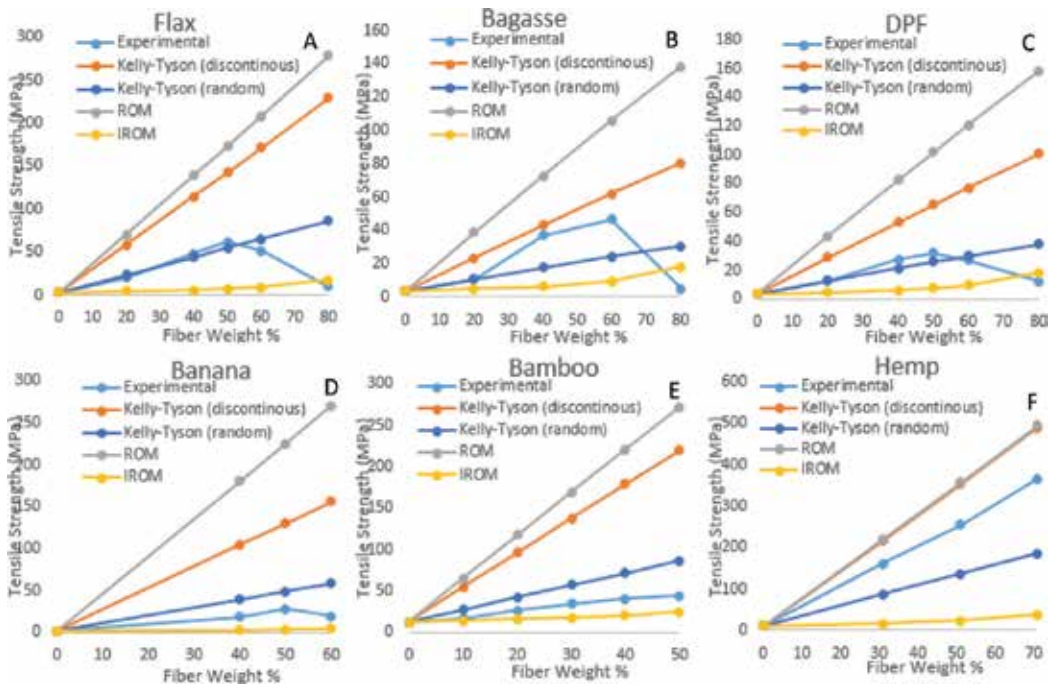


Figure 1. Experimental and theoretical tensile strength of starch-based lignocellulosic fiber composites for different fibers: (a) flax, (b) bagasse, (c) DPF, (d) banana, (e) bamboo, and (f) hemp.

severely deteriorated tensile properties due to lack of matrix material; hence, the load cannot be transferred from fiber to another. For the last two types, the trials did not continue to recognize the maximum possible fiber content for maximal strength (no reduction in strength after maximum strength point). Hemp fiber composite recorded 365 MPa for 70% of the fibers, the high strength of hemp fiber (above 700 MPa), and availability of hemp in long bundles are reasons for this high strength. Kelly-Tyson’s (random 2d) was the closest model to experimental results for flax, bagasse, and DPF composites. In the case of banana and bamboo fibers, the experimental results were between Kelly-Tyson (random 2d) and IROM, with more inclined trend to IROM, and this can be due to higher levels of randomness (3d), especially for shorter fibers (banana). Hemp fibers were continuous fibers; hence, the results were close to ROM model.

2.1.2. Elasticity

Similar to ROM and IROM strength models, the two models predict longitudinal and transversal elasticity values for unidirectional continuous fiber composites in which the actual composite elasticity value must lie between. ROM equation predicts elastic modulus in longitudinal direction (E_L):

$$E_L = E_F V_F + E_M V_M \tag{6}$$

And IROM equation predicts elastic modulus in transversal direction (E_T):

$$E_T = \frac{E_F E_M}{V_M E_F + V_F E_M} \quad (7)$$

where E_F is the fibers modulus of elasticity, E_M is the matrix modulus of elasticity, V_F is the fibers volume fraction, and V_M is the matrix volume fraction.

Another model used to predict discontinuous fiber composite behavior was called Halpin-Tsai. The composite elastic modulus in longitudinal direction (E_L) can be obtained as follows [15, 19]:

$$E_L = E_M \frac{(1 + \xi_L \eta_L V_F)}{(1 - \eta_L V_F)} \quad (8)$$

where (ξ) is a factor dependant on the shape and distribution of the reinforcement. The parameter (η) is a function of the ratio of the relevant fiber and matrix moduli with respect to the reinforcement factor (ξ). In this model, they can be calculated by the following formulas:

$$\eta_L = \frac{(E_F - E_M)}{(E_F + \xi_L E_M)} \quad (9)$$

$$\xi_L = 2 \left(\frac{L}{d} \right) + 40 V_F^{10} \quad (10)$$

Also, the composite elastic modulus in transversal direction (E_T) can be obtained as follows:

$$E_T = E_M \frac{(1 + \xi_T \eta_T V_F)}{(1 - \eta_T V_F)} \quad (11)$$

where

$$\eta_T = \frac{(E_F - E_M)}{(E_F + \xi_T E_M)} \quad (12)$$

$$\xi_T = 2 + 40 V_F^{10} \quad (13)$$

The two previous moduli are for oriented fibers, the following equation is a result of an averaging process made by Tsai and Pagano [21] to predict the modulus of an isotropic composite (E_c) based on random fibers reinforcement.

$$E_C = \frac{3}{8} E_L + \frac{5}{8} E_T \quad (14)$$

Figure 2 shows the modulus of elasticity for the first four composite types discussed in the strength section. Young's modulus followed the same pattern as tensile strength. Modulus increased with fiber content till an optimum point (50–60%), then property deterioration took place at higher content (80%) due to the scarcity of resin and inability to transfer load between fibers. Flax composite exhibited the highest modulus (4.7 GPa) in comparison with other types. Superior mechanical properties for flax were realized elsewhere and attributed to high

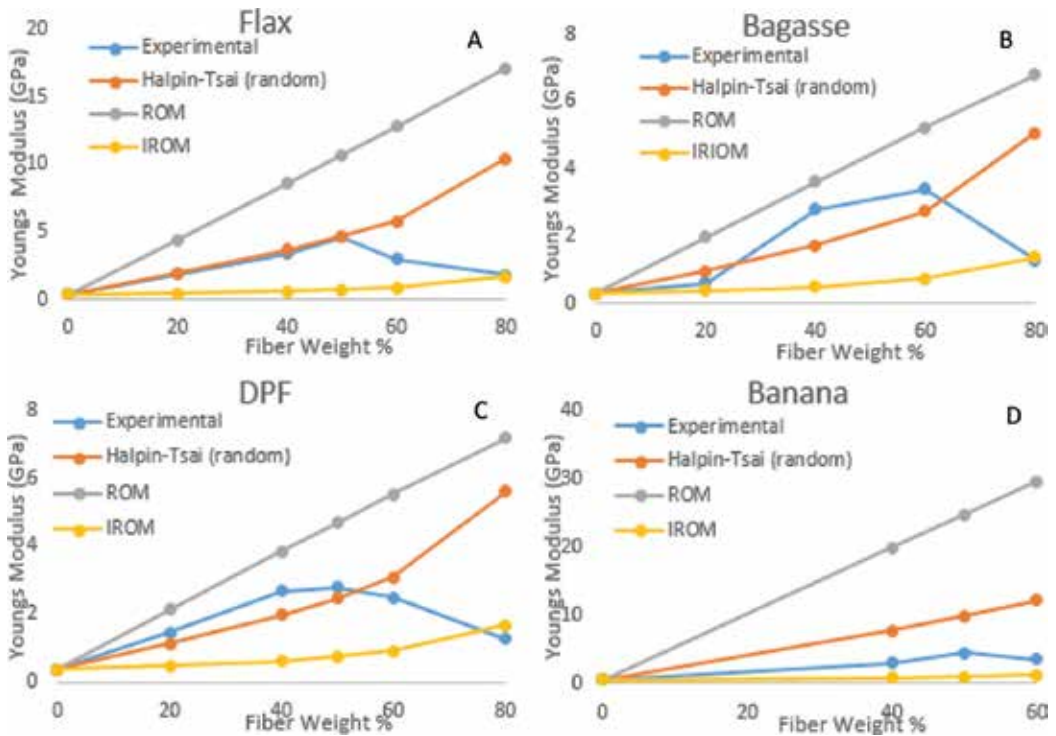


Figure 2. Experimental and theoretical tensile modulus of starch-based lignocellulosic fiber composites for different fibers: (a) flax, (b) bagasse, (c) DPF, and (d) banana.

cellulose content and low fiber diameter. Halpin-Tsai was the best model to predict the composite behavior, and this is due to the randomness of the fibers used to prepare these composites.

2.2. Moisture absorption behavior

Owing to its natural abundance and low cost, starch-based biodegradable “green” polymers have attracted great attention. Unfortunately, the use of these plastics in a wide range of applications has been restricted by its low water resistance. Therefore, in order to overcome this disadvantage while preserving the biodegradability and the green property of this polymer, natural lignocellulosic fibers are being used as a biodegradable and eco-friendly reinforcement [22–25]. The incorporation of natural lignocellulosic fibers, which are mainly made up of hydrophilic cellulose, into starch-based matrix is responsible for the reduction of moisture absorption of the resultant composite. This reduction in the moisture absorption of the two hydrophilic materials is attributed to the good interfacial adhesion between starch and cellulose which leads to decreasing the free volume of the starch molecular chains and thus reduce the water absorption; the less hygroscopicity of cellulose when compared with starch; formation of fibrous network around starch thus hinder the moisture penetration; and the high crystallinity of cellulose when compared with starch [26–29].

2.2.1. Mechanism of moisture absorption in polymer/natural fiber composites

Polymer/natural fiber composites tend to absorb moisture in humid atmosphere. Therefore, this moisture absorption affects the fiber matrix interface leading to low stress transfer between matrix and fiber. The transport of water in a polymer/fiber composite can be attributed to the imperfections of the matrix (voids, pores, and cracks). The water absorbed in a matrix can be divided into two types, free water and bound water. Free water is the water molecules moving freely through the voids, and bound water is the water molecules bonded to the polar groups of a matrix [30]. **Figure 3** shows the two types of absorbed water in polymeric matrix.

When water molecules penetrate polymer/fiber composite, it attaches to the hydrophilic group of the fiber creating intramolecular hydrogen bonds. Thus, this interaction reduces the interfacial adhesion between fiber and matrix which leads to deterioration in the mechanical properties of the composite [30, 31]. **Figure 4** explains how moisture absorption by fiber affects the composite.

Polymeric matrices, especially, starch-based reinforced with natural lignocellulosic fibers are sensitive to moisture. Moisture absorption will deteriorate their functionality. Therefore, aspects should be considered when manufacturing such a composite that would be used in a humid atmosphere. The most important aspect is the proper selection of the fiber type according to its moisture resistance.

2.2.2. Effect of fiber type and content on moisture absorption

According to literature, the moisture absorption of starch/natural fiber composites is highly affected by the fiber type and its content. Each type of fibers has its own cellulose content; thus fibers with high cellulose content highly diminish the moisture absorption of the resultant composite. Mehanny *et al.* [13] studied the effect of reinforcing thermoplastic starch (TPS) matrix with different contents of NaOH-treated bagasse fiber on the moisture absorption of the resultant composite. **Figure 5** shows the moisture absorption of composites reinforced with 0, 20, 40, 60, and 80% bagasse fiber. Their results showed that the moisture absorption after reaching equilibrium of the starch-based matrix with 0% fiber reached more than 53%,

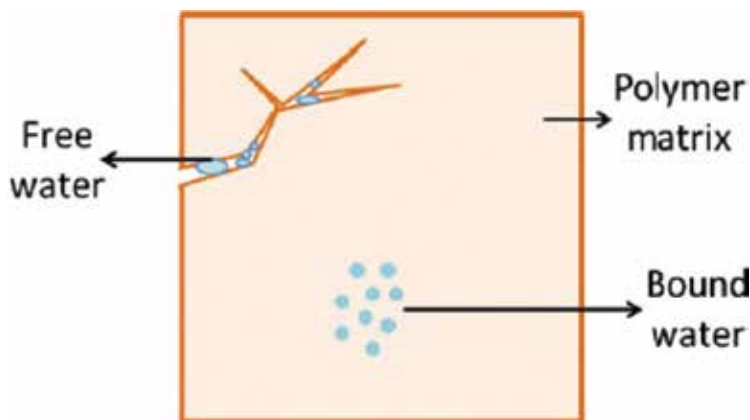


Figure 3. Free water and bound water in polymer matrix. Adopted from Ref. [30].

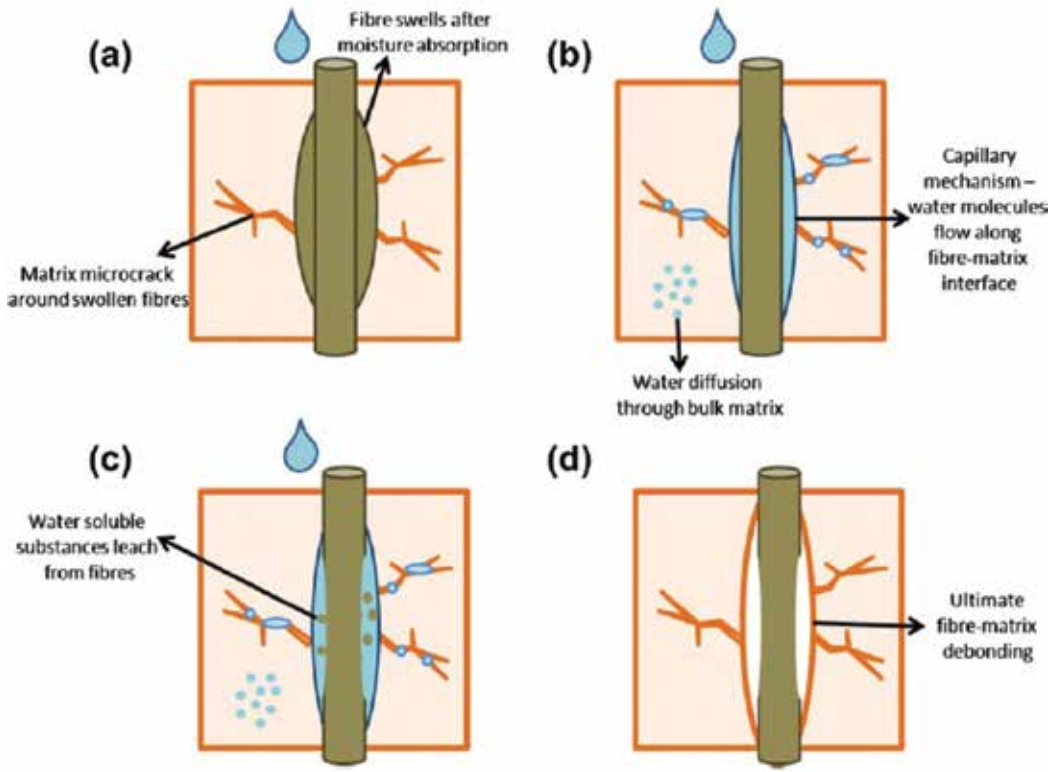


Figure 4. Effect of water on fiber-matrix interface. Adopted from Ref. [30].

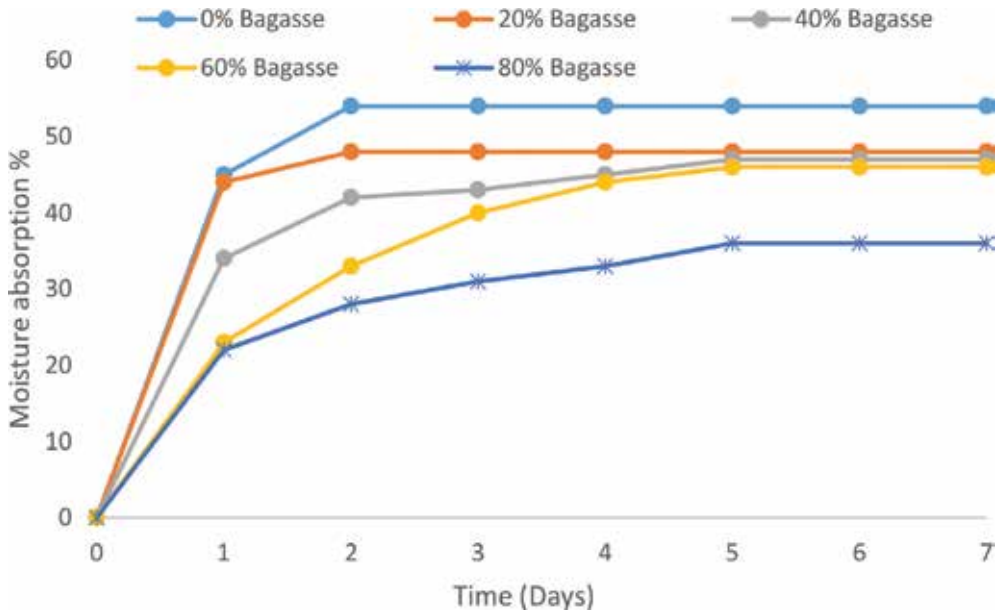


Figure 5. Moisture absorption of TPS/bagasse fiber composites with different fiber wt%. Adopted from Ref. [13].

whereas with the lowest fiber content 20% it reached 48%. By increasing the fiber content up to 80%, the moisture absorption dropped to 36%.

According to Elsayed *et al.* [14, 15], increasing the NaOH-treated flax fiber content from 0 up to 60% resulted in reducing the moisture absorption of the TPS/flax composite from 48 to 38% as shown in **Figure 6**. The authors proposed investigating, as well, the effect of changing

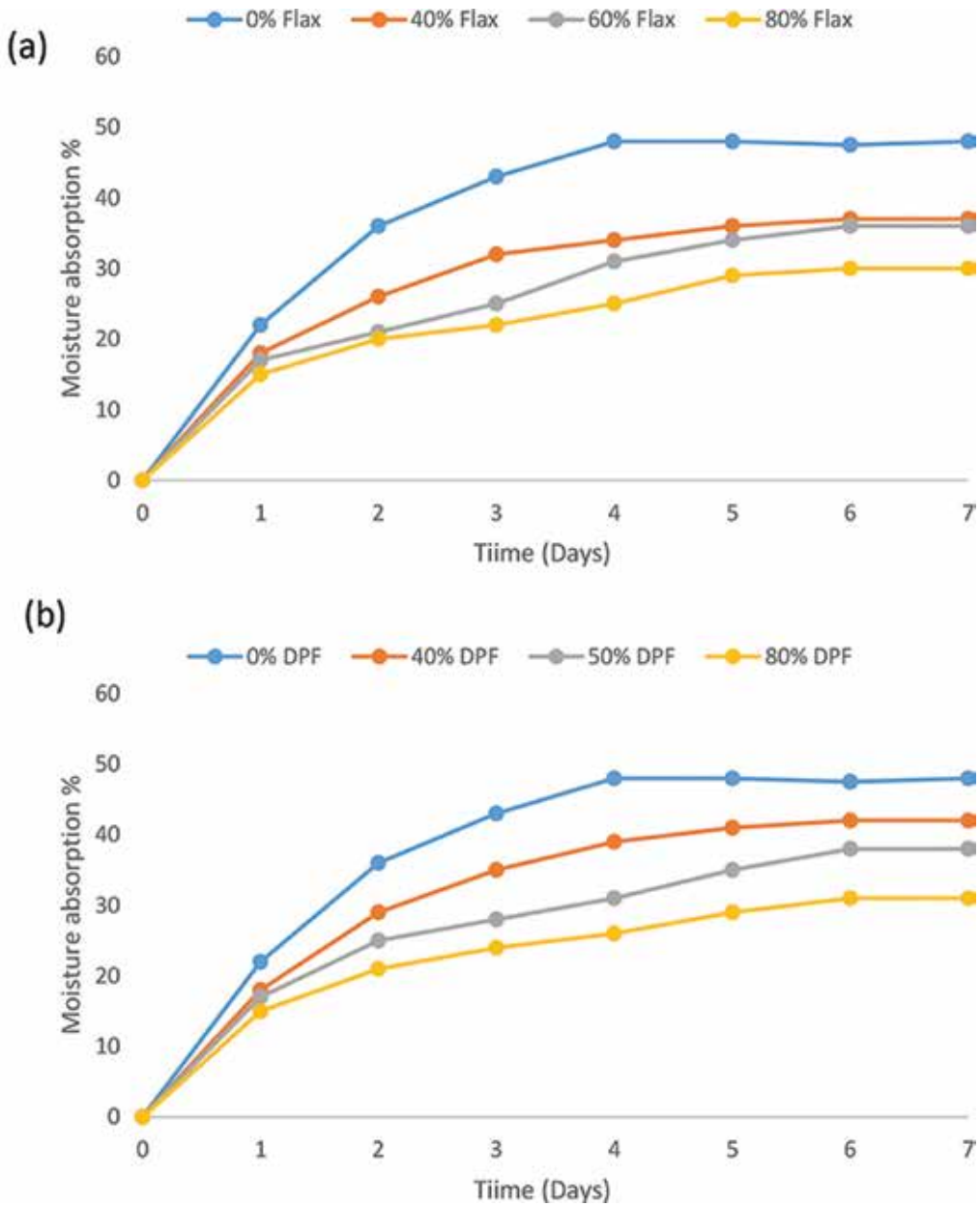


Figure 6. Moisture absorption of (a) TPS/flax fiber and (b) TPS/DPF composites with different fiber wt%. Adopted from Refs. [14, 15].

the reinforcement fiber on the moisture absorption of the resultant composite. NaOH-treated date palm fiber (DPF) with different contents was used. They demonstrated that changing the fiber type caused a slight effect on the moisture absorption property of the resultant composite. The authors attributed this slight difference to the convergence of the cellulosic content of both fibers.

Darwish *et al.* [16] investigated the effect of increasing the content of the NaOH-treated banana fiber (BF) reinforcement on the moisture absorption property of the starch/BFs composites as shown in **Figure 7**. The starch matrix was reinforced with 40, 50, and 60% BFs. The moisture absorption dropped from 70 to 41% with increasing the BF content from 0 to 60%.

Figure 8 shows a comparison between the moisture absorption of the TPS composites reinforced with 60 wt% fibers at the equilibrium plateau from the previously stated studies [13–16]. From **Figure 8**, it can be concluded that the moisture absorption is highly dependent on the fiber type, hence the cellulose content of the fibers. Therefore, flax with the highest cellulose content diminished the moisture absorption of the composite to 35%.

2.2.3. Fick's law and moisture absorption of TPS/natural fiber composites

Fick's second law of diffusion has been widely used to model and characterize the absorption of moisture in many materials. Fick's second law depicts the process of one dimension moisture absorption with respect to exposure time as shown in Eq. (1) [32–35]:

$$\frac{dC}{dt} = D \frac{d^2C}{dX^2} \quad (15)$$

where C is the water concentration, t is the time of diffusion, and D is the diffusion coefficient normal to the surface in the x -direction.

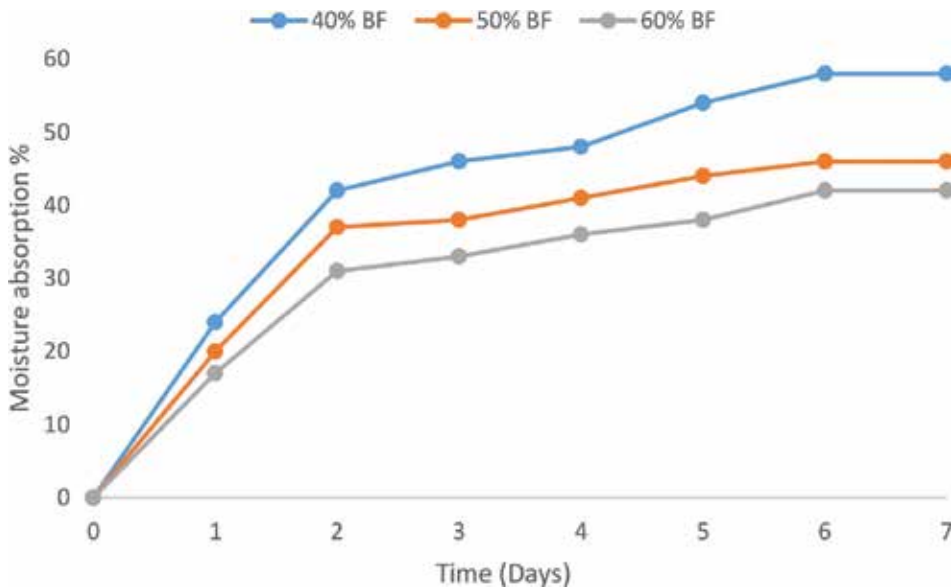


Figure 7. Moisture absorption of TPS/banana fiber composites with different fiber wt%. Adopted from Ref. [16].

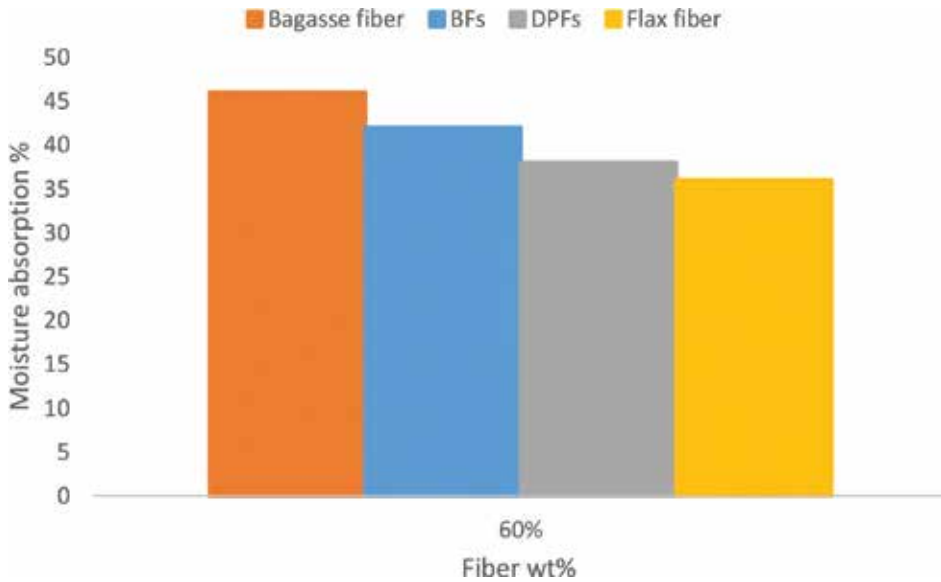


Figure 8. Moisture absorption of TPS composites reinforced with 60% fibers at the equilibrium plateau.

Diffusion behavior, Fickian or non-Fickian, can be recognized theoretically by the shape of the absorption curve represented by

$$\frac{M_t}{M_m} = K \cdot t^n \quad (16)$$

where M_t and M_m are moisture absorption at time t and at equilibrium state, respectively. K and n are the diffusion kinetic parameters. M_t can be calculated from

$$M_t = \frac{W_t - W_0}{W_0} 100(\%) \quad (17)$$

where W_0 is the weight of dry sample and W_t is the weight of wet sample at time t [32–35].

The diffusion parameter n indicates whether the diffusion is Fickian or non-Fickian. When $n = 0.5$, the diffusion is Fickian. When $n \geq 1$, the diffusion is non-Fickian. Moisture absorption in lignocellulosic fiber-reinforced polymer composites always follows Fickian behavior [32–36].

One-dimensional approach of Fick's law shows that the moisture absorption is directly proportional to the square root of time, then slows down until an equilibrium plateau is reached. For values of $M_t/M_m < 0.6$, the initial part of the curve can be deduced by [36]:

$$\frac{M_t}{M_m} = \frac{4}{h} \sqrt{\frac{D \cdot t}{\pi}} \quad (18)$$

where h is the thickness of the sample.

For the second half of the absorption curve, where $M_t/M_m > 0.6$, Springer [37] proposed the following approximation:

$$\frac{M_t}{M_m} = 1 - \exp \left[-7.3 \left(\frac{D \cdot t}{h^2} \right)^{0.75} \right] \quad (19)$$

Figure 9 shows a comparison between the Fick's law predicted and the experimental moisture absorption test results of TPS composites reinforced with 60 wt% of different fibers (banana, bagasse, DPF, and flax). The four curves show that the experimental data are in a good agreement with the predicted values. Thus, TPS/lignocellulosic fiber composites follow a Fickian behavior.

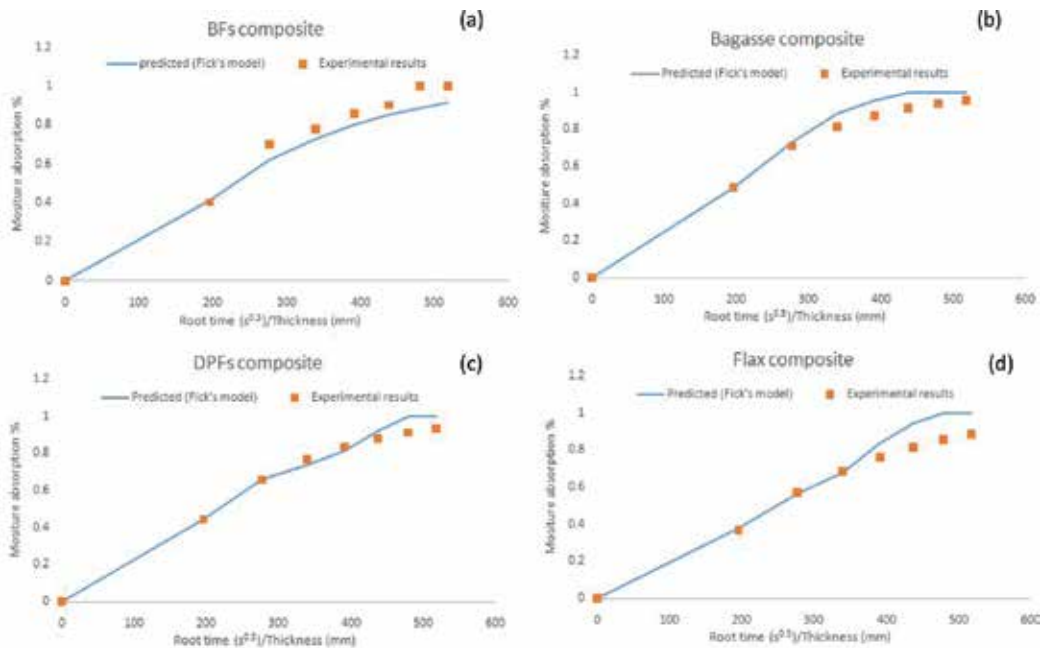


Figure 9. Experimental and predicted moisture absorption of TPS composites reinforced with 60% (a) BFs, (b) bagasse fibers, (c) DPFs, and (d) flax fibers.

2.2.4. Effect of moisture absorption on mechanical properties of composites

Mechanical properties deterioration is one of the drawbacks of moisture absorption on polymer/natural fiber composites. This deterioration is attributed to the swelling of the cellulose fibers. Due to this swelling, development of shear stress at the fiber/matrix interface occurs. Therefore, this leads to debonding of the fibers, delamination, and loss of structural integrity [30, 38]. Fiber surface chemical treatments are proven to promote the moisture resistance by reducing fiber hydrophilicity. Moreover, these treatments improve the interfacial adhesion between matrix and fiber thus, tightens the water penetration pathways and consequently, lowers the moisture absorption [30, 39–41].

In Ref. [25], the authors studied the effect of moisture absorption on the mechanical properties of starch-based composites reinforced with different contents of NaOH-treated flax and DP fibers. Tensile strength test results showed that the strength of both flax and DPFs composites decreased to the half of its original value as shown in **Figure 10**.

In sum, from the previously illustrated studies, moisture absorption of TPS/lignocellulosic fiber composites is affected by the type and the content of the reinforcement fiber. Moreover, different fiber surface treatment techniques highly modify its water resistance. Therefore, proper selection of fiber type, content, and surface treatment technique is of crucial importance while manufacturing a composite exposed to humid atmosphere in order to preserve its strength and structural integrity.

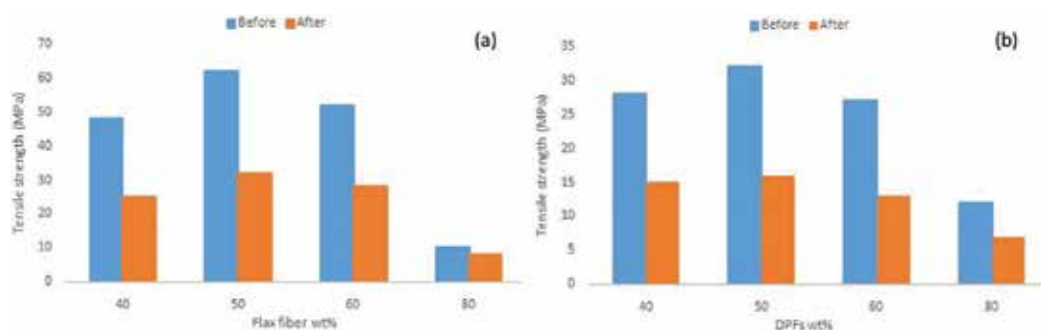


Figure 10. Effect of moisture absorption on the tensile strength of (a) flax composites and (b) DPFs composite. Adopted from Ref. [42].

2.3. Thermal properties

Thermogravimetric analysis (TGA) is a widely used thermal technique due to its high accuracy in determining the decomposition temperature and thermal stability of materials. TGA measures the rate and amount of weight change of a material as a function of time or temperature in a controlled atmosphere. This technique proved to be useful in studying the thermal characteristics of polymeric materials such as thermoplastics, composites, films, and fibers [43]. The thermogravimetric graph for thermoplastic starch matrix is shown in **Figure 11**. The authors in references [13–16] reported that the thermal decomposition of thermoplastic starch occurs in three main steps. The initial weight loss that occurred in the TGA curve between room temperature and 100°C represents the first step. This weight loss was attributed to the evaporation of water. It can be observed as a small peak around 100°C in the DTG curve. The second step appeared as a peak in the DTG curve around 200°C. This peak was attributed to the evaporation of glycerin. The last step appeared as a major peak around 330°C in the DTG curve. This peak was attributed to thermal decomposition of starch.

TGA and DTG curves for different lignocellulosic fibers are comparable due to their chemical composition similarity. On the other hand, chemical surface treatments affect the thermal stability of the fibers [40, 45]. Darwish *et al.* [16] studied the effect of NaOH treatment on the thermal stability of BFs. Their results showed that TGA and DTG curves were shifted to the

right after treatment (**Figure 12**). This shift indicated that the treated fiber exhibited an increased thermal stability relative to the untreated fiber.

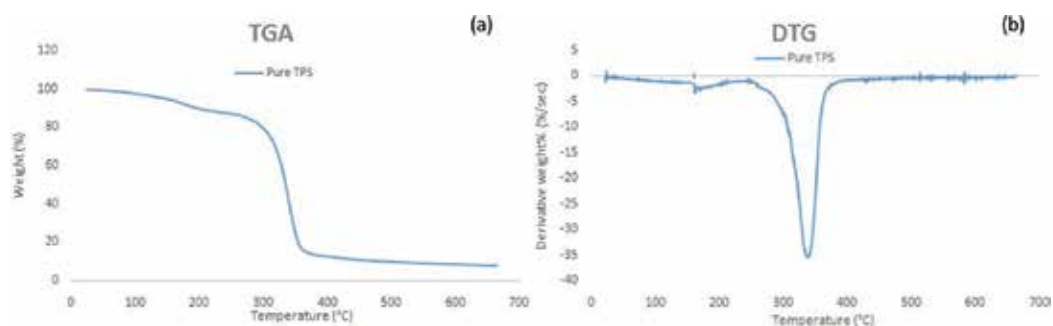


Figure 11. (a) TGA and (b) DTG of TPS matrix. Adopted from Refs. [13, 14, 44].

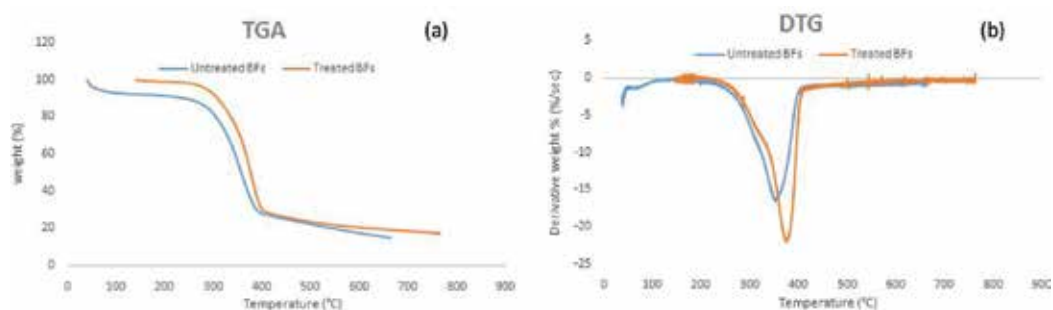


Figure 12. (a) TGA and (b) DTG of untreated and treated BFs. Adopted from Ref. [44].

TGA and DTG curves were plotted by the authors in references [13–16] to analyze the thermal degradation of starch-based composites reinforced with different contents of NaOH-treated lignocellulosic fibers (bagasse, flax, DPF, and banana) (**Figure 13**). The authors reported that the decomposition of TPS/natural fiber composites has two main peak regions. From the DTG curves, peaks, Group I represents the first decomposition region which is attributed to the decomposition of starch. These peaks appeared at the temperature range of 300–340°C. The second decomposition region appeared in the DTG curves as peaks Group II in the temperature range of 340–400°C. These peaks are attributed to the decomposition of the lignocellulosic fibers.

The authors in references [11–14] reported that the small peak that is related to the evaporation of water disappeared at high fiber contents. They attributed this disappearance to the improvement of the moisture absorption resistance of the composites with higher fiber contents. Also, the authors noted that as the fiber content increases, the residual weight decreases, which imply that starch-based matrix contains more inorganic inclusions. The authors noticed that the onset degradation temperature of starch increased with increasing the fibers' content. They assigned this improvement to the possible formation of hydrogen bond linkage between starch

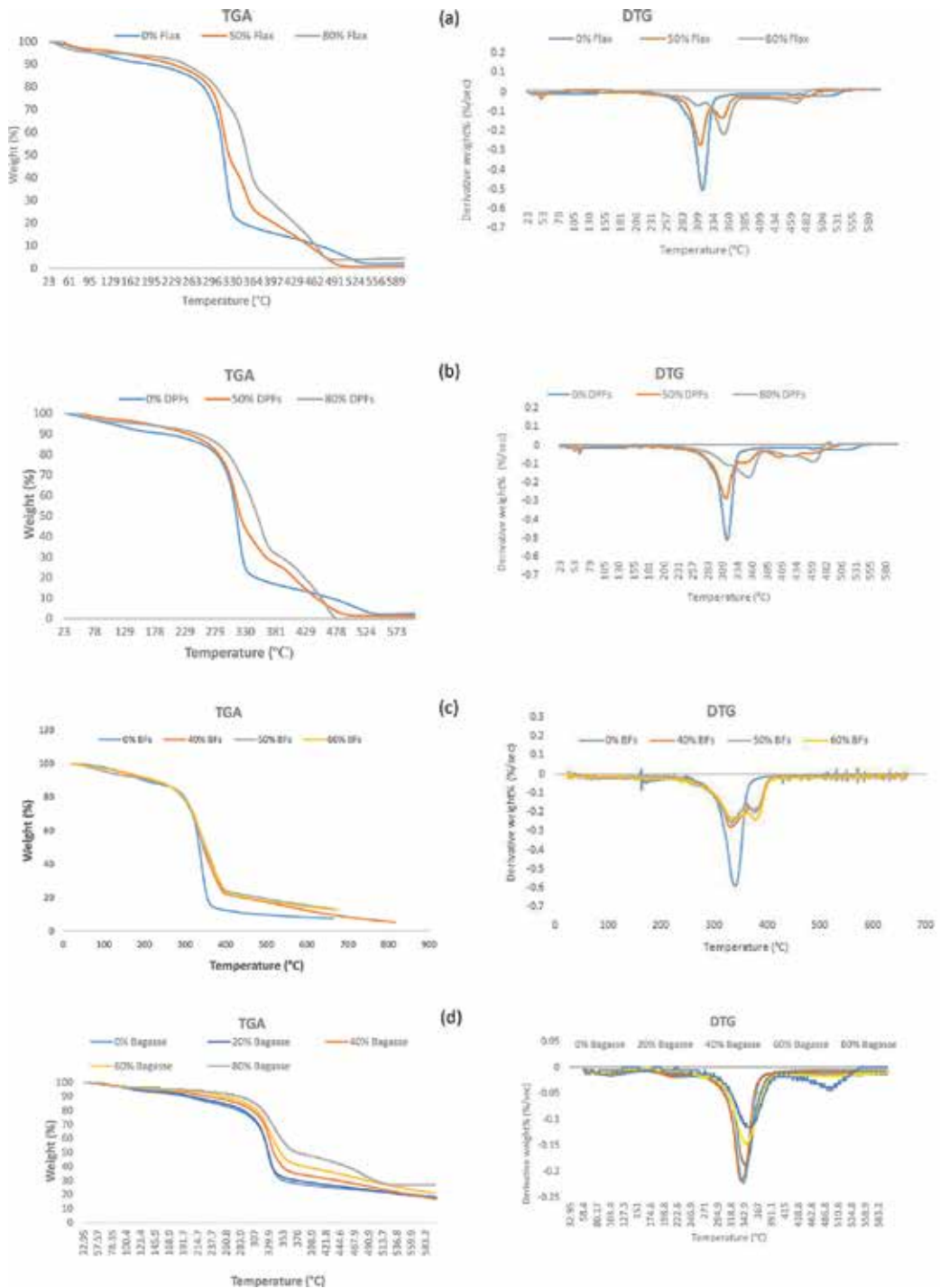


Figure 13. TGA and DTG curves for TPS composites reinforced with (a) flax fibers, (b) DPFs, (c) banana fibers, and (d) bagasse fibers. Adopted from Refs. [13–16, 46].

and fibers. The mentioned studies [13–16] reported that with increasing the fiber content, the onset degradation temperature of the composites increased and the weight loss decreased. Thus, the thermal stability of the composites improved with increasing the fibers content. This improvement was attributed to the higher thermal stability of the cellulosic fibers when compared with starch and the good compatibility of both polysaccharides. Moreover, proper selection of the surface treatment technique of the fibers plays a prominent role in improving the thermal stability of the resultant composite.

In short, the parameters obtained from the thermal characterization of TPS/lignocellulosic fiber composites are useful in identifying the temperature limits of treatment, processing, or operating both matrix and fibers. Moreover, these parameters are useful in comparing the thermal performance of various TPS/lignocellulosic fiber composites.

3. Conclusion

- For flax, bagasse, DPF, and banana composites, samples with 50-60 wt% fibers manifest the highest tensile strength of 8-15 times what was recorded by 0% composite (less than 4 MPa strength for 0% fiber content).
- In 80 wt% composite, insufficient matrix is unable to transfer load and fill the gaps between fibers, leading to severely deteriorated tensile properties.
- Kelly-Tyson (random) model shows the best fit for the mentioned composites, which can be attributed to the realistic assumptions that count for the randomness of the fibers during preparation.
- For hemp composite, strength can be increased to 365 MPa, when increasing fiber content to 70%. Small diameter and continuous fibers with such high strength (702 MPa) led to the significant composite strength improvement.
- ROM model can be used for tensile strength and modulus prediction for hemp composites in case of fiber continuity in the composite.
- Halpin-Tsai (random) is the most suitable model to predict starch composite behavior.
- The moisture absorption of TPS/lignocellulosic fiber composites is affected by the fiber type and content. Increasing the fiber content and choosing a fiber with high cellulose content improve the moisture resistance of the composites. Moreover, proper selection of the surface treatment technique of the fiber highly modifies its water resistance.
- The moisture absorption behavior can be modeled successfully by Fick's law of diffusion.
- The thermal stability of the TPS/lignocellulosic fiber composites is improved with increasing the fiber content. This is attributed to the high thermal stability of cellulose when compared to starch. Furthermore, proper selection of the surface treatment technique of the fiber enhances the thermal stability of the fiber itself and the resultant composite.

- To further improve moisture resistance properties, hydrophobic modified starch, or hydrophobic coating can be implemented.
- Starch-based lignocellulosic fiber can be a good candidate for regenerating broken bones (producing bone plates) due to the biocompatibility of starch plastics (especially after modifying the moisture uptake issue).
- Starch-fiber panels can be a good candidate for many paneling applications relevant to housing, cars, and decorative applications.

Author details

Sherif Mehanny^{1*}, Lamis Darwish², Hamdy Ibrahim¹, Mohamed Tarek El-Wakad² and Mahmoud Farag³

*Address all correspondence to: smehanny@gmail.com

1 Faculty of Engineering, Cairo University, Giza, Egypt

2 Faculty of Engineering, Helwan University, Egypt

3 School of Science and Engineering, American University in Cairo, Egypt

References

- [1] A. Bourmaud, Y.-M. Corre, and C. Baley, Fully biodegradable composites: Use of poly-(butylene-succinate) as a matrix and to plasticize l-poly-(lactide)-flax blends, *Ind. Crops Prod.*, vol. 64, pp. 251–257, 2015.
- [2] Y.-X. Weng, Y.-J. Jin, Q.-Y. Meng, L. Wang, M. Zhang, and Y.-Z. Wang, Biodegradation behavior of poly(butylene adipate-co-terephthalate) (PBAT), poly(lactic acid) (PLA), and their blend under soil conditions, *Polym. Test.*, vol. 32, no. 5, pp. 918–926, 2013.
- [3] K. A. Iyer and J. M. Torkelson, Dispersion and property enhancements in polyolefin/Soy flour biocomposites prepared via melt extrusion followed by solid-state shear pulverization, *Macromol. Mater. Eng.*, vol. 300, no. 8, pp. 772–784, 2015.
- [4] V. Koushal, R. Sharma, M. Sharma, R. Sharma, and V. Sharma, Plastics: Issues challenges and remediation, *Int. J. Waste Resour.*, vol. 4, no. 1, pp. 1–6, 2014.
- [5] R. C. Thompson, C. J. Moore, F. S. vom Saal, and S. H. Swan, Plastics, the environment and human health: Current consensus and future trends, *Philos. Trans. R. Soc. Lond. B. Biol. Sci.*, vol. 364, no. 1526, pp. 2153–2166, 2009.

- [6] J.-F. Zhang and X. Sun, Mechanical properties of poly(lactic acid)/starch composites compatibilized by maleic anhydride, *Biomacromolecules*, vol. 5, no. 4, pp. 1446–1451, 2004.
- [7] J. Maitra and N. Singh, Swelling behavior of starch chitosan polymeric blend, *An Int. J.*, vol. 4, no. 2, pp. 22–27, 2014.
- [8] O. Vilpoux and L. Averous, Chapter 18—Starch-based plastics.
- [9] K. G. Satyanarayana, G. G. C. Arizaga, and F. Wypych, Biodegradable composites based on lignocellulosic fibers—An overview, *Prog. Polym. Sci.*, vol. 34, no. 9, pp. 982–1021, 2009.
- [10] K. Oksman, M. Skrifvars, and J.-F. Selin, Natural fibres as reinforcement in polylactic acid (PLA) composites, *Compos. Sci. Technol.*, vol. 63, no. 9, pp. 1317–1324, 2003.
- [11] M. M. Haque, M. Hasan, M. S. Islam, and M. E. Ali, Physico-mechanical properties of chemically treated palm and coir fiber reinforced polypropylene composites, 2009.
- [12] F. Le Digabel, N. Boquillon, P. Dole, B. Monties, and L. Averous, Properties of thermo-plastic composites based on wheat-straw lignocellulosic fillers, *J. Appl. Polym. Sci.*, vol. 93, no. 1, pp. 428–436, 2004.
- [13] S. Mehanny, M. Farag, R. M. Rashad, and H. Elsayed, Fabrication and characterization of starch based bagasse fiber composite, in *Volume 3: Design, Materials and Manufacturing, Parts A, B, and C*, 2012, p. 1345.
- [14] H. Elsayed, M. Farag, H. Megahed, and S. Mehanny, Influence of flax fibers on properties of starch-based composites, in *Volume 3: Design, Materials and Manufacturing, Parts A, B, and C*, 2012, p. 1397.
- [15] H. Ibrahim, M. Farag, H. Megahed, and S. Mehanny, Characteristics of starch-based biodegradable composites reinforced with date palm and flax fibers, *Carbohydr. Polym.*, vol. 101, pp. 11–19, 2014.
- [16] L. R. Darwish, M. T. El-Wakad, M. Farag, and M. Emara. “The use of starch matrix-banana fiber composites for biodegradable maxillofacial bone plates.” RECENT ADVANCES in BIOLOGY, MEDICAL PHYSICS, MEDICAL CHEMISTRY, BIOCHEMISTRY and BIOMEDICAL ENGINEERING, Sep 2013, p.70.
- [17] H. Takagi and Y. Ichihara, Effect of fiber length on mechanical properties of “green” composites using a starch-based resin and short bamboo fibers, *JSME Int. J. Ser. A*, vol. 47, no. 4, pp. 551–555, 2004.
- [18] S. Ochi, Development of high strength biodegradable composites using Manila hemp fiber and starch-based biodegradable resin, *Compos. Part A Appl. Sci. Manuf.*, vol. 37, no. 11, pp. 1879–1883, 2006.
- [19] B. Harris, Engineering composite materials.
- [20] Mechanics of Composite Materials. [Online]. Available from: <http://www.springer.com/materials/characterization+%26+evaluation/journal/11029>.
- [21] M. R. Piggott and M. R. Piggott, 4—Composite Mechanics, in *Load-Bearing Fibre Composites*, 1980, pp. 62–82.

- [22] A. Kaushik, M. Singh, and G. Verma, Green nanocomposites based on thermoplastic starch and steam exploded cellulose nanofibrils from wheat straw, *Carbohydr. Polym.*, vol. 82, no. 2, pp. 337–345, 2010.
- [23] Y. Lu, L. Weng, and X. Cao, Morphological, thermal and mechanical properties of ramie crystallites—reinforced plasticized starch biocomposites, *Carbohydr. Polym.*, vol. 63, no. 2, pp. 198–204, 2006.
- [24] J. Prachayawarakorn, P. Sangnitivej, and P. Boonpasith, Properties of thermoplastic rice starch composites reinforced by cotton fiber or low-density polyethylene, *Carbohydr. Polym.*, vol. 81, no. 2, pp. 425–433, 2010.
- [25] Y. Z. Wan, H. Luo, F. He, H. Liang, Y. Huang, and X. L. Li, Mechanical, moisture absorption, and biodegradation behaviours of bacterial cellulose fibre-reinforced starch biocomposites, *Compos. Sci. Technol.*, vol. 69, no. 7, pp. 1212–1217, 2009.
- [26] J. Prachayawarakorn, S. Chaiwatyothin, S. Mueangta, and A. Hanchana, Effect of jute and kapok fibers on properties of thermoplastic cassava starch composites, *Mater. Des.*, vol. 47, no. 47, pp. 309–315, 2013.
- [27] J. P. López, P. Mutjé, A. J. F. Carvalho, A. A. S. Curvelo, and J. Gironès, Newspaper fiber-reinforced thermoplastic starch biocomposites obtained by melt processing: Evaluation of the mechanical, thermal and water sorption properties, *Ind. Crops Prod.*, vol. 44, pp. 300–305, 2013.
- [28] S. Karimi, A. Dufresne, P. Md. Tahir, A. Karimi, and A. Abdulkhani, Biodegradable starch-based composites: Effect of micro and nanoreinforcements on composite properties, *J. Mater. Sci.*, vol. 49, no. 13, pp. 4513–4521, 2014.
- [29] M. George, M. Chae, and D. C. Bressler, Composite materials with bast fibres: Structural, technical, and environmental properties, *Prog. Mater. Sci.*, vol. 83, pp. 1–23, 2016.
- [30] Z. N. Azwa, B. F. Yousif, A. C. Manalo, and W. Karunasena, A review on the degradability of polymeric composites based on natural fibres, *Mater. Des.*, vol. 47, pp. 424–442, 2013.
- [31] T. Kunanopparat, P. Menut, M.-H. Morel, and S. Guilbert, Reinforcement of plasticized wheat gluten with natural fibers: From mechanical improvement to deplasticizing effect, *Compos. Part A Appl. Sci. Manuf.*, vol. 39, no. 5, pp. 777–785, 2008.
- [32] W. Wang, M. Sain, and P. A. Cooper, Study of moisture absorption in natural fiber plastic composites, *Compos. Sci. Technol.*, vol. 66, no. 3, pp. 379–386, 2006.
- [33] C. J. Pérez, V. A. Alvarez, I. Mondragón, and A. Vázquez, Water uptake behavior of layered silicate/starch-polycaprolactone blend nanocomposites.
- [34] R.-H. Hu, M. Sun, and J.-K. Lim, Moisture absorption, tensile strength and microstructure evolution of short jute fiber/polylactide composite in hygrothermal environment, *Mater. Des.*, vol. 31, no. 7, pp. 3167–3173, 2010.
- [35] V. A. Alvarez, R. A. Ruscekaite, and A. Vazquez, Mechanical properties and water absorption behavior of composites made from a biodegradable matrix and alkaline-treated sisal fibers, *J. Compos. Mater.*, vol. 37, no. 17, pp. 1575–1588, 2003.

- [36] D. Scida, M. Assarar, C. Poilâne, and R. Ayad, Influence of hygrothermal ageing on the damage mechanisms of flax-fibre reinforced epoxy composite, *Compos. Part B Eng.*, vol. 48, pp. 51–58, 2013.
- [37] C.-H. Shen and G. S. Springer, Moisture absorption and desorption of composite materials, *J. Compos. Mater.*, vol. 10, no. 1, pp. 2–20, 1976.
- [38] A. Athijayamani, M. Thiruchitrabalambam, U. Natarajan, and B. Pazhanivel, Effect of moisture absorption on the mechanical properties of randomly oriented natural fibers/polyester hybrid composite, *Mater. Sci. Eng. A*, vol. 517, no. 1, pp. 344–353, 2009.
- [39] P. A. Sreekumar, S. P. Thomas, J. Marc Saiter, K. Joseph, G. Unnikrishnan, and S. Thomas, Effect of fiber surface modification on the mechanical and water absorption characteristics of sisal/polyester composites fabricated by resin transfer molding, *Compos. Part A Appl. Sci. Manuf.*, vol. 40, no. 11, pp. 1777–1784, 2009.
- [40] S. Kalia, B. S. Kaith, and I. Kaur, Pretreatments of natural fibers and their application as reinforcing material in polymer composites—a review, *Polym. Eng. Sci.*, vol. 49, no. 7, pp. 1253–1272, 2009.
- [41] M. J. John and R. D. Anandjiwala, Recent developments in chemical modification and characterization of natural fiber-reinforced composites, *Polym. Compos.*, vol. 29, no. 2, pp. 187–207, 2008.
- [42] H. Ibrahim, *Characteristics of Corn Starch-Based Composites Reinforced with Flax and Date Palm Fibers*, Cairo University, 2012.
- [43] G. J. Marosi, A. Menyhárd, G. Regdon, and J. Varga, Thermal analysis of multiphase polymer systems, in *Handbook of Multiphase Polymer Systems*, Chichester, UK: John Wiley & Sons, Ltd, 2011, pp. 359–385.
- [44] LM. Darwish, “MECHANICAL CHARACTERIZATION OF PREPARED COMPOSITE MATERIALS FOR BIODEGRADABLE BONE PLATES,” Helwan University, 2014.
- [45] S. Sultana Mir, M. Hasan, S. M. N. Hasan, M. J. Hossain, and N. Nafsin, Effect of chemical treatment on the properties of coir fiber reinforced polypropylene and polyethylene composites, *Polym. Compos.*, 2015.
- [46] S. Mehanny, *Fabrication and Characterization of Starch Based Sugar Cane Bagasse Fibers Composite*, Cairo University, 2012.

Polysaccharides as Composite Biomaterials

Izzati Fatimah Wahab and Saiful Izwan Abd Razak

Additional information is available at the end of the chapter

<http://dx.doi.org/10.5772/65263>

Abstract

Polysaccharide-based composite materials have been the recent research focus in the field of material science and engineering because of their biocompatibility, renewability, and sustainability. In this chapter, the authors attempt to review and discuss recent works in developing polysaccharide-based composites in applications of tissue engineering, drug delivery, and biopolymer-based film packaging. This chapter focuses on carrageenan, alginate, chitosan, starch, and cellulose composites. Introduction on these types of polysaccharides used as biomaterials is briefly discussed.

Keywords: polysaccharide, biomaterials, composites, renewable, biocomposites

1. Introduction

Biomaterials are defined as materials that are used in therapeutic or diagnostic procedure by interactions with components of living systems [1]. Over the years, synthetic polymers, ceramics, and metals were preferred for these types of applications due to their reproducibility and better performance. However, the growing concern on environment and health side-effects have promoted researches to look for naturally derived polymers. Biomaterials are designed to be inert and not to interact in biological systems and not to cause any harmful changes to the body. Polysaccharides are natural polymers found in plant and organism. The abundance of polysaccharide as a renewable resource promised its sustainability and economic value for biomaterials. Their production cost is less than any synthetic polymers and is easily processable.

Polysaccharides are polymeric carbohydrate molecules consisting of long chains of monosaccharide units bound by glycosidic linkages. The fact that these polymers are extracted from natural resources has led to the impression of good biocompatibility and biodegradability. Chemically, nearly all materials from plants are carbohydrate in nature and composed of repeating unit of monosaccharides. Thus, they are nontoxic. Its biocompatible nature is also attributed to the structural similarity of glycosaminoglycans (GAGs), which is a vital component of extracellular matrix in tissue. There is an emerging interest in reducing the amount of undisposible plastic waste that often leads to serious environmental problem. Polysaccharides are potential alternative for replacing conventional petroleum-based plastics which are able to biodegrade naturally in soil. Polysaccharides are famous for their used in the food and dairy industries. However, its unique structure and versatile modification can be explored for other important fields.

Polysaccharide can be categorized into structural and storage polysaccharides. Examples of structural polysaccharides are cellulose in plant and chitin in the shells of crustacean, while storage polysaccharides include starch and glycogen. Polysaccharides are present in most living organisms. In fact, polysaccharides comprise about 70% of the dry weight of the total biomass [2]. Although polysaccharide is advantageous as biomaterials as they are more ecofriendly than petro-polymers, there are still critical drawbacks that need special attention to make it an ideal choice. Polysaccharide exhibits poorer mechanical properties than the conventional plastics. Some polysaccharides also have strong hydrophilic behavior that may cause early rupture. Thus, polysaccharide composites have been extensively studied in regard to counter this problem and obtain additional properties for specific application.

2. Types of polysaccharide

Several types of polysaccharide were widely studied over the past decades due to their potential in numerous research areas. Some of the polysaccharides being explored as biomaterials are carrageenan, alginate, chitosan, starch, and cellulose.

2.1. Carrageenan

Carrageenan is a sulfated polysaccharide extracted from red algae. Marine organisms from *Rhodophycea* family like *Hypnea*, *Euchema*, *Chondrus*, *Crispus*, and *Gigartina* are the main type of red seaweeds manufactured for carrageenan sources. Different types of red seaweed is used to extract different carrageenan, namely, kappa (κ), iota (ι), lambda (λ), nu (η), mu (μ), ksi (ξ), and theta (ϕ). The structures of the three most prevalent and commercialized carrageenans are shown in **Figure 1**. Examples of some different sources of carragenans are *Euchomadenticulatum* (spinosum) for ι -carrageenan, *Kappaphycusalvarezzi* (cottoni) for κ -carrageenan, and *Gigartinaradula* and *Chondruscrispus* for extraction of both ι - and κ -carrageenans [3]. All types of carrageenans are water-soluble.

Carrageenans contain alternate units of D-galactose and 3, 6-anhydro-galactose linked glycosidically. As can be seen in **Figure 1**, κ -carrageenan has only one sulfate group per

disaccharide chain, two for κ -carrageenan, whereas λ -carrageenan got three. This resulted in anionic polysaccharide that is often neutralized by cations like sodium, potassium, calcium, magnesium, and ammonium. Interesting to note that the structure of λ -carrageenan does not have 3,6-anhydro-bridge like in the κ - and ι -carrageenans. This structure gives κ - and ι -carrageenans gelling ability in response to thermal condition. The location of ester sulfate group affects the solubility and gel strength of carrageenan, while existence of 3,6-anhydro-bridge results in polysaccharide gelation [5]. Besides galactose and sulfate units, other carbohydrate residues that commonly exist in carrageenan are xylose, glucose, and uronic acids [6]. Carrageenans are used in a variety of commercial applications as gelling, thickening, and stabilizing agents, especially in food products and sauces. Aside from these functions, carrageenans are being explored in experimental medicine, pharmaceutical formulations, cosmetics, and industrial applications.

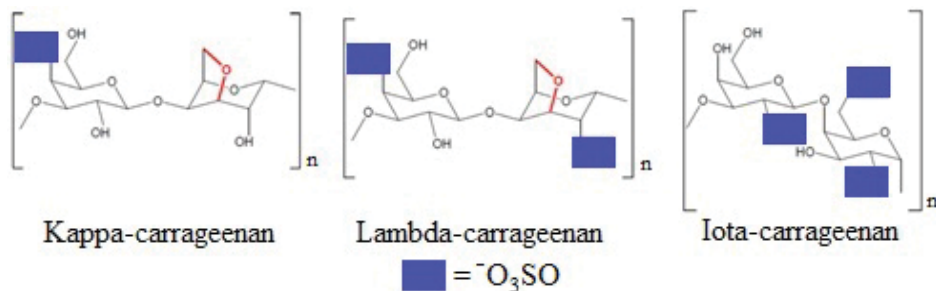


Figure 1. Structure of carrageenan [4].

2.2. Alginate

Alginate, or also called alginic acid, can be derived from both algal and bacterial sources. Current commercial alginates are mostly from the cell walls of brown algae (*Phaeophyceae*) [7] such as *Laminaria hyperborea*, *Laminaria lessonia*, *Macrocystis pyrifera*, and *Ascophyllum nodosum*. They are harvested to be converted into raw material commonly known as sodium alginate. On the other hand, alginates that are synthesized by bacterial biosynthesis obtain more defined chemical structures and physical properties than that of seaweed-derived alginates [8]. These bacterial alginates can be produced from *Azotobacter* and *Pseudomonas*. Other common forms of alginates are potassium alginate and calcium alginate. Alginates are anionic polysaccharides that can form viscous gum when bound with water. They are composed of linear unbranched copolymers containing blocks of (1,4)-linked β -D-mannuronic acid (M) and α -L-guluronate (G) residues, covalently linked in different sequences or blocks. The blocks can be consecutive MMMMM or GGGGG, or alternating GMGMGM. The amount of G and M blocks and the length depends on the alginate origin. The gel formation of alginate occurs when two G blocks of adjacent chains chelate with cations like Ca^{2+} with their carboxylic groups [9].

Alginate is also another popular material used in foods as a thickening agent, gelling agent, emulsifier, stabilizer, and texture improver. It can be added to color paste for textile printing

and act as binder of flux in welding rod production. Alginates are also established as biomaterials in the pharmaceutical industry where they can be compounded into tablets to accelerate disintegration of tablet for faster release of drugs. In cosmetic field, alginate can help to retain the color of lipstick on lip surface by forming gel network.

2.3. Chitosan

Chitosan is a natural aminopolysaccharide produced from partial alkaline deacetylation of chitin. Chitin, the second largest natural polymer after cellulose, is the structural element found in the exoskeleton of crustaceans, insects, and fungi. Just like plants produce cellulose in their cell walls, insects and crustaceans produce chitin in their shells. Chitosan is composed of linear copolymer of β (1–4) linked 2-acetamido-2-deoxy- β -D-glucopyranose and 2-amino-2-deoxy- β -D-glycopyranose. Different factors, such as alkali concentration, incubation time, ratio chitin to alkali, temperature, atmosphere, source of chitin, and particle size, play a role in affecting the properties of chitosan [10]. Chitin possesses poor solubility in aqueous solution and organic solvents mainly because of the highly extended hydrogen bonded semicrystalline structure of chitin, thus limiting its practical application in biomaterials [11]. Chitin has the degree of acetylation (DA) of 0.90 [12]. Whereas chitosan possess primary amino groups with pKa value of 6.3. These amines get protonated and form water-soluble and bioadhesive chitosan which readily bind to negatively charged surfaces [13].

Unlike chitin, chitosan has highly sophisticated functionality and wide range of applications in biomedical and other industrial areas. The advantage of chitosan over other polysaccharides is because of its cationic character and primary amino group [14]. Although they exhibit similar structure, chitosan display different properties from that of cellulose. When the degree of deacetylation of chitin reaches about 50%, it becomes chitosan and soluble in aqueous acidic media [15]. Chitosan has been applied in agriculture, water and waste management, food and beverages, cosmetics and toiletries, and biopharmaceutics.

2.4. Starch

Starch comprises of two main components: (1) amylose (**Figure 2a**), a nonbranching helical polymer consisting of α -1, 4 linked D-glucose monomers and (2) amylopectin (**Figure 2b**), a highly branched polymer consisting of both α -1,4 and α -1,6 linked D-glucose monomers. All starches are biosynthesized as semicrystalline granules with small amount of water [16]. There are amorphous and crystalline growth rings arranged alternately encircling hilum which is the point of initiation of the granule. Starch gelatinization is done by heating native starch in water [17]. After heating, starch granules start to swell and burst. The semicrystalline structure is disrupted and smaller amylose molecules start to leach out of the granules. Gelatinization irreversibly dissolves starch granule in water where water acts as a plasticizer. It forms network that holds water and increase the solution viscosity.

Starch is a resourceful natural polymer where it can be found in many plant roots, crop seeds, stalks, and staple crops. Main sources of native starch are maize (82%), wheat (8%), cassava (5%), and potatoes (5%) [18]. Starch is produced by all green plants as source of stored energy.

They were used in many applications in the form of native and modified starches. Starches are popular in food making including bakery, dairy products, confectionery, and processed foods. Other nonfood industries using starches are papermaking, adhesives, clothing, and cosmetics. Starch also involves in production of antibiotics, vitamins, penicillin, and dialysis solutions.

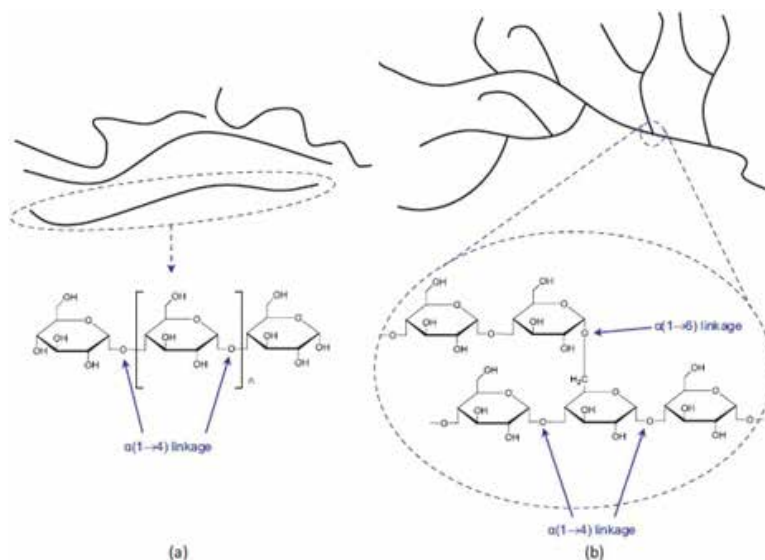


Figure 2. Structures of (a) amylose and (b) amylopectin [17].

2.5. Cellulose

Cellulose is a linear chain of ringed glucose molecules and has a flat ribbon-like conformation. It has the formula $(C_6H_{10}O_5)_n$ where n depended on the source of cellulose linked by $\beta(1\rightarrow4)$ glycosidic bonds. Cellulose is an essential structural component of cell walls in higher plants and is the most abundant organic polymer on the Earth. It is relatively stiff and rigid because of the intramolecular hydrogen bonding that can be reflected from its tendency to crystallize, high viscosity, and ability to form fibrillary strands [19]. Cellulose is insoluble in water and indigestible by the human body [20]. The glucose units in cellulose are linked by β glycosidic bonds, different than the α glycosidic bonds found in glycogen and starch. Cellulose has more hydrogen bonds between adjacent glucose units, both within a chain and between adjacent chains, making it a tougher fiber than glycogen or starch. This is why wood is so tough. Wood, paper, and cotton are the most common forms of cellulose. The purest natural form of cellulose is cotton. Other than these, cellulose can also be produced by certain types of bacteria and they are called bacterial cellulose. While cellulose is a basic structural component in most plants, it is also produced in *Acetobacter*, *Sarcina ventriculi*, and *Agrobacterium*. Bacterial cellulose contains higher purity and water uptake capability compared to plant cellulose [21]. It has a tensile strength that is almost comparable to the Kevlar and steel and it can achieve stress-strain behavior resembling that of a soft tissue in never dried form [22].

Being the largest natural polymer available is the most advantageous character for material sustainability and renewability. Cellulose has been tremendously applied in the production of cardboard and paper [19]. Current development of cellulose shows its potential in biomedical and biotechnological implementation. It is used in bioseparation, adsorbent for sewage treatment, cell suspension culture, and wound healing system.

3. Applications of polysaccharide composite biomaterials

Fabrications of polysaccharide-based composites containing different kind of reinforcements were subjected to many applications.

3.1. Tissue engineering

Tissue engineering and regenerative medicine have been important research areas that aim to repair and replace malfunction tissues or organs [23]. Assistive material or system is produced in order to support tissue generation which then can continue growing and functioning like original tissue in the body. Ideal three-dimensional (3D) tissue scaffolds must have certain characters to promote new tissue formation. Polymer-based material for 3D tissue scaffolds needs to possess high porosity, high surface area, suitable biodegradability, and good structural integrity. Human bodies are made up of complex and sensitive biological systems. Therefore, thorough attention needs to be taken in developing materials for tissue regeneration. Polysaccharide-based materials have since been of interest because of their important properties for biomedical application such as biocompatibility, biodegradability, and low cost [24]. They have acceptable response to the host and have ability to promote cell proliferation and adhesion. The emerging technology has investigated and explored many potential new forms of biomaterials for this purpose.

Halloysite nanotubes have been of interest since decades as biomaterials and fillers in composite scaffolds. A study by Liu et al. used this clay in alginate matrix to construct porous tissue engineered scaffolds [25]. They have successfully produced scaffold with 96% porosity. The composite scaffolds showed increased mechanical properties of alginate where higher compressive strength and modulus than pure alginate scaffold were obtained in dry and wet states. Halloysite nanotubes assisted in cell attachment and improved the stability against enzymatic degradation. Another attempt reported that chitosan/alginate/halloysite nanotube undergo amine treatment which later showed better cell growth and adherence than nonaminated composite scaffold [26]. Biomimetic synthetic scaffold was fabricated with inclusion of amorphous silica into alginate hydrogel [27]. They embedded bone cells, osteoblast-related SaOS-2 cells, and osteoclast-like RAW 264.7 cell into the hydrogel beads. The bead encapsulation of bone cells is a useful technique to produce bioactive programmable hydrogels. It is observed that it does not impair the viability of the encapsulated cells. Furthermore, incorporation of nanoceramic may improve the capability of polymeric scaffold for tissue regeneration. A study found that as-fabricated alginate/nano-TiO₂ needles nanocomposites by lyophiliza-

tion technique contain well controlled swelling and degradation compared to neat alginate scaffold [28].

A unique honeycomb composite of mollusca shell matrix and calcium alginate was fabricated to carry cells for soft tissue, skin, bone, and cartilage tissue regenerative therapies [29]. The composite was produced by frozen and treated mixture of *Anodonta woodiana* shell powder and sodium alginate with hydrochloric acid. It was transplanted into rats for 7, 14, 42, and 70 days. The composite displayed honeycomb structure under laser confocal microscope. This composite has significant mechanical properties, good biological safety over 70-day period, and lower degradation rate compared to the calcium carbonate (control). The regeneration of soft tissue requires substitutes that exhibit mechanical properties similar to native tissue. Thin saloplastic membranes from chitosan/alginate polyelectrolyte complexes containing different concentration of sodium chloride were prepared [30]. The membranes are resistant to degradation by lysozyme and stable at different pH. With high salt concentration, the water uptake and tensile moduli were increased, but decreasing the ultimate strength. High proliferation rates and viability of L929 fibroblasts were demonstrated. Structural modification to bacterial cellulose/alginate scaffold was constructed by two procedures, first is producing composite sponge bacterial cellulose/alginate (BCA) by crosslinking and freeze drying, and second is by reversing the previous procedure [31]. These procedures resulted in open and interconnected porous structure and thus lift up the problem of limited *in vivo* application due to dense outer layer of scaffolds.

3.1.1. Bone tissue engineering

Scaffolds fabrication in bone tissue engineering becomes preferable alternative to autografts and allografts which require surgical transplant of tissue or bone whether from the patient's own body or from a donor, respectively. These procedures often suffer from limited availability and risks of immunogenicity [32]. The performance of scaffolds for hard tissue critically depends on their mechanical and biological properties. Reinforcement of nanomaterials inside polysaccharide matrix is always proposed to increase the material surface area for enhanced cell adhesion and proliferation.

A blend of alginate and chitosan was added with nanosized bioactive silica (SiO_2) particles to provide biomineralization capability and polymer stiffness [33]. The composite scaffolds showed increased protein adsorption, controlled swelling ability, and improved apatite deposition without significant cytotoxicity toward osteolineage cells. Nanoscale fibers have been suggested to be effective reinforcing agents because of their resemblance to the fibrous structures of bone tissue bone extracellular matrix (ECM). A composite was developed by unique combination of wet electrospinning, particulate leaching, and freeze drying of starch/silk fibroin [34]. Silk fibroin has slow degradation rate with high oxygen permeability and thus is suitable for slow regeneration of tissue. Hadisi et al. fabricated the silk fibroin nanofibers by wet spinning directly via wet electrospinning using methanol coagulation bath before incorporating the chopped electrospun nanofibers into the starch matrix, followed by particulate leaching and freeze drying. The silk fibroin-containing starch hydrogel was further coated with calcium phosphates for better compatibility with the surrounding tissues. The

viability of osteoblast-like cells (MG63) exposed to the composites' extracts was significantly higher than that of the pure starch.

Hydroxyapatite (HAp) is the main inorganic component of natural bone that has been extensively used in many biocomposites to boost osteoconductivity and reinforce the structure of polymer-based bone scaffolds [35, 36]. The formation of bone-like apatite on scaffolds can be seen through the detection of calcium phosphates on the material surfaces. Incorporation of HAp nanoparticles in carrageenan [37], alginate [38, 39], cellulose [40, 41], and chitosan [42] displayed favorable site for bone cell adhesion and tissue regeneration compared to the neat polysaccharide scaffolds. The preparation of HAp-containing composites can be carried out either by using conventional mixing technique or by precipitating HAp crystals on the polymer matrices [36]. Mixture of two or more types of polysaccharides with HA like in Sharma et al. were believed to generate more synergistic effect to better mimic to the bone extracellular matrix, which comprises a variety of components [43].

3.1.2. Skin tissue engineering

Skin is the largest organ of human body. It serves as the first protection to human from environmental and surrounding threat. Fabrication of quaternary composite scaffold using chitosan, alginate, gelatin, and silk fibroin has successfully produced scaffold of 88% porosity with good mechanical stability [44]. L929 fibroblast cell cultured onto this quaternary composite scaffold showed good viability, adhesion, and proliferation, thus indicating the great prospect of the scaffold for skin tissue engineering. Boateng et al. studied two different methods for wound dressing to test their adhesive properties [45]. Solvent cast films and freeze-dried wafers containing polyethylene oxide (polyox) and carrageenan or sodium alginate. Wafers and films produced demonstrated high detachment force indicating strong interactions between polymers and the model wound surface. The adhesive properties were evaluated using attenuated reflectance Fourier transform infrared spectroscopy by monitoring the diffusion of mucin solution. The diffusion of mucin solution as model protein was faster for the wafer form than the film.

Wound dressings with antimicrobial and antiinflammatory properties are favorable besides the general noncytotoxic requirement. The gel-forming ability of polysaccharide materials helps in dressing application and removal without much pain to the skin. Incorporation of certain fillers to the dressing can provide additional function to the wound dressing to meet patients' needs. Encapsulation of antimicrobial and antiinflammatory drugs into wound dressing is the most common attempt for this purpose. The previous polyox/carrageenan composite has been loaded with diclorofenac and streptomycin to enhance the healing effect of wound [46]. The dressing showed higher zones of inhibition against three microbes compared to the individual drugs zones of inhibition. The insertion of diclorofenac can prevent inflammation while streptomycin can prevent the wound infections. However, adding multiple drugs into wound dressing without disturbing the healing function of the dressing is quite challenging. Thus, several studies have been done to incorporate other materials as antimicrobial agents, such as essential oil [47] and metal oxide [48], inside wound dressing to support its purpose.

3.1.3. Neural tissue engineering

Central nervous system diseases are usually caused by the death of neurons and progressive loss of its function. Current developments in neural technology have opened up possibilities of nerve tissue regeneration. Two potential natural polymers for nerve tissue engineering were combined with hyaluronic acid and heparan sulfate via freeze-drying technique [49]. The composite scaffolds demonstrated highly homogenous and interconnected pores with porosity above 96%. The presence of hyaluronic acid and heparan sulfate has promoted the adhesion of initial neural stem and progenitor cells. Nanofiber-hydrogel of polycaprolactone (PCL) and sodium alginate composite was prepared by electrospinning [50]. The fibrous form of this scaffold is to provide suitable environment for regeneration of the peripheral nerve injury. This kind of combination of natural and synthetic polymers has long been worked on to utilize the mechanical properties of PCL while preserving alginate hydrophilicity to support cell adhesion. The composite displayed that a good suture pulled out strength and assists the human mesenchymal stem cells (hMSCs) viability, adhesion, proliferation, and neurogenic differentiation in neural induction media.

3.2. Drug delivery

Drug delivery area involves an art of transporting drugs or therapeutic compounds to human body. It is a critical research field where the transported compounds must achieve the optimum therapeutic effect to protect or heal from any kind of disease. The use of polysaccharide materials in drug delivery systems is increasing mainly because of their ability to form hydrogel with stimuli-responsive properties [51, 52]. Besides being mechanically deficient, polysaccharide-based drug carrier normally have initial burst problem in the delivery system. Therefore, controlled delivery systems were proposed by addition of various fillers into polysaccharide matrix. This includes incorporation of Fe_3O_4 [53], CaCO_3 [54], silica nanoparticle [55], graphene oxide [56], gold nanoparticle [57], and montmorillonite [58].

Oral drug administration is one of the preferred routes since it is convenient and has no cross-infection. However, drugs taken through oral route have to pass through different phases of gastrointestinal tract, where pH values vary greatly. The change in pH may lead to loss of mechanical strength and fast degradation. To protect the drugs from the harsh environment in stomach before they can be absorbed in the intestine, pH-sensitive polysaccharide composites were developed. Protein drugs were encapsulated in inorganic carrier [59, 60] and gel beads [61, 62] to prolong their release. Series of pH-sensitive composite hydrogel composites of alginate and chitosan base were prepared with addition of attapulgite [61], bone ash [63], and other polymer-like pectin [64] that clearly showed their release dependence to pH condition. It was found that cross-linking and nanofiller loading can significantly improve the targeted release [65, 66] in the pH-sensitive polysaccharide composites.

Polysaccharides like starch and carrageenan are thermoresponsive polymers. They can be utilized in drug delivery with thermal sensitivity. λ -carrageenans were incorporated with Au [67] and silica [68] nanoparticles. The effect of both nanoparticles on the microstructure and strength of the hydrogel had implications in the mechanism of controlled release as demonstrated by *in vitro* release studies using a drug model and displayed potential for thermally

controlled drug delivery. Schmitt et al. loaded aqueous drug containing 5-aminosalicylic acid (5-ASA) into halloysite nanotubes and dispersed them well in thermoplastic starch matrix [69]. The swelling of the produced nanocomposite strongly depends on the temperature but not on pH. Furthermore, λ -carrageenans were also studied for a triple-response hydrogel by simultaneous formation of super paramagnetic iron oxide nanoparticles (SPION) and crosslinking of polyacrylic acid (PAA) [70]. The swelling capacity and drug release of λ -carrageenan-PAA/SPION hydrogel were tested to different temperature, pH, and magnetic field to assess the sensitivity of the hydrogel. They have successfully synthesized biocompatible hydrogel with considerable temperature, pH, and external magnetic field sensitivity using simple and convenient one-pot strategy. Another interesting functional hydrogel of λ -carrageenan was prepared by reinforcing with multiwalled carbon nanotubes (MWCNT) [71]. This hydrogel composite shows increased release of a model drug in *in vitro* conditions due to the near-infrared (NIR) photothermal effect of MWCNTs, thus demonstrating its promising role as carrier for remotely activated drug delivery.

Apart from being too focused on the additional function on drug carrier material, excipients must have the ability to encapsulate and protect the drugs. Some drugs have some specific needs to achieve targeted release. Targeted release is very important to ensure optimum drug effects. Aceclofenac is an orally administered phenyl acetic acid derivative with effects on a variety of inflammatory mediators. Its frequent administration and prolonged treatment was associated with various side effects. The use of *Boswellia* gum resin into chitosan polymer to deliver nonsteroidal antiinflammatory drug has caused significant improvement in drug entrapment efficiency (~40%) of the polymer composites [72]. Highly hydrophobic drug like curcumin frequently has poor solubility in polysaccharide excipients. An attempt to add pluronic F127 into alginate/chitosan matrix found to have increased the encapsulation efficiency of curcumin inside the composite, indicating better dispersion of curcumin inside matrix [73]. Local avascular delivery to treat orthopedic infections caused by Methicillin-resistant *Staphylococcus aureus* (MRSA) was developed by fabrication of porous chitosan/bioceramic β -tricalcium phosphate (CS/ β -TCP) [74]. The composite was then coated with poly(ϵ -caprolactone) (PCL) to retard the release of vancomycin for 6 weeks at levels to inhibit MRSA proliferation. Recently, the potential application of deferoxamine (DFO) in several iron dysregulation diseases has been highlighted. However, DFO presents significant limitations in clinical use due to its poor absorption in the gut and very short plasma half-life. Inclusion of poly(D,L-lactide-co-glycolide) microspheres into preformed chitosan/alginate hydrogel provided strong DFO entrapment in the hydrogel network and slow release [75].

3.3. Packaging films

The disability of conventional plastic material used in packaging to biodegrade has led to serious solid waste problem. Polysaccharide materials are fully recognized as potential alternative for petroleum-based plastics, mainly contributed by its biodegradability and environmental friendly properties. Packaging basically functions as container and external preserver or protector to consumer goods including food. Materials used in packaging need

to possess excellent mechanical properties and barrier properties so they will be able to maintain the condition for the products to extend their shelf-life. Therefore, several reinforcements have been identified to be good fillers for polysaccharide films.

Clay minerals have received extensive study as reinforcing filler in polysaccharide-based packaging film and coating [76]. Nanoclays have been a subject of interest nowadays considering their high aspect ratio and surface area, alongside with biocompatibility feature. The inclusion of clays showed good dispersion in polysaccharide matrix and resulted in superior mechanical and barrier properties. Incorporation of montmorillonite (MMT) nanoclay into alginate film has shown increase in tensile strength of up to 36% [77]. MMT may also enhance the thermal stability, storage modulus, and barrier properties of chitosan [78]. A comparative study of nanobiocomposite of carrageenan/zein and carrageenan/mica found mica clay to be more efficient as an additive to carrageenan for clay has better dispersion in carrageenan composite [79]. Cellulose nanocomposite foam containing MMT was investigated as a substitution for synthetic polymer foam trays. The presence of nanoclay caused more uniformity in the structure of the foam, thus resulted in higher compressive strength, Young's modulus, and density [80]. The use of sepiolite and palygorskite fibrous clays in some polysaccharides of different types was reported [81]. The good compatibility between these fibrous clays with the polymers resulted in improved mechanical properties, barrier to UV light, stability in water, and reduction of water absorption, which make them very attractive bionanocomposite in the food packaging sector. Other fillers included into polysaccharide-based packaging films are nanosilica [82], zinc oxide [83], and copper [84] nanoparticles.

In terms of polysaccharide composites, certain fillers were added to the packaging films not only to improve their mechanical and barrier properties, but special characteristics can also be instilled for the production of active packaging films. Active packaging refers to the packaging systems used for products like foods and pharmaceuticals that have extra function to extend their shelf-life, in addition to the general purpose of providing external protective barrier. Introduction of different kinds of natural and synthetic antimicrobial agents into packaging have been studied against various pathogens such as *Listeria monocytogenes*, *Escherichia coli*, *Clostridium perfringens*, *Staphylococcus aureus*, *Salmonella pullorum*, *Bacillus cereus*, and *Pseudomonas aeruginosa*. The inhibitory effect of the films was determined by measuring the bacterial growth inhibition zones. Preparation of polysaccharide-based packaging films with incorporation of nanometals, organically modified clay minerals, plant essential oils and extracts, and other natural antibacterial agent were tested for their antimicrobial properties.

Clays are organically modified to increase their hydrophobicity since the polysaccharide matrix is already water sensitive and has low water vapor barrier properties. They also exhibit biocompatibility, bioactivity, and can be used as antibacterial materials. The inclusion of modified clay Cloisite 30B in carrageenan/locust bean gum matrix [85] and zeolite-A inside chitosan matrix [86] have demonstrated high antimicrobial efficiency compared to neat polysaccharide. A combination of halloysite nanotube and nisin had been expected synergistic effect in active packaging [87]. Nisin is an antimicrobial agent recognized to fight against

Listeria and spores of *Bacilli* and *Clostridia*. However, a study by Lu et al. showed the formation of 3% alginate solution containing nisin-ethylenediaminetetraacetic acid (EDTA) might have limited the release of nisin [88]. Lower concentration of alginate was proposed to see the effect of alginate concentration to nisin performance. Another study included silver (Ag) nanoparticles combined with Cloisite 30B in γ -carrageenan as antimicrobial bionanocomposite films [89]. Ag nanoparticles have attracted considerable attention for packaging application for their antibacterial activities, high thermal stability, and low toxicity. Ag/clay mineral was prepared to overcome the tendency of Ag nanoparticles to agglomerate when used alone. While organically modified nanoclay exhibited strong antibacterial activity against Gram-positive bacteria, Ag nanoparticles exhibited strong antimicrobial activity against Gram-negative bacteria. Thus, the combination of these two antibacterial agents helps in providing polymer packaging with strong antimicrobial properties. Shankar et al. investigated different types of Ag particles incorporated into alginate-based films [90]. They found Ag zeolite and citrate reduced Ag nanoparticles provide better antimicrobial activity than metallic silver and laser-ablated Ag nanoparticles in alginate compared to the neat films.

Strong antimicrobial activities can also be induced inside packaging films by plant extracts and essential oils. Extracts of green and black tea were added into chitosan displayed good antioxidant and antimicrobial capacity [91]. Natural extract from the seeds, pulps, and peel of grapefruit was also put inside carrageenan film to encourage the antibacterial, antifungal, and antioxidant properties [92]. However, addition of plant extracts showed decreased tensile strength and elongation at break of the packaging films. In addition, oregano, thyme, and *Satureja hortensis* essential oils were used in carrageenan films to overcome the poor water vapor barrier and as possible substitutes for synthetic antioxidant-antimicrobial agents to achieve oxidative and microbial stability [93, 94]. The tensile strength was lowered with increasing essential oil concentration. They suggested it happened because of the replacement of strong polymer-polymer interaction with oil-polymer interaction in the film network.

4. Conclusions

Polysaccharide-based composites are attractive biomaterials because of their chemical structure and ease of manipulation. They are easily processable and abundant in nature, forming a vast potential economical application compared to other synthetic biomaterials. Moreover, they are highly environmental friendly and nontoxic to humans and animals. Preserving the nature while taking advantage of its application leads to promising future for renewable and sustainable materials. Polysaccharide-based composites are mainly to overcome the problem of low mechanical and water barrier properties of common natural polymers. Many studies have been done and successfully associated different reinforcements and fillers to polysaccharides for variety of fabrication purposes. Polysaccharide-based composites are thus a favorable alternative to the commercial petroleum-based polymers and highly recommended for renewable and sustainable composite materials.

Author details

Izzati Fatimah Wahab^{1,2} and Saiful Izwan Abd Razak^{1,2*}

*Address all correspondence to: saifulizwan@utm.my

1 IJN-UTM Cardiovascular Engineering Centre, University of Technology, Malaysia, Johor, Malaysia

2 Faculty of Biosciences and Medical Engineering, University of Technology, Malaysia, Johor, Malaysia

References

- [1] D. F. Williams, "On the nature of biomaterials," *Biomaterials*, vol. 30, no. 30, pp. 5897–5909, 2009.
- [2] J. N. BeMiller, "Polysaccharides: Occurrence, significance, and properties," in *Glycoscience*, B. Fraser-Reid, K. Tatsuta, and J. Thiem, Eds., Springer, Berlin Heidelberg, 2008, pp. 1431–1435.
- [3] V. D. Prajapati, P. M. Maheriya, G. K. Jani, and H. K. Solanki, "Carrageenan: A natural seaweed polysaccharide and its applications," *Carbohydr. Polym.*, vol. 105, no. 1, pp. 97–112, 2014.
- [4] J. Liu, X. Zhan, J. Wan, Y. Wang, and C. Wang, "Review for carrageenan-based pharmaceutical biomaterials: Favourable physical features versus adverse biological effects," *Carbohydr. Polym.*, vol. 121, pp. 27–36, 2015.
- [5] V. L. Campo, D. F. Kawano, D. B. da Silva, and I. Carvalho, "Carrageenans: Biological properties, chemical modifications and structural analysis – A review," *Carbohydr. Polym.*, vol. 77, no. 2, pp. 167–180, 2009.
- [6] F. van de Velde, S. H. Knutsen, A. I. Usov, H. S. Rollema, and A. S. Cerezo, "1H and 13C high resolution NMR spectroscopy of carrageenans: Application in research and industry," *Trends Food Sci. Technol.*, vol. 13, no. 3, pp. 73–92, 2002.
- [7] S. N. Pawar and K. J. Edgar, "Alginate derivatization: A review of chemistry, properties and applications," *Biomaterials*, vol. 33, no. 11, pp. 3279–3305, 2012.
- [8] K. Y. Lee and D. J. Mooney, "Alginate: Properties and biomedical applications," *Prog. Polym. Sci.*, vol. 37, no. 1, pp. 106–126, 2012.
- [9] A. D. Augst, H. J. Kong, and D. J. Mooney, "Alginate hydrogels as biomaterials," *Macromol. Biosci.*, vol. 6, no. 8, pp. 623–633, 2006.

- [10] L. A. M. Van Den Broek, R. J. I. Knoop, F. H. J. Kappen, and C. G. Boeriu, "Chitosan films and blends for packaging material," *Carbohydr. Polym.*, vol. 116, pp. 237–242, 2015.
- [11] M. Dash, F. Chiellini, R. M. Ottenbrite, and E. Chiellini, "Chitosan—A versatile semi synthetic polymer in biomedical applications," *Prog. Polym. Sci.*, vol. 36, no. 8, pp. 981–1014, 2011.
- [12] C. K. S. Pillai, W. Paul, and C. P. Sharma, "Chitin and chitosan polymers: Chemistry, solubility and fiber formation," *Prog. Polym. Sci.*, vol. 34, no. 7, pp. 641–678, 2009.
- [13] D. W. Lee, C. Lim, J. N. Israelachvili, and D. S. Hwang, "Strong adhesion and cohesion of chitosan in aqueous solutions," *Langmuir*, vol. 29, no. 46, pp. 14222–14229, 2013.
- [14] M. A. Elgadir, M. S. Uddin, S. Ferdosh, A. Adam, A. J. K. Chowdhury, and M. Z. I. Sarker, "Impact of chitosan composites and chitosan nanoparticle composites on various drug delivery systems: A review," *J. Food Drug Anal.*, vol. 23, no. 4, pp. 619–629, 2015.
- [15] M. Rinaudo, "Chitin and chitosan: Properties and applications," *Prog. Polym. Sci.*, vol. 31, no. 7, pp. 603–632, 2006.
- [16] N. Lin, J. Huang, P. R. Chang, D. P. Anderson, and J. Yu, "Preparation, modification, and application of starch nanocrystals in nanomaterials: A review," *J. Nanomater.*, vol. 2011, pp. 20, 2011.
- [17] F. Xie, E. Pollet, P. J. Halley, and L. Averous, "Starch-based nano-biocomposites," *Prog. Polym. Sci.*, vol. 38, pp. 1590–1628, 2013.
- [18] D. Le Corre, J. Bras, and A. Dufresne, "Starch nanoparticles: A review," *Biofabrication*, vol. 11, pp. 1139–1153, 2010.
- [19] T. L. B. Ha, T. M. Quan, D. N. Vu, and D. M. Si, "Naturally derived biomaterials: Preparation and application," in *Regenerative Medicine and Tissue Engineering*, J. A. Andrades, Ed., InTech, Croatia, 2013, pp. 247–274.
- [20] V. Kulkarni, K. Butte, and S. Rathod, "Natural polymers—A comprehensive review," *Int. J. Res. Pharm. Biomed. Sci.*, vol. 3, no. 4, pp. 1597–1613, 2012.
- [21] N. Shah, M. Ul-Islam, W. A. Khattak, and J. K. Park, "Overview of bacterial cellulose composites: A multipurpose advanced material," *Carbohydr. Polym.*, vol. 98, no. 2, pp. 1585–1598, 2013.
- [22] H. Ullah, F. Wahid, H. A. Santos, and T. Khan, "Advances in biomedical and pharmaceutical applications of functional bacterial cellulose-based nanocomposites," *Carbohydr. Polym.*, vol. 150, pp. 330–352, 2016.
- [23] P. X. Ma, "Biomimetic materials for tissue engineering," *Adv. Drug Deliv. Rev.*, vol. 60, no. 2, pp. 184–198, 2008.

- [24] F. Khan and S. R. Ahmad, "Polysaccharides and their derivatives for versatile tissue engineering application," *Macromol. Biosci.*, vol. 13, no. 4, pp. 395–421, 2013.
- [25] M. Liu, L. Dai, H. Shi, S. Xiong, and C. Zhou, "In vitro evaluation of alginate/halloysite nanotube composite scaffolds for tissue engineering," *Mater. Sci. Eng. C. Mater. Biol. Appl.*, vol. 49, pp. 700–712, 2015.
- [26] H. Amir Afshar and A. Ghaee, "Preparation of aminated chitosan/alginate scaffold containing halloysite nanotubes with improved cell attachment," *Carbohydr. Polym.*, vol. 151, pp. 1120–1131, 2016.
- [27] U. Schloßmacher, H. C. Schröder, X. Wang, Q. Feng, B. Diehl-Seifert, S. Neumann, A. Trautwein, and W. E. G. Müller, "Alginate/silica composite hydrogel as a potential morphogenetically active scaffold for three-dimensional tissue engineering," *RSC Adv.*, vol. 3, no. 28, p. 11185, 2013.
- [28] V. V. D. Rani, R. Ramachandran, K. P. Chennazhi, H. Tamura, S. V. Nair, and R. Jayakumar, "Fabrication of alginate/nanoTiO₂ needle composite scaffolds for tissue engineering applications," *Carbohydr. Polym.*, vol. 83, no. 2, pp. 858–864, 2011.
- [29] H. J. You, J. Li, C. Zhou, B. Liu, and Y. G. Zhang, "A honeycomb composite of mollusca shell matrix and calcium alginate," *Colloid Surf. B Biointerfaces*, vol. 139, pp. 100–106, 2016.
- [30] R. R. Costa, A. M. S. Costa, S. G. Caridade, and J. F. Mano, "Compact saloplastic membranes of natural polysaccharides for soft tissue engineering," *Chem. Mater.*, vol. 27, no. 21, pp. 7490–7502, 2015.
- [31] S. Kirdponpattara, A. Khamkeaw, N. Sanchavanakit, P. Pavasant, and M. Phisalaphong, "Structural modification and characterization of bacterial cellulose-alginate composite scaffolds for tissue engineering," *Carbohydr. Polym.*, vol. 132, pp. 146–155, 2015.
- [32] E. Chiarello, M. Cadossi, G. Tedesco, P. Capra, C. Calamelli, A. Shehu, and S. Giannini, "Autograft, allograft and bone substitutes in reconstructive orthopedic surgery," *Aging Clin. Exp. Res.*, vol. 25, no. 1 Suppl., pp. 101–103, 2013.
- [33] J. A. Sowjanya, J. Singh, T. Mohita, S. Sarvanan, A. Moorthi, N. Srinivasan, and N. Selvamurugan, "Biocomposite scaffolds containing chitosan/alginate/nano-silica for bone tissue engineering," *Colloid Surf. B Biointerfaces*, vol. 109, pp. 294–300, 2013.
- [34] Z. Hadisi, J. Nourmohammadi, and J. Mohammadi, "Composite of porous starch-silk fibroin nano fiber-calcium phosphate for bone regeneration," *Ceram. Int.*, vol. 41, pp. 10745–10754, 2015.
- [35] J. Li, H. Sun, D. Sun, Y. Yao, F. Yao, and K. Yao, "Biomimetic multicomponent polysaccharide/nano-hydroxyapatite composites for bone tissue engineering," *Carbohydr. Polym.*, vol. 85, no. 4, pp. 885–894, 2011.

- [36] J. Venkatesan, I. Bhatnagar, P. Manivasagan, K. Kang, and S. Kim, "Alginate composites for bone tissue engineering: A review," *Int. J. Biol. Macromol.*, vol. 72C, pp. 269–281, 2014.
- [37] A. L. Daniel-Da-Silva, A. B. Lopes, A. M. Gil, and R. N. Correia, "Synthesis and characterization of porous K-carrageenan/calcium phosphate nanocomposite scaffolds," *J. Mater. Sci.*, vol. 42, no. 20, pp. 8581–8591, 2007.
- [38] D. Porrelli, A. Travan, G. Turco, E. Marsich, M. Borgogna, S. Paoletti, and I. Donati, "Alginate-hydroxyapatite bone scaffolds with isotropic or anisotropic pore structure: Material properties and biological behavior," *Macromol. Mater. Eng.*, vol. 300, no. 10, pp. 989–1000, 2015.
- [39] G. Turco, E. Marsich, F. Bellomo, S. Semeraro, I. Donati, F. Brun, M. Grandolfo, A. Accardo, and S. Paoletti, "Alginate/hydroxyapatite biocomposite for bone ingrowth: A trabecular structure with high and isotropic connectivity," *Biomacromolecules*, vol. 10, pp. 1575–1583, 2009.
- [40] S. Zadegan, M. Hossainipour, H. Ghassai, H. R. Rezaie, and M. R. Naimi-Jamal, "Synthesis of cellulose–nanohydroxyapatite composite in 1-n-butyl-3-methylimidazolium chloride," *Ceram. Int.*, vol. 36, no. 8, pp. 2375–2381, 2010.
- [41] C. Tsiptsias and C. Panayiotou, "Preparation of cellulose-nanohydroxyapatite composite scaffolds from ionic liquid solutions," *Carbohydr. Polym.*, vol. 74, no. 1, pp. 99–105, 2008.
- [42] J. Zhang, J. Nie, Q. Zhang, Y. Li, Z. Wang, and Q. Hu, "Preparation and characterization of bionic bone structure chitosan/hydroxyapatite scaffold for bone tissue engineering," *J. Biomater. Sci. Polym. Ed.*, vol. 25, no. 1, pp. 61–74, 2014.
- [43] C. Sharma, A. K. Dinda, P. D. Potdar, C. F. Chou, and N. C. Mishra, "Fabrication and characterization of novel nano-biocomposite scaffold of chitosan-gelatin-alginate hydroxyapatite for bone tissue engineering," *Mater. Sci. Eng. C*, vol. 64, pp. 416–427, 2016.
- [44] C. Sharma, A. K. Dinda, P. D. Potdar, and N. C. Mishra, "Fabrication of quaternary composite scaffold from silk fibroin, chitosan, gelatin, and alginate for skin regeneration," *J. Appl. Polym. Sci.*, vol. 132, no. 42743, pp. 1–12, 2015.
- [45] J. S. Boateng, H. V. Pawar, and J. Tetteh, "Evaluation of in vitro wound adhesion characteristics of composite film and wafer based dressings using texture analysis and FTIR spectroscopy: A chemometrics factor analysis approach," *RSC Adv.*, vol. 5, no. 129, pp. 107064–107075, 2015.
- [46] J. S. Boateng, H. V. Pawar, and J. Tetteh, "Polyox and carrageenan based composite film dressing containing anti-microbial and anti-inflammatory drugs for effective wound healing," *Int. J. Pharm.*, vol. 441, no. 1–2, pp. 181–191, 2013.

- [47] I. Liakos, L. Rizzello, D. J. Scurr, P. P. Pompa, I. S. Bayer, and A. Athanassiou, "All natural composite wound dressing films of essential oils encapsulated in sodium alginate with antimicrobial properties," *Int. J. Pharm.*, vol. 463, no. 2, pp. 137–145, 2014.
- [48] K. T. Shalumon, K. H. Anulekha, S. V. Nair, K. P. Chennazhi, and R. Jayakumar, "Sodium alginate/poly(vinyl alcohol)/nano ZnO composite nanofibers for antibacterial wound dressings," *Int. J. Biol. Macromol.*, vol. 49, no. 3, pp. 247–254, 2011.
- [49] S. Guan, X. Zhang, and X. L. T. L. X. Ma, "Chitosan/gelatin porous scaffolds containing hyaluronic acid and heparan sulfate for neural tissue engineering," *J. Biomater. Sci. Polym. Ed.*, vol. 24, no. 8, pp. 999–1014, 2013.
- [50] N. B. Shelke, P. Lee, M. Anderson, N. Mistry, R. K. Nagarale, X. Ma, and X. Yu, "Neural tissue engineering: Nano fiber-hydrogel based composite scaffolds," *Polym. Adv. Technol.*, vol. 27, pp. 42–51, 2016.
- [51] H. H. Tønnesen and J. Karlsten, "Alginate in drug delivery systems," *Drug Dev. Ind. Pharm.*, vol. 28, no. 6, pp. 621–630, 2002.
- [52] A. Bernkop-Schnürch and S. Dünnhaupt, "Chitosan-based drug delivery systems," *Eur. J. Pharm. Biopharm.*, vol. 81, pp. 463–469, 2012.
- [53] H. Hamidian and T. Tavakoli, "Preparation of a new Fe₃O₄/starch-g-polyester nano-composite hydrogel and a study on swelling and drug delivery properties," *Carbohydr. Polym.*, vol. 144, pp. 140–148, 2016.
- [54] M. L. Cacicedo, K. Cesca, V. E. Bosio, L. M. Porto, and G. R. Castro, "Self-assembly of carrageenin-CaCO₃ hybrid microparticles on bacterial cellulose films for doxorubicin sustained delivery," *J. Appl. Biomed.*, vol. 13, no. 3, pp. 239–248, 2015.
- [55] M. Zhu, Y. Zhu, L. Zhang, and J. Shi, "Preparation of chitosan/mesoporous silica nanoparticle composite hydrogels for sustained co-delivery of biomacromolecules and small chemical drugs," *Sci. Technol. Adv. Mater.*, vol. 14, no. 4, p. 045005, 2013.
- [56] Y. Chen, Y. Qi, X. Yan, H. Ma, J. Chen, B. Liu, and Q. Xue, "Green fabrication of porous chitosan/graphene oxide composite xerogels for drug delivery," *J. Appl. Polym. Sci.*, vol. 131, no. 6, pp. 1–11, 2014.
- [57] K.S.Oh,R.S.Kim,J.Lee,D.Kim,S.H.Cho,andS.H.Yuk,"Gold/chitosan/pluroniccomposite nanoparticlesfordrugdelivery,"*J.Appl.Polym.Sci.*,vol.108,pp.3239–3244,2008.
- [58] P. L. Nayak and D. Sahoo, "Chitosan-sodium alginate nanocomposites blended with cloisite 30b as a novel drug delivery system for anticancer drug curcumin," *Int. J. Appl. Biol. Pharm. Technol.*, vol. 2, no. 3, pp. 402–411, 2011.
- [59] P. Savitha, "Fabrication and in vitro evaluation of starch/MWCNT composites as drug delivery device," *J. Pharm. Sci. Res.*, vol. 7, no. 9, pp. 753–754, 2015.

- [60] H. Kaygusuz, M. Uysal, V. Adimcilar, and F. B. Erim, "Natural alginate biopolymer montmorillonite clay composites for vitamin B2 delivery," *J. Bioact. Compat. Polym.*, vol. 30, no. 1, pp. 48–56, 2015.
- [61] Q. Wang, J. Zhang, and A. Wang, "Preparation and characterization of a novel pH sensitive chitosan-g-poly (acrylic acid)/attapulgit/sodium alginate composite hydrogel bead for controlled release of diclofenac sodium," *Carbohydr. Polym.*, vol. 78, no. 4, pp. 731–737, 2009.
- [62] Y. Hu, J. Peng, L. Ke, D. Zhao, H. Zhao, and X. Xiao, "Alginate/carboxymethyl chitosan composite gel beads for oral drug delivery," *J. Polym. Res.*, vol. 23, no. 7, p. 129, 2016.
- [63] N. Alemdar, "Fabrication of a novel bone ash-reinforced gelatin/alginate/hyaluronic acid composite film for controlled drug delivery," *Carbohydr. Polym.*, vol. 151, pp. 1019–1026, 2016.
- [64] C. Y. Yu, B. C. Yin, W. Zhang, S. X. Cheng, X. Z. Zhang, and R. X. Zhuo, "Composite microparticle drug delivery systems based on chitosan, alginate and pectin with improved pH-sensitive drug release property," *Colloids Surf. B Biointerfaces*, vol. 68, no. 2, pp. 245–249, 2009.
- [65] M. S. Hasnain, A. K. Nayak, M. Singh, M. Tabish, M. T. Ansari, and T. J. Ara, "Alginate based bipolymeric-nanobioceramic composite matrices for sustained drug release," *Int. J. Biol. Macromol.*, vol. 83, pp. 71–77, 2016.
- [66] H. Hezaveh and I. I. Muhamad, "The effect of nanoparticles on gastrointestinal release from modified K-carrageenan nanocomposite hydrogels," *Carbohydr. Polym.*, vol. 89, no. 1, pp. 138–145, 2012.
- [67] A. M. Salgueiro, A. L. Daniel-Da-Silva, S. Fateixa, and T. Trindade, "K-Carrageenan hydrogel nanocomposites with release behavior mediated by morphological distinct Au nanofillers," *Carbohydr. Polym.*, vol. 91, no. 1, pp. 100–109, 2013.
- [68] S. F. Soares, T. Trindade, and A. L. Daniel-Da-Silva, "Carrageenan-silica hybrid nanoparticles prepared by a non-emulsion method," *Eur. J. Inorg. Chem.*, vol. 2015, no. 27, pp. 4588–4594, 2015.
- [69] H. Schmitt, N. Creton, K. Prashantha, J. Soulestin, M. F. Lacrampe, and P. Krawczak, "Melt-blended halloysite nanotubes/wheat starch nanocomposites as drug delivery system," *Polym. Eng. Sci.*, vol. 55, pp. 573–580, 2015.
- [70] G. R. Bardajee and Z. Hooshyar, "Kappa carrageenan-g-poly (acrylic acid)/SPION nanocomposite as a novel stimuli-sensitive drug delivery system," *Colloid Polym. Sci.*, vol. 291, pp. 2791–2803, 2013.
- [71] A. C. Estrada, A. L. Daniel-Da-Silva, and T. Trindade, "Photothermally enhanced drug release by k-carrageenan hydrogels reinforced with multi-walled carbon nanotubes," *RSC Adv.*, vol. 3, no. 27, pp. 10828–10836, 2013.

- [72] S. Jana, B. Laha, and S. Maiti, "Boswellia gum resin/chitosan polymer composites: Controlled delivery vehicles for aceclofenac," *Int. J. Biol. Macromol.*, vol. 77, pp. 303–306, 2015.
- [73] R. K. Das, N. Kasoju, and U. Bora, "Encapsulation of curcumin in alginate-chitosan pluronic composite nanoparticles for delivery to cancer cells," *Nanomed. Nanotechnol. Biol. Med.*, vol. 6, no. 1, pp. 153–160, 2010.
- [74] T. Fang, J. Wen, J. Zhou, Z. Shao, and J. Dong, "Poly (ε-caprolactone) coating delays vancomycin delivery from porous chitosan/B-tricalcium phosphate composites," *J. Biomed. Mater. Res. B Appl. Biomater.*, vol. 100 B, no. 7, pp. 1803–1811, 2012.
- [75] G. Rasso, A. Salis, E. P. Porcu, P. Giunchedi, M. Roldo, and E. Gavini, "Composite chitosan/alginate hydrogel for controlled release of deferoxamine: A system to potentially treat iron dysregulation diseases," *Carbohydr. Polym.*, vol. 136, pp. 1338–1347, 2016.
- [76] F. Uddin, "Clays, nanoclays, and montmorillonite minerals," *Metall. Mater. Trans. A Phys. Metall. Mater. Sci.*, vol. 39, no. 12, pp. 2804–2814, 2008.
- [77] M. Alboofetileh, M. Rezaei, H. Hosseini, and M. Abdollahi, "Effect of nanoclay and cross-linking degree on the properties of alginate-based nanocomposite film," *J. Food Process. Preserv.*, vol. 38, no. 4, pp. 1622–1631, 2014.
- [78] Y. Kasirga, A. Oral, and C. Caner, "Preparation and characterization of chitosan/montmorillonite-K10 nanocomposites films for food packaging applications," *Polym. Compos.*, vol. 33, no. 11, pp. 1874–1882, 2012.
- [79] M. D. Sanchez-Garcia, L. Hilliou, and J. M. Lagaron, "Nanobiocomposites of carrageenan, zein, and mica of interest in food packaging and coating applications," *J. Agric. Food Chem.*, vol. 58, no. 11, pp. 6884–6894, 2010.
- [80] S. Ahmadzadeh, J. Keramat, A. Nasirpour, N. Hamdami, T. Behzad, L. Aranda, M. Vilasi, and S. Desobry, "Structural and mechanical properties of clay nanocomposite foams based on cellulose for the food-packaging industry," *J. Appl. Polym. Sci.*, vol. 133, no. 2, p. 42079, 2016.
- [81] A. C. S. Alcantara, M. Darder, P. Aranda, A. Ayrál, and E. Ruiz-Hitzky, "Bionanocomposites based on polysaccharides and fibrous clays for packaging applications," *J. Appl. Polym. Sci.*, vol. 133, no. 2, 2016.
- [82] L. R. Rane, N. R. Savadekar, P. G. Kadam, and S. T. Mhaske, "Preparation and characterization of K-carrageenan/nanosilica biocomposite film," *J. Mater.*, vol. 2014, pp. 1–8, 2014.
- [83] M. Shafiq, T. Yasin, M. A. Rafiq, and Shaista, "Structural, thermal, and antibacterial properties of chitosan/ZnO composites," *Polym. Polym. Compos.*, vol. 16, no. 2, pp. 101–113, 2008.

- [84] V. Sadanand, N. Rajini, A. Varada Rajulu, and B. Satyanarayana, "Preparation of cellulose composites with in situ generated copper nanoparticles using leaf extract and their properties," *Carbohydr. Polym.*, vol. 150, pp. 32–39, 2016.
- [85] J. T. Martins, A. I. Bourbon, A. C. Pinheiro, B. W. S. Souza, M. A. Cerqueira, and A. A. Vicente, "Biocomposite films based on K-carrageenan/locust bean gum blends and clays: Physical and antimicrobial properties," *Food Bioprocess Technol.*, vol. 6, no. 8, pp. 2081–2092, 2013.
- [86] L. Yu, J. Gong, C. Zeng, and L. Zhang, "Preparation of zeolite-A/chitosan hybrid composites and their bioactivities and antimicrobial activities," *Mater. Sci. Eng. C*, vol. 33, no. 7, pp. 3652–3660, 2013.
- [87] S. M. M. Meira, G. Zehetmeyer, J. M. Scheibel, J. O. Werner, and A. Brandelli, "Starch halloysite nanocomposites containing nisin: Characterization and inhibition of *Listeria monocytogenes* in soft cheese," *LWT Food Sci. Technol.*, vol. 68, pp. 226–234, 2016.
- [88] F. Lu, D. Liu, X. Ye, Y. Wei, and F. Liu, "Alginate-calcium coating incorporating nisin and EDTA maintains the quality of fresh northern snakehead (*Channa argus*) fillets stored at 4°C," *J. Sci. Food Agric.*, vol. 89, no. 5, pp. 848–854, 2009.
- [89] J. Rhim and L. Wang, "Preparation and characterization of carrageenan-based nanocomposite films reinforced with clay mineral and silver nanoparticles," *Appl. Clay Sci.*, vol. 97–98, pp. 174–181, 2014.
- [90] S. Shankar, L.-F. Wang, and J.-W. Rhim, "Preparations and characterization of alginate/silver composite films: Effect of types of silver particles," *Carbohydr. Polym.*, vol. 146, pp. 208–216, 2016.
- [91] Y. Peng, Y. Wu, and Y. Li, "Development of tea extracts and chitosan composite films for active packaging materials," *Int. J. Biol. Macromol.*, vol. 59, pp. 282–289, 2013.
- [92] P. Kanmani and J.-W. Rhim, "Development and characterization of carrageenan/grapefruit seed extract composite films for active packaging," *Int. J. Biol. Macromol.*, vol. 68, pp. 258–266, 2014.
- [93] A. Soni, G. Kandeepan, S. K. Mendiratta, V. Shukla, and A. Kumar, "Development and characterization of essential oils incorporated carrageenan based edible film for packaging of chicken patties," *Nutr. Food Sci.*, vol. 46, no. 1, pp. 82–95, 2016.
- [94] S. Shojaee-Aliabadi, H. Hosseini, M. A. Mohammadifar, A. Mohammadi, M. Ghasemlou, S. M. Ojagh, S. M. Hosseini, and R. Khaksar, "Characterization of antioxidant antimicrobial K-carrageenan films containing *Satureja hortensis* essential oil," *Int. J. Biol. Macromol.*, vol. 52, no. 1, pp. 116–124, 2013.

Thermoplastic Starch (TPS)-Cellulosic Fibers Composites: Mechanical Properties and Water Vapor Barrier: A Review

Emilio Pérez-Pacheco, Jorge Carlos Canto-Pinto,
Víctor Manuel Moo-Huchin,
Iván Alfredo Estrada-Mota,
Raciel Javier Estrada-León and Luis Chel-Guerrero

Additional information is available at the end of the chapter

<http://dx.doi.org/10.5772/65397>

Abstract

Current research studies have been focusing on the procurement of environmentally friendly materials, with the aim of resolving the problems created by materials derived from petroleum. Starch is a promising biopolymer for producing biocomposite materials because it is renewable, completely biodegradable, and easily available at a low cost. Thermoplastic starch (TPS), by itself, exhibits poor mechanical properties such as low tensile strength and severe deformations, which limits its application in packaging or films. In addition, TPS presents high hygroscopicity. The use of reinforcing agents in the starch matrix is an effective means to overcome these drawbacks and several types of biodegradable reinforcements, such as cellulosic fibers, whiskers, and nanofibers, have been utilized to develop new and inexpensive starch biocomposites. This chapter provides the latest advances in green composite materials based on TPS and cellulose fibers and includes information on compositions, preparations, and the properties of “green” composite materials elaborated from TPS and cellulose fibers, with the focus on using undervalued natural resources.

Keywords: Thermoplastic Starch, Cellulose Fibers, Sustainable Green, Biopolymer, Natural Resource

1. Introduction

Current research studies have been focusing on the procurement of environmentally friendly materials with the aim of resolving the problems created by materials derived from petroleum. Starch is a promising biopolymer used in the production of biocomposite materials because it is renewable, completely biodegradable, and easily available at a low cost. Starch, in the form of its thermoplastic derivative (TPS), has been revealed as an appropriate candidate to be employed as a substitute of synthetic polymers traditionally used for packaging. Starch is not a real thermoplastic polymer, but can be processed after its gelatinization by mixing it with enough water and/or plasticizers [1, 2]. In most investigations the plasticization of the material is carried out by casting a dispersion of starch with glycerol [1, 3].

TPS films are reported to have low permeability to gases, poor water vapor barrier properties, and must resist the tensions arising from their use in packaging [4].

Therefore, improving the resistance of TPS films to traction forces is a factor that must be taken into consideration for their use [5, 6]. The use of reinforcing agents in the starch matrix is an effective means of overcoming these drawbacks and several types of biodegradable reinforcements such as cellulosic fibers, whiskers, and cellulose nanofibers (CNF) have been utilized to develop new and inexpensive starch biocomposites. Cellulose is the most abundant, renewable polymer in the world; it is found in plant cell walls and it can also be synthesized by some bacteria. Its reinforcing property is remarkable [7]. Basically two types of nanoreinforcements can be obtained from cellulose: microfibrils (or CNF) and whiskers.

Improving the mechanical and water barrier properties by the addition of CNF (extracted from different botanical sources) can depend on the correct dispersion and the generation of an active nanoreinforcement/matrix interface.

This chapter provides the latest advances in green composite materials based on TPS and cellulose fibers and includes information on compositions, preparations, and the properties of “green” composite materials elaborated from TPS and cellulose fibers, with the focus on using undervalued natural resources.

2. Starch

Starch is a biodegradable and widely available natural resource [8], and constitutes the main source of carbohydrate reserves in plants. This polysaccharide is found in different parts of the plants and can be isolated from seeds, fruits, leaves, tubers, and roots [9].

The functionality of starch is largely due to its two components of high molecular weight: amylose and amylopectin. Most of the starches contain between 20 and 30% of amylose and 70 and 80% of amylopectin; these proportions depend on the plant source. Amylose molecules consist of approximately 200–20,000 glucose units joined by α -1,4 glycoside bonds (**Figure 1**) in unbranched chains or coiled helix [10].

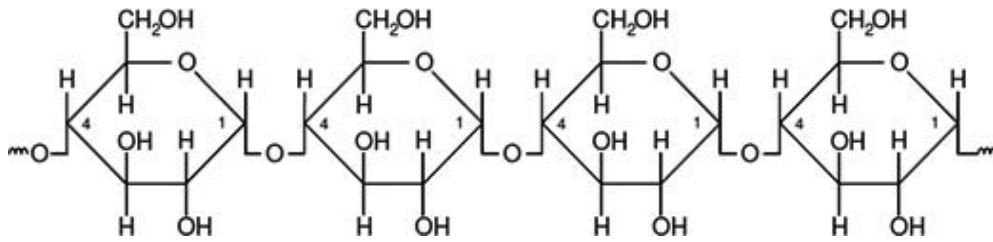


Figure 1. Segment of an amylose molecule [10].

The structure of amylopectin is different from that of amylose; amylopectin molecules contain α -1,4 and α -1,6 glycosidic bonds, as can be seen in Figure 2. The glycosidic bonds join the glucose molecules in the main amylopectin chain. Branches of the main chain are often found, which are due to the α -1,6 glycosidic bonds with other glucose molecules.

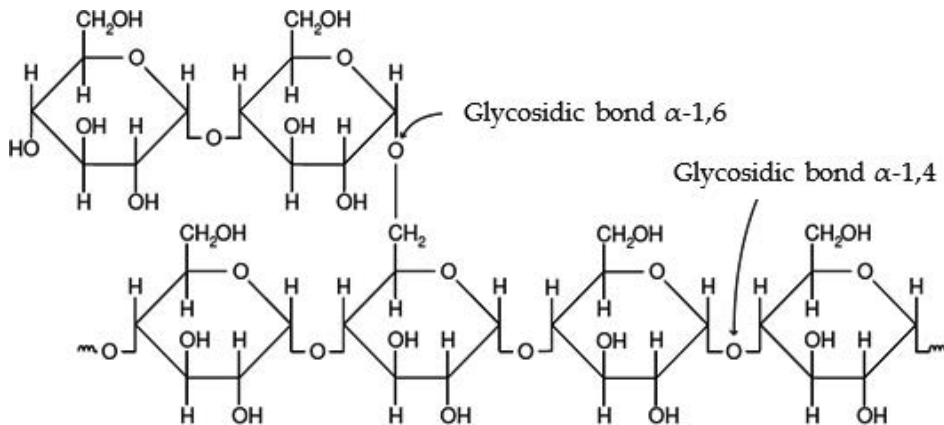


Figure 2. Segment of an amylopectin molecule [10].

The bonding points of the branches constitute between 4 and 5% of all the bonds [11]. Amylopectin molecules are significantly larger than the amylose molecules; some contain between 10,000 and 20,000,000 glucose units. The molecular weight of amylose is between 0.1 and 1 million g/mol while that of amylopectin ranges between 10,000 and 1000 million g/mol [10].

One of the most important properties of natural starch is its semicrystallinity and amylopectin is the dominant component for crystallization in most starches. The significant commercial properties of starch, such as mechanical resistance and flexibility, depend on the resistance and character of the crystalline region, which in turn depend on the amylose/amylopectin ratio and thus on the type of plant; these properties also depend on the distribution of molecular weight, degree of branching, and the conformation process of each polymeric component [12].

Starch is versatile due to its variety of uses; it is also one of the most important ingredients at an industrial level. In the food industry, starch is used to provide a wide range of functional

properties and is probably the most utilized hydrocolloid [13]. It can be used in flavor encapsulation, as a thickening agent or a filling agent, in bakery products, production of syrups, etc. Starch is also included in many other industries such as textiles, paper, cosmetics, plastics, pharmaceutical, and adhesives.

Currently, the negative environmental impact caused by synthetic polymer wastes, denominated plastic materials, is well known and there is now a growing interest in biodegradable materials like starch to substitute the conventional plastic materials, such as polyethylene and polystyrene. A number of studies have reported the use of starch in the manufacture of fast food utensils and packaging material [14].

It is clear that one of the alternatives is the use of starch from nonconventional sources, particularly in countries where there is a high production of raw material for the production of this polymer. Nonconventional sources of starch have attracted much attention, given their diversity of properties, which allow their application in different industries, including the food industry.

Table 1 shows the amylose content, granule size, and gelatinization temperature of a few starches from nonconventional sources such as chestnut [15], kudzu [16], ramon [17], chayote [18], -parota [19], makal [20], sorghum [21], mango [22], and okenia [23], which could be considered for the production of biodegradable materials. In general, the new botanical sources are always widely available in the countries, which produce them.

Type of starch	Amylose (%)	Granule size (μm)	Gelatinization temperature ($^{\circ}\text{C}$)	Reference
Chestnut	26.6	4–21	61.9	[15]
Kudzu	22	2–20	64–83	[16]
Ramon	25.3	6.5–15	83.05	[17]
Chayote	12.9	7–50	67.7	[18]
Parota	17.5–21.3	20–28	76–78	[19]
Makal	23.6	12.4	78.4	[20]
Sorghum	11.2–28.5	Not reported	70–75	[21]
Mango	9–16	7–28	77–80	[22]
Okenia	26	Not reported	71.3	[23]

Table 1. Characteristics of starches from different botanical sources.

3. Thermoplastic starch (TPS)

To produce a film based on starch, a high content of water or plasticizer is required (glycerol, sorbitol). These plasticized materials (application of mechanical and thermal energy) are known as thermoplastic starches [8].

The development and production of TPS is considered to be important for the reduction of the total quantity of synthetic plastic wastes in the world [24].

TPS is a material which is obtained through the structural disruption (modification) occurring inside the starch granule when it is processed with a low water content and the action of shear force and temperature in the presence of plasticizers which do not evaporate easily during the processing [25].

To date, it is known that the techniques (extrusion, injection molding, and film casting) for processing starch-based materials are similar to those used for conventional polymers. However, it is important to note that although the processing of starch is complicated, it can be achieved successfully if an appropriate formulation is developed and adequate processing conditions are established [26].

A simple and well-established technique for producing sheets or films by extrusion is the use of a twin-screw extruder with a slit or flat film die, followed by a takeoff device for orientation and collection [27, 28].

Foaming extrusion has mainly been used to produce loose-fill packaging materials, in a similar way to the production of extruded expanded snack foods [29].

Twin-screw extrusion is the most widely used and is preferred because of its ease of feeding, longer residence time, more extensive shear, and more flexible temperature control [30, 31].

The high viscosity and poor flow properties of starch-based materials present difficulties during injection molding, while the lack of reliable parameters makes it difficult to design the optimum processing conditions [26].

Compression molding has been intensively investigated for processing starch-based plastics, particularly in the production of foamed containers, and generally involves starch gelatinization, expanding, and drying. Apart from gelatinization agents, mold-releasing agents such as magnesium stearate and stearic acid are also often used in formulations to prevent the starch sticking to the mold [26].

The casting technique for preparing starch films includes the preparation of a dispersion, gelatinization at 95°C, casting in acrylic or Teflon plates, and a drying period of approximately 24 h at 40–75°C [32–34]. Glycerol is the most used plastifier in the preparation of starch films. The resulting starch film can have a thickness between 0.02 and 0.10 mm [26].

Over the last few years, much research has focused on the modification of the starch in the production of a good thermoplastic material [35, 36]. A number of mixtures of TPS with biopolymers based on thermoplastic starch are being commercialized with a certain degree of success, by companies such as Mater Bi® (Novamont S.P.A., Italia) in Italy [www.mater-bi.com], Cargill-Down® in the U.S., and by others in Spain, Germany, France, Japan, Denmark, and Canada [37].

4. Cellulose

Cellulose is the most abundant renewable biomass material in nature and is also a major component of plant cell walls. It has been widely used in the form of wood and plant fibers as an energy source, for building materials, and for clothing. Cellulose can be used as feedstocks for producing biofuels, bio-based chemicals, and high value-added bio-based materials. In the past, much attention has been given to the conversion of cellulose-to-cellulose-based composites due to its properties relating to mechanical strength, biocompatibility, biodegradation, and bioactivity, as well as its potential applications which include biomedical, antibacterial, water pretreatment, and in the field of functional materials for photocatalysis [38].

The basic building block of cellulose is β -D-glucose ($C_6H_{12}O_6$) (Figure 3). To form the “cellobiose” molecule, one water molecule is eliminated for every two glucose molecules. Then, from the condensation of various cellobiose molecules, the cellulose molecule is formed. The cellulose chains are found very close to each other due to their hydrophilic character [39].

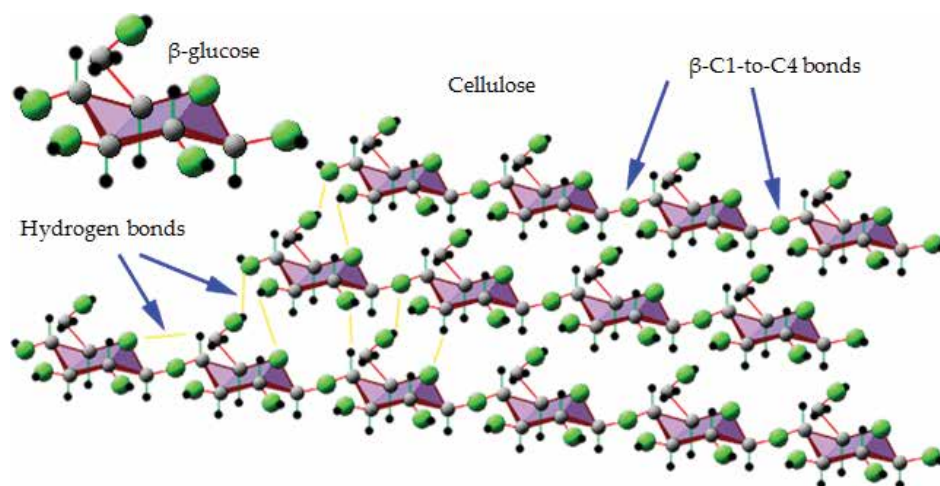


Figure 3. Segment of a cellulose molecule.

The elemental composition of cellulose was discovered in 1842 by the French chemist Anselme Payen [40] and cellulose consists of: 44.0–45.0% carbon (C), 6.0–6.5% hydrogen (H), and 48.5–50.0% oxygen (O).

Table 2 presents a list of the chemical composition of several materials containing cellulose [41].

In plants, cellulose can be found in the form of microfibrils in the primary, secondary, and tertiary cell walls, organized either unidirectional or as a woven mesh. Cellulose microfibrils are 5 nm thick strands of glucopyranose molecular chains, whose Young's modulus is 134 GPa, with a density of 1.5 g/cm³, and a tensile strength (TS) estimated at approximately 2 GPa. Cellulose microfibrils have a diameter of 20–200 Å, while the length can reach several dozen microns. These characteristics are responsible for the interesting mechanical properties of the

microfibers, which are extracted from the biomass by means of a chemical treatment followed by a mechanical treatment; the aim being to obtain a homogenous suspension of individual microfibers [42, 43].

Composition (%)				
Source	Cellulose	Hemicellulose	Lignin	Extract
Hardwood	43–47	25–35	16–24	2–8
Softwood	40–44	25–29	25–31	1–5
Cotton	95	2	1	0.4
Bagasse	40	30	20	10
Coconut fiber (coir)	32–43	10–20	43–49	4
Corn cobs	45	35	15	5
Corn stalks	35	25	35	5
China grass (ramie)	76	17	1	6
Flax (unretted)	63	12	3	13
Flax (retted)	71	21	2	6
Hemp	70	22	6	2
Jute	71	14	13	2
Sisal	73	14	11	2
Kenaf	36	21	18	2
Sunn	80	10	6	3

Table 2. Chemical composition of materials containing cellulose [41].

In this process, the disintegration of the cellulose was achieved by the generation of high shear forces. As a consequence of the above, the microfibers detach from the surrounding material and remain united to other microfibers, thereby forming a network of fibers with nanometric dimensions. The cellulose obtained from this procedure is denominated cellulose nanofibers. These CNF are packages of fibers on a nanometric scale. It has been determined that, within the plant, these CNF are capable of supporting the pressure exerted by the water contained in the plant cells and thus the interest in using cellulose in this form for nanocomposites, based on the concept of introducing nanometric loads (fillings) in a polymeric matrix [44].

4.1. Extraction of cellulose nanofillers

Several processes have been used to extract highly purified CNF from cellulosic materials. All these methods lead to different types of magnesium stearate and stearic acid, depending on the cellulose raw material and its pretreatment, and more importantly, depending on the disintegration process itself [45]. CNF extraction can be divided into: chemical hydrolysis and extraction by mechanical force.

4.1.1. Extraction by chemical hydrolysis

A commonly used extraction methodology of CNF is acidic hydrolysis of the amorphous regions surrounding the embedded CNF and cleavage of the bundles, followed by filtration or centrifugation to exclude dissolved noncrystalline elements [46, 47]. The methodology is beneficial in that it can be performed on very small quantities of cellulose, it requires only the simplest laboratory equipment, and the CNF can be obtained without any induced imperfections caused by mechanical processing. The conditions typically involve the use of aqueous solutions of sulfuric acid, stirred at 45–60°C at atmospheric pressure until a homogeneous beige solution is obtained [48, 49]. After acid hydrolysis, the suspension is diluted with water in order to stop the chemical reaction. This suspension is subjected to centrifugation to obtain the cellulose and eliminate excess acids. The resulting cellulose is washed with water using centrifugation and is finally dialyzed using membranes to reach a neutral pH [50].

This procedure results in CNF having anionic groups on the surfaces (leading to electrostatic stabilization of the nanocrystals in suspension) with the ability to form chiral nematic liquid crystalline phases in concentrated solutions [51]. The form of cellulose obtained was denoted microcrystalline cellulose (MCC) by Battista in 1975 [52].

Exaggerated hydrolysis can typically be noted as the solutions turn dark or black in color as the degradation of the CNF occurs. This phenomenon was reported by Roman et al. in 2004 [53], who assigned the crystal degradation to potential induced thermal degradation related to the sulfate groups, introduced as a functional surface on the CNF when sulfuric acid is used for hydrolysis.

4.1.2. Extraction by mechanical force

The mechanical methods to extract CNF from wood pulp and parenchyma cells typically involve a high-pressure homogenizer treatment [42, 54], a microfluidizer [55, 56], a high-pressure refiner, a super-grinder treatment [57], or ultrasonication [58]. The form of cellulose obtained was denoted microfibrillated cellulose (MFC) by Herrick et al. and Turbak et al. in 1983 [42, 43]. These processing methodologies have in common the fact that they rely on the application of high shear forces on cellulose fiber suspensions in order to mechanically liberate the CNF from the original plant cell wall structure. In a high-pressure homogenizer this is achieved by allowing a cellulose suspension to pass under high pressure through a thin slit where it is subjected to high shear forces. The shear forces serve to disintegrate the microfibrils or microfibril bundles in the plant cell wall, resulting in CNF with diameters of about 5–100 nm [59].

High-intensity ultrasonication consists of a combination of chemical pretreatment and high-intensity ultrasonication. To obtain the cellulose fiber, first, the lignin is eliminated from the samples by immersion for 1 h at 75°C in a solution of sodium chlorite, previously acidified [60, 61]. After the bleaching, the samples are treated with potassium hydroxide (3%) at boiling point for 2 h. After which, they are subjected once again to a treatment with potassium hydroxide at a different concentration (6%), the aim being to eliminate hemicellulose, residual starch, and pectin. After the application of the chemical treatment, the samples are washed

with distilled water and the resulting cellulose fibers are immersed in distilled water. A total of 120 ml of this solution containing purified cellulose fibers is placed in an ultrasound generator of 20–25 kHz in frequency equipped with a cylindrical titanium alloy probe tip of 1.5 cm in diameter. The subsequent ultrasonication is conducted for 30 min to isolate the CNF.

4.2. Green composites of TPS and cellulose fibers

Human beings are known to be highly dependent on synthetic polymers derived from petroleum for the elaboration of diverse packaging and utensils, giving rise to environmental problems [45]. However, reports have been published of the combination of natural fibers, which are completely biodegradable, for the development of green composites. These materials are environmentally friendly and their use can reduce contamination on a global level [45].

Nanocomposites contain materials with a nanometric dimension ranging between 1 and 100 nm. These materials surpass conventional composite materials due to their superior thermal, mechanical, and barrier properties [62, 63]. Biodegradable polymers, in particular, may require improvement in terms of brittleness, low thermal stability, and poor barrier properties [63].

The physical and mechanical properties of the polymeric material reinforced with cellulose are strongly dependent on their structure, relaxation, and morphological processes, as well as a good dispersion of the fiber in order to achieve the minimization of holes. Indeed, a good dispersion of fibers in the polymer matrix has been reported as something very difficult to achieve [64].

The processing of TPS reinforced with cellulose fibers processing is similar to most conventional synthetic thermoplastic processing [65]. Most thermoplastic operations involve heating and forming into desired shapes, and then cooling. Processing techniques used on thermoplastics can also be used in the TPS reinforced with cellulose fibers. These include extrusion, injection molding, internal mixing, compression molding, and others [66].

4.3. Preparation of green composites: mechanical properties and water vapor barrier

From a tensile test, basic mechanical properties of a TPS can be obtained such as tensile strength (the maximum tensile stress a TPS can withstand before it breaks), percentage of elongation at breakage (E) (flexibility), percentage of elongation at yield (EY), and modulus of elasticity (EM) (stiffness) [67, 68].

It has been reported that the mechanical properties of a starch film is affected by the glass transition temperature, degree of crystallinity of the films, amylose content, plastifier type, and content and the storage conditions.

Studies of the barrier properties of starch films are important in order to estimate the shelf life of a food product. This barrier property depends on the starch source, and on the quantity and type of plastifier used, among the most important. Gas barrier properties for a TPS film include water vapor permeability (WVP), oxygen permeability [14], and aroma permeability. WVP is used to describe the ability of the film to control water vapor transportation between a food system and its surrounding. TPS films are not considered good water vapor barriers [68].

The use of CNF has shown to be a viable option for the improvement of mechanical and barrier properties of TPS films. **Table 3** presents a number of studies on the use of starch from different botanical sources to obtain TPS films reinforced with CNF from different materials. However, there are in fact very few reports relating to the use of CNF as reinforcement materials in TPS films. A number of studies have researched the use of undervalued residues as source material for the procurement of cellulose fibers or CNF such as cassava bagasse, barley husk, and sugarcane bagasse, as shown in **Table 3**.

Type of starch	Type of fiber	Preparation of CNF or isolation of cellulose fiber	Preparation of TPS reinforced with CNF or cellulose fibers	Most important results	Reference
Cassava	Cassava bagasse	Acidic hydrolysis with sulfuric acid (H ₂ SO ₄) at 60°C for 40 min. Excess acid was removed by centrifugation. Dialysis of the suspension and ultrasonic treatment	A mixture containing starch, glycerol or a mixture of glycerol with sorbitol, stearic acid and different quantities of CNF from cassava bagasse. The films were prepared by compression molding at 140°C	The addition of 10% and 20% of CNF significantly reduced the elastic module of the TPS films	[49]
Barley grain	Barley husk	Removal of lipids from the barley husk. Removal of lignin and hemicellulose by alkaline treatment at 80°C for 4 h. Bleaching to remove residual lignin in sodium acetate buffer and a solution of sodium chlorite at 95°C for 4 h	The films were prepared by <i>casting</i> . A suspension containing 3% starch in distilled water, 0.30 g of glycerol/g dry starch, 0.01 g of guar gum/g dry starch, 10 and 20 g of cellulose fiber/100 g dry starch. The solution was heated at 90°C for 10 min and poured onto acrylic plaques	The addition of cellulose fibers in the films increased the TS and decreased elongation. The WVP of the starch film with 20% of cellulose fibers was lower than that of the film without fibers	[72]
Potato	Wood flour	To obtain the cellulose, the wood flour was treated with acetic acid and sodium chlorite between 70 and 75°C for 58 h. The CNF were obtained from delignified wood flour through mechanical fibrillation	A mixture of starch, sorbitol, stearic acid and CNF (5, 10, 15, and 20 g/100 g dry starch). The TPS films with CNF were manufactured using a twin screw extruder. Pieces of the extruded materials were compression molded into thin films with a thickness of 0.3 mm	An increase in TS of TPS films was observed with the addition of CNF	[74]

Type of starch	Type of fiber	Preparation of CNF or isolation of cellulose fiber	Preparation of TPS reinforced with CNF or cellulose fibers	Most important results	Reference
Cassava	Wood cellulose fibers	Not reported	The films were prepared by casting. Film-forming solutions were prepared with 3% w/w of cassava starch, 0.30 g glycerol/g dry starch, 0.01 g guar gum/g dry starch (to avoid fiber sedimentation) and three concentrations of cellulose fibers: 0.10, 0.30, and 0.50 g of fiber/g dry starch. The film forming solution was placed in a Petri dish and dried at 40°C for 16 h	The incorporation of cellulose fibers mechanically reinforces the films, resulting in high TS, low deformation and low WVP	[4]
Corn	Eucalyptus wood fiber	Acid hydrolysis of eucalyptus wood fiber at 50°C for 50 min. The hydrolyzed material was subjected to centrifugation, washing, dialysis, and ultrasonication	The films were prepared by casting. The filmogenic solution was composed of 3% starch, 20% glycerol, gelatin, and CNF. The solution was placed in Petri dishes and dried at 25°C to 50% relative humidity (RH)	The films with gelatin and CNF have greater resistance.	[75]
Chayote	Starch	Acid hydrolysis of the cellulose fiber (H ₂ SO ₄ , 60%) at 45°C for 30 min	The films were prepared by casting. The filmogenic solution consisted of 4% starch, 2% glycerol, cellulose, or CNF and water. The solution was heated to 90°C for 10 min. The solution was placed in Petri dishes and dried at 40°C for 24 h. The films were placed at 25°C and 57% RH	The addition of CNF reinforced the film matrix, improving TS, EM, and E. The mechanical properties of the starch films with CNF were better than those for films with cellulose. Starch films added with CNF presented the lowest WVP values	[48]
Tamarind seeds	Sugarcane bagasse	Not reported	A mixture of tamarind starch (12%, w/v) and cellulose	The cellulose used	[77]

Type of starch	Type of fiber	Preparation of CNF or isolation of cellulose fiber	Preparation of TPS reinforced with CNF or cellulose fibers	Most important results	Reference
			(4% w/v) in 100 ml of deionized water. 1.5% of acetic acid and 2.5% of glycerol were added. The mixture was gelatinized at 105°C for a period of 15–20 min. The mixture was placed on glass trays at 50°C, for 6 h	as filler improves the mechanical properties of the film (TS and E)	
Potato tuber	Potato tuber	Potato pulp was treated with NaOH (2%) at 80°C for 2.5 h. The cellulose was submitted to a bleaching process with a solution of sodium chlorite (NaClO ₂). The resultant cellulose was washed with distilled water and lyophilized. The cellulose microfibrils were obtained by submitting the cellulose to a homogenization process with distilled water at 500 bars and 90–95°C	A suspension of cellulose microfibrils (3.3%) was mixed with a gelatinized solution of starch (3.1%). Glycerol was used as plasticizer. The mixture was homogenized and air bubbles were eliminated at reduced pressure. The suspension was poured into a Teflon mold.	The cellulose microfibrils reinforce the starch matrix in the film (greater tension module in comparison with the film without cellulose microfibrils)	[73]
Corn	–	Extraction of the crystalline region of the cellulose was carried out by acid hydrolysis (H ₂ SO ₄ , 64%) for 30 min at 45°C. The CNF obtained was washed and neutralized by dialysis. Finally, the	The nanocomposites were obtained by <i>casting</i> . A solution was prepared containing 3.58 g of normal corn starch, 1.93 g glycerol, 35 g of distilled water, and different quantities of waxy corn starch nanocrystals (0, 50, and 100%) and CNF (0, 50, and 100%). The solution was gelatinized at 90°C. The mixture	The addition of waxy starch nanocrystals and CNF increased the TS and reduced WVP of TPS films. Moreover, with the addition of the CNF, deformation values decreased and	[76]

Type of starch	Type of fiber	Preparation of CNF or isolation of cellulose fiber	Preparation of TPS reinforced with CNF or cellulose fibers	Most important results	Reference
		suspension was sonicated for 15 min	was placed in Petri dishes and dried at 55°C. The samples were stored at 43% RH for 2 weeks	Young's module increased	
Wheat	Cotton	The cotton CNF were obtained by acid hydrolysis with H ₂ SO ₄ (64%) at 45°C for 4 h. After hydrolysis, the suspension was neutralized and washed by dialysis	A suspension was prepared containing 7% wheat starch, 3% glycerol, and 90% water. The suspension was gelatinized at 100°C for 20 min. After gelatinization, a dispersion of CNF (0, 2.5, 5, 10, 15, 20, 25, and 30%) was added to the suspension and mixed for 20 min. The mixture was degassed in a vacuum and placed in a polystyrene mold. The nanocomposites were dried at 40°C with 50% RH	As the CNF content increased, deformation diminished and both Young's module and TS of TPS films increased	[78]

Table 3. Research work on the use of starch from different botanical sources to obtain TPS films reinforced with CNF.

Table 3 presents information regarding the isolation of cellulose fibers, CNF preparation, the preparation of TPS films reinforced with CNF or with cellulose fibers, and indicates the most significant results.

In general, one can observe that the isolation of cellulose fiber consists in exposing the plant material to high temperatures by means of an alkaline treatment, with the purpose of eliminating lignin and hemicellulose. In addition, the material is exposed to a bleaching process at high temperatures with a solution of sodium chlorite.

For the procurement of CNF, the cellulose fibers are treated with hydrolysis between 45 and 60°C. After hydrolysis, the CNF are recovered by centrifugation, dialysis, and subsequent treatment with ultrasonic bath.

Diverse studies are available which report the use of the casting technique for the production of biodegradable starch films. The most commonly used plasticizer is glycerol. To prepare the solution used to form the films, the starch is mixed with glycerol, water, and different quantities of CNF (between 2.5 and 50% with respect to the starch) as reinforcing agents. In some cases, guar gum is used to avoid sedimentation of the fibers. The solution for film formation is heated in order to achieve gelatinization of the starch for a specific period of time. After gelatinization,

the solution is poured into Petri dishes for the formation of the films, and conditioned for evaluation. Very few studies have been published reporting on the use of injection molding and extrusion to obtain TPS films reinforced with CNF.

The mechanical properties and water barrier properties of TPS films reinforced with CNF have been reported in a number of publications. In general, CNF facilitates an increase in tensile strength, a decrease in deformation values, an increase in Young's module, and a decrease in WVP of TPS films. The chemical structure of cellulose and starch is similar. When they are mixed to produce a filmogenic solution, interactions among the OH groups of both polymers are produced by hydrogen bridges, producing a rigid network that increases the TS [4, 5, 69]. The addition of CNF favors high values of TS for TPS films. This may be due to the fact that a greater contact surface is produced between CNF and the starch chains [70].

The nanometric size of CNF allows a low WVP value of the starch films, which favors the generation of a network of hydrogen bridges between the starch chains and the CNF, causing the water molecule to follow a path with many "curves and bends" and thus reducing its diffusion through the starch films [71]. In addition, the cellulose is less hydrophilic than starch, due to its higher crystallinity and compact microfibrillar arrangement, making it more hydrophobic [69].

Table 3 shows research works on the use of starch from different botanical sources, such as cassava [4, 49], barley grain [72], potato [73, 74], corn [75, 76], chayote [48], tamarind seeds [77], and wheat [78], to obtain TPS films reinforced with CNF.

5. Conclusions

The knowledge that the ecosystem is already considerably contaminated as a consequence of the use of synthetic polymers derived from petroleum, environmental initiatives have now been put in place to promote research work on new products which will be compatible with the environment. The development of biocomposites of TPS with cellulose can reduce the dependency on oil reserves.

In recent times, science and technology has centered on the use of more environmentally friendly, raw materials; emphasizing the importance of the advances in such research on "green" composite materials and cellulose fibers for use in the industry.

It is important to mention that cellulose on a nanometric scale is used as a biodegradable reinforced material to improve the mechanical properties as well as the water barrier properties of the TPS.

According to reports in the literature, the technique for the preparation of cellulose fibers from different materials is very similar, whereas the technique for the preparation of TPS reinforced with CNF presents some differences depending on the type of material processed.

Starches from different sources which do not include corn and potato are used in the development of the green composite material, while the cellulose fibers are obtained from waste

material produced by the industries, the aim being to attain the sustainability of natural resources.

Extrusion is one of the most promising methods for processing “green” composite materials and cellulose fibers (TPS-cellulose); however, very little information is available with respect to this.

Based on information found in the literature, it is reported that the incorporation of CNF mechanically reinforces the films, which display high tensile strength, low deformation, and low WVP.

Within the next few years, it is highly likely that the production of biocomposites of TPS films-cellulose will intensify with techniques that are normally used in synthetic polymer processing.

Author details

Emilio Pérez-Pacheco^{1*}, Jorge Carlos Canto-Pinto¹, Víctor Manuel Moo-Huchin¹, Iván Alfredo Estrada-Mota¹, Raciél Javier Estrada-León¹ and Luis Chel-Guerrero²

*Address all correspondence to: eperez@itescam.edu.mx

1 Cuerpo Académico Bioprocesos, Instituto Tecnológico Superior de Calkiní, en el Estado de Campeche Av. Ah Canul SN por Carretera Federal, Campeche, Mexico

2 Facultad de Ingeniería Química, Universidad Autónoma de Yucatán, Colonia Chuburná de Hidalgo Inn, Mérida, Yucatán, Mexico

References

- [1] Carvalho AJ. Starch: major sources, properties and applications as thermoplastic materials. Elsevier, Amsterdam; 2008.
- [2] García NL, Ribba L, Dufresne A, Aranguren M, Goyanes S. Effect of glycerol on the morphology of nanocomposites made from thermoplastic starch and starch nanocrystals. *Carbohydrate Polymers*. 2011;84(1):203–10.
- [3] Yan Q, Hou H, Guo P, Dong H. Effects of extrusion and glycerol content on properties of oxidized and acetylated corn starch-based films. *Carbohydrate Polymers*. 2012;87(1): 707–12.
- [4] Müller CM, Laurindo JB, Yamashita F. Effect of cellulose fibers on the crystallinity and mechanical properties of starch-based films at different relative humidity values. *Carbohydrate Polymers*. 2009;77(2):293–9.

- [5] Gaspar M, Benko Z, Dogossy G, Reczey K, Czigany T. Reducing water absorption in compostable starch-based plastics. *Polymer Degradation and Stability*. 2005;90(3):563–9.
- [6] Müller CM, Yamashita F, Laurindo JB. Evaluation of the effects of glycerol and sorbitol concentration and water activity on the water barrier properties of cassava starch films through a solubility approach. *Carbohydrate Polymers*. 2008;72(1):82–7.
- [7] Tashiro K, Kobayashi M. Theoretical evaluation of three-dimensional elastic constants of native and regenerated celluloses: role of hydrogen bonds. *Polymer*. 1991;32(8):1516–26.
- [8] Peelman N, Ragaert P, De Meulenaer B, Adons D, Peeters R, Cardon L, et al. Application of bioplastics for food packaging. *Trends in Food Science & Technology*. 2013;32(2):128–41.
- [9] Rincón AM, Rached LB, Aragoza LE, Padilla F. Efecto de la acetilación y oxidación sobre algunas propiedades del almidón de semillas de Fruto de pan (*Artocarpus altilis*). *Archivos Latinoamericanos de Nutrición*. 2007;57(3):287.
- [10] Matzinos P, Bikiaris D, Kokkou S, Panayiotou C. Processing and characterization of LDPE/starch products. *Journal of Applied Polymer Science*. 2001;79(14):2548–57.
- [11] Whistler RL, BeMiller JN. *Carbohydrate chemistry for food scientists*. Eagan Press, St. Paul, Minn. (USA); 1997.
- [12] Fritz H-G, Schroeter J. Study on production of thermoplastics and fibres based mainly on biological materials: European Commission, Directorate-General XII, Science, Research and Development, Agro-Industrial Research Division; 1994.
- [13] Tharanathan RN. Starch—value addition by modification. *Critical Reviews in Food Science and Nutrition*. 2005;45(5):371–84.
- [14] Manek RV, Kunle OO, Emeje MO, Builders P, Rao GVR, Lopez GP, et al. Physical, thermal and sorption profile of starch obtained from *Tacca leontopetaloides*. *Starch-Stärke*. 2005;57(2):55–61.
- [15] Cruz BR, Abraão AS, Lemos AM, Nunes FM. Chemical composition and functional properties of native chestnut starch (*Castanea sativa* Mill). *Carbohydrate Polymers*. 2013;94(1):594–602.
- [16] Hung PV, Maeda T, Morita N. Study on physicochemical characteristics of waxy and high-amylose wheat starches in comparison with normal wheat starch. *Starch-Stärke*. 2007;59(3–4):125–31.
- [17] Pérez-Pacheco E, Moo-Huchin V, Estrada-León R, Ortiz-Fernández A, May-Hernández L, Ríos-Soberanis C, et al. Isolation and characterization of starch obtained from *Brosimum alicastrum* Swarts Seeds. *Carbohydrate Polymers*. 2014;101:920–7.

- [18] Jiménez-Hernández J, Salazar-Montoya J, Ramos-Ramírez E. Physical, chemical and microscopic characterization of a new starch from chayote (*Sechium edule*) tuber and its comparison with potato and maize starches. *Carbohydrate Polymers*. 2007;68(4):679–86.
- [19] Estrada-León R, Moo-Huchin V, Ríos-Soberanis C, Betancur-Ancona D, May-Hernández L, Carrillo-Sánchez F, et al. The effect of isolation method on properties of parota (*Enterolobium cyclocarpum*) starch. *Food Hydrocolloids*. 2016;57:1–9.
- [20] Hernandez-Medina M, Torruco-Uco JG, Chel-Guerrero L, Betancur-Ancona D. Physicochemical characterization of starch tuber grown in Yucatan, Mexico. *Ciencia e Tecnologia de Alimentos*. 2008;28(3):718–26.
- [21] Singh J, Dartois A, Kaur L. Starch digestibility in food matrix: a review. *Trends in Food Science & Technology*. 2010;21(4):168–80.
- [22] Kaur L, Singh N, Singh J. Factors influencing the properties of hydroxypropylated potato starches. *Carbohydrate Polymers*. 2004;55(2):211–23.
- [23] González-Reyes E, Méndez-Montealvo G, Solorza-Feria J, Toro-Vazquez J, Bello-Perez LA. Rheological and thermal characterization of *Okenia hypogaea* (Schlech. & Cham.) starch. *Carbohydrate Polymers*. 2003;52(3):297–310.
- [24] Ma X, Yu J. The plasticizers containing amide groups for thermoplastic starch. *Carbohydrate Polymers*. 2004;57(2):197–203.
- [25] Bastioli C. Global status of the production of biobased packaging materials. *Starch-Stärke*. 2001;53(8):351–5.
- [26] Liu H, Xie F, Yu L, Chen L, Li L. Thermal processing of starch-based polymers. *Progress in Polymer Science*. 2009;34(12):1348–68.
- [27] Dean K, Yu L, Wu DY. Preparation and characterization of melt-extruded thermoplastic starch/clay nanocomposites. *Composites Science and Technology*. 2007;67(3):413–21.
- [28] Walenta E, Fink HP, Weigel P, Ganster J, Schaaf E. Structure-property relationships of extruded starch, 2 extrusion products from native starch. *Macromolecular Materials and Engineering*. 2001;286(8):462–71.
- [29] Chinnaswamy R. Basis of cereal starch expansion. *Carbohydrate Polymers*. 1993;21(2–3):157–67.
- [30] Guan J, Eskridge KM, Hanna MA. Acetylated starch-poly(lactic acid) loose-fill packaging materials. *Industrial Crops and Products*. 2005;22(2):109–23.
- [31] Xu Y, Kim KM, Hanna MA, Nag D. Chitosan–starch composite film: preparation and characterization. *Industrial crops and Products*. 2005;21(2):185–92.

- [32] Lawton, J. W., in: Campbell, G. M., Webb, C., McKee, S. L. (Eds.), *Cereals: Novel Uses and Processes*, Springer US, Boston, MA; 1997, pp. 43-47.
- [33] Mali S, Grossmann MVE, Garcíá, Martino MN, Zaritzky NE. Mechanical and thermal properties of yam starch films. *Food Hydrocolloids*. 2005;19(1):157-64.
- [34] Shen Y-d, Lai X-j. Structure and mechanical properties of polyethylene glycol modified poly (lactic acid)/thermoplastic starch blend films. *Modern Chemical Industry*. 2006;26(5):35.
- [35] Averous L, Boquillon N. Biocomposites based on plasticized starch: thermal and mechanical behaviours. *Carbohydrate Polymers*. 2004;56(2):111-22.
- [36] Bangyekan C, Aht-Ong D, Srikulkit K. Preparation and properties evaluation of chitosan-coated cassava starch films. *Carbohydrate Polymers*. 2006;63(1):61-71.
- [37] Bastioli C. Properties and applications of Mater-Bi starch-based materials. *Polymer Degradation and Stability*. 1998;59(1):263-72.
- [38] Ma X, Yu J, Kennedy JF. Studies on the properties of natural fibers-reinforced thermoplastic starch composites. *Carbohydrate Polymers*. 2005;62(1):19-24.
- [39] Wuestenberg, T., *Cellulose and Cellulose Derivatives in the Food Industry: Fundamentals and Applications*, Wiley, Weinheim, Germany; 2014.
- [40] Stana-Kleinschek K, Ribitsch V, Kreze T, Fras L. Determination of the adsorption character of cellulose fibres using surface tension and surface charge. *Materials Research Innovations*. 2002;6(1):13-8.
- [41] Zugenmaier P. *Crystalline cellulose and derivatives: characterization and structures*. 1st ed. Springer-Verlag, Berlin Heidelberg; 2008. 285 p.
- [42] Herrick FW, Casebier RL, Hamilton JK, Sandberg KR, editors. *Microfibrillated cellulose: morphology and accessibility*. *J Appl Polym Sci: Appl Polym Symp (United States)*; 1983: ITT Rayonier Inc., Shelton, WA.
- [43] Turbak AF, Snyder FW, Sandberg KR, editors. *Microfibrillated cellulose, a new cellulose product: properties, uses, and commercial potential*. *J Appl Polym Sci: Appl Polym Symp (United States)*; 1983: ITT Rayonier Inc., Shelton, WA.
- [44] Arroyo RK., *Biocompósitos de Almidón Termoplástico con Microfibras de Celulosa*. Instituto Politécnico Nacional, Altamira, Tamaulipas, México. 2008, p. 77.
- [45] Khalil HA, Bhat A, Yusra AI. Green composites from sustainable cellulose nanofibrils: a review. *Carbohydrate Polymers*. 2012;87(2):963-79.
- [46] de Souza Lima MM, Borsali R. Static and dynamic light scattering from polyelectrolyte microcrystal cellulose. *Langmuir*. 2002;18(4):992-6.

- [47] Dong XM, Kimura T, Revol J-F, Gray DG. Effects of ionic strength on the isotropic-chiral nematic phase transition of suspensions of cellulose crystallites. *Langmuir*. 1996;12(8):2076–82.
- [48] Aila-Suárez S, Palma-Rodríguez HM, Rodríguez-Hernández AI, Hernández-Uribe JP, Bello-Pérez LA, Vargas-Torres A. Characterization of films made with chayote tuber and potato starches blending with cellulose nanoparticles. *Carbohydrate Polymers*. 2013;98(1):102–7.
- [49] Teixeira EdM, Pasquini D, Curvelo AA, Corradini E, Belgacem MN, Dufresne A. Cassava bagasse cellulose nanofibrils reinforced thermoplastic cassava starch. *Carbohydrate Polymers*. 2009;78(3):422–31.
- [50] Cranston ED, Gray DG. Morphological and optical characterization of polyelectrolyte multilayers incorporating nanocrystalline cellulose. *Biomacromolecules*. 2006;7(9):2522–30.
- [51] Fleming K, Gray D, Prasanna S, Matthews S. Cellulose crystallites: a new and robust liquid crystalline medium for the measurement of residual dipolar couplings. *Journal of the American Chemical Society*. 2000;122(21):5224–5.
- [52] Battista O.A. *Microcrystal polymer science*. McGraw-Hill, New York; 1975.
- [53] Roman M, Winter WT. Effect of sulfate groups from sulfuric acid hydrolysis on the thermal degradation behavior of bacterial cellulose. *Biomacromolecules*. 2004;5(5):1671–7.
- [54] Saito T, Nishiyama Y, Putaux J-L, Vignon M, Isogai A. Homogeneous suspensions of individualized microfibrils from TEMPO-catalyzed oxidation of native cellulose. *Biomacromolecules*. 2006;7(6):1687–91.
- [55] Pääkkö M, Ankerfors M, Kosonen H, Nykänen A, Ahola S, Österberg M, et al. Enzymatic hydrolysis combined with mechanical shearing and high-pressure homogenization for nanoscale cellulose fibrils and strong gels. *Biomacromolecules*. 2007;8(6):1934–41.
- [56] Zimmermann T, Pöhler E, Geiger T. Cellulose fibrils for polymer reinforcement. *Advanced Engineering Materials*. 2004;6(9):754–61.
- [57] Chakraborty A, Sain M, Kortschot M. Cellulose microfibrils: a novel method of preparation using high shear refining and cryocrushing. *Holzforschung*. 2005;59(1):102–7.
- [58] Zhao H, Kwak JH, Zhang ZC, Brown HM, Arey BW, Holladay JE. Studying cellulose fiber structure by SEM, XRD, NMR and acid hydrolysis. *Carbohydrate Polymers*. 2007;68(2):235–41.
- [59] Olsson RT, Fogelström L, Martínez-Sanz M, Henriksson M. Cellulose nanofillers for food packaging. *Multifunctional and Nanoreinforced Polymers for Food Packaging*. 2011 ed. Cambridge: Woodhead Publishing Limited; 2011. pp. 86–107.

- [60] Abe K, Yano H. Comparison of the characteristics of cellulose microfibril aggregates of wood, rice straw and potato tuber. *Cellulose*. 2009;16(6):1017–23.
- [61] Abe K, Yano H. Comparison of the characteristics of cellulose microfibril aggregates isolated from fiber and parenchyma cells of Moso bamboo (*Phyllostachys pubescens*). *Cellulose*. 2010;17(2):271–7.
- [62] Oksman K, Mathew A, Bondeson D, Kvien I. Manufacturing process of cellulose whiskers/poly(lactic acid) nanocomposites. *Composites Science and Technology*. 2006;66(15):2776–84.
- [63] Sorrentino A, Gorrasi G, Vittoria V. Potential perspectives of bio-nanocomposites for food packaging applications. *Trends in Food Science & Technology*. 2007;18(2):84–95.
- [64] Raj R, Kokta B, Dembele F, Sanschagrain B. Compounding of cellulose fibers with polypropylene: effect of fiber treatment on dispersion in the polymer matrix. *Journal of Applied Polymer Science*. 1989;38(11):1987–96.
- [65] Janssen, L., Moscicki, L., *Thermoplastic starch*, John Wiley & Sons, Weinheim, Germany; 2009.
- [66] Wattanakornsiri A, Tongnunui S. Sustainable green composites of thermoplastic starch and cellulose fibers. *Songklanakarin Journal of Science and Technology*. 2014;36(2):149–61.
- [67] Mali S, Sakanaka L, Yamashita F, Grossmann M. Water sorption and mechanical properties of cassava starch films and their relation to plasticizing effect. *Carbohydrate Polymers*. 2005;60(3):283–9.
- [68] Zhang Y, Rempel C, Liu Q. Thermoplastic starch processing and characteristics—a review. *Critical Reviews in Food Science and Nutrition*. 2014;54(10):1353–70.
- [69] Curvelo A, De Carvalho A, Agnelli J. Thermoplastic starch–cellulosic fibers composites: preliminary results. *Carbohydrate Polymers*. 2001;45(2):183–8.
- [70] Teixeira EdM, Lotti C, Corrêa AC, Teodoro KB, Marconcini JM, Mattoso LH. Thermoplastic corn starch reinforced with cotton cellulose nanofibers. *Journal of Applied Polymer Science*. 2011;120(4):2428–33.
- [71] De Azeredo HM. Nanocomposites for food packaging applications. *Food Research International*. 2009;42(9):1240–53.
- [72] El Halal SLM, Colussi R, Deon VG, Pinto VZ, Villanova FA, Carreño NLV, et al. Films based on oxidized starch and cellulose from barley. *Carbohydrate Polymers*. 2015;133:644–53.
- [73] Dufresne A, Dupeyre D, Vignon MR. Cellulose microfibrils from potato tuber cells: processing and characterization of starch–cellulose microfibril composites. *Journal of Applied Polymer Science*. 2000;76(14):2080–92.

- [74] Hietala M, Mathew AP, Oksman K. Bionanocomposites of thermoplastic starch and cellulose nanofibers manufactured using twin-screw extrusion. *European Polymer Journal*. 2013;49(4):950–6.
- [75] Freitas F, Alves VD, Reis MA, Crespo JG, Coelho IM. Microbial polysaccharide-based membranes: current and future applications. *Journal of Applied Polymer Science*. 2014;131(6). doi: 10.1002/app.40047
- [76] Gonzalez JS, Ludueña LN, Ponce A, Alvarez VA. Poly(vinyl alcohol)/cellulose nanowhiskers nanocomposite hydrogels for potential wound dressings. *Materials Science and Engineering: C*. 2014;34:54–61.
- [77] Sudharsan K, Mohan CC, Babu PAS, Archana G, Sabina K, Sivarajan M, et al. Production and characterization of cellulose reinforced starch (CRT) films. *International Journal of Biological Macromolecules*. 2016;83:385–95.
- [78] Lu Y, Weng L, Cao X. Biocomposites of plasticized starch reinforced with cellulose crystallites from cottonseed linter. *Macromolecular Bioscience*. 2005;5(11):1101–7.

Composite Coatings Based on Renewable Resources Synthesized by Advanced Laser Techniques

Anita-Ioana Visan, Carmen-Georgeta Ristoscu and
Ion N. Mihailescu

Additional information is available at the end of the chapter

<http://dx.doi.org/10.5772/65260>

Abstract

This chapter reviews the progress and perspectives of composite materials in the form of thin films based on renewable resources for biofabrication of a new generation of medical implants with antibacterial properties. The chapter starts with an overview of the types of renewable materials that were currently studied and of the unique properties which make them perfect candidates for numerous bio-related applications. A briefing of recent progresses in the field of advanced laser synthesis of composites from renewable and sustainable materials, as well as the relevant results in our researches is made. The discussion spans composite coatings based on renewable resources, [e.g., chitosan (CHT) and lignin (Lig)] as biomaterials intended for metallic implants. A particular attention is given to lignin synthesis in the form of thin films due to its ability to functionalize the medical implant surface while preserving the similar composition and the structural properties of the raw, renewable biomaterial. We focused on recent technological advancements (e.g., matrix-assisted pulsed laser evaporation (MAPLE) and Combinatorial-MAPLE) which have brought the spotlight onto renewable biomaterials, by detailing the relevant engineering data of processing. This chapter concludes that the extensions of advanced laser techniques are viable fabrication methods of a new generation of metallic implants.

Keywords: Renewable, Chitosan, Lignin, MAPLE, C-MAPLE

1. Introduction

In this section, we made a short overview regarding classification of biocomposites, emphasizing the motivation of using biomaterials derived from renewable resources and highlighting

the current challenges in natural-derived biomaterials and their biomedical-related applications. We present relevant data regarding the properties of natural-derived and renewable biomaterials.





Biocomposites/biofibers			
Natural biopolymers			
Animal-based fibers		Wood-based natural fibers	Nonwood natural fibers
Proteins, like wool, spider, and silkworm <i>silk fibroin</i> [2]	Polysaccharides, chitin/ <i>chitosan</i> , glucose [3]	Cellulose, hemicellulose, and <i>lignin</i> , like flax, jute, sisal, and kenaf [4]	Straw fibers, bast, leaf, seed/fruit, grass fibers [5]
			

Table 1. Classification of renewable biopolymers used for biocomposites fabrication.

Biocomposites are a combination of natural fibers (e.g., wood fibers: hard and soft wood) or nonwood fibers (e.g., rice straw, pineapple, sugar cane, jute, flax, banana, etc.) with polymer matrices from both of the renewable and nonrenewable resources [1]. **Table 1** includes a classification of biocomposite biomaterials based on renewable resources [2–5].

In recent years, researchers focused on environmentally friendly composite based on natural fibers [6]. Because of their advantages, recent developments in composite based on renewable resources lead to improved biomaterials biofabrication with enhanced support for global sustainability [7].

In particular case of medical applications, biocomposite based on renewable materials have ability to support cell adhesion, migration, proliferation and differentiation; therefore, they can induce extracellular matrix formation and promote tissue repair [8]. An overview of recent reviews, book chapters and articles published in the field of renewable biomaterials is given in **Table 2**.

Relevant data regarding the properties of natural renewable biomaterials with related results presented in this chapter are introduced.

Polysaccharide-based biopolymers are of considerable interest as a source of renewable materials with applications in the biomedical, food, textile and energy industries [22].

Between them, chitin derivatives are widely studied [e.g., chitosan (CHT)]. Since chitosan is biocompatible and biodegradable, an ample diversity of interesting studies based on chitosan were reported [22].

Chitosan has been explored as a scaffold for tissue engineering due to its significant osteoconductivity, but minimal osteoinductive property [23, 24]. Chitosan has been prepared in various geometries such as thin films, scaffolds, sponges, fibers or other complex structures, for biomedical applications [25, 26].

The chitosan incorporation in composite biomaterials enhances the mechanical property of the basic biomaterial. In Ref. [27], it was proved an increase in compressive strength by 33.07% and an enhancement of the proliferation of mouse preosteoblastic cells (MC3T3-E1) upon addition of nano-hydroxyapatite (nHA) to chitosan. Another example is given by Venkatesan et al. [28] which evidenced that the blending chitosan with an anionic polysaccharide alginate may stabilize the system by electrostatic interaction of them.

Renewable materials	Applications	References
Thermosetting materials, plant oils, polysaccharides, lignin, phenolics, epoxy, unsaturated polyester and polyurethane resins and proteins	Non-food applications	[9]
Polysaccharides and their derivatives, lignin, suberin, vegetable oils, tannins, natural monomers like terpenes, and monomers derived from sugars, with particular emphasis on furan derivatives and lactic acid, bacterial cellulose, and poly(hydroxyalkanoates)	Biomedical application Biomass	[10]
Vegetable oils, lignin, proteins, natural polysaccharides	Bioplastics; bioasphalt; biofuel; biomass; medical applications	[11]
Biocomposites natural fiber bioplastic cellulosic plastic polyactides poly(hydroxyalkanoates) soybean-based plastic fiber-matrix interface	Industrial ecology; green chemistry; agricultural and biomass feedstock	[12]
Plant oil-clay hybrid materials	Green nanocomposites	[13]
Ryegrass (<i>Lolium perenne</i> X <i>multiflorum</i>) and alfalfa (<i>medicago sativa</i> subsp. <i>Sativa</i>)	Production of leaf protein concentrate; green biorefinery	[14]
Cellulose nanocrystals (CNC)	Biomedical application	[15]
Oil palm	Biofuel production	[16]
Lignin	Production of chemicals, materials, and fuels from renewable plant resources	[17]
Algae-derived hybrid polyester	Scaffolds for bone, cartilage, cardiac and nerve tissue regeneration	[18]
Polymers from biomass; polysaccharides; lignin; plant oils; terpenes and rosin; glycerol; sugars; furans	Bioplastics; bioasphalt; biofuel; biomass; medical applications	[19]
Chitosan; poly(vinyl butyral)	Anti-corrosion coatings	[20]
Polysaccharide-based biopolymers especially starch, cellulose, chitin, chitosan, alginate	Waste-water treatment; drug-delivery systems	[21]

Table 2. Overview of recent reviews, book chapters and articles published in the field of renewable biomaterials.

Other studies have been dedicated to chitosan and its biocomposite scaffolds investigations under *in-vivo* conditions. Ma et al. [29] demonstrated that chitosan/gelatin scaffolds degraded completely in 12 weeks, while promoted osteoblast proliferation *in-vivo*.

As well as chitosan, lignin (Lig) is a renewable and a natural polymer [30]. This complex, amorphous organic polymer consists in a natural matrix which binds the strong and stiff cellulose units together, generally in natural wood. Lignin has been studied due to its antioxidant and antimicrobial properties, making it the perfect candidate for biomedical applications [31].

In the study of X. Pan et al. [32], lignin prepared from hybrid poplar wood chips exhibited higher antioxidant activities based on 1,1-diphenyl-2-picrylhydrazyl (DPPH) assay. In the same time, in Ref. [33], it is reported that Kraft lignin from wood sources in pulp industry can protect the oxidation of corn oil, being as efficient as vitamin E.

Nada et al. [34] demonstrated the lignin antimicrobial activities toward some bacteria and fungi-like Gram-positive bacteria (*Bacillus subtilis* and *Bacillus mycoides*).

The lignin incorporation in composite biomaterials led to biofabrication of new compounds with enhanced bioactivity and osteoconductivity [35, 36]. An unaltered incorporation of lignin provides a composite with enhanced stability and improved interconnected structure, while increasing the coating cohesion, as showed in Refs [37, 38].

Renewable resources have therefore a functional role in providing easily available and often cheap biomaterials for biofabrication of new generation of implants.

2. Laser-assisted strategies for renewable resources with medical applications

In this section, we present the current strategy in laser-assisted synthesis (emphasizing the challenges and limitations) and the potential biomedical applications of deposited/obtained coatings. An up-to-date example of composites based on natural biopolymers for medical applications by means of laser-assisted processing is given.

The development of bionanotechnology based on laser techniques holds out great promise of improvements in the quality of life, including new treatments for disease providing a high potential for the fabrication of antimicrobial coatings for orthopedic implants [39].

Several techniques for the synthesis of thin films based on renewable resources such as spin-coating [40], dip-coating [41], spray-coating [42], as well as laser methods, such as laser-induced forward transfer [43], matrix-assisted pulsed laser evaporation (MAPLE) [44], Combinatorial-MAPLE [45]; resonant infrared (RIR) MAPLE [46] and MAPLE direct write [47] are currently used.

In spite of the vast list reported in the literature of biomaterials deposited in form of thin films, each of the above-mentioned methods have some limitations in terms of coating thickness, multilayer deposition, adherence, composition or crystallinity. **Table 3** summarizes the generally used biomaterials based on renewable resources and deposition methods along with specific advantages and drawbacks.

Biomaterials and performance/application	Deposition method	Advantages	Disadvantages
Lignin extracted from sugar cane bagasse [48]	Physical vapor deposition (PVD)	High temperature and good impact strength, excellent abrasion resistance, improved corrosion resistance	Line-of-sight transfer, operate at very high temperatures and vacuums, requires a cooling water system to dissipate large heat loads
Silver/hydroxyapatite/lignin [49]	Electrophoretic deposition (EPD)	Lower costs, simpler and less complex control requirements; application to both organic and inorganic coatings	Poor coating adhesion
Nano-TiO ₂ /silk fibroin [50]	Sol-gel (SG)	Macroporous bioactive scaffold	Poor coating adhesion; involvement of liquid media limit multi-layer assembling (affect interfaces)
Lignin [51]	Spin coating	Simple, uniform coatings	Solvent issue during multilayers, adherence
Acacia lignin-gelatin [52]	Casting	Monolayers	Limited to very thin films
Simple and silver-doped hydroxyapatite lignin [53]	Matrix assisted pulsed laser evaporation (MAPLE)	Application to both organic and inorganic coatings, multilayers and multistructures	Small covering areas
Fibronectin (FN) and poly-dl-lactide (PDLLA) [45] Chitosan/biomimetic apatite [54]	Combinatorial matrix-assisted pulsed laser evaporation (C-MAPLE)	Simple, single step, fabrication route which can easily limit the time of manipulation and biomaterials consumption	Composition gradient is hard to discriminate in case of compounds with similar chemical structures

Table 3. Biomaterials from renewable resources, deposition methods, advantages and drawbacks.

Between all techniques, laser-based technologies are exhibiting a lot of advantages, as: fabrication of a wide range of different biomaterials, controlled film thickness, good adhesion to substrate [55]. Furthermore, laser-based technologies imply a low material consumption and ensure the stoichiometry preservation of the growing films [39].

Next, relevant data regarding the laser processing techniques used for fabrication of medical implants based on renewable materials are presented. Concretely, the discussion spans the MAPLE and C-MAPLE techniques.

MAPLE technique proved to be a safe approach for transporting and depositing delicate, heat sensitive molecules. Recent comprehensive reviews on MAPLE deposition of organic, biological and nanoparticle thin films exemplified a large potential in medicine, biology, pharmaceuticals or drug delivery applications of thin coatings obtained by this method [56].

The MAPLE experimental setup is presented in **Figure 1**.

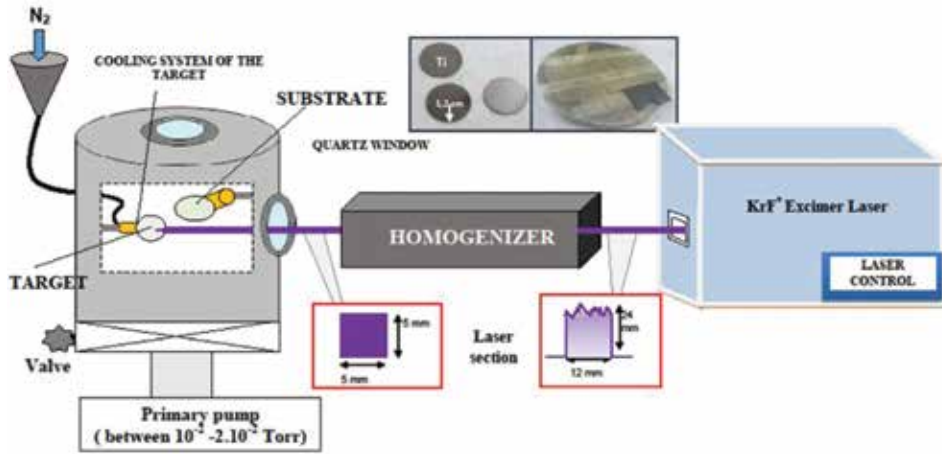


Figure 1. MAPLE experimental setup.

MAPLE target consists of starting material (<10 wt.%) dissolved or suspended into a laser wavelength absorbing solvent when in frozen state. The biomaterial molecules achieve enough kinetic energy by collective collisions with the evaporating solvent molecules, guarantying a controlled transfer on the substrate while being efficiently pumped away by the vacuum system.

By most favorably adjusting the MAPLE deposition parameters (e.g., laser wavelength, laser fluence, repetition rate, solvent type, solute concentration, substrate temperature, background gas nature and pressure), the process can be performed without considerable biomaterial decomposition [38, 57].

Concomitantly, remarkable efforts were recently focused on the development of combinatorial processes for biofabrication of new biomaterials with innovative properties. Typically, the fabrication of a composite layer is carried out by premixing of biopolymer solutions followed by heating of coating [58] or film casting/solvent evaporation [59]. The combinatorial technology for the blending of two different biomaterials [45, 60–62] is based on MAPLE process (Figure 2).

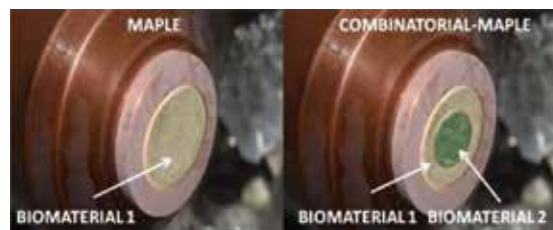


Figure 2. Target holder in the case of MAPLE (left) and combinatorial-MAPLE (right) techniques.

This brand new developed technique—Combinatorial-MAPLE—stands for a simple, single step, biofabrication path which can easily limit the time of manipulation and biomaterials consumption [55].

In C-MAPLE experiments, the two targets (e.g., Biomaterial 1 and Biomaterial 2) were concurrently evaporated by the laser beam, which was divided into two beams (**Figure 3**) by an optical splitter. The two beams were focused in parallel onto the surface of each target, containing the frozen solutions to be irradiated. A gradient of composition from 100% Biomaterial 1 to 100% Biomaterial 2 is thus obtained on a substrate, as schematically represented in **Figure 4**.

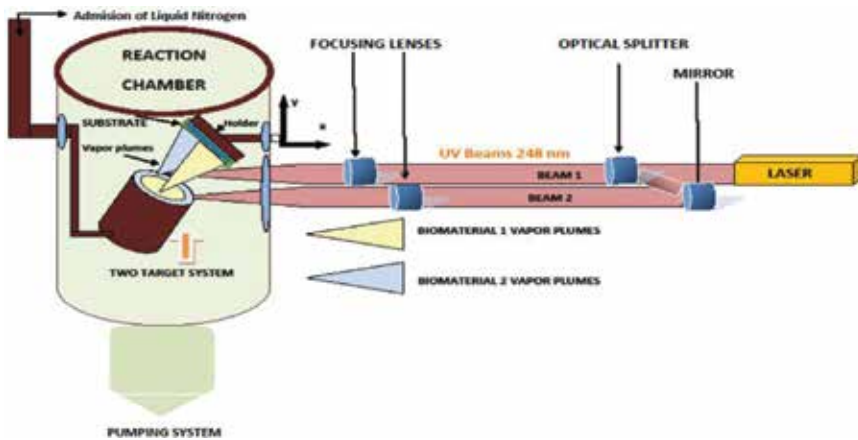


Figure 3. Combinatorial-MAPLE experimental setup.

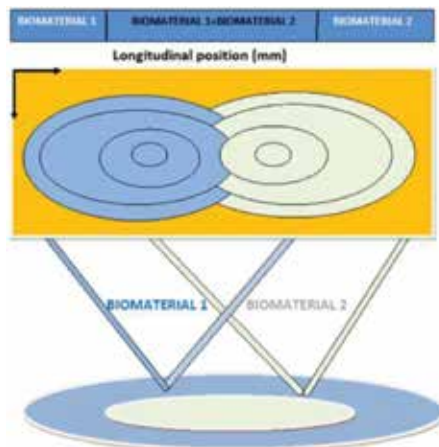


Figure 4. Schematic representation of the thin film gradient structure growth and components intermixing developed by C-MAPLE.

C-MAPLE technique offers the possibility to combine and immobilize two or more biomaterials, dissolved in different solvents, using diverse wavelengths. Next, by physical, chemical and biological characterization of the obtained structures, one may select the best compositions that can be synthesized from the two biomaterials.

MAPLE and C-MAPLE techniques could unlock the research frontiers in biofabrication of composite based on renewable resources with great potential for various applications.

3. Relevant results regarding renewable materials deposited by advanced laser techniques: trends and challenges

In this section, relevant data regarding the engineering of novel renewable materials by laser processing and their applications are detailed.

3.1. The literature survey of renewable materials-based composites deposited by laser techniques

In this chapter, we focused biomaterials based on renewable resources in form of thin films fabricated by laser-based concepts for obtaining functionalized medical implants. The first example refers to silk fibroin and composite HA-fibroin coatings deposited by MAPLE [63]. Silks are fibrous proteins synthesized in specialized epithelial cells of Lepidoptera larvae such as silkworms, spiders, scorpions, flies and mites.

The studies of Miroiu et al. [63] showed that compared to the simple fibroin or HA thin films, obtained implants exhibit an intermediary topography, favorable to bone cells anchorage and proliferation. On the same time, it resulted that the fibroin content in films was a mixture of preponderantly random coil with crystalline forms, β -sheet and α -helix. The renewable silk fibroin composite evidenced by *in-vitro* viability tests appropriate bone cell behavior nontoxicity, good spreading and normal cell morphology [63].

Next, biocomposite silk fibroin-poly(3-hydroxybutyric-acid-co-3-hydroxyvaleric-acid) biodegradable functionalized implants were grown by MAPLE [64]. Silk fibroin and poly(3-hydroxybutyric-acid-co-3-hydroxyvaleric-acid—PHVB) are both natural biopolymers with excellent biocompatibility, but different biodegradability rates and tensile strength properties. They were combined in a composite in order to improve their properties as coatings for biomedical uses. The physical-chemical properties of the composite coatings and principally their degradation behavior in simulated body fluid were investigated as primary step of applicability in local controlled drug release. It was demonstrated that higher PHBV contents enhance the resistance and lead to a slower degradation rate of composite coatings [64].

Another MAPLE studies related to synthesis of poly(D,L-lactide-co-glycolide) (PLGA) particle systems were reported by Socol et al. [65]. PLGA + polyvinyl alcohol (PVA), PLGA + PVA + bovine serum albumin (BSA) and PLGA + PVA + chitosan nanoparticles were prepared by an

oil-in-water emulsion-diffusion-evaporation method and afterwards were transferred in form of thin film for local-controlled drug delivery. *In vitro* investigations exhibited that the distribution and morphology of osteoblast-like SaOs-2 cells on some PLGA particle coatings were comparable with that of control [65].

Further, considerable attention has been focused on development and utilization of secondary metabolites of plants (phytochemicals) as a substitute to and/or in combination with traditional antibiotics for treating infections. Between the phytochemicals, flavonoids are perfect candidates because they are extensively distributed in edible plants and possess broad pharmacologic activity [66]. Flavonoids are a group of heterocyclic organic compounds frequently found in vegetables, fruit, flowers, nuts, wine, seeds, stems, tea, honey and propolis [66]. Composite thin films of biopolymer (polyvinylpyrrolidone), flavonoid (quercetin dihydrate and resveratrol)-biopolymer and silver nanoparticles biopolymer were deposited using MAPLE method demonstrating the anti-inflammatory, antispasmodic, anti-allergic and antimicrobial properties obtained effects [66].

Furthermore, C-MAPLE was used for transfer and immobilization of Fibronectin (FN) and poly-D,L-lactide as a new strategy for the controlled release applications of biologically active substances as proteins and drugs [45].

3.2. Case study: lignin-based biocomposites

This subsection is intended to summarize the recent progresses and concerns involving the use of lignin in the development of new polymer biocomposite materials for high performance medical implants applications.

Until now, biocomposite coatings based on the renewable lignin were studied by electrophoretic deposition (EPD) only [36, 37], and the results revealed that the obtained composite exhibited enhanced stability and improved interconnected structure, with an increased coating cohesion [53]. For electrophoretic deposition (EPD) method, it was applied a constant voltage (at optimized parameters 60 V for 45 s), and it were obtained uniform composite coatings with good adhesion and mechanical properties without any phase transformation [67].

In our studies, we report MAPLE deposited a large macromolecule of undefined molecular weight-organosolv lignin (Lig) embedded in a simple hydroxyapatite (HA) or silver (Ag) doped hydroxyapatite film matrix [53]. A pulsed KrF* laser source ($\lambda = 248 \text{ nm}$, $\zeta_{\text{FWHM}} = 25 \text{ ns}$) operating at 10 Hz was used for the Ag/HA/Lig and its counterpart without silver (HA/Lig) composite frozen targets evaporation. Pure titanium foils or silicon wafers were used as substrates. A total number of 20,000 pulses at a fluence of 0.7 Jcm^{-2} were applied for the deposition of each structure while the spot size was of 25 mm^2 . Then, the structures were subjected to analysis by scanning electron microscopy (SEM), energy-dispersive X-ray spectroscopy (EDS), X-ray diffraction analysis (XRD), X-ray photoelectron spectroscopy (XPS) and attenuated total reflectance-Fourier transform infrared (ATR-FTIR) [53].

Smooth, uniform Lig-based thin films adherent to substrate were revealed by typical top-view SEM images (Figure 5). As a first observation, rough surface of the films was reported starting

from the same nano-hydroxyapatite powder composite with Lig, when using the electrophoretic deposition [67] (**Figure 6**).

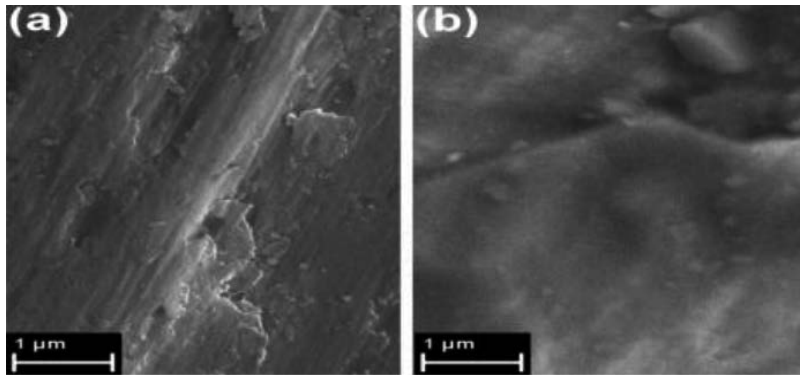


Figure 5. Top-view SEM micrographs of the HA-Lig (a) and Ag:HA-Lig films (b) deposited by MAPLE on Ti substrates. Reproduced with permission from Ref. [53].

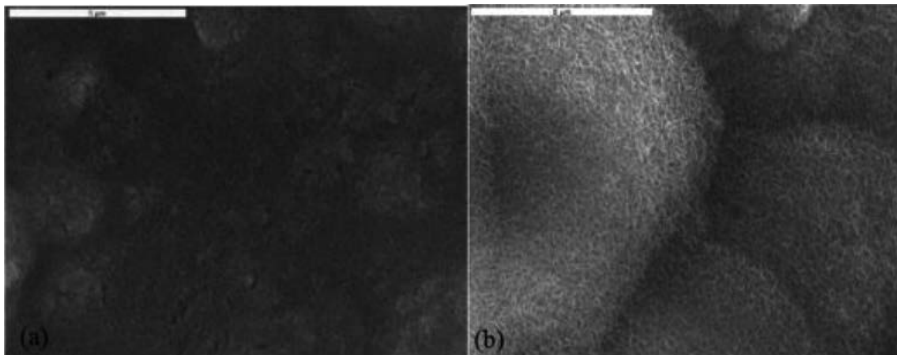


Figure 6. SEM micrographs of sintered Ag/HAP/Lig coating (a) before and (b) after immersion in SBF solution at 37°C. Scale bar: 5 μm. Reprinted from Ref. [67] with permission. Copyright American Chemical Society 2013.

EDS analyses revealed the presence of HA components but also evidences of traces of Ag and lignin. The deposited HA was Ca deficient, which denotes a film with increased solubility. Recorded X-ray patterns (data not presented) were characteristic to amorphous films. Lignin presence in composite films was undoubtedly proved by both XPS and FTIR. The XPS spectra were achieved for two films: the composite Ag:HA-Lig and the pure HA film one (**Figure 7**). The lignin dispersion in HA matrix was evidenced by the massive increase in the C-bonded carbon signature, accompanied by a slight raise of the constituent connected with oxygen-bonded C or oxygen-containing radicals. These enhancements were attributed to the lignin presence. The certain proof that lignin has been successfully transferred into the HA composite film consist in calculated experimental data regarding the stoichiometry fraction $x\text{C}:y\text{O}$ considering the addition of 10% lignin into the HA matrix.

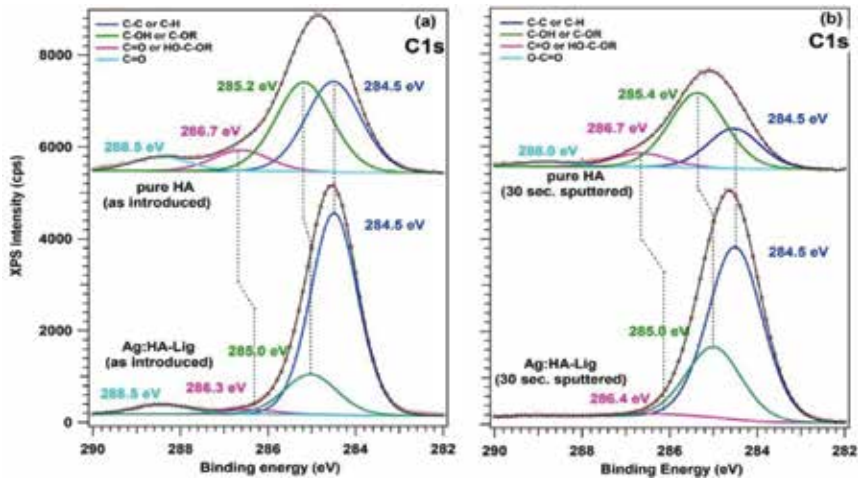


Figure 7. C 1s core level high resolution XPS spectra for the pure HA (a) and Ag:HA-Lig (b) MAPLE films. Reproduced with permission from Ref. [53].

HAP/Lig, wt.% Lig	Thermal treatment	Ca	P	C	Ca/P
HAP	Non-sintered	19.4	11.3	7.2	1.72
	Sintered	16.5	5.5	21.7	3.00
0.5	Non-sintered	19.1	11.3	8.2	1.69
	Sintered	18.4	7.9	15.9	2.33
1	Non-sintered	19.3	10.8	10.5	1.79
	Sintered	18.7	8.9	11.3	2.10
3	Non-sintered	18.4	12.0	11.7	1.53

Adapted from Ref. [67] with permission. Copyright Elsevier 2016.

Table 4. Quantitative XPS analysis data for Synthetic hydroxyapatite, $\text{Ca}_{10}(\text{PO}_4)_6(\text{OH})_2$ (HAP) and hydroxyapatite/lignin (HAP/Lig) (0.5–10) wt.% Lig electrophoretic coatings.

According to the Ref. [67], in the electrophoretic deposition case, lignin limited the decomposition of the apatite lattice of sintered composite coatings based on Lig with (1–10) wt.% Lig. This was designated by the smaller increase in carbon content and decreased Ca/P ratio, compared to pure apatite coating and HAP/Lig coating with 0.5 wt.% Lig (Table 4).

In addition, FTIR investigations advocated a certain improvement of Lig-based films mechanical properties due to lignin incorporation (Figure 8). In good agreement with FTIR observations in the case of MAPLE method, it is also noticed for electrophoretic deposition that does not occur with any alteration of the initial material. This fact could be associated with the binding of hydroxyls from apatite lattice, preventing the decomposition and/or ion diffusion on substrate surface, demonstrating that Lig protects HAP/Lig coatings [68].

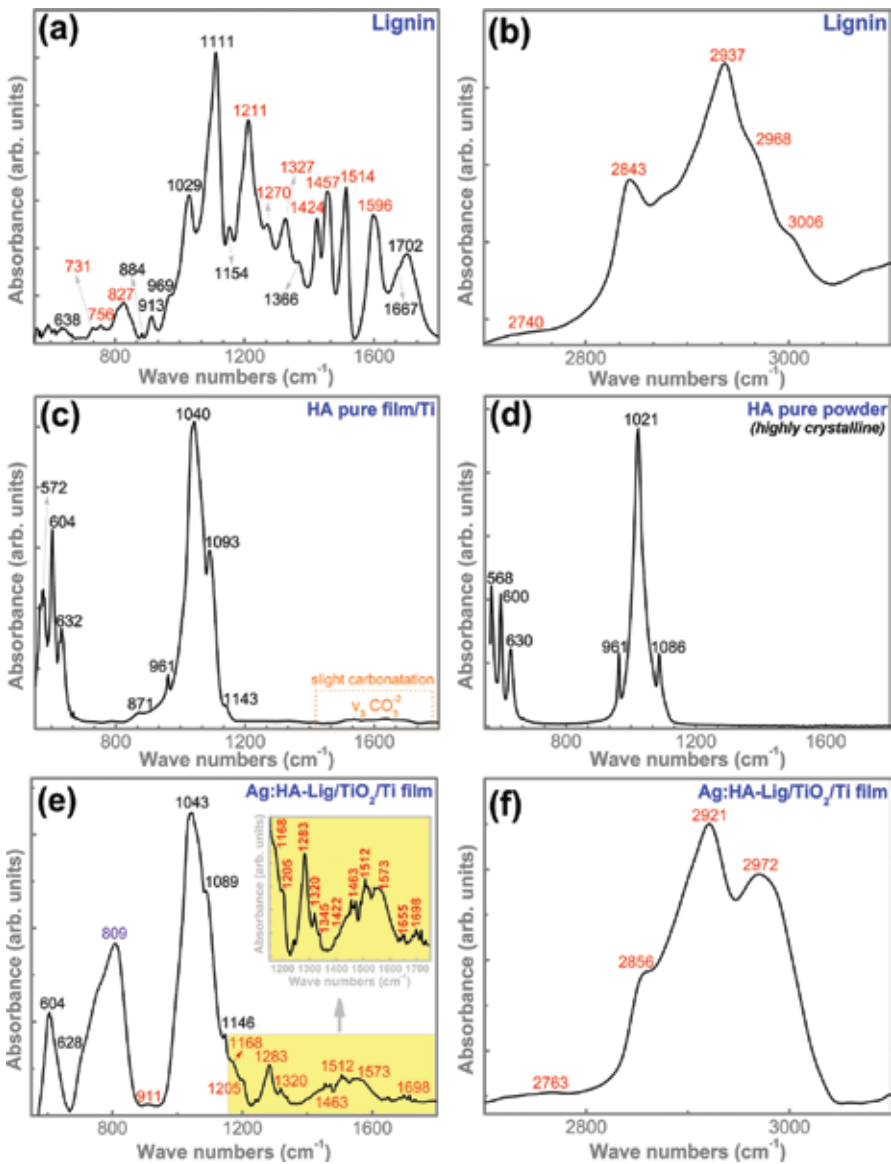


Figure 8. ATR-FTIR spectra of Lig powder (a,b), pure HA film (c), pure HA powder (Sigma-Aldrich) (d) and Ag:HA-Lig film (e,f) in the spectral regions: 1800 – 550 cm⁻¹ (a,c,d,e) and 3100 – 2700 cm⁻¹ (b,f). Reproduced with permission from Ref. [53].

The validation of the MAPLE technique was demonstrated for deposition of such delicate renewable biomaterial, as suggested by EDS, XPS, FTIR, biological and microbial results. The MAPLE obtained biocomposites-based Lig were found noncytotoxic, promoting the proliferation of the adhered human mesenchymal cells (figure not shown here) [53], while the microbiological assays revealed that the coated composite assured a prolonged release of silver

ions, exhibiting a high both bacterial and fungal behavior (**Figure 9**). The same comportament was noticed in the case of the other reported electrophoretic case (**Table 5**) [68], where lignin addition both boosted the antimicrobial activity and supported the normal development and growth of the adhered cells [68].

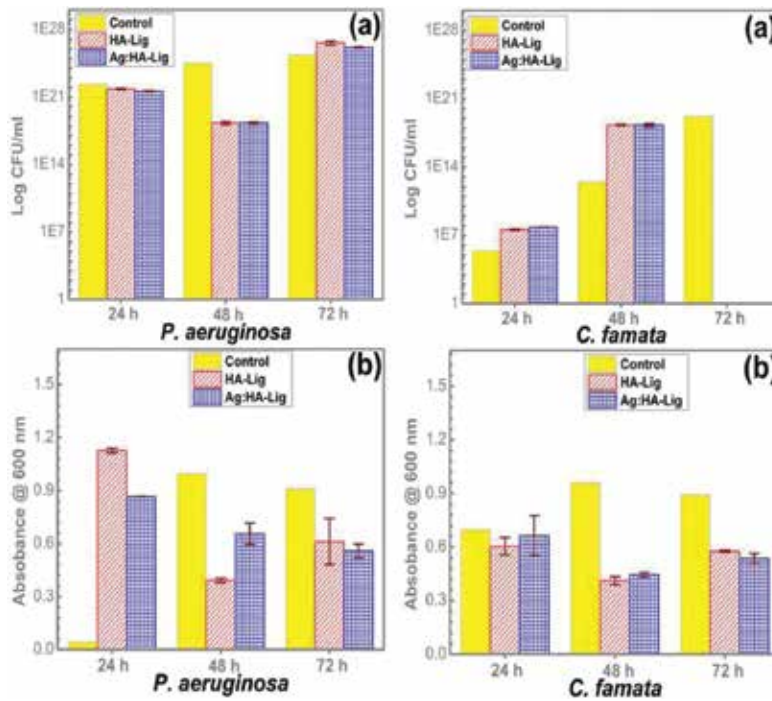


Figure 9. (a) Number of *Pseudomonas aeruginosa* and *C. famata* viable cells recovered from the biofilms growing on the tested specimens after 24, 48 and 72 h, respectively (b) Absorbance values at 600 nm of the *P. aeruginosa* and *C. famata* bacterial biofilm developed on the tested specimens after 24, 48 and 72 h, respectively. Adapted with permission from Ref. [53].

Bacteria strain type	<i>Staphylococcus aureus</i> TL		
Initial	1 h	24 h	
Control (CFU mL ⁻¹)	1.0 × 10 ⁵	3.0 × 10 ⁴	9.9 × 10 ⁴
Ag/HAP/Lig (CFU mL ⁻¹)	2.5 × 10 ⁴	2.0 × 10 ³	No bacteria

Reprinted from Ref. [68] with permission. Copyright Elsevier 2016.

Table 5. Reduction of viable cell number of *Staphylococcus aureus* TL after incubation with Ag/HAP/Lig coating for 0, 1 and 24 h.

Biofabrication of composites based on Lig-renewable resources have a great potential for medical applications, supporting the osteogenic cell proliferation while assuring an antibacterial behavior.

3.3. Case study: chitosan-based biocomposites

This subsection is intended to summarize the recent progresses and concerns involving the use of chitosan in the development of new biocomposite materials for high performance medical implants applications.

Although many authors have reported the preparation of mixtures of chitosan and calcium phosphates in the form of powders [69], membranes [70], scaffolds [71] or microspheres [72], only few publications were dedicated on developing new procedures allowing the concomitant preparation of a biocomposite material containing the two components, which is predicted to assure a more close contact between them [73–75]. For this reason, further we will exemplify the biofabrication of the compositional map of chitosan (CHT) and biomimetic apatite (BmAp) by the innovative C-MAPLE technique. In the experiments, an excimer laser source (KrF*, $\lambda = 248$ nm, $\zeta_{FWHM} = 25$ ns) operated at 10 Hz frequency repetition rate was used for the cryogenic targets evaporation. As deposition substrates were used as follows: 12 mm diameter Ti (grade 4) disks, Si wafers or glass slides. The coated samples areas deposited onto the substrate selection formed of five consecutive 12 mm Ti disks which are further denoted S1–S5; where S1 stands for the coating area having CHT as major component, S5 represents the coating area with richer content of BmAp. S2–S3–S4 series indicates blended coating areas with decreasing CHT/BmAp ratios. For comparison reasons, simple CHT and BmAp films have been also deposited on the same type of substrates [54]. After preliminary studies, deionized water was chosen as solvent to prepare solutions of 1 and 2 wt.% for CHT and BmAp, respectively. A parametric study in order to find the optimum laser energy (70, 100, 120 and 150 mJ) for which the materials are deposited unaltered was performed. The selected laser energy was as follows: 100 mJ in the case of CHT target and of 70 mJ for the BmAp one.

C-MAPLE composite coatings have a homogeneous spongy appearance all over the substrate, which is known to be beneficial for cell adhesion as revealed by SEM micrographs (results not presented here). While CHT particulates preserve their spherical morphology, elongated filiform structures can be also noticed in the blended regions of the film (S2–S4). One can assume that these thread-like structures may support some toughness improvements similar to the one provided by fiber reinforcing in the biocomposite materials, ensuring the desired mechanical behavior for tissue substitution [76].

The C-MAPLE synthesized biocomposite-based CHT thin films are amorphous, rough, with a morphology characteristic to laser deposited structures. Next, by high resolution AFM investigations, we disclose information about the nanostructuring of the film grains and their morphological evolution (**Figure 10**). One notices that a progressive increase in roughness (R_{RMS}) occurs with the CHT concentration in the C-MAPLE composite films [54].

For each combinatorial surface, the Ca/P molar ratio was in the range ~ 1.3 – 1.5 , lower than the stoichiometric theoretical value of hydroxyapatite (i.e., 1.67), pointing to the calcium-deficient state of biomimetic apatite synthesized.

The Raman spectra of BmAp, HA (pure and highly crystalline) and CHT raw materials are presented comparatively in **Figure 11a** and **b** [54]. Similar vibration bands to the ones revealed by FTIR investigations (data not shown here) [54] have been also identified by micro-Raman

analyses for the CHT and BmAp source materials. However, in the case of Raman spectra the symmetric stretching bands are now the dominant ones (e.g., symmetric stretching ν_1 of $(\text{PO}_4)^{3-}$ $\sim 956 \text{ cm}^{-1}$; symmetric stretching of aliphatic (C–H) bonds $\sim 2929 \text{ cm}^{-1}$). This is owned to the fact that in Raman spectroscopy, the vibration bands intensity is dependent on the polarizability induced dipole, and not on the variation of the dipole moment of the molecule, as is the case of FTIR spectroscopy. Thereby, this was to be expected, as for a given centrosymmetric molecule, the vibration modes which are symmetric to the inversion center of the molecule generate higher Raman intensity bands. Moreover, the electronic density between the carbon atoms in aliphatic C–H bonds that can be deformed under the action of the radiation electric field should be large. If the vibrational mode involved in the Raman scattering process is not totally symmetric, then the polarization of the photon can be partially (e.g., antisymmetric stretching modes) or even totally reduced.

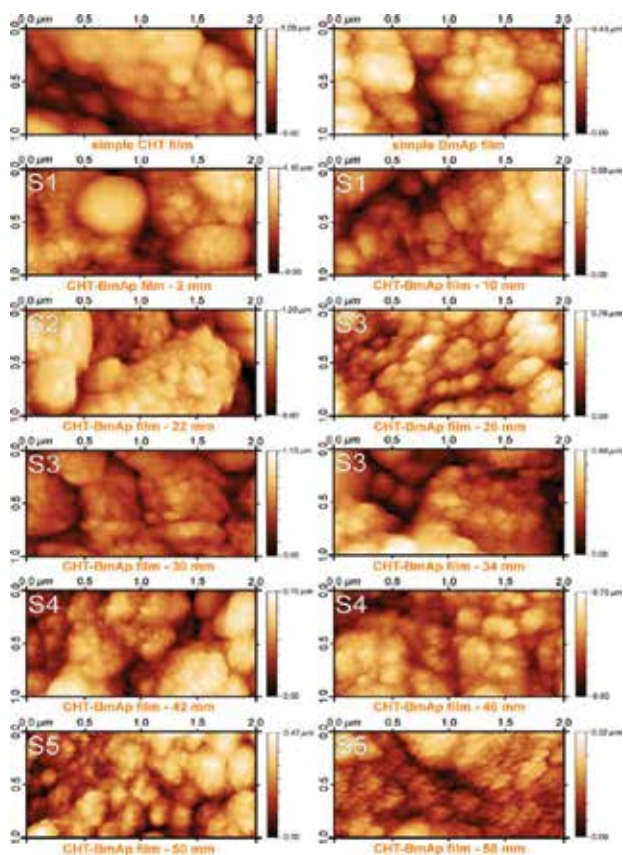


Figure 10. Comparative AFM images recorded on the surface of: simple CHT and BmAp films deposited by MAPLE, and in various regions of the C-MAPLE composite film starting from the CHT-rich edge. The coated samples areas deposited onto the substrate array composed of five consecutive 12 mm Ti disks were denoted S1 to S5; where S1 stands for the coating area having CHT as major component, S5 represents the coating area with richer content of BmAp. S2-S3-S4 series indicates blended coating areas with decreasing CHT/BmAp ratios.

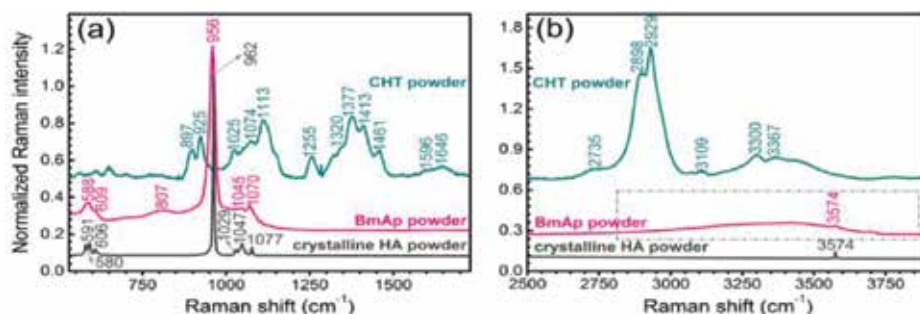


Figure 11. Comparative Raman spectra of BmAp, crystalline HA and CHT powders presented in the fingerprint (a) and functional groups (b) regions. The spectra have been normalized to the highest intensity peak (i.e., $\nu_1(\text{PO}_4)^{3-}$ vs. C-H bands in the case hydroxyapatite and chitosan, respectively).

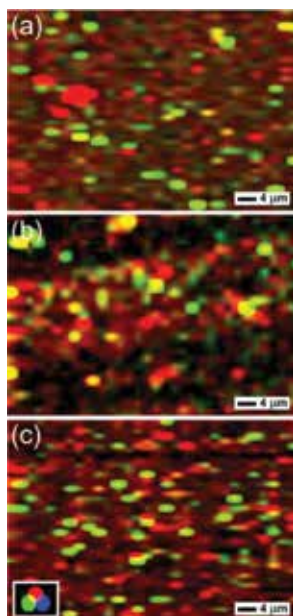


Figure 12. 2D Raman maps obtained from $(80 \times 100) \mu\text{m}^2$ areas of the CHT-BmAp composite C-MAPLE film, based on the characteristic Raman stretching vibration bands of C-H bond in aliphatic and aromatic groups ($3000\text{--}2850 \text{ cm}^{-1}$ wave numbers region) of CHT (red colored), and ν_1 symmetric stretching of orthophosphate groups ($965\text{--}950 \text{ cm}^{-1}$ wave numbers region) of BmAp (green colored). (a) CHT-rich edge region (b) CHT-BmAp central region (c) BmAp-richer edge region.

In perfect agreement with the FTIR results, the Raman spectra indicated that the BmAp material elicit a decreased ordering (indicated by the broader aspect of the bands) and a certain level hydration with respect to the pure and crystalline HA.

The CHT vibration bands in the $1250\text{--}1000 \text{ cm}^{-1}$ wave numbers region are screened by the more intense superimposed Si-O-Si stretching band of the glass substrate (**Figure 12**). Overall, the

CHT and BmAp bands in the case of the composite C-MAPLE films are less conspicuous and defined with respect to the ones of the source powders. The shift of ν_1 symmetric stretching band of $(\text{PO}_4)^{3-}$ groups close to $\sim 956 \text{ cm}^{-1}$ with respect to the stoichiometric crystalline compound (i.e., $\sim 962\text{--}961 \text{ cm}^{-1}$) suggest a higher degree of disordering, similarly to the source BmAp material.

Subsequently, X-Y Raman mapping measurements have been performed in three relevant regions (with areas of $(80 \times 100) \mu\text{m}^2$) of the C-MAPLE synthesized biocomposite-based CHT thin films deposited onto glass substrate (**Figure 12**), in order to generate detailed chemical images (in red-green-blue colors) of the spatial distribution of the two species (i.e., CHT and BmAp). The CHT phase (red colored) has been integrated with the stretching vibration bands of C–H bond in aliphatic and aromatic groups ($3000\text{--}2850 \text{ cm}^{-1}$ wave numbers region), while the BmAp phase (green colored) has been assigned with the prominent Raman band of HA (i.e., $\nu_1(\text{PO}_4)^{3-}$ symmetric stretching) situated in the $965\text{--}950 \text{ cm}^{-1}$ range. The distribution of CHT seems to be homogenous in all analyzed composite film regions, whilst the BmAp phase is rather distributed in randomly dispersed aggregates.

XPS analysis confirmed the chemical composition of the C-MAPLE synthesized biocomposite-based CHT thin films. XPS survey spectra collected on the surface of CHT-BmAp samples (not presented) indicated the presence of C 1s, O 1s, N 1s, Ca 2s, Ca 2p, P 2s and P 2p photoelectron peaks [54], while **Figure 13** showed the atomic ratio N 1s/(N 1s + Ca 2p) evolution depending on the position of material deposited along the CHT-BmAp blended sample. As predicted, the atomic ratio (N 1s/N 1s + Ca 2p) is decreasing from CHT to BmAp compounds, evidencing the composition gradient of the combinatorial films.

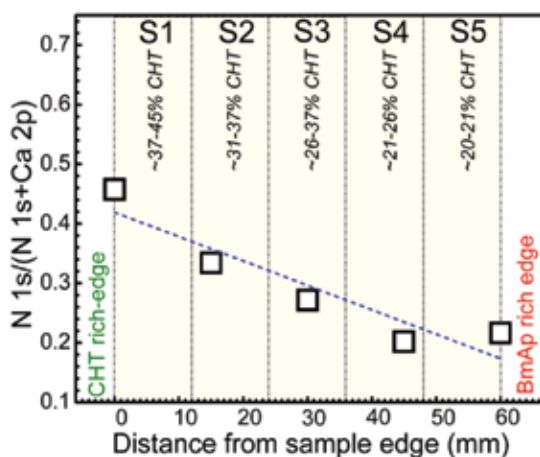


Figure 13. Typical XPS measurement along the composite CHT-BmAp C-MAPLE films. Reproduced with permission from Ref. [54].

The antimicrobial activity was controlled by the concentration of chitosan, the most efficient antimicrobial activity, against Gram-positive and Gram-negative strains, was assigned to blended S3 and S4 samples (**Figure 14**).

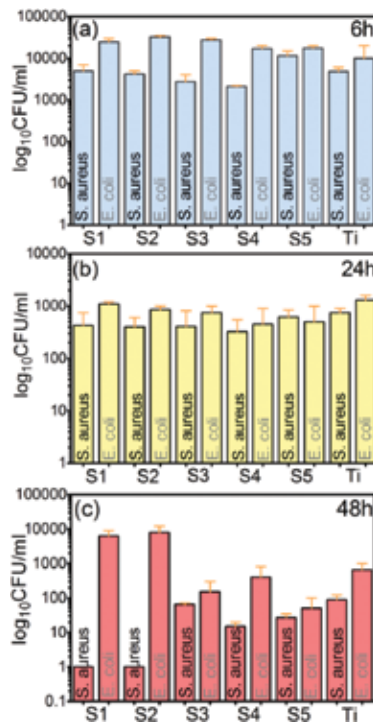


Figure 14. Graphic representation of the number of viable microbial cells adhered to the surface of CHT-BmAp composite film after (a) 6 h (b) 24 h and (c) 48 h of incubation. Reproduced with permission from Ref. [54].

The composition gradient of the chitosan-to-biomimetic hydroxyapatite has been confirmed longwise the combinatorial films by FTIR and XPS analyses, validating the used C-MAPLE technique.

C-MAPLE technique used in this study proves to be a prospective and viable method for the fabrication of biomimetic and bioactive antimicrobial orthopedic coatings based on renewable resources which resemble the native bone extracellular matrix while creating a favorable living environment for osteogenic cells, in the same time assuring protection from microbial colonization.

4. Conclusions and future perspectives

This chapter is intended to provide a brief outline of work that covers biocomposites based on renewable resources which have been studied and applied in medical applications, capable of supporting cell proliferation and biodegradability.

The raw substances used for depositions are renewable and the whole procedure is very accurate due to the cumulative advantages of substances origin and applied laser procedures. A credible demonstration for the conservation of biomaterial composition, structure, mor-

phology and the most probably functionality was made of the MAPLE and C-MAPLE transferred films.

In this way, multifunctional structures could be deposited with combined bioactive osteoinductive and/or antimicrobial action. The synthesized multistructures were considered for use as biomimetic coatings of advanced implants but also as a shield against infections including microbial biofilms. This feature can play a key role in the development of a new generation of drug delivery systems based on renewable resources free of infection with microbial biofilms which cannot be annihilated with the existing generation of antibiotics.

Acknowledgements

The authors acknowledge the financial support of UEFISCDI under the France-Romania bilateral contract: 778/2014, 19_RO-Fr/2014, PCCA 244/2014 Contracts and the National Authority for Research and Innovation in the frame of Nucleus Programme – contract 4N/2016.

Author details

Anita-Ioana Visan, Carmen-Georgeta Ristoscu and Ion N. Mihailescu*

*Address all correspondence to: ion.mihailescu@inflpr.ro

National Institute for Laser, Plasma and Radiation Physics, Magurele-Ilfov, Romania

References

- [1] Kalita D, Netravali AN. Interfaces in green composites: a critical review. *Reviews of Adhesion Adhesives*. 2015;3:4.
- [2] Serum Silk Fibroin [Internet]. 2016. Available from: <http://www.a6k6n6.com/Serum-Silk-Fibroin-p-8821.html> [Accessed: 2016-07-28].
- [3] Chitosan Powder [Internet]. 2016. Available from: <http://www.pureherbextract.com/chitosan-powder.html> [Accessed: 2016-07-28].
- [4] Lignin Powder [Internet]. 2016. Available from: <http://www.domtar.com/en/pulp/lignin/10387.asp> [Accessed: 2016-07-28].
- [5] Green Leaves, images free downloaded [Internet]. 2016. Available from: http://pngimg.com/upload/green_leaves_PNG3660.png [Accessed: 2016-07-28].

- [6] Sahari J, Sapuan SM. Natural fibre reinforced biodegradable polymer composites. *Reviews on Advanced Materials Science*. 2011;30:166–174.
- [7] Mohanty AK, Misra M, Drzal LT. (ed.). *Natural Fibers, Biopolymers, and Biocomposites*. Taylor & Francis Group; ISBN 9780849317415, United Kingdom, 2005.
- [8] Ha TL, Quan TM, Vu DN, Si DM. Naturally Derived Biomaterials: Preparation and Application. In: Andrades JA. (ed.). Chapter 11 in *Regenerative Medicine and Tissue Engineering*. InTech; Croatia; 2013. p. 247–274. ISBN 978-953-51-1108-5. <http://dx.doi.org/10.5772/55668>
- [9] Raquez J-M, Deléglise M, Lacrampe M-F, Krawczak P. Thermosetting (bio) materials derived from renewable resources: a critical review. *Progress in Polymer Science*. 2010;35:487–509.
- [10] Gandini A. Polymers from renewable resources: a challenge for the future of macromolecular materials. *Macromolecules*. 2008;41(24):9491–9504.
- [11] Belgacem MN, Gandini A. (ed.). *Monomers, Polymers and Composites from Renewable Resources*. Elsevier; Netherlands; 2008. ISBN:978-0-08-045316-3.
- [12] Mohanty AK, Misra M, Drzal LT. Sustainable bio-composites from renewable resources: opportunities and challenges in the green materials world. *Journal of Polymers and the Environment*. 2002;10(1):19–26.
- [13] Uyama H, Kuwabara M, Tsujimoto T, Nakano M, Usuki A, Kobayashi S. Green nanocomposites from renewable resources: plant oil–clay hybrid materials. *Chemistry of Materials*. 2003;15(13):2492–2494.
- [14] Koschuh W, Povoden G, Thang VH, Kromus S, Kulbe KD, Novalin S, Krotscheck C. Production of leaf protein concentrate from ryegrass (*Lolium perenne* × *multiflorum*) and alfalfa (*Medicago sativa* subsp. *sativa*). Comparison between heat coagulation/centrifugation and ultrafiltration. *Desalination*. 2004;163(1–3):253–259.
- [15] Yanamala N, Farcas MT, Hatfield MK, Kisin ER, Kagan VE, Geraci CL, Shvedova AA. *In Vivo* evaluation of the pulmonary toxicity of cellulose nanocrystals: a renewable and sustainable nanomaterial of the future. *ACS Sustainable Chemistry and Engineering*. 2014;2(7):1691–1698. doi:10.1021/sc500153k
- [16] Kurnia JC, Jangam SV, Akhtar S, Sasmito AP, Mujumdar AS. Advances in biofuel production from oil palm and palm oil processing wastes: a review. *Biofuel Research Journal*. 2016;3(1):332–346.
- [17] Zhang LM, You TT, Zhou T, Zhang L, Xu F. Determining Lignin degradation in white-rot fungi-treated sacrau poplar: lignin structural changes and degradation compound analysis. *Bioresources*. 2016;11(2):3972–3986.
- [18] Noreen A, Zia KM, Zuber M, Ali M, Mujahid M. A critical review of algal biomass: a versatile platform of bio-based polyesters from renewable resources. *International*

- Journal of Biological Macromolecules. 2016;86:937–949. doi:10.1016/j.ijbiomac.2016.01.067
- [19] Gandini A, Lacerda TM. From monomers to polymers from renewable resources: recent advances. *Progress in Polymer Science*. 2015;48:1–39. doi:10.1016/j.progpolymsci.2014.11.002
- [20] Luckachan GE, Mittal V. Anti-corrosion behavior of layer by layer coatings of cross-linked chitosan and poly(vinyl butyral) on carbon steel. *Cellulose*. 2015;22(5):3275–3290. doi:10.1007/s10570-015-0711-2
- [21] Zia KM, Zia F, Zuber M, Rehman S, Ahmad MN. Alginate based polyurethanes: a review of recent advances and perspective. *International Journal of Biological Macromolecules*. 2015;79:377–387. doi:10.1016/j.ijbiomac.2015.04.076
- [22] Logith Kumar R, KeshavnNarayan A, Dhivya S, Chawla A, Saravanan S, Selvamurugan N. A review of chitosan and its derivatives in bone tissue engineering. *Carbohydrate Polymers*. 2016;151:172–188. doi:10.1016/j.carbpol.2016.05.049
- [23] Costa-Pinto AR, Reis RL, Neves NM. Scaffolds based bone tissue engineering: the role of chitosan. *Tissue Engineering Part B: Reviews*. 2011;17(5):331–347.
- [24] Saravanan S, Sameera DK, Moorthi A, Selvamurugan N. Chitosan scaffolds containing chicken feather keratin nanoparticles for bone tissue engineering. *International Journal of Biological Macromolecules*. 2013;62:481–486.
- [25] Jiang T, James R, Kumbar SG, Laurencin CT. Chitosan as a biomaterial: structure, properties, and applications in tissue engineering and drug delivery. *Natural and Synthetic Biomedical Polymers*. 2014;5:91–113.
- [26] Niranjana R, Koushik C, Saravanan S, Moorthi A, Vairamani M, Selvamurugan N. A novel injectable temperature-sensitive zinc doped chitosan/ β -glycerophosphate hydrogel for bone tissue engineering. *International Journal of Biological Macromolecules*. 2013;54:24–29.
- [27] Zhang BG, Myers DE, Wallace GG, Brandt M, Choong PF. Bioactive coatings for orthopaedic implants—recent trends in development of implant coatings. *International Journal of Molecular Sciences*. 2014;15(7):11878–11921.
- [28] Venkatesan J, Bhatnagar I, Manivasagan P, Kang KH, Kim SK. Alginate composites for bone tissue engineering: a review. *International Journal of Biological Macromolecules*. 2015;72:269–281.
- [29] Ma K, Cai X, Zhou Y, Zhang Z, Jiang T, Wang Y. Osteogenetic property of a biodegradable three-dimensional macroporous hydrogel coating on titanium implants fabricated via EPD. *Biomedical Materials*. 2014;9(1):015008.
- [30] Schorr D, Diouf PN, Stevanovic T. Evaluation of industrial lignins for biocomposites production. *Industrial Crops and Products*. 2014;52:65–73.

- [31] Cazacu G, Capraru M, Popa VI. Advances Concerning Lignin Utilization in New Materials. In: Thomas S, Visak PM, Mathew AP. (eds). *Advances in Natural Polymers: Composites and Nanocomposites*. New York, Heidelberg: Springer; 2013. p. 255–312.
- [32] Pan X, Gilkes N, Kadla J, Pye K, Saka S, Gregg D, Ehara K, Xie D, Lam D, Saddler J. Bioconversion of hybrid poplar to ethanol and co-products using an organosolv fractionation process: optimization of process yields. *Biotechnology and Bioengineering*. 2006;94(5):851–861.
- [33] Catignani GL, Carter ME. Antioxidant properties of lignin. *Journal of Food Science*. 1982;47:1745–1748.
- [34] Nada AMA, El-Diwanya AI, Elshafei AM. Infrared and antimicrobial studies on different lignins. *Acta Biotechnologica*. 1989;9(3):295–298.
- [35] Eraković S, Janković A, Veljović DJ, Palcevskis E, Mitrić M, Stevanović T, Janačković DJ, Mišković-Stanković V. Corrosion stability and bioactivity in simulated body fluid of silver/hydroxyapatite and silver/hydroxyapatite/lignin coatings on titanium obtained by electrophoretic deposition. *The Journal of Physics Chemistry B*. 2013;117:1633–43. doi:10.1021/jp305252a
- [36] Eraković S, Veljović DJ, Diouf PN, Stevanović T, Mitrić M, Janačković DJ, Matic IZ, Juranić ZD, Mišković-Stanković V. Investigation of silver impact on hydroxyapatite/lignin coatings electrodeposited on titanium. *Progress in Organic Coatings*. 2012;75:275–83. doi:10.1016/j.porgcoat.2012.07.005
- [37] Santillán MJ, Quaranta NE, Boccaccini AR. Titania and titania–silver nanocomposite coatings grown by electrophoretic deposition from aqueous suspensions. *Surface and Coating Technology*. 2010;205:2562–71. doi:10.1016/j.surfcoat.2010.10.001
- [38] Pique A. Deposition of Polymers and Biomaterials Using the Matrix-Assisted Pulsed Evaporation (MAPLE) Process. In: Eason R. (ed.). *Pulsed Laser Deposition of Thin Films. Applications-Led Growth of Functional Materials*. Hoboken, NJ: Wiley Interscience; 2007. p. 63–84.
- [39] Mihailescu IN, Ristoscu C, Bigi A, Mayer I. Advanced Biomimetic Implants Based on Nanostructured Coatings Synthesized by Pulsed Laser Technologies. In: Miotello A, Ossi PM. (eds.). *Laser-Surface Interactions for New Materials Production Tailoring Structure and Properties*, Series: Springer Series in Materials Science; Springer; New York City; USA; 2010. p. 235–260.
- [40] Lawrence CJ. The mechanics of spin coating of polymer-films. *Physics of Fluids*. 1988;31(10):2786–2795. doi:10.1063/1.866986
- [41] Brinker CJ, Frye GC, Hurd AJ, Ashley CS. Fundamentals of sol-gel dip coating. *Thin Solid Films*. 1991;201:97–108.

- [42] Berger LM. Coatings by Thermal Spray. *Comprehensive Hard Materials*, vol. 1. 2014. p. 471–506. 1st Edition from Vinod Sarin. ISBN-9780080965277, Elsevier; Netherlands; 2014.
- [43] Duocastella M, Fernández-Pradas JM, Morenza J, Serra P. Printing biological solutions through laser induced forward transfer. *Applied Physics A*. 2008;93:941.
- [44] Mihailescu IN, Bigi A, Gyorgy E, Ristoscu C, Sima F, Toksoy Oner E. Biomaterial Thin Films by Soft Pulsed Laser Technologies for Biomedical Applications. In: Ossi PM, Castillejo M, Zhigilei L. (eds.). *Lasers in Materials Science: Springer Series Materials in Science*. Springer; London; 2014. p. 271–291.
- [45] Sima F, Axente E, Iordache I, Luculescu C, Gallet O, Anselme K, Mihailescu IN. Combinatorial matrix assisted pulsed laser evaporation of a biodegradable polymer and fibronectin for protein immobilization and controlled release. *Applied Surface Science*. 2014;306:75–79.
- [46] McCormick RD, Lenhardt J, Stiff-Roberts AD. Effects of emulsion-based resonant infrared matrix assisted pulsed laser evaporation on the molecular weight of polymers. *Polymers*. 2012;4(1):341–354.
- [47] Gittard SD, Narayan R. Laser direct writing of micro- and nano-scale medical devices. *Expert Review of Medical Devices*. 2010;7(3):343–356.
- [48] Volpati D, Machado AD, Olivati CA, Alves N, Curvelo AAS, Pasquini D, Constantino CJL. Physical vapor deposited thin films of Lignins extracted from sugar cane bagasse: morphology, electrical properties, and sensing applications. *Biomacromolecules*. 2011;12(9):3223–3231. doi:10.1021/bm200704m
- [49] Eraković S, Janković A, Matić IZ, Juranić ZD, Vukašinović-Sekulić M, Stevanović T, Mišković-Stanković V. Investigation of silver impact on hydroxyapatite/lignin coatings electrodeposited on titanium. *Materials Chemistry and Physics*. 2013;142(2–3): 521–53.
- [50] Xin-Xing F, Li-Li Z, Jian-Yong C, Hua-Peng Z. Preparation, characterization, and properties of nano-TiO₂/silk fibroin hybrid films by sol-gel processing. *Journal of Biomedical Materials Research Part A*. 2008;84A(3):761–768.
- [51] Hoeger IC, Filpponen I, Martin-Sampedro R, Johansson LS, Österberg M, Laine J, Kelley S, Rojas OJ. Bicomponent lignocellulose thin films to study the role of surface lignin in cellulolytic reactions. *Biomacromolecules*. 2012;13(10):3228–3240. doi:10.1021/bm301001q
- [52] Aadil KR, Barapatre A, Jha H. Synthesis and characterization of Acacia lignin-gelatin film for its possible application in food packaging. *Bioresources and Bioprocessing*. 2016;3(27). doi:10.1186/s40643-016-0103-y; in press <http://link.springer.com/article/10.1186/s40643-016-0103-y> (last access September 6, 2016).

- [53] Janković A, Eraković S, Ristoscu C, Mihailescu Serban N, Duta L, Visan A, Stan GE, Popa AC, Husanu MA, Luculescu CR, Srdić VV, Janačković DJ, Mišković-Stanković V, Bleotu C, Chifiriuc MC, Mihailescu IN. Structural and biological evaluation of lignin addition to simple and silver-doped hydroxyapatite thin films synthesized by matrix-assisted pulsed laser evaporation. *Journal of Materials Science: Materials in Medicine*. 2015;26(1):5333. doi:10.1007/s10856-014-5333-y
- [54] Visan A, Stan GE, Ristoscu C, Popescu-Pelin G, Sopronyi M, Besleaga C, Luculescu C, Chifiriuc MC, Hussien MD, Marsan O, Kergourlay E, Grossin D, Brouillet F, Mihailescu IN. Combinatorial MAPLE deposition of antimicrobial orthopedic maps fabricated from chitosan and biomimetic apatite powders. *International Journal of Pharmaceutics*. 2016;511(1):505–515. doi:10.1016/j.ijpharm.2016.07.015
- [55] Axente E, Sima F, Ristoscu C, Mihailescu N, Mihailescu IN. Biopolymer Thin Films Synthesized by Advanced Pulsed Laser Techniques. In: Parveen F.K. (ed.). Chapter 4 in book *Recent Advances in Biopolymers*. ISBN 978-953-51-2255-5. InTech; Croatia; 2016.
- [56] Chrisey D, Pique A, McGill R, Horwitz J, Ringeisen B, Bubb D. Laser deposition of polymer and biomaterial films. *Chemical Reviews*. 2003;103(2):553–76.
- [57] Cristescu R, Mihailescu IN, Jelinek M, Chrisey D. Functionalized Thin Films and Structures Obtained by Novel Laser Processing Issues. *Functional Properties of Nanostructured Materials*. Springer; New York City; USA; 2006. p. 211–26.
- [58] Meredith JC, Karim A, Amis EJ. High-throughput measurement of polymer blend phase behavior. *Macromolecules*. 2000;33:5760–5762.
- [59] Li X, Nan K, Shi S, Chen H. Preparation and characterization of nano-hydroxyapatite/chitosan cross-linking composite membrane intended for tissue engineering. *International Journal of Biological Macromolecules*. 2012;50:43–49.
- [60] Torricelli P, Sima F, Axente E, Fini M, Mihailescu IN, Bigi A. Strontium and zoledronate hydroxyapatites graded composite coatings for bone prostheses. *Journal of Colloid Interface Science*. 2015;448:1–7.
- [61] Axente E, Sima F, Sima LE, Erginer M, Eroglu MS, Serban N, Ristoscu C, Petrescu SM, Oner ET, Mihailescu IN. Combinatorial MAPLE gradient thin film assemblies signaling to human osteoblasts. *Biofabrication*. 2014;6:035010.
- [62] Sima F, Axente E, Sima LE, Tuyel U, Eroglu MS, Serban N, Ristoscu C, Petrescu SM, Oner ET, Mihailescu IN. Combinatorial matrix-assisted pulsed laser evaporation: single-step synthesis of biopolymer compositional gradient thin film assemblies. *Applied Physics Letters*. 2012;101:233705.
- [63] Miroiu FM, Socol G, Visan A, Stefan N, Craciun D, Craciun V, Dorcioman, Mihailescu IN, Sima LE, Petrescu SM, Andronie A, Stamatini I, Moga S, Ducu C. Composite biocompatible hydroxyapatite–silk fibroin coatings for medical implants obtained by

- matrix assisted pulsed laser evaporation. *Materials Science and Engineering B*. 2010;169:151–158.
- [64] Miroiu FM, Stefan N, Visan A, Nita C, Luculescu C, Rasoga O, Socol M, Zgura I, Cristescu R, Craciun D, Socol G. Composite biodegradable biopolymer coatings of silk fibroin – poly(3-hydroxybutyric-acid-co-3-hydroxyvaleric-acid) for biomedical applications. *Applied Surface Science*. 2015;355:1123–1131.
- [65] Socol G, Preda N, Socol M, Sima L, Luculescu CR, Sima F, Miroiu M, Axente E, Visan A, Stefan N, Cristescu R, Dorcioman G, Stanculescu A, Radulescu L, Mihailescu IN. MAPLE deposition of PLGA micro-and nanoparticles embedded into polymeric coatings. *Digest Journal of Nanomaterials and Biostructures*. 2013;8(2):621–630.
- [66] Cristescu R, Visan A, Socol G, Surdu AV, Oprea AE, Grumezescu AM, Chifiriuc MC, Boehm RD, Yamaleyeva D, Taylor M, Narayan RJ, Chrisey DB. Antimicrobial activity of biopolymeric thin films containing flavonoid natural compounds and silver nanoparticles fabricated by MAPLE: a comparative study. *Applied Surface Science*. 2015;336:234–239. doi:10.1016/j.apsusc.2015.11.252
- [67] Erakovic S, Jankovic A, Tsui GCP, Tang C-Y, Miskovic-Stankovic V, Stevanovic T. Novel bioactive antimicrobial Lignin containing coatings on titanium obtained by electrophoretic deposition. *International Journal of Molecular Sciences*. 2014;15(7):12294–12322. doi:10.3390/ijms150712294
- [68] Erakovic S, Veljovic D, Diouf PN, Stevanovic T, Mitric M, Milonjic S, Miskovic-Stankovic VB. Electrophoretic deposition of biocomposite Lignin/hydroxyapatite coatings on titanium. *International Journal of Chemical Reactor Engineering*. 2009;7:A62.
- [69] Yoshida A, Miyazaki T, Ishida E, Ashizuka M. Preparation of bioactive chitosan-hydroxyapatite nanocomposites for bone repair through mechanochemical reaction. *Materials Transactions*. 2004;45:994–998.
- [70] Ito M, Hidaka Y, Nakajima M, Yagasaki H, Kafrawy AH. Effect of hydroxyapatite content on a physical properties and connective tissue reactions to a chitosan-hydroxyapatite composite membrane. *Journal of Biomedical Materials Research*. 1999;45:204–208.
- [71] Zhang Y, Zhang M. Calcium/phosphate composite scaffolds for controlled *in vitro* antibiotic drug release. *Journal of Biomedical Materials Research*. 2002;62:378–386.
- [72] Sivakumar M, Manjubala I, Panduranga Rao K. Preparation, characterization and *in vitro* release of gentamicin from coralline hydroxyapatite-chitosan composite microspheres. *Carbohydrate Polymers*. 2002;49:281–288.
- [73] Hu Q, Li B, Wang M, Shen J. Preparation and characterization of biodegradable chitosan/hydroxyapatite nanocomposite rods via *in situ* hybridization: a potential material as internal fixation of bone fracture. *Biomaterials*. 2004;25:779–785.

- [74] Davidenko N, Carrodeguas RG, Peniche C, Solís Y, Cameron RE. Chitosan/apatite composite beads prepared by *in situ* generation of apatite or Si-apatite nanocrystals. *Acta Biomaterialia*. 2010;6:466–476.
- [75] Thein-Han WW, Misra RDK. Biomimetic chitosan–nanohydroxyapatite composite scaffolds for bone tissue engineering. *Acta Biomaterialia*. 2009;5:1182–1197.
- [76] Boyan BD, Lincks J, Lohmann CH, Sylvia VL, Cochran DL, Blanchard CR, Dean DD, Schwartz Z. Effect of surface roughness and composition on costochondral chondrocytes is dependent on cell maturation state. *Journal of Orthopaedic Research*. 1999;17:446–457.

Biodegradable Polylactide-Based Composites

Ester Zuza, Emilio Meaurio and Jose-Ramon Sarasua

Additional information is available at the end of the chapter

<http://dx.doi.org/10.5772/65468>

Abstract

The aim of this chapter is to introduce to the use and possible applications of polylactide-based composites. Polylactides are biodegradable aliphatic polyesters, which are widely used in medical and ecological-friendly fields. First of all, a deep description of main characteristics of polylactides is shown. This chapter summarizes many concepts, which comprehend a general view of polylactide biopolymers such as synthesis and structures, physical-chemical and mechanical characterization and possible applications of final products. Then, an overview of composites based on polylactides and their benefits compared with bare polylactides are described.

Keywords: Polylactide, poly(lactic acid), composite, biodegradable, biopolymer, polyester, biocompostable, bone repair, nanocomposite

1. Introduction

Poly(lactide or poly(lactic acid) (PLA) is the front runner in the emerging biopolymer market with the best availability and the most attractive cost structure [1]. Although PLA existed for several decades, its use has been limited to biomedical applications due its high cost. However, in the new century processing of PLA has been developed in the industry in a large-scale production promoting its commercialization as a commodity plastic [2].

To date, PLA is one of the most used biodegradable polymers in the field of biomedical applications and eco-friendly industrial production. A clear advantage of this polymer is its possibility of polymerization coming from renewable resources as starch, but it is not the only one: stiffness of polylactides are similar to some commodity polymers as polyethylene,

polypropylene and polystyrene [3] and products derived from its degradation process are nontoxic for the human body and also do not leave any footprint in the landfills [4].

2. Synthesis

The monomer of PLA is lactic acid. Although this monomer can synthesize from petroleum, almost all lactic acid available on the market is produced by fermentation. During fermentation a suitable carbohydrate is converted to lactic acid by microorganisms without the presence of oxygen, hence, under anaerobic conditions. Fermentation of sour whey resulted in the discovery of lactic acid in 1780, when it was isolated by C. W. Scheele [5].

Lactic acid is the simplest α -hydroxyacid that contains a chiral carbon atom and exists in the following two enantiomeric forms: L-lactic acid and D-lactic acid. Monomer forms a stable cycled dimer, that is, lactide. Consequently, dimer presents three different structures, namely L-lactide, D-lactide and DL-lactide. Isotactic, optically active and crystalline homopolymers are obtained if either L- or D-lactide dimers are polymerized. However, DL-lactide or copolymers of L- and D-dimers polymerize obtain atactic, nonactive optically and amorphous polymers [6].

Polymerization of this lactic acid is carried out by polycondensation [7], instead of polymerization of the dimer that occurs by ring opening polymerization [8]. Polymerization started from lactide dimer allows to obtain high level of molecular mass due to a chain polymerization mechanism and this is the mechanism that is normally used for production.

3. Polylactide characterization

3.1. Physical-chemical and mechanical characterization

Poly lactides have a glass transition (T_g) value around 60°C. This characteristic point refers to a change in the mobility of amorphous chains. Hence, atactic homopolymer shows a value of 60°C, but crystalline homopolymers that have some restriction in the mobility of amorphous phase could present T_g values up to 70°C depending on the thermal treatment used for crystallization [9, 10].

Isotactic polylactides (pure PLLA and PDLA have same properties) crystallize forming a homocrystal, which melts in the range of 160–190°C depending on the molecular mass and shows a crystallinity fraction around 35% [9]. This value is calculated using one of the different values for theoretic melting enthalpy extrapolated from experimental analysis by different researches, being the most common values 93.6 [11] and 106 J/g [12].

Depending on the crystallization conditions, PLLA can crystallize in α , β or γ polymorphs [13, 14]. The most common form usually is the orthorhombic α crystal [15], while trigonal β form is obtained under high drawing conditions and high temperatures [16, 17]. Besides, γ poly-

morph is obtained through epitaxial crystallization on special substrates with organic solvents [18]. Recently, the existence of a α' crystal has been reported, which can be identified as a disordered α form, with the same 10_3 helical conformation but different lateral packing [19].

As with other enantiomeric polymers occurs [20], polylactides also form thermally stable crystals when 50–50 wt.% of PLLA and PDLA enantiomers are blended [21]. The formation of stereocomplex crystals is favored with low molecular mass [22, 23] or isothermal treatments above homocrystal melting [24, 25]. These crystals melt at 50°C above the homocrystals and their formation is favored if a pretreatment at temperatures above the melting temperature of α crystals is carried out. This pretreatment allows the formation of homocrystal nuclei and increases the crystallization rate of stereocomplex during the isothermal crystallization step [26].

In regard to the mechanical properties, PLAs display high tensile modulus (3 GPa [27]) and yield strength (50–70 MPa [28]) but low elongation at break (5–7%) that result in a brittle behavior of the material.

3.2. Biodegradability

Ester groups in polylactides allow hydrolytic degradation of polymer chains. The degradation mechanism depends on factors, which can be assigned to two groups: (a) related to material as molecular weight, crystallinity, comonomer structure, porosity, etc; and (b) related to the media: temperature, pH, solute concentration, enzymes, etc. [29].

For bulky materials, there are three kinds of degradation mechanisms: surface erosion, bulk erosion and core-accelerated bulk erosion [30]. A surface erosion mechanism takes place when the hydrolytic degradation rate of the material surface in contact with water (containing catalytic substances as alkalis and enzymes) is much higher than the diffusion within the material. In contrast, a bulk erosion mechanism occurs when hydrolytic degradation takes place homogeneously, irrespective of the depth from the material surface. As it can be foreseen, the hydrolytic degradation mechanism changes from the bulk to surface erosion when material thickness becomes higher than the critical [31]. On the other hand, some authors report that polylactides degradation mechanism proceeds via core-accelerated bulk erosion, when the material is thicker than 0.5–2 mm, due to the accelerated degradation sustained by oligomers and monomers trapped and accumulated in the core part of the materials [32]. Hence, depending of the thickness of the PLA piece, the degradation mechanism proceeds via bulk (<0.5–2 mm), core accelerated (between 0.5–2 and 74 mm) and surface erosion (>7.4 cm). In general, chains in the crystalline region are hydrolysis resistant compared to those in the amorphous regions because the access of water molecules to the chains inside the rigid crystalline regions is prohibited. Such crystalline regions are called “crystalline residues.”

Concerning to enzymatic degradation, no study of specific enzymes for the biodegradation of polylactides has been reported [33]. Williams reported the enzymatic hydrolysis of polylactides in the presence of proteases as pronase, bromelain and proteinase K, being the latter a protease with a strong activity in hydrolizing proteins, particularly keratin [34, 35].

4. Strategies to changes polylactide properties

4.1. Blending

Easier strategy to change properties of a pure polymer is blending with other polymers. These blends could be miscible or immiscible depending on solubility parameters and specific interactions established between counterparts. Miscibility of blends is governed by thermodynamic law, in which the free energy of mixing in the blend must be negative [30]. Polylactide is miscible with polyvinylphenol (PVPh) [36–39], poly(styrene-co-vinylphenol) [40, 41], polyhydroxybutirate (PHB) [42], poly(methyl methacrylate) (PMMA) [43], poly(vinyl acetate) [44] and poly(ethylene oxide) [45].

Phase separation induced by immiscible blends has been commonly used for improving fragile commodity polymers as PS and PMMA with a rubber modification leading into HIPS [46] and high impact PMMA [47]. However, the modifications in polylactides with biodegradable polymers as polycaprolactone (PCL) are an efficient way to toughen polylactides [48].

4.2. Copolymerization

Modification in the synthesis process with other monomers is other way to tune the properties of polylactides. Comonomers as ethylenglycol or ethylene oxide [49, 50], propylene oxide [51] and trimethylcarbonate [52] have been reported for polymerization with lactide units. However, cyclic comonomers are suitable to polymerize by ring opening polymerization (ROP) with lactide such as lactones or macrolactones. The most investigated systems are poly(glycolide-lactide) [53, 54] and poly(lactide-co-caprolactone) copolymers [55–57]. Recently, some studies in search of more biodegradable copolymers are using macrolactones as γ -valerolactone [58].

Moreover, starting the polymerization of lactide or lactic acid with polymer containing hydroxyl groups leads into graft copolymers. This strategy is welcomed to increase the miscibility with other polymers and hydrophobicity as it occurs with poly(vinyl alcohol) [59].

5. Polylactide-based composites

Composites combine two (or more) different components: a continuous phase, called matrix, acts as binder and distributes homogeneously the forces through whole composite; and a discontinuous phase, called reinforcement, fundamentally is used to carry the applied load. Depending on the form of the reinforcements, they are arranged in different groups, of which two most important are fibers and particles. Normally, the aim of the reinforcements is to enhance the stiffness and tensile strength of the matrix, although sometimes fillers are used to reduce the price of the final product or modify the physical, rheological, optical or other properties. However, more important is the interface between both components to assure good transmission among constituents of the composite.

Efforts made for advancing in technology lead to the scientific community to introduce nanoscale in material science and consequently in polymer science. It must pay special attention in nanocomposites, because it is foreseen remarkable improvement in properties with less quantity of reinforcement than micro or macroscale composites.

Different families of reinforcements can be classified into function of their chemical nature and it is analyzed the effect that induces in polylactides.

5.1. Organic reinforcements

5.1.1. Natural fibers

These composites are very attractive because both matrix and reinforcement are obtained from renewable resources. But comparing to synthetic ones they have some characteristics to take into account [60]:

- Natural fibers degrade at low temperatures (<200°C). Hence, processing of polylactide/natural fibers composite must be made carefully.
- Natural fibers are hydrophilic and absorb moisture easily. Polylactides can degrade faster and wettability of fibers produces swelling and distorsion in the interface due to a lack in dimensional stability.
- Natural fibers have low microbial resistance. Long-time storages are not ideal for these composites.

Environmental friendly materials with a full degradation capability promote the interest of these composites, especially in the automotive industry. Different natural plant fibers have been used to obtain polylactide-based composites: agricultural natural fibers as jute, kenaf, sisal and flax and also inexpensive agricultural residues as wheat straw, corn stover, soy stalks and their hybrids [61].

- Jute/polylactide [62]: Alkali-, permanganate- and peroxide-treated composites exhibit lower thermal stability, whereas silane-treated composites show a higher thermal stability when compared to untreated composites. However, a better fiber matrix adhesion improves the abrasive wear resistance of the jute fiber-reinforced composites.
- Kenaf/polylactide [63]: The effects of the silane-coupling agent on composite properties is highly beneficial leading to increased moduli and heat deflection temperatures as well as reduced water swelling. Moreover, an optimal formulation comprised of 50% kenaf and 50% PLA fibers with three parts of silane-coupling agent represents an optimal formulation to manufacture automotive headliners.
- Sisal/polylactide [64]: Mechanical properties of PLLA/sisal fiber composites (improved with caustic soda treatment) confer high strength, high modulus sisal-PLLA composites, because of effective stress transfer at well-bonded fiber to matrix interfaces.
- Flax/polylactide [65]: Mechanical properties of polylactide and its composites with flax are greater than those of related polypropylene/flax fiber composites and concretely the specific

tensile strength and modulus have demonstrating to be very close to values obtained in glass fiber polyester composites.

Moreover, micro- and nanoscale improve the mechanical properties of natural fiber-based composites; hence, cellulose microfibrils (CMF), cellulose nanofibrils (CNF) and cellulose nanocrystals (CNC) are the new tendencies.

Composites of polylactide with silane-modified cellulose microfibrils (CMFs) coming from sisal fiber (SF) showed a maximum impact strength which was 24% higher than that of virgin PLA [66].

However, the most important feature of using nanofibrils is the dispersion in the matrix, because fibrils are hydrophilic and the matrix hydrophobic. To overcome this, feature some researches disperse CNF in polylactides by a new method obtaining increments in the modulus and strength (up to 58 and 210%, respectively) demonstrated the load-bearing capability of the CNF network in the composites [67].

Although crystallinity degree of polylactide/CNC nanocomposites remain similar to that of neat homopolymer, the crystallization rate has been notably increased (1.7–5 times) boosted by the presence of CNC, which act as nucleating agents during the crystallization process. In addition, structural relaxation kinetics of PLLA chains has been drastically reduced by 53 and 27% with the addition of CNC [68].

5.1.2. Synthetic fibers, nanofibers and nanotubes

5.1.2.1. Carbon-based reinforcements

Carbon fiber (CF) is made from organic polymers, where hexagonal carbon structures acquired a fibrillate form. Helped by their excellent specific properties supported by low weight (high stiffness, tensile strength, chemical resistance, thermal stability and low thermal expansion) carbon fibers have a widespread application in different sectors such as aerospace, civil engineering, military and competition sports. However, still remain to overcome the price because they are relatively expensive when correlated with natural fibers, glass fibers or polymeric fibers. However, most futurist than carbon fiber composites are these with nanofibers, nanotubes or graphene.

- Carbon nanotubes (CNT)

Since the discovery by Iijima in 1991 [69], carbon nanotubes have been investigated as their unique properties [70, 71, 72] make them interesting fillers to develop polymer nanocomposites. CNTs influence in the physical-chemical properties, as well as in the mechanical, electrical and biocompatible properties of polylactides.

It has been reported that CNT influence in the crystallinity without changes in dimension of the crystal assisting in the disorder-to-order (α' -to- α) transition. However, results obtained from Hoffman-Weeks plot reveal that equilibrium melting temperature increase with CNT content, while thickness of crystal layer and amorphous layer of PLLA both decreased with increasing CNT contents of polylactide matrix [73]. Moreover, structural

aspects as physical aging [74] and thermal degradation [75] of polylactide matrix is notably affected by the presence of these CNTs.

However, compatibilization of CNTs increment the efficiency of the composites [76]. Pyrene-end-polylactide has been founded as a good interface stabilizer in polylactide/CNT composites. Therefore, modified CNT influence in polylactides in much greater manner than comparing results obtained without modification of CNTs [77].

Besides, polylactide stereocomplexation is clearly favored by CNT content [78]. The addition of small amounts of MWCNTs combined with a mild thermal treatment extends the processing window for the preparation of polylactides exclusively crystallized in the stereocomplex form, instead of the homocrystal formation.

With other point of view, conductivity of polymer matrices with nanofiller addition has been increased even with very low percentages of conductive carbon nanotubes composites [79].

In the biomedical field, also, polylactide/MWCNT composites have been carefully analyzed due to the possible cytocompatibility of the CNTs when polylactide matrix degrades [80, 81]. Instead of nanocomposite system shows adequate biocompatibility, degradation products may induce adverse effects on cell metabolism and proliferation, paying special attention in lactic acid presence and the quality of the MWCNT suspension [82]. However, an extensive *in vitro* evaluation including final degradation products is needed to enable a comprehensive prediction of the overall success or failure of newly developed degradable nanocomposites.

- Graphene

Graphene is a single-atom thick graphite sheet. It is structurally very similar to silicate layers and chemically analogous to carbon nanotubes, due to its huge specific surface area is considered as ideal reinforcing nanofiller in the fabrication of multifunctional polymer nanocomposites, superior mechanical strength, remarkable electronic and thermal properties [83]. As it could be expected to achieve its maximal reinforcing efficiency, graphene sheets must be homogeneously dispersed in the polymer matrix to prompt the interfacial stress transfer between graphene and polymer matrix [84].

An effective nanofiller has been found when graphene is functionalized with octadecylamine (ODAG) in well-exfoliated solution/casting process. Due to the good hydrophobic compatibility between organic counterparts, interfacial adhesion and consequently crystallization, mechanical properties and thermal stability are improved [85].

5.1.2.2. Other organic reinforcements

Slit die extrusion, hot stretching and quenching is proposed as a new technique to construct well-aligned, stiff poly(butylene succinate) (PBS) nanofibrils in the PLA matrix for the first time [86]. The high strength, modulus and ductility are unprecedented for PLA and are in great potential need for packaging applications. However, this technique opens a new way for the development of new composite materials based on polymeric fibers.

5.1.3. Inorganic reinforcements

Bioresorbable polymers play great relevance in biomedical field. Due to its excellent mechanical properties related to stiffness and tensile strength, polylactides are proposed for using in implants with safety-critical applications [87]. Hence, fixation and bone reconstruction are compulsory for a good health and reconstruction of the damaged zone. Most of implants based on polylactide polymer are focused on bone repair; however, radiopacity and other properties are too of great interest.

5.1.3.1. Bone repair

In this context, inorganic reinforcements play the most important role, because the natural bone is formed up to 70 wt. % by calcium phosphate very similar to hydroxyapatite (HA) [88]. HA is an inorganic compound, which helps the differentiation of osteoblasts in regeneration of the bone structure [89]. For this reason, incorporation of HA into PLA matrices has been widely reported [90, 91, 92, 93].

Tricalcium phosphate (β -TCP) has been also widely used due its bioactivity and biodegradability. Its degradation rate is incremented 3–12 times compared with HA [94] and this favors bonding of bone to the bioceramic [95]. However, combination of β -TCP and HA in denominated biphasic calcium phosphates (BCP) shows the advantages of both components: reactivity of β -TCP and stability of HA. BCP with 60–40% of HA-TCP incubated in simulated body fluid produces the precipitation of needle-shaped apatite crystals [96], allowing polylactide/BCP composites for fracture fixation plates [97].

Furthermore, discovery of bioactive glasses by L. L. Hench in 1969 catapults the use of these inorganic particles in tissue engineering due to their excellent biocompatibility and the ability of bone bonding [98]. A common characteristic of bioactive glasses and ceramics is a time-dependent kinetic modification of the surface that occurs upon implantation [99]. Bioactive glasses originate a superficial layer of calcium deficient carbonate, which permits a chemical adhesion to bone. This adhesion is appealed as bioactivity and is associated with the formation of carbonated hydroxyapatite (HCA) when glass is implanted or in contact with simulated body fluids [100, 101]. The HCA layers formed on a scaffold made of 45S5Bioglass® immersed in SBF takes a “cauliflower” typical morphology [99] and allows osteogenic formation [102].

Some researches of PLA/bioactive glass composites have been reported [103, 104]. However, melt processing of bioglass with polylactides affects the thermal stability of the composite [105], and to overcome this handicap, protection of bioactive ceramic with and acrylic plasma treatment has been proposed [106]. An easier treatment than plasma has been proposed by A. Larrañaga by covering these particles with a mussel inspired polydopamine coating, which results in a bioactive composite [107].

5.1.3.2. Radiopacity

Although alternative radiopacifiers have been proposed in bibliography [108, 109], barium sulfate (BaSO_4) is still the gold standard for medical applications [110]. Incorporation of BaSO_4

particles to polymer matrices enables surgeons to accurately place and to monitor any migration of the implant over time.

Singularly, barium sulfate submicron particles added to polylactide matrix enhance deformation at rupture and confer high toughness to fragile polylactides [111]. Consequently, the addition of these submicron barium sulfate particles enables a radiopaque and tough polylactide composite.

5.1.3.3. Nucleating effect

The influence of the nature of the filler on the mechanical properties of PLA has been reported for two silicated clays, both having a platelet-like shape [112]. Talc is a more efficient filler regarding mechanical reinforcement of PLA as compared to kaolin. This better reinforcing effect in the case of talc is ascribed to its higher affinity with the PLA. It was also evidenced that talc has a nucleating effect on the PLA crystallization [113], while kaolin has no or very limited effect on the crystallization behavior of PLA. In conclusion, the existence of crystallographic relationships between the structures of the filler and the polymer crystals is also a key parameter for the observation of a nucleating effect.

6. Future trends and perspectives

Although polylactide has been researched for various decades, still remain being the gold standard in biodegradable polymers. In fact, development of new techniques as 3D printing includes in its commercial version polylactide material. It seems as if polylactides will be investigated for long years and could carve out a place in commodity plastics.

7. Conclusions

Polylactide composites broaden the possibilities of application of neat polylactides. Biodegradable matrix allows validity for ecological packaging and biomedical applications and their composites improve the potential use of these materials.

Author details

Ester Zuza*, Emilio Meaurio and Jose-Ramon Sarasua

*Address all correspondence to: ester.zuza@ehu.eus

Faculty of Engineering, University of the Basque Country (UPV-EHU) and POLYMAT, Bilbao, Spain

References

- [1] Auras R., Lim L.T., Selke S.E.M., Tsuji H. editors. Poly(lactic acid): synthesis, properties and applications. New Jersey: Wiley; 2010. 499 p.
- [2] Auras R., Harte B., Selke S. An overview of polylactides as packaging materials. *Macromolecular Bioscience*. 2004;4(835-864).
- [3] Sinclair R.G. The case for polylactic acid as a commodity packaging plastic. *Journal of Macromolecular Science-Pure and Applied Chemistry*. 1996;A33(585-597).
- [4] Musiol M., Sikorska W., Adamus G., Janeczek H., Richert J., Malinowski R., Jiang G.Z., Kowalczyk M. Forensic engineering of advanced polymeric materials. Part III - Biodegradation of thermoformed rigid PLA packaging under industrial composting conditions. *Waste Management*. 2016;52(69-76).
- [5] Dobbin L. The collected papers of Carl Wilhelm Scheele. London: G. Bell & Sons Ltd.; 1931. 367p.
- [6] Sarasua J.R., Prud'homme R.E., Wisniewski M., Leborgne A., Spassky N. Crystallization and melting behavior of polylactides. *Macromolecules*. 1998;12(3895-3905).
- [7] Bendix D. Chemical synthesis of polylactides and its copolymers for medical applications. *Polymer Degradation and Stability*. 1998;59(129-135).
- [8] Kricheldorf H.R., Kreiser-Sunders I., Stricker, A. Polylactones: 48. SnOct₂-initiated polymerizations of lactide: a mechanistic study. *Macromolecules*. 2000;33(702-709).
- [9] Zuza E., Ugartemendia J.M., Lopez A., Meaurio E, Lejardi A., Sarasua J.R. Glass transition behavior and dynamic fragility in polylactides containing mobile and rigid amorphous fractions. *Polymer*. 2008;48(4427-4432).
- [10] Sarasua J.R., Zuza E., Imaz N., Meaurio E. Crystallinity and crystalline confinement of the amorphous phase in polylactides. *Macromolecular symposia*. 2008;272(81-86).
- [11] Fischer E.W., Sterzel H.J., Wegner G. Investigation of structure of solution grown crystals of lactide copolymers by means of chemical-reactions. *Kolloid-Zeitschrift and Zeitschrift für Polymere*. 1973;251(980-990).
- [12] Cho T.Y., Strobl G. *Polymer*. Temperature dependent variations in the lamellar structure of poly(l-lactide). 2006;47(1036-1043).
- [13] Lizundia E., Petisco S., Sarasua J.R. Phase-structure and mechanical properties of isothermally melt- and cold-crystallized poly (L-lactide). *Journal of the Mechanical Behavior of Biomedical Materials*. 2012;17(242-251).
- [14] Meaurio E., Zuza E., Lopez-Rodriguez N., Sarasua J.R. Conformational behavior of poly(l-lactide) studied by infrared spectroscopy. *Journal of Physical Chemistry B*. 2006;110(5790-5800).

- [15] Del Rio J., Etxeberria A., Lopez-Rodriguez N., Lizundia E., Sarasua J.R. A PALS contribution to the supramolecular structure of poly(L-lactide) Macromolecules. 2010;43(4698-4707).
- [16] Engelberg I., Kohn J. Physicomechanical properties of degradable polymers used in medical applications—a comparative-study. Biomaterials. 1991;12(292-304).
- [17] Hoogsteen W., Postema A.R., Pennings A.J., Brinke G.T., Zugenmaier P. Macromolecules. Crystal structure, conformation and morphology of solution-spun poly(L-lactide) fibers. 1990;23(634).
- [18] Furuhashiv Y., Iwata T., Kimura Y., Doi Y. Structural characterization and enzymatic degradation of alpha-, beta-, and gamma-crystalline forms for poly(beta-propiolactone). Macromolecular Bioscience. 2003;3(462-470).
- [19] Meaurio E., Martinez de Arenaza I., Lizundia E., Sarasua J.R. Analysis of the C=O stretching band of the alpha-crystal of poly(L-lactide). Macromolecules. 2009;42(5717-5727).
- [20] Marín R., Martínez de Ilarduya A., Romero P., Sarasua J.R., Meaurio E., Zuza E., Muñoz-Guerra S. Spectroscopic evidence for stereocomplex formation by enantiomeric polyamides derived from tartaric acid. Macromolecules. 2008;41(3734-3738).
- [21] Sarasua J.R., Lopez-Arraiza A., Balerdi P., Maiza I. Crystallization and thermal behaviour of optically pure polylactides and their blends. Journal of Materials Science. 2005;40:1855-1862.
- [22] Tsuji H., Ikada Y. Polymer. Stereocomplex formation between enantiomeric poly(lactic acid)s. XI. Mechanical properties and morphology of solution-cast films. 1999;40(6699-6708).
- [23] Tsuji H.. Poly(lactide) stereocomplexes: formation, structure, properties, degradation, and applications. Macromolecular Bioscience. 2005;5(569-597).
- [24] Sarasua J.R., López-Rodríguez N., Lopez-Arraiza A., Meaurio E. Stereoselective crystallization and specific interactions in polylactides. Macromolecules. 2005;38(8362-8371).
- [25] Sarasua J.R., Lopez-Arraiza A., Balerdi P., Maiza I. Crystallinity and mechanical properties of optically pure polylactides. Polymer Engineering and Science. 2005;45(745-753).
- [26] López-Rodríguez N., Martinez de Arenaza I., Meaurio E., Sarasua J.R. Efficient stereocomplex crystallization in enantiomeric blends of high molecular weight polylactides. RSC Advances. 2015;5(34525-34534).
- [27] Bergstroem J.S., Hayman D. Annals of Biomedical Engineering. An Overview of Mechanical Properties and Material Modeling of Polylactide (PLA) for Medical Applications. 2016; 44(330-340).

- [28] Sodergard A., Stolt M. *Progress in Polymer Science. Properties of lactic acid based polymers and their correlation with composition.* 2002;27(1123-1163).
- [29] Tsuji H. *Degradation of polylactide-based biodegradable materials.* New York: Nova Science Publishers; 2007.
- [30] Tsuji H. *Polylactides.* In: Doiand Y., Steinbüchel A. editors. *Biopolymers.* Weinheim: Wiley-VCH; 2002. p. V/129ff.
- [31] von Bukersroda F, Schedl L., Göpferich A. *Biomaterials. Why degradable polymers undergo surface erosion or bulk erosion.* 2002;23(4221-4231).
- [32] Li S.M., Vert M. *Biodegradation of aliphatic polyesters.* In: Scott G., Gilead D. editors. *Biodegradable polymers: principles and applications.* Cambridge: Chapman & Hall; 1995. pp. 43-87.
- [33] Iwata T., Abe H. Kikkawa Y. *Enzymatic degradation.* In: Auras R., Lim L.T., Selke S.E.M., Tsuji H. editors. *Poly(lactic acid): synthesis, properties and applications.* New Jersey: Wiley; 2010. pp. 383-399.
- [34] Williams D.F. *Engineering Medicine. Enzymatic hydrolysis of poly(lactic acid).* 1981;10(5-7).
- [35] Ebeling W., Hennrich N.M., Klockow M., Orth H.D., Lang H. *European Journal of Biochemistry. Proteinase K from Tritirachium album Limber.* 1974;47(91-97).
- [36] Meaurio E., Hernández-Montero N., Zuza E., Sarasua J.R. *Miscible blends based on biodegradable polymers.* In: Interfaces S. Thomas, Y. Grohens, and P. Jyotishkumar editors. *Characterization of polymer blends: miscibility, morphology, and interfaces.* Weinheim: Wiley-VCH; 2014.
- [37] Meaurio E., Zuza E., Sarasua J.R. *Miscibility and specific interaction of poly(L-lactide) with poly(vinyl phenol).* *Macromolecules.* 2005;38(1207-1215).
- [38] Meaurio E., Zuza E., Sarasua J.R. *Direct measurement of the enthalpy if mixing in miscible blends of poly(DL-lactide) with poly(vinyl phenol).* *Macromolecules.* 2005;38(9221-9228).
- [39] Zuza E., Meaurio E., Etxebarria A., Sarasua J.R. *Exothermal process in miscible polylactide/poly(vinyl phenol) blends: mixing enthalpy or chemical reaction?* *Macromolecules.* 2006;27(2026-2031).
- [40] Zuza E., Lejardi A., Ugartemendia J.M., Monasterio N., Meaurio E., Sarasua J.R. *Compatibilization through specific interactions and dynamic fragility in poly(DL-lactide)/polystyrene blends.* *Macromolecular Chemistry and Physics.* 2008;209(5354-5358).

- [41] Zuza E., Lejardi A., Meaurio E., Sarasua J.R. Phase behavior and interactions in poly(DL-lactide)/poly(styrene-co-vinylphenol) blends. *European Polymer Journal*. 2015;63(58-66).
- [42] Focarate M.L., Scandola M., Dobrzynski P., Kowalczyk M. Miscibility and mechanical properties of blends of (L-lactide copolymers with atactic poly(3-hydroxybutyrate). *Macromolecules*. 2002;35(8472-8477).
- [43] Eguiburu J.L., Iruin J.J., Fernandez-Berridi M., San Roman J. Blends of amorphous and crystalline polylactides with poly(methyl methacrylate) and poly(methyl acrylate): a miscibility study. *Polymer*. 1998;39(6891-6897).
- [44] Gajra A.M., Dave V., Gross R.A., McCarthy S.P. Miscibility and biodegradability of blends of poly(lactic acid) and poly(vinyl acetate). *Polymer*. 1999;40(2303-2313).
- [45] Nakafuku C., Sakoda M. Melting and crystallization of poly(L-lactic acid) and poly(ethylene oxide) binary mixture. *Polymer Journal*. 1993;25(909-917).
- [46] Zhu L.D., Yang H.Y., Di Cai G., Chao Z., Wu G.F., Zhang M.Y., Gao G.H., Zhang H.X. *Journal of Applied Polymer Science*. Submicrometer-sized rubber particles as "craze-bridge" for toughening polystyrene/high-impact polystyrene. 2013; 129(224-229).
- [47] Lalande L., Plummer C.J.G., Manson J.A.E., Gerard P. *Polymer*. The Influence of Matrix Modification on Fracture Mechanisms in Rubber Toughened Polymethylmethacrylate. 2006; 47(2389-2401).
- [48] López-Rodríguez N., Lopez-Arraiza A., Meaurio E., Sarasua J.R.. Crystallization, morphology and mechanical behavior of polylactide/poly(ϵ -caprolactone) blends. *Polymer Engineering and Science*. 2006;46(1299-1308).
- [49] Li S.M., Vert M. Synthesis, characterization, and stereocomplex-induced gelation of block copolymers prepared by ring-opening polymerization of L(D)-lactide in the presence of poly(ethylene glycol). *Macromolecules*. 2003;36(8008-8014).
- [50] Yu G.H., Ji J., Zhu H.G., Shen J.C. Poly(D,L-lactic acid)-block-(ligand-tethered poly(ethylene glycol)) copolymers as surface additives for promoting chondrocyte attachment and growth. *Journal of Biomedical Materials Research Part B-Applied Biomaterials*. 2006;76B(64-75).
- [51] Yang D., Lu Q., Fan Z., Li S.M., Tu J.J., Wang W. Synthesis and characterization of degradable triarm low unsaturated poly(propylene oxide)-block-polylactide copolymers. *Journal of Applied Polymer Science*. 2010;118(2304-2313).
- [52] Pospiech D., Komber H., Jehnichen D., Haussler K., Eckstein K., Scheibner H., Janke A., Kricheldorf H.R., Petermann O. *Biomacromolecules*. Multiblock Copolymers of L-Lactide and Trimethylene Carbonate. 2005;6(439).

- [53] Khang G., Choe J.H., Rhee J.M., Le H.B. Interactions of different types of cells on physicochemically treated poly (L-lactide-glycolide) surfaces. *Journal of Applied Polymer Science*. 2002;85(1253-1262).
- [54] Barakat I., Dubois P., Grandfils C., Jerome R. Poly(epsilon-caprolactone-b-glycolide) and poly(D,L-lactide-b-glycolide) diblock copolyesters: controlled synthesis, characterization, and colloidal dispersions. *Journal of Polymer Science Part A-Polymer Chemistry*. 2001;39(294-306).
- [55] Fernandez J., Etxeberria A., Ugartemendia J.M., Petisco S., Sarasua J.R. Effects of chain microstructures on mechanical behavior and aging of poly(L-lactide-co-epsilon-caprolactone) biomedical thermoplastic-elastomer. *Journal of the mechanical behavior of biomedical materials*. 2012;12(29-38).
- [56] Fernandez J., Larrañaga A., Etxeberria A., Sarasua J.R. Effects of chain microstructures and derived crystallization capability on hydrolytic degradation on poly(L-lactide/-epsilon-caprolactone) copolymer. *Polymer Degradation and stability*. 2013;98(481-489).
- [57] Fernandez J., Etxeberria A., Sarasua J.R. Effects of repeat unit sequence distribution and residual catalyst on thermal degradation of poly(L-lactide-co-epsilon-caprolactone) statistical copolymers. *Polymer Degradation and Stability*. 2013;98(1293-1299).
- [58] Fernandez J., Larrañaga A., Etxeberria A., Sarasua J.R. Tensile behavior and dynamic analysis of novel poly(lactide/valerolacton) statistical copolymers. *Journal of the Mechanical Behavior of Biomedical Materials*. 2014;35(39-50).
- [59] Lejardi A., Etxeberria A., Meaurio E., Sarasua J.R. Novel poly(vinyl alcohol)-g-poly(hydroxy acid) copolymers: synthesis and characterization. *Polymer*. 2012;53(50-59).
- [60] Ghosh S.B., Bandyopadhyay-Ghosh S., Sain M. Composites. In: Auras R., Lim L.T., Selke S.E.M., Tsuji H. editors. *Poly(lactic acid): synthesis, properties and applications*. New Jersey: Wiley; 2010. pp. 293-310.
- [61] Nyambo C., Mohanty A.K., Misra M. Polylactide-based renewable green composites from agricultural residues and their hybrids. *Biomacromolecules*. 2010;11(1654-1660).
- [62] Goriparthi B.K., Suman K.N.S., Rao N.M. Effect of fiber surface treatments on mechanical and abrasive wear performance of polylactide/jute composites. *Composites Part A-Applied Science and Manufacturing*. 2012;43(1800-1808).
- [63] Lee B.H., Kim H.S., Lee S., Kim H.J., Dorgan, J.R. Bio-composites of kenaf fibers in polylactide: role of improved interfacial adhesion in the carding process. *Composites Science and Technology*. 2009;69(2573-2579).
- [64] Prajer M., Ansell M.P. Bio-composites for structural applications: poly-L-lactide reinforced with long sisal fiber bundles. *Journal of Applied Polymer Science*. 2014;131(40999).

- [65] Bodros E., Pillin I., Montrelay N., Baley C. Could biopolymers reinforced by randomly scattered flax fibre be used in structural applications? *Composites Science and Technology*. 2007;67(462-470).
- [66] Johari A.P., Mohanty S., Kurmvanshi S.K., Nayak S.K.. Influence of different treated cellulose fibers on the mechanical and thermal properties of poly(lactic acid). *ACS Sustainable Chemistry & Engineering*. 2016;4(1619-1629).
- [67] Wang T., Drzal L.T. Cellulose-nanofiber-reinforced poly(lactic acid) composites prepared by a water-based approach. *ACS Applied Materials and Interfaces*. 2012;4(5079-5085).
- [68] Lizundia E., Vilas J.L., Leon L.M. Crystallization, structural relaxation and thermal degradation in poly(L-lactide)/cellulose nanocrystal renewable nanocomposites. *Carbohydrate Polymers*. 2015;123(256-265).
- [69] Iijima S. Helical microtubules of graphitic carbon. *Nature* 1991;6348(56).
- [70] Ruoff R.S., Lorents D.C. Mechanical and thermal properties of carbon nanotubes. *Carbon*. 1995;7(925).
- [71] Berber S., Kwon Y., Tomanek D. *Physical Review Letters*. Unusually High Thermal Conductivity of Carbon Nanotubes. 2000;20(4613).
- [72] Treacy M.M.J., Ebbesen T.W., Gibson J.M. *Nature*. Exceptionally high Young's modulus observed for individual carbon nanotubes. 1996;6584(678).
- [73] Shieh Y.T., Liu G.L., Twu Y.K., Wang T.L., Yang C.H. Effects of carbon nanotubes on dynamic mechanical property, thermal property, and crystal structure of poly(L-lactic acid). *Journal of Polymer Science Part B-Polymer Physics*. 2010;48(145-152).
- [74] Lizundia E., Sarasua J.R. Physical aging in poly(L-lactide) and its multiwall carbon nanotube composites. *Macromolecular Symposia*. 2012;1(321-322).
- [75] Lizundia E., Sarasua J.R. Improvement of thermal degradation of PLLA/MWCNT composites by nanotube purification. *SPE EUROTEC: Barcelona*; 2011.
- [76] Tunckol M., Zuza E., Sarasua J.R., Durand J., Serp P. Polymerized ionic liquid functionalized multi-walled carbon nanotubes/polyetherimide composites. *European Polymer Journal*. 2013;49(3370-3377).
- [77] Martínez de Arenaza I., Obarzanek-Fojt M., Sarasua J. R., Meaurio E., Meyer F., Raquez J. M., Dubois P., Bruinink A. Pyrene-end-functionalized poly(L-lactide) as efficient carbon nanotube dispersing agent in poly(L-lactide): mechanical performance and biocompatibility study. *Biomedical Materials*. 2015;10(1-9).
- [78] I. Martínez de Arenaza, H. Amestoy, N. López-Rodríguez, E. Zuza, E. Meaurio, J.R. Sarasua, F. Meyer, J.I. Santos, J.M. Raquez, P. Dubois. Polylactide stereocomplex crystallization prompted by multiwall carbon nanotubes. *Journal Applied of Polymer Science*. 2013; 130(4327-4337).

- [79] Lizundia E., Oleaga A., Salazar A., Sarasua J.R. Nano- and microstructural effects on thermal properties of poly (L-lactide)/multi-wall carbon nanotube composites. *Polymer*. 2012;53(2412-2421).
- [80] I. Martínez de Arenaza, M. Obarzanek-Fojt, J. R. Sarasua, E. Meaurio, F. Meyer, J. M. Raquez, P. Dubois, A. Bruinink Pyrene-end-functionalized poly(L-lactide) as efficient carbon nanotube dispersing agent in poly(L-lactide): mechanical performance and biocompatibility study. *Biomedical Materials*. 2015; 10(1-9).
- [81] Lizundia E., Sarasua J. R., D'Angelo F., Martino S., Orlacchio A., Kenny J.M., Armentano I. Biocompatible poly(L-lactide)/MWCNT nanocomposites: morphological characterization, electrical properties and stem cell interaction. *Macromolecular Bioscience*. 2012;12(870-888).
- [82] Obarzanek-Fojt M., Elbs-glatz Y., Lizundia E., Diener L., Sarasua J.R., Bruinink A. From implantation to degradation— are poly (L-lactide)/multiwall carbon nanotube composite materials really cytocompatible? *Nanomedicine*. 2014;10(1041-1051).
- [83] Huang X., Qi X.Y., Boeyab F., Zhang H. Graphene-based composites. *Chemical Society Reviews*. 2012;41(666-686).
- [84] M. Fang, Wang K.G., Lu H.B., Yang Y.L., Nutt S. Single-layer graphene nanosheets with controlled grafting of polymer chains. *Journal of Material Chemistry*. 2010;20(1982-1992).
- [85] Zhang L., Li Y., Wang H., Qiao Y., Chen J., Cao S. Strong and ductile poly(lactic acid) nanocomposite films reinforced with alkylated graphene nanosheets. *Chemical Engineering Journal*. 2015;264(538-546).
- [86] Xie L., Xu H., Niu B., Ji X., Chen J., Li Z.M., Hsiao B.S., Zhong G.J. Unprecedented access to strong and ductile poly(lactic acid) by introducing in situ nanofibrillar poly(butylene succinate) for green packaging. *Biomacromolecules*. 2014;10(4054-4064). doi: 10.1021/bm5010993.
- [87] Sarasua J.R., López-Rodríguez N., Zuza E., Petisco S., Castro B., Del Olmo M., Palomares T., Alonso-Varona A. Crystallinity assessment and in vitro cytotoxicity of polylactide scaffolds for biomedical applications. *Journal of Materials Science—Materials in Medicine*. 2011;22(2513-2523).
- [88] Junqueira L.C., Carneiro J. In: Foltin J., Lebowitz H., Boyle P.J. editors. *Basic histology, text and atlas* (10th ed.). McGraw-Hill Companies; New York. 2003. p. 144.
- [89] Rizzi S.C., Heath D.T., Coombes A.G.A., Bock N., Texto M., Downes S. Biodegradable polymer/hydroxyapatite composites: surface analysis and initial attachment of human osteoblasts. *Journal of Biomedical Materials Research*. 2001;55(475-486).
- [90] Kasuga T., Ota Y., Nogami M., Abe Y. Preparation and mechanical properties of polylactic acid composites containing hydroxyapatite fibers. *Biomaterials*. 2001;22(19-23).

- [91] Deng X.M., Hao J.Y., Wang C.S. Preparation and mechanical properties of nanocomposites of poly (D,L-lactide) with Ca-deficient hydroxyapatite nanocrystals. *Biomaterials*. 2001;22(2867-2873).
- [92] Kothapalli C.R., Shaw M.T., Wei M. Biodegradable HA-PLA 3-D porous scaffolds: effect of nano-sized filler content on scaffold properties. *Acta Biomaterialia*. 2005;1(653-662).
- [93] Jeong S.I., Ko E.K., Yum J., Jung C.H., Lee Y.M., Shin H. Nanofibrous poly(lactic acid)/hydroxyapatite composite scaffolds for guided tissue regeneration. *Macromolecular Bioscience*. 2008;8(328-338).
- [94] Oonishi H., Oomamiuda K. Degradation/resorption in bioactive ceramics in orthopaedics. In: Black J., Hastings G.W. editors. *Handbook of Biomaterial Properties*. London: Chapman & Hall; 1998. pp. 406-419.
- [95] Wang J., Chen W., Li Y., Fan S., Weng J., Zhang X. Biological evaluation of biphasic calcium phosphate ceramic vertebral laminae. *Biomaterials*. 1998;19(1387-1392).
- [96] Rohanzadeh R., Padrines M., Bouler J.M., Couchourel D., Fortun Y., Daculsi G. Apatite precipitation after incubation of biphasic calcium phosphate ceramic in various solutions: influence of seed species and proteins. *Journal of Biomedical Materials Research*. 1998;42(530-539).
- [97] Bleach N.C., Nazhat S.N., Tanner K.E., Kellomaki M., Tormala P. Effect of filler content on mechanical and dynamic mechanical properties of particulate biphasic calcium phosphate-polylactide composites. *Biomaterials*. 2002;23(1579-1585).
- [98] Hench L.L., Splinter R.J., Allen W.C. Bonding mechanisms at the interface of ceramic prosthetic materials. *Journal of Biomedical Material Research Symposia*. 1971;5(117-141).
- [99] Rezwana K., Chena Q.Z., Blakera J.J., Boccaccini A.R. Biodegradable and bioactive porous polymer/inorganic composite scaffolds for bone tissue engineering. *Biomaterials*. 2006;27(3413-3431).
- [100] L.L. Hench. *Bioceramics*. *Journal of American Ceramic Society*. 1998;81(1705-1728).
- [101] Wilson J., Pigott G.H., Schoen F.J., Hench L.L. Toxicology and biocompatibility of bioglass. *Journal of Biomedical Material Research*. 1981;15(805-811).
- [102] Larrañaga A., Martín F.J., Aldazabal P., Palomares T., Alonso-Varona A., Sarasua J.R. Effect of bioactive glass particles on osteogenic differentiation of adipose-derived mesenchymal stem cells seeded on lactide and caprolactone based scaffolds. *Journal of Biomedical Materials Research Part A*. 2015;103(3815-3824).
- [103] Kim H.W., Lee H.H., Chun G.S. Bioactivity and osteoblast responses of novel biomedical nanocomposites of bioactive glass nanofiber filled poly(lactic acid). *Journal of Biomedical Materials Research Part A*. 2008;85A(651-663).

- [104] Zhang K., Wang Y.B., Hillmyer M.A., Francis L.F. Processing and properties of porous poly(L-lactide)/bioactive glass composites. *Biomaterials*. 2004;25(2489-2500).
- [105] Larrañaga A., Sarasua J.R. Effect of bioactive glass particles on the thermal degradation behaviour of medical polyesters. *Polymer Degradation and Stability*. 2013;98(751-758).
- [106] Larrañaga A., Petisco S., Sarasua J.R. Improvement of thermal stability and mechanical properties of medical polyester composites by plasma surface modification of the bioactive glass particles. *Polymer Degradation and Stability*. 2013;98(1717-1723).
- [107] Larrañaga A., Ramos D., Amestoy H., Zuza E., Sarasua J.R. Coating of bioactive glass particles with mussel-inspired polydopamine as a strategy to improve the thermal stability of poly (L-lactide)/bioactive glass composites. *RSC Advances*. 2015;5(65618-65626).
- [108] Ruddy A.C., McNally G.M. Annual Technical Conference – Society of Plastic Engineering. Rheological, Mechanical and Thermal Behaviour of Radiopaque Filled Polymers. 2005;63(3078–3082).
- [109] Kusiak E., Zaborski M. Composite Interfaces. Characteristic of natural rubber composites absorbing X-radiation. 2012;19(7)(433–439).
- [110] Meagher M.J., Leone B., Turnbull T.L., Ross R.D., Zhang Z., Roeder R.K. *Journal of Nanoparticles Research*. Dextran-encapsulated barium sulfate nanoparticles prepared for aqueous dispersion as an X-ray contrast agent. 2013;15(2146/1–2146/10).
- [111] Martínez de Arenaza I., Sadaba N., Larrañaga A., Zuza E., Sarasua J.R. High toughness biodegradable radiopaque composites based on polylactide and barium sulphate. *European Polymer Journal*. 2015;73(88-93).
- [112] Ouchiar S., Stoclet G., Cabaret C., Georges E., Smith A., Martias C., Addad A., Gloaguen V. Comparison of the influence of talc and kaolinite as inorganic fillers on morphology, structure and thermomechanical properties of polylactide based composites. *Applied Clay Science*. 2015;116-117(231-240).
- [113] Ouchiar S., Stoclet G., Cabaret C., Gloaguen V. Influence of the filler nature on the crystalline structure of polylactide-based nanocomposites: new insights into the nucleating effect. *Macromolecules*. 2016;49(2782-2790).

The Role of Biopolymers in Obtaining Environmentally Friendly Materials

Rodolfo Rendón-Villalobos, Amanda Ortíz-Sánchez,
Efraín Tovar-Sánchez and
Emmanuel Flores-Huicochea

Additional information is available at the end of the chapter

<http://dx.doi.org/10.5772/65265>

Abstract

Polymeric materials have had a boom in the global industry over the past two decades, because of its adaptability, durability, and price so much so that now we cannot imagine a product that does not contain it. However, many synthetic polymers that have been developed are mainly derived from petroleum and coal as raw material, which make them incompatible with the environment, since they cannot be included in what is a natural recycling system. Aware of the environmental impacts that produce synthetic polymers, a solution could be the mixtures with different types and sources of biological materials, called biopolymers, such as starch, cellulose, chitosan, zein, gelatin among others and that gradually replace synthetic polymers to address and resolve these problems. The development of new applications, such as composite materials by incorporation of alternative materials, found in nature that has similar properties to oil-based polymers, but its main feature is its biodegradability and offering competitive to current material costs. In this sense, various investigations are aimed at decreasing the amounts of plastic waste and to manufacture products with less aggressive environment since the synthetic plastics are difficult to recycle and can remain in nature for over a century.

Keywords: biopolymers, biodegradability, friendly materials

1. Introduction

Use of polymers has increased significantly over other types of materials, this more than anything because of its many possible applications, true reflection of the ease offered to the design of new compositions with very different properties.

However, conventional polymers remain subject to very specific investigations, primarily aimed at improving their properties, as well as modifications that allow the expansion of its range of applications.

That is, materials can be prepared with very different properties, for example, polymers with a great structural rigidity, due to a high proportion of aromatic structures in the molecular skeleton or flexible polymers with chains exclusively of the concatenation of aliphatic groups.

These polymers are primarily used for their advantages being chemically inert, lightweight, durable, comfortable and hygienic, and submit versatility of shape and size. It is undeniable that the introduction and advancement in the technology of synthetic polymer-based petroleum have brought many benefits to humanity.

But nevertheless, to be synthetic compounds, nonbiodegradable and based on petroleum, use poses serious ecological problems, mainly due to the environmental pollution they cause, by manufacturing and incineration as its contribution to the generation and accumulation of waste.

Since the last decades there has been a growing demand of friendly products environment, promoting the development of biodegradable materials based on biopolymers as lipids, polysaccharides, and proteins, which have been studied being renewable raw materials and inexpensive considered as an alternative to plastic nonbiodegradable and based on petroleum.

The replacement of synthetic plastics by biodegradable materials to obtain friendly products environment has not been achieved so far. However, if some synthetic polymers are replaced by other natural, in specific applications such as films, foams, covering, dishes, cups, spoons, and bags.

2. Classification of polymers

Although there are several elements that can be molecules of synthetic organic polymers, the main elements are carbon (C), hydrogen (H), oxygen (O), and nitrogen (N).

According to the process of obtaining, the polymers may be classified in to the following types:

- Synthetic polymers are obtained by polymerization processes from raw materials of low molecular weight, for example nylon, polystyrene, polyvinyl chloride, and polyethylene.
- Semisynthetic polymers are the resultant product of chemical processes of some natural polymers. Examples of these are nitrocellulose, etonita, vulcanized rubber, to name a few.

- Natural polymers obtained directly from the plant or animal kingdom, for example, cellulose, starch, protein, natural rubber, nucleic acid, chitin, lignin, among others.

Within this classification, the synthetic-based polymers have induced the accumulation of plastic in our environment, pollution sources of atmospheric, visual, and also contamination of soil and marine environments [1].

Thus, natural polymers, also known as polymers, are in complete growth, although their properties limit their applications compared to conventional polymers, but nevertheless, the market for biodegradable polymers is growing every year [2, 3] mainly by increasing access limited to nonrenewable fossil resources has contributed toward finding renewable natural sources for chemical synthesis of polymers with similar properties those based on petroleum, but its main feature is its biodegradability.

2.1. Biodegradable polymers

Biopolymers are a new generation of materials that are still in development and that have attracted attention as possible replacement-based materials of conventional plastics due to an increased interest in sustainable development [4–6].

These have been part of humanity since it exists, being that have been part of basic daily needs as fundamental as food and clothing, as well as medical materials, packaging, food additives, engineering plastics, chemicals for water treatment, among many others [7, 8].

Biopolymers used to obtain biodegradable materials have diverse provenances, such as products from vegetable origin (starches, celluloses, pectins, chitosan, zein, etc.); animal origin (casein, whey protein, and gelatin); microbial products (polyhydroxybutyrate and polyhydroxyvalerate) and chemically synthesized polymers from the monomers of natural origin (polylactic acid) [9, 10].

Natural polymers more prominent have been sugar derivatives, polysaccharides, being starch the most used and representative. This is a thermoplastic biodegradable polymer highly hydrophilic, low cost, and high availability [11]. Starch is found in a variety of tissues botanicals, including fruits, seeds, leaves, and tubers [12]. It consists essentially of a mixture of polysaccharides comprised of amylose and amylopectin and, a minority fraction (from 1 to 2%) not forming glycosidic [13]. Most starches in their glycosidic structure is made up of 20% amylose and the remaining 80% amylopectin.

Some application with this biopolymer has been its combination with synthetic polymers (such as polyvinyl alcohol, polyethylene), plasticizers (glycerin, sorbitol), nitrogenous bases, etc., to obtain a material partially biodegradable.

However, there are others polysaccharides obtained from various sources of natural resources (e.g., cellulose and chitosan) that also have been used by both its structure and its functional diversity [14].

The mixture of chitosan with aldehydes produces a harder material, biodegradable, insoluble in water and with high resistance to fats and oils [15]. Cellulose derivatives obtained by

chemical modification by esterification of glucose, such as carboxymethylcellulose (CMC), hydroxypropylcellulose, and methylcellulose (MC), are used as food additives in the case of CMC, and in the pharmaceutical industry, the MC and hydroxypropylcellulose are used in pharmaceutical tablets for sustained release of granules.

The most important sectors that are intended to the biodegradable polymers are as follows:

- Containers and bags used in stores.
- Disposables (razors, dishes, spoon, and other items).
- Electric and electronic (computers, photography).
- Automotive (internal lining, mudguards).
- Sanitary (prosthesis).
- Agricultural (plastic greenhouses).

However, the market of biodegradable polymers is an alternative market or replacement, intended to replace as a percentage of conventional materials for biodegradable materials. The demand is being generated from own production companies, appealing to a more ecological sense and responsible consumption, through the use of biodegradable materials. Nevertheless, given the evolution of the oil market with a view to 2020, it is estimated that replacement could reach almost 10% by weight, this involves managing areas for the cultivation of raw materials of which biopolymers are obtained and may present in a way as competitors in agricultural area for biofuels, livestock feed, and human food.

Even if the biopolymers are widely distributed in the nature, only limited number of plants and animals are used extensively for the production of commercial biopolymers. It points to a “exploitation” of natural resources that if not treated as a “management” of these; could become an excessive and irresponsible consumption on natural resources. So, all renewable resource must be replenished twice to meet the needs of current and future generations, and then, things that sustain life should also last in time, should be sustainable.

2.2. The role of sustainable in the use of biopolymers

The effects of pollution from nonbiodegradable plastics have been found in both terrestrial ecosystems and water, which has changed behavior, morphology and physiology of individuals, the distribution and abundance of populations, the structure of communities and dynamics of ecosystems. The increasing incorporation of these materials and its impact on the environment are due largely to having resistance to corrosion, weathering, and degradation by microorganisms.

Every year several million tons of plastic are produced in the world, for example, it has been documented that global production in 2013 increases to 299 million tons [16]. On the other hand, the deposition of plastic particles less than 5 mm has increased in the ecosystems, which may be acrylic, polyethylene, polypropylene, polystyrene, etc., and can have an impact on different levels of ecological organization having a knock-on effect and affecting biodiversity in terms of genes, species, or ecosystems.

Therefore, recent studies focus on finding new technologies to use biodegradable natural products (natural polymers), allowing replace conventional materials and significantly reduce the production and accumulation of garbage (plastic). The integrated use of natural resources as a source of conservation and recycling, becomes an excellent choice and innovation in the development of new biodegradable products.

Also, biopolymers have the characteristic of being thermoplastics and have properties similar to petroleum-based plastics. Its total biodegradation by bacteria that produce, fungi, and algae yield products such as CO₂, water and then composted is a great advantage over synthetic [17].

Biopolymers synthesized by microorganisms, polyhydroxyalkanoates (PHA), have the characteristic of being biodegradable, with physical properties similar to petroleum-based plastics (e.g., are rigid, brittle, or flexible). This has led to an increased research on studies with PHA, and it is proved by [18] Lemoigne (1926), since he documented that the bacteria *Bacillus megaterium* yields PHA and it has been that more than 300 bacteria can produce this biopolymer.

Species such as *Alcaligenes latus*, *Azotobacter vinelandii*, *Herbaspirillum seropedicae*, *Pseudomonas oleovorans*, and *Wautersia eutropha* are mostly used, because they are easily grown and can accumulate a large amount of PHA in the form of granules within the bacterial cell, and up to 90% of the biomass. Despite this, tracking new producing strains, optimization in strategies culture and the production of PHA using strains of recombinant bacteria, remains challenging to reduce production costs and increase productivity using various strategies.

With emphasis on reducing environmental degradation caused by unnatural polymers, innovation studies are performed on cultivation technologies, processing, and application. The studies focus on using plants available as side products in agriculture to obtain biopolymers, for example: *Ananas commusus*, *Hevea*, *Lycopersicon esculentum*, *Manihot esculenta*, *Opuntia ficus-indica*, *Saccharum*, *Solanum quitoense*, *Zea mayz*.

Plants are an excellent alternative in the production of biopolymers, because they can be grown in large tracts of land generating high levels of biomass, as they use sunlight as an energy source.

The disturbances caused by high levels of pollution produced by plastic are another factor that set in crisis the biodiversity of genes, species, and ecosystems on the planet. Therefore, the effort to search for new alternatives of natural polymers, which allow contaminated environments return to their state of pre-disturbance, is essential. More studies are necessary with an integrative approach to enable sustainable development, defined as “which meets the needs of the present generation without compromising the ability of future generations to provide their own needs” [19, 20]. This sustainable development is a key element for the management of natural resources [21], involving environmental, economic and social aspects.

To take a direction to the management systems of natural resources more sustainable, it is necessary to adjust the economic model with the conviction that security, the welfare, and survival of the planet depend on these changes [19]. Thus, from the 1960s, it began to start to have a sense of comprehension of serious environmental problems, and therefore, the consequences for economic and social development [19, 22], resulting several years later in the

approval of the global Earth Charter and the formation of the World Commission on Environment and Development. This commission presented in 1987 the Brundtland Report which is distinguished by describing for the first time the concept of sustainable development.

Conservation of biodiversity in the world is crucial not only in the socioeconomic and industry development of a country, but also maintain environmental stability, including the protection of water resources, flora and fauna [23]. Particularly, forest biodiversity focusing in the struggle for the sustainable conservation of biodiversity embedded in the convention on biological diversity (CBD), because the forests contain most photosynthetically active biomass and contain the greatest diversity of species in terrestrial ecosystems, in addition to providing an important source of food, medicines, energy and building materials, provides esthetic and cultural values [23].

Returning to the above, we have a disorderly growth and an imminent ecological, social and environmental imbalance, insomuch is established a direct correlation between economic growth and environmental degradation. Thus, there is a need to develop synergies between economic subsystems, social, and environmental [24].

It is necessary to have an ecological mentality and changing consumption patterns; guide efforts towards the efficient use and recycling of resources; develop more efficient technologies that mainly use renewable resources; conserve natural ecosystems and promote the participation of all social actors [21, 22, 24]. With this new model, imbalance can be handled with a holistic approach to the development [24].

Currently, there is a need to evaluating socioenvironmental system and guide actions and policies for the sustainable management of natural resources. The concept of sustainability or sustainable development is clearly on the basis of assessment of sustainability [20]. Indicators are a central element in practice the concept of sustainability. They represent a link between the theoretical development of the concept and its practical application [21].

The concept of sustainable development has gained attention locally, nationally, and internationally to guide planning and policy in the transition to the sustainable development. This performs every aspect of human life, one of which is education. Education for sustainability was recognized by the UNESCO in 1975, and today, it is found that this can help to change attitudes and behavior of people as consumers, producers, and citizens to carry out their responsibilities. Agenda 21, (Action plan proposed by the United Nations Organization), reaffirmed the importance of education for sustainability and the need to consider all social, economic, and political aspects of sustainable development, in addition to environmental protection [22].

3. Conclusions

Due to the characteristic features of biodegradability, eco-friendly manufacturing processes and its wide application ranges, biopolymers are important alternatives to unsustainable products.

Therefore, it is noted that all efforts on obtaining materials from sustainable sources, which also have a high rate of biodegradation in the environment, occupying roles, and displacing traditional plastics, are of great importance, in order to restore the environment that has been damaged so far by the indiscriminate use of synthetic polymers and prevent deterioration onwards.

But nevertheless, obtaining these biopolymers must be based on an integrated environmental perspective to increase the sustainability of materials and processes throughout its lifetime, obtaining materials from products that do not compete with traditional food sources, and also reduce dependence on non-renewable resources in long term.

Author details

Rodolfo Rendón-Villalobos^{1*}, Amanda Ortíz-Sánchez², Efraín Tovar-Sánchez² and Emmanuel Flores-Huicochea¹

*Address all correspondence to: rrendon@ipn.mx; rendonrodolfo23@gmail.com

1 National Polytechnic Institute, Center for Development of Biotic Products, Yautepec, Morelos, Mexico

2 Autonomous University of Morelos, Biodiversity and Conservation Research Center, Cuernavaca, Morelos, Mexico

References

- [1] Webb HK, Arnott J, Crawford RJ, Ivanova EP. Plastic degradation and its environmental implications with special reference to poly (ethylene terephthalate). *Polymers*. 2012;5:1–18.
- [2] O’Brine T, Thompson RC. Degradation of plastic carrier bags in the marine environment. *Marine Pollution Bulletin*. 2010;60:2279–2283. DOI: 10.1016/j.marpolbul.2010.08.005.
- [3] Ammala A, Bateman S, Dean K, Petinakis E, Sangwan P, Wong S, Leong KH. An overview of degradable and biodegradable polyolefins. *Progress in Polymer Science*. 2011;36:1015–1049.
- [4] Martucci JF, Ruseckaite RA. Biodegradable bovine gelatin/Na⁺ - montmorillonite nanocomposite films. Structure, barrier and dynamic mechanical properties. *Polymer-Plastics Technology and Engineering*. 2010;49:581–588.

- [5] Chandra R, Rustgi R. Biodegradable polymers. *Progress in Polymer Science*. 1998;23:1273–1335.
- [6] Flieger M, Kantorova M, Prell A, Řezanka T, Votruba J. Biodegradable plastics from renewable sources. *Folia Microbiológica*. 2003;48:27–44.
- [7] Hill J.W, Kolb D.K. *Chemistry for Changing Time*. 14th ed. Malaysia:Prentice Hall; 2015. 816 p.
- [8] Marsh K, Bugusu B. Food packaging-roles, materials, and environmental issues. *Journal of Food Science*. 2007;72:39–55.
- [9] Vieira MGA, da Silva MA, dos Santos LO, Beppu M. Natural-based plasticizers and biopolymer films: a review. *European Polymer Journal*. 2011;47:254–263.
- [10] Tharanathan R. Biodegradable films and composite coating: past, present and future. *Critical Review in Food Science and Technology*. 2003;14:71–78.
- [11] Cha DS, Chinnam M. Biopolymers-based antimicrobial packaging: a review. *Critical Reviews in Food Science and Nutrition*. 2004;44:223–237.
- [12] Taylor BC. Synthesizing Starch: Roles for Rugosus5 and Dull1. *The Plant Cell*. 1998;10:311–314.
- [13] French D. Organization of starch granules. In: Whistler R.L, BeMiller J.N, Paschall E.F, editors. *Starch: Chemistry and Technology*. 2nd ed. Orlando: Academic Press; 1984. p. 183–247.
- [14] Stawski R, Jantas R. Preparation and characterisation of (meth)acryloyloxystarch. *AUTEX Research Journal*. 2003;3:85–89.
- [15] Srinivasa P, Ramesh M, Kumar K, Tharanathan R. Properties of chitosan films prepared under different drying conditions. *Journal of Food Engineering*. 2004;63:79–85.
- [16] PlasticEurope. *Plastics-the material for the 21st century*. Brussels:Association of Plastics Manufactures in Europa. 2015. 34 p.
- [17] Bastioli C. Global status of the production of biobased packaging materials. *Starch/ Stärke*. 2001;53:351–355.
- [18] Lemoigne M. Products of dehydration and polymerization of β -hydroxybutyric acid. *Bulletin de la Societe de Chimie Biologique*. 1926;8:770–782.
- [19] Gómez de Segura B. From the sustainable development to sustainability as biomimesis according to Brundtland. *Hegoa*; 2014. 60 p.
- [20] Pope J, Annandale D, Morrison-Saunders A. Conceptualising sustainability assessment. *Environmental Impact Assessment Review*. 2004;24:595–616. DOI: 10.1016/j.eiar.2004.03.001.
- [21] Astier M, Masera O, Galván-Miyoshi Y. Sustainability evaluation. A dynamic and multidimensional approach. 1^a ed. SEAE / CIGA / ECOSUR / CIEco / UNAM / GIR A /

Mundiprensa / Fundación Instituto de Agricultura Ecológica y Sustentable: España; 2008. 200 p.

- [22] Martins A, Mata T, Costa C. Education for sustainability: challenges and trends. *Clean Technologies and Environmental Policy*. 2008;8:31–37. DOI: 10.1007/S 10098-005-0026-3.
- [23] Izatul W, Mohd N, Lokman M. Sustainable management of forest biodiversity and the present Malaysian policy and legal framework. *Journal of Sustainable Development*. 2012;5:76–83. DOI: 5539/jsd.v5n3p76.
- [24] Scheel C, Vazquez M. The role of innovation technology in industrial ecology systems for the sustainable development of emerging regions. *Journal of Sustainable Development*. 2011;4:197–210. DOI: 10.5539/jsd.v4n6p197.

Waste and Recycled Materials and their Impact on the Mechanical Properties of Construction Composite Materials

Gonzalo Martínez-Barrera, Nelly González-Rivas,
Enrique Viguera-Santiago, Ángel Martínez-López,
Jorge A. Tello-González and
Carmina Menchaca-Campos

Additional information is available at the end of the chapter

<http://dx.doi.org/10.5772/65433>

Abstract

In a world increasingly fixated on the demands of sustainable development, too much attention has been focused on the widely used building materials, mainly on those tools and strategies for their reuse and those characteristics for considering them as environmental-friendly materials. Among the strategies are the following: (a) increased reliability on waste and recycled materials—such action will have to incorporate the substitution of recycled for virgin materials; (b) improved durability through reduction of materials needed for their replacement; and (c) improved mechanical properties, which reduces the use of raw materials. Extensive research and development activities in recycling composite materials have been conducted, and various technologies have been developed: (a) mechanical recycling, (b) thermal recycling, and (c) chemical recycling. However, gamma radiation is an innovative and clean technology, alternative to conventional recycling procedures. Gamma irradiation has proved to be an adequate tool for modifications of the physicochemical properties of polymers, through different effects: (a) scission, branching as well as cross-linking of polymer chains and (b) oxidative degradation. Moreover, the reuse and recycling of waste materials and the use of gamma radiation are useful tools for improving the mechanical properties of concrete. In this chapter, we show results of the effects of gamma irradiation on the physicochemical properties of waste and recycled materials and their reuse to enhance the properties of construction composite materials.

Keywords: waste, recycled materials, composite materials, mechanical properties, gamma radiation

1. Introduction

In recent years, due to high demand of construction materials, some actions have been developed such as extraction of large amounts of raw materials, development of new materials, use of recycled and demolition waste; all of them generating higher costs and environmental problems. Special attention on the development of economic and ecological materials through the use of waste materials has generated a novel research area. Moreover, in order to reduce the ecological impact, many efforts have been made for reducing the consumption of nonrenewable resources in the production of construction materials, one of these is the production or addition of waste or recycled materials into the mixture in substitution of the common mineral aggregates, taking care of the final quality that includes parameters such as resistance, modulus of elasticity, and durability, among others.

Although some advantages are obtained when adding waste or recycled materials for improvement of the toughness of construction materials, they present some disadvantages such as lower values on the compressive strength, which should be attended. One alternative is the use of gamma radiation. Recent works have studied the effects of gamma radiation on compressive properties; in one of them, the results show more resistance to crack propagation; moreover, compressive strain and the elasticity modulus depend on the combination of the particle sizes and the radiation dose. This chapter attempts to use gamma irradiation as modifier of the physicochemical properties of waste and recycled materials, and use them as reinforcements of construction composites and as a consequence improve their mechanical properties. This chapter promotes the use of waste and recycled materials in the construction industry, as one alternative for reducing environmental pollution.

2. Waste and recycling materials in the research area of construction

Discovered and patented in England in 1941, polyethylene terephthalate (PET) has been used in the packaging industry for a broad range of applications. Annual average consumption per person of 234 l of bottled water is reported. As it has become a widely used material, all disposed bottles are actually a serious environmental issue. Pollution caused by PET bottles includes not only the final disposal of them, but also the by-products obtained during PET fabrication process. Plastic bottles take centuries to decompose and if they are incinerated, toxic by-products, such as chlorine gas and dioxins, are released into the atmosphere. Solid handles of materials have experienced an important impact because of the nonbiodegradability nature of PET. The world consumption of PET is about 15 million tons, of which 3.5 million tons are used in the manufacture of packaging materials, including jars and bottles.

Two methods for recycling of polyethylene terephthalate (PET) bottles are mechanical process and chemical process. (1) Mechanical process includes three well-defined stages such as separation, washing, and grinding. The recycled PET is used for elaborated laminates, metal sheets, and food and nonfood packages. Moreover, recycled PET flakes can be directly employed to elaborate pellets in the creation of products by injection or extrusion. (2) Chemical process consists of separation of the basic components or monomers. The methanolysis, glycolysis, and hydrolysis are the elemental processes to achieve this transformation.

PET can be recycled many times and can be used in a variety of products, such as fibers for clothes, fiberfill for bags, or industrial strapping. One interesting alternative to recycled PET materials consists of using them as a substitute of concrete aggregates; in this, silica sand is partially substituted by waste PET particles. The main goal is improvement of mechanical properties, including compressive strength, deformation, and modulus of elasticity. Demand of technological development in different construction areas makes possible the generation of alternative materials that can be applied with increasing functionality, low costs, and better physical, chemical, and mechanical properties than conventional materials. Fiber-reinforced concrete, in which new materials are applied in order to obtain more efficient crack-resistant concrete, is an important research field these days. PET has been widely used to produce fibers, particles, or flakes to obtain cement-based products with improved properties.

Different kinds of fibers have been used in the concrete, including steel, glass, carbon, nylon, polyester, propylene, among others; however, in order to reduce the environmental impact of industrial or postconsumer waste, recycled fibers have been used. They offer advantages in reducing waste and conserving resources.

Another waste with potential applications in different technological areas is that related with the automotive tires. The typical components of automotive tires are synthetic and natural elastomers, sulfur and its compounds, phenolic resins, oils, and steel wires among others; while zinc oxide, titanium dioxide, and carbon black are used as pigments. Moreover, manufactured tire includes: synthetic elastomers (27%), natural elastomers (14%), carbon black (28%), steel (15%), as well as fabric, infill materials, accelerators, and anti-ionizer (16%) [1, 2].

The most common method to dispose waste tires is to burn them for vapor, heat, or electricity. The usage of waste tires as alternative fuel in cement furnaces is generalized across the U.S. and Europe. However, these practices result in the generation of organic and inorganic compounds such as zinc oxide (ZnO) and zinc sulfide (ZnS), in hydrocarbon gas, aromatic volatile compounds, and liquids formed by heavy and light oils, all these by-products which are highly polluting.

Recycling of automotive tire includes reuse in plastic and rubber products as well as alternative fuel in cement furnace or as material in the carbon black production. Another approach for the application of waste tires includes hot bituminous mixes as pneumatic dust for the agglutinative modification in asphalt pavements. This application has been more or less effective, but not enough for reducing the reserves of waste tires, since these novel technologies are more expensive than conventional methods. Moreover, components of the recycled waste tires have been used in the construction industry, for example: (a) waste steel fibers as mechanical

reinforcement of concrete [3] and (b) recovered rubber as replacement of natural aggregates (fine and coarse), in which the elasticity features are improved and a lower diminution on the compressive strength and brittleness values is found [4–6]. In general, use of them as a substitute of fine or coarse aggregate can improve mechanical properties of concrete such as strength and modulus of elasticity, instead of those achieved by sand or stone.

Addition of particles into concrete produces internal stresses, which promote sooner cracking and subsequent failure, which can be avoided with the control of the particle sizes. Early studies pointed out that those elastomeric particles can reduce propagation of cracks, show increment in tensile strength, and have capacity in energy absorption. One advantage of the rubber particles is concerning energy absorption through ultrasonic waves, in order to benefit the concrete elasticity. However, differences in the values of Young's modulus between rubber particles and concrete matrix, besides concentration of rubber particles into concrete, could promote great deformations when applying loads and thus results in progressive diminution of the mechanical properties. Other properties of concern for concrete workability include diminution of slump and increment of air content when increasing the elastomeric concentration, which promotes a low unit weight.

Tetra Pak is an aseptic packaging material, elaborated of several laminated layers of three raw materials: paper (75%), low-density polyethylene (20%), and aluminum (5%). The barriers consist of six layers of these materials. After recycling Tetra Pak packages through hydropulping process, cellulosic fibers are recuperated, which have superior quality when compared to those found in the waste paper market. Moreover, they are used in the production of tissue and paper towels. Percentage of recovery of the Tetra Pak components in a separate way shows 63 wt% for paper, 30% for polyethylene, and 7% for aluminum.

Recycling of these materials is based on mechanical milling and chemical attack, from which it is possible to obtain size reduction and component separation. In the case of the cellulosic fibers, the surface energy is closely related to the hydrophilicity of the fiber. Another important parameter is concerning reduction of the moisture adsorption of cellulose fibers, which are involved in reduction of the number of cellulose hydroxyl groups and the hydrophilicity of the fiber's surface, as well as restraint of the swelling of the fiber. Moreover, degradation produces water-soluble or insoluble oxygenated compounds.

Cellulose is the most abundant, inexpensive, and readily available carbohydrate polymer in the world, traditionally extracted from plants or their wastes. Currently about 30 million tons of natural fibers are produced by year around the world. The current interest for using such fibers is based on the environmental preservation; there is great interest for replacing synthetic fibers for natural ones [7, 8]. However, due to environmental problems caused by products made using cellulose (boxes, bags, containers, office supplies, etc.), different ways to recycle those materials have been developed.

Some natural fibers are composed mainly of cellulose (54%), hemicellulose (20%), and lignin (15%). Natural fibers are a resource that is environmentally clean, renewable, and biodegradable; one of them that has captured attention in applied research is Luffa fiber, due to its physicochemical properties. They are obtained from a subtropical plant of the Cucurbitaceae

family, which produces a fruit with a fibrous vascular system (luffa), with sizes between 1.5 cm and 1.5 m and an average diameter 8–10 cm [9]. Their morphological surfaces show roughness surfaces, containing width channels (4–12 μm), and particles with different lignin shapes (indicated by arrow), and thin layers of lignin and hemicellulose covering the cellulosic fibers (Figure 1).

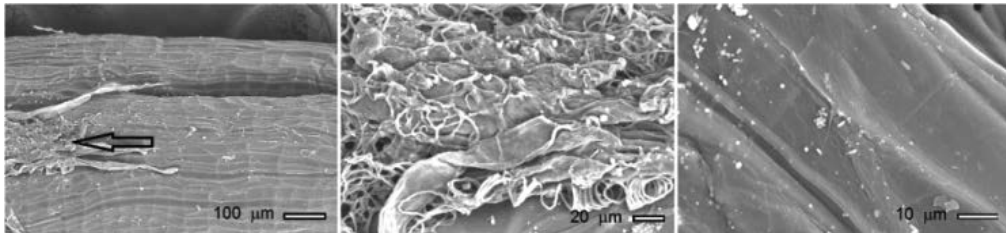


Figure 1. Morphological surfaces of Luffa fibers.

One of the main characteristics of raw luffa fibers (without surface treatment) is its capacity to absorb moisture easily and its high potential as reinforced material in hybrid composites, mainly on the mechanical properties. In the case of Tetra Pak packaging, an optional recycling way for this is based as a substitute of mineral aggregates in the elaboration of composite materials, which improving its properties, including lower weight and density, higher mechanical strength and toughness [10].

Some investigations are concerning use of natural fibers, such as cellulose, for elaboration of composite materials. Different thermosetting polymers, namely polymeric resins, have been used for such purpose. The main idea is to use inexpensive and abundantly available fibers. Mechanical properties, including tensile strength, flexural strength, compressive strength, and wear resistance, increase their values when increasing the concentration of the cellulosic fibers. Moreover, the impact properties significantly increase. Such behavior is due to an excellent dispersion of the reinforcements. But for higher content of fibers, decrement on the values is observed; this is due to agglomeration of the fibers. Composite elaborated with cellulose fibers has light weight. Surface modification of the cellulose fibers facilitates elaboration of composites. Silane and alkali treatments are used for such proposal, having higher fiber-matrix adhesion strength. Moreover, reduction of water absorption is observed, as a consequence of the strong interface. Another treatment is referred to coupling agents; the presence of double bonds is necessary to obtain the formation of covalent bonds between fiber and matrix. Residue cellulose can act as a natural coupling agent and improve the interfacial bonding by reducing the hydrophilicity of the fiber. The water absorption increases with an increase in fiber content. Moreover, fibers can be further subdivided into microfibrils with high elastic modulus by hydrolysis, followed by mechanical disintegration. Such fibers are produced commercially by the pulp and paper industry.

3. Structural modification by using gamma irradiation

As it is known that environmental problems caused by waste materials are in a constant growth and as a consequence different methods have been developed, some of them are consuming money and time. One novel alternative is to use ionizing radiation, such as gamma rays.

Gamma radiation has many advantages over other conventional methods such as chemical attack or thermal process. For example, initiation process is different; gamma particles only are necessary if that material is in contact with radioactive source, while in a chemical reaction, catalysts or additives are required; another important aspect is referred to the production of free radicals, when using chemicals these are produced through decomposition of the initiator in fragments, while in the case of irradiation process free radicals are produced by the absorption of energy of the polymer; moreover, with irradiation process the reaction can be controlled and be free from contamination. With respect to the temperature, gamma irradiation shows better behavior, because in the case of a chemical reaction often local overheating of the initiator is produced, while for irradiation no activation energy is found [11–13].

Applying gamma radiation for recycling polymers has increased its acceptance as a current technology due to the ecologic and economical features and mainly its capacity to modify physicochemical properties of the wastes without introducing any chemical initiators or the need to dissolve them [14]. In principle the molecular structure of materials can be modified by using gamma irradiation; this creates free radicals which will often chemically react in various ways, sometimes at slow reaction rates. The free radicals can recombine, forming the cross-links.

A competing process, called scissioning, occurs when polymers are irradiated. In this case, the polymer chains are broken and molecular mass decreases. The other process is called cross-linking, which depends on kind of polymer, and the number of cross-links can be controlled by the amount of irradiation dose. Scissioning and cross-linking occur at the same time where one may predominate over the other, depending upon the polymer and the dose. Both phenomena change the physical, chemical, and mechanical properties of polymer materials. In fact, more benefits can be obtained from recovered scrap polymer cross-linking by using gamma radiation [15, 16].

In the case of polyethylene terephthalate (PET), different opinions about radiation stability have been reported. Some authors report fair stability in the mechanical and physicochemical properties at high doses (900 kGy), with changes from cross-linking processes up to 35% from the starting values. Some authors have reported changes due to the chain scission process at low dose (from 0 to 10 kGy) while others have reported such events at a high dose (from 120 kGy to 5 MGy). The degradation mechanism for PET fibers or PET bulk is the same. No chemical degradation for PET fibers is found up to 200 kGy [17–20].

The recycling and reutilization of cross-linked elastomers are difficult due to their 3D formed network; nevertheless, it is necessary to find wise-strategies for reuse and to avoid ground contamination. The natural and synthetic rubbers such as styrene-butadiene-styrene (SBS) and

styrene-butadiene-rubber (SBR) are the raw materials in the production of tires; the natural rubbers provide elastic properties while the synthetics provide thermal stability.

In the case of elastomers (such as tire rubber), gamma radiation causes morphological deterioration and chemical changes, including accelerated oxidation [21]. Physicochemical properties of blends of rubber stocks and virgin or recycled elastomers are improved after irradiating with gamma particles. For example, rubber stocks blended with recycled and irradiated butyl crumb show shortened vulcanization period and antitearing properties. Moreover, improvement on the plasticity of crumb rubber, as well as great moldability of virgin rubber and recycled crumb blends, when they are irradiated at 70 kGy.

Vulcanization of chlorine butyl rubbers by using gamma radiation decreases the tensile strength and elongation-at-break up to 25 kGy, but after this dose, stability of such properties is observed, up to 200 kGy. Moreover, thermal stability is reduced through the degradation and scission of molecular chains [22]. Other study is based on the effects of gamma irradiation in polydimethylsiloxane rubber foams and their relationship with mechanical properties and chemical structure, which are measured by compression strength, infrared attenuated total reflectance (ATR) spectroscopy and X-ray-induced photoelectron spectroscopy (XPS). The results show a higher cross-linking of polymer chains when increasing the irradiation dose, thus foams became harder [22].

By using gamma radiation, ground tire rubber (GTR) and recycled high-density polyethylene (HDPE) blends can be functionalized through higher interaction between elastomer and acrylamide functional groups, allowing improvement of their mechanical properties for doses from 25 to 50 kGy. Elongation-at-break and Charpy impact strength of the blends are significantly increased due to the presence of GTR; moreover, blends' Young's modulus values are only slightly decreased due to the radiation-induced cross-linking of the HDPE matrix [22, 23].

The use of gamma radiation as a mechanism for reaction initiation and accelerator of the polymerization of a monomer in a ceramic matrix can bring considerable advantages. One of the most important objectives is to obtain higher adhesion between fibers and the matrix. In the case of the Tetra Pak components, the first investigations focused on the influence of gamma radiation on lignocellulose materials, in terms of increasing the solubility of insoluble high-polymerized sugars such as cellulose. Application of gamma irradiation on cellulose results in decrease in molecular weight and crystallinity, as well as formation of oxidation products, because cellulose is a predominantly chain-scissioning polymer. After irradiation, changes in the main chain of the cellulose are observed, where radicals provoke random cleavage of glycoside bonds, as well as splitting of carbon-bonded hydrogen and dehydrogenation reactions. Another studied parameters are the degree of polymerization (DP) and specific gravity. Such changes are beneficial for manufacturing products such as medical grade cellulose.

As it is known, the cross-linking reaction is affected by the initial degree of crystallinity, crystal size distribution, and molecular weight. In general terms, crystallinity increases and reaches a maximum at certain irradiation dose, but it decreases on further increase of irradiation dose. Microfibrils are composed of cellulose crystals and amorphous zones, in which more pene-

tration of chemicals is observed. Such zones have different appearances such as cracks and irregular morphological shapes.

Tetra Pak panel boards (TPPBs) show decrease in the mass up to 200°C which is related to the evaporation of physical water. In general, thermal degradation of paper is located between 200°C and 400°C, particularly two decomposition peaks are observed. The first one at 300°C due to hemicellulose and the second at 360°C due to thermal degradation of α -cellulose. For higher temperature from 400°C to 461°C, degradation of remaining paper and LDPE is considered. After thermal process can be found two kinds of residues, char and aluminum foil [24].

In the case of irradiated polyester resin some physicochemical properties are affected, for example, when increasing the dose a better thermal stability is obtained at low temperatures, because its glass transition temperature increases. But at high temperatures, the decomposition temperature is unaffected. After analyzing both thermal and mechanical properties a relationship is observed. Moreover, a typical behavior is observed: improvement of the compressive strength depends on the increment of the irradiation dose [23].

4. Modified waste and recycled materials and their uses in construction materials

In this section different studies concerning the structural modification of waste and recycling materials by using ionizing irradiation and their possibilities as reinforced materials of hydraulic and polymer concrete are shown.

For recycled PET, nonirradiated concrete follows a typical behavior for compressive strain: it increases progressively as PET particle concentration increases, but it does not happen for compressive strength or elasticity modulus. In the case of irradiated concrete, different behaviors are observed regarding nonirradiated ones. When increasing PET concentration, the compressive strength values diminish; it is more notable: the diminution of compressive strain. In general, irradiated concrete containing PET particles had similar modulus of elasticity, higher compressive strength, and lower compressive strain values compared to nonirradiated concrete.

Compressive strength and Young's modulus of concrete specimens containing waste PET particles of beverage bottles were evaluated before and after irradiation. Three different sizes of waste PET particles (0.5, 1.5, and 3.0 mm) were considered, and for each size, three different concentrations of waste PET particles were used (1.0, 2.5, and 5.0% by volume). Concrete specimens after 28 days of moist curing were irradiated at 100 kGy with gamma rays at 3 kGy/h ratio.

In the case of irradiated concrete, different behaviors are observed regarding nonirradiated ones. When increasing PET concentration, the compressive strength values diminish; it is more notable: the diminution of compressive strain. Nevertheless, elasticity modulus has an opposite behavior to that shown for nonirradiated concrete. In terms of the particle sizes,

different behaviors are observed; at the lowest sizes, compressive strength has minimal values; whereas for highest sizes, both compressive strength and modulus of elasticity have the maximal values. Such situations are similar for irradiated specimens because modulus of elasticity, higher compressive strength, and lower strain values are maximal.

Irradiation effects are caused over PET particles, as it is well known that irradiation causes chain scission and generation of free radicals, which can produce a hard material instead of a ductile. In the case of irradiated PET particles (at 150 kGy), a smooth and homogeneous surface is observed (**Figure 2**); when increasing the irradiation dose, morphological changes are produced; small particles and cracks are observed (at 400 kGy). For the highest irradiation dose, more defined cracks and particles of different sizes are observed (at 800 kGy); in general, a roughness surface is obtained (**Figure 2**).

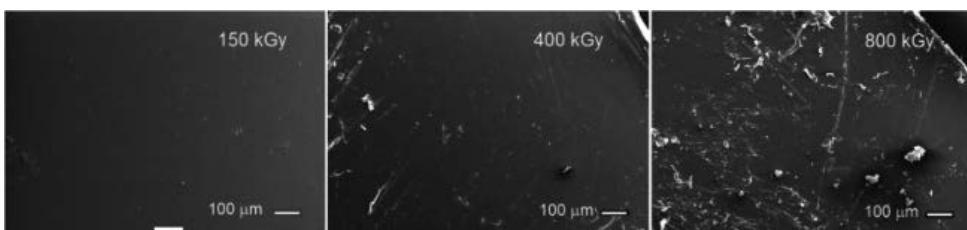


Figure 2. SEM images of irradiated PET at different application doses.

Generally speaking, as waste PET concentration increases in the concrete specimens, a decreasing tendency on the mechanical properties is observed. Moreover, irradiated concrete specimens show higher compressive strength values, similar elasticity modulus values, but lower deformations when compared to nonirradiated specimens.

Some studies covered the effects of gamma radiation on composite materials, for example, on the mechanical properties and durability of cement concretes. Some applications include concrete as material for nuclear power reactors; for this purpose, the specimens were submitted to dosages from 227 and 470 MGy with a dose rate of 5.0 kGy/h. The results show a diminution of about 10% on the elastic and tensile properties, as well as loss of weight, caused by one or more of the following mechanisms: (a) “natural” drying (including gamma heating); (b) radiolysis-induced accelerated drying (where large gas is released); (c) radiolysis-induced carbonation; and (d) degradation of the calcium-bearing cement hydrates.

In hydraulic concrete where silica sand is partially replaced by recycled automotive tire fibers. Both tire fibers and modified concrete are irradiated at different gamma doses. Main mechanical properties are studied before and after irradiation process. These include compression and flexural strength. The mechanical properties of concrete depend on the waste tire particle sizes and their concentration. Compressive and tensile strength values decrease due to waste tire particles, because they promote stress concentration zones, as well as, generation of tensile stresses into concrete, resulting in a fast cracking and soon failure. Nevertheless, when applying gamma radiation to waste tire particles, in some cases, improvements on mechanical

properties are found. Concrete with irradiated particles can be support up to 30% of tire particles, making possible to reduce the final cost of the concrete.

In the case of polymer concrete with recycled tire fibers, strength and strain results show improvements of mechanical properties according to the tire fiber concentration as well as gamma irradiation dose. In general terms, addition of recycled tire fibers as well as higher radiation doses generate greater ductility on the polymer concrete; features no common for ordinary polymer concrete.

In **Figure 3**, surface characteristics of the recycled tire particles are shown. Nonirradiated particles have different sizes; some of them show roughness on their surface and others smooth surfaces. Average size of recycled particles varies from 30 to 600 μm . In general, when recycled particles are added to concrete, a poor elastomer-matrix adherence is found, but when increasing the volume fraction of particles, mechanical interactions are augmented, therefore improvements on the mechanical properties are obtained. For irradiated tire particles, at 200 kGy, rough surfaces are created, with some small and disperse particles. According to the literature, sometimes smooth surfaces are generated after irradiation as a consequence of the cross-linking of polymer chains, while for higher dose, scissions of the polymer chains are done, which is manifested by appearances of cracks on the surfaces; as it is shown for irradiated particles at 250 kGy (**Figure 3**).

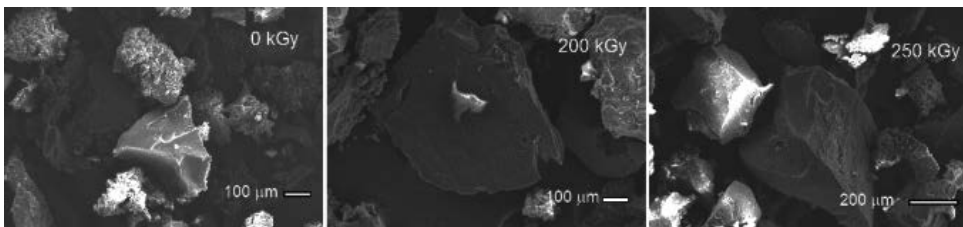


Figure 3. SEM images of nonirradiated and irradiated tire rubber.

In polymer concrete elaborated with polyester resin and silica sand; partial replacement of the silica sand by recycled tire fibers at concentration from 0.3 to 1.2% in volume, was done. Such concrete was submitted to gamma rays at doses from 50 to 100 kGy, and studied its mechanical properties, including compression and flexural strengths, as well as elasticity modulus. The results show noticeable improvements on the mechanical deformation, which are related with morphological and structural changes of the recycled tire fibers.

The effects of gamma irradiation on the compressive properties of polymer concretes show that the compressive strain and the elasticity modulus depend on the particle sizes used and the applied radiation dose; in particular, more resistance to crack propagation is obtained. In studies based on two parameters, use of recycled polymers and gamma radiation shows that: (a) polymer concrete with recycled high-density polyethylene (HDPE) and tire rubber particles, irradiated from 25 to 50 kGy, has significant increase on the impact strength as well as in the elongation-at-break; such improvements are attributed to the good adhesion between

tire rubber particles and the polymer matrix [21]; (b) polymer concrete with waste tire rubber and styrene-butadiene-rubber (SBR) improves its tensile strength, elongation, and heat resistance up to 75 kGy [25].

In some experiments, waste Tetra Pak particles obtained from trash beverage bottles are used as reinforcements in polymer concrete; they partially substitute the mineral aggregates. The effects of the concentration and size of them on the compressive and flexural strength of polymer concrete are evaluated. The results show that the compressive and flexural strength as well as modulus of elasticity values decreases gradually when increasing the addition of waste particle concentration. A slight increment on the flexural strength values is observed for polymer concrete with smallest particle size. It is convenient to mention that to improve the mechanical properties of polymer concrete, gamma irradiation has been an adequate tool, because this improves the interfacial interaction between polymer concrete and Tetra Pak particles. However, improvements in compressive and flexural strength, as well as modulus of elasticity, when irradiating the concrete specimens, are observed.

Through SEM images the influence of gamma radiation on waste cellulose obtained from Tetra Pak packaging and its effect on the mechanical properties of concrete can be observed. As it is appreciated, a smooth and homogeneous surface, as well as agglomerations of particles is appreciated for polymer concrete. There are no chemical interactions between polyester resin and waste cellulose particles, and as a consequence, decrements of mechanical properties can be observed (**Figure 4**). For irradiated polymer concrete, deformation decreases which can be attributed to the stress transfer between polymer matrix and waste cellulose particles. The greater contact area between the particles and the concrete matrix, thus the greater stress transfer; moreover, rough surface and irregular distribution of the particles are observed (**Figure 4**).

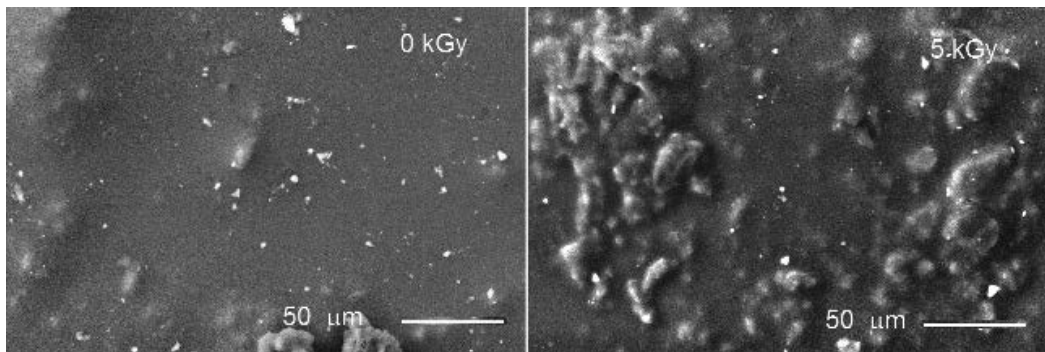


Figure 4. SEM images of nonirradiated and irradiated polymer concrete.

The effects of the concentration of Tetra Pak` particles as mechanical reinforcements and gamma irradiation as a tool for improvement of interfacial coupling in polyester-based composite are evaluated. The main proposal is to find a material with improved ductility, that is, with more elasticity instead of a rigid property. After irradiation, the deformation increased

substantially, having a maximum value at 400 kGy when compressive evaluation is done; while for flexural test, maximal deformation is obtained at 500 kGy. Such improvements are due to the cross-linking and degradation processes in both cellulose and polyester resin.

In the case of polymer concrete for improvement of the interfacial surface, gamma irradiation is a novel proposal. As it is known that in a composite material only physical interactions are present between matrix and aggregates, nevertheless, by using gamma irradiation, chemical bonds can be obtained [26]. In **Figure 5**, the irradiation process in the polyester resin causes chain scission and it also produces some cross-linking, chain relaxation, and cage breaking. As a consequence, the formation of bonds into polymer chains increases the degree of polymerization of the resin matrix. Homogenous surface is affected by gamma radiation because a higher number of chemical bonds are established and a rougher surface is observed (**Figure 5**), and for higher radiation dose, voids and small particles created from the cross-linking of the resin are observed. One can achieve good control of the dimensions and the elimination of internal stress, which cause reduction in mechanical strength [27, 28].

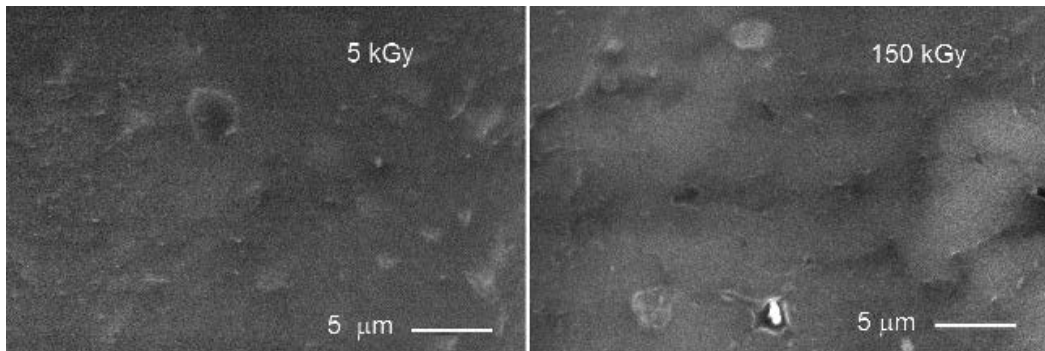


Figure 5. SEM images of irradiated polyester resin.

Other studies show different behaviors, for example: (a) molecular defects on mineral aggregates such as calcium bentonite have been observed [29]; (b) compressive strength values increased while total porosity and water absorption values decreased with increasing irradiation dose, in polymer-modified cement mortar specimens, with styrene-acrylic ester as adding polymer [30]; and (c) improvement on mechanical properties such as compressive strength and Young's modulus was observed for concrete reinforced with polypropylene fibers [31].

5. Conclusions

The main aim of this chapter is to show how both waste and recycled materials as well as gamma irradiation are adequate tools for improvement of mechanical properties of construction composites. Such materials are reused to replace partially those component concrete

materials, such as mineral aggregates. Gamma irradiation is an adequate tool for modification of the physicochemical properties of waste and recycling materials. Moreover, such modified materials act as reinforcements of concrete and as a consequence improve their mechanical properties, through the improvement of interfacial interaction between the matrix and waste or recycled materials. Mechanical properties include compressive and flexural strength, and Young's modulus among others. In general, the results are depending on the particle sizes and concentrations of waste or recycled materials, as well as on irradiation and ratio doses. We believe that this kind of work opens several possibilities in research area of construction with great benefits, in order to ensure economic earnings in the context of sustainable development, by solving environmental pollution problems. Moreover, a simple and inexpensive process based on gamma irradiation is expected.

Acknowledgements

Financial support of the Autonomous University of the State of Mexico (UAEM), located at Toluca City, is acknowledged.

Author details

Gonzalo Martínez-Barrera^{1*}, Nelly González-Rivas², Enrique Vigueras-Santiago¹, Ángel Martínez-López¹, Jorge A. Tello-González¹ and Carmina Menchaca-Campos³

*Address all correspondence to: gonzomartinez02@yahoo.com.mx

1 Laboratory of Research and Development of Advanced Materials (LIDMA), College of Chemistry, Autonomous University of the State of Mexico, Toluca-Atlacomulco, San Cayetano, Mexico

2 Joint Center of Research in Sustainable Chemistry (CCIQS) UAEM-UNAM, Toluca-Atlacomulco, San Cayetano, Mexico

3 Center of Research in Engineering and Applied Sciences (CIICAp), Autonomous University of the State of Morelos, Cuernavaca Morelos, México

References

- [1] Siddique R, Naik TR, Properties of concrete containing scrap-tire rubber – an overview. *Waste Management*. 2004; 24: 563-569.

- [2] Fattuhi NI, Clark LA, Cement-based materials containing shredded scrap truck tyre rubber. *Construction and Building Materials*. 1996; 10: 229-236.
- [3] Aiello MA, Leuzzi F, Centonze G, Maffezzoli A. Use of steel fibres recovered from waste tyres as reinforcement in concrete: pull-out behaviour, compressive and flexural strength. *Waste Management*. 2009; 29: 1960-1970.
- [4] Mohammed BS, Anwar Hossain KM, EngSwee JT, Wong G, Abdullahi M. Properties of crumb rubber hollow concrete block. *Journal of Cleaner Production*. 2012; 23: 57-67.
- [5] Pelisser F, Zavarise N, Longo TA, Bernardin AM. Concrete made with recycled tire rubber: effect of alkaline activation and silica fume addition. *Journal of Cleaner Production*. 2011; 19 (6): 757-763.
- [6] Bravo M, de Brito J. Concrete made with used tyre aggregate: durability related performance. *Journal of Cleaner Production*. 2012; 25: 42-50.
- [7] Altinisik A, Gur E, Seki Y. A natural sorbent, *Luffa cylindrica* for the removal of a model basic dye. *Journal of Hazardous Materials*. 2010; 179: 658-664.
- [8] Ghali L, Aloui M, Zidi M, Bendaly H, Msahli S, Sakli F. Effect of chemical modification of *luffa cylindrica* fibers on the mechanical and hygrothermal behaviours of polyester/*luffa* composites. *BioResources*. 2011; 6: 3836-3849.
- [9] Zaska OC. Unsaturated polyester and vinylester resins. In: Goodman SH, editor. *Handbook of Thermoset Plastics*. USA: Noyes Publications; 1986. p. 59-111.
- [10] Ávila Córdoba L, Martínez-Barrera G, Barrera Díaz C, Ureña Nuñez F, LozaYañez A. Effects on mechanical properties of recycled-PET in cement-based composites, *International Journal of Polymer Science*. 2013; 2013: p.6, Article ID 763276, DOI: 10.1155/2013/763276
- [11] Cruz-Zaragoza E, Martínez-Barrera G. Ionizing radiation effects on the matter and its applications in research and industry. In: Barrera-Díaz C., Martínez-Barrera G., editors. *Gamma radiation effects on polymeric materials and its applications*. Kerala, India: Research Signpost; 2009. p. 1-14
- [12] Dobo J. Some features of radiation processing in the plastics industry. *Radiation Physics and Chemistry*. 1985; 26: 555-558.
- [13] Clough RL. High-energy radiation and polymers: a review of commercial processes and emerging applications. *Nuclear Instruments and Methods in Physics Research Section B*. 2001; 185: 8-33.
- [14] Martínez-Barrera G, Menchaca-Campos C, Barrera-Díaz CE, Avila-Cordoba LI. Recent developments in polymer recycling. In: Istvan Bikit, editor. *Gamma Rays: Technology, Applications and Health Implications*. Hauppauge NY, USA: Nova Science Publishers Inc.; 2013, p. 237-255.

- [15] Burillo G, Clough RL, Czvikovszky T, Guven O, Le Moel A, Liu W, Singh A, Yang J, Zaharescu T. Polymer recycling: potential application of radiation technology. *Radiation Physics & Chemistry*. 2012; 6: 41-51.
- [16] Dispenza C, Alessi S, Spadaro G. Carbon fiber composites cured by γ -radiation-induced polymerization of an epoxy resin matrix. *Advances in Polymer Technology*. 2008; 27: 163-171.
- [17] Burillo G, Tenorio L, Bucio E, Adem E, Lopez GP. Electron beam irradiation effects on poly(ethylene terephthalate). *Radiation Physics & Chemistry*. 2007; 76: 1728-1731.
- [18] Mariani M, Ravasio U, Consolati G, Buttafava A, Giola M, Faucitano A. Gamma irradiation of polyethylene terephthalate and polyethylene naphthalate. *Nuclear Instruments and Methods in Physics Research Section B*. 2007; 265: 245-250.
- [19] Razek TMA, Said HM, Khafaga MR, El-Naggar MAW. Effect of gamma irradiation on the thermal and dyeing properties of blends based on waste poly(ethylene terephthalate) blends. *Journal of Applied Polymer Science*. 2010; 117: 3482-3490.
- [20] Shiv-Govind P, Abhijit D, Udayan D. Structural and optical investigations of radiation damage in transparent PET polymer films. *International Journal of Spectroscopy*. 2011; 201: 1-7.
- [21] Sonnier R, Leroy E, Clerc L, Bergeret A, Lopez-Cuesta JM. Compatibilisation of polyethylene/ground tyre rubber blends by γ irradiation. *Polymer Degradation and Stability*. 2006; 91: 2375-2379.
- [22] Sui HL, Liu XY, Zhong FC, Li XY, Wang L, Ju X. Gamma radiation effects on polydimethylsiloxane rubber foams under different radiation conditions. *Nuclear Instruments and Methods in Physics Research B*. 2013; 307: 570-574.
- [23] Fainleib A, Grigoryeva O, Martínez-Barrera G. Radiation induced functionalization of polyethylene and ground rubber for their reactive compatibilization in thermoplastic elastomers. In: Barrera-Díaz CE, Martínez-Barrera G, editors. *Gamma Radiation Effects on Polymer Materials and its Applications*. Kerala, India: Research Signpost; 2009, p. 63-85.
- [24] AyselK F, Evren T, Nural Y, Saip NK, Sabriye PK. Thermal degradation characteristic of Tetra Pak panel boards under inert atmosphere. *Korean Journal of Chemical Engineering*. 2013; 30: 878-890.
- [25] Yasin T, Khan S, Shafiq M, Gill R. Radiation crosslinking of styrene-butadiene rubber containing waste tire rubber and polyfunctional monomers. *Radiation Physics and Chemistry*. 2015; 106: 343-347.
- [26] Martínez-Barrera G, Giraldo LF, López BL, Brostow W. Effects of gamma radiation on fiber-reinforced polymer concrete. *Polymer Composites*. 2008; 29: 1244-1251.

- [27] Bobadilla-Sánchez EA, Martínez-Barrera G, Brostow W, Datashvili T. Effects of polyester fibers and gamma irradiation on mechanical properties of polymer concrete containing CaCO₃ and silica sand. *eXPRESS Polymer Letters*. 2009; 3: 615-620.
- [28] Menchaca C, Alvarez-Castillo A, Martínez-Barrera G, López-Valdivia H, Carrasco H, Castaño VM. Mechanisms for the modification of nylon 6,12 by gamma irradiation. *International Journal of Materials and Product Technology*. 2003; 19: 521-529.
- [29] Dies J, de las Cuevas C, Tarrasa F, Miralles L, Pueyo JJ, Santiago JL. Thermoluminescence response of heavily irradiated calcic bentonite. *Radiation Protection Dosimetry*. 1999; 85: 481-486.
- [30] Khattab MM. Effect of gamma irradiation on polymer modified white sand cement mortar composites. *Journal of Industrial and Engineering Chemistry*. 2014; 20: 1-8.
- [31] Martínez-Barrera G, Menchaca-Campos C, Ureña-Núñez F. Gamma Radiation as a Novel Technology for Development of New Generation Concrete. InTech: Rijeka Croatia; 2012, p. 91-114.

Renewable Biocomposite Properties and their Applications

Thimmapuram Ranjeth Kumar Reddy,
Hyun-Joong Kim and Ji-Won Park

Additional information is available at the end of the chapter

<http://dx.doi.org/10.5772/108445>

Abstract

Recently, with increasing environmental awareness and expanding global waste problems, eco-friendly biofillers have been recognized as a promising alternative to inorganic fillers in the reinforcement of thermoplastic and biodegradable plastics. Therefore, many industries are seeking more eco-friendly materials that will decrease the level of environmental contamination and economic cost. Bacteria cellulose, rice straw, rice husk, natural fiber, lignocellulose, cellulose, and paper sludge are renewable resources owing many beneficial properties; these materials were used to manufacture composite products such as sound absorbing wooden construction materials, interior of bathrooms, wood decks, window frames, decorative trim, automotive panels, and industrial and consumer applications. This chapter elucidates the different renewable biocomposite properties and their applications.

Keywords: renewable materials, composites, properties, applications

1. Introduction

Over several years, fiber-reinforced composites have been attracting great interest because of their many superior properties and applications. The well-known fact is that the reinforcement of fibers in different polymers significantly increases the mechanical properties of the composites. Generally, aircraft and automobile industries prefer to use synthetic fibers such as glass and carbon fibers for reinforcement in polymers. In addition, the increasing performance of composites has been identified by advanced research with two or three polymers/reinforcements or fillers. However, the recycling of these composites is difficult due to difficulty for separation of their components. On the other side, these composites cause

severe environment issues during the landfills or burning. Most of these composites are made from petroleum-based nonrenewable resources [1]. In order to replace the petroleum-based nonrenewable resource-based composites, the eco-friendly biocomposites need to reduce environmental impact. Generally, biocomposites are formed with one or more phases of reinforcement of natural fibers with organic matrix or biopolymers. These reinforcements (cotton, hemp, flax, sisal, jute, and kenaf or recycled wood and paper) and biopolymers (natural biopolymers such as gelatin, corn zein and soy protein; synthetic biopolymers such as poly(lactic acid) (PLA), poly(vinyl alcohol) (PVA); and other microbial fermentation such as microbial polyesters) are renewable and degradable [2, 3]. Meanwhile, in another approach, these biocomposites are formed from the renewable, recyclable, and sustainable agricultural and forestry feedstocks but not food or feed, this can make better change in an environment day-to-day. Systematically, the utilization of bio-based polymers as a reinforced matrix to form biocomposites increases more and more. The spectacular effect on developments of biopolymer-based composites, which lead the rapid growth of biocomposites in the market place, can be seen. In the duration of 2003–2007, globally the average annual growth rate was 38%. During the same period, the annual growth rate was as high as 48% in Europe. On the other hand, from 2007 to 2013, the capacity of utilization of these biocomposites was projected from 0.36 to 2.33 million metric ton by 2013 and 3.45 million metric ton in 2020. Indeed, PLA, PHA, and starch-based plastics were large volumes of production in biocomposites [4]. The U.S. Department of Energy (DOE) had sponsored the Technology Road Map for Plant/Crop-based Renewable Resources 2020. The main intention of this program is to use plant-derived renewable resources for making 10% of basic chemical building blocks by 2020, and further this concept should be extended to achieve 50% by 2050. The U.S. agricultural, forestry, life sciences, and chemical communities have developed a strategic vision for using crops, trees, and agricultural residues to manufacture industrial products, and have identified major barriers to its implementation [5].

The reinforcement of many agricultural and forestry feedstocks with biopolymers comprises change in mechanical, thermal, and biodegradable properties of the composites. This chapter elucidates the properties of renewable biocomposites and their applications.

2. Properties of biocomposites

The most important characteristic feature of selection materials for various applications is depending on its properties. The properties of materials are often dependent on the isotropic and anisotropic nature of the materials. The properties of materials that relate to different physical phenomena often behave linearly (or approximately so) in a given operating range. Modeling them as linear can significantly simplify the differential constitutive equations that the property describes. On the other hand, the relevant equations are also used to determine the material properties. If we know the original length of a material, then we can determine the gain or loss of its original length by calculating change of the length. Material properties are most reliably measured by standardized test methods. Many such test methods have been documented by their respective user communities and published through ASTM

International [6]. We noted the most important properties of the renewable biocomposites from several researchers' investigations that are listed below.

(1) Mechanical properties, (2) thermal properties, (3) optical properties, (4) degradable properties, and (5) electrical properties.

2.1. Mechanical properties

Most of the plastic materials are used because they have desirable mechanical properties at an economical cost. For this reason, several polymers were used in numerous applications. Indeed, several research studies have focused on such materials to gain knowledge on mechanical behavior of numerous structural factors depending on polymers. Moreover, these mechanical properties of the materials depend on the applied load. For this reason, most of the materials can be predictable their service life for future needs. In addition, mechanical properties were also useful in identification and classification of materials for different applications. The considerable properties of mechanical tests are tensile strength, modulus, impact resistance, compression, hardness, and toughness. These properties also depend on the orientation of the reinforcements and atmospheric conditions.

Generally, the properties of biocomposites depend on a matrix, natural filler, and interfacing between them. For this reason, the stress transfers between the two components. The presence of hydroxyl groups in natural fillers exhibits poor interfacial bonding with the matrix. This result concludes that biocomposites exhibit poor mechanical properties. This effect could be reduced by introducing a suitable compatibilizing agent. The effect of different compatibilizing agents on mechanical properties of natural flour filled [bamboo flour (BF) and wood flour (WF)] with biodegradable polymers [poly(lactic acid) (PLA) and poly(butylene succinate) (PBS)]. The maleic anhydride (MA) grafted biopolymers significantly improved the tensile strength of PBS-BF, PBS-WF, and PLA-BF and PLA-WF composites compared to the untreated biopolymers. This tensile strength can be improved by 25–35 MPa [7].

A novel biodegradable hybrid biocomposite system developed with the reinforcement of kenaf fiber (KF) and corn husk flour and investigated the role of the aspect ratio of natural fibers against their tensile properties. **Figure 1** shows the influence of the aspect ratio reinforcement on mechanical properties before and after passing through the extrusion process. The difference between theoretical and experimental values of the tensile modulus was not significant and the aspect ratio determined after extrusion did not influence the predicted values [8].

The use of petroleum-based polymers in composites creates serious environmental problems; it is necessary to replace it with green composites. Baek et al. [9] developed the green composites using coffee ground (CG) and bamboo flour (BF) as a reinforcement to poly(lactic acid) (PLA) and investigated mechanical, thermal, optical properties. Because of the tensile and flexural properties, BF/PLA and CG/PLA composites decrease with addition of CG and BF fillers, but pure PLA showed a tensile strength of 60.1 MPa and the tensile strength of BF/PLA and CG/PLA composites is decreased from 48 to 27 MPa. The addition of a coupling agent

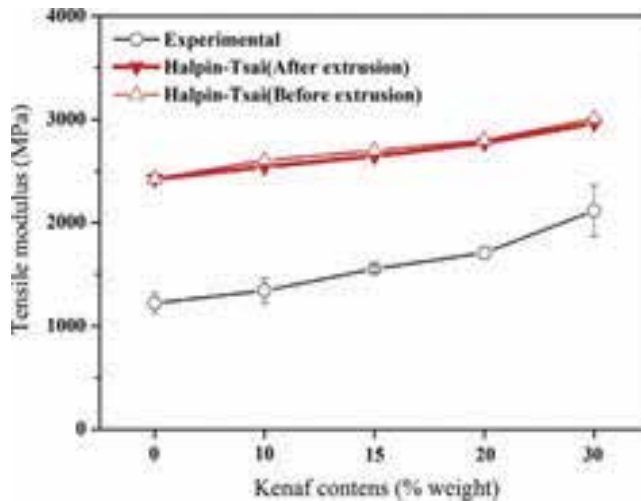


Figure 1. Comparisons of the predicted tensile modulus before and after extrusion.

improved the interfacial adhesion between the filler and PLA, and the tensile strength of the composites increases with increasing 4, 40-methylene diphenyl diisocyanate (MDI), as shown in **Figure 2**.

The similar results obtained in flexural strength of these composites. Without the coupling agent in composites, the flexural strength varies from 98 to 28 MPa, and it is low when compared with pure PLA. With the addition of the coupling agent, the flexural strength might be increased with the increase of MDI, which is shown in **Figure 3** [9].

A similar result was obtained by Kim et al. [10] for cassava and pineapple flour-filled PLA biocomposites. The tensile and flexural strength of the PLA biocomposites decreased with the increasing amount of flour. However, a 3% loading of the compatibilizer in the PLA biocomposite increased the strength up to that observed with the 10% loading flour [10]. To generate the sustainable biocomposites, Sukyai et al. [11] developed the biocomposites with the reinforcement of kenaf fiber (KF) and bacterial cellulose (BC) using the PLA matrix. In particular, BC is nanocellulose, which was anticipated to increase the interfacial area and therefore low volume fractions of additives. That was consequently to attain mechanical property improvement. The elastic modulus of the composites increased concurrently with the increasing KF content. Remarkably, the incorporation of 1 wt% of BC to 60/39 wt% of PLA/KF significantly improved the tensile and flexural strength, which indicates that the BC makes good compatibility between PLA and KF [11]. The tropical crop residues such as particular starch containing bioflours were used for producing biocomposites and the feasibility and industrial potential of using biocomposites were investigated. Polypropylene (PP) and poly(butylene succinate) (PBS) were compounded with bioflours from pineapple skin (P) and from nondestarched (CS) and destarched (C) cassava root by twin-screw extrusion. The impact on mechanical properties observed when the proportion of bioflour was increased to 40% w/w, it reduced the tensile strength by 26–48% and impact strength by 14–40%. However, the different flexural

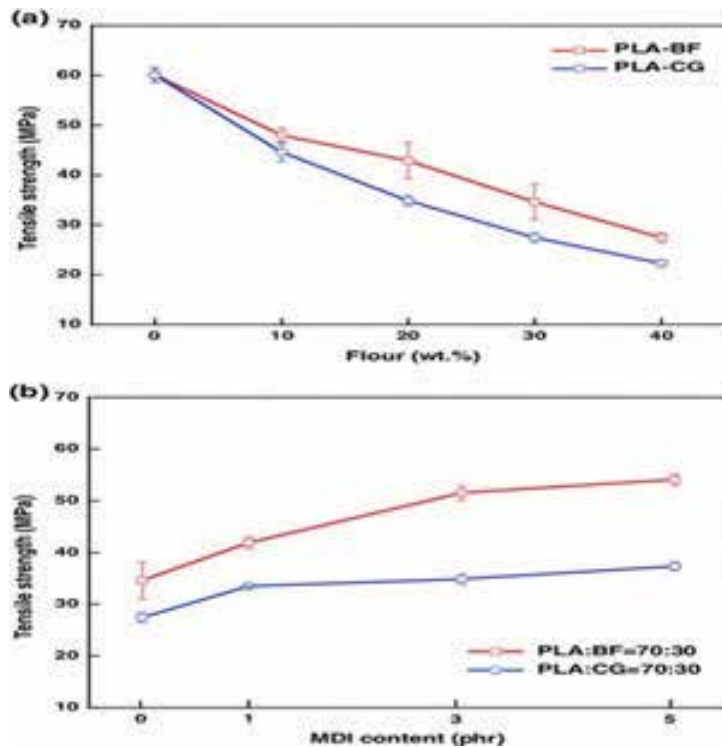


Figure 2. Tensile strength of the green composites with (a) natural fillers (bamboo flour and coffee grounds) and (b) MDI.

strength appeared upon the addition of bioflours; it increased initially but then decreased at higher loads. This effect was also studied by using a compatibilizer of maleic anhydride polypropylene (MAPP), it enhances the flexural strength compared to pure PP, and this resultant material becomes stronger and less flexible [12]. A similar effect was observed while adding 3-glycidoxypropyltrimethoxysilane (GPS) as a coupling agent in the PLA/kenaf fiber biocomposites. The flexural strength and flexural modulus of the composites increased with increasing the content of GPS, while compared with pure PLA. This coupling agent significantly increases the interfacial strength between resin and fibers [13]. There are many value-added composite products obtained from the raw materials of biomass and it consist most promising beneficial resources, for example rice straw, rice husk, and paper sludge are the by-products and industrial waste and are beneficial resources as raw biomass. Kim et al. [14] investigated mechanical properties by adding rice straw, rice husk, and paper sludge to wood composites to replace wood particles for manufacturing green pallets using urea-formaldehyde (UF) resin. The obtained mechanical properties of the composites showed the decrement, upon increasing the contents of rice straw and rice husk flours. The presence of wax and silicate creates less interfacial bonding with UF resin. Moreover, the mechanical properties of wood-paper sludge composites are similar to wood particles so it was replaced with paper sludge [14]. Yang et al. [15] studied the effect of compatibilizing agents on rice-husk flour-reinforced polypropylene (PP) composites. The mechanical properties of these composites were studied

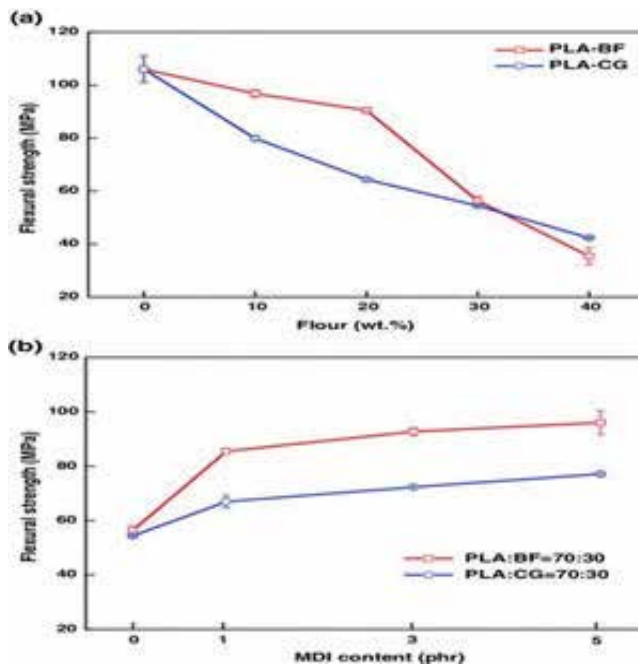


Figure 3. Flexural strength of the green composites with (a) natural fillers (bamboo flour and coffee grounds) and (b) MDI.

at different filler loadings, temperatures, and crosshead speeds. The obtained results indicated that tensile strength of the composites decreased with increasing filler contents in the absence of compatibilizing agent, whereas in the presence of compatibilizing agents, these mechanical properties were significantly increased [15]. Another report showed that the bio-flour-filled [rice husk flour (RHF), wood flour (WF)] maleic anhydride grafted polypropylene (MAPP) composites have good mechanical properties compared with pure polypropylene (PP) composites. The enhancement of mechanical properties was strongly dependent on the amount of MA graft (%) and the MAPP molecular weight, which is shown in **Figure 4** [16].

The most interesting study proved the manufacturing effect on mechanical properties of lignocellulosic material-filled polypropylene biocomposites. The obtained results of tensile strength and modulus of the biocomposites significantly improved with a fabricated twin-screw extruding system compared with a single-screw extruding system [17]. The mechanical properties of the biodegradable polymers and PBS-WF, PBS-BF biocomposites were analyzed with increasing hydrolysis time at 50°C and 90% relative humidity (RH). The resultant properties of these polymers and biocomposites show decrement with the increasing hydrolysis time, due to the easy hydrolytic degradation of the ester linkage of the biodegradable polymers. However, when the antihydrolysis agent trimethylolpropane triacrylate (TMPTA) was treated with PBS, tensile strength was significantly increased with the increasing hydrolysis time as compared to the nontreated PBS. The same results were observed for the PBS-based biocomposites [18]. The addition of paper sludge to thermoplastic polymer composites significantly improved the tensile properties with increasing mixing ratios, and tensile strength

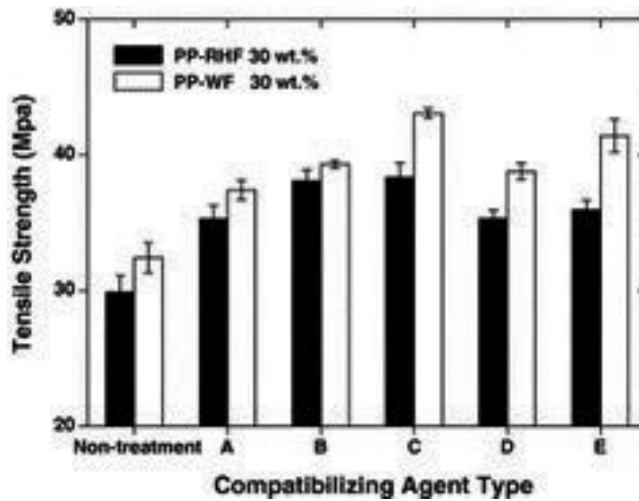


Figure 4. Tensile strength of RHF- and WF-filled PP composites as a function of different MAPP types. A, Polybond 3150; B, Polybond 3200; C, G-3003; D, E-43; E, Bondyram 1004.

vary from 230 to 280 MPa. Moreover, tensile modulus improved with the increasing paper sludge content. On the other hand, flexural properties showed a similar trend as tensile properties [19]. A similar effect was observed in the tensile strength properties of lignocellulosic filler-reinforced polyethylene biocomposites [20].

2.2. Thermal properties

Fiber-reinforced polymer composites are often used as structural components that are exposed to extremely high or low heats. These applications include the following:

- a. Automotive engine components
- b. Aerospace and military products
- c. Electronic and circuit board components
- d. Oil and gas equipment, etc.

In this section, we explore the thermal properties of different natural fiber-reinforced biocomposites.

Lee et al. [21] studied the polymerization of aniline on bacterial cellulose and characterization of bacterial cellulose/polyaniline nanocomposite films. In this study, the thermal stability of the composites is described by thermogravimetric analysis (TGA). The spectacular effect indicated that the pure bacterial cellulose has good thermal stability compared with combination of bacterial cellulose and polyaniline composites. The weight loss occurred in two stages for composites. First stage was obtained at 200°C, due to the combination result of bacterial cellulose and the side chain or impurities of polyaniline. The obtained result at this stage indicates the change in macromolecule of cellulose in smaller one. For these reasons, the weight

reduction pertains at low temperatures. On the other hand, due to thermaloxidative degradation of the main polyaniline chain, it establishes the second stage of weight loss at around 300°C [21]. In most of the automotive, military, aerospace applications, thermal expansion and coefficient of thermal expansion (CTE) are determined by thermomechanical analysis (TMA). Kim et al. observed this effect on natural flour-filled biodegradable polymer composites. The TMA method for determining CTE is useful for understanding the dimensional changes of biocomposite materials as well as the thermal stresses caused by increasing temperature. The effect of porous, inorganic filler treated and nontreated PBS-WF biocomposites as a function of inorganic filler type reveals that the slight decrement of thermal expansion and CTE value of PBS-WF hybrid composites was observed with the addition of 3 wt% porous inorganic filler in the biocomposites. This indicates the prevention of thermal expansion at high temperature due to the addition of lower thermal expansion porous inorganic fillers in the biocomposites. A similar effect was also observed in CTE by Kim et al. [22]. Pineapple skin (P) bioflour, nondestarched, and destarched (C) cassava root bioflours were used for the preparation of polypropylene (PP) and poly(butylene succinate) (PBS) biocomposites. TGA analysis reveals that the thermal stability of the composites decreased, as compared with pure PP and PBS materials, due to the lower degradation temperature of the bioflours (261–351°C). Differential scanning calorimetry (DSC) analysis indicated that bioflours improved nucleation and crystallinity [12]. The compatibilizing effect was also considered for improving the interface between the matrix and filler. This can also affect the thermal properties of the final product. Yang et al. [15] observed the thermal analysis of lignocellulosic material-filled PP biocomposites. With the increasing filler content, there was no change in glass transition temperature (T_g) and melting temperature (T_m) of the biocomposites. This indicates that there is no interface between the matrix and natural filler. However, there was significant change found when the compatibilizing agent was introduced between the matrix and natural filler. The storage modulus of the biocomposite increases with the increasing filler (RHF, WF) content and it is higher than neat PP [23]. The similar effect was also observed with addition of the compatibilizing agent, which is shown in **Figure 5**.

For the fabrication of thermosetting polycardanol biocomposite, the surface was treated with jute fibers using GPS and 3-aminopropyltriethoxy silane (APS). The fiber treatment with GPS and APS were improved the interfacial adhesion between jute fibers and polycardanol resin, compared with untreated jute fiber. This result indicates that the thermal stability and thermomechanical stability also improved [24]. The influence of a zeolite type on thermal properties of natural flour-filled PP composites revealed that the addition of the zeolite content to the PP-RHF and PP-WF composites had peculiar behavior on thermal stability. With the increasing content of natural and synthetic zeolite contents, the thermal stability and degradation temperature also increase. In the presence of 3 and 5% of natural and synthetic zeolite at PP-RHF and PP-WF composites, the thermal stability for 5% mass loss was in the range of 303–329°C and 322–331°C, respectively. However, the thermal stability and degradation temperature was not significantly changed with the increasing natural zeolite content. Interestingly, this property significantly improved in the presence of quartz and the formation of metal oxides in the pozzolan content on the PP and natural flour surface. These results suggest that the addition of inorganic porous materials to reinforcing fillers enhanced the thermal

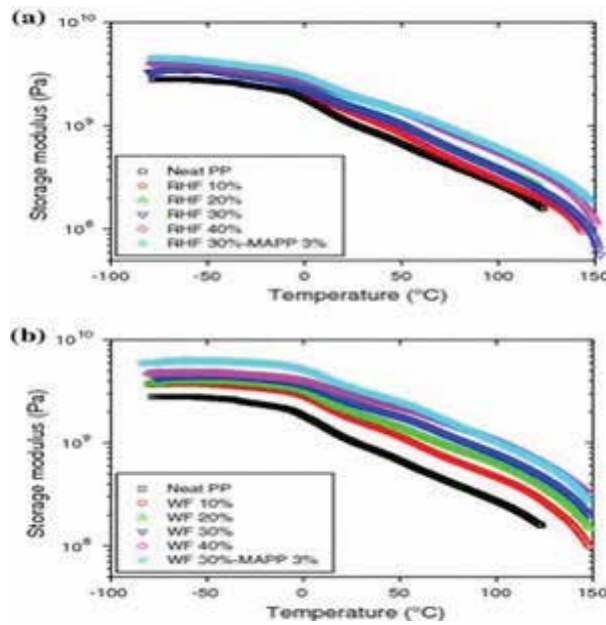


Figure 5. Storage modulus of biocomposites from -80 to 100°C as a function of temperature. (a) RHF filled biocomposite; (b) WF filled biocomposite.

stability of the hybrid composites [25]. In the same manner, the thermal stability and thermal expansion study was performed for bioflour-filled PP biocomposites with different pozzolan contents. With the increasing pozzolan content, at 5% mass loss the thermal stability of the biocomposite increased. On the other hand, the CTE and thermal expansion of the biocomposites decreased with the increasing pozzolan content. There is no significant change in glass transition temperature (T_g), melting temperature (T_m), and percentage of crystallinity (X_c) of the biocomposites. However, the enhancement of interfacial adhesion was observed in maleic anhydride-grafted PP (MAPP)-treated biocomposites, which showed higher thermal stability, thermal expansion, and X_c compared with nontreated biocomposites even at 1% pozzolan content [26]. Another study revealed the effect of the addition of two different compatibilizing agents on thermal properties, maleic anhydride (MA)-grafted polypropylene (MAPP) and MA-grafted polyethylene (MAPE) to bioflour-filled polypropylene (PP) and low-density polyethylene (LDPE) composites. With the increasing MAPP and MAPE content, the thermal stability, storage modulus (E'), $\tan \delta_{\max}$ peak temperature (glass transition temperature: T_g), crystallinity (X_c), and loss modulus (E''_{\max}) peak temperature (β relaxation) were slightly increased except melting temperature (T_m). The improvement in these properties encountered due to good interfacial adhesion between the bioflour and PP matrix in the presence of compatibilizing agent treatment [27]. It is well-known fact that the composite systems must have good thermal stability and thermal expansion properties, which affect the quality of the final products. For example, during the summer, dashboard is affected by the high temperature inside vehicle. On the other hand, the thermal stability of these composite systems is very important because these materials must withstand against heat during the fire. To study this

effect, Yang et al. [15] studied the effect of lignocellulosic filler on thermoplastic polyester polymer biocomposites. In TGA study, the thermal stability slightly decreased and the ash content increased with increasing the filler loading. This result revealed that there is no interfacial bonding between the filler and matrix. To improve the interface adhesion, a suitable compatibilizer was used for improving the thermal properties. In TMA analysis, the thermal expansion of the composites was found to decrease with increasing the filler and incorporating compatibilizing agent. This result elucidates that the thermal expansion of the composite materials was prevented by using the lignocellulosic filler under different atmospheric conditions. These results are shown in **Figures 6 and 7** [28].

Another study on thermal properties of rice husk flour (RHF)-filled polypropylene (PP) and high-density polyethylene (HDPE) composites revealed that the thermal stability of PP and HDPE was higher than RHF. Moreover, with the increasing RHF content, the thermal stability decreases and the ash content increases. On the other hand, the activation energy of the RHF-filled PP composites increased slowly in the initial stage and thereafter remained almost constant, whereas that of the RHF-filled HDPE composites decreased between 30 and 40 mass% of RHF contents. This is due to the interfacial adhesion and dispersion of RHF in the PP and HDPE matrix [29].

2.3. Biodegradation properties

In this modern society, petroleum-based synthetic polymers are widely used for many applications, such as polyolefin in packaging, bottle, and molding products. Globally, the annual disposal of petrochemical plastics reached nearly 150 million tons, which creates serious environment problems, especially with the continuously increasing production and consumption

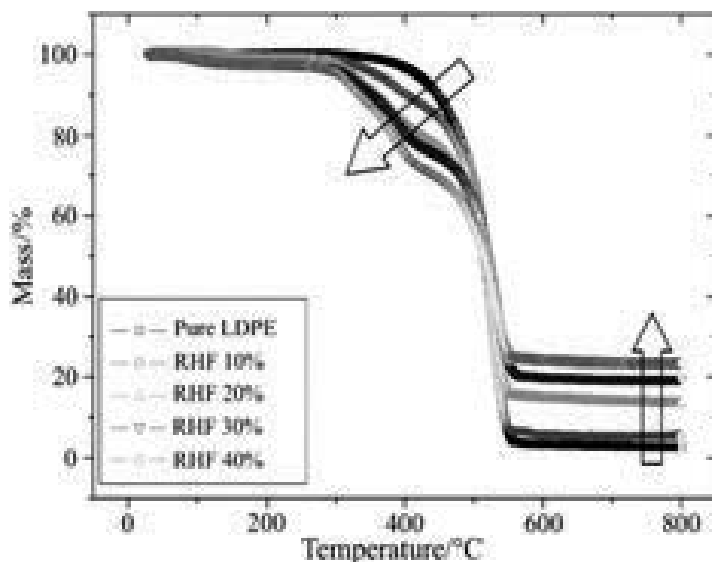


Figure 6. TG curves of RHF-filled LDPE composites at a heating rate of $40^{\circ}\text{C min}^{-1}$ in an N_2 atmosphere.

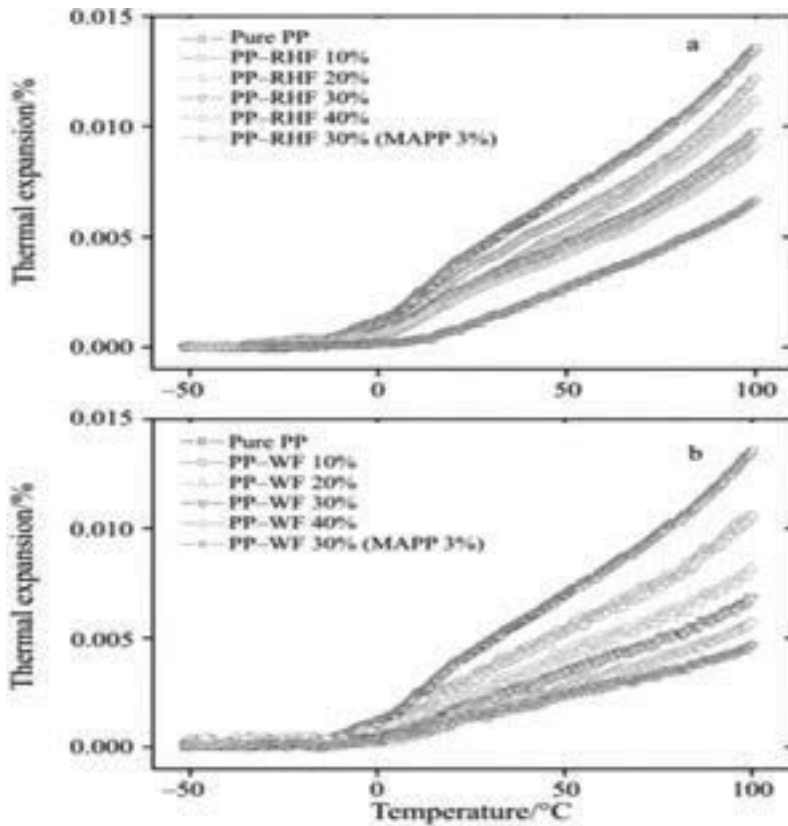


Figure 7. Thermal expansion of the RHF-PP and WF-PP composites: (a) RHF-PP composites, (b) WF-PP composites.

of these materials. Moreover, these plastic wastes capable of resistance of microbial attack, this caused undesired pollutant in soil, rivers and marine. Nowadays eco-friendly biodegradable polymers receive great attention in order to replace the consumption of petroleum-based plastic materials. These biodegradable polymer materials have potential to complete degradation into natural ecosystems such as active sludge, natural soil, lake, and marine. On the other hand, these eco-friendly polymers are capable chemical transformation by the action of biological enzymes or microorganisms. Several researchers are reported that the biodegradability of the biocomposites was most important factor for many composites.

Kim et al. [30] investigated the biodegradability of PBS and bioflour, which is a poly(butylene succinate) (PBS) biocomposite filled with rice-husk flour (RHF) reinforcing in natural and aerobic compost soil. This result indicated the percentage of weight loss of HDPE, PBS, and biocomposites, which is shown in **Figure 8**. The percentage weight loss of biocomposites decreased rapidly with increasing the RHF content. This indicates that the cellulosic materials were easily attacked by microorganisms and enhanced by the degradation capability of the composites compared with PBS and HDPE matrix. On the other hand, the significant comparison identified the percentage weight loss of the biocomposites in a natural and compost

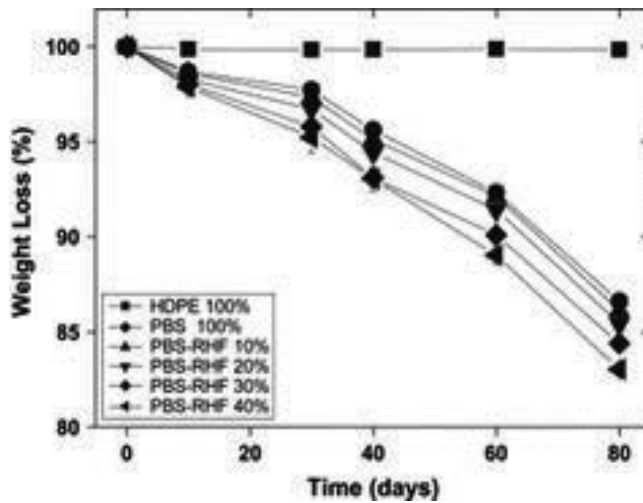


Figure 8. Percentage weight loss of HDPE, PBS, and biocomposites for 80 days.

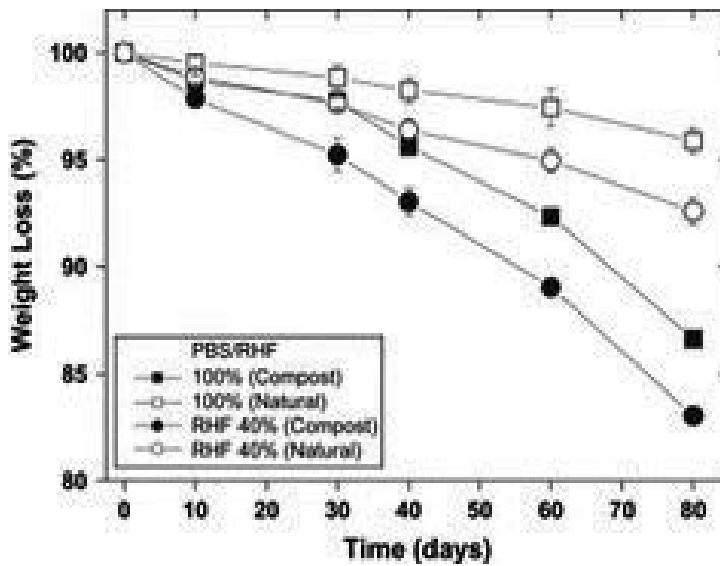


Figure 9. Comparison of the percentage weight loss of PBS and biocomposites at 40 wt% filler loading in natural and compost soil.

soil environment with 40 wt% filler loading. Herein, the faster degradation rate was identified in a compost soil burial test compared with a natural soil burial test over 80 days. Due to the composting environment in the chamber, the enhanced biodegradation rate of biocomposites is shown in **Figure 9** [30].

A similar study investigated the biodegradability of agro-filled PBS biocomposites and their weight loss percentage. Biodegradation generally caused by microorganisms involves

hydrolytic depolymerization of cellulose materials to lower molecular weight compounds, yielding monomeric glucose units. In addition, major deterioration of cellulose and wood-based lignocellulosic materials is caused by microorganisms. **Figure 10** shows the effect of filler particle size on weight loss of the agro-flour-filled PBS biocomposites at 40 wt% filler loading. The significant effect of size variation of filler particle size on weight loss can be seen. Generally, the smaller particle size possesses a higher surface area that makes better contact with the PBS matrix, this indeed the weight loss of the larger particle size (80–100 mesh) filled-PBS biocomposites was slightly greater than that of the smaller particle size (200 mesh) filled PBS biocomposites.

Iovino et al. [31] investigated the biodegradation of poly(lactic acid)/starch/coir biocomposites under controlled composting conditions. The composite formed by reinforced thermoplastic starch (TPS) and short natural fiber (coir) with poly(lactic acid) (PLA), with and without the incorporation of maleic anhydride (MA) as a coupling agent. The biodegradation test was carried on materials of TPS and matrix (containing 75% of PLA and 25% of TPS). The result of the incubation period reveals that the TPS matrix showed a higher level of biodegradation (higher amounts of evolved CO₂) than PLA, this might be arise due to attack of microorganisms on TPS. The fibers seemed to play a secondary role in the process as confirmed by the slight differences in carbon dioxide produced. The compatibilized composite revealed a lower percentage of evolved CO₂ than the uncompatibilized one [31]. Similarly, the degradation of sago-starch-filled linear low-density polyethylene (LLDPE) composites under a soil burial test was observed the presence of holes on samples due to microbial activity. Moreover, the loss in properties (tensile strength, elongation at break and weight loss) of the composites was identified. After 12 months of soil burial, the tensile strength and elongation at break of the composites decreased. Weight loss of the composites changed from 0.6% during the first month to 2% in the 12 month [32]. Pradhan et al. [33] studied the compostability and

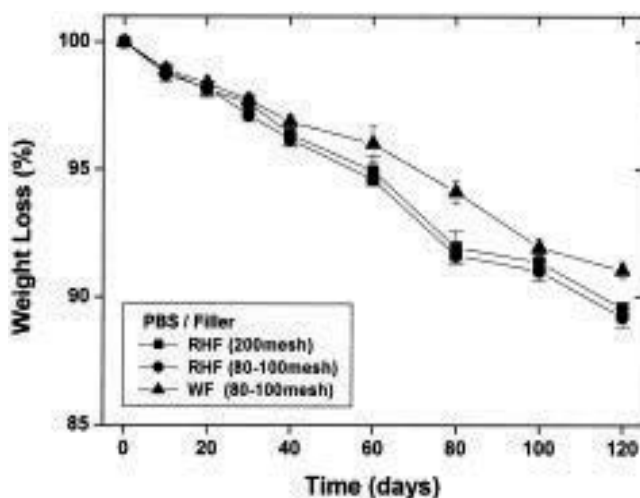


Figure 10. Comparison of the percentage weight loss of agro-flour-filled PBS biocomposites in natural soil at 40 wt% filler loading.

biodegradability of PLA-wheat straw and PLA-soy straw-based green composites. The result of this study elucidates that under aerobic composting the soy and wheat straw degraded rapidly over 70% within 45 days. The similar result obtained in the process of composites degradation irrespective of the biomass used, this rate of degradation was higher than that of pure PLA. Indeed, the faster rate degradation in composites may be due to the presence of degradable natural biomass in composites and due to reduced average molecular weight of PLA [33]. Lu et al. observed the biodegradation behavior of PLA/distiller's dried grains with soluble (DDGS) composites. These materials consist of bio-based and strong potential for industrial applications. The composites were made by adding 20% DDGS to the 80% of PLA and biodegradation experiments were conducted in soil under landscape conditions. The result of this experiment shows that during 24 weeks of degradation time the weight loss of the composites was 10.5%, while the weight loss of pure PLA was only 0.1% during the same time interval. With increasing the degradation time, the surface cracks and voids caused by erosion and loss of polymer chain length were clearly observed as shown in **Figure 11** [34].

The untreated and treated with acetic anhydride-treated (AA-) abaca fibers were reinforced with aliphatic polyesters (poly (ϵ -caprolactone) (PCL), poly (3-hydroxybutyrate-co-3-hydroxyvalerate) (PHBV), PBS, and PLA). The biodegradability of obtained composites was studied by the soil-burial test. The result of the test reveals that the presence of abaca fiber or AA-abaca did not show any effect of weight loss on PCL composites, because PCL itself has a relatively high biodegradability. However, the addition of abaca fibers was shown to accelerate the weight loss of PBS and PHBV composites. Moreover, no weight loss was observed in pure PLA and PLA/AA-abaca composites, but PLA/untreated abaca composites showed 10% weight loss after 60 days due to degradation of fiber by microbial activity [35]. Yussuf et al. [36] investigated the biodegradability difference between PLA/kenaf fibers (KF) and PLA/rice husk flour (RHF) composites by natural soil burial test. The result of this test elucidates that the biodegradability of these composites slightly increased and reached 1.2 and 0.8% for PLA-KF and PLA-RHF, respectively, for a period of 90 days. Moreover, this percentage change in biodegradability of composites is higher as compared to pure PLA, because microorganisms are easily attacked in the presence of natural fibers [36]. Another study emphasized the effect

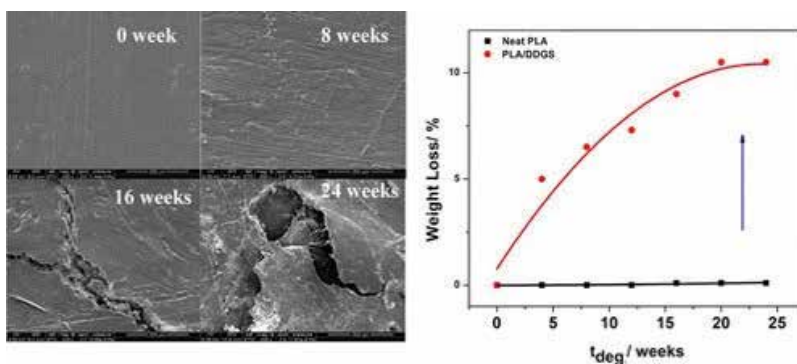


Figure 11. SEM micrographs of PLA/DDGS 80/20 composites after 0, 8, 16, and 24 weeks. Biodegradation time dependence of weight loss of pure PLA and PLA/DDGS (80/20) composites in soil medium [34].

of starch on biodegradability of PLA and poly (hydroxyester-ether) (PHEE) composite bars in soil for 1 year. Due to the fast attack of microorganisms on starch, the rates of weight loss increased in the order pure PLA (~0%/year) < starch/PLA (0–15%/year) < starch/PHEE/ PLA (4–50%/year) and increased with increasing starch and PHEE contents [37]. Alimuzzaman et al. [38] studied the biodegradability of nonwoven flax fiber-reinforced PLA biocomposites under soil burial test during 120 days. The obtained result of the test emphasized that the percentage of weight loss of the PLA, flax fibers, and biocomposites increases with increasing the soil burial time for all samples. The weight loss of PLA and flax fibers after 120 days is found to be 3.08 and 91.41%, respectively. This indicates that the flax fibers show more biodegradability than PLA. The similar result obtained in composites due to presence of flax fibers. Moreover, the weight loss also increases with increasing the content of flax fibers to the pure PLA. During the soil burial test, the presence of various microorganisms and water in the soil can attack flax composites easily. This induces the fiber degradation and resulted degradation of composites [38].

3. Applications of renewable biocomposites

Biocomposites materials, which were formed by a matrix (resin) with the reinforcement of natural fibers such as wood fibers (soft wood, hard wood, newspaper, and magazine fibers) and nonwood fibers (kenaf, flax, jute, hemp, coir, cotton, sisal, and pineapple). These composite materials exhibit ultimate mechanical, thermal, and biodegradable properties. Because of the presence of these superior properties, the composite materials have significant applications in various fields such as automobile, military, aerospace, naval, construction, and packaging.

3.1. Automobile applications

The usage of the biocomposite makes the car lighter, renders greater resistance to heat, external impact, and improves fuel capacity. This leads further to manufacture mid-end and low-end cars as well. The pioneering research on composites and large mass production techniques forced to decline the prices and increase demand for various applications including the automotive sector [39].

Akampunguza et al. [2] reviewed the application of biocomposites in the automotive industry. In this review, they identified future significance of biocomposites in the automotive industry through bioconcept cars. Though these seldom make it to the market, they are useful to give an idea to the industry on the possibilities of particular materials and designs. In 2001, Toyota Motor Corporation brought eco-friendly model an ES3 concept car made with polyester reinforced with hemp fibers composite parts such as carpets, lightweight seats, body panels, and other interior parts exhibited to give awareness of this cleaner manufacturing process. With this inspiration and response in 2003, they bring another model Toyota Raum, which had its interior parts made by using hemp fibers and its springboard was made from potato-derived PLA reinforced with sugarcane bagasse. In 2008, at British Motor Show in London, U.K.-based Lotus car displayed lotus Eco Elise green technology with aimed at making the use of eco-friendly materials and a cleaner manufacturing process in accordance to achieve

weight and carbon miles reduction with the features of components made from bioplastic and biofibers such as sweet potatoes and sugarcane. Renault has been developing a series of bioconcept cars for the racetrack with the first generation introduced in 2006. Volkswagen Scirocco a bioconcept car was configured as a racing car. Several parts of the car body such as the rear hatch, the driver's door, and the front lid have been produced by eco-friendly materials by compression molding. In March 2014, at 84th Geneva International Motor Show, UPM Company displayed biofore concept car with the collaborated Helsinki University of Applied Sciences. The improved manufacturing methods and brilliant technology drive the car's weight reduction by more than 15%. The researchers believed that the biofore car would be the role model for the advance development in manufacturing and technology of actual car making [2]. Four Motors GmbH of Reutlingen, Germany, was presented with the composites in the third generation of bioconcept cars in 2015, which has an extremely efficient TDI engine and travels with a novel, low-pollutant biodiesel based on rapeseed oil. The lightweight body is made from a reinforced natural fiber thermoset, and other components in the interior and the engine compartments are made from bio-based plastics [40].

3.2. Marine applications

Several researchers discovered that the biocomposites have potential marine applications due to their good mechanical properties and biodegradability. Due to these properties, the biocomposites become an alternative to the synthetic fiber-reinforced composites. Le et al. [41] conducted the experiment on seawater aging of flax/PLA biocomposites. The obtained result of this experiment describes that under seawater aging mechanism the absorption of water determined the degradation of hydrolysis of the matrix, structural change, degradation of the fiber/matrix interface, different swelling at composite interfaces and the degradation of fibers reduced the mechanical properties of the composites. However, the matrix and fiber cracks also appear at longer periods. This accomplishes that a special care is needed to integrate marine structures due to biodegradable nature of biocomposites. Indeed, with the eco-friendly impact of usage recyclable materials, now the extensive research is continuing in this area for optimizing lifetime, degradation control, and inherent losses of properties [41]. In the similar study, for the innovation in sailing yacht design must include the current environmental concerns such as depletion and waste management. This leads to incorporate natural fibers into the matrix to form eco-friendly composite materials for possible usage in marine applications. Moreover, they offer high specific stiffness and low environment footprint. The aging mechanism of flax/PLA biocomposites was observed under natural seawater for the period of 2 years. This study elucidates that biocomposites suffer from relatively high moisture absorption, which is controlled by the vegetal fibers [42]. There is necessity to control aging of biocomposites in a seawater environment of both natural fiber and matrix. The extra coating layer of the similar biopolymer on biocomposite may enhance the reduction of weight gain by the interface of the fiber and matrix. The mechanical and thermal properties of the biocomposites after immersion show that the protective layers reduce hydrolysis of the matrix, retain the composite properties, and enhance their durability [43]. DuPont™ specially made marine composite with Kevlar, which is useful to provide an ideal balance of strength, stiffness, and lightweight properties for many marine applications. This enhances the higher

speeds in patrol and service boats that can be achieved by increasing engine power. These composites made with Kevlar be lighter yet tougher, damage tolerant and perform better under hydrodynamic fatigue loading [44]. Davies [45] studied the environmental degradation of composites for marine structures and reported that the use of composites in highly loaded marine components, such as tidal turbine blades or composite propellers, is increasing and requires a detailed understanding of coupling between stress and seawater. A very few experimental data available rather than the theoretical framework, and the time being process for conducting couple of experiments and require specific test equipment. This is an area where further work is urgently required [45].

4. Conclusions

We conclude that renewable biocomposites play a vital role in manufacturing many of the interior and exterior part of automobile, marine, sound absorbing wooden construction materials, and consumer applications. Indeed, several researchers reported that the reinforcement of natural fibers with biopolymers shows good mechanical, thermal, and biodegradable properties. Moreover, the enhancement of these properties was found with the incorporation of a compatibilizing agent. Nevertheless, the renewable biocomposites made from bacteria cellulose, rice straw, rice husk, natural fiber, lignocellulose, cellulose, and paper sludge renewable resources possess many beneficial properties compared to other inorganic fillers. The biocomposites are best alternatives and eco-friendly compared with petroleum-based composites.

Author details

Thimmapuram Ranjeth Kumar Reddy, Hyun-Joong Kim* and Ji-Won Park

*Address all correspondence to: hjokim@snu.ac.kr

Laboratory of Adhesion & Bio-Composites, Program in Environmental Materials Science, College of Agriculture and Life Sciences, Seoul National University, Seoul, Republic of Korea

References

- [1] Ramamoorthy SK, Skrifvars M, Persson A. A review of natural fibers used in biocomposites: plant, animal and regenerated cellulose fibers. *Polymer Reviews*. 2015 Jan 2;55(1):107–62. DOI: 10.1080/15583724.2014.971124
- [2] Akampumuza O, Wambua P, Ahmed A, Li W, Qin X. Review of the applications of biocomposites in the automotive industry. *Polymer Composites*. 2016 Feb 1. DOI 10.1002/pc.23847
- [3] Misra M, Nagarajan V, Reddy J, Mohanty AK. Bioplastics and green composites from renewable resources: where we are and future directions. 18th International

- Conference on Composite Materials, The Korean Society of Composite Materials, Korea. 21–26 Aug 2011.
- [4] Faruk O, Bledzki AK, Fink HP, Sain M. Biocomposites reinforced with natural fibers: 2000–2010. *Progress in Polymer Science*. 2012 Nov 30;37(11):1552–96.
- [5] Mohanty AK, Misra M, Drzal LT. Sustainable bio-composites from renewable resources: opportunities and challenges in the green materials world. *Journal of Polymers and the Environment*. 2002 Apr 1;10(1–2):19–26.
- [6] https://en.wikipedia.org/wiki/List_of_materials_properties
- [7] Kim HS, Lee BH, Lee S, Kim HJ, Dorgan JR. Enhanced interfacial adhesion, mechanical, and thermal properties of natural flour-filled biodegradable polymer bio-composites. *Journal of Thermal Analysis and Calorimetry*. 2010 Nov 11;104(1):331–8.
- [8] Kwon HJ, Sunthornvarabhas J, Park JW, Lee JH, Kim HJ, Piyachomkwan K, Sriroth K, Cho D. Tensile properties of kenaf fiber and corn husk flour reinforced poly(lactic acid) hybrid bio-composites: role of aspect ratio of natural fibers. *Composites Part B: Engineering*. 2014 Jan 31;56:232–7.
- [9] Baek BS, Park JW, Lee BH, Kim HJ. Development and application of green composites: using coffee ground and bamboo flour. *Journal of Polymers and the Environment*. 2013 Sep 1;21(3):702–9.
- [10] Kim KW, Lee BH, Kim HJ, Sriroth K, Dorgan JR. Thermal and mechanical properties of cassava and pineapple flours-filled PLA bio-composites. *Journal of thermal analysis and calorimetry*. 2011 Feb 13;108(3):1131–9.
- [11] P. Sukyai, K. R. Sriroth, B. H. Lee, J. K. Hyun, “The Effect of Bacterial Cellulose on the Mechanical and Thermal Expansion Properties of Kenaf/Poly(lactic acid) Composites”, *Applied Mechanics and Materials*, Vols. 117–119, pp. 1343–1351, 2012.
- [12] Tran T, Lee BH, Yang HS, Chotineeranat S, Sriroth K, Kim HJ. Use of starch granules melting to control the properties of bio-flour filled polypropylene and poly(butylene succinate) composites: mechanical properties. *Starch-Stärke*. 2011 Oct 1;63(10):637–48.
- [13] Lee BH, Kim HS, Lee S, Kim HJ, Dorgan JR. Bio-composites of kenaf fibers in polylactide: role of improved interfacial adhesion in the carding process. *Composites Science and Technology*. 2009 Dec 31;69(15):2573–9.
- [14] Kim S, Kim HJ, Park JC. Application of recycled paper sludge and biomass materials in manufacture of green composite pallet. *Resources, Conservation and Recycling*. 2009 Oct 31;53(12):674–9.
- [15] Yang HS, Kim HJ, Park HJ, Lee BJ, Hwang TS. Effect of compatibilizing agents on rice-husk flour reinforced polypropylene composites. *Composite Structures*. 2007 Jan 31;77(1):45–55.
- [16] Kim HS, Lee BH, Choi SW, Kim S, Kim HJ. The effect of types of maleic anhydride-grafted polypropylene (MAPP) on the interfacial adhesion properties of bio-flour-filled

- polypropylene composites. *Composites Part A: Applied Science and Manufacturing*. 2007 Jun 30;38(6):1473–82.
- [17] Yang HS, Wolcott MP, Kim HS, Kim S, Kim HJ. Properties of lignocellulosic material filled polypropylene bio-composites made with different manufacturing processes. *Polymer Testing*. 2006 Aug 31;25(5):668–76.
- [18] Yang HS, Wolcott MP, Kim HS, Kim S, Kim HJ. Effect of different compatibilizing agents on the mechanical properties of lignocellulosic material filled polyethylene bio-composites. *Composite Structures*. 2007 Jul 31;79(3):369–75.
- [19] Son J, Yang HS, Kim HJ. Physico-mechanical properties of paper sludge-thermoplastic polymer composites. *Journal of Thermoplastic Composite Materials*. 2004 Nov 1;17(6):509–22.
- [20] Kim HS, Kim HJ. Enhanced hydrolysis resistance of biodegradable polymers and bio-composites. *Polymer Degradation and Stability*. 2008 Aug 31;93(8):1544–53.
- [21] Lee BH, Kim HJ, Yang HS. Polymerization of aniline on bacterial cellulose and characterization of bacterial cellulose/polyaniline nanocomposite films. *Current Applied Physics*. 2012 Jan 31;12(1):75–80.
- [22] Kim HS, Lee BH, Kim HJ, Yang HS. Mechanical–thermal properties and VOC emissions of natural-flour-filled biodegradable polymer hybrid bio-composites. *Journal of Polymers and the Environment*. 2011 Sep 1;19(3):628–36.
- [23] Yang HS, Gardner DJ, Kim HJ. Viscoelastic and thermal analysis of lignocellulosic material filled polypropylene bio-composites. *Journal of thermal analysis and calorimetry*. 2009 Nov 1;98(2):553–8.
- [24] Zhou Q, Cho D, Song BK, Kim HJ. Novel jute/polycardanol biocomposites: effect of fiber surface treatment on their properties. *Composite Interfaces*. 2009 Jan 1;16(7–9):781–95.
- [25] Kim HS, Kim HJ. Influence of the zeolite type on the mechanical–thermal properties and volatile organic compound emissions of natural-flour-filled polypropylene hybrid composites. *Journal of Applied Polymer Science*. 2008 Dec 5;110(5):3247–55.
- [26] Kim HS, Choi SW, Lee BH, Kim S, Kim HJ, Cho CW, Cho D. Thermal properties of bio flour-filled polypropylene bio-composites with different pozzolan contents. *Journal of Thermal Analysis and Calorimetry*. 2007 Sep 1;89(3):821–7.
- [27] Kim HS, Kim S, Kim HJ, Yang HS. Thermal properties of bio-flour-filled polyolefin composites with different compatibilizing agent type and content. *Thermochimica Acta*. 2006 Dec 1;451(1):181–8.
- [28] Yang HS, Wolcott MP, Kim HS, Kim HJ. Thermal properties of lignocellulosic filler-thermoplastic polymer bio-composites. *Journal of Thermal Analysis and Calorimetry*. 2005 Sep 1;82(1):157–60.
- [29] Kim HS, Yang HS, Kim HJ, Park HJ. Thermogravimetric analysis of rice husk flour filled thermoplastic polymer composites. *Journal of Thermal Analysis and Calorimetry*. 2004 May 1;76(2):395–404.

- [30] Kim HS, Kim HJ, Lee JW, Choi IG. Biodegradability of bio-flour filled biodegradable poly(butylene succinate) bio-composites in natural and compost soil. *Polymer Degradation and Stability*. 2006 May 31;91(5):1117–27.
- [31] Iovino R, Zullo R, Rao MA, Cassar L, Gianfreda L. Biodegradation of poly (lactic acid)/starch/coir biocomposites under controlled composting conditions. *Polymer Degradation and Stability*. 2008 Jan 31;93(1):147–57.
- [32] Danjaji ID, Nawang R, Ishiaku US, Ismail H, Ishak ZM. Degradation studies and moisture uptake of sago-starch-filled linear low-density polyethylene composites. *Polymer Testing*. 2002 Dec 31;21(1):75–81.
- [33] Pradhan R, Misra M, Erickson L, Mohanty A. Compostability and biodegradation study of PLA–wheat straw and PLA–soy straw based green composites in simulated composting bioreactor. *Bioresource Technology*. 2010 Nov 30;101(21):8489–91.
- [34] Lu H, Madbouly SA, Schrader JA, Srinivasan G, McCabe KG, Grewell D, Kessler MR, Graves WR. Biodegradation behavior of poly(lactic acid)(PLA)/distiller's dried grains with solubles (DDGS) composites. *ACS Sustainable Chemistry & Engineering*. 2014 Oct 23;2(12):2699–706.
- [35] Teramoto N, Urata K, Ozawa K, Shibata M. Biodegradation of aliphatic polyester composites reinforced by abaca fiber. *Polymer Degradation and Stability*. 2004 Dec 31;86(3):401–9.
- [36] Yussuf AA, Massoumi I, Hassan A. Comparison of polylactic acid/kenaf and polylactic acid/rise husk composites: the influence of the natural fibers on the mechanical, thermal and biodegradability properties. *Journal of Polymers and the Environment*. 2010 Sep 1;18(3):422–9.
- [37] Shogren RL, Doane WM, Garlotta D, Lawton JW, Willett JL. Biodegradation of starch/poly(lactic acid)/poly (hydroxyester-ether) composite bars in soil. *Polymer Degradation and Stability*. 2003 Mar 31;79(3):405–11.
- [38] Alimuzzaman S, Gong RH, Akonda M. Biodegradability of nonwoven flax fiber reinforced polylactic acid biocomposites. *Polymer Composites*. 2014 Nov 1;35(11):2094–102.
- [39] <http://www.marketsandmarkets.com/Market-Reports/automotive-composite-market-10869121.html>
- [40] http://www.fourmotors.com/2_bioconcept-cars/0_scirocco/
- [41] Le Duigou A, Davies P, Baley C. Seawater ageing of flax/poly(lactic acid) biocomposites. *Polymer Degradation and Stability*. 2009 Jul 31;94(7):1151–62.
- [42] Le Duigou A, Bourmaud A, Davies P, Baley C. Long term immersion in natural seawater of Flax/PLA biocomposite. *Ocean Engineering*. 2014 Nov 1;90:140–8.

- [43] Le Duigou A, Deux JM, Davies P, Baley C. Protection of flax/PLLA biocomposites from seawater ageing by external layers of PLLA. *International Journal of Polymer Science*. 2011 Sep 21;2011:140-148.
- [44] <http://www.dupont.com/products-and-services/fabrics-fibers-nonwovens/fibers/uses-and-applications/composites.html>
- [45] Davies P. Environmental degradation of composites for marine structures: new materials and new applications. *Philosophical Transactions of the Royal Society A*. 2016 Jul 13;374(2071):20150272.

Epoxy Composites Using Wood Pulp Components as Fillers

Douglas M. Fox, Noy Kaufman, Jeremiah Woodcock,
Chelsea S. Davis, Jeffrey W. Gilman, John R. Shields,
Rick D. Davis, Szabolcs Matko and
Mauro Zammarano

Additional information is available at the end of the chapter

<http://dx.doi.org/10.5772/65261>

Abstract

The components of wood, especially lignin and cellulose, have great potential for improving the properties of polymer composites. In this chapter, we discuss some of the latest developments from our lab on incorporating wood-based materials into epoxy composites. Lignosulfonate was used as a flame retardant and cellulose nanocrystals were used as reinforcing materials. Lignosulfonate will disperse well in epoxy, but phase separates during curing. An epoxidation reaction was developed to immobilize the lignosulfonate during curing. The lignosulfonate–epoxy composites were characterized using microcombustion and cone calorimetry tests. Cellulose also has poor interfacial adhesion to hydrophobic polymer matrices. Cellulose fibers and nanocrystals aggregate when placed in epoxy resin, resulting in very poor dispersion. The cellulose nanocrystal surface was modified with phenyl containing materials to disrupt cellulose interchain hydrogen bonding and improve dispersion in the epoxy resin. The cellulose nanocrystal – epoxy composites were characterized for mechanical strength using tensile tests, water barrier properties using standardized water absorption, glass transition temperatures using differential calorimetry, and aggregation and dispersion using microscopic techniques.

Keywords: cellulose, lignosulfonate, flammability, reinforcement, epoxy

1. Introduction

Wood is comprised of three of the most abundant natural polymers on earth: cellulose, lignin, and hemicellulose. Wood fibers and extracted cellulose fibers have good structural characteristics, and their use in polymers as an inexpensive filler for strength and stiffness improvements is well documented [1–5]. Lignin can also be used as a reinforcing filler, though its irregular structure and natural composition variability can lead to reduced toughness, while the phenolic moieties can promote heat instability [6–9]. Nevertheless, there are benefits, such as sustainability, cost reduction, and improved stiffness, to incorporating wood-based fibers into polymers.

Fiber composites can be prepared using either thermoplastics or thermosets. Thermoplastics have higher impact strength, are recyclable, and can be molded into a variety of shapes, while thermosets are typically stronger, easier to process, and less expensive. Most fiber-reinforced plastics in use today are thermosets. One of the most versatile and widely used thermosets is bisphenol-A-based epoxy systems [10, 11]. These polymers suffer from poor impact strength and are typically reinforced with glass, polymer, or carbon fibers.

Lignin has been used to increase stiffness and toughness in thermoset composites [7, 9, 12]. The addition of lignin was found to toughen neat epoxy [12] and hemp-reinforced epoxy composites [13]. And, lignin was found to increase the flexural strength in flax-epoxy composites [14]. Lignin has also been used as a condensed phase flame retardant. Initially, it was used as an additive to other flame retardants to reduce the flammability of polypropylene [15–17] and polylactic acid [18, 19]. More recently, lignin has been modified with phosphorous to enhance its flame retardancy, then blended with epoxy [20, 21], polybutylene succinate [22], poly(acrylonitrile-butadiene-styrene) [23], and wood plastic composites [24]. And, lignosulfonate has been used unmodified to reduce the flammability of epoxy composites [25]. More often, however, lignin is used as a raw material for the preparation of polymers. Due to the phenolic structure of lignin, it is most often used as a prepolymer for epoxy composites. Typically, the lignin is depolymerized, then epoxidated with epichlorohydrin to produce polyglycidyl phenolic monomers and oligomers [11, 26, 27]. In some cases, it has been aminated to act as a hardener in epoxy composites [28–30]. Recently, lignin has been fractionated using ethanol, then epoxidated using epichlorohydrin in the presence of a phase transfer salt, such as tetramethylammonium hydroxide [31, 32]. This isolates the lower molecular weight lignin to produce a liquid epoxy and minimize segregation between the lignin and the epoxy composite. The use of the phase transfer salt does add toxicity to the process and requires an additional liquid–liquid extraction step to remove it.

The main component of plant fiber that adds strength and stiffness is cellulose, making it a good reinforcement agent for polymer nanocomposites. Recently, cellulose nanocrystals, which are the short, highly crystalline regions in a cellulose fiber, have been identified as good candidates to add reinforcement while simultaneously reducing the weight and increasing the sustainability of the reinforced composite [5, 33–35]. Unfortunately, cellulose is hydrophilic while most polymers are hydrophobic, leading to poor adhesion and water absorption problems when blending the two. In addition, when the cellulose nanocrystals are dried they aggregate, and it is extremely difficult to reparate these aggregates [36, 37].

There have been a variety of approaches to overcome this obstacle. In most studies, a covalently bonded coupling agent is used to improve the adhesion between the crystal and the polymer. Another approach for is to use solvent exchange and solvent casting or thermosetting with the aid of a solvent. In a two-component thermoset, each component can have significantly different chemistries and surface energies, creating opportunities to use processing techniques to improve dispersion of less compatible fillers. One of the most commonly studied epoxy composites are based on diglycidyl ether of bisphenol A epoxy resin and aliphatic diamines. Polyether diamines are typically used to improve flexibility, toughness, and color fastness of the composite. These diamines are significantly more hydrophilic than the epoxy resin or the final epoxy composite, and will have better adhesion with cellulose. Tang and Weder [38] prepared cellulose nanocrystal–epoxy composites by solvent exchange into dimethylformamide and Peng et al. [39] used acetone to create a nanocrystal gel network prior to adding a hydrophilic curing agent, followed by an epoxy resin. These approaches all suffer from laborious and high-energy processing steps. Further, the solvent is difficult to remove, can lead to the loss of desirable composite properties, and add an environmental burden to the process. And, Emami et al. [40] used a polypropylene oxide–polyethylene oxide block copolymer as a surfactant. Although dispersion was improved, there was a loss in tensile strength and elongation by adding the surfactant. We have recently developed a simple, scalable, ion-exchange method to alter the surface energy of cellulose nanocrystals while retaining much of the cellulose surface intact [41].

In this study, we modified wood components using simple procedures to improve their dispersion in epoxy matrices. Lignosulfonate was used as a flame retardant in epoxy composites. The lignosulfonate was epoxidized using epichlorohydrin and sodium hydroxide, then fractionated by extraction in ethanol to minimize migration in the epoxy during curing. The flammability was examined using microcombustion and cone calorimeters and the glass transition temperature was measured using differential scanning calorimetry (DSC). We also prepared cellulose nanocrystal–epoxy composites. A novel ion exchange method was used to eliminate the need for a reaction solvent, reduce the aggregation of the nanocrystals, and improve dispersion throughout the epoxy matrix. The glass transition temperatures were measured using DSC and the dispersion was visualized using confocal fluorescent microscopy.

2. Materials and methods¹

All the chemicals were used as-received unless otherwise indicated. A sulfonated ethoxylated kraft lignin (REAX825E) was provided by MeadWestvaco Corporation (Richmond, VA). Two forms of cellulose nanocrystals were obtained from the University of Maine: (a) an aqueous solution prepared using sulfuric acid, neutralized to the sodium form, and containing 0.95 % mass fraction sulfur on a dry basis and (b) freeze-dried powder, freeze-dried from an aqueous

¹ The policy of NIST is to use metric units of measurement in all its publications, and to provide statements of uncertainty for all original measurements. In this document however, data from organizations outside NIST are shown, which may include measurements in non-metric units or measurements without uncertainty statements.

solution containing a 9 % mass fraction *t*-butanol. Ammonium polyphosphate (APP, Clariant EXOLIT AP422, $(\text{NH}_4\text{PO}_3)_{1000+}$) was used as control filler. Ammonium tartrate (AT, Aldrich) and melamine (ML, Melamine 003 fine, DSM) were used as blowing agents. An epoxy monomer (DER331, Dow Plastics) was cross-linked with a diamine-terminated polypropylene glycol (JA230, Jeffamine D230, Huntsman Corp.). Alkali lignin, Dowex 50 W-X2 (50–100 mesh, H^+ form) cation exchange resin and Rhodamine 6G (Rh, 95 %) were obtained from Sigma Aldrich. Methyltriphenylphosphonium bromide (MePh_3PBr , 98 + %) was supplied by Alfa Aesar.

Lignin sulfonate (Reax 825E, 20.6 g) was dispersed in 400 mL of 15 % mass fraction sodium hydroxide solution and stirred for 3 h. After stirring, the solution was filtered using vacuum filtration and a glass fiber filter to remove any undissolved lignin, yielding a dark red solution. The lignin solution was then heated to 50 °C and epichlorohydrin was added (60 g, 0.63 mol). The reaction was stirred for 4 h and then brought to room temperature. The reaction solution was again filtered to remove any precipitates. The majority of water and unreacted epichlorohydrin was removed under high vacuum. The glycidyl lignin sulfonate was extracted from the resulting opaque solid using ethanol (200 proof). The excess sodium hydroxide was removed through repetitive washings of the lignin sulfonate with 50/50 ethanol/isopropanol (volume fraction). Excess ethanol was removed under vacuum at 50 °C. The product was isolated as a viscous red oil (30.8 g). Epoxide content (275 g/equiv) was determined by titration with 0.1 N HBr in acetic acid using a crystal violet endpoint. Cellulose nanocrystals were exchanged using the process described previously [41]. The epoxy composites were prepared by in the following manner. For most composites, fillers were added to either the epoxy resin or amine curing agent using a high shear mixer (FlackTek Inc. SpeedMixer) for 10 min at 260 rad/s (2500 rpm). The other epoxy composite component was added in stoichiometric amounts and mixed again in a high shear mixer for 10 min at 2500 rpm. For some of the composites, fillers were added using a mechanical stirrer and final mixtures were placed in a sonication bath for 30 min. For all composites, the mixture was degassed for 5 min under vacuum and immediately transferred to silicone molds for cone calorimetry (25 g, 75 cm diameter disk), optical properties (22 mm diameter, 1 mm thick), tensile properties (type V, ASTM D 638-02a), and water absorption analysis (51 mm diameter \times 3.2 mm thick). Samples were also extracted using a 1 mL Teflon syringe before and after transferring to the silicone molds for thermal property measurements. These syringes were kept upright during the curing process. All epoxy samples were cured at room temperature for 24 h and 80 °C for 2 h. For lignosulfonate containing composites, the total filler content was kept constant at 10 % mass fraction, and for cellulose containing composites, the filler content varied between 0.5 % and 5 % mass fraction.

Combustion properties were examined using microcombustion calorimetry (MCC) and cone calorimetry. The microcombustion calorimetry (MCC) samples (5 ± 0.1 mg) were tested with a Govmark MCC-2 microcombustion calorimeter at 1 °C/sec heating rate under nitrogen from 200 to 600 °C using method A of ASTM D7309 (pyrolysis under nitrogen). Each sample was run in triplicate to evaluate reproducibility of the flammability measurements. Cone calorimetry was conducted according to a standard testing procedure (ASTM E-1354-07) on a National Institute of Standards and Technology (NIST) prototype calorimeter. The cone was operated with an incident target flux of 35 kW/m² and an exhaust flow of 24 L/s. The sample was placed

in a pan constructed from heavy-gauge aluminum foil (Reynolds Heavy Gauge Aluminum Foil). The sides and bottom of the sample were covered by aluminum foil so that only the top surface of the sample was exposed to the Cone heater. The aluminum foil height was 5 mm higher than the sample to allow for expansion of intumescent samples. Exposure to the 35 kW/m² external heater caused pyrolysis of the sample. Once sufficient fuel (pyrolysis products) was released, ignition occurred, which was activated by a spark igniter. The test was over when there were no visible flames. The standard measurement uncertainty was $\pm 10\%$ of the reported reduction values and ± 2 s in time.

Optical images were obtained using a Zeiss ID03 inverted microscope, equipped with LD10, LD20, and LD32 phase contrast objectives and an AmScope 5.0MP Microscope USB Camera. A confocal laser scanning microscope (LSM 510 META Carl Zeiss, Germany) was used to examine the aggregation and dispersion of cellulose in epoxy. The excitation source was a 405 nm diode laser (30 mW) and an emission band pass filter (420–480 nm) was used. Images were collected at 5 \times , 50 \times , and 100 \times magnification. A TA Instruments Q-2000 differential scanning calorimetry (DSC) was used to determine extent of curing and glass transition temperatures. For each epoxy, 5.0 mg \pm 0.4 mg samples were placed in aluminum pans with unsealed lids and the cell was purged with nitrogen at a flow rate of 50 mL/min. The samples were equilibrated at $-30\text{ }^{\circ}\text{C}$, heated to $200\text{ }^{\circ}\text{C}$ at a scan rate of $10\text{ }^{\circ}\text{C}/\text{min}$, and cooled to $-30\text{ }^{\circ}\text{C}$. The cycle was repeated five times, with the final four showing no changes between cycles. The uncertainties are $\sigma = \pm 0.4\text{ }^{\circ}\text{C}$ for the reported temperatures and $\sigma = \pm 0.3\text{ J/g}$ for the heat flow. Tensile tests were performed on an MST Criterion Model 45 hydraulically driven test frame with a 5 kN load cell in accordance to the ASTM D 638-02a norm at a speed rate of 0.05 mm/s with a gauge length of 14 mm. All tests were averaged over a minimum of five measurements for each sample with a standard deviation of $\sigma = \pm 10\%$. Water absorption was measured after submersion in water for 1 day at $23\text{ }^{\circ}\text{C}$, according to the ASTM D570 standard.

3. Lignosulfonate–epoxy composites

3.1. Migration of lignosulfonate

In a previous study, the flammability of epoxy composites containing lignosulfonate was initially measured using a radiative gasification apparatus [25]. This is a nonflaming technique used to study condensed phase flammability reductions in composites. The measured mass loss rate and time to peak mass loss rate are related to the heat release rate and time to peak heat release rate (PHRR) of materials in a standard cone calorimetry experiment. The results indicated that ethoxylated lignosulfonate can reduce the flammability of epoxy composites through the formation of char. Further, the addition of naturally derived gas-forming agents, such as melamine or ammonium tartrate, initially reduced mass loss rates by enhancing the quality of char rather than by inducing intumescence behavior. The addition of these gas-forming agents also induces cracks and debonding later in the burning process, leading to a loss of protection partway through the experiment.

The flammability of these materials was re-examined using cone calorimetry. The shape and relative heat release values mirrored the mass loss rate curves obtained using the gasification apparatus for all samples. The strong correlation observed indicates the reduced flammability when adding lignosulfonate is almost entirely through a condensed phase mechanism. The cone calorimetry data are summarized in **Figure 1**. The peak heat release rate (PHRR), which estimates how intense a fire will be and can help predict the time to flashover, is reduced by 24 % by adding 10 % lignin, 34 % by adding 10 % REAX825E, and 36 % by adding 7 % REAX825E + 3 % AT. The addition of ML instead of AT leads to an increase in PHRR compared to pure epoxy. Melamine produces more gases, leading to more cracks to the char layer, reducing its protective ability. The total heat release is reduced by as much as 14 % when using REAX825E. Since MCC suggests that 30 % to 40 % of lignosulfonate will volatilize during pyrolysis, this indicates an ability to prevent some of the epoxy from burning. One disadvantage to using lignin is that the time to ignition is significantly reduced. A number of factors contribute to the ignition time, including heat capacity, thermal conductivity, surface emissivity, oligomeric decomposition products, melt viscosity, and permeability of the solid. Pure epoxy is transparent with low surface emissivity, whereas lignin is brown or black in color with high surface emissivity. Accordingly, t_{ign} is reduced going from pure epoxy to epoxy + 10 % lignin to epoxy + 10 % REAX825E. The addition of gas-forming compounds, which degrade at temperatures lower than the pure epoxy, leads to a more porous solid as the sample heats up. So, it is not surprising that t_{ign} is further reduced going from epoxy + 10 % REAX825E to epoxy + 7 % REAX825E + 3 % AT to epoxy + 7 % REAX825E + 3 % ML.

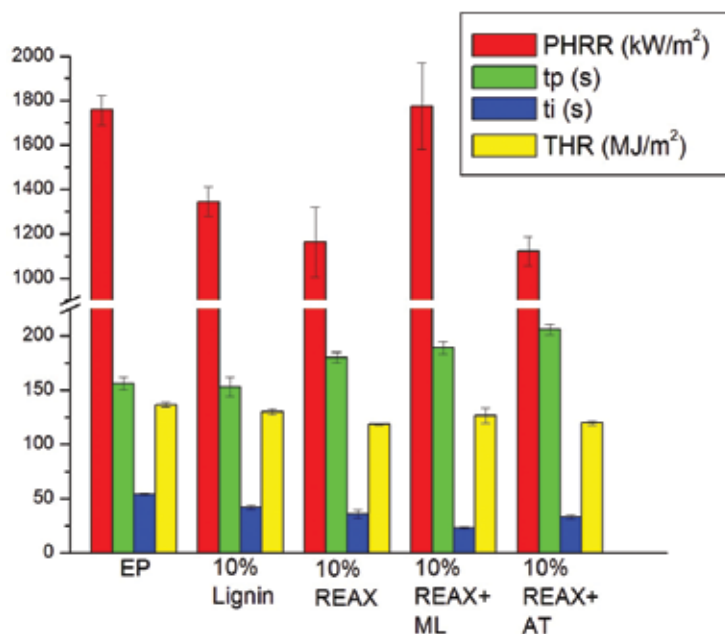


Figure 1. Cone calorimetry data for epoxy + lignosulfonate composites. Error bars represent 2σ .

The observed peeling of the char layer during combustion in the cone calorimeter suggested the lignin migrated and separated from the epoxy matrix during curing. The migration was verified using microcombustion calorimetry. Microcombustion calorimetry is a small scale (3 mg to 10 mg samples) test, where a sample is heated in nitrogen, similar to thermogravimetric analysis, and the pyrolyzed gases are mixed with oxygen and combusted in a separate chamber. The amount of oxygen consumed can be correlated to heat released. The heat release capacity (HRC) and heat of combustion (H_c) measured by the MCC are correlated to several flammability parameters obtained from other measurements, including peak heat release rate (PHRR) and total heat released (THR) from cone calorimetry experiments. As shown in **Table 1**, ethoxylated lignosulfonate has a lower flammability and higher char yield than alkali lignin, which is why it was chosen as the primary flame retardant in this study. Lignin and ethoxylated lignosulfonate have much lower flammabilities than epoxy. The use of these materials in epoxy significantly reduces the HRC by up to 45 % and the H_c by up to 20 %. A 5 mg sample was taken from the top and the bottom of an 8 mm thick epoxy + 10 % REAX825E sample. The results show that the lignosulfonate migrates to the top surface of the epoxy during the curing process. The higher char yield and lower apparent heat capacity are likely due almost entirely to the lignin, rather than uncombusted epoxy. The low H_c and char yield for AT verifies that it has potential as a gas-forming agent in intumescent formulations.

Sample	HRC (J/g · K)	H_c (kJ/g)	T_{peak} (°C)	Char (mass-%)
Epoxy	703	24.4	391	0
Lignin	29	3.5	252	56
Ethoxylated lignosulfonate (REAX825E)	19	1.7	251	64
Ammonium tartrate (AT)	233	4.3	250	6
Epoxy + 10% REAX825E (top)	385	19.7	393	24
Epoxy + 10% REAX825E (bottom)	489	24.8	398	14

Table 1. Microcombustion analysis of epoxy + lignosulfonate samples.

3.2. Variability of lignosulfonate

Additional ethoxylated lignosulfonate was obtained from the same source. Composites were prepared and tested in a cone calorimeter. Even though the exact same product was used, the two lots had significantly different properties. As shown in **Figure 2**, lot #RI27 had a later ignition time, but a 10 % higher PHRR and THR than lot #NK22. The addition of ammonium tartrate lowered the PHRR and reduced the time to PHRR to the same extent, so its interaction with the salt did not change. Most of the difference is due to the natural variability of the lignin composition. The color of lot #RI27 was darker than that of #NK22. In addition, the number of phenolic groups, sulfate groups, or average molecular weight may be different, depending on the source of the lignin and sulfonation process. Although there are variations, the general properties and potential use of lignosulfonate as a flame retardant remain promising.

3.3. Immobilization of lignosulfonate

To prevent the migration of the lignosulfonate, it was epoxidated using epichlorohydrin. It was then used to prepare epoxy + 10 % eLS composites, which were still opaque, but lighter in color than the REAX825E composites. The addition of glycidyl moieties did add to the fuel content of the lignin. Using MCC, eLS was found to have $H_c = 5.1$ kJ/g, $HRC = 72$ J/g · K, $T_{peak} = 340$ °C, and 44 % mass fraction residue. This is only a modest increase in flammability and the immobilization was expected to have a greater effect. As shown in **Figure 3**, by incorporating the lignosulfonate within the epoxy matrix, the char layer was more effective at reducing the heat released. The PHRR was reduced by 63 % and the THR was reduced by 27 % over neat epoxy. The one disadvantage is that the composite ignited the earliest of all composites tested. To improve the efficiency of the epoxidation process, the starting material was dissolved in ethanol and filtered to remove any insoluble material. The solubility of lignin in ethanol decreases as the molecular weight of lignin increases, so this likely removes the highest molecular weight lignin. This may account for the earlier time to ignition, though residual ethanol will also lower this characteristic. The char formed during the decomposition was thicker and did not peel away from the composite, which helps explain how it could effectively reduce the heat released during combustion.

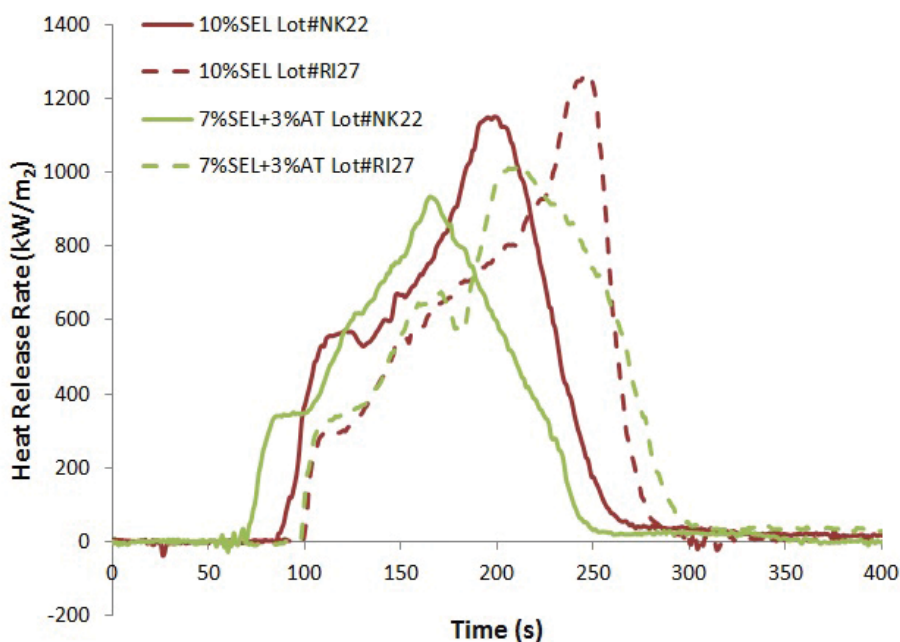


Figure 2. Heat release rate as measured in a cone calorimeter of epoxy flame retarded with lignosulfonate, using two different batches of ethoxylated lignosulfonate.

The addition of lignosulfonate significantly changed the glass transition temperatures (T_g). The measured T_g were 81.2 °C for neat epoxy, 88.7 °C for epoxy + 10 % REAX825E, and 75.7 °C for epoxy + 10 % eLS. Increases in T_g are typically associated with enthalpic interactions between

the filler and epoxy matrix. This may be π - π interactions between lignosulfonate and DGEBA or hydrogen bond interactions with the poly(propylether)diamine curing agent.

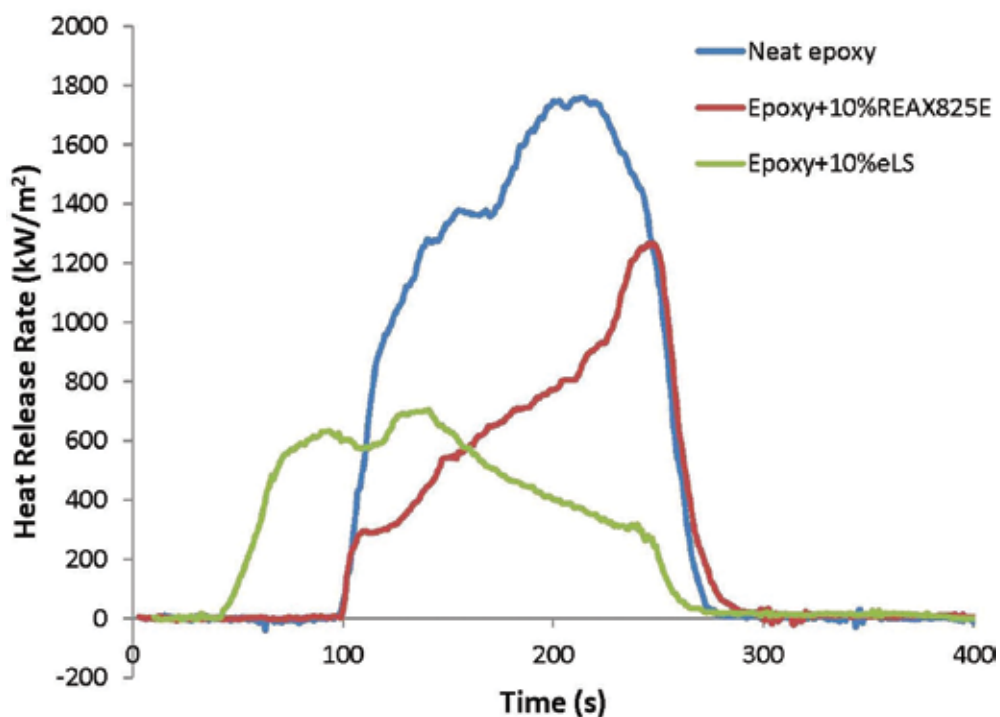


Figure 3. Heat release rate as measured in a cone calorimeter of epoxy + epoxidated lignosulfonate.

4. Cellulose–epoxy composites

4.1. Effects of processing methods of dispersion

The order of addition and the use of high speed centrifugal mixing were investigated to improve dispersion of unmodified sulfated cellulose nanocrystals (Na-CNC) in epoxy composites. The Na-CNC nanocrystals that were obtained as a dried powder were freeze dried in the presence of 9 % mass fraction t-butyl alcohol. This reduces the water crystal size during the freezing process and adds a small amount of an organic solvent to the crystal structure of the cellulose, which improves the microscopic dispersion of the crystals. Since these represent the “best case scenario” for dispersing unmodified sulfated cellulose nanocrystals in hydrophobic matrices, these were used to assess the effects of processing methods on dispersion. All the composites exhibited cellulose aggregation that was visible without magnification. Mechanical stirring and sonication resulted in the largest aggregates and high shear mixing with addition of cellulose to the diamine followed by addition of the epoxy resin resulted in

the smallest aggregates. In previous studies, both a polar, nonaqueous solvent and ultrasonication were required to form transparent composites free from visible aggregates.

4.2. Ion exchange of cellulose nanocrystals

A method has recently been developed to modify the surface of sulfated cellulose nanocrystals using a simple, scalable ion exchange process [41]. In this approach, rather than adding a surfactant, the sodium cation is exchanged with a surfactant cation. The exchange reduces the surface energy, reduces the water uptake, increases the thermal stability, and improves the polymer adhesion of the nanocrystals. This method also allows co-exchange of cations. In this study, the column was loaded with 1 % mass fraction rhodamine 6G and 99 % mass fraction methyl(triphenyl)phosphonium, (MePh₃P/Rh)-CNC. A Na-CNC control was prepared by using a column that was loaded with 1 % mass fraction rhodamine 6G and 99 % mass fraction Na⁺. The fluorescence of 2 % mass fraction cellulose nanocrystals in water is shown in Figure 4.

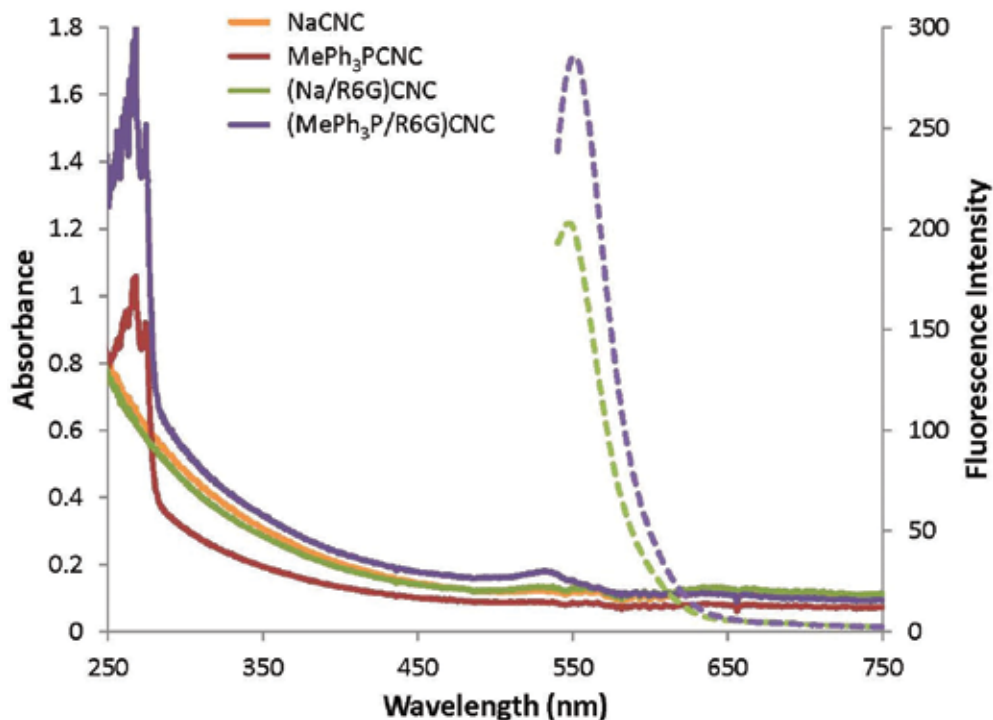


Figure 4. UV and fluorescence spectra of aqueous solutions of cellulose nanocrystals.

4.3. Improved dispersion with exchanged cellulose nanocrystals

The exchanged cellulose nanocrystals disperse readily in the epoxy resin, even without significant shear. Composites were initially prepared using a high shear, speed mixer. Optical

images (**Figure 5**) show large microscopic agglomeration for the Na-CNC composites, which disappear when using MePh₃P-CNC. There is still some agglomeration, but the lengths of the aggregates are smaller than 50 μm and the width of the aggregates is on the submicron scale.

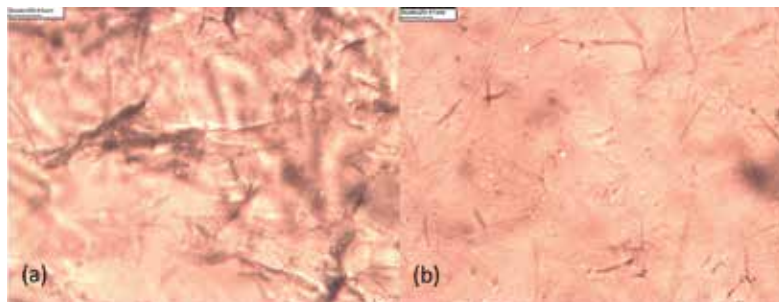


Figure 5. Optical images (20× magnification) of (a) 0.5 % Na-CNC in epoxy and (b) 0.5 % MePh₃P-CNC in epoxy.

When using an optical microscope, it is often difficult to differentiate cellulose crystals from matrix defects, such as cracks, bubbles, or impurities. To obtain a better representation of cellulose distribution, laser scanning fluorescent confocal microscopy was used to image epoxies containing rhodamine co-exchanged crystals (cf **Figure 6**). These images show larger Na-CNC agglomerates, since the (Na/Rh)-CNCs were freeze dried without *t*-butyl alcohol. They also show fewer microscopic (MePh₃P/Rh)-CNC than the optical images of MePh₃P-CNC containing epoxies (**Figure 5b**). The visible crystal sizes are similar to those observed for MePh₃P-CNC. This suggests that some of the features observed in the light microscope images are defects rather than cellulose crystals. It also indicates that there are crystals that are smaller than the limit of detection of optical microscopes, likely nanoscale in size. This mixed micro-scale/nanoscale size distribution of nanocellulose in polymer matrices has been observed previously [42].

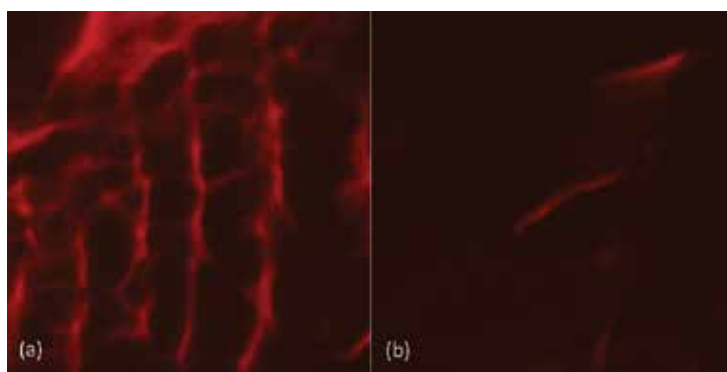


Figure 6. Fluorescent confocal images (100× magnification) of (a) 0.5 % Na-CNC in epoxy and (b) 0.5 % MePh₃P-CNC in epoxy.

Composites were also prepared by gently heating the epoxy resin to reduce viscosity, blending the cellulose using a stir plate, and use of a sonication bath to help separate some of the slower dispersing particles. Epoxies containing 2 % MePh₃P-CNC were visibly transparent, and the microscopic images (not shown) suggest similar levels of crystal separation and dispersion throughout the epoxy.

The differences in particle size and surface energy of the crystals resulted in differences in the glass transition temperatures (cf **Figure 7**). The cellulose nanocrystals interact strongly with the epoxy matrix, leading to a 5 °C increase in the glass transition temperature at 2 % NaCNC loading. This behavior is consistent with other studies incorporating cellulose nanofibers [43] or nanocrystals [44]. The addition of MePh₃PCNC does not change the glass transition temperature relative to neat epoxy. The MePh₃P⁺ functionality lowers the surface energy of the cellulose, reducing both crystal–crystal interactions (less aggregation), and cellulose–polymer interactions (lower T_g). The differences in T_g between the epoxies prepared using high shear mixing and those using mechanical mixing were not statistically significant.

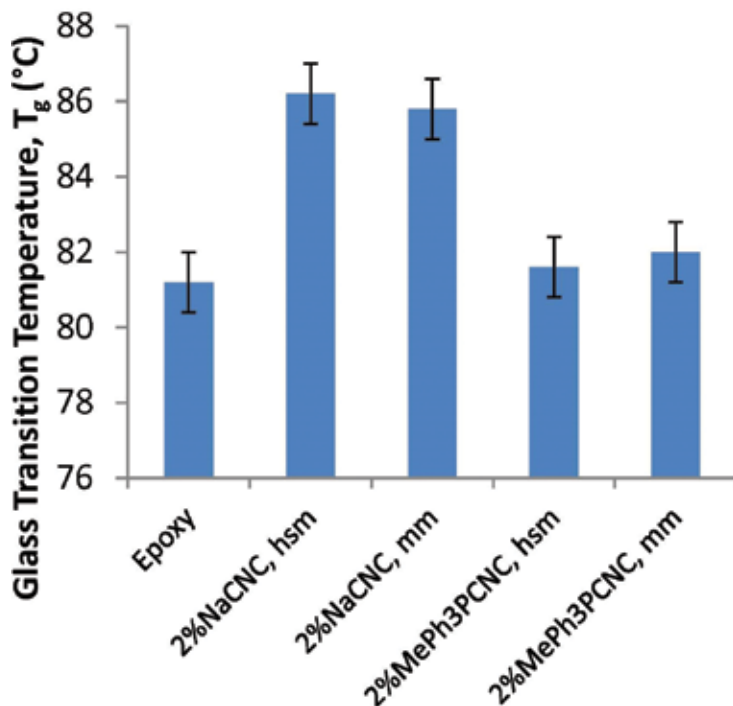


Figure 7. Glass transition temperatures of epoxy-cellulose nanocrystal composites using DSC. Error bars represent 2σ .

The tensile properties of the epoxy composites are provided in **Table 2**. As expected, the incorporation of stiff crystals increased the modulus (E) of the epoxy composites. The addition of MePh₃P-CNC had a greater effect than the addition of Na-CNC, likely due to the smaller size of aggregates and better dispersion in these composites. The peak tensile strength (σ_p) of

the composites decreased, which may be due to heterogeneity in the cross-linking due to the presence of the crystals. The use of MePh₃P-CNC also reduced the tensile strength, but only half as much in the Na-CNC composites. A key advantage to using the modification is the reduction in hydrophobicity due to the presence of large, hydrophobic cations. The water absorption in Na-CNC epoxy after 1 day of water immersion (W_{1d}) was significantly higher than in neat epoxy, but the MePh₃P-CNC filled epoxies had nearly the same water absorption as neat epoxy.

Sample	E (GPa)	σ_p (MPa)	W_{1d} (% mass fraction)
Epoxy	2.03 ± 0.09	61.2 ± 2.1	0.24 ± 0.04
Epoxy + 1% NaCNC	2.10 ± 0.04	43.7 ± 2.6	0.33 ± 0.01
Epoxy + 1% MePh ₃ PCNC	2.15 ± 0.17	48.5 ± 3.7	0.25 ± 0.02
Epoxy + 5% NaCNC	2.23 ± 0.05	39.9 ± 2.3	0.53 ± n.d.
Epoxy + 5% MePh ₃ PCNC	2.33 ± 0.06	49.5 ± 3.9	0.30 ± n.d.

n.d. – not determined due to insufficient number of samples.

Table 2. Tensile properties and water absorption of cellulose nanocrystal–epoxy composites.

5. Conclusions

Epoxy composites were filled with lignocellulosic materials to improve their flammability and mechanical properties. Lignosulfonate was used as a condensed phase flame retardant. The lignosulfonate migrated during the curing process and resulted in delamination, reducing its effectiveness at maintaining a protective char layer during combustion. The lignosulfonate was successfully epoxidated and incorporated within the epoxy matrix. This reduced the migration and improved the fire performance of the composite. Cellulose nanocrystals were successfully incorporated in an epoxy composite without the aid of a solvent by modifying the crystals with a simple ion exchange process. This process minimized aggregation of cellulose without the use of nonaqueous solvents. The resulting composites were transparent, were stiffer, had a smaller loss in tensile strength, and absorbed less water than the composites with unmodified Na-CNC.

Acknowledgements

This material is based upon work supported by the NIST-EL Extramural Fire Research Grants Program. Research was carried out at the National Institute of Standards and Technology (NIST), an agency of the U.S. government and by statute is not subject to copyright in the United States. Certain commercial equipment, instruments, materials or companies are identified in this paper in order to adequately specify the experimental procedure. Such

identification is not intended to imply recommendation or endorsement by the National Institute of Standards and Technology, nor is it intended to imply that the materials or equipment identified are necessarily the best available for this purpose.

Author details

Douglas M. Fox^{1*}, Noy Kaufman¹, Jeremiah Woodcock², Chelsea S. Davis², Jeffrey W. Gilman², John R. Shields³, Rick D. Davis³, Szabolcs Matko³ and Mauro Zammarano³

*Address all correspondence to: dfox@american.edu

1 Department of Chemistry, American University, Washington, DC, USA

2 Materials Science and Engineering Division, Materials Measurement Laboratory, National Institute of Standards and Technology, Gaithersburg, MD, USA

3 Fire Research Division, Engineering Laboratory, National Institute of Standards and Technology, Gaithersburg, MD, USA

References

- [1] Pickering K.L., editors. *Properties and Performance of Natural-Fibre Composites*. Cambridge, England: Woodhead Publishing; 2008. 576 p.
- [2] Hodzik A., Shanks R., editors. *Natural Fibre Composites: Materials, Processes and Properties*. Cambridge, England: Woodhead Publishing; 2014. 408 p.
- [3] Thomas S., Pothan L.A. *Natural Fibre Reinforced Polymer Composites: From Macro to Nanoscale*. Philadelphia, PA: Old City Publishing; 2009. 539 p.
- [4] Nabi Saheb D., Jog J.P. Natural fiber polymer composites: a review. *Advances in Polymer Technology* 1999;18:351–363.
- [5] Miao C., Hamad W.Y. Cellulose reinforced polymer composites and nanocomposites: a critical review. *Cellulose*. 2013;20(5):2221–2262.
- [6] Belgacem M.N., Gandini A., editors. *Monomers, Polymers and Composites from Renewable Resources*. Amsterdam: Elsevier; 2008. 552 p.
- [7] Faruk O., Sain M. *Lignin in Polymer Composites*. Amsterdam: Elsevier; 2015. 350 p.
- [8] Lora J.H., Glasser W.G. Recent industrial applications of lignin: a sustainable alternative to nonrenewable materials. *Journal of Polymers in the Environment*. 10;2002:39–48.

- [9] Thakur V.K., Thakur M.K., Raghavan P., Kessler M.R. Progress in green polymer composites from lignin for multifunctional applications: a review. *ACS Sustainable Chemistry & Engineering* 2014;2:1072–1092.
- [10] Auvergne R., Caillol S., David G., Boutevin B. Pascault J.-P. Biobased thermosetting epoxy: present and future. *Chemical Reviews* 2014;114:1082–1115.
- [11] Ferdosian F., Yuan Z., Anderson M., Xu C. Sustainable lignin-based epoxy resins cured with aromatic and aliphatic amine curing agents: curing kinetics and thermal properties. *Thermochimica Acta* 2015;618:48–55.
- [12] Liu W., Zhou R., Goh H.L.S., Huang S., Lu X. From waste to functional additive: toughening epoxy resin with lignin. *ACS Applied Materials & Interfaces* 2014;6:5810–5817.
- [13] Wood B.M., Coles S.R., Maggs S., Meredith J., Kirwan K. Use of lignin as a compatibiliser in hemp/epoxy composites. *Composites Science and Technology* 2011;71:1804–1810.
- [14] Thielemans W., Wool R.P. Butyrate kraft lignin as compatibilizing agent for natural fiber reinforced thermoset composites. *Composites Part A: Applied Science and Manufacturing* 2004;35:327–338.
- [15] Gregorova A., Kosikovka B., Osvald A. The study of lignin influence on properties of polypropylene composites. *Wood Research*. 2005;50(2):41–48.
- [16] Galina A., Bravin E., Badalucco C., Audisio G., Armanini M., De Chirico A., Provasoli F. Application of cone calorimeter for the assessment of class of flame retardants for polypropylene. *Fire and Materials*. 1998;22(1):15–18.
- [17] De Chirico A., Armanini M., Chini P., Cioccolo G., Provasoli F., Audisio G. Flame retardants for polypropylene based on lignin. *Polymer Degradation and Stability* 2003;79:139–145.
- [18] Reti C., Casetta M., Duquesne S., Bourbigot S., Delobel R. Flammability properties of intumescent PLA including starch and lignin. *Polymers for Advanced Technologies*. 2008;19(6):628–635.
- [19] Zhang R., Xiao X., Tai Q., Huang H., Yuan H. Modification of lignin and its application as char agent in intumescent flame-retardant poly(lactic acid). *Polymer Engineering and Science* 2012;52:2620–2626.
- [20] Alalykin A.A., Vesnin R.L., Kozulin D.A. Preparation of modified hydrolysis lignin and its use for filling epoxy polymers and enhancing their flame resistance. *Russian Journal of Applied Chemistry*. 2011;84(9):1616–1622.
- [21] Howarter J.A., Mendis G.P., Bruce A.N., Youngblood J.P., Dietsberger M.A., Hasburgh L. Flame retardancy of chemically modified lignin as functional additive to epoxy nanocomposites. In: Wilkie C.A., editors. 26th Annual Conference on Recent Advances in Flame Retardancy of Polymeric Materials; May 18–20, 2015; Stanford, CT. BCC

- Research; 2015. p. Session 3: Nanocomposites, 2–1 through Session 3: Nanocomposites, 2–8.
- [22] Ferry L., Dorez G., Taguet A., Otazaghine B., Lopez-Cuesta J.M. Chemical modification of lignin by phosphorus molecules to improve the fire behavior of polybutylene succinate. *Polymer Degradation and Stability* 2005;113:135–143.
- [23] Prieur B., Meub M., Wittemann M., Klein R., Bellayer S., Fontaine G., Bourbigot S. Phosphorylation of lignin to flame retard acrylonitrile butadiene styrene (ABS). *Polymer Degradation and Stability* 2016;127:32–43.
- [24] Liu L., Qian M., Song P., Huang G., Yu Y. Fu S. Fabrication of green lignin-based flame retardants for enhancing the thermal and fire retardancy properties of polypropylene/wood composites. *ACS Sustainable Chemistry & Engineering* 2016;4:2422–2431.
- [25] Zammarano M., Fox D.M., Matko S., Kashiwagi T., Gilman J.W., Davis R.D. Sustainable flame retardants: bio-derived products as intumescent materials. In: *Fire & Materials* 2011; San Francisco, CA. 2011. p. 337–342.
- [26] Koike T. Progress in development of epoxy resin systems based on wood biomass in Japan. *Polymer Engineering and Science* 2012;52:701–717.
- [27] Sun G., Sun H., Liu Y., Zhao B., Zhu N., Hu K. Comparative study on the curing kinetics and mechanism of a lignin-based-epoxy/anhydride resin system. *Polymer* 2007;48:330–337.
- [28] Pan H., Sun G., Zhao T. Synthesis and characterization of aminated lignin. *International Journal of Biological Macromolecules* 2013;59:221–226.
- [29] Mendis G.P., Hua I., Youngblood J.P., Howarter J.A. Enhanced dispersion of lignin in epoxy composites through hydration and Mannich functionalization. *Journal of Applied Polymer Science*. 2015;132(1):41263.
- [30] Pan H., Sun G., Zhao I., Wang G.H. Thermal properties of epoxy resins crosslinked by an aminated lignin. *Polymer Engineering and Science*. 2015;55(4):924–932.
- [31] Sasaki C., Wanaka M., Takagi H., Tamura S., Asada C., Nakamura Y. Evaluation of epoxy resins synthesized from steam-exploded bamboo lignin. *Industrial Crops and Products* 2013;43:757–761.
- [32] Asada C., Basnet S., Otsuka M., Sasaki C., Nakamura Y. Epoxy resin synthesis using low molecular weight lignin separated from various lignocellulosic materials. *International Journal of Biological Macromolecules* 2015;74:413–419.
- [33] Habibi Y., Lucia L.A., Rojas O.J. Cellulose nanocrystals: chemistry, self-assembly, and applications. *Chemical Reviews* 2010;110:3479–3500.
- [34] Moon R.J., Martini A., Nairn J., Simonsen J., Youngblood J. Cellulose nanomaterials review: structure, properties, and nanocomposites. *Chemical Society Reviews* 2011;40:3941–3994.

- [35] Samir M., Alloin F., Dufresne A. Review of recent research into cellulosic whiskers, their properties, and their application in nanocomposite field. *Biomacromolecules* 2005;6:612–626.
- [36] Beck S., Bouchard J., Berry R. Dispersibility in water of dried nanocrystalline cellulose. *Biomacromolecules* 2012;13:1486–1494.
- [37] Khoshkava V., Kamal M.R. Effect of drying conditions on cellulose nanocrystal (CNC) agglomerate porosity and dispersibility in polymer nanocomposites. *Powder Technology* 2014;261:288–298.
- [38] Tang L., Weder C. Cellulose whisker/epoxy resin nanocomposites. *ACS Applied Materials & Interfaces* 2010;2:1073–1080.
- [39] Peng S.X., Youngblood J.P., Moon R.J. Design and characterization of cellulose nanocrystal-enhanced epoxy hardeners. *Green Materials* 2014;2:1–13.
- [40] Emami Z., Meng Q., Pircheraghi G., Mana-Zloczower I. Use of surfactants in cellulose nanowhisker/epoxy nanocomposites: effect on filler dispersion and system properties. *Cellulose* 2015;22:3161–3176.
- [41] Fox, D.M., Rodriguez, R.S., Devilbiss, M.N., Woodcock, J., Davis, C.S., Gilman, J.W. Simultaneously Tailoring Surface Energies and Thermal Stabilities of Cellulose Nanocrystals Using Ion Exchange: Effects on Polymer Composites Properties for Transportation, Infrastructure, and Renewable Energy Applications. *ACS Applied Materials & Interfaces*. <http://dx.doi.org/10.1021/acsami.6b06083>.
- [42] Zammarano M., Maupin P.H., Sing L.-P., Gilman J.W., McCarthy E.D., Kim Y.S., Fox D.M. Revealing the interface in polymer composites. *ACS Nano*. 2011;5(4):3391–3399.
- [43] Omrani A., Simonb L.C., Rostami A.A. Influences of cellulose nanofiber on the epoxy network formation. *Materials Science and Engineering A* 2008;490:131–137.
- [44] Xu S., Girouard N., Schueneman G., Shofner M.L., Meredith J.C. Mechanical and thermal properties of waterborne epoxy composites containing cellulose nanocrystals. *Polymer* 2013;54:6589–6598.

Bio-Based Composites for Sound Absorption

Eulalia Gliścińska, Izabella Krucińska,
Marina Michalak, Michał Puchalski,
Danuta Ciechańska, Janusz Kazimierczak and
Arkadiusz Bloda

Additional information is available at the end of the chapter

<http://dx.doi.org/10.5772/65360>

Abstract

The acoustic thermoplastic composites and a method for their production with the participation of the bio-components were presented. To form composite matrix polylactide fibres (PLA) were used. Natural fibres (flax (LI) and cotton (CO)), straw and cellulose ultra-short/ultra-fine fibres obtained from biomass were used as a reinforcement. Cellulose ultra-short/ultra-fine fibres were obtained from the flax fibres or straw by enzymatic treatment and optionally modified by silane. The tensile stress at maximum load of composites with the sub-microfibres obtained from waste flax fibres after silane modification is twice higher than that of the composite with the sub-microfibres without the silane modification.

The effect of different kinds of natural materials on the acoustic composites was studied. The addition of the straw increases the values of the sound absorption coefficient are higher because of the additional voids caused by the particles of straw. If as a reinforcement the CO fibres and cellulose sub-microfibres are used, the sound absorption of the composite is higher than for composite with only CO fibres. In the case of sub-microfibres obtained from the waste flax fibres the highest sound absorption and tensile stress of the composites gives the modification by solution of silane in ethanol and water.

Keywords: biomass, composite, sound absorption, fibre

1. Introduction

Composites are more and more popular products present in our lives. An extensive use of composites results from the diversity of their functional properties, what is connected with the combination of different components, diversified in terms of materials and forms, and with diversity of the final structures. Recently, the composites have been produced from renewable and sustainable materials. Renewable materials are natural, environmentally friendly and usually cheap. The composites produced from such materials are called 'green composites', but this concept is much broader and should concern their production and usage. Now the filling components in composites should be waste and the matrix material should be recyclable such as, for example, thermoplastics. Sustainability concerns three aspects: environmental, economic and social. The use of biomass, paper, fibres, wood as a waste filling material and bio-based thermoplastic polymers as a matrix can be the optimal material's solution [1].

The production of environmentally friendly composites on the basis of materials obtained from renewable resources is important for the economy and the environment. Recently, new materials on the basis of different plants are more and more popular and used in many industrial and life fields. Materials on the basis of straw, reeds, cattails and bent grass stalks are used in the ecological building sector [2]. The natural fibres can be used as a reinforcement or as a filling in composites, but also can give some new functions to them. Moreover, there is observed a growing trend towards replacing high-modulus reinforcing fibres with natural fibres [3–5]. Many technologies of composites based on different plants, natural fibres and even fibres isolated from plants are developed. The cellulose micro- or nanofibres, or micro-fibrils can be obtained through the chemical, mechanical, ultrasonic and enzymatic treatment of plants, such as jute [6, 7], soya bean source [8], wheat straw [9], soy hulls [10], rice straw [11], regenerated wood fibres [12] and canola straw [13].

Due to the great variety of plants, the properties of composites made of natural components are much diversified what favors different applications. Natural fibre-reinforced composites are used not only for construction but also for new uses, e.g., attenuation of sounds. Sound-absorbing composites can show a high degree of sound absorption, especially at high frequencies [14–19].

The commercially available porous sound-absorbing materials are usually fibrous. The fibres used are mostly synthetic, but recently, natural fibres are more and more popular as a raw material of the sound-absorbing products. Natural fibres are biodegradable and safer for human health than most mineral or polymer synthetic fibres. Introduction of the cellulose ultra-short/ultra-fine fibres prepared from different kinds of biomasses into functional composite structures causes increase in their sound absorption. Conversion of biomass to ultra-short/ultra-fine fibres perfectly fits into the current trends of cellulose nanostructures receiving by a top-down method. Depending on the size of the structures the obtained cellulose is suitably named, for example: microcrystalline cellulose, nanocrystalline cellulose or nano-whiskers.

Ultra-short/ultra-fine fibres, i.e., fibres not only extremely thin, but also extremely short, can be obtained by the enzymatic treatment of flax fibres and different kinds of straw. This form of fibres provides a greater surface area but causes application problems different from the case of electrospun filament fibres. A dust form requires direct screening of fibres onto the substrate. The use of ultra-short/ultra-fine fibres means larger area than in the case of longer fibres, in particular standard fibres. This form of fibres is advantageous from sound absorption point of view. The energy of the sound wave propagating in the material is reduced, and the internal energy of the material increases. Sound waves cause vibration of the fibres in the material and as a result of friction the created energy is converted into heat. A larger fibre surface promotes greater energy loss of the sound wave [16].

The virgin straw can also be used in sound-absorbing composites as an absorption enhancer. Independent of straw type, the values of the sound absorption coefficient increase because of the additional voids caused by the particles of straw and internal channels [20].

The aim of this work is to develop acoustic thermoplastic composites and the method for their production with the participation of the above-mentioned bio-based components. The effect of different kinds of natural materials on the acoustic composites was studied. Both waste natural fibres, straw and cellulose ultra-short/ultra-fine fibres, obtained from biomass can be used as an acoustic component increasing sound absorption of the composites.

In this work, the thermoplastic composites were obtained on the basis of textiles, i.e., nonwovens and above-mentioned natural materials in a thermal pressing process.

2. Materials

In order to thermally connect the composite constituents, one of them, forming the composite matrix, should be thermoplastic. The other ones are reinforcing/filling constituents.

To have a broader view of the acoustic properties of the composites the different raw materials and different combinations of reinforcing materials were used.

As a matrix material, the polylactide (PLA) fibres (6.7 dtex/64 mm) with a melting point in the range of 165–170°C have been selected. These fibres, Ingeo Fiber type SLN2660D, finished with polylactide resin without any hazardous substances, were delivered by Far Eastern Textile Ltd., Taipei, Taiwan.

As a reinforcement the following materials were used:

(a) waste natural fibres, **Figure 1**:

- flax fibres delivered by Safilin Ltd., Miłakowo, Poland,

- Tadjikistan cotton fibres 1.7 dtex/11 mm in the form of noils, delivered by Alto Ltd. (Gorzów Śląski, Poland), quality/degree of maturity is III/1.66 in a scale from 0 to 5.

(b) straws:

Three kinds of straw: grinded sunflower straw (SS), grinded corn straw (CS) and random cut wheat straw (WS) were cultivated and prepared by University of Agriculture in Cracow, Poland. The reinforcing materials are presented in **Figure 2**.



Figure 1. Photographs of the waste natural fibres reinforcement.



Figure 2. Photographs of the straw reinforcement.

Each kind of reinforcing material is characterized by diversified length and width. The length results from the random cutting process. The width is dependent on the native fibre or straw stem. Moreover, in the case of sunflower straw, two kinds of the particles can be distinguished, oblong particles coming from a hard envelope and more rounded particles coming from the soft inner parts. The corn straw particles are similar to sunflower ones but with smaller part of soft almost round particles. The wheat straw particles have the hollow channels.

(c) cellulose ultra-short/ultra-fine fibres obtained from:

- flax fibres 5.2 dtex/102 mm in the form of bleached roving, delivered by Safilin Ltd., Miłakowo, Poland,

- straw of retted fibre flax (SRFF), straw of oil flax (SOF) and hemp straw (HS) delivered by University of Agriculture in Cracow, Poland,

as a result of different processes depending on raw materials.

In order to obtain cellulose ultra-short/ultra-fine fibres, the flax fibres or straw were cut to the pieces of several centimetres and treated by enzyme preparation. The enzymatic treatment causes the decrease in length and fineness of starting materials. The fibres obtained, called as sub-microfibres, were dried at an ambient temperature and ground in a disk mill and then treated or not by 3-aminopropyltriethoxysilane STRUKTOL® SCA 1100 (Struktol Company of America, USA). That modification usually is used to increase adhesion of fibres to a hydrophobic matrix. In this case, silane modification was used also to prevent fibres connection in the polymer matrix. In the case of sub-microfibres obtained from waste flax fibres, two kinds of silane modifications were used, i.e., by 10 wt% solution of 3-aminopropyltriethoxysilane in ethanol or by 10 wt% solution of 3-aminopropyltriethoxysilane in mixture of ethanol and water to obtain additional activation. The surface of sub-microfibres obtained from straw was modified by 10 wt% solution of 3-aminopropyltriethoxysilane in acetone. That modification causes an agglomeration of sub-microfibres.

After silane modification, the cellulose sub-microfibres were ground in a disk mill. The sub-microfibres obtained from waste flax fibres and straw are presented in **Figures 3** and **4**, respectively.

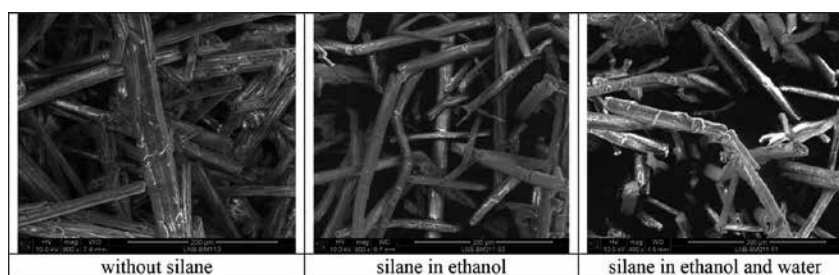


Figure 3. SEM images of cellulose sub-microfibres from waste flax fibres.

Characteristics of all cellulose sub-microfibres, with and without silane modification, are presented in **Table 1**.

The silane modification of the cellulose sub-microfibres obtained from waste flax fibres has not influence their morphological properties. The fineness of the sub-microfibres without modification is 11.36 μm and the length is 146.55 μm . The fineness of the sub-microfibres after the silane modification in solution of silane in ethanol is 12.28 μm and the fineness of the sub-microfibres after modification in solution of silane in mixture of ethanol and water is 13.46 μm . The length of the sub-microfibres after modification is 117.21 μm and 138.83 μm , corre-

spondingly. Because of high values of variation coefficients of these parameters, the above differences are non-essential. The silane modification results in increase in the value of degree of crystallinity of cellulose sub-microfibres by about 6% apart from the conditions of silane modification. The degree of crystallinity of sub-microfibres without the silane modification is 79% and after the silane modification takes the value above 85%.

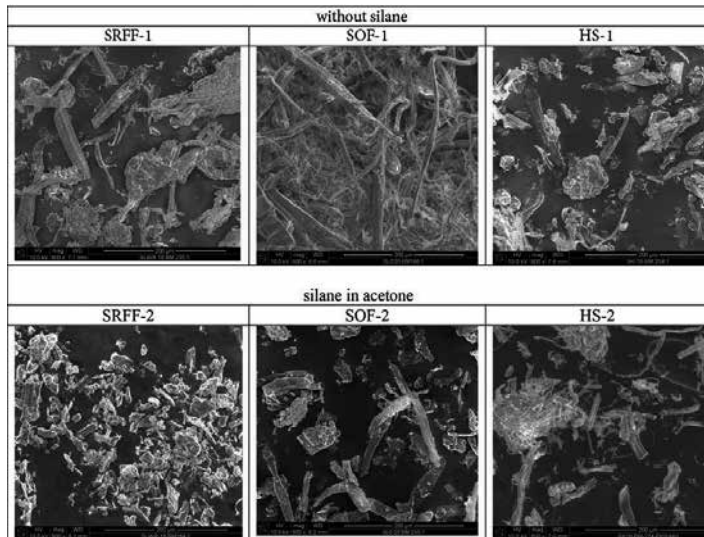


Figure 4. SEM images of cellulose sub-microfibres from straw (straw of retted fibre flax, SRFF, straw of oil flax, SOF, hemp straw, HS).

Symbol of sub-microfibres	Silane modification of sub-microfibres	Fineness		Length		Degree of crystallinity %
		Mean value (μm)	CV (%)	Mean value (μm)	CV (%)	
Cellulose sub-microfibres from waste flax fibres						
LI-1	Without	11.36	81.0	146.55	73.7	79.0
LI-2	Silane in ethanol	12.28	37.5	117.21	54.3	85.1
LI-3	Silane in ethanol+water	13.46	35.7	138.83	61.4	85.3
Cellulose sub-microfibres from straw						
SRFF-1	Without	5.62	48.40	70.00	53.16	68.3
SRFF-2	Silane in acetone	1.64	56.7	16.1	55.1	59.4
SOF-1	Without	11.09	46.80	89.07	61.65	63.2
SOF-2	Silane in acetone	8.94	55.06	46.35	35.77	61.3
HS-1	Without	6.33	40.13	55.24	64.30	65.8
HS-2	Silane in acetone	2.43	36.67	19.64	33.11	65.3

Table 1. Characteristics of cellulose sub-microfibres [21].

The silane modification of the cellulose sub-microfibres obtained from different kinds of straw causes the reduction of fibre dimensions. The fineness of the sub-microfibres from the SRFF straw without silane modification is 5.62 μm , from the SOF straw it is 11.09 μm and from HS it is 6.33 μm . The fineness of the sub-microfibres from SRFF straw after silane modification is 1.64 μm , from SOF straw it is 8.94 μm and from HS it is 2.43 μm . The length of the sub-microfibres after the enzymatic treatment is 70.00 μm for SRFF, 89.07 μm for SOF, and 55.24 μm for SOF straw. The length of the sub-microfibres from straw after silane modification is 16.1 μm for SRFF straw, 46.35 μm for SOF straw and 19.64 μm for HS straw. The values of variation coefficients of these parameters are very high. The silane modification has not significant influence on the degree of crystallinity of the cellulose sub-microfibres obtained from SOF and HS straws. For these sub-microfibres, the values of the degree of crystallinity change from 63.2 to 61.3% for SOF straw and from 65.8 to 65.3% for HS straw. In the case of sub-microfibres obtained from SRFF straw, the values of the degree of crystallinity are lower by 9% after silane modification.

The dimensions of the cellulose sub-microfibres obtained from flax fibres can be further reduced during the mechanical treatment in an aqueous suspension by means of a homogenizer. The length decreases to about 6 μm and diameter to about 300 nm. These fibres, **Figure 5**, referred to as sub-micro/nanofibres, were not dried to prevent their agglomeration.

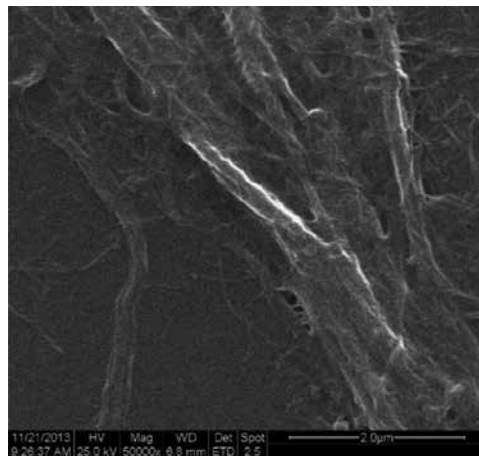


Figure 5. SEM image of the sub-micro/nanofibres from flax fibres [16].

3. Manufacturing of composites

Thermoplastic composites were obtained from the multilayer structures in a hydraulic press machine using a water-cooling system from Hydromega (Poland). The press conditions for all multilayer structures were the same, i.e., temperature 170–175°C, time 5 min and pressure 0.275

MPa. The multilayer structure was wrapped with Teflon foil to prevent molten polymer propagation during the pressing process.

It was assumed to obtain composite samples with similar thicknesses to allow for assessment of the effect of the reinforcement type. Each multilayer structure was composed of several layers of nonwovens either separated alternately or not by layers of grinded straw or cellulose ultra-short/ultra-fine fibres. The appropriate mass of straw/cellulose ultra-short/ultra-fine fibres was divided in portions, which were put uniformly onto consecutive layers of nonwoven and the top of multilayer structure was covered by nonwoven.

The needle-punched nonwovens were manufactured from matrix fibres 'PLA (100%)' or from a blend consisting of matrix fibres 'PLA' and reinforcing waste flax fibres 'LI' or waste cotton fibres 'CO'.

In order to manufacture needle-punched nonwovens the fleeces with a cross-system of fibre arrangement were obtained on the roller card. Needle punching of the fleece layers was carried out on an Asselin needle punching machine (France), with the following technological parameters: type of needles – $15 \times 18 \times 40 \times 3\frac{1}{2}$ RB (Groz-Beckert®), number of needle punches – $40/\text{cm}^2$, depth of needle punching – 12 mm [16].

4. Methods

The thickness of composites was determined according to the standard procedure ISO 9073-2:1995 and their apparent density was determined as the ratio of mass to volume of samples. The mechanical properties of composites were estimated in unidirectional tensile test by means of testing machine type 3119-410 (Instron, UK) according to the standard ISO 527-4:1997. The sound absorption coefficient was determined according to the standard procedure ISO 10534-2:1998 within the frequency range of 500–6400 Hz. A small size impedance tube (Kundt tube) type 4206 (Brüel&Kjaer, Denmark) was used (**Figure 6**). The diameter of the investigated samples was equal to 29 mm.



Figure 6. The Kundt device for acoustic measurements.

5. Results

The values of mass per square meter were similar for all nonwovens, i.e., in the range of 115–120 g/m². The composites obtained were rigid with a small thickness of a few millimetres, ‘green’, and designed among others from cheap components coming from renewable resources. Each composite was manufactured from the system consisting of 80 wt% of nonwoven (PLA (100%) or PLA/LI (80/20%) or PLA/CO (90/10%)) and 20 wt% of straw or cellulose ultra-short/ultra-fine fibres.

5.1. Composite structure: organoleptic assessment

The most uniform and homogeneous structure is observed for matrix materials. In the case of the composites, the structure depends on the reinforcement type. The photographs in **Figure 7** present the structure of the selected composites.

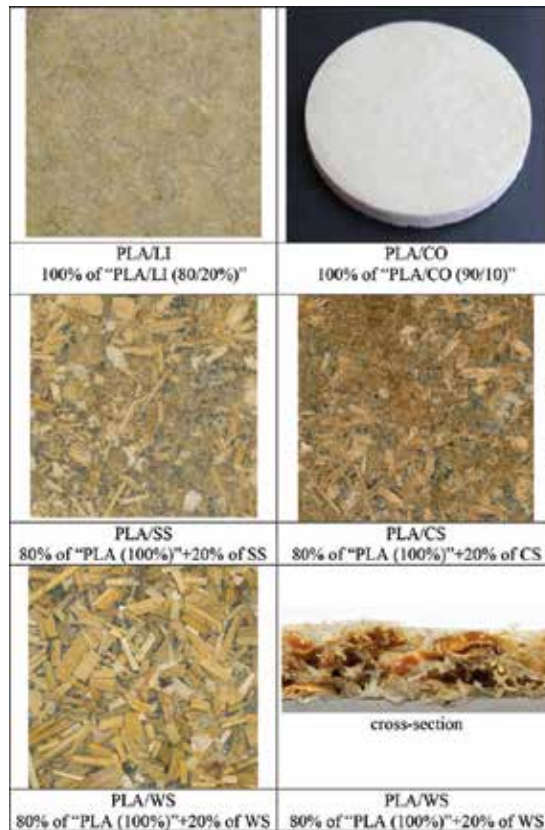


Figure 7. Photographs of the composites.

If the fibres are used as a reinforcement, the composite structure is more uniform. It results from the uniform structure of nonwoven composed of reinforcing and matrix fibres and from

their high mixing level. The external and internal layers of nonwoven are pressed giving uniform, homogeneous porous structure. On the composite surface, the reinforcing fibres, matrixes and voids are visible. If the fibres and straw are used as a reinforcement, the composite structure is more diversified. The addition of straw particles leads to the formation of larger voids inside the composite structure. If only the straw is used as a reinforcement, the layers of matrix and straw can be visible. Inside the composite structure, the straw particles are partially bound with the matrix, and the voids exist. The composite surfaces are formed from the matrix without visible voids. Generally, the straw gives larger voids than the fibres and the larger straw particles give larger voids. In the case of composite, on the basis of the wheat straw, the additional voids are inside the straw particles. In the case of composites with cellulose ultra-short/ultra-fine fibres, the variants with standard fibres give more uniform structures than without, because standard fibres prevent their agglomeration.

5.2. Physical and mechanical properties

The physical properties as a thickness and apparent density and mechanical properties as a tensile stress at the maximum load are presented in **Table 2**. The thickness and density of the material are the most important factors determining its acoustic properties [21]. In this work, it was assumed to obtain composites of very low thickness and low density. A small thickness of millimetres is important when the composite material is combined with other materials. The low density is important to produce light materials.

5.2.1. Composites on the basis of flax fibres and straw

The thickness of the composites is in the range from 3.52 to 4.71 mm. The thickness of the PLA/straw composites is higher on average by 26.90% than thickness of the PLA/LI/straw composites, and because of that the density is correspondingly lower. The tensile stress at maximum load of the composites depends on a reinforcement type. The highest value of tensile stress, i.e., 2.69 MPa, is determined for the PLA/LI composite characterized by the medium value of apparent density. If the matrix material is used in the form of fibres, their mixing with reinforcing fibres can be excellent, especially in the needle-punched nonwoven. It results in the higher tensile stress of the composite. The lower mixing level of the thermoplastic fibres with straw particles, or with straw particles and reinforcing fibres, gives lower tensile stress of the composite. It means that flax fibres are better reinforcing materials than straw and the level of mixing of reinforcing and matrix materials in nonwoven is high what leads to suitable consolidation. This is confirmed by the PLA/LI/straw composites, for which the values of tensile stress at maximum load are higher than for the PLA/straw composites and lower than PLA/LI composites. The differences in apparent density of the composites have no significant effect on the tensile stress [20].

5.2.2. Composites on the basis of cotton fibres and cellulose ultra-short/ultra-fine fibres

The composites obtained (**Table 2**) were characterized by similar, very low thickness on the level of about 4.7–5.5 mm. These differences in the thickness of composites are insignificant for their acoustical properties [16].

Variant of the composite	Thickness (mm)	Apparent density (kg/m ³)	Tensile stress at maximum load (MPa)
PLA	3.80	1321.00	–
PLA/LI (80/20%)	3.92	313.43	2.69
PLA/CO (90/10%)	4.5	264.32	0.79
PLA + straw			
PLA/SS	4.65	271.76	1.12
PLA/CS	4.65	276.20	1.22
PLA/WS	4.71	258.63	1.54
PLA+LI+straw			
PLA/LI/SS	3.77	393.60	1.98
PLA/LI/CS	3.52	341.22	1.75
PLA/LI/WS	3.75	337.75	1.60
PLA+CO+sub-microfibres from LI			
LI-1	5.3	260.61	1.20
LI-2 silane in ethanol	4.9	287.57	2.27
LI-3 silane in ethanol and water	4.8	299.87	2.27
PLA+CO+sub-microfibres from straw			
SRFF-1	5.4	267.30	1.29
SRFF-2 silane in acetone	4.8	299.87	1.79
SOF-1	4.9	242.42	1.04
SOF-2 silane in acetone	4.7	273.39	1.13
HS-1	5.5	236.01	1.19
HS-2 silane in acetone	4.8	287.17	1.54

SS, grinded sunflower straw; CS, grinded corn straw; WS, random cut wheat straw.

Table 2. Characteristics of the composites [20, 21].

For studied composites, the 20% addition of cellulose sub-microfibres results in increase in their mechanical properties. The composite manufactured under the same technological conditions but without the addition of sub-microfibres (PLA/CO) has the lowest tensile stress at maximum load equals to 0.79 MPa. The results show the relationship between the mechanical properties of the composites with cellulose sub-microfibres and the method of the sub-microfibres preparation.

For the composites with sub-microfibres obtained from waste flax fibres, the tensile stress at maximum load is diversified depending on the sub-microfibres preparation. The tensile stress at maximum load for the composite manufactured with sub-microfibres obtained from waste

flax fibres gains the value of 1.20 MPa and for the composites with sub-microfibres additionally modified by silane (LI-2, LI-3), the value of 2.27 MPa is twice higher apart from the conditions of silane modification. These results correspond to the degree of crystallinity of the cellulose sub-microfibres. The same relationship is observed for the composites manufactured with sub-microfibres from straws, after silane modification the cellulose sub-microfibres give better reinforcement than without silane modification. The values of tensile stress at maximum load of the composites with sub-microfibres obtained from each kind of straw after silane treatment are from 9.05 to 38.76% higher than the values of tensile stress of composites with corresponding sub-microfibres obtained without silane modification. The best results of tensile stress are observed for composites with sub-microfibres obtained from SRFF straw.

The tensile stress at maximum load for the composites manufactured with sub-microfibres obtained from the straw of retted fibre flax is 1.29 MPa and for the composites with sub-microfibres additionally modified by silane (SRFF-2) reaches the value of 1.79 MPa. It means that silane modification gives favorable conditions for adhesion between the cellulose sub-microfibres and the PLA matrix. It results advantageously in tensile strength of composites. This effect is more distinct for the composites with sub-microfibres from flax fibres than with sub-microfibres from straws. The tensile strength is the highest for composites with sub-microfibres obtained from waste flax fibres and modified by silane (LI-2, LI-3). Both the silane modification favoring good adhesion to polymer and a high degree of crystallinity of sub-microfibres resulted in the highest values of tensile stress at maximum load for these composites.

In the case of apparent density, which is a very important factor deciding about sound absorption, the differences are more considerable. Density of the composites with cellulose sub-microfibres obtained from waste flax fibres and modified by silane with additional water activation (LI-3) is higher by 4% than the density of the composites with the same cellulose sub-microfibres but modified by silane without water activation (LI-2), and by 15% higher than the density of the composites with the sub-microfibres not modified by silane (LI-1).

Density of the composites with cellulose sub-microfibres obtained from straws and modified by solution of silane in acetone is higher by 12.1% for SRFF straw, 12.8% for SOF straw, and 21.6% for HS straw than the density of the corresponding composites with sub-microfibres not modified by silane [22]. For the studied composites, these differences in material density are not significant from their sound absorption point of view [16].

5.3. Acoustic properties

Acoustic properties were characterized by sound absorption coefficient, which values can be in the range from 0 (total reflection) to 1.00 (total absorption). According to EN ISO 11654, low absorption is from 0.15, absorption from 0.30, high absorption from 0.60 and very high absorption from 0.80.

For studied materials not only the value of sound absorption coefficient is important, but also the sound frequency range of high absorption.

5.3.1. Composites on the basis of flax fibres and straw

The biomass is very diversified and gives a very diversified effect from the acoustical point of view. **Figures 8–10** present the most characteristic dependences of the sound absorption coefficient-sound frequency for PLA materials, PLA/LI fibres, PLA/straw and PLA/LI fibres/straw composites. Among studied composites, the highest values of the sound absorption coefficient, even in the range of 0.8–0.9, are determined for the PLA/straw composites [20].

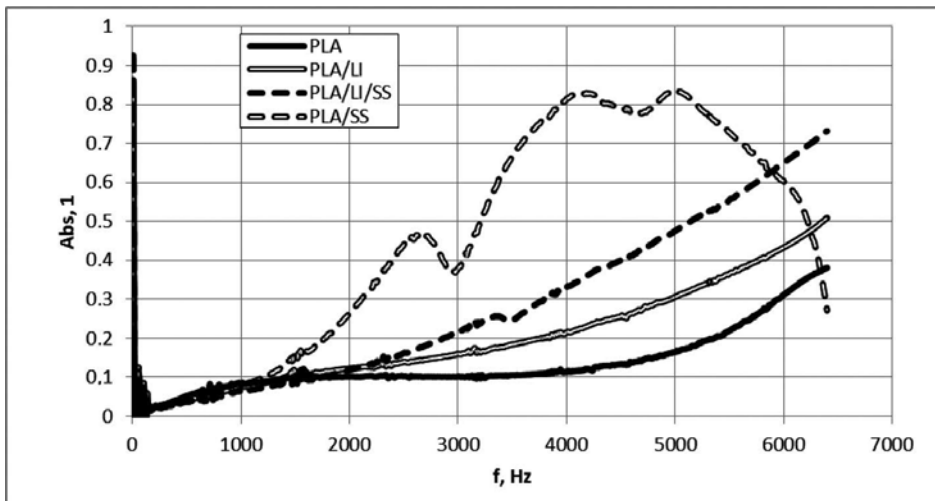


Figure 8. Sound absorption coefficient of the composite-waste flax fibres and sunflower straw as a reinforcement.

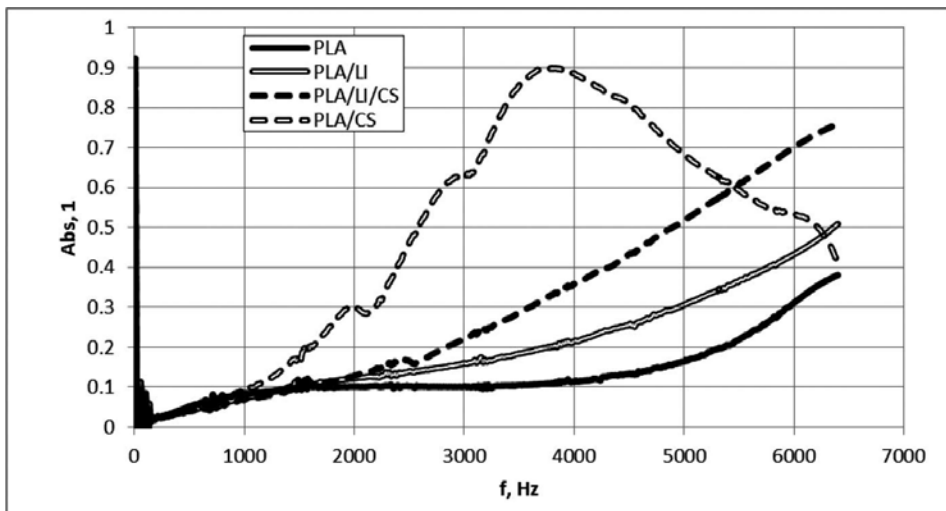


Figure 9. Sound absorption coefficient of the composites-waste flax fibres and corn straw as a reinforcement.

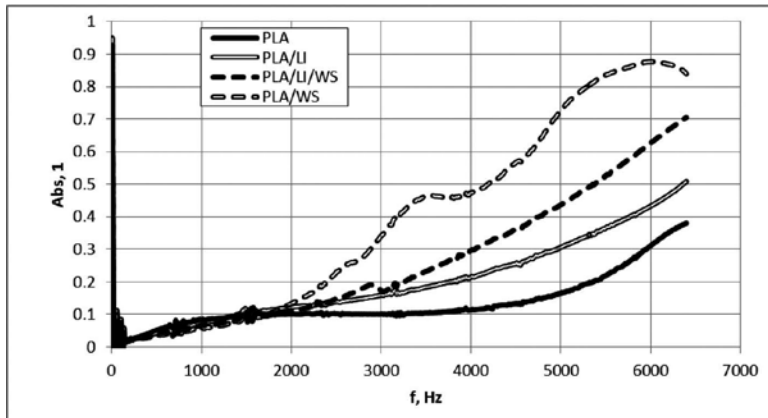


Figure 10. Sound absorption coefficient of the composites-waste flax fibres and wheat straw as a reinforcement.

The sound absorption coefficient of the PLA matrix material is the lowest and has the value of about 0.1 at the low and mid-frequencies, at high frequencies it increases to 0.38 at 6400 Hz. This material cannot be used as a sound absorber of frequencies lower than 6000 Hz.

If nonwoven from blend of PLA matrix fibres and diversified waste flax fibres is used, the sound absorption of the composite is growing with frequency. The sound absorption coefficient of the composite from the 'PLA/LI (80/20%)' nonwoven is higher and depends linearly on a sound frequency arriving maximum value of 0.40 at a maximum studied frequency of 6400 Hz. This almost linear dependence is typical for fibre-based composites [19]. Even addition of particles thicker than fibres gives similar dependence, but with higher sound absorption. If the 20% of 'PLA/LI (80/20%)' nonwoven is replaced by straw, the sound absorption is more higher in the range from 3000 to 6400 Hz. It probably results from the fact that beside of small voids in composite, the bigger voids are formed. The sound waves of such frequencies can be reverberated repeatedly inside the diversified voids until soundproofing. The upward trend is evident and similar for all three kinds of composites with straw, as shown in **Table 3**. For the composite from a multilayer structure consisting of 80% of PLA/LI nonwoven and 20% of corn straw, the sound absorption coefficient increases linearly with sound frequency, and at 6400 Hz it is equal to 0.76. For the composites with sunflower or wheat straw as a reinforcement, the maximum value is 0.71 and 0.68 at 6400 Hz, respectively.

If PLA nonwoven and straw are used, the acoustic characteristic of the composite is totally different. The curve of the sound absorption coefficient-sound frequency dependence has another course. For each PLA/straw composite this course is slight different, because the kind of particle of each straw is slight different. Generally, the maximum values of sound absorption coefficient occur at medium (for PLA/SS and PLA/CS composites) and high (for PLA/WS composite) values of the studied frequency range. It means that the PLA/straw composites can be used as a material absorbing the sound of medium and high frequencies. The maximum values of the sound absorption coefficient of the PLA/straw composites are higher than those of PLA/LI or PLA/LI/straw composites. The sound absorption coefficient reaches the values of

0.8–0.9. For the PLA/straw composites, the frequency range of the maximum values of the sound absorption coefficient is wider than for PLA/LI or PLA/LI/straw composites.

Variant of the composite	Sound absorption coefficient						
	Frequency (Hz)						
	1000	2000	3000	4000	5000	6000	6400
PLA/LI	0.061	0.122	0.138	0.196	0.310	0.434	0.496
PLA/LI/SS	0.067	0.105	0.202	0.315	0.459	0.628	0.706
PLA/LI/CS	0.071	0.133	0.221	0.360	0.515	0.702	0.757
PLA/LI/WS	0.059	0.095	0.168	0.281	0.422	0.617	0.684

Table 3. The sound absorption coefficients of the PLA/LI/straw composites.

All of the obtained composites of such small thickness and apparel density show the sound absorption, wherein the values of the sound absorption coefficient depend on the reinforcement type and sound frequency.

5.3.2. Composites on the basis of cotton fibres and cellulose ultra-short/ultra-fine fibres

The CO fibres used as a reinforcement give better effect on sound absorption of the PLA composites than cellulose sub-microfibres. If as a reinforcement the CO fibres and cellulose sub-microfibres are used the sound absorption is more better. Increase in sound absorption over the whole range of investigated frequency is observed for 10% and optimal for 20% by ieswt. sub-microfibre content. The addition of sub-microfibres changes the character of the curve of the sound absorption coefficient in a function of sound frequency (**Figure 11**).

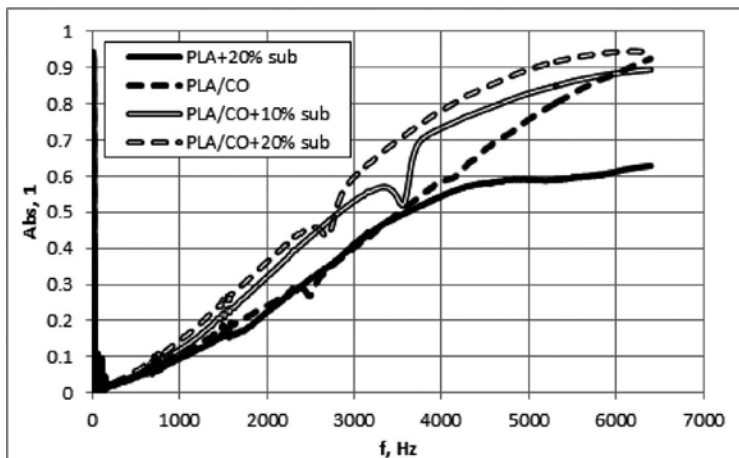


Figure 11. Sound absorption coefficient of the composites with/without sub-microfibres.

Among composites with sub-microfibres obtained from flax fibres, the composites with fibres without silane (LI-3) are characterized by the highest sound absorption, **Figure 12**, and the highest tensile stress at maximum load, **Table 2** [21]. Among studied composites with cellulose sub-microfibres obtained from straws, the best results, similar to composites LI-1, are observed for composites with sub-microfibres from SOF straw (SOF-1), **Figure 13**.

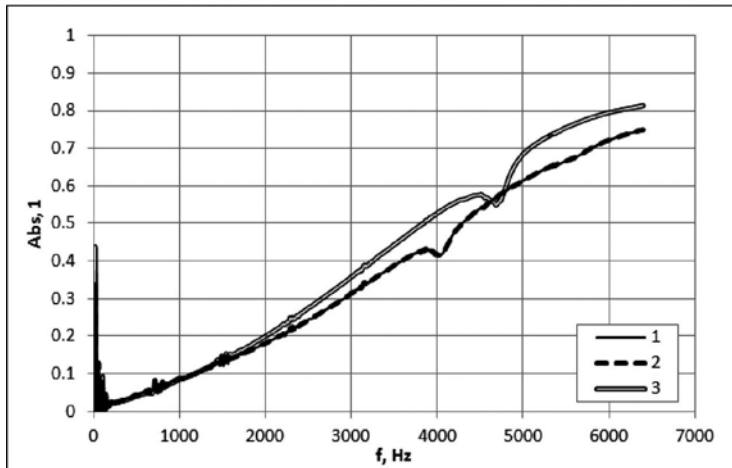


Figure 12. The sound absorption coefficient in the function of sound frequency for the composites: 1, LI-1 (without silane); 2, LI-2 (silane in ethanol); and 3, LI-3 (silane in ethanol and water).

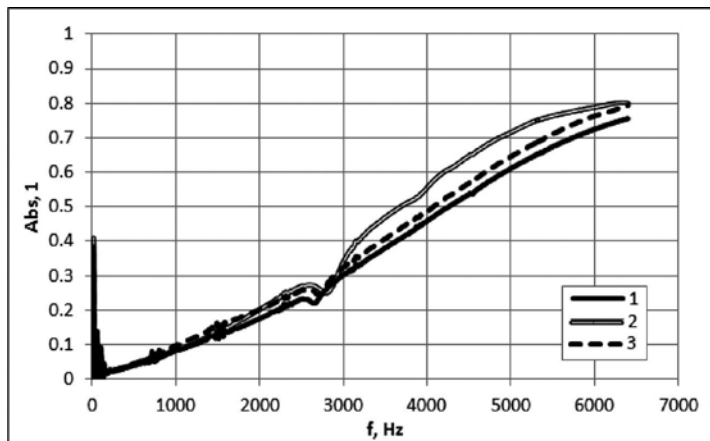


Figure 13. The sound absorption coefficient in the function of sound frequency for the composites: 1, SRFF-1; 2, SOF-1; 3, HS-1.

For the composites with sub-microfibres obtained from straws and then modified by solution of silane in acetone, the best results of the sound absorption are observed for the composites with sub-microfibres obtained from SRFF straw (SRFF-2), **Figure 14**. The silane modification

of sub-microfibres obtained from SOF and HS straws does not change the sound absorption coefficient of the composites with them. In the case of SRFF, the difference between the sound absorption of composites with sub-microfibres modified by silane and without modified by silane is the highest, **Figures 15–17**. The composites with sub-microfibres obtained from SRFF straw modified with silane (SRFF-2) are characterized by the best results in sound absorption and tensile stress among the composites with sub-microfibres obtained from straws.

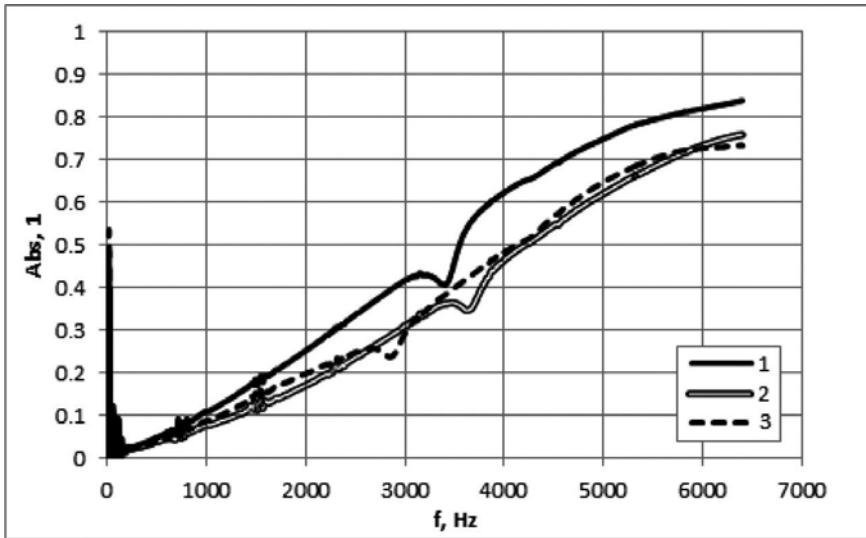


Figure 14. The sound absorption coefficient in the function of sound frequency for the composites: 1, SRFF-2; 2, SOF-2; 3, HS-2.

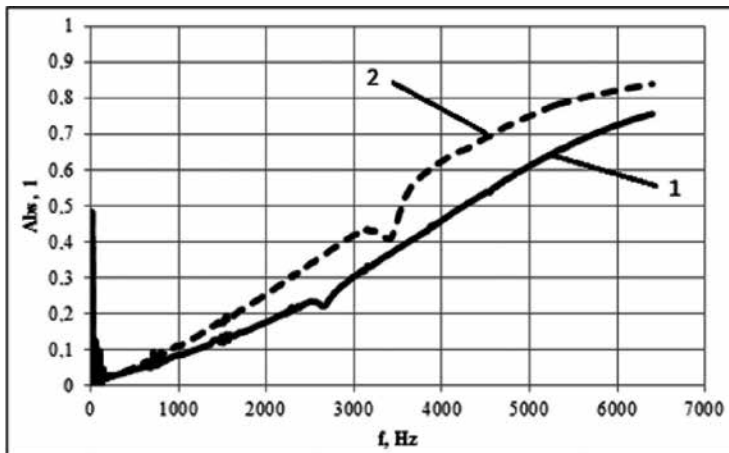


Figure 15. The sound absorption coefficient in the function of sound frequency for the composites with SRFF sub-microfibres: 1, SRFF-1; 2, SRFF-2.

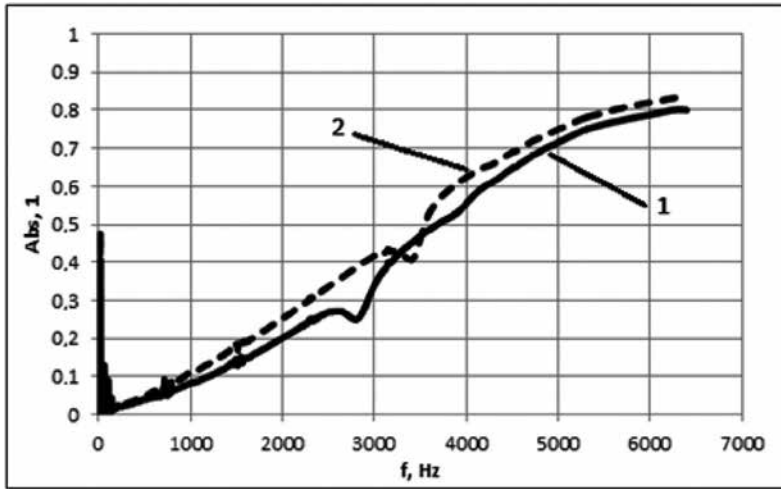


Figure 16. The sound absorption coefficient in the function of sound frequency for the composites with SOF sub-microfibres: 1, SOF-1; 2; SOF-2.

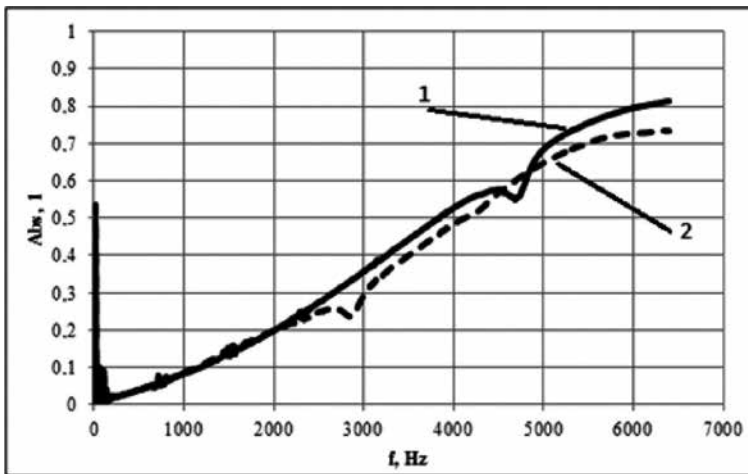


Figure 17. The sound absorption coefficient in the function of sound frequency for the composites with HS sub-microfibres: 1, HS-1; 2, HS-2.

The silane modification of sub-microfibres obtained from straws gives the best effect for SRFF straw because of the highest increase in tensile stress and in sound absorption coefficient. The sound absorption coefficient of the SRFF-1 composite was the lowest among all composites with sub-microfibres without silane modification but absorption coefficient of SRFF-2 composite is the highest in the whole range of investigated frequencies. The increase in stress at maximum load of the SRFF-2 composite is the highest among other composites with sub-microfibres from straws and is 38.8% higher than that of SRFF-1 composite.

For composites with sub-microfibres obtained both from waste flax fibres and from straws, the silane modification of sub-microfibres gives probably higher arrangement of fibres and their better adhesion to the polymer matrix, what is observed in high sound absorption and high tensile stress. In the case of sub-microfibres obtained from waste flax fibres, the highest sound absorption and the highest tensile stress of the composites give the modification by solution of silane in ethanol and water.

In the case of the composites with cotton fibres and sub-micro/nanofibres, **Figure 18**, the sound absorption increases rapidly to a value of 0.8 in the range of 500–4000 Hz and in the range of 4000–6400 Hz slightly increases. The absorption coefficient at a frequency of 6400 Hz is equal to 0.95. If the content of CO fibres was increased to 50%, the sound absorption coefficient increases in the range of 500–2500 Hz to approximately 0.8, and in the range of 4000–6000 Hz it is almost constant.

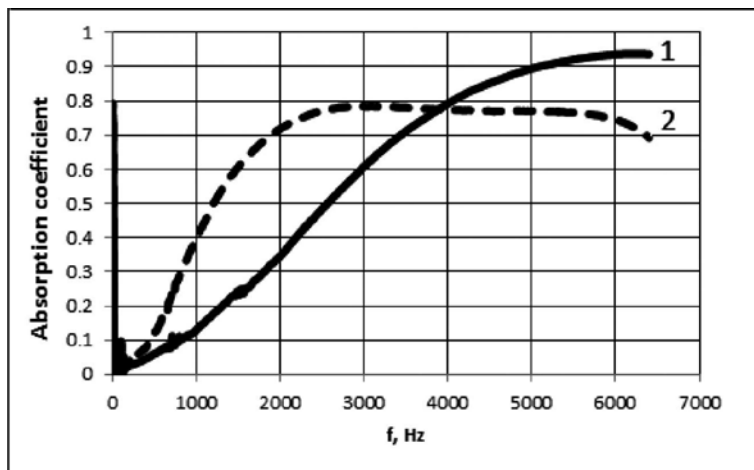


Figure 18. Sound absorption coefficient of the composites: 1, 80%PLA/CO (90/10) + 20% cel. Sub-micro/nano; 2, 80%PLA/CO (50/50) + 20% cel. Sub-micro/nano [16].

Results show that sound absorption of the composite depends on the content of reinforcing fibres. For higher percentage of these fibres, the higher sound absorption is observed. The sound wave causes the fibres vibration and as a result of friction the created energy of sound wave is converted to heat conversion. Larger total fibre surface leads to greater interaction of sound wave with the fibres. This effect of interaction between sound wave and fibre surface is stronger if the standard fibres are replaced by ultra-short/ultra-fine fibres [16].

6. Conclusions

The study included not only development of a method for manufacturing sound-absorbing composites, but also determination of the requirements for the characteristics of reinforcing

materials, optimal from the point of view of sound absorption. A comparison was made to the raw material used, and its treatment, with respect to the sound absorption of the composite as well as its strength. Silane modification does not significantly affect change fibre dimensions, and the manner of its implementation and the origin of the fibres show no effect on the sound absorption of the composite. The use of fibres coated by silane preparation is preferred from the viewpoint of mechanical properties. Tensile strength of composites containing fibres coated with the silane preparation is about twice higher than that of the composites with the unmodified fibres.

Composites could be prepared from the layers of needled nonwoven formed from the matrix fibres or a mixture of matrix fibres and reinforcing standard fibres and layers of straw or ultra-short/ultra-fine fibres alternately arranged. In the case of composite reinforced by straw, the presence of the standard fibres is inadvisable. The addition of the straw, independent of straw type, increases the values of the sound absorption coefficient because of the additional voids caused by the particles of straw. Both grinded sunflower straw, grinded corn straw and random cut wheat straw reduce the tensile stress at maximum load of the composites, but increase the sound absorption even to 0.8–0.9 in some frequency ranges.

Studies have shown that the composite structure produced by compressing the fibrous layer system is most advantageous from the point of view of its sound absorption when the standard fibres are as a reinforcement with ultra-short/ultra-fine fibres. The addition of sub-microfibres in an amount of 10–20% by weight of this system gives the significant effect on the composite sound absorption in the entire tested range of sound frequencies, i.e., up to 6400 Hz. The rapid increase of the absorption coefficient to the value of approx. 0.8 is in the range of 500–4000 Hz, followed by a further but slower increase is observed. If, however, as ultra-short/ultra-fine fibres will be used sub-micro/nanofibres, obtained by additional mechanical treatment of sub-microfibres, giving further fragmentation, then this relationship may adopt a different character. For a composite containing approx. 50% of the standard fibres and 20% of sub-micro/nanofibres sound absorption coefficient reaches a high value of 0.75–0.80 even at lower frequencies, i.e., from 2500 Hz and maintains at such a high level at higher frequencies.

Studies have shown that the best effect on the sound absorption of the composite, i.e., high sound absorption coefficient over a wide frequency range, may be obtained using next the standard reinforcing fibres the ultra-short/ultra-thin fibres with a minimum dimensions, because the larger the surface of the fibres, the greater the impact of the sound wave with fibres, and therefore greater its attenuation.

The developed composites are thin (several mm thick), lightweight, rigid, washable, high sound-absorbing of middle and high frequencies, which can be produced from waste fibres and straw, and may be designed to eliminate sound from various sources, for example in devices, vehicles and other means of transport, and for sound absorption in the rooms.

These ecological composites have characteristics in line with European trends and can be used as a stand-alone screen or to fill sound-absorbing panels, as a sound-absorbing contribution under the plaster in the construction of walls and ceilings suspended or in silenced car door, hatch, wheel arches, headliner and trunk.

Acknowledgements

This work has been supported by the Project 'Utilization of biomass for the preparation of environmentally friendly polymer materials' (Biomass)—POIG.01.01.02-10-123/09.

Author details

Eulalia Gliścińska^{1*}, Izabella Krucińska¹, Marina Michalak¹, Michał Puchalski¹,
Danuta Ciechańska², Janusz Kazimierczak² and Arkadiusz Bloda²

*Address all correspondence to: klata@p.lodz.pl

1 Department of Material and Commodity Sciences and Textile Metrology, Faculty of Material Technologies and Textile Design, Lodz University of Technology, Łódź, Poland

2 Institute of Biopolymers and Chemical Fibres, Łódź, Poland

References

- [1] Mohanty A.K., Misra M., Drzal L.T. Sustainable bio-composites from renewable resources: opportunities and challenges in the green materials world. *Journal of Polymers and the Environment*. 10, 1(2002) 19–26.
- [2] Vėjelienė J., Gailius A., Vėjelis S., Vaitkus S., Balčiūnas G. Evaluation of structure influence on thermal conductivity of thermal insulating materials from renewable resources. *Materials Science (Medžiagotyra)*. 17, 2(2011) 208–212.
- [3] Mohanty AK. Natural fibre composites for a sustainable and low-carbon economy: where we are and our future directions. In: *Proceedings of 1st International Conference on Natural Fibers – Sustainable Materials for Advanced Applications*. Guimarães. 9–11 June 2013, pp. 5 and CD.
- [4] Bodur MS, Bakkal M, Sonmez HE. Silane treatment effect on the mechanical performance of the waste cotton fiber reinforced composites. *Composites Week @ Leuven and TexComp-11*. Leuven. 16–20 September 2013. CD. Form 20.03.2014 online.
- [5] Zimniewska M, Myalski J, Kozioł M, et al. Natural fiber textile structures suitable for composite materials. *Journal of Natural Fibers*. 9 (2012) 229–239.
- [6] Padal KTB, Ramji K, Prasad VVS. Mechanical properties of jute nanofibres reinforced composites. *Global Journal of Researches in Engineering: A. Mechanical and Mechanics Engineering*. 14 (2014) 1–6.

- [7] Baheti V., Militky J., Marsalkova M. Mechanical properties of polylactic acid composite films reinforced with wet milled jute nanofibers. *Polymer Composites*. Vol. 34, 12(2013) 2133–2141.
- [8] Wang B., Sain M. Isolation of nanofibers from soybean source and their reinforcing capability on synthetic polymers. *Composites Science and Technology*. 67 (2007) 2521–2527.
- [9] Alemdar A., Sain M. Biocomposites from wheat straw nanofibers: morphology, thermal and mechanical properties. *Composites Science and Technology*. 68 (2008) 557–565.
- [10] Alemdar A., Sain M. Isolation and characterization of nanofibers from agricultural residues – wheat straw and soy hulls. *Bioresource Technology*. 99 (2008) 1664–1671.
- [11] Nasri-Nasrabadi B., Behzad T., Bagheri R. Preparation and characterization of cellulose nanofiber reinforced thermoplastic starch composites. *Fibers and Polymers*. 15 (2014) 347–354.
- [12] Panaitescu D.M., Frone A.N., Ghiurea M., Spataru C.I., Radovici C., Iorga M.D. Properties of polymer composites with cellulose microfibrils. Brahim Attaf, *Materials Science Composite Materials, Advances in Composite Materials—Ecodesign and Analysis*, ISBN 978-953-307-150-3, 2011 under CC BY-NC-SA 3.0 license. Chapter 5, 103–122.
- [13] Yousefi H., Faezipour M., Nishino T., Shakeri A., Ebrahimi G. All-cellulose composite and nanocomposite made from partially dissolved micro-and nanofibers of canola straw. *Polymer Journal*. 43 (2011) 559–564.
- [14] Jayamani E., Hamdan S. Sound absorption coefficients natural fibre reinforced composites. *Advanced Materials Research*. 701 (2013) 53–58.
- [15] Koizumi T, Tsujiuchi N and Adachi A. The development of sound absorbing materials using natural bamboo fibers. *WIT Press 2002*; Vol. 59. 672–81.
- [16] Krucińska I., Gliścińska E., Michalak M., Ciechańska D., Kazimierzczak J., Bloda A. Sound-absorbing green composites based on cellulose ultra-short/ultra-fine fibers. *Textile Research Journal*. Vol. 85, 6(2015) 646–657.
- [17] Gliścińska E., Michalak M., Krucińska I., Kazimierzczak J., Bloda A., Ciechańska D. Sound absorbing composites from nonwoven and cellulose submicrofibres. *Journal of Chemistry and Chemical Engineering*. 7 (2013) 942–948.
- [18] Krucińska I., Gliścińska E., Michalak M., Kazimierzczak J., Bloda A., Ciechańska D. The influence of cellulose submicrofibres reinforcement on the sound absorption behavior of thermoplastic composites, in: R. Fangueiro, *Book of Abstracts*, pp. 385, ISBN 978-989-20-3872-8, 1st International Conference on Natural Fibers, 09–11 June 2013, Guimarães, Portugal.

- [19] Gliścińska E., Michalak M., Krucińska I. Sound absorption property of nonwoven based composites. *AUTEX Research Journal*. 13 (2013) 150–155.
- [20] Krucińska I., Gliścińska E., Michalak M. Efficient utilization of biomass to produce sound-absorbing composites, 2nd International Conference on Natural Fibers, 2015, Azores, Portugal, CD Proceedings ISBN: 978-989-98468-4-5, 1–9.
- [21] Parikh D.V., Chen Y., Sun L. Reducing automotive interior noise with natural fiber nonwoven floor covering systems. *Textile Research Journal*. 76 (2006) 813–820.
- [22] Gliścińska E., Krucińska I., Michalak M., Puchalski M., Kazimierczak J., Bloda A., Ciechańska D. Sound absorption of composites with waste cellulose submicrofibres, 14th AUTEX World Textile Conference, 2014, Bursa, Turkey, CD, ISBN 978-605-63112-4-6, poster, 1–6.

Nano-Rheological Behaviour of Cassava Starch-Zinc Nanocomposite Film under Dynamic Loading for High Speed Transportation of Packaged Food

Adeshina Fadeyibi, Zinash D. Osunde, Gbabo Agidi,
Evans C. Egwim and Peter A. Idah

Additional information is available at the end of the chapter

<http://dx.doi.org/10.5772/64984>

Abstract

This research was undertaken to determine the nano-rheological behaviours of cassava starch-zinc-nanocomposite films under dynamic loading for assessing their suitability as food packaging materials in high speed transportation. The films, with thickness ranging between 15 ± 0.22 – 17 ± 0.13 μm , were prepared by casting mixtures of 24 g cassava starch, 45–55% (w/w) glycerol and 0–2% (w/w) zinc nanoparticles in plastic moulds of 8–12 mm depths. The effects of the nanoparticles, thickness and glycerol on the rheological properties of the films, including the Young's modulus, creep, hardness and plasticity index were determined using nanoindentation technique. The results show that the Young's modulus and hardness of the films varied inconsistently with glycerol concentration and nanoparticles due probably to their isotropic nature and sensitivity to slight change in load. The plasticity index was lower for 15 μm film, which absorbed 40 pNm and dissipated 0.5 pNm during loading and unloading stages, respectively. The response of the 15 μm film to creep was higher than 16 μm and 17 μm films, and this may be consequence of lower wear at higher loads. This implies that the nanocomposite film might be suitable for high speed transportation of packaged food.

Keywords: rheological behaviour, hysteresis loop, zinc nanocomposite film, food packaging

1. Introduction

Flexible films (<100 μm), such as low-density polyethylene and polyvinyl chloride, are widely applied in the food industry [1]. The handling of the flexible films in the packaging and

transportation of food and food products over long distances is an issue bordering the agricultural products processing engineers, due to the dynamic loading experienced by the materials in the process [2]. The viscoelastic behaviour often exhibited by this material has great influence on its degree of wear and tear, especially during high speed transportation of packaged foods. The low mechanical impedance of the flexible films has rendered measurement of the rheological behaviour difficult to achieve using the universal tensile testing equipment but can be measured using nanoindentation analysis [3, 4]. The indirect measurement of the area of contact between the indenter and flexible film under investigation is called nanoindentation. The method provides an avenue of touching the flexible film, whose rheological properties are unknown, with another material of known property. The penetration depth of the indenter, which allowed for proper measurement of the penetration rate in the flexible film, is usually measured in nanometres, thus considering the process as non-destructive because of its relatively smaller area of contact. The accurate measurement of the rheological properties has been made possible using the nanoindentation technique. It is easier to measure the rheological properties of flexible films by this process due probably to the high response of the material to the depth sensing device. The knowledge of the response of flexible films to this device can be used to study their behaviour with respect to deformation or wear [5].

The rheological behaviour of flexible films, under static and dynamic loading, has been reported by some researchers [6–8]. Jian et al. [6] studied the load-displacement behaviour of Cu_2O thin films by nanoindentation. The authors observed that the regions of loading and unloading appeared distinct on the hysteresis loop of the films. Also, Syed et al. [7] studied the nanoindentation behaviour of ultra-thin polymeric films and use the finite element modelling to characterise their mechanical properties. The authors observed that the Young's modulus and hardness of the flexible film increased with the indentation depth and the projected area of the deformed region. The nano-rheological properties of flexible films including the hardness and elastic modulus have been studied by Chateauminois and Briscoe [8]. The authors observed a progressive wearing of the flexible film due to compaction brought about by increasing load at the contact area. The intensity of the wearing process was interpreted by considering the evolving load carrying capacity of the contact, which was characterised by progressive redistribution of the contact pressure within the flexible film. However, the behaviour of the flexible films, as reported, does not account for the viscoelasticity, elastic and plastic works of the materials. It was also difficult to determine the plasticity index and creep of the materials because of their inconsistent strain rate sensitivity under dynamic loading. The hardness and Young's modulus of the materials were practically inadequate to withstand the dynamic vibrational loading usually experienced on rough roads. Many of the flexible films therefore are limited in their application for high speed transportation, where higher hardness, Young's modulus and elastic behaviours of the materials are required for food packaging. Hence, there is the need for a suitable food packaging material with the required characteristics for potential application in high speed transportation of packaged foods.

The addition of zinc nanoparticles to renewable resource like starch provides an alternative flexible film with improved rheological properties. The new material offers opportunity to

package food under dynamic loading at high speed due to their improved rheological behaviour. The improvement of these properties may be explained by the fundamental length scales of the nanoparticles, whose uniform dispersion with the starch results in ultra-large interfacial area between the constituents. The interface between the organic and inorganic materials alters the mobility of the molecules and thus the rheological behaviour of the nanocomposite material. Thus, the objective of this research was to determine the nano-rheological behaviour of cassava starch-zinc nanocomposite film, such as hardness, Young's modulus, creep, elastic and plastic works, under dynamic loading for high speed transportation of packaged food.

2. Materials and methods

2.1. Source of materials

The cassava used in this investigation was bought from Kasuwan Gwari Market in Minna, Niger State. The method described by Fadeyibi et al. [9] was used to prepare the starch slurry, which was dried under the Sun for 1 week until a moisture content of 2 % (wb) was achieved.

2.2. Preparation and size analysis of zinc nanoparticles

The method described by Fadeyibi et al. [10] was used to prepare the zinc nanoparticles. The method involves mixing two homogeneous solutions prepared separately. The first solution was prepared by adding 30 mL of distilled water to 20 mL of triethanolamine with constant stirring while adding 2 mL (100 drops) of ethanol in drop wise. The second solution was prepared by adding 5.39 g of zinc acetate di-hydrate to 50 mL distilled water with continuous stirring, to form a 0.5 M solution. The two solutions were mixed together in 500 mL beaker and a solution of ammonium hydroxide and 10 mL distilled water were added (in drop wise). The mixture was left undisturbed for 30 minutes to form a white bulky solution, which was washed 8–10 times with distilled water and filtered in a filter paper. The resulting residue was dried in the oven at 95°C for 8 hours. Also, the zetasizer equipment (version 7.01) was used to carry out size analysis of the synthesised zinc particles to establish their size range in nanometre. The tests were carried out at the Centre of Genetic Engineering and Biotechnology of the Federal University of Technology Minna, Nigeria.

2.3. Preparation of cassava starch-zinc nanocomposite film and thickness determination

The starch composite was prepared by adding analytical grade glycerol (45–55%, w/w) and zinc nanoparticles (0–2%, w/w) to 24 g of the prepared cassava starch. The mixtures were homogenised using a locally fabricated screw extruder to form the nanocomposites. The resulting nanocomposites were dispersed into 600 mL of distilled water to form suspensions and heated for 30 minutes until viscous thermoplastic liquid were formed. The thickness of the film was determined by casting the thermoplastic solution in plastic mould of 8, 10 and 12 mm depths. In the design of the plastic mould, the surface area was first determined by

wrapping 50 g of biomaterials (50 mm major and 10 mm minor axial dimensions) using aluminium foil and the layout was traced on the graph paper. The size of the plastic mould was computed from the empirical relationship expressed in Eq. (1).

$$TSA = Na + e \quad (1)$$

where N is the number of equivalent biomaterials (50 g), a is the surface area of the mould mm^2 , e is the allowance (assumed 600 mm^2) and TSA is the total surface area of the mould (mm^2).

Based on the expression in Eq. (1), the total surface area of the mould measured was $350 \times 180 \text{ mm}$ and this was used to cast the thermoplastic solutions into films. The thickness of the dried film, whose moisture content was 4% (db), was determined at the four edges of the films and the average taken. The plastic mould with 8 mm depth gave an average dried thickness of $15.14 \pm 0.22 \mu\text{m}$, whereas those with 10 and 12 mm depths were 16.21 ± 0.36 and $17.38 \pm 0.13 \mu\text{m}$, respectively. Twenty-seven samples of the cassava starch-zinc nanocomposite film, obtained from the 3^3 full factorial experiments (three levels from each of the zinc nanoparticles, glycerol and thickness), were prepared and stored in separate polyethylene bags to avoid subsequent hydration.

2.4. Determination of rheological properties of the film

The nanoindenter was used to determine the rheological properties of the nanocomposite films. A typical profile of the load-displacement curve of the film, obtained from the nanoindenter, is shown in **Figure 1**. The profile shows loading, unloading and holding stages from which other rheological behaviours such as the hardness, Young's modulus and creep were computed (Eqs. 2 and 3). Also, the strain rate sensitivity, which corresponds to creep response of the films, was determined at the holding stage of the profile (stage 2). The elastic and plastic works correspond to the areas under the loading and the unloading stages of the hysteresis loop [7, 11]:

$$H = \frac{P_{\max}}{A_c h_c} \quad (2)$$

where P_{\max} is the maximum load, A_c is the contact area (nm^2), h_c is the contact depth (nm) and H is the hardness of the nanocomposite film.

$$\frac{1}{E_r} = \frac{1-\nu^2}{E} + \frac{1-\nu_i^2}{E_i} \quad (3)$$

where E_r is the reduced modulus (MPa), ν is the Poisson's ratio of the nanocomposite film, which was obtained by assuming that the material is isotropic in nature with the elastic modulus

evenly distributed in all crystallographic directions = 0.5, ν_i is the Poisson's ratio of the diamond indenter = 0.25, E_i is the elastic modulus of the diamond indenter = 1140 GPa and E is the elastic modulus of the nanocomposite film [6, 7].

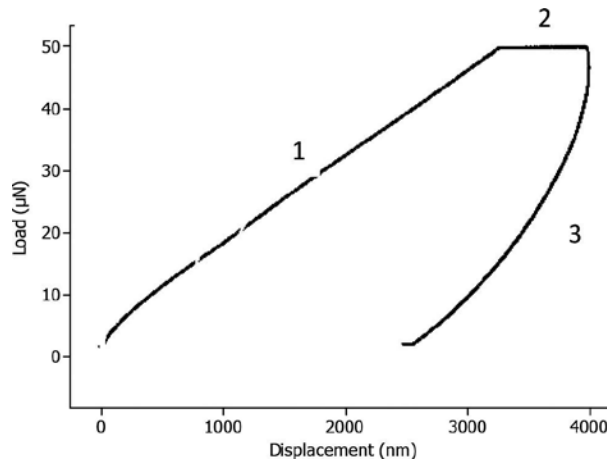


Figure 1. Load-displacement profile of a typical nanocomposite film (1, loading stage; 2, holding stage; 3, unloading stage).

3. Results and discussion

3.1. Response of cassava starch-zinc nanocomposite film to dynamic loading

The responses of the thickness and the various concentrations of glycerol and zinc nanoparticles on the rheological behaviour of the cassava starch-zinc nanocomposite films to dynamic loading are shown in **Figures 2–10**. It can be seen that the nanocomposite films behave differently under the various glycerol concentration and zinc nanoparticles at 15, 16 and 17 μm . The holding rate sensitivity of the nanocomposite film, which corresponds to the creep behaviour, was more pronounced in the 16 and 17 μm of the 45% glycerol film than the 15 μm counterpart, as shown in **Figure 2**. This may suggest that the strain rate sensitivity of the 15 μm nanocomposite film, which is a quantitative representation of a film's ability to stretch and the amount of energy absorbed when stretched [12], was lower than the other two nanocomposite films with 45% glycerol and 0% zinc nanoparticles formulation. The addition of 1% zinc nanoparticles in the formulation abruptly increased the strain rate sensitivity of the 15 μm film, as can be seen in **Figure 3**. The presence of the nanoparticles in the 15 μm film formulation might have caused an improvement in the ability of the material to withstand dead load, as exhibited by its high holding rate sensitivity in comparison to the other two thicknesses. The responses of the nanocomposite films to dynamic loading were somewhat conspicuous with a further increase in the concentration of the zinc nanoparticles to the matrix of the 45% glycerol films (**Figure 4**). It can be seen that the 15 μm film responded to dynamic

loading and strain rate sensitivity than both the 16 and 17 μm films due probably to its lower brittle nature. Sanyang et al. [13] observed similar decrease in the strain energy of biodegradable films based on sugar palm at 45% glycerol concentration. It is possible that the high amount of the dry matter in the matrix of the films, which may be associated with the increased thickness [9], might have been responsible for the higher brittle nature and hence the poor responses to dynamic loading of the 16 and 17 μm films. Interestingly, the responses of the nanocomposite films containing 50% glycerol at the various concentrations of the zinc nanoparticles and thicknesses were slightly different from those containing 45% glycerol with respect to the strain rate sensitivity (Figures 5–7). For instance, the nanocomposite films responded to dynamic loading almost in the same manner irrespective of their distinct thickness, as shown in Figure 5. It is likely that the 10% increment in the glycerol concentration might have led to the improvement in the strain rate sensitivities of the nanocomposite films.

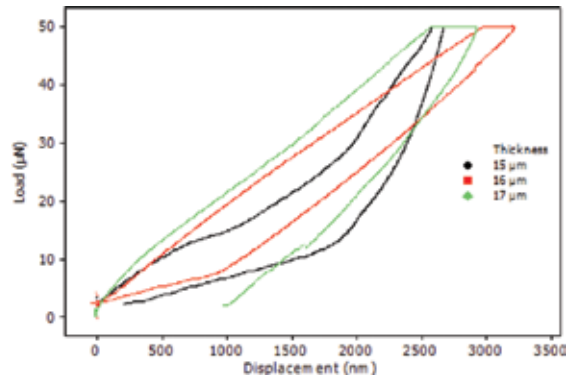


Figure 2. Response of the 45% glycerol–0% zinc nanocomposite films of different thickness to dynamic loading causing wear.

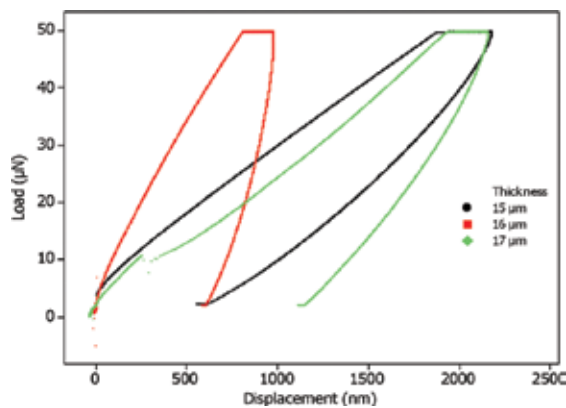


Figure 3. Response of the 45% glycerol–1% zinc nanocomposite films of different thickness to dynamic loading causing wear.

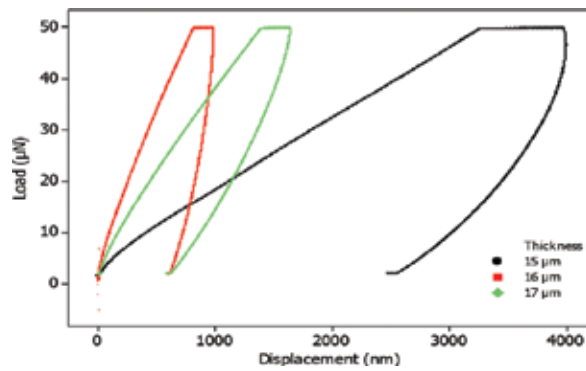


Figure 4. Response of the 45% glycerol-2% zinc nanocomposite films of different thickness to dynamic loading causing wear.

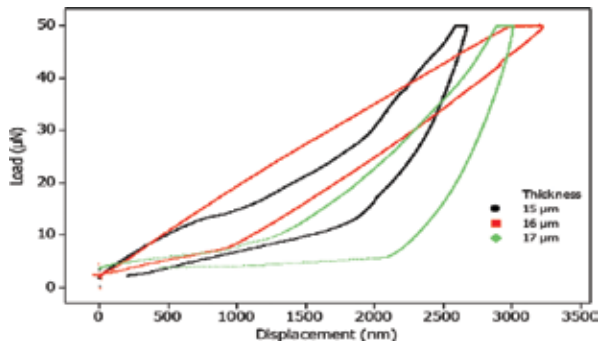


Figure 5. Response of the 50% glycerol-0% zinc nanocomposite films of different thickness to dynamic loading causing wear.

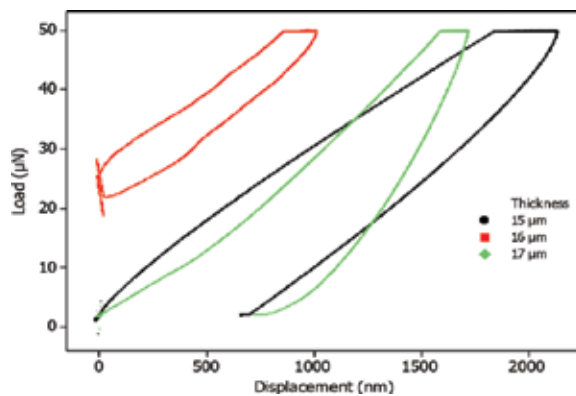


Figure 6. Response of the 50% glycerol-1% zinc nanocomposite films of different thickness to dynamic loading causing wear.

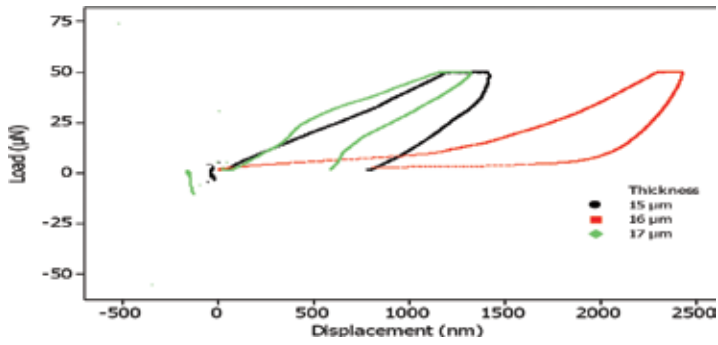


Figure 7. Response of the 50% glycerol–2% zinc nanocomposite films of different thickness to dynamic loading causing wear.

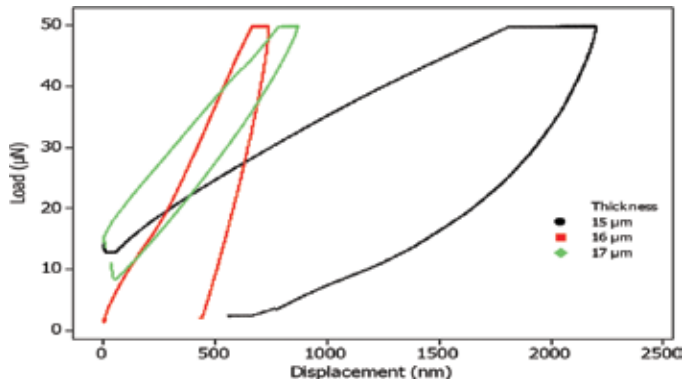


Figure 8. Response of the 55% glycerol–0% zinc nanocomposite films of different thickness to dynamic loading causing wear.

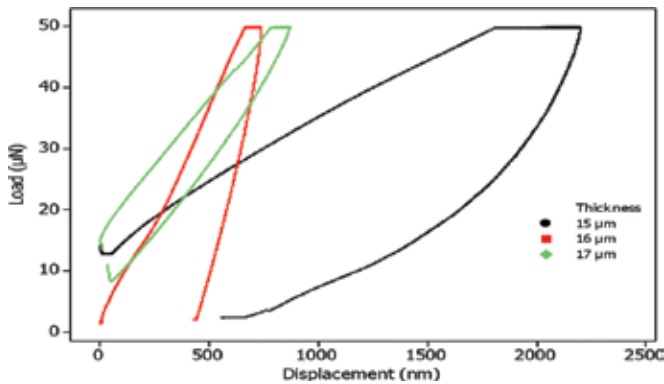


Figure 9. Response of the 55% glycerol–1% zinc nanocomposite films of different thickness to dynamic loading causing wear.

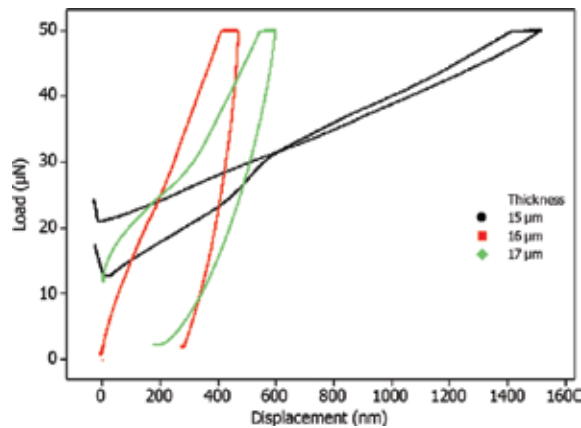


Figure 10. Response of the 55% glycerol-2% zinc nanocomposite films of different thickness to dynamic loading causing wear.

The addition of 1% zinc nanoparticles might have caused the nanocomposite films to behave differently (**Figure 6**), with the 16 μm film responding inconsistently to dynamic loading with a further increase in the concentration of the nanoparticles (**Figure 7**). The addition of 1% zinc nanoparticles to the nanocomposite films containing 55% glycerol does not show any improvement from those with 0% of the nanoparticles, as shown in **Figures 8** and **9**. An improvement was noticed when 2% zinc nanoparticle was used in the film formulation; where the strain rate sensitivity was considerably lower (**Figure 10**). As pointed out previously, here again the 15 μm film responded considerably to dynamic loading than the other two counterpart films. Tall et al. [11], in a similar research noted the response of Ni-Ti thin films to dynamic loading and unloading with distinct strain rate sensitivity. Additionally, the strain energy released during the loading part of the hysteresis loop is in the range of 40–190 pNm, and this varies with thickness and glycerol concentration (**Figures 2–10**). In all cases, the energy dissipated was recovered into the system during the unloading part of the loop. Also, the energy dissipated by the nanocomposite films was lower than those with 0% zinc nanoparticles, irrespective of the concentration of the glycerol but decreases with the thickness of the films. This corroborates the works of Tall et al. [11] who observed regions of loading and unloading of the hysteresis loop of the Ni-Ti thin films. Also, regions of loading and unloading were observed in Cu_2O thin films [7]. This behaviour might be associated with the increased displacement of the film with a slight change in the applied load as the concentration of the glycerol and zinc nanoparticles increased. The rheological properties are important parameters for the formation, application and quality of the films. The measure of wear and tear of the films, and its knowledge informs the engineer on the choice of appropriate films to withstand high mechanical load at nanoscale, especially during transportation on rough roads.

3.2. Effects of the processing parameters on rheological properties of the films

The effects of the processing parameters (thickness, zinc nanoparticles and glycerol concentration) on the rheological properties of the cassava starch nanocomposite films are shown in

Figures 11 and 12. It can be seen that the hardness and Young's modulus varied inconsistently with the concentrations of glycerol and zinc nanoparticles at 15, 16 and 17 μm thickness (**Figure 11**). This implies that an increase in the applied load does not necessarily reduce the area of cross-section due to the influence exerted by the zinc nanoparticles and the glycerol on the crystalline lattice of the films. The elastic and plastic works, which determines the plasticity indices of the nanocomposite films, decreased generally with the thickness, zinc nanoparticles and glycerol concentration (**Figure 12**). Higher plasticity index was obtained for 15 μm film than 16 and 17 μm films irrespective of the concentrations of glycerol and zinc nanoparticles. It is likely that the high amount of the dry matter in the matrix of the films, which is associated with the increased thickness [9], might have been responsible for the decreased elastic and plastic works of the 16 and 17 μm films. Jorge et al. [14], who studied the mechanical properties of gelatine nanocomposite films and investigated the effect of montmorillonite concentration on the properties, corroborated our findings. The authors revealed that the hardness and Young's modulus of the films were inconsistent with montmorillonite concentration, thus indicating the reinforcement of the film matrix by the nanoparticle. The lower values of plasticity indices of the films might also be associated with the plasticising effect of the absorbed glycerol during formulation. Thus, the zinc nanoparticles can be said to enhance the rheological properties, particularly stress and Young's modulus for high speed packaging application [15].

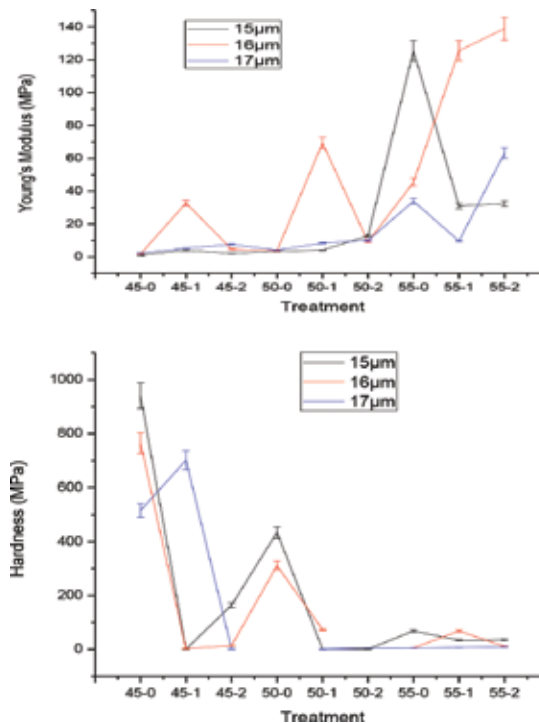


Figure 11. Effect of experimental variables on creep and Young's modulus of the films.

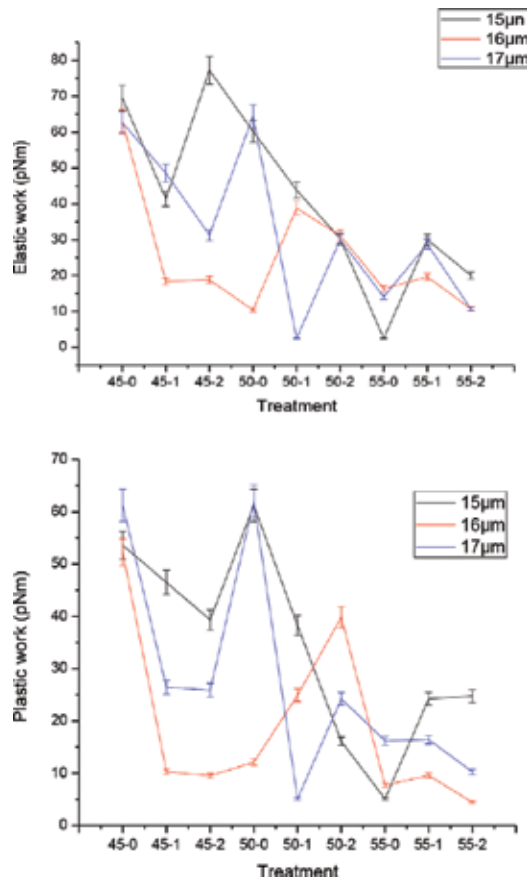


Figure 12. Effect of experimental variables on the elastic and plastic works of the films.

There is a correlation between the elastic work done during dynamic loading and the viscoelasticity of the nanocomposite films [16–18]. Thus, since the elastic work is affected by the concentration of glycerol and thickness of the film formulation, the viscoelastic behaviour of the nanocomposite film might as well be influenced. It is possible that the increased thickness of the nanocomposite films, which can affect their flexibility, might be associated with their poor viscoelasticity. Therefore, in order to adapt to the possible deformation or wear, occurring especially on rough roads [19, 20], the viscoelasticity of the nanocomposite films must be high enough so that the elastic work done during the dynamic loading is subsequently recovered in the unloading part of the cycle.

4. Conclusions

The dynamic behaviour of nanocomposite film, which is associated with viscoelastic behaviour, has not being well understood and characterised. This has often caused wears and

consequent damages of the packaging materials, particularly during the handling and transportation of food. Nanoindentation provides a convenient tool for probing the basic rheological properties and the extent of stress-induced phase transition in small volumes of nanocomposite materials. Thus, this research was carried out to determine the nano-rheological behaviour of cassava starch-zinc nanocomposite films under dynamic loading for high speed transportation of packaged food. The films, whose dried thicknesses were in the range of 15–16 μm , were prepared by casting mixtures of 24 g of cassava starch, 45–55% w/w of glycerol and 0–2% w/w of zinc nanoparticles. The responses of cassava starch-zinc nanocomposite films to dynamic loading were determined, thus assessing their suitability for high speed packaging application. The increase in the concentrations of glycerol (>45%) and zinc nanoparticles (>1%) in the formulation might be responsible for the increased strain rate sensitivity of the 15 μm film. The hardness and Young's modulus of the films varied inconsistently with the concentrations of glycerol and zinc nanoparticles at 15, 16 and 17 μm thickness, because of the increased displacement with a slight change in the applied load. The strain energy absorbed was lower for the 15 μm film, which absorbed 40 pNm during the loading part of the hysteresis loop, than for the 16 and 17 μm films. Also, only 0.5 pNm of the strain energy was finally dissipated during the unloading part of the loop. The creep response of the 15 μm film makes it viscoelastic enough to withstand death loads or wear at higher loads. Consequently, the film can be used for the high speed packaging of food and food products.

Acknowledgements

The authors like to thank the Tertiary Education Trust Fund (TETFund) of the Federal Ministry of Education, Nigeria (TETFUND/FUTMINNA/2014/09) and the management of the Federal University of Technology, Minna, Nigeria for providing the grant and work space for this research.

Author details

Adeshina Fadeyibi^{1*}, Zinash D. Osunde², Gbabo Agidi², Evans C. Egwim³ and Peter A. Idah²

*Address all correspondence to: adeshina.fadeyibi@kwasu.edu.ng

1 Department of Agricultural and Biological Engineering, Kwara State University Malete, Nigeria

2 Department of Agricultural and Bioresources Engineering, Federal University of Technology Minna, Minna, Nigeria

3 Department of Biochemistry, Federal University of Technology Minna, Minna, Nigeria

References

- [1] Luo, H., Chen, W., & Lu, H. 2008. Tensile Behaviour of a Polymer Film at High Strain Rates. Proceedings of the XIth International Congress and Exposition. Society for Experimental Mechanics Inc. June 2–5, 2008, Orlando, Florida, USA.
- [2] Good, J.K., & Roisum, D.R. 2008. Winding Machines: Mechanics and Measurement. Destech Publications. 439 N Duke St, Lancaster, PA 17602, UK.
- [3] Lu, H., Luo, H., & Gan, R. 2007. Measurements of Young's Modulus of Human Eardrum at High Strain Rates Using a Miniature Split Hopkinson Tension Bar. Proceedings of the SEM Annual Conference and Exposition on Experimental and Applied Mechanics, pp. 190–194.
- [4] Casem, D., Weerasooriya, T., & Moy, P. 2003. Split Hopkinson (Kolsky) Bar: Design, Testing and Applications. *Experimental Mechanics*, 45:368.
- [5] Zhang, J., & Fox, B.L. 2006. Characterization and Analysis of Delamination Fracture and Nanocrep Properties in Carbon Epoxy Composites Manufactured by Different Processes. *Journal of Composite Materials*, 40(14): 1287–1299. doi: 10.1177/0021998305057438
- [6] Jian, S., Chen, G., & Hsu, W. 2013. Mechanical Properties of Cu O Thin Films by Nanoindentation. *Materials*, 6(1):4505–4513. doi:10.3390/ma6104505.
- [7] Syed, V.A.H., Nagamani, A., Yeshwanth, A., & Sundaram, S. 2013. Nano-indentation Behaviour of Ultrathin Polymeric Films. *Advances in Aerospace Science and Applications*, ISSN 2277-3223, 3(3):235–238.
- [8] Chateauminois, A., & Briscoeb, B.J. 2003. Nano-Rheological Properties of Polymeric Third Bodies Generated Within Fretting Contacts. *Surface and Coatings Technology*, 163(164):435–443.
- [9] Fadeyibi, A., Osunde, Z.D., Agidi, G., & Egwim, E.C. 2014a. Development and Dynamic Simulation of a Single Screw Extruder for the Production of Cassava and Yam Starch Nanocomposite. Theme: Agricultural Infrastructures for Wealth Creation. In: Proceedings of the 2014 International Conference of the Nigerian Institution of Agricultural Engineers held at the Federal University of Technology, Akure, Nigeria, 22–26, September, 2014. pp. 870–879.
- [10] Fadeyibi, A., Osunde, Z.D., Agidi, G., & Evans, E.C. 2014b. Flow and Strength Properties of Cassava and Yam Starch-Glycerol Composites Essential in the Design of Handling Equipment for Granular Solids. *Journal of Food Engineering*, 129:38–46. DOI: 10.1016/j.jfoodeng.2014.01.006.
- [11] Tall, P.D., Ndiaye, S., Beye, A.C., Zong, Z., Soboyejo, W.O., Lee, H.J., Ramirez, A.G., & Rajan, K. 2007. Nanoindentation of Ni-Ti Thin Films. *Materials and Manufacturing Processes*, 22:175–179.

- [12] Park, H.J., Weller, C.L., Vergano, P.J., & Testin, R.F. 1993. Permeability and Mechanical Properties of Cellulose Based Edible Films. *Journal of Food Science*, 58(1):1361–1365.
- [13] Sanyang, M.L., Sapuan, S.M., Jawaid, M., Ishak, M.R. & Sahari, J. 2015. Effect of Plasticiser Type and Concentration on Tensile, Thermal and Barrier Properties of Biodegradable Films Based on Sugar Palm (*Arenga pinnata*) Starch. *Polymers*, 7(1):1106–1124. DOI:10.3390/polym7061106.
- [14] Jorge, M.F.G., Vanin, F.M., de Carvalho, R.A., Moraes, I.C.F., Bittante, A.M.Q.B., Nassar, S.F., & Sobral, P.J.A. 2014. Mechanical Properties of Gelatin Nanocomposite Films Prepared by Spreading: Effect of Montmorillonite Concentration. Unknown publisher.
- [15] Lagaron, J.M., & Sanchez-Garcia, M. 2008. Thermoplastic Nanobiocomposites for Rigid and Flexible Food Packaging Applications. In: E. Chiellini (Ed.), *Environmentally Friendly Food Packaging*, Woodhead Publishers, Boca Raton, FL, 2008, pp. 62–89.
- [16] Siracusaa, V., Pietro, R., Romanib, S., & Rosa, M.D. 2008. Mechanical stability of biobased food packaging materials. *Trends in Food Science & Technology*, 10(1):52–68.
- [17] Auras, R., Singh, S.P., & Singh, J.J. 2005. Evaluation of Oriented (Poly-Lactide) Polymers vs. Existing PET and Oriented PS for Fresh Food Service Containers. *Packaging Technology and Science*, 18:207–216.
- [18] Chen, W., Zhang, B., & Forrestal, M.J. 1995. Dynamic Behaviour of Material. In: *Proceeding of the 2014 Annual Conference on Experimental and Applied Mechanics*, 39(1):81.
- [19] Guilbert, S., Gontard, N., & Gorris, G.M. 1996. Prolongation of the Shelf Life of Perishable Food Products Using Biodegradable Films and Coatings. *Lebensm-Wiss. University of Technology*, 29(1):10–17.
- [20] Auras, R., Harte, B., Selke, S., & Hernandez, R. 2003. Mechanical, Physical and Barrier Properties of Poly (Lactide) Films. *Journal of Plastic Film and Sheeting*, 19(2):123–135.

Multifunctional Wound-Dressing Composites Consisting of Polyvinyl Alcohol, Aloe Extracts and Quaternary Ammonium Chitosan Salt

Yang Hu, Yongjun Zhu and Xin Zhou

Additional information is available at the end of the chapter

<http://dx.doi.org/10.5772/65476>

Abstract

Wound dressings are materials generally made of gauze, synthetic, and natural polymers that are able to protect wound from microorganism, absorb exudates, and provide compression to minimize edema as well as a temporary substrate for tissue cells to grow. The multifunction of wound dressing exhibiting antibacterial and anti-inflammatory properties and conducive to skin-tissue regeneration is highly desired. In this study, we developed such a multifunctional wound-dressing composite consisting of polyvinyl alcohol, aloe extracts, and quaternary ammonium chitosan salt (PVA/AE/QCS, PAQ). The mass ratio of PAQ composites was controlled at three different levels of 6:3:1, 7:2:1, and 8:1:1. The as-prepared PAQ composites exhibited a porous profile on both surface and cross-section areas with 3–60- μm pore size and a three-dimensional (3D) porous network inside. Such a porous structure could effectively prevent the invasion of microorganism, as well as readily absorb extrudes from wound. The PAQ composites exhibited a good competency of moisture maintenance, excellent antibacterial characteristics, and a good biocompatibility of fibroblasts, and they would become a competitive multifunctional wound dressing.

Keywords: wound dressing, aloe extracts, chitosan, antibacterial, moisture maintenance

1. Introduction

The occurrence of wound is a cause of break in the skin that generally results from physical, mechanical, and thermal damage, or medical surgery and physiological disorder [1]. It

accompanies cell death, destruction of extracellular connective tissue components, and loss of blood vessel integrity [2]. Wound healing is a dynamic process including inflammatory, proliferative, and remodeling phases. Each phase involves numerous biochemical activities and is overlapped with other phases until the completion of wounded-tissue regeneration [3]. When serious tissue injuries can hardly heal themselves, human interventions are required [4]. The use of wound dressings is such a first step of human interventions to first contribute the hemostasis and prevent wound from deteriorating. Wound dressings are materials generally made of gauze, synthetic, and natural polymers that are able to control moisture content, provide gaseous permeability, protect wound from microorganism, absorb exudates, exhibit low adherence, and provide compression to minimize edema as well as a temporary substrate for tissue cells to grow [1, 5]. Different types of wound need separate wound dressings exhibiting different functions according to various healing objectives. In order to obtain optimal healing result, wound dressings containing integrated functions such as antibacterial and anti-inflammatory properties, and contribution to skin-tissue regeneration are highly desired.

Inorganic materials generally used in wound healing can be selected from a wide range of materials, such as silicone-based bioglasses. Most of them exhibit either high-elastic module satisfying the mechanical requirement of skin tissue or certain biodegradability to release beneficial elements for wound care, such as borate or siloxane bioglasses [6, 7]. Polymeric materials are contributed to most of wound-dressing materials because of their processibility, moldability, low toxicity, biocompatibility, and low cost [8]. Both synthetic and natural polymers can be used to prepare appropriate wound dressings. Some typical synthetic polymers, such as polypropylene (PP) and polylactic acid (PLA), although showing excellent molding ability and certain biodegradability, present inadequate biocompatibility and unpleasant side effects [9–13]. Naturally generated polymers are derived from biomacromolecules such as alginate, chitin/chitosan, gelatin, heparin, collagen, chondroitin, fibrin, keratin, silk fibroin, and bacterial cellulose (BC), and most of them show desirable properties of biocompatibility, biodegradability, nontoxicity, fluid exchange, and moldable prototypes during the synthetic process [14–20], although some unavoidable defects, such as high cost, inappropriate mechanical properties, and untunable biodegradability, are still present [14, 21]. Therefore, blending or compositing synthetic polymers with natural polymers using facile but advanced technologies [22] is highly recommended to integrate advantages of both synthetic and natural polymers and minimize their disadvantages for wound care and other medical uses.

Chitosan is the deacetylated derivative of chitin that is a linear polysaccharide composed of β -1,4-D glucosamine and β -1,4-D-N-acetylglucosamine [23]. Due to numerous amino groups, chitosan becomes a significant polysaccharide carrying positive charges. Such a character offers chitosan an impressive antibacterial property because negatively charged cytoplasmic membrane is neutralized by positive charge which leads to the destruction of the function of bacterial cell membrane [24]. Meanwhile, many studies have also demonstrated the effectiveness of chitosan in wound care that specifically exhibits merits in providing the hemostasis, accelerating the fibroblastic synthesis of collagen, and promoting the tissue regeneration [25]. Due to relatively high cost and difficulties in fiber/film forming as compared to the traditional

gauze-type wound dressing, incorporating chitosan as one of active components of wound care into cheap and easily processible material substrates has become an alternative to prepare wound dressing. The typical examples are electrospinning chitosan with polyethylene oxide (PEO) [26], polyvinyl alcohol (PVA) [27], and (PLA) [28], respectively, for antibacterial application and scaffold construction to promote tissue regeneration. Additionally, blending chitosan with other biomacromolecules, such as collagen [29], pullulan [30], and BC [31], can synergistically contribute to the enhancement of biocompatibility and reduce the toxicity of chitosan to normal tissue cells.

Aloe (*Aloe vera*) is a succulent plant and its extracts mainly consisting of carbohydrates and glycoproteins have been found to contribute to the anti-inflammatory and wound-healing activity [32]. The most beneficial effect of Aloe extracts (AEs) is its function in healing burned wound in which the instant reduction of painful feeling may be easily attained [33, 34]. In addition, AE can be added as a bioactive agent to other material substrates and combine other bioactive agents such as curcumin to exert a synergistic function of moisture maintenance, antibacterial, and anti-inflammation, and thereby promote the wound healing [35]. Nowadays, AE has been successfully commercialized and found in many consumer products for either cosmetic or medicinal purposes.

Although the combination of CS and AE has shown the advantage in wound healing, the effectiveness of modified chitosan combining AE as bioactive agents of wound healing incorporated into PVA matrix has not been investigated yet. Therefore, we aimed to develop such a multifunctional wound-dressing composite consisting of PVA, AE, and quaternary ammonium chitosan salt (QCS, 3-chloro-2-hydroxypropyl trimethylammonium chloride-functionalized chitosan) which was expected to exhibit antibacterial property, ability of moisture maintenance, and good biocompatibility for the growth of skin tissue. Three different mass ratios of QCS, AE, and PVA were selected to investigate the effectiveness of wound-dressing composites prepared. Material characterization of as-prepared wound-healing composites was performed to investigate the porous profile, functional groups of materials, thermal stability, and water absorbability. Cell culture study and antibacterial assay were conducted to investigate the antibacterial activity and biocompatibility in an in vitro wound-healing environment.

2. Materials and methods

2.1. Materials

Quaternary ammonium chitosan salt (QCS, 3-chloro-2-hydroxypropyl trimethylammonium chloride-functionalized chitosan, HACC-101) was purchased from Tianhua Bioagents (Dongying, Shandong, China). Aloe extracts (AE, lyophilized powder, FBE013) were purchased from Five Brothers Bioproducts (Haikou, Hainan, China). Poly(vinyl alcohol) (PVA, 341584 Aldrich) was purchased from Sigma-Aldrich (Saint Louis, MO, USA). All the chemicals were received as it is and used without further purification. L929 mouse fibroblast cells (ATCC CCL-1), human fibroblast cells (HFCs, ATCC CCL110), and *Staphylococcus aureus* (*S. aureus*, ATCC

9213) were purchased from the American-Type Culture Collection (Manassas, VA, USA). *Escherichia coli* (*E. coli*, Trans5 α) was purchased from Transgen Biotech (Beijing, China).

2.2. Preparation of QCS/AE/PVA composites

An amount of PVA, AE, and QCS was dissolved in deionized (DI) water with a final concentration of 5% (m:v). The mass ratios of PVA, AE, and QCS in the PVA/AE/QCS (PAQ) mixture were selected at three levels which were 6:3:1 (PAQ1), 7:2:1 (PAQ2), and 8:1:1 (PAQ3). The mixture was poured into a mold with a depth of 0.5 mm and kept at 4°C for 4 h. The cold mixture was then frozen at -20°C for 4 h following a defrozen operation at room temperature for 4 h. This freezing-defreezing operation was repeated three times until a homogeneous gel was achieved. Next, the gel was lyophilized and cut into an identical size for next studies.

2.3. Material characterization by SEM, FTIR, TGA

PAQ composite samples prepared in the last section were coated with gold and then were imaged by the scanning electron microscopy (SEM, FEI Nova NanoSEM450, USA) operating at 5 kV. Both surface and cross section of samples were examined by SEM. Examination of Fourier transform infrared spectroscopy (FTIR, Bruker Vertex 70, USA) spectra for all composite samples was performed under conditions that FTIR data were taken from 500 to 4000 cm^{-1} . OMNIC software (Thermo Electron Corporation) was used to correct and normalize the baseline of FTIR spectra. Thermogravimetric analyses (TGA) of all composite samples were performed by the TGA Q600 (TA Instrument, USA). Thermograms of samples were recorded between 36 and 600°C at a heating rate of 10°C/min and a nitrogen flow of 100 mL/min. TA Universal Analysis 2000 (TA Instrument, USA) was used to calculate the percentage of weight loss, the first derivatives of the thermograms (DTG), and the decomposition temperatures.

2.4. Water absorbability

The lyophilized PAQ composite samples were soaked in phosphate-buffered saline (PBS, pH 7.4) and acetic acid/sodium acetate buffer (HAc-NaAc, pH 5.0). At different assigned times, the sample was taken out and the excessive solution on the surface of the sample was removed by Kimwipes. The water absorbability was the ratio of weight difference of lyophilized sample before and after the soaking versus the weight of lyophilized sample (the amount of adsorbed water vs. dry weight of lyophilized sample).

2.5. Antibacterial assays

E. coli and *S. aureus* were activated and diluted to the desired concentration of 10^8 CFU/mL (CFU is an abbreviation of colony-forming unit). The inoculum of 10 μL *E. coli* and 10 μL *S. aureus* was separately added to the 1-L growth broth consisting of 30-g tryptic soy broth (BD 211825) and 1-L DI water. Two broth media were shaken at 37°C overnight. The bottom-layer media were taken and rinsed by sterile PBS via the centrifugation at 4000 revolutions per minute (rpm) for 3 min, and the rinsing process was repeated three times. The bacterial pellets obtained for two bacteria were re-dispersed, respectively, in the fresh growth broth

and then adjusted to achieve 0.1 of optical density (OD) value for bacterial media (equal to 10^8 CFU/mL). The composite materials prepared were cut into identical round size with a diameter (D) of 10.5 mm. One piece of sample was placed into 12-well culture plate and UV sterilized for 1 h. Each bacterial medium of 16 μ L was dripped onto the sample and another piece of sample was immediately covered on the bacterial medium. The culture plate with samples and bacterial media was cultivated at 37°C for 2 h. Next, the samples and the culture plate were rinsed by sterile PBS at least three times. The collected bacterial solution was centrifuged at 4000 rpm for 3 min and the bacterial pellet was re-dispersed in 250- μ L fresh broth. The as-prepared bacterial medium of 100 μ L was taken and spread out on the agar medium consisting of 40 g of tryptic soy agar (BD 236950) in 1-L DI water. The bacteria with the agar medium were cultivated at 37°C for 15 h. The number of bacteria growing on the agar was counted. The antibacterial ability was calculated according to Eq. (1).

$$\text{antibacterial ability (\%)} = \frac{\text{CFU}_{\text{blank}} - \text{CFU}_{\text{composite}}}{\text{CFU}_{\text{blank}}} \times 100 \quad (1)$$

where $\text{CFU}_{\text{blank}}$ is the number of bacterial colonies growing on the agar medium without the presence of composite samples and $\text{CFU}_{\text{composite}}$ is the number of bacterial colonies growing on the agar medium in the presence of composite samples.

2.6. Biocompatibility

The effect of the composite samples on the proliferation of L929 mouse fibroblast was first examined. The composite samples of 10.5-mm D round size were sterilized under UV light for 1 h and then activated in the α -minimum essential media (α -MEM, ThermoFisher 11095072) at 37°C and 5% CO_2 for 24 h. The activated samples were placed in a 12-well culture plate and 100 μ L of activated L929 cells (20,000 cells/mL/well) was then added to the culture plate. The growth media were exchanged to α -MEM plus 10% of fetal bovine serum (FBS, ATCC 30-2021, USA) and added to the culture plate. The cultivation was conducted at 37°C and 5% CO_2 for 5 days. At days 1, 3, and 5, the culture medium in the culture plate was taken out and rinsed by sterile PBS via centrifugation at 120 \times g relative centrifugal force (RCF), respectively. The collected cell pellet was added to the cell-counting kit-8 (CCK-8, Sigma 96992, USA) consisting of 10% CCK-8 plus 90% α -MEM. The cell mixture was cultivated at 37°C and 5% CO_2 for 2 h and then OD value of cell mixture was examined by ultraviolet-visible (UV-VIS) spectrometry (Shimadzu UV-3600, Japan).

For the cell attachment and morphology of HFCs on the composite samples, HFCs were first activated according to the protocol described in our previous study [18]. The complete growth medium of HFCs was composed by Eagle's minimum essential medium (EMEM) (ATCC 30-2003, USA) plus 10% of FBS. The composite samples were sterilized under UV light for 1 h and then activated by growth medium of HFCs in a 16-well culture plate. Next, the initial cell suspension (2000 cells/mL/well) was added directly onto the samples following the addition of adequate growth medium to each well, and the cultivation was conducted at 37°C and 5%

CO₂. At the assigned day, the culture medium was removed and the attached cells on the samples were rinsed by PBS. The samples were subsequently fixed with 2.5% glutaraldehyde PBS solution at room temperature for 2 h and stained by a small drop of fluorescent isothiocyanate dye (FITC) at 4°C for 1 h. Laser scanning confocal microscope (LSCM, Leica SD AF) with an excitation wavelength of 488 nm was used to examine the cell attachment and morphology.

3. Results and discussion

3.1. Material characterization and water absorbability of wound-dressing composites

SEM images in **Figures 1** and **2** show distinct surface and cross-section morphologies of PAQ composites prepared at different mass ratios of components. Overall, the PAQ composites display a porous morphology and the cross-section images reveal a three-dimensional (3D) porous network inside PAQ composites. It is noticed that the difference lies in the pore size in each composite. Due to the addition of different amounts of AE and QCS, the PVA fibers inside the 3D structural network are covered by AE and QCS. The pore size of 20–30 μm in PAQ2 appears to be more homogeneous on the surface and cross-section areas than PAQ1 and PAQ2. The PAQ1 exhibits smaller pore size of 5–20 μm and the PAQ3 exhibits larger pore size of 20–60 μm. Too smaller pore may inhibit the air exchange and too larger pores may not effectively prevent the adverse microorganism from infection to wound [36]. In order to prepare a satisfactory wound-dressing material, the porous profile of PAQ2 with a mass ratio of PVA:AE:QCS (7:2:1) seems more qualified.

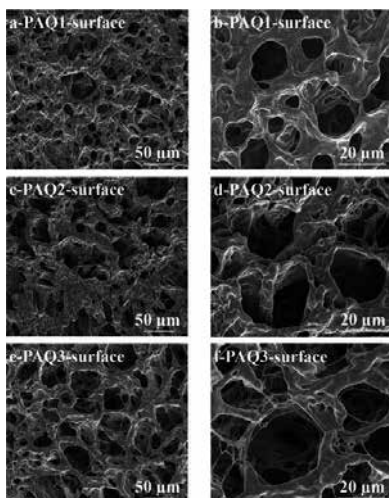


Figure 1. SEM images of surface of PAQ composites with different mass ratios of components: (a, b) PVA:AE:QCS = 6:3:1; (c, d) PVA:AE:QCS = 7:2:1; (e, f) PVA:AE:QCS = 8:1:1. Images b, d, and f indicate higher magnifications of images a, c, and e, respectively.

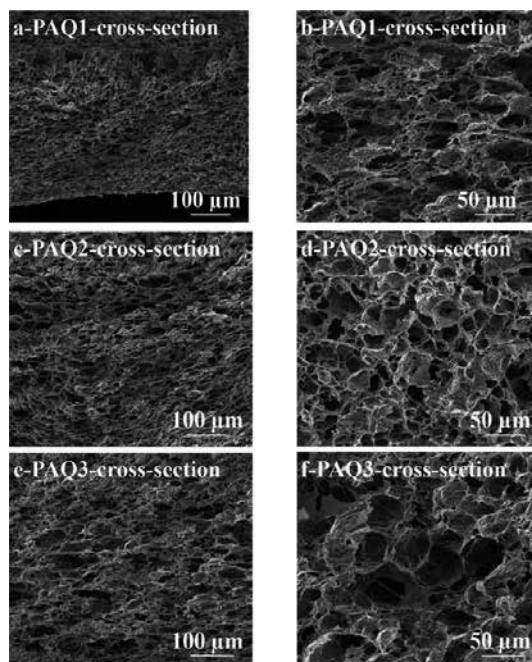


Figure 2. SEM images of cross-section of PAQ composites with different mass ratios of components: (a, b) PVA:AE:QCS = 6:3:1; (c, d) PVA:AE:QCS = 7:2:1; (e, f) PVA:AE:QCS = 8:1:1. Images b, d, and f indicate higher magnifications of images a, c, and e, respectively.

The FTIR spectra of pure PVA, AE, QCS, and PAQ composite samples are illustrated in **Figure 3**. Vertically numerical peaks at 3433 and 2908 cm^{-1} on the pure PVA spectrum may be typical characters of hydroxyl groups and alkyl long chain of PVA, respectively [37]. The strong peak at 3433 cm^{-1} indicates the proof of numerous existing interchain and intrachain hydrogen bonds in the samples of AE and QCS [38]. This peak in three PAQ composite samples shows a limited enhancement as compared to PVA and a remarkable reduction as compared to AE and QCS, suggesting that AE and QCS have been physically bound to PVA and possible hydrogen bonding may have been formed among them. PAQ1 shows a stronger peak at 3433 cm^{-1} than PAQ2 and PAQ3 because of the highest AE component in its composition. The peaks at 1485 and 1230 cm^{-1} are associated with amino groups and they slightly shift to 1400 and 1200 cm^{-1} with the reduction of peak intensity in PAQ composite samples, which is the proof of the presence of QCS in the composites [39, 40]. The strong peaks at 1722 and 1624 cm^{-1} are associated with carbonyl groups existing in AE and they are both present in PAQ composites with the reduction of peak intensity, which is another proof of the incorporation of AE into PVA [40]. The peak at 1120 cm^{-1} is associated with ether groups representing the presence of sugar rings in the PAQ composites, suggesting the successful binding of AE and QCS onto the PVA substrate [40]. The above FTIR analysis chemically demonstrates that AE and QCS have been bound to PVA matrix, although the ratio of AE and QCS in the composites is far below PVA, and as-prepared PAQ composites exhibit all characteristic peaks regarding specific functions that AE and QCS possess.

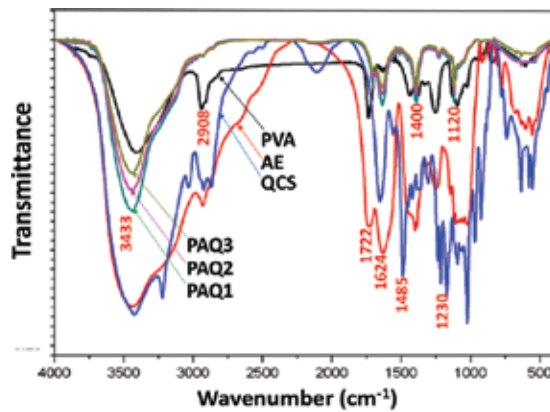


Figure 3. FTIR spectra of pure PVA, pure Aloe, pure QCS, and PAQ composites with different mass ratios of components: PAQ1, PVA:AE:QCS = 6:3:1; PAQ2, PVA:AE:QCS = 7:2:1; PAQ3, PVA:AE:QCS = 8:1:1.

The TGA thermograms of pure PVA and PAQ composites are shown in **Figure 4a** and DTG curves regarding the maximum decomposition temperature and decomposition rate of material components are shown in **Figure 4b**. All the samples show four stages of weight loss in **Figure 4a**. The first stage between 36 and 100°C is associated with the weight loss of absorbed water of samples [19]. Pure PVA exhibits around 8% weight loss in this stage as compared to 9.82% for PAQ3, 15.42% for PAQ2, and 18.51% for PAQ1, suggesting that the competency of moisture maintenance of PAQ composites increases according to the increasing content of AE and QCS in the composition. The second stage between 150 and 300°C is associated with the disintegration of intermolecular breaking of molecular structure which is believed to be the disassociation of physical binding among material components [41]. In this stage, the weight losses of composites are around 25% for pure PVA, 27.25% for PAQ3, 30.36% for PAQ2, and 29.91% for PAQ1, which suggests that AE and QCS bound to PVA start the disassociation from PVA matrix. Although the weight loss does not have a big difference among PAQ composites, due to the addition of AE and QCS, the maximum decomposition temperature of PAQ composites as shown in **Figure 4b** increases as compared with pure PVA, which results in the increase of thermal stability of PAQ composites. The third stage between 300 and 380°C shows the highest weight loss of materials which are associated with the decomposition of molecular structure of PVA, AE, and QCS [38]. As shown in **Figure 4b**, in this stage, the maximum decomposition temperature is increased from 328.7°C for pure PVA to 335.5°C for PAQ3, 341.7°C for PAQ2, and 342.4°C for PAQ1. This means that the addition of AE and QCS increases the thermal stability of PAQ composites. Meanwhile, the decomposition rate of PAQ3 composites is greatly reduced as the increasing content of AE in the composite. The fourth stage between 380 and 450°C is associated with the decomposition of material proportion with higher crystalline structure in AE or QCS [42]. PAQ2 and PAQ3 containing higher amount of AE and QCS exhibit higher weight losses than pure PVA and PAQ. The above TGA analysis indicates that the addition of AE and QCS in PAQ composites is conducive to the enhancement of thermal stability of materials and beneficial to the moisture maintenance of PAQ composites.

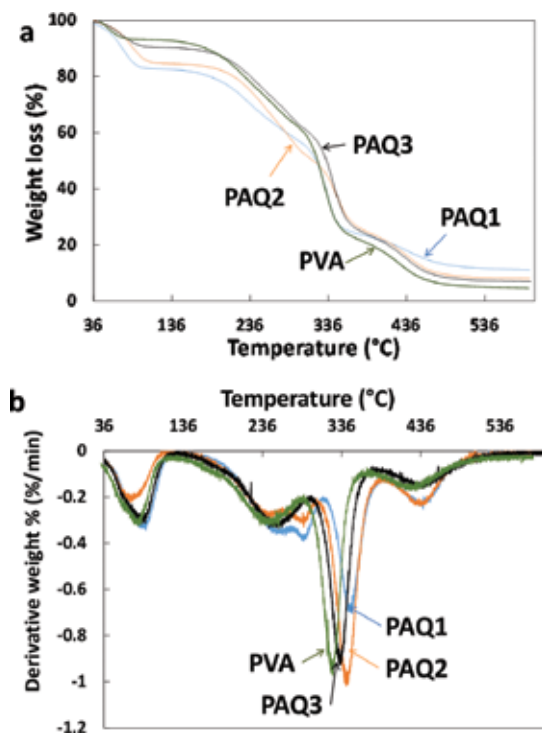


Figure 4. TGA (a) and DTG (b) curves of pure PVA and PAQ composites with different mass ratios of components: PAQ1, PVA:AE:QCS = 6:3:1; PAQ2, PVA:AE:QCS = 7:2:1; PAQ3, PVA:AE:QCS = 8:1:1.

The water absorbability of PAQ composites was investigated using two physiological solutions, PBS (pH 7.4) and HAc-NaAc (pH 5.0), at 37°C, to evaluate their potential to be used for fluid exchange and moisture maintenance because a real wound-healing process generally involves a variation of pH values from pH 5.0 for wound occurrence to pH 7.4 for wound closure [15, 16]. As shown in **Figure 5**, all the PAQ composites exhibit strong water absorbability over 10 times higher than their dry weight, as well as higher than pure PVA. This suggests that the incorporation of AE and QCS could significantly enhance the water absorbability of pure PVA. Owing to the maximum content of AE in PAQ1 composite, the maximum water absorption is 23.85 ± 0.76 for PAQ1 soaked in PBS, which means that this composite material could absorb 23.85 times its dry weight. As compared to PBS (pH 7.4), the PAQ composites exhibited a slight decline of water absorbability in HAc-NaAc (pH 5.0), partly because of the presence of QCS with a competency of proton donor neutralizing the acidic effect in HAc-NaAc buffer. Overall, the water absorption tends to be stable after soaking the composites for over 240 min and can be maintained until 720 min, which suggests that the optimal time to exchange new PAQ composites is somewhere between 240 and 720 min because old composites may lose persistent competency to absorb exudates from wound, whereas it can maintain the high moisture for wound. In consideration of both high water absorbability and relatively low cost resulted from less addition of AE and QCS, the composition of PAQ2 (PVA:AE:QCS, 7:2:1) may be the best choice.

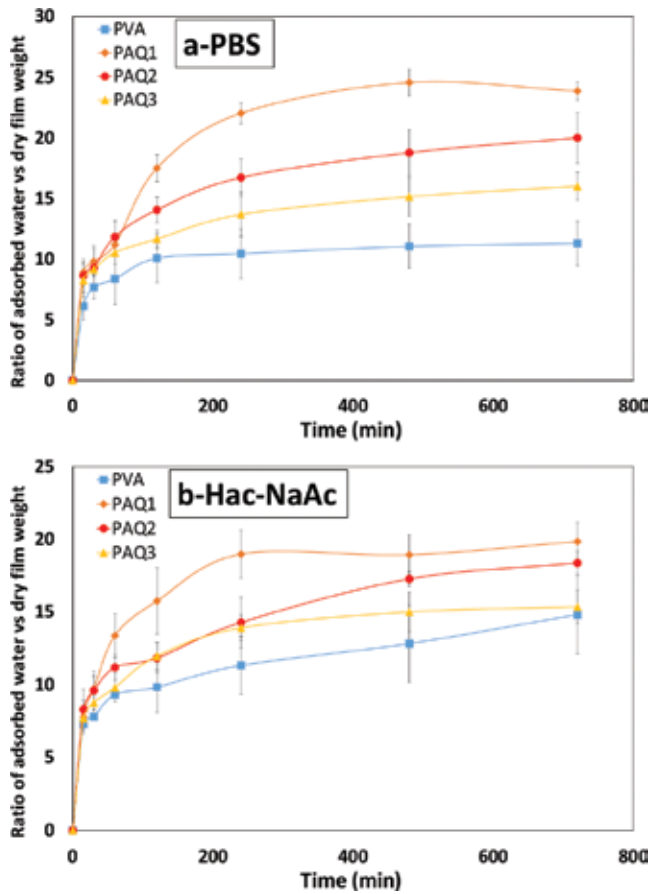


Figure 5. Water absorbability of pure PVA and PAQ composites with different mass ratios of components: PAQ1, PVA:AE:QCS = 6:3:1; PAQ2, PVA:AE:QCS = 7:2:1; PAQ3, PVA:AE:QCS = 8:1:1.

3.2. Antibacterial property and biocompatibility of wound-dressing composites

As shown in **Figure 6**, PAQ composites exhibit significant antibacterial property as compared to pure PVA because of the presence of QCS which is generally documented as a strong and bio-safe antibacterial agent. PAQ1 in **Figures 6e** and **f** exhibits a slightly better antibacterial property against both *E. coli* and *S. aureus* than PAQ2 and PAQ3, although their antibacterial effects are quite similar. This may be a reason of a higher amount of AE present in PAQ1 composite. All the PAQ composites show the excellent antibacterial outcomes over 99% after cell counting and calculation, which are 99.85% for PAQ1, 99.58% for both PAQ2 and PAQ3 against *E. coli*, and 99.80% for PAQ1, 99.69 for PAQ2, and 99.52% for PAQ3 against *S. aureus*. The proliferation of L929 mouse fibroblasts in the presence of pure PVA and PAQ composites over time is shown in **Figure 7**. No significant difference is present in the proliferation of L929 fibroblasts for PAQ composites, which suggests that the addition of QCS and AE to PVA matrix did not significantly influence the proliferation of L929 cells.

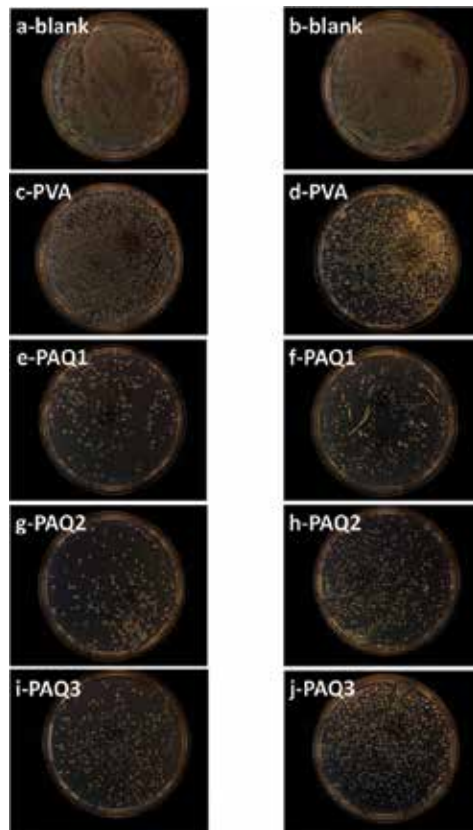


Figure 6. Antibacterial assays using *E. coli* (a, c, e, g, h) and *S. aureus* (b, d, f, h, j) for (c, d) pure PVA and PAQ composites with different mass ratios of components: (e, f) PAQ1, PVA:AE:QCS = 6:3:1; (g, h) PAQ2, PVA:AE:QCS = 7:2:1; (i, j) PAQ3, PVA:AE:QCS = 8:1:1. Images a and b are blank samples.

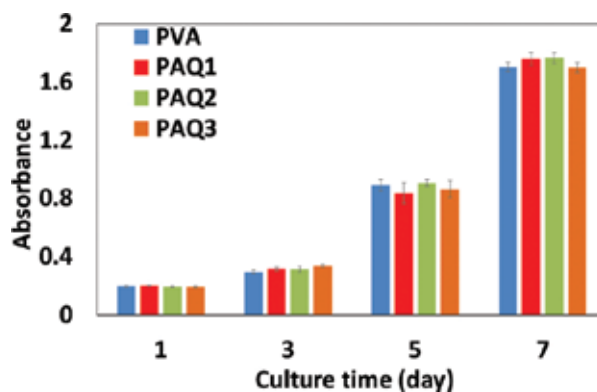


Figure 7. The effect of pure PVA and PAQ composites with different mass ratios of components on the proliferation of L929 mouse fibroblasts: PAQ1, PVA:AE:QCS = 6:3:1; PAQ2, PVA:AE:QCS = 7:2:1; PAQ3, PVA:AE:QCS = 8:1:1.

The attachment and morphology observation in the 3-day cultivation of HFCs on pure PVA and PAQ composites were analyzed as shown in **Figure 8**. All the samples show good attachment of HFCs on their substrates. A slightly preferable viability of HFCs is found in PAQ composites as compared to pure PVA, although no significant viability is present, suggesting that the impact of QCS against cell growth has been offset by AE which shows a potential of facilitating the growth of fibroblasts. L929 fibroblasts show a good morphology of extended shape on all the substrates, which suggests that either pure PVA or PAQ composites are satisfied substrates for the attachment and growth of L929 fibroblasts. In the light of the results from antibacterial assays and biocompatibility plus the analyses from SEM, FTIR, TGA, and water absorbability, considering the cost, the PAQ2 with a mass ratio of PVA:AE:QCS (7:2:1) exhibits relatively satisfactory properties and thereby it should become the optimal material composition.

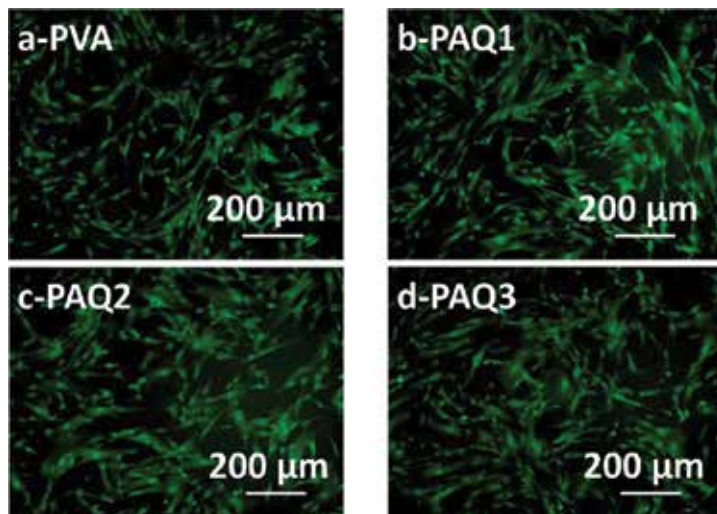


Figure 8. The attachment and morphology of HFCs on (a) pure PVA and PAQ composites with different mass ratios of components on the proliferation of L929 mouse fibroblasts on day 3: (b) PAQ1, PVA:AE:QCS = 6:3:1; (c) PAQ2, PVA:AE:QCS = 7:2:1; (d) PAQ3, PVA:AE:QCS = 8:1:1.

4. Conclusion

This work used a facile approach to prepare PVA/AE/QCS composites used as a multifunctional wound-dressing materials exhibiting strong antibacterial property, good moisture maintenance, and excellent biocompatibility for wound healing. The mass ratio of PAQ composites was controlled at three different levels of 6:3:1, 7:2:1, and 8:1:1 (PVA/AE/QCS). Material characterization of PAQ composites shows that PAQ composites possess a porous profile on both surface and cross-section areas with 3–60- μm pore size and a 3D porous network inside, in which PAQ composite with a mass ratio of 7:2:1 exhibits more homogeneous

porous structure. Such a homogeneous porous structure could effectively prevent the invasion of microorganism, as well as readily absorb extrudes from wound. FTIR and TGA results indicate that AE and QCS have been successfully bound to PVA matrix, and the addition of AE and QCS to PVA is conducive to the enhancement of thermal stability of composites. All the PAQ composites exhibit excellent water absorbability over 10 times higher than their dry weight in both PBS (pH 7.4) and HAc-NaAc buffer (pH 5.0). The PAQ composites exhibited an excellent antibacterial characteristic and a good biocompatibility of fibroblasts. In consideration of cost and results from material characterization plus antibacterial property and biocompatibility, the PAQ2 composite with a mass ratio of 7:2:1 exhibits relatively satisfactory thermal stability and antibacterial property plus fewer amounts of AE and QCS, and thereby it would become a competitive multifunctional wound dressing.

Acknowledgements

This work was financially supported by the National Natural Science Foundation of China no. 31570967 and 31370978; the Shenzhen Science and Technology Program no. JCYJ20140610152828698; the Shenzhen Peacock Program no. 110811003586331.

Author details

Yang Hu^{1,2*}, Yongjun Zhu¹ and Xin Zhou¹

*Address all correspondence to: yang.hu@siat.ac.cn

1 Center for Human Tissue and Organs Degeneration and Shenzhen Key Laboratory of Marine Biomedical Materials, Institute of Biomedicine and Biotechnology, Shenzhen Institutes of Advanced Technology, Chinese Academy of Sciences, Shenzhen, Guangdong, China

2 Department of Plant and Soil Science, Fiber and Biopolymer Research Institute, Texas Tech University, Lubbock, TX, USA

References

- [1] Thomas S. Wound Management and Dressings. London: The Pharmaceutical Press; 1990. p. 1–2.
- [2] Dee KC, Puleo DA, Bizios R. An Introduction to Tissue-biomaterial Interactions. Hoboken, NJ: John Wiley and Sons; 2003. p. 1–10.

- [3] Archana D, Dutta PK, Dutta J. Chitosan: A potential therapeutic dressing material for wound healing. In: Dutta PK, editors. *Chitin and Chitosan for Regenerative Medicine*. New York, NY: Springer; 2016. pp. 193–227. DOI: 10.1007/978-81-322-2511-9.
- [4] Lionelli GT, Lawrence WT. 2003. Wound dressings. *Surgical Clinics of North America*. 2003; 83: 617–638. DOI: 10.1016/S0039-6109(02)00192-5.
- [5] Boateng JS, Matthews KH, Stevens HNE, Eccleston GM. Wound healing dressings and drug delivery systems: a review. *Journal of Pharmaceutical Sciences*. 2008; 97: 2892–2923. DOI: 10.1002/jps.21210.
- [6] Gonyon Jr DL, Zenn MR. Simple approach to the radiated scalp wound using INTEGRA skin substitute. *Annals of Plastic Surgery*. 2003; 50: 315–320.
- [7] Sebastian K, Fellman J, Potter R, Bauer J, Searl A, DE Meringo A, Maquin B, DE Reydellet A, Jubb G, Moore M, Preininger R. EURIMA test guideline: in-vitro acellular dissolution of man-made vitreous silicate fibres. *Glass Science and Technology*. 2002; 75: 263–270.
- [8] Puppi D, Chiellini F, Piras AM, Chiellini E. Polymeric materials for bone and cartilage repair. *Progress in Polymer Science*. 2010; 35: 403–440. DOI: 10.1016/j.progpolymsci.2010.01.006.
- [9] McCullen SD, Hanson AD, Lucia LA, Lobo EG. Development and application of naturally renewable scaffold materials for bone tissue engineering. In: Lucia LA, Rojas OJ, editors. *The Nanoscience and Technology of Renewable Biomaterials*. India: Wiley; 2009. pp. 293–314.
- [10] Bhattarai N, Matsen FA, Zhang M. PEG-grafted chitosan as an injectable thermoreversible hydrogel. *Macromolecular Bioscience*. 2005; 5: 107–111. DOI: 10.1002/mabi.200400140.
- [11] Middleton JC, Tipton AJ. Synthetic biodegradable polymers as orthopedic devices. *Biomaterials*. 2000; 21: 2335–2346. DOI:10.1016/S0142-9612(00)00101-0.
- [12] Temenoff JS, Mikos AG. Injectable biodegradable materials for orthopedic tissue engineering. *Biomaterials*. 2000; 21: 2405–2412. DOI:10.1016/S0142-9612(00)00108-3.
- [13] Mohanty AK, Misra M, Hinrichsen G. Biofibres, biodegradable polymers and biocomposites: an overview. *Macromolecular Materials and Engineering*. 2000; 276: 1–24. DOI: 10.1002/(SICI)1439-2054(20000301)276:1<1::AID-MAME1>3.0.CO;2-W.
- [14] Malafaya PB, Silva GA, Reisa RL. Natural-origin polymers as carriers and scaffolds for biomolecules and cell delivery in tissue engineering applications. *Advanced Drug Delivery Reviews*. 2007; 9: 207–233. DOI:10.1016/j.addr.2007.03.012.
- [15] Hu Y, Catchmark JM. Integration of cellulases into bacterial cellulose: toward bioabsorbable cellulose composites. *Journal of Biomedical Materials Research Part B: Applied Biomaterials*. 2011; 97: 114–123. DOI: 10.1002/jbm.b.31792.

- [16] Hu Y, Catchmark JM. In vitro biodegradability and mechanical properties of bioabsorbable bacterial cellulose incorporating cellulases. *Acta Biomaterialia*. 2011; 7: 2835–2845. DOI:10.1016/j.actbio.2011.03.028.
- [17] Hu Y, Catchmark JM, Vogler, EA. Factors impacting the formation of sphere-like bacterial cellulose particles and their biocompatibility for human osteoblast growth. *Biomacromolecules*. 2013; 14: 3444–3452. DOI: 10.1021/bm400744a.
- [18] Hu Y, Catchmark JM, Zhu Y, Abidi N, Zhou X, Wang J, Liang N. Engineering of porous bacterial cellulose toward human fibroblasts ingrowth for tissue engineering. *Journal of Materials Research*. 2014; 29: 2682–2693. DOI: <http://dx.doi.org/10.1557/jmr.2014.315>.
- [19] Hu Y, Zhu Y, Zhou X, Ruan C, Pan H, Catchmark JM. Bioabsorbable cellulose composites prepared by an improved mineral-binding process for bone defect repair. *Journal of Materials Chemistry B*. 2016; 4: 1235–1246. DOI: 10.1039/C5TB02091C.
- [20] Hu Y, Catchmark JM. Formation and characterization of spherelike bacterial cellulose particles produced by *Acetobacter xylinum* JCM 9730 strain. *Biomacromolecules*. 2010; 7: 1727–1734. DOI: 10.1021/bm100060v.
- [21] Lin J, Yu W, Liu X, Xie H, Wang W, Ma X. In vitro and in vivo characterization of alginate-chitosan-alginate artificial microcapsules for therapeutic oral delivery of live bacterial cell. *Journal of Bioscience and Bioengineering*. 2008; 105: 660–665. DOI:10.1263/jbb.105.660.
- [22] Huang S, Liang N, Hu Y, Zhou X, Abidi N. Polydopamine-assisted surface modification for bone biosubstitutes. *BioMed Research International*. 2016: 1–9. DOI: <http://dx.doi.org/10.1155/2016/2389895>.
- [23] Jayakumar R, Prabakaran M, Kumar PS, Nair SV, Tamura H. Biomaterials based on chitin and chitosan in wound dressing applications. *Biotechnology Advances*. 2011; 29: 322–337. DOI:10.1016/j.biotechadv.2011.01.005.
- [24] Jayakumar R, Menon D, Manzoor K, Nair SV, Tamura H. Biomedical applications of chitin and chitosan based nanomaterials—a short review. *Carbohydrate Polymers*. 2010; 82: 227–232. DOI:10.1016/j.carbpol.2010.04.074.
- [25] Mi FL, Shyu, SS, Wu YB, Lee ST, Shyong JY, Huang RN. Fabrication and characterization of a sponge-like asymmetric chitosan membrane as a wound dressing. *Biomaterials*. 2001; 22: 165–173. DOI:10.1016/S0142-9612(00)00167-8.
- [26] Pakravan M, Heuzey MC, Aji A. A fundamental study of chitosan/PEO electrospinning. *Polymer*. 2011; 52: 4813–4824. DOI:10.1016/j.polymer.2011.08.034.
- [27] Jia Y, Gong J, Gu X, Kim H, Dong J, Shen X. Fabrication and characterization of poly(vinyl alcohol)/chitosan blend nanofibers produced by electrospinning method. *Carbohydrate Polymers*. 2007; 67: 403–409. DOI:10.1016/j.carbpol.2006.06.010.

- [28] Xu J, Zhang J, Gao W, Liang H, Wang H, Li J. Preparation of chitosan/PLA blend micro/nanofibers by electrospinning. *Materials Letters*. 2009; 63: 658–660. DOI:10.1016/j.matlet.2008.12.014.
- [29] Chen Z, Mo X, Qing F. Electrospinning of collagen–chitosan complex. *Materials Letters*. 2007; 61: 3490–3494. DOI:10.1016/j.matlet.2006.11.104.
- [30] Xu F, Weng B, Gilkerson R, Materon LA, Lozano K. Development of tannic acid/chitosan/pullulan composite nanofibers from aqueous solution for potential applications as wound dressing. *Carbohydrate polymers*. 2015; 115: 16–24. DOI:10.1016/j.carbpol.2014.08.081.
- [31] Lin WC, Lien CC, Yeh HJ, Yu CM, Hsu SH. Bacterial cellulose and bacterial cellulose–chitosan membranes for wound dressing applications. *Carbohydrate Polymers*. 2013; 94: 603–611. DOI:10.1016/j.carbpol.2013.01.076.
- [32] Davis RH, Donato JJ, Hartman GM, Haas RC. Anti-inflammatory and wound healing activity of a growth substance in Aloe vera. *Journal of the American Podiatric Medical Association*. 1994; 84: 77. DOI: 10.7547/87507315-84-2-77.
- [33] Choi SW, Son BW, Son YS, Park YI, Lee SK, Chung MH. The wound – healing effect of a glycoprotein fraction isolated from Aloe vera. *British Journal of Dermatology*. 2001; 145: 535–545. DOI: 10.1046/j.1365-2133.2001.04410.x.
- [34] Farzadinia P, Jofreh N, Khatamsaz S, Movahed A, Akbarzadeh S, Mohammadi M, Bargahi A. Anti-inflammatory and Wound Healing Activities of Aloe vera, Honey and Milk Ointment on Second-Degree Burns in Rats. *The International Journal of Lower Extremity Wounds*. 2016; 15: 241–247. DOI: 10.1177/1534734616645031.
- [35] Tummalapalli M, Berthet M, Verrier B, Deopura BL, Alam MS, Gupta B. Composite wound dressings of pectin and gelatin with Aloe vera and curcumin as bioactive agents. *International Journal of Biological Macromolecules*. 2016; 82: 104–113. DOI:10.1016/j.ijbiomac.2015.10.087.
- [36] Rees A, Powell LC, Chinga-Carrasco G, Gethin DT, Syverud K, Hill KE, Thomas DW. 3D bioprinting of carboxymethylated-periodate oxidized nanocellulose constructs for wound dressing applications. *BioMed research international*. 2015; 2015: 1–7. DOI: 10.1155/2015/925757.
- [37] Anicuta SG, Dobre L, Stroescu M, Jipa I. Fourier transform infrared (FTIR) spectroscopy for characterization of antimicrobial films containing chitosan. *Analele Universităţii Ńii din Oradea, Fascicula Ecotoxicologie, Zootehnie şi Tehnologii de Industrie Alimentară*. 2010: 1234-1240. Available from: [https://www.researchgate.net/profile/Iuliana_Jipa/publication/267248659_Fourier_Transform_Infrared_\(FTIR\)_spectroscopy_for_characterization_of_antimicrobial_films_containing_chitosan/links/544de4df0cf2bcc9b1d8f44b.pdf](https://www.researchgate.net/profile/Iuliana_Jipa/publication/267248659_Fourier_Transform_Infrared_(FTIR)_spectroscopy_for_characterization_of_antimicrobial_films_containing_chitosan/links/544de4df0cf2bcc9b1d8f44b.pdf) [Accessed: 2016-09-22].

- [38] Pereira R, Carvalho A, Vaz DC, Gil MH, Mendes A, Bártolo P. Development of novel alginate based hydrogel films for wound healing applications. *International Journal of Biological Macromolecules*. 2013; 52: 221–230. DOI: 10.1016/j.ijbiomac.2012.09.031.
- [39] El Miri N, Abdelouahdi K, Zahouily M, Fihri A, Barakat A, Solhy A, El Achaby M. Bio-nanocomposite films based on cellulose nanocrystals filled polyvinyl alcohol/chitosan polymer blend. *Journal of Applied Polymer Science*. 2015; 132: 1–13. DOI: 10.1002/app.42004.
- [40] Abidi N, Cabrales L, Haigler CH. Changes in the cell wall and cellulose content of developing cotton fibers investigated by FTIR spectroscopy. *Carbohydrate Polymers*. 2014; 100: 9–16. DOI:10.1016/j.carbpol.2013.01.074.
- [41] Lewandowska K. Miscibility and thermal stability of poly (vinyl alcohol)/chitosan mixtures. *Thermochimica Acta*. 2009; 493: 42–48. DOI: 10.1016/j.tca.2009.04.003.
- [42] Mohamed RR, Elella MHA, Sabaa MW. Synthesis, characterization and applications of N-quaternized chitosan/poly (vinyl alcohol) hydrogels. *International Journal of Biological Macromolecules*. 2015; 80: 149–161. DOI: 10.1016/j.ijbiomac.2015.06.041.

Production and Characterization of Hybrid Polymer Composites Based on Natural Fibers

Wendy Rodriguez-Castellanos and Denis Rodrigue

Additional information is available at the end of the chapter

<http://dx.doi.org/10.5772/64995>

Abstract

In this chapter, a review is made on the processing and properties of hybrid composites based on a polymer matrix and a blend of different natural (lignocellulosic) fibers. In particular, the processing methods are described and comparisons are made between the general properties with a focus on physical, mechanical and thermal properties. A discussion is presented on the effect of the polymer and fiber types, as well as reinforcement content. Properties improvement is also discussed using fiber surface treatment or the addition of coupling agents. Finally, auto-hybrid composites are presented with conditions leading to a positive deviation from the rule of hybrid mixture (RoHM) model.

Keywords: hybrid composites, polymer matrices, natural fibers, fiber concentration, mechanical properties

1. Introduction

Composites are materials containing at least two constituents, each one with different chemical composition. Their combination provides a new material with better functional properties than each of the components separately [1].

The main component in the composite is the matrix, which can be a metal, ceramic or polymer, while the other part is a reinforcement which can be in particulate, laminate, short fiber or long fiber form [2]. Composite materials are widely used in construction, aerospace, aircraft, medicine, electrical and automotive industries [2–5]. Here, a focus is made on fiber reinforced composites made from a polymer matrix reinforced with fibers having a natural origin [6].

2. Natural fibers

Natural fibers are biosourced materials extracted from plants (lignocellulosic) or animals [7]. Lignocellulosic fibers are produced by plants for which, on a dry basis, the cell walls are mainly composed of cellulose, with hemicelluloses, lignins, pectins and extractives in lower amounts. Chemical composition and distribution mostly depend on fiber source and varies within different parts even of the same type or family [7, 8]. According to their source, lignocellulosic fibers can be classified as bast fibers, leaf fibers, fruits-seeds fibers, grass-reed fibers and wood fibers [7, 9–12]. **Table 1** presents some examples of each category [13].

Fiber type	Characteristics	Examples
Bast	High cellulose content, flexible, obtained from plants phloem	Kenaf, hemp, flax
Seed	Fibers that have grown around seeds	Cotton, kapok
Fruit	Obtained from fruit shells	Coir, oil palm
Stalk	Cereal stalks byproducts	Wheat and corn straw
Grass	Obtained from grass plants	Bamboo, wild cane, esparto grass
Leaf	Obtained by decortication of plants leaves	Banana, sisal, pineapple, agave
Wood	Extracted from flowering and conifers trees	Maple, pine

Table 1. Lignocellulosic fibers classification [13].

Due to natural fibers' strength, stiffness, availability, low cost, biodegradability and lower density (1.2–1.5 g/cm³) compared to synthetic fillers such as talc (2.5 g/cm³) and glass fiber (2.5 g/cm³) [14–16], they can be effectively used in lightweight composites production [8, 9, 17].

3. Natural fiber composites

Natural fiber composites are materials based on a polymer matrix reinforced with natural fibers [9]. The polymer matrix can be a thermoplastic or a thermoset, the main difference being that once thermoplastics are molded they can be remelted and reprocessed by applying heat and shear, while this is not the case for thermosets [14, 15]. But thermoset matrices generally provide higher rigidity and are more chemically stable. This is why they are more difficult to recycle. The main thermoset matrices used for natural fiber composite production are polyester, vinyl ester, phenolic, amino, derived ester and epoxy resins. Thermoset composites are commonly processed via resin transfer molding (RTM), sheet molding compound (SMC), pultrusion, vacuum-assisted resin transfer molding (VARTM) and hand lay-up. All these manufacturing processes do not need high pressure requirements. Another advantage of thermoset matrices is that fiber loading can be higher than for thermoplastics since the resin

is initially in a liquid form. So, lower viscosity improves fibers introduction and dispersion via different mixing equipment [18–22]. Fiber orientation as well as fiber content might improve mechanical properties in thermoset composites. Grass, leaf and bast fibers are more effective to increase the matrix mechanical properties, while surface treatment improves interfacial interactions. **Table 2** summarizes some work on natural fiber thermoset composites with their manufacturing process, fiber content, fiber treatments and fiber source, as well as the main results obtained from each work.

Matrix	Natural fiber source	Manufacturing process	Fiber content (%)	Fiber treatment	Mechanical properties					References	
					E (GPa)	TS (MPa)	FM (GPa)	FS (MPa)	IS (J/m)		
Epoxy	Banana	Hand lay-up	10	NaOH solution	0.6–1.4	12.1–33.6	15–34	26–69	2–12	[23]	
	Recycled cellulose	RTM	19, 28, 40, 46	–	–	–	0.5–5.5	60–140	5–22	[21]	
	Flax	RTM	40–50	–	–	17.3–33.6	–	–	–	–	[19]
		Hand lay-up	50	–	–	8.6	–	–	–	–	[24]
		Compression molding and pultrusion	40	NaOH solution	2.7–32	50–283	8–27	0.4–4.1	–	–	[25]
	Oil palm	Compression molding	5, 10, 15, 20	NaOH solution	–	11–17	–	–	–	–	[26]
	Hemp	Hand lay-up	30	H ₂ PO ₃ solution NH ₄ OH Geniosil GF-9 Toluene solution aminosilane	3–4.8	49.1–66.5	3–5.2	69–92.8	–	–	[27]
	Date palm	Hand lay-up	10	NaOH solution	1.5–2.5	10–40	–	–	–	–	[28]
	Sansevieria cylindrical leaf	Molding	1, 5, 7, 9	NaOH solution	–	98.3–114.9	–	17–26	–	–	[29]
Polyester	Jute	Hand lay-up	NA	–	–	–	–	–	3.8–4.1	[30]	
	Macadamia nut shell	Hand lay-up	10, 20, 30, 40	–	–	–	4.1–4.6	26–38	–	–	[31]
	Flax	VARTM	20	–	15.3–20.3	188.6–230.7	2.1–2.3	16.3–17.5	–	–	[32]
	Curaua	RTM	0–40	–	–	–	0.1	–	20–190	–	[33]
	Wild cane grass	Hand lay-up	0–40	NaOH solution KMnO ₄ solution	–	–	1.8–7	–	–	–	[34]
	Sisal	Mixing and compression molding	10, 20, 30, 40	NaOH solution	–	–	1.49–2.68	–	–	–	[35]
	Typha leaf	Compression molding	7.3, 10.3, 12.6	NaOH solution Sea water	–	–	3.5–6	25–70	–	–	[36]

Matrix	Natural fiber source	Manufacturing process	Fiber content (%)	Fiber treatment	Mechanical properties					References
					E (GPa)	TS (MPa)	FM (GPa)	FS (MPa)	IS (J/m)	
	Rice husk	Mixing and compression molding	57	GMAMAHSAAH solutions	0.4–1.6	2.5–19	0.1–1.9	3–42	9.5–40	[22]
	Elephant grass	Hand lay-up	30.4, 31.3, 31.5	NaOH, KMnO ₄ solutions	0.6–2.2	31.5–118.1	–	–	–	[37]
	Bamboo	Mixing and compression molding	NA	H ₂ O ₂ +DTPA +Na ₂ O ₃ Si +NaOH solution, IEM +DBTDL	–	39–65	–	75–105	–	[38]
	Coir	Hand lay-up	NA	NaOH solutions	–	17.9–23.6	–	18.7–48	–	[39]
			10, 20, 30	–	–	–	10.6–15.6	–	25.9–38.5	25.6–161.9
Polyurethane	Kraft cellulose	Compression molding	5, 10, 15, 20	–	0–0.2	–	–	–	–	[41]
Phenolic	Bagasse	Compression molding	17.6	HClO ₂ solution Furfuryl alcohol	–	–	–	–	17–28	[42]
	Curaua	Compression molding	17.6	HClO ₂ solution Furfuryl alcohol	–	–	–	–	39–88	[42]
	Cellulose from eucalyptus	Molding	1, 3, 5, 7	NaOH solution, propyl-trimethoxy-silane	0.7–0.9	9.5–16.5	5.1–1.0	18.5–28.0	–	[43]
	Ramie	Compression molding	40.4	–	3.3, 1.2	72.3, 158	–	90–145	–	[44]
	Jute	Pultrusion	N/A	–	–	25–38	–	28–63	–	[45]
	Bamboo	Compression molding	15	–	21.2–30.1	–	–	210–320	–	[46]
Vinyl ester	Silk	Hand lay-up	0–15	–	0.9–1.3	40–71	–	–	–	[47]
	Cellulose	VARTM	20, 30, 40, 50	–	3–7	–	–	40–160	–	[20]
	Sisal	RTM	10, 15, 20, 25, 30	NaOH solution	1.7–2.9	38–75	2.1–4.5	75–180	–	[48]
	Kenaf	Pultrusion	40	–	9–12.5	135–145	1.6–1.9	150–190	–	[49]
	Pineapple leaf	Molding	20	NaOCl solution	–	–	1.9–3.9	68–119	19–105	[50]

E: Tensile modulus; TS: tensile strength; FM: flexural modulus; FS: flexural strength; IS: impact strength; GMA: glycidyl methacrylate; MAH: maleic anhydride; SAH: succinic anhydride; DTPA: diethylenetriaminepenta-acetic acid; IEM: isocyanatoethyl methacrylate; DBTDL: dibutyltin dilaurate.

Table 2. Mechanical and thermal properties of natural fiber composites based on thermoset matrices.

The most common thermoplastic matrices used for natural fiber composites production are the different grades of polypropylene (PP) and polyethylene (PE), as well as polycarbonate (PC), nylon (PA), polysulfones (PSU), polyethylene terephthalate (PET) and polystyrene (PS). More recently, biopolymers such as polylactic acid (PLA) have gained interest to produce 100% biosourced materials [51–55]. Typical manufacturing processes for these composites are extrusion, injection, calendaring, compression molding and thermoforming. Some advantages of using thermoplastic matrices are their recyclability and the production can be continuous [56–61]. Depending on the matrix, fiber and additives content, fiber treatment and manufacturing process, the mechanical and thermal properties of these composites can be adjusted as presented in **Table 3**, with the main results obtained.

The main objective of adding natural fibers in polymer matrices is to increase mechanical properties regardless of polymer and fiber type [21, 26, 31, 40, 52, 54, 55, 61–68]. Since natural fibers have lower density (1.2–1.5 g/cm³) compared to synthetic/inorganic reinforcement such as glass fibers (2.5 g/cm³), lightweight composites can be produced [28, 69, 70]. Nevertheless, lignocellulosic fibers are hydrophilic and polar which causes some incompatibility with the most common polymer matrices which are hydrophobic and nonpolar. This effect leads to poor mechanical properties due to a lack of interfacial adhesion between the fibers and the matrix. Furthermore, the high amount of hydroxyl groups available on the fiber surface is increasing water absorption, even when inside a composite [65, 71, 72]. These problems can be resolved by modification of the fibers surface such as mercerization (treatment in sodium hydroxide solution to remove lignins and hemicellulose) with subsequent addition of coupling agents [22, 73–75]. There is also the possibility to combine thermomechanical refining with coupling agent addition [71, 72]. More recently, fiber treatment with a coupling agent in solution has been proposed [76].

Matrix	Fiber source	Processing	Fiber content (%)	Fiber surface treatment	Additive		Mechanical properties					TD (°C)	References
					CA	BA	E (MPa)	TS (MPa)	FM (MPa)	FS (MPa)	IS (J/m)		
HDPE	Flax	Injection molding	0, 15, 30–		–	ACA	220–470	14–24	500–1600	15–26	60–230	–	[66]
	Wood	Compression molding	0–40	Thermo-mechanical refining		MAPEACA	–	–	0.9–3.9	–	–	–	[72]
	Wood	Extrusion	20, 30, 40	–		MAPE–	2300–2900	–	1900–3400	–	–	–	[56]
	Wood	Extrusion	50, 60, 70, 80	–		MAPE–	3130–4600	11.1–30.2	2470–3370	25.0–58.8	–	–	[77]
	Wood	Injection molding	40	Ethanol and toluene extraction NaClO ₂ treatment NaOH solution		MAPE–	3570–4940	23.8–48	–	–	–	–	[78]

Matrix	Fiber source	Processing	Fiber content (%)	Fiber surface treatment	Additive		Mechanical properties					TD (°C)	References
					CA	BA	E (MPa)	TS (MPa)	FM (MPa)	FS (MPa)	IS (J/m)		
	Wood	Injection molding	25, 35, 45	-	-	-	1200-2000	18.5-27.5	1200-2700	27.5-43	-	-	[59]
	Oil palm	Compression molding	30, 40	-	MAPP-	-	650-1050	10-15	-	-	-	-	[65]
	Hemp	Compression molding	0-40	-	-	ACA	-	-	1093-1634	18.8-23	-	-	[55]
	Agave	Injection molding	0-20	-	-	ACA	225-550	15-24	1-2.7	-	-	-	[79]
	Hemp	Compression molding	40	Thermo-mechanical refining	MAPE-MAH	-	-	2-2.6	-	-	-	-	[71]
	Argan nut shell	Injection molding	5, 10, 15, 20, 25	NaOH solution	-	-	1136-1795	27.2-29.3	-	-	-	-	[80]
UHMWPE	Wood powder	Compression molding	0-30	-	-	-	195-280	-	650-1260	-	-	-	[67]
LMDPE	Agave	Rotomolding	5, 10, 15-	-	-	-	255-440	13-18.8	495-590	12.5-16.5	0.9-7.5	-	[81]
	Agave	Rotomolding	15	Solutions of: MAPE, NaOH, Aldehyde, Acrylic acid, Methyl methacrylate, Silane	-	-	167-217	13-18	420-520	13-17.8	83.8-148.5	-	[76]
	Hemp	Injection molding	30	Solutions of: MAPE, NaOH, MAPE	MAPE-	-	241-668	13.1-17.9	-	-	-	-	[73]
LLDPE	Maple wood	Rotomolding	0-20	-	-	ACA	26-184	3-16.4	1119-680	-	-	-	[52]
	Wood	Injection molding	47	-	MAPP-	-	-	30.2	-	-	-	-	[82]
	Agave	Compression molding	0-40	Solutions of: NaOH, MAPE	-	-	224-381	10-22	389-1027	14-31	123-260	-	[75]
PS	Agave	Compression molding	10, 20, 30	-	-	ACA	3345-4929	30-62	-	-	-	400	[83]
	Wood fiber	Extrusion	10, 20, 30, 40	MAPS	-	-	-	31-49	-	54-94.5	-	-	[84]
	Wood flour	Extrusion	10, 20, 30, 40	MAPS	-	-	-	31-41.5	-	55-68	-	-	
PP	Argan nut shell	Injection molding	0-30	-	SEBS-g-MA	-	1034-1593	26.5-30	-	-	-	-	339.4-350 [85]
	Flax	Compression molding	10, 20, 26, 30	-	MAPP-PPAA	-	1000-3200	-	-	-	-	-	[86]

Matrix	Fiber source	Processing	Fiber content (%)	Fiber surface treatment	Additive		Mechanical properties					TD (°C)	References
					CA	BA	E (MPa)	TS (MPa)	FM (MPa)	FS (MPa)	IS (J/m)		
	Abaca	Injection molding	10, 15, 20, 25	Benzene diazonium treatment, NaOH solution	-	-	800-2700	24.5-31	800-3100	43-55	22.5-50	-	[87]
	Coir bagasse	Injection molding	5, 10, 15, 20, 25, 30	NaOH solution	-	-	1100-1700	27.5-34.7	1400-2000	35-53	-	-	[88]
	Wood	Compression molding	10, 20, 30, 40	-	MAPP	-	600-1600	-	2100-2400	44-52	10-17	-	[89]
	NNC	Compression molding	1	-	MAPP	-	450-663	32.3-39.1	1809-2238	-	-	-	[90]
	Sisal	Injection molding	10, 20, 30	NaOH solution	MAPP	-	500-1100	23-28	-	-	-	363.2-434.5	[91]
	Pine cone	Injection molding	5, 10, 15, 20, 25, 30	NaOH solution	SEBS-g-MA SBS	-	1020-1550	21-27.5	-	-	-	321-355	[92]
	Wood cotton	Compression molding	10, 20, 30	-	MAPP	-	-	28-50	-	37-152	-	-	[93]
PLA	Flax	Injection molding	15, 25, 40	-	-	-	-	2500-6000	-	-	-	282-340	[54]
	Maple wood	Injection molding	15, 25, 40	-	-	-	-	2400-5900	-	-	-	282.3-342.7	[62]
	Maple wood	Injection molding	5, 10, 15, 20, 25	-	-	-	1250-1890	59.8-61.5	3650-5260	96.6-107	21.7-34.3	250-360	[94]
	Wood	Injection molding	20, 30, 40, 50, 55, 60, 65	-	-	-	5270-10300	56.8-64.6	5400-1088	77-91.8	-	-	[58]
	Cotton	Injection molding	10, 20, 30, 40, 50	-	-	-	1260-2500	58.1-62.6	3690-8220	97.9-106.2	17.5-24.3	250-360	[94]
	Agave Coir Pine	Injection molding	10, 20, 30	-	-	-	1242-1865	43-60	2300-3110	55-96	30-49	-	[95]
Post consumer PP+HDPE	Wood flour	Compression molding	0-40	-	MAPP-MAPE	-	247-394	12.7-15.3	950-1889	-	38-65.6	-	[61]
	Wood flour	Compression molding	0-40	-	POE-MAPP-MAPE	-	-	-	1073-1958	16.6-22.4	-	-	[96]
	Flax	Injection molding	30	-	MAPP-EO-g-MAH	-	608-579	-	3090-2921	-	-	-	[97]
							332-608	-	1114-3090	-	-	-	[99]
Post consumer HDPE	Pine wood	Compression molding	30	-	MAPE-CAPE	-	-	21.4-30.6	-	-	-	341.3-342.4	[60]

Matrix	Fiber source	Processing	Fiber content (%)	Fiber surface treatment	Additive		Mechanical properties					TD (°C)	References
					CA	BA	E (MPa)	TS (MPa)	FM (MPa)	FS (MPa)	IS (J/m)		
	Bagasse	Compression molding	30	-	TDM								
					MAPE-	-	22.3-	-	-	-	348.5-	[60]	
					CAPE		36.1				353.3		
					TDM								
	Wood	Compression molding	50, 60	-	MAPE-	-	9-18	-	-	20-	-	[100]	
										35			
Post consumer PP	Wood	Extrusion	-	-	MAPP-	450-	27.3-	2230-	43-51	-	285-	[101]	
						490	29.8	2940			499		
	Oil palm	Extrusion	-	-	MAPP-	340-	18.7-	1870-	30.1-	-	268-	[101]	
						380	19	2150	33.8		495		

CA: coupling agent; BA: blowing agent; TD: thermal degradation; ACA: Azodicarbonamide; MAPE: Maleic anhydride-grafted polyethylene; MAPP: maleic anhydride-grafted polypropylene; MAH: maleic anhydride, SEBS-g-MA: styrene-(ethylene-octene)-styrene triblock copolymer grafted with maleic anhydride; PPAA: acrylic acid grafted polypropylene; POE: ethylene-octene copolymer; EO-g-MAH: maleic anhydride grafted ethylene-octene metallocene copolymer; CAPE: carboxylated polyethylene; TDM: titanium-derived mixture.

Table 3. Mechanical and thermal properties of natural fiber composites based on thermoplastic matrices.

Coupling agents are usually copolymers containing functional groups compatible with the fibers (hydroxyl groups) and the polymer matrix [74]. These reactions (chemical or physical) are increasing interfacial adhesion leading to improved mechanical properties and water absorption reduction [22, 65, 71–73, 75, 76, 99, 102, 103]. Coupling agents can be mixed with the polymer matrix by extrusion previously to fibers addition [65, 74, 92] but can also be added during composite compounding, i.e. mixing the matrix, fiber and coupling agent all together [55, 72, 83, 90, 97–99, 102–104]. Likewise, natural fibers can be functionalized by treating them with a coupling agent in solution, to increase compatibility with the polymer matrix [22, 71, 73–76].

Since natural fibers start to degrade at lower temperature (150–275°C) than most polymer matrices (350–460°C) [60, 63, 74, 83, 105], fiber mercerization and coupling agent addition were shown to improve the thermal stability of the fibers and therefore of the final composites [24, 29, 73, 75, 85, 91, 92].

4. Hybrid composites

To improve on the properties of natural fiber composites and/or overcome some of their limitations such as moisture absorption, thermal stability, brittleness and surface quality, the concept of hybrid composite was developed. The idea is to combine natural fibers with other fibers or particulate reinforcements, which can be of natural or synthetic origin such as glass fibers or rubber particles [15, 51, 63, 106–109]. The main purpose of blending different reinforcements is to obtain a material with better properties than using a single reinforcement. Assuming there is no chemical/physical interaction between each type of fibers, the resulting

properties of hybrid composites (P_H) should follow the rule of hybrid mixtures (RoHM) given as [106, 110, 111]:

$$P_H = P_{C1}V_{C1} + P_{C2}V_{C2} \tag{1}$$

where P_{C1} and P_{C2} are the properties of composite C1 and C2, respectively, while V_{C1} and V_{C2} are their respective volume fractions such that:

$$V_{C1} + V_{C2} = 1 \tag{2}$$

Naturally, the model can be generalized for more than two types of reinforcement.

Natural and synthetic reinforcements combination has showed to improve several composite characteristics such as thermal stability [106, 112–114], impact strength [63, 115–117] and water uptake [70, 112–114, 118, 119]. But the combination of two different types of lignocellulosic fibers was shown to control water absorption [53, 103, 110] and increased impact strength [103, 120], especially when using coupling agents.

The final properties of hybrid composites depend are function of different factors [53, 74, 104, 120], and **Table 4** summarizes some of the most important mechanical and thermal properties of hybrid composites based on thermoset matrices. The effect of fiber and matrix type, as well as fiber surface treatment is reported with their mechanical properties and thermal degradation temperature. Similarly, **Table 5** reports the corresponding information for hybrid composites based on thermoplastic matrices. In general, it is observed that combining natural fibers with inorganic reinforcements leads to improved thermal stability and impact strength, as well as higher flexural and tensile moduli. Moreover, **Table 6** shows that water uptake decreases by combining two natural fibers from different sources, or using natural fibers with inorganic reinforcements in hybrid composites based on thermoplastics matrices.

Matrix	Fibers	Manufacturing process	Fiber treatment	Mechanical properties					TD (°C)	References
				E (GPa)	TS (MPa)	FS (MPa)	FM (GPa)	IS (kJ/m ²)		
Polyester	Hemp/wool	Pultrusion	–	16.84	122.12	180	11	–	–	[18]
	Palmyra palm leaf/jute	Compression molding	NaOH solution	2.3–	–	–	15.3–	24.7–	–	[121]
				5.1			19.3	36.4		
	Banana/sisal	Hand lay-up + compression molding	–	1.1–	–	–	2.7–	~16–	–	[122]
1.5				4.2			37			
Coir/silk	–	–	NaOH solution	–	11.4–	–	37.4–	–	–	[123]
					17.4		42			

Matrix	Fibers	Manufacturing process	Fiber treatment	Mechanical properties					TD (°C)	References
				E (GPa)	TS (MPa)	FS (MPa)	FM (GPa)	IS (kJ/m ²)		
Epoxy	Oil palm/glass	Compression molding	-	~2.5-5.5	~20-75	~30-138	~1.5-8	~7-16	-	[124]
	Banana/kenaf	Hand lay-up	Solutions of: NaOH SLS	-	45-139	75-172.2	-	~15-28	-	[125]
	Ramie/cotton	Compression molding	-	-	24.2-118	-	6.3-27.4	-	-	[126]
	Sisal/roselle	RTM	-	-	30.1-58.7	48.4-63.5	-	1.39-1.41	-	[127]
	Sisal/glass	Hand lay-up	-	-	~78-95	~70-265	~2.1-11	~66-88	-	[128]
	Sisal/jute/glass	Hand lay-up	-	-	111.2-232.1	214.1-308.6	-	-	-	[118]
	Hemp/glass fibers	Hand lay-out + compression molding	NaOH solution	-	-	-	-	-	345	[107]
	Banana/jute	Hand lay-up + compression molding	-	0.6-0.7	16.6-19	57.2-59.8	8.9-9.1	13.44-18.23	376.5-380	[108]
	Banana/sisal	Hand lay-up	-	0.6-0.7	16.1-18.6	57.3-62	8.9-9.3	13.2-17.9	-	[129]
	Jute/bagasse	Hand lay-up	NaOH HCl solution	0.3-0.7	0.6-1.7	6.9-15.9	0.6-1.7	6.9-15.9	438.2-475.9	[109]
	Jute/coir	Hand lay-up	NaOH Cyclohexane/ethanol Furfuryl alcohol	~0.3-0.7	~8.5-35	~39-37	~0.5-1.5	-	-	[130]
Polyurethane	Banana/silica	Hand lay-up	-	6.5-9.1	-	-	-	-	-	[111]
	Sisal/silica	Hand lay-up	-	4.7-6.1	-	-	-	-	-	[111]
Polyurethane	Hemp/wool	Pultrusion	-	18.91	122.66	~142	~12	-	-	[18]
Vinyl ester	Hemp/wool	Pultrusion	-	15.27	112.54	~143	~13	-	-	[18]
	Jute/ramie	VARTM	-	6.7-6.8	6.2-6.7	-	-	18-19	-	[131]
	Coconut/sisal/glass	Molding	-	-	-	-	-	1993-16373	-	[117]

Matrix	Fibers	Manufacturing process	Fiber treatment	Mechanical properties					TD (°C)	References
				E (GPa)	TS (MPa)	FS (MPa)	FM (GPa)	IS (kJ/m ²)		
	Vetiver/glass	Hand lay-up	NaOH solution	1-2.4	53.2-69.8	97.3-131.9	2-3.6	-	-	[116]
	Jute/vetiver	Hand lay-up	NaOH solution	1.7-1.9	63.3-71.7	114.8-133.1	2.9-3.6	-	-	[116]

E: tensile modulus, TS: tensile strength, FS: flexural strength, FM: flexural modulus, IS: impact strength, TD: thermal degradation.

Table 4. Mechanical and thermal properties of natural fiber hybrid composites based on thermoset matrices.

Manufacturing process	Composite	Coupling agent	Filler content (%)	Filler surface treatment	Mechanical properties					TD (°C)	References
					E (MPa)	TS (MPa)	FS (MPa)	FM (GPa)	IS (J/m)		
	PP-glass/ flax fibers	MAPP (5%)	40 (vol)	-	522-629	21.9-25.5	-	-	37.9-49.6	-	[106]
	MAPE-GTR/ rubber/ hemp fiber	-	10, 30, 50, 60	-	120-243	9.8-14.3	-	363-781	139.6-294-239.8	465	[63]
	PP-Kenaf/ coir/MMT	MAPP (5%)	30	-	300-360	11-12	-	-	-	-	[132]
	PP-NNC/ Maple fibers	MAPP (2%)	21	-	444.9	25.4	-	1735.2	-	-	[104]
	PP-wood/ CaCO ₃ / PP-wood/ milled glass fibers	MAPP (4.5%)	50	-	-	32-45	48-65	2400-3540	-	348	[133]
	PP-sisal/ glass fibers	MAPP (1%, 2%, 3%)	30	-	41.75-55.1	970-1686	47.4-67.5	1900-2800	59.3-81.6	346-384	[70]
	PP-jute/ flax fibers	MAPP (19.12%)	25.96%	PP/jute and MAPP/ flax woven fabrics were treated with NaOH solution	29.7-42.6	2437.3-2852.4	50.1-68.8	1399.7-2331.8	-	-	[134]

Manufacturing process	Composite	Coupling agent	Filler content (%)	Filler surface treatment	Mechanical properties					TD (°C)	References
					E (MPa)	TS (MPa)	FS (MPa)	FM (GPa)	IS (J/m)		
	LDPE-banana/coir fibers	MAPP (5%)	15	Solutions of: NaOH Acetylation bleaching with H ₂ SO ₄	36.2–50	29.5–52.4	–	9.3–13.6	473	[135]	
	HDPE-coir/Oil palm fibers	MAPE (2%, 4%)	40	Hot water and soap	8–13.5	550–630	17–27	1570–2380	–	[120]	
	HDPE-kenaf/pineapple leaf fibers (PALF)	–	40	–	27–30	550–680	23–28	1700–2100	–	[110]	
	PS-banana/glass fibers	–	20	Solutions of: NaOH Benzoyl chloride PSMA	29–38.8	1462.2–1558.3	7.9–11.3	489.7–698.8	–	[136]	
Injection + compression	PP-SBR rubber/birch wood	MAPP (3%, 5%)	0–40	–	10.5–25	520–1560	–	–	–	[51]	
Injection molding	PP-sisal/glass fiber	N/A (3.5%)	10, 20, 30	Boiled in methanol and benzene mixture and with NaOH solution	–	–	–	100	190–230	[112]	
	PP-sisal/glass fibers	MAPP (3%)	30	–	29.2–31.6	2330–2430	66.7–68.8	4.03–4.14	16.7–20	331.3–464.7	[113]
	RPP-date palm wood/glass fiber	–	30	–	19.5–21	1100–1300	–	–	–	361.8–479.4	[114]
	PP-hemp/glass fibers	MAPP (5%)	40	–	52.5–59	3800–4300	97–101	5000–5400	49–55.4	360–474	[57]
	PP-wood flour/glass fiber	MAPP PP-g-MA POE-g-MA	40	–	28–45.4	–	39.7–62.8	2680–3497	–	345–363	[137]

Manufacturing process	Composite	Coupling agent	Filler content (%)	Filler surface treatment	Mechanical properties					TD (°C)	References
					E (MPa)	TS (MPa)	FS (MPa)	FM (GPa)	IS (J/m)		
		SBS-g-MA (3%, 6%)									
	PP-wood/kenaf fibers	MAPP (1%)	40	-	39-44	2771-3008	-	-	-	-	[138]
	PLA-kenaf/corn husk	-	30	NaOH solution Sodium lauryl sulfate solution Silane and potassium permanganate	-	1547	-	-	-	-	[139]
	PLA-banana/nano-clay	-	33	-	67	4965-5577	105-108	7715-7725	119-120	295-397	[140]
	HDPE-Pine/agave fibers	MAPE (3%)	20, 30	-	20.5-26.5	415-650	24-32	670-1180	37-47	-	[53]
	HDPE-coir/agave fibers	MAPE (3%)	20, 30	NaOH solution	19.5-25.9	355-500	23.3-31.9	890-1190	42-68	-	[103]
	HDPE-sisal/hemp	MA solution (10%)	25, 30	NaOH solution	15.7-19.2	-	-	-	-	-	[141]
	PP-coir-shell/coir fibers	SEBS-g-MA (8%)	20	NaOH solution Benzoyl peroxide solution	26.5-29.5	1050-1300	-	-	-	344-349	[74]
	PLA-banana/sisal fibers	-	30	-	57-79	1700-4100	91-125	4200-5600	-	-	[142]
	PLA-hemp/lyocell	-	40	-	41.4-71.5	4643-7035	-	-	-	-	[143]
	PLA-hemp/kenaf fibers	-	40	-	34.4-61	4920-7039	-	-	-	-	
	HDPE-wood/hollow	-	50	-	26.2-31	3300-3600	-	-	-	-	[119]

Manufacturing process	Composite	Coupling agent	Filler content (%)	Filler surface treatment	Mechanical properties					TD (°C)	References
					E (MPa)	TS (MPa)	FS (MPa)	FM (GPa)	IS (J/m)		
Extrusion	glass microspheres	–	60	Vinyl triethoxysilane	42–44	650–700	73–77	4900–	–	–	[144]
	HDPE-wood/bast fibers	–	60	Allyl and 3-trimethoxy silyl-propyl	13.8–19.8	3050–4100	24.5–3600	2200–3400	–	–	[145]
Extrusion calendaring	PP-jute/glass	–	20, 30, 40	–	42–63	4660–7170	72.8–102.5	3550–5950	–	–	[69]

MAPP: maleic anhydride-grafted PP; MAPE: maleic anhydride-grafted PE; GTR: ground tire rubber; LDPE: low density polyethylene; HDPE: high density polyethylene; PS: polystyrene; SBR: styrene butadiene rubber; RPP: recycled polypropylene; PP-g-GMA: glycidyl methacrylate-grafted PP; POE-g-MA: maleic anhydride-grafted ethylene-octene copolymer; SEBS-g-MA: maleic anhydride-grafted hydrogenated styrene-butadiene-styrene; PLA: polylactic acid.

Table 5. Mechanical and thermal properties of hybrid composites based on thermoplastic matrices.

Matrix	Reinforcements	Observations	References
MAPE	GTR rubber/hemp fiber	GTR decreases water uptake	[63]
PP	Kenaf/coir/MMT	Water uptake is reduced by hybridization	[132]
	Wood/SiO ₂	SiO ₂ , CaCO ₃ and milled grass decreased water uptake	[133]
	Wood/CaCO ₃		
	Milled glass fibers		
	Hemp/glass fibers	Glass fiber reduced water uptake	[57]
	Wood/glass fibers	Increasing fiber glass weight ratio, water uptake was reduced.	[146]
HDPE	Pine/agave fibers	Pine fiber decreased water uptake in hybrid composites	[53]
	Coir/agave fibers	Coir reduced water uptake in hybrid composites	[103]

PP: polypropylene; HDPE: high density polyethylene; MAPE: maleic anhydride-grafted polyethylene; GTR: ground tire rubber; MMT: montmorillonite.

Table 6. Water uptake in hybrid composites using thermoplastic matrices.

5. Auto-hybrid composites

Composites reinforced with two sizes of the same type of reinforcement are referred to as auto-hybrid composites. As these composites only have a single type of reinforcement, they are

easier to recycle. But most importantly, these materials were shown to exhibit a positive deviation from the RoHM depending on fiber concentration, weight ratio, size and type [64, 102, 147]. Nevertheless, the auto-hybridization effect seems to be more influenced by the total fiber content than coupling agent addition [64, 147]. However, coupling agent addition is always important to improve tensile strength [102]. As total fiber content, fiber type and coupling agent content, all affect the level of deviation from the RoHM, and optimization of these parameters is a new challenging field of research to develop better composite performances. **Table 7** summarizes the limited amount of work on auto-hybrid composites using natural fibers as reinforcement.

Processing	Composite	Coupling agent	Fiber diameter (μm)	Fiber content (%)	Crystallinity index (%)	Main results	References
Injection	PP-hemp fibers	MAPP (3%, 5%)*	Fiber: 300–710 Powder: 45–180	20, 30	–	Hybridization more effective at 20 wt.% reinforcement Optimum weight ratio of 20/80 (powder/fibers) 3% of coupling agent was more efficient Ductility and impact strength decreased with fiber content Tensile and flexural modulus increased with fiber content	[147]
	HDPE-pine fibers	MAPE (3%)	Short fiber: 40–105	10, 20, 30	56.2–61.1	Coupling agent increased tensile strength, and decreased tensile modulus, flexural strength and impact strength of auto-hybrids	[102]
	HDPE-agave fibers	–	Long fiber: 300–425	–	53.3–57.4	Total fiber concentration affected hybridization being more effective at 20 and 30 wt.% Higher values of mechanical properties were obtained at 30/70 (short/long) weight ratio (without coupling agent) in auto-hybrids Crystallinity index decreased with coupling agent addition	
	PP-pine fiber – PP-agave fibers	–	Short fiber: 50–212	10, 20, 30	–	Hybridization did not affect flexural and tensile strength Hybridization was more effective at 30/70 (short/	[64]

Processing	Composite	Coupling agent	Fiber diameter (μm)	Fiber content (%)	Crystallinity index (%)	Main results	References
			Long fiber: 300–425			long) and 50/50 (short/long) weight ratio Positive hybridization effect was higher at 20 and 30 wt.% fiber content Impact strength was higher at 20 wt.% with a 30/70 (short/long) weight ratio Water absorption was not affected by fiber size	
Compression molding	LLDPE-maple fibers	MAPE (3%)	Short fibers: 0–45 Medium fibers: 125–250 Long fibers: 355–450	5, 10, 15, 20	13–32	Positive deviation of RoHM at 30/70 (smaller/longer) weight ratio, regardless of fiber size 20 wt.% showed higher RoHM positive deviation and auto-hybridization was more effective Positive deviation of RoHM is affected by fiber size and total fiber content Tensile and flexural modulus increased with fiber content, but not with fiber size Impact strength and torsion modulus of hybrid composites are affected by fiber weight ratio	[148]

MAPP was not used in auto-hybrid composites.

Table 7. Overview of the different investigations on auto-hybrid composites based on natural fibers.

6. Conclusion

Natural fibers are now interesting alternative to replace synthetic fibers due their good specific properties (per unit weight). They have been used to develop different composites based on thermoset and thermoplastic matrices. As for any composite, their mechanical, thermal and physical properties are function of the properties of the matrix and the reinforcement, as well as fiber loading, fiber source and manufacturing process. Nevertheless, interfacial conditions are always important to optimize the general properties.

The main disadvantages of using natural fibers are water uptake, low thermal stability, as well as low mechanical properties due to fiber agglomeration and poor interfacial adhesion, especially at high concentration. The problem is usually more important in thermoplastics than

thermosets due to their difference in initial resin viscosity. But most of the limitations associated to natural fiber composites can be controlled or overcome by the addition of coupling agents and/or fiber surface modifications.

Finally, another possibility to improve the properties of natural fiber composites is to add a second reinforcement to produce hybrid composites. These materials were shown to have improved mechanical and thermal properties over neat natural fiber composites as they follow the rule of hybrid mixture (RoHM) regardless of the matrix, manufacturing processing and fiber combination. Based on this concept, different class of materials was also developed such as all natural fiber hybrid composites (combination of two different natural fibers) and auto-hybrid composites (combination of two different sizes of the same fiber). The latter is highly interesting as positive deviations from the RoHM were reported. This is usually the case around 20 wt.% of total fiber content with around 30/70 short/long fiber ratio regardless of coupling agent addition, fiber type and processing method. This opens the door to a new field of investigation as several parameters can be controlled to optimize the final properties of the materials and to design new applications for these multi-functional composites.

Acknowledgements

The authors would like to thank the financial support of the Natural Sciences and Engineering Research Council of Canada (NSERC) and the Research centre for high performance polymer and composite systems (CREPEC), as well as Centre de recherche sur les matériaux avancés (CERMA) and Centre de recherche sur les matériaux renouvelables (CRMR) of Université Laval for technical help.

Author details

Wendy Rodriguez-Castellanos and Denis Rodrigue*

*Address all correspondence to: Denis.Rodrigue@gch.ulaval.ca

Department of Chemical Engineering and CERMA, Université Laval, Quebec, QC, Canada

References

- [1] Josmin PJ, Kuruvilla J. Advances in polymer composites: Macro-and microcomposites-state of the art, new challenges, and opportunities. In: Jose JP, Malhotra SK, Thomas S, Kuruvila J, Goda K, Sreekala MS, editors. *Polymer Composites*. Weinheim, Germany: Wiley-VCH Verlag GmbH & Co. KGaA; 2012. p. 1–16. DOI: 10.1002/9783527645213.ch1

- [2] Wang RM, Zheng SR, Zheng YP. Introduction to polymer matrix composites. In: Wang RM, Zheng SR, Zheng YP, editors. *Polymer Matrix Composites and Technology*. Cambridge, UK; Sawston: Elsevier; 2011. p. 1-25. DOI: 10.1533/9780857092229.1
- [3] Naebe M, Abolhasani MM, Khayyam H, Amini A, Fox B. Crack damage in polymers and composites: A review. *Polym Rev*. 2016; 56:31–69. DOI: 10.1080/15583724.2015.1078352
- [4] Yan L, Kasal B, Huang L. A review of recent research on the use of cellulosic fibres, their fibre fabric reinforced cementitious, geo-polymer and polymer composites in civil engineering. *Compos Part B Eng*. 2016;92:94–132. DOI: 10.1016/j.compositesb.2016.02.002
- [5] Scholz M-S, Blanchfield JP, Bloom LD, Coburn BH, Elkington M, Fuller JD, et al. The use of composite materials in modern orthopaedic medicine and prosthetic devices: A review. *Compos Sci Technol*. 2011;71:1791–803. DOI: 10.1016/j.compositesb.2016.02.002
- [6] Wang J, Gangarao H, Liang R, Liu W. Durability and prediction models of fiber-reinforced polymer composites under various environmental conditions : A critical review. *J Reinf Plast Compos*. 2015;35:179–211. DOI: 10.1177/0731684415610920
- [7] Kicińska-Jakubowska A, Bogacz E, Zimniewska M. Review of natural fibers. Part I—vegetable fibers. *J Nat Fibers*. 2012;9:150–67. DOI: 10.1080/15440478.2012.703370
- [8] Fuqua MA, Huo S, Ulven CA. Natural fiber reinforced composites. *Polym Rev*. 2012;52:259–320. DOI: 10.1080/15583724.2012.705409
- [9] Mohammed L, Ansari MNM, Pua G, Jawaid M, Islam MS. A review on natural fiber reinforced polymer composite and its applications. 2015;2015:1-15. DOI: 10.1155/2015/243947
- [10] Faruk O, Bledzki AK, Fink HP, Sain M. Biocomposites reinforced with natural fibers: 2000-2010. *Prog Polym Sci*. 2012;37:1552–96. DOI: 10.1016/j.progpolymsci.2012.04.003
- [11] Jayavani S, Harekrishna D, Varghese TO, Nayak SK. Recent development and future trends in coir fiber reinforced green polymer composites: Review and evaluation. *Polym Compos*. DOI: 10.1002/pc.23529
- [12] Sathishkumar T, Naveen J, Satheeshkumar S. Hybrid fiber-reinforced polymer composites—A review. *J Reinf Plast Compos*. 2014;33:454–71. DOI: 10.1177/0731684413516393
- [13] Gurunathan T, Mohanty S, Nayak SK. A review of the recent developments in biocomposites based on natural fibres and their application perspectives. *Compos Part A Appl Sci Manuf*. 2015;77:1–25. DOI:10.1016/j.compositesa.2015.06.007
- [14] Yan L, Chouw N, Jayaraman K. Flax fibre and its composites - A review. *Compos. A review of recent research on the use of cellulosic fibres, their fibre fabric reinforced cementitious, geo-polymer and polymer composites in civil engineering. Compos Part B Eng*. 2016;92:94–132.doi:10.1016/j.compositesb.2016.02.002

- [15] Zhang Y, Li Y, Ma H, Yu T. Tensile and interfacial properties of unidirectional flax/glass fiber reinforced hybrid composites. *Compos Sci Technol.* 2013;88:172–7. DOI:10.1016/j.compscitech.2013.08.037
- [16] Nekhlaoui S, Essabir H, Kunal D, Sonakshi M, Bensalah MO, Bouhfid R, et al. Comparative study for the talc and two kinds of moroccan clay as reinforcements in polypropylene-SEBS-g-MA matrix. *Polym Compos.* 2014;36:675–84. DOI 10.1002/pc.22986
- [17] Koronis G, Silva A, Fontul M. Green composites: A review of adequate materials for automotive applications. *Compos Part B Eng.* 2013;44:120–7. DOI:10.1016/j.compositesb.2012.07.004
- [18] Peng X, Fan M, Hartley J, Al-Zubaidy M. Properties of natural fiber composites made by pultrusion process. *J Compos Mater.* 2011;46:237–46. DOI: 10.1177/0021998311410474
- [19] Poilâne C, Cherif ZE, Richard F, Vivet A, Ben Doudou B, Chen J. Polymer reinforced by flax fibres as a viscoelastoplastic material. *Compos Struct.* 2014;112:100–12. DOI: 10.1016/j.compstruct.2014.01.043
- [20] Alhuthali A, Low IM. Mechanical properties of cellulose fibre reinforced vinyl-ester composites in wet conditions. *J Mater Sci.* 2013;48:6331–40. DOI: 10.1007/s10853-013-7432-4
- [21] Alamri H, Low IM. Mechanical properties and water absorption behaviour of recycled cellulose fibre reinforced epoxy composites. *Polym Test.* 2012;31:620–8. DOI: 10.1016/j.polymertesting.2012.04.002
- [22] Rozman HD, Musa L, Abubakar A. Rice husk-polyester composites: The effect of chemical modification of rice husk on the mechanical and dimensional stability properties. *J Appl Polym Sci.* 2005;97:1237–47. DOI 10.1002/app.21268
- [23] Venkateshwaran N, Elaya Perumal A, Arunsundaranayagam D. Fiber surface treatment and its effect on mechanical and visco-elastic behaviour of banana/epoxy composite. *Mater Des.* 2013;47:151–9. DOI: 10.1016/j.matdes.2012.12.001
- [24] Gindl-Altmatter W, Keckes J, Plackner J, Liebner F, Englund K, Laborie MP. All-cellulose composites prepared from flax and lyocell fibres compared to epoxy-matrix composites. *Compos Sci.* 2012;72:1304–9. DOI: 10.1016/j.compscitech.2012.05.011
- [25] Van de Weyenberg I, Chi Truong T, Vangrimde B, Verpoest I. Improving the properties of UD flax fibre reinforced composites by applying an alkaline fibre treatment. *Compos Part A Appl Sci Manuf.* 2006;37:1368–76. DOI: doi:10.1016/j.compositesa.2005.08.016
- [26] Bakri MK Bin, Jayamani E, Heng SK, Hamdan S. Reinforced oil palm fiber epoxy composites: An investigation on chemical treatment of fibers on acoustical, morphological, mechanical and spectral properties. *Mater Today Proc.* 2015;2:2747–56. DOI: 10.1016/j.matpr.2015.07.266

- [27] Szolnoki B, Bocz K, Soti PL, Bodzay B, Zimonyi E, Toldy A, et al. Development of natural fibre reinforced flame retarded epoxy resin composites. *Polym Degrad Stab.* 2015;119:68–76. DOI: 10.1016/j.polymdegradstab.2015.04.028
- [28] Abdal-hay A, Suardana NPG, Jung DY, Choi K-S, Lim JK. Effect of diameters and alkali treatment on the tensile properties of date palm fiber reinforced epoxy composites. *Int J Precis Eng Manuf.* 2012;13:1199–206. DOI: 10.1007/s12541-012-0159-3
- [29] Ashok Kumar M, Hemachandra Reddy K, Ramachandra Reddy G, Vishnu Mahesh KR. Characterization of light weight epoxy composites from short *Sansevieria Cylindrica* fibers. *Fibers Polym.* 2012;13:769–74. DOI: 10.1007/s12221-012-0769-5
- [30] Dobah Y, Bourchak M, Bezazi A, Belaadi A, Scarpa F. Multi-axial mechanical characterization of jute fiber/polyester composite materials. *Compos Part B Eng.* 2016;90:450–6. DOI: 10.1016/j.compositesb.2015.10.030
- [31] Dong C, Davies IJ. Flexural properties of macadamia nutshell particle reinforced polyester composites. *Compos Part B Eng.* 2012;43:2751–6. DOI: 10.1016/j.compositesb.2012.04.035
- [32] Fuentes CA, Ting KW, Dupont-Gillain C, Steensma M, Talma AG, Zuijderduin R, et al. Effect of humidity during manufacturing on the interfacial strength of non-pre-dried flax fibre/unsaturated polyester composites. *Compos Part A Appl Sci Manuf.* 2016;84:209–15. DOI: 10.1016/j.compositesa.2016.01.023
- [33] Monteiro SN, Lopes FPD, Nascimento DCO, da Silva Ferreira A, Satyanarayana KG. Processing and properties of continuous and aligned curaua fibers incorporated polyester composites. *J Mater Res.* 2013;2:2–9. DOI: 10.1016/j.jmrt.2013.03.006
- [34] Prasad AVR, Rao KM, Gupta AVSSKS, Reddy B V. A Study on flexural properties of wildcane grass fiber-reinforced polyester composites. *J Mater Sci.* 2011;46:2627–34. DOI 10.1007/s10853-010-5117-9
- [35] Wu CS, Yen FS, Wang CY. Polyester/natural fiber biocomposites: Preparation, characterization, and biodegradability. *Polym Bull.* 2011;67:1605–19. DOI 10.1007/s00289-011-0509-9
- [36] Sana R, Foued K, Yosser BM, Mounir J, Slah M, Bernard D. Flexural properties of typha natural fiber-reinforced polyester composites. *Fibers Polym.* 2015;16:2451–7. DOI: 10.1007/s12221-015-5306-x
- [37] Rao KMM, Prasad AVR, Babu MNVR, Rao KM, Gupta AVSSKS. Tensile properties of elephant grass fiber reinforced polyester composites. *J Mater Sci.* 2007;42:3266–72. DOI 10.1007/s10853-006-0657-8
- [38] Liu W, Chen T, Wen X, Qiu R, Zhang X. Enhanced mechanical properties and water resistance of bamboo fiber-unsaturated polyester composites coupled by isocyanatoethyl methacrylate. *Wood Sci Technol.* 2014;48:1241–55. DOI 10.1007/s00226-014-0668-6

- [39] Jayabal S, Sathiyamurthy S, Loganathan KT, Kalyanasundaram S. Effect of soaking time and concentration of NaOH solution on mechanical properties of coir-polyester composites. *Bull Mater Sci.* 2012;35:567–74. DOI: 10.1007/s12034-012-0334-2
- [40] Jayabal S, Natarajan U. Influence of fiber parameters on tensile, flexural, and impact properties of nonwoven coir-polyester composites. *Int J Adv Manuf Technol.* 2011;54:639–48. DOI: DOI 10.1007/s00170-010-2969-8
- [41] Hadjadj A, Jbara O, Tara A, Gilliot M, Malek F, Maafi EM, et al. Effects of cellulose fiber content on physical properties of polyurethane based composites. *Compos Struct.* 2015;135:217–23. DOI: 10.1016/j.compstruct.2015.09.043
- [42] Trindade WG, Hoareau W, Megiatto JD, Razera IAT, Castellan A, Frollini E. Thermoset phenolic matrices reinforced with unmodified and surface-grafted furfuryl alcohol sugar cane bagasse and curaua fibers: Properties of fibers and composites. *Biomacromolecules.* 2005;6:2485–96. DOI: 10.1021/bm058006+
- [43] Rojo E, Alonso MV, Oliet M, Del Saz-Orozco B, Rodriguez F. Effect of fiber loading on the properties of treated cellulose fiber-reinforced phenolic composites. *Compos Part B Eng.* 2015;68:185–92. DOI: 10.1016/j.compositesb.2014.08.047
- [44] Wang H, Xian G, Li H, Sui L. Durability study of a ramie-fiber reinforced phenolic composite subjected to water immersion. *Fibers Polym.* 2014;15:1029–34. DOI 10.1007/s12221-014-1029-7
- [45] Singh B, Gupta M. Performance of pultruded jute fibre reinforced phenolic composites as building materials for door frame. *J Polym Environ.* 2005;13:127–37. DOI: 10.1007/s10924-005-2944-x
- [46] Xie J, Qi J, Hu T, De Hoop CF, Hse CY, Shupe TF. Effect of fabricated density and bamboo species on physical–mechanical properties of bamboo fiber bundle reinforced composites. *J Mater Sci.* 2016;51:7480–90. DOI 10.1007/s10853-016-0024-3
- [47] Ravindra Rama S, Rai SK. Performance analysis of waste silk fabric-reinforced vinyl ester resin laminates. *J Compos Mater.* 2011;45:2475–80. DOI: 10.1177/0021998311401097
- [48] Mahato K, Goswami S, Ambarkar A. Morphology and mechanical properties of sisal fibre/vinyl ester composites. *Fibers Polym.* 2014;15:1310–20. DOI 10.1007/s12221-014-1310-9
- [49] Fairuz AM, Sapuan SM, Zainudin ES, Jaafar CNA. The effect of gelation and curing temperatures on mechanical properties of pultruded kenaf fibre reinforced vinyl ester composites. *Fibers Polym.* 2015;16:2645–51. DOI 10.1007/s12221-015-5535-z
- [50] Mohamed AR, Sapuan SM, Khalina A. Mechanical and thermal properties of josapine pineapple leaf fiber (PALF) and PALF-reinforced vinyl ester composites. *Fibers Polym.* 2014;15:1035–41. DOI 10.1007/s12221-014-1035-9

- [51] Kakroodi AR, Leduc S, González-Núñez R, Rodrigue D. Mechanical properties of recycled polypropylene/SBR rubber crumbs blends reinforced by birch wood flour. *Polym Polym Compos.* 2012;20:439–44.
- [52] Raymond A, Rodrigue D. Foams and wood composite foams produced by rotomolding. *Cell Polym.* 2013;32:199–212.
- [53] Perez-Fonseca AA, Robledo-Ortiz JR, Ramirez-Arreola DE, Ortega-Gudino P, Rodrigue D, Gonzalez-Nunez R. Effect of hybridization on the physical and mechanical properties of high density polyethylene-(pine/agave) composites. *Mater Des.* 2014;64:35–43. DOI: 10.1016/j.matdes.2014.07.025
- [54] Teymoorzadeh H, Rodrigue D. Biocomposites of wood flour and polylactic acid : Processing and properties. *J Renew Mater.* 2015;9:1–6.
- [55] Kavianiboroujeni A, Cloutier A, Rodrigue D. Mechanical characterization of asymmetric high density polyethylene/hemp composite sandwich panels with and without a foam core. *J Sandw Struct Mater.* 2015;17:748–65. DOI: 10.1177/1099636215597667
- [56] Migneault S, Koubaa A, Erchiqui F, Chaala A, Englund K, Krause C, et al. Effect of fiber length on processing and properties of extruded wood-fiber/HDPE composites. *J Appl Polym Sci.* 2008;110:1085–92. DOI 10.1002/app.28720
- [57] Panthapulakkal S, Sain M. Injection-molded short hemp fiber/glass fiber-reinforced polypropylene hybrid composites—Mechanical, water absorption and thermal properties. *J Appl Polym Sci.* 2007;103:2432–41. DOI 10.1002/app.25486
- [58] Sykacek E, Hrabalova M, Frech H, Mundigler N. Extrusion of five biopolymers reinforced with increasing wood flour concentration on a production machine, injection moulding and mechanical performance. *Compos Part A Appl Sci Manuf.* 2009;40:1272–82. DOI:10.1016/j.compositesa.2009.05.023
- [59] Bouafif H, Koubaa A, Perré P, Cloutier A. Effects of fiber characteristics on the physical and mechanical properties of wood plastic composites. *Compos Part A Appl Sci Manuf.* 2009;40 :1975–81. DOI:10.1016/j.compositesa.2009.06.003
- [60] Lei Y, Wu Q, Yao F, Xu Y. Preparation and properties of recycled HDPE/natural fiber composites. *Compos Part A Appl Sci Manuf.* 2007;38:1664–74. DOI:10.1016/j.compositesa.2007.02.001
- [61] Kazemi Y, Cloutier A, Rodrigue D. Mechanical and morphological properties of wood plastic composites based on municipal plastic waste. *Polym Compos.* 2013;34:487–93. DOI 10.1002/pc.22442
- [62] Teymoorzadeh H, Rodrigue D. Biocomposites of wood flour and polylactic acid : Processing and properties. *J Biobased Mater Bioenergy.* 2015;9:1–6. doi:10.1166/jbmb.2015.1510 1

- [63] Ramezani Kakroodi A, Kazemi Y, Rodrigue D. Mechanical, rheological, morphological and water absorption properties of maleated polyethylene/hemp composites: Effect of ground tire rubber addition. *Compos Part B Eng.* 2013;51:337–44. DOI: 10.1016/j.compositesb.2013.03.032
- [64] Perez-Fonseca AA, Robledo-Ortiz J, Moscoso-Sanchez FJ, Rodrigue D, Gonzalez-Nunez R. Injection molded self-hybrid composites based on polypropylene and natural fibers. *Polym Compos.* 2014;35:1798–806. DOI 10.1002/pc.22834
- [65] Kakou CA, Arrakhiz FZ, Trokourey A, Bouhfid R, Qaiss A, Rodrigue D. Influence of coupling agent content on the properties of high density polyethylene composites reinforced with oil palm fibers. *Mater Des.* 2014;63:641–9. DOI: 10.1016/j.matdes.2014.06.044
- [66] Tissandier C, Gonzalez-Nunez R, Rodrigue D. Asymmetric microcellular composites: Mechanical properties and modulus prediction. *J Cell Plast.* 2015;50:1–34. DOI: 10.1177/0021955X14528191
- [67] Mahfoudh A, Cloutier A, Rodrigue D. Characterization of UHMWPE/wood composites produced via dry-blending and compression molding. *Polym Compos.* 2013;34:510–6. DOI 10.1002/pc.22455
- [68] Moscoso-Sanchez FJ, Mendizabal E, Jasso-Gastinel CF, Ortega-Gudino P, Robledo-Ortiz JR, Gonzalez-Nunez R, et al. Morphological and mechanical characterization of foamed polyethylene via biaxial rotational molding. *J Cell Plast.* 2015;51:489–503. DOI: 10.1177/0021955X14566207
- [69] Uawongsuwan P, Yang Y, Hamada H. Long jute fiber-reinforced polypropylene composite: Effects of jute fiber bundle and glass fiber hybridization. *J Appl Polym Sci.* 2015;132:1–13. DOI: 10.1002/app.41819
- [70] Nayak SK, Mohanty S. Sisal Glass Fiber Reinforced PP hybrid composites: Effect of MAPP on the dynamic mechanical and thermal properties. *J Reinf Plast Compos.* 2009;29:1551–68. DOI: 10.1177/0731684409337632
- [71] Fang H, Zhang Y, Deng J, Rodrigue D. Effect of fiber treatment on the water absorption and mechanical properties of hemp fiber/polyethylene composites. *J Appl Polym Sci.* 2013;127:942–9. DOI: 10.1002/app.37871
- [72] Tissandier C, Zhang Y, Rodrigue D. Effect of fibre and coupling agent contents on water absorption and flexural modulus of wood fibre polyethylene composites. In: Altstädt V, Keller J-H, Fathi A, editors. *Proceedings of PPS-29: The 29th International Conference of the Polymer Processing Society.* Nuremberg, Germany: AIP Publishing; 2014. p. 411–5. DOI: 10.1063/1.4873810
- [73] Chimeni DY, Toupe JL, Dubois C, Rodrigue D. Effect of hemp surface modification on the morphological and tensile properties of linear medium density polyethylene

- (LMDPE) composites. *Compos Interfaces*. 2016;23:405–21. DOI: 10.1080/09276440.2016.1144163
- [74] Essabir H, Bensalah MO, Rodrigue D, Bouhfid R, Qaiss A. Structural, mechanical and thermal properties of bio-based hybrid composites from waste coir residues: Fibers and shell particles. *Mech Mater*. 2016;93:134–44. DOI: 10.1016/j.mechmat.2015.10.018
- [75] Cisneros-Lopez EO, Aznaldo J, Fuentes-Talavera FJ, Gonzalez-Nunez R, Robledo-Ortíz JR, Rodrigue D. Effect of agave fiber surface treatment on the properties of polyethylene composites produced by dry-blending and compression molding. *Polym Compos*. DOI 10.1002/pc.23564
- [76] Cisneros-Lopez EO, Pérez-Fonseca AA, Fuentes-Talavera FJ, Aznaldo J, Gonzalez-Nunez R, Rodrigue D, et al. Rotomolded polyethylene-agave fiber composites: Effect of fiber surface treatment on the mechanical properties. *Polym Eng Sci*. 56: 856–65. DOI: 10.1002/pen.24314
- [77] Li Y. Effect of coupling agent concentration, fiber content, and size on mechanical properties of wood/HDPE composites. *Int J Polym Mater*. 2012;61:882–90. DOI: 10.1080/00914037.2011.617338
- [78] Ou R, Xie Y, Wolcott MP, Yuan F, Wang Q. Effect of wood cell wall composition on the rheological properties of wood particle/high density polyethylene composites. *Compos Sci Technol*. 2014;93:68–75. DOI: 10.1016/j.matdes.2014.02.018
- [79] Tissandier C, Vazquez R, González R, Rodrigue D. Microcellular agave fiber-high density polyethylene composites produced by injection molding. *Mater Sci Eng*. 2012;2:677–92.
- [80] Essabir H, Achaby ME, Hilali EM, Bouhfid R, Qaiss A. Morphological, structural, thermal and tensile properties of high density polyethylene composites reinforced with treated Argan nut shell particles. *J Bionic Eng*. 2015;12:129–41. DOI: 10.1016/S1672-6529(14)60107-4
- [81] López-Bañuelos RH, Moscoso FJ, Ortega-Gudiño P, Mendizabal E, Rodrigue D, Gonzalez-Nuñez R. Rotational molding of polyethylene composites based on agave fibers. *Polym Eng Sci*. 2012;52:2489–97. DOI: 10.1002/pen.23168
- [82] Kuo PY, Wang SY, Chen JH, Hsueh HC, Tsai MJ. Effects of material compositions on the mechanical properties of wood-plastic composites manufactured by injection molding. *Mater Des*. 2009;30:3489–96. DOI: 10.1016/j.matdes.2009.03.012
- [83] Moscoso FJ, Martínez L, Canche G, Rodrigue D, González-Núñez R. Morphology and properties of polystyrene/agave fiber composites and foams. *J Appl Polym Sci*. 2013;127:599–606. DOI: 10.1002/app.37843

- [84] Aggarwal PK. Influence of maleated polystyrene on the mechanical properties of bio-based fibers-polystyrene composites. *J Indian Acad Wood Sci.* 2011;8:184–9. DOI 10.1007/s13196-012-0034-y
- [85] Essabir H, Bensalah MO, Rodrigue D, Bouhfid R, Qaiss A el kacem. Biocomposites based on Argan nut shell and a polymer matrix: Effect of filler content and coupling agent. *Carbohydr Polym.* 2016;143:70–83. DOI: 10.1016/j.carbpol.2016.02.002
- [86] Sojoudiasli H, Heuzey M-C, Carreau PJ. Rheological, morphological and mechanical properties of flax fiber polypropylene composites: influence of compatibilizers. *Cellulose.* 2014;21:3797–812. DOI 10.1007/s10570-014-0375-3
- [87] Rahman MR, Huque MM, Islam MN, Hasan M. Mechanical properties of polypropylene composites reinforced with chemically treated abaca. *Compos Part A Appl Sci Manuf.* 2009;40:511–7. DOI: 10.1016/j.compositesa.2009.01.013
- [88] Arrakhiz FZ, Malha M, Bouhfid R, Benmoussa K, Qaiss A. Tensile, flexural and torsional properties of chemically treated alfa, coir and bagasse reinforced polypropylene. *Compos Part B Eng.* 2013;47:35–41. DOI: 10.1016/j.compositesb.2012.10.046
- [89] Ashori A, Nourbakhsh A. A comparative study on mechanical properties and water absorption behavior of fiber-reinforced polypropylene composites prepared by OCC fiber and aspen fiber. *Polym Compos.* 2008;29:574–8. DOI 10.1002/pc.20582
- [90] Hassanabadi HM, Alemdar A, Rodrigue D. Polypropylene reinforced with nanocrystalline cellulose: Coupling agent optimization. *J Appl Polym Sci.* 2016; 132: 42438. DOI: 10.1002/app.42438
- [91] Kaewkuk S, Sutapun W, Jarukumjorn K. Effects of interfacial modification and fiber content on physical properties of sisal fiber/polypropylene composites. *Compos Part B Eng.* 2013;45:544–49. doi:10.1016/j.compscitech.2012.05.011
- [92] Arrakhiz FZ, El Achaby M, Benmoussa K, Bouhfid R, Essassi EM, Qaiss A. Evaluation of mechanical and thermal properties of pine cone fibers reinforced compatibilized polypropylene. *Mater Des.* 2012;40:528–35. DOI: 10.1016/j.matdes.2012.04.032
- [93] Kim S-J, Moon J-B, Kim G-H, Ha C-S. Mechanical properties of polypropylene/natural fiber composites: Comparison of wood fiber and cotton fiber. *Polym Test.* 2008;27:801–6. DOI: 10.1016/j.polymertesting.2008.06.002
- [94] Way C, Wu DY, Cram D, Dean K, Palombo E. Processing stability and biodegradation of polylactic acid (PLA) composites reinforced with cotton linters or maple hardwood fibres. *J Polym Environ.* 2013;21:54–70. DOI 10.1007/s10924-012-0462-1
- [95] Pérez-Fonseca AA, Robledo-Ortíz JR, González-Núñez R, Rodrigue D. Effect of thermal annealing on the mechanical and thermal properties of polylactic acid-cellulosic fiber biocomposites. *J Appl Polym Sci.* 2016;133(31):1–10. DOI: 10.1002/app.43750

- [96] Kazemi Y, Cloutier A, Rodrigue D. Design analysis of three-layered structural composites based on post-consumer recycled plastics and wood residues. *Compos Part A Appl Sci*. 2013;53:1–9. DOI: 10.1016/j.compositesa.2013.06.002
- [97] Toupe JL, Trokourey A, Rodrigue D. Simultaneous optimization of the mechanical properties of postconsumer natural fiber/plastic composites: Phase compatibilization and quality/cost ratio. *Polym Compos*. 2014;35:730–46. DOI 10.1002/pc.22716
- [98] Toupe JL, Trokourey A, Rodrigue D. Simultaneous optimization of the mechanical properties of postconsumer natural fiber/plastic composites: processing analysis. *J Compos Mater*. 2015;49:1355–67. DOI: 10.1177/0021998314533714
- [99] Toupe JL, Chimeni DY, Trokourey A, Rodrigue D. Optimizing the performance of natural fiber reinforced plastics composites : Influence of combined optimization paths on microstructure and mechanical properties. *Polym Polym Compos*. 2015;23:535–44.
- [100] Cruz-Estrada RH, Martínez-Tapia GE, Canché-Escamilla G, González-Chí PI, Martín-Barrera C, Duarte-Aranda S, et al. A preliminary study on the preparation of wood-plastic composites from urban wastes generated in Merida, Mexico with potential applications as building materials. *Waste Manag Res*. 2010; 28:838–47. DOI: 10.1177/0734242X09350059
- [101] Ratanawilai T, Nakawirok K, Deachsrijan A, Homkhiew C. Influence of wood species and particle size on mechanical and thermal properties of wood polypropylene composites. *Fibers Polym*. 2014;15:2160–8. DOI 10.1007/s12221-014-2160-1
- [102] Pérez-Fonseca AA, Robledo-Ortíz JR, Moscoso-Sánchez FJ, Fuentes-Talavera FJ, Rodrigue D, González-Núñez R. Self-hybridization and coupling agent effect on the properties of natural fiber/HDPE composites. *J Polym Environ*. 2015;23:126–36. DOI 10.1007/s10924-014-0706-3
- [103] Perez-Fonseca AA, Arellano M, Rodrigue D, Gonzalez-Nunez R, Robledo-Ortiz JR. Effect of coupling agent content and water absorption on the mechanical properties of coir-agave fibers reinforced polyethylene hybrid composites. *Polym Compos*. DOI 10.1002/pc.23498
- [104] Yousefian H, Ben Azouz K, Rodrigue D. New multi-scale hybrid system based on maple wood flour and nano crystalline cellulose: Morphological, mechanical and physical study. *J Polym Environ*. 2016;24:48–55. DOI 10.1007/s10924-016-0752-0
- [105] Arrakhiz FZ, El Achaby M, Malha M, Bensalah MO, Fassi-Fehri O, Bouhfid R, et al. Mechanical and thermal properties of natural fibers reinforced polymer composites: Doum/low density polyethylene. *Mater Des*. 2013;43:200–5. DOI: 10.1016/j.matdes.2012.06.056

- [106] Ghasemzadeh-Barvarz M, Duchesne C, Rodrigue D. Mechanical, water absorption, and aging properties of polypropylene/flax/glass fiber hybrid composites. *J Compos Mater.* 2015;49: 3781–98. DOI: 10.1177/0021998314568576
- [107] Dhakal HN, Zhang ZY, Bennett N. Influence of fibre treatment and glass fibre hybridisation on thermal degradation and surface energy characteristics of hemp/unsaturated polyester composites. *Compos Part B Eng.* 2012;43:2757–61. DOI: 10.1016/j.compositesb.2012.04.036
- [108] Boopalan M, Niranjana M, Umopathy MJ. Study on the mechanical properties and thermal properties of jute and banana fiber reinforced epoxy hybrid composites. *Compos Part B Eng.* 2013;51:54–7. DOI: 10.1016/j.compositesb.2013.02.033
- [109] Saw SK, Datta C. Thermomechanical properties of jute/bagasse hybrid fibre reinforced epoxy thermoset composites. *BioResources.* 2009;4:1455–76.
- [110] Aji I, Zainudin E, Abdan K, Sapuan S, Khairul M. Mechanical properties and water absorption behavior of hybridized kenaf/pineapple leaf fibre-reinforced high-density polyethylene composite. *J Compos Mater.* 2013;47:979–90. DOI: 10.1177/0021998312444147
- [111] da Silva LJ, Panzera TH, Christoforo AL, Rubio JCC, Scarpa F. Micromechanical analysis of hybrid composites reinforced with unidirectional natural fibres, silica microparticles and maleic anhydride. *Mater Res.* 2012;15:1003–12. DOI: 10.1590/S1516-14392012005000134
- [112] Birat KC, Panthapulakkal S, Kronka A, Agnelli JAM, Tjong J, Sain M. Hybrid biocomposites with enhanced thermal and mechanical properties for structural applications. *J Appl Polym Sci.* 2015;132, 42452. DOI: 10.1002/app.42452
- [113] Jarukumjorn K, Suppakarn N. Effect of glass fiber hybridization on properties of sisal fiber-polypropylene composites. *Compos Part B Eng.* 2009;40:623–7. DOI: 10.1016/j.compositesb.2009.04.007
- [114] AlMaadeed MA, Kahraman R, Noorunnisa Khanam P, Madi N. Date palm wood flour/glass fibre reinforced hybrid composites of recycled polypropylene: Mechanical and thermal properties. *Mater Des.* 2012;42:289–94. DOI: 10.1016/j.matdes.2012.05.055
- [115] Kumar MA, Reddy GR, Rao HR, Reddy KH, Reddy BHN. Assessment of glass/drumstick fruit fiber (*Moringa oleifera*) reinforced epoxy hybrid composites. *Int J Polym Mater.* 2012;61:759–67. DOI: 10.1080/00914037.2011.610046
- [116] Vinayagamoorthy R, Rajeswari N. Mechanical performance studies on *Vetiveria zizanioides*/jute/glass fiber-reinforced hybrid polymeric composites. *J Reinf Plast Compos.* 2013;33:81–92. DOI: 10.1177/0731684413495934
- [117] Nicolai FNP, Botaro VR, Cunha Lins VF. Effect of saline degradation on the mechanical properties of vinyl ester matrix composites reinforced with glass and natural fibers. *J Appl Polym Sci.* 2008;108:2494–502. DOI 10.1002/app.27909

- [118] Ramesh M, Palanikumar K, Reddy KH. Influence of fiber orientation and fiber content on properties of sisal-jute-glass fiber-reinforced polyester composites. *J Appl Polym Sci.* 2015; 133, 42968. DOI: 10.1002/app.42968
- [119] Yalcin B, Amos SE, D'Souza AS, Clemons CM, Gunes IS, Ista T ro. K. Improvements in processing characteristics and engineering properties of wood flour-filled high density polyethylene composite sheeting in the presence of hollow glass microspheres. *J Plast Film Sheeting.* 2012;28:165–80. DOI: 10.1177/8756087911434185
- [120] Kakou CA, Essabir H, Bensalah M-O, Bouhfid R, Rodrigue D, Qaiss A. Hybrid composites based on polyethylene and coir/oil palm fibers. *J Reinf Plast Compos.* 2015;34:1684–97. DOI: 10.1177/0731684415596235
- [121] Shanmugam D, Thiruchitrabalam M. Static and dynamic mechanical properties of alkali treated unidirectional continuous Palmyra palm leaf stalk fiber/jute fiber reinforced hybrid polyester composites. *Mater Des.* 2013;50:533–42. DOI: 10.1016/j.matdes.2013.03.048
- [122] Idicula M, Neelakantan NR, Oommen Z, Joseph K, Thomas S. A study of the mechanical properties of randomly oriented short banana and sisal hybrid fiber reinforced polyester composites. *J Appl Polym Sci.* 2005;96:1699–709. DOI: 10.1002/app.21636
- [123] Noorunnisa Khanam P, Ramachandra Reddy G, Raghu K, Venkata Naidu S. Tensile, flexural, and compressive properties of coir/silk fiber-reinforced hybrid composites. *J Reinf Plast Compos.* 2010;29:2124–7. DOI: 10.1177/0731684409345413
- [124] Khalil HPSA, Hanida S, Kang CW, Fuaad NAN. Agro-hybrid Composite: The effects on mechanical and physical properties of oil palm fiber (EFB)/glass hybrid reinforced polyester composites. *J Reinf Plast Compos.* 2007;26:203–18. DOI: 10.1177/0731684407070027
- [125] Alavudeen A, Rajini N, Karthikeyan S, Thiruchitrabalam M, Venkateshwareen N. Mechanical properties of banana/kenaf fiber-reinforced hybrid polyester composites: Effect of woven fabric and random orientation. *Mater Des.* 2015;66:246–57. DOI: 10.1016/j.matdes.2014.10.067
- [126] Paiva Júnior C, de Carvalho L, Fonseca V, Monteiro S, d'Almeida JR. Analysis of the tensile strength of polyester/hybrid ramie–cotton fabric composites. *Polym Test.* 2004;23:131–5. DOI: 10.1016/S0142-9418(03)00071-0
- [127] Athijayamani A, Thiruchitrabalam M, Natarajan U, Pazhanivel B. Effect of moisture absorption on the mechanical properties of randomly oriented natural fibers/polyester hybrid composite. *Mater Sci Eng A.* 2009;517:344–53. DOI: 10.1016/j.msea.2009.04.027
- [128] Amico SC, Angrizani CC, Drummond ML. Influence of the stacking sequence on the mechanical properties of glass/sisal hybrid composites. *J Reinf Plast Compos.*

- [129] Venkateshwaran N, ElayaPerumal A, Alavudeen A, Thiruchitrambalam M. Mechanical and water absorption behaviour of banana/sisal reinforced hybrid composites. *Mater Des.* 2011;32:4017–21. DOI: 10.1016/j.matdes.2011.03.002
- [130] Misra RK, Saw SK, Datta C. The influence of fiber treatment on the mechanical behavior of jute-coir reinforced epoxy resin hybrid composite plate. *Mech Adv Mater Struct.* 2011;18:431–45. DOI: 10.1080/15376494.2010.528157
- [131] Li Y, Xie L, Ma H. Permeability and mechanical properties of plant fiber reinforced hybrid composites. *Mater Des.* 2015;86:313–20. DOI: 10.1016/j.matdes.2015.06.164
- [132] Islam MS, Talib ZA, Hasan M, Ramli I, Haafiz MKM, Jawaid M, et al. Evaluation of mechanical, morphological, and biodegradable properties of hybrid natural fiber polymer nanocomposites. *Polym Compos.* 2015. DOI 10.1002/pc.23616
- [133] Lin ZD, Hong XJ, Chen C, Guan ZX, Zhang XJ, Tan SZ, et al. Polypropylene hybrid composites with wood flour and needle-like minerals. *Plast Rubber Compos.* 2012;41:114–9. DOI: 10.1179/1743289811Y.0000000026
- [134] Karaduman Y, Onal L, Rawal A. Effect of stacking sequence on mechanical properties of hybrid flax/jute fibers reinforced thermoplastic composites. *Polym Compos.* 2015;36:2167–73. DOI 10.1002/pc.23127
- [135] Arifuzzaman Khan GM, Alam Shams MS, Kabir MR, Gafur MA, Terano M, Alam MS. Influence of chemical treatment on the properties of banana stem fiber and banana stem fiber/coir hybrid fiber reinforced maleic anhydride grafted polypropylene/low-density polyethylene composites. *J Appl Polym Sci.* 2013;128:1020–9. DOI:10.1002/app.38197
- [136] Haneefa A, Bindu P, Aravind I, Thomas S. Studies on tensile and flexural properties of short banana/glass hybrid fiber reinforced polystyrene composites. *J Compos Mater.* 2008;42:1471–89. DOI: 10.1177/0021998308092194
- [137] Zhang X, Yang H, Lin Z, Tan S. Polypropylene hybrid composites filled by wood flour and short glass fiber: Effect of compatibilizer on structure and properties. *J Thermoplast Compos Mater.* 2013;26:16–29. DOI: 10.1177/0892705711417030
- [138] Mirbagheri J, Mehdi T, John C. H, Ismaeil G. Tensile properties of wood flour/kenaf fiber polypropylene hybrid composites. *J Appl Polym Sci.* 2007;105:3054–9. DOI 10.1002/app.26363
- [139] Kwon HJ, Sunthornvarabhas J, Park JW, Lee JH, Kim HJ, Piyachomkwan K, et al. Tensile properties of kenaf fiber and corn husk flour reinforced poly(lactic acid) hybrid bio-composites: Role of aspect ratio of natural fibers. *Compos Part B Eng.* 2014;56:232–7. DOI: 10.1016/j.compositesb.2013.08.003
- [140] Sajna V, Mohanty S, Nayak SK. Hybrid green nanocomposites of poly(lactic acid) reinforced with banana fibre and nanoclay. *J Reinf Plast Compos.* 2014;33:1717–32. DOI: 10.1177/0731684414542992

- [141] Pal N, Aggarwal L, Gupta VK. Tensile behavior of sisal/hemp reinforced high density polyethylene hybrid composite. *Mater Today Proc.* 2015;2:3140–8. DOI: 10.1016/j.matpr.2015.07.102
- [142] Asaithambi B, Ganesan G, Ananda Kumar S. Bio-composites: Development and mechanical characterization of banana/sisal fibre reinforced poly lactic acid (PLA) hybrid composites. *Fibers Polym.* 2014;15:847–54. DOI 10.1007/s12221-014-0847-y
- [143] Graupner N, Herrmann AS, Müssig J. Natural and man-made cellulose fibre-reinforced poly(lactic acid) (PLA) composites: An overview about mechanical characteristics and application areas. *Compos Part A Appl Sci Manuf.* 2009;40:810–21. DOI: 10.1016/j.compositesa.2009.04.003
- [144] Lu G, Wang W, Shen S. Mechanical properties of wood flour reinforced high density polyethylene composites with basalt fibers. *Mater Sci.* 2014;20:464–7. DOI: 10.5755/j01.ms.20.4.6441
- [145] Ou R, Zhao H, Sui S, Song Y, Wang Q. Reinforcing effects of Kevlar fiber on the mechanical properties of wood-flour/high-density-polyethylene composites. *Compos Part A Appl Sci Manuf.* 2010;41:1272–8. DOI: 10.1016/j.compositesa.2010.05.011
- [146] Mohebbi B, Younesi H, Ghotbifar A, Kazemi-Najafi S. Water and moisture absorption and thickness swelling behavior in polypropylene/wood flour/glass fiber hybrid composites. *J Reinf Plast Compos.* 2010;29:830–9. DOI: 10.1177/0731684408100702
- [147] Ramezani Kakroodi A, Leduc S, Rodrigue D. Effect of hybridization and compatibilization on the mechanical properties of recycled polypropylene-hemp composites. *J Appl Polym Sci.* 2012;124:2494–500. DOI 10.1002/app.35264
- [148] Rodriguez-Castellanos W, Rodrigue D. Auto-hybridization of polyethylene/maple composites: The effect of fiber size and concentration. *Polym Polym Compos.* 2016.

Viscoelastic Performance of Biocomposites

Miguel Ángel Hidalgo Salazar

Additional information is available at the end of the chapter

<http://dx.doi.org/10.5772/66148>

Abstract

The viscoelastic behavior and performance to creep of biocomposites made from fique natural fiber and low-density polyethylene-aluminum (LDPE–Al) obtained from recycled long-life packages were studied. A relationship was observed between the creep mechanical responses of biocomposites with respect to natural fibers. Additionally, the four and six parameters of the mathematical model were calculated from the creep curves. A very good agreement between the experimental data and the theoretical curves was obtained in the fluency region. The relationship between interfacial fiber or filler and the polymer matrix is an indicator of mechanical performance of biocomposite, regardless of the application that you want to give. It is known that the mechanical and viscoelastic properties depend on the application time of loading, the type of load, temperature, micromechanics relationship between the natural fiber and the matrix, the type of anchor prevailing for the transfer effort to micro- and nano-levels and cannot be treated mathematically only by the laws of solids or fluids, viscoelastic behavior of biocomposites. It is possible to obtain mathematical models that fit different rheological phenomena; for example, creep and stress relaxation can be modeled and correlated with biocomposite experiment using dynamic mechanical analysis (DMA).

Keywords: biocomposites, DMA, natural fiber, fique fiber, viscoelastic behavior, mathematical models

1. Introduction

One biocomposite is a material formed by a polymer matrix and a filler or reinforcement, with the characteristic that both the matrix and the filler or reinforcement, one should at least be of biological origin. Now, it is known that the concept of sustainability has managed to motivate industries to seek alternative and sustainable materials using natural fibers that can reinforce or fill materials for different applications. Similarly, efforts are made to the development of

compound parts that could become an option to supply the irregular use of wood, and 100% the use of synthetic polymers and origin of oil. Biocomposites are already accepted, viable, and sustainable alternative, are characterized by one of its phases, and are of biological origin may be fibers or natural fillers or polymer that can obtained from renewable resources such as sugar cane, corn, and among others. Various natural fibers have been used for strengthening plastic matrices due to their low cost compared to synthetic fibers. In this context, we have already conducted several investigations that have developed new composite materials using natural fibers from different sources [1–7], the composites of thermoplastic matrix reinforced with natural fibers or fillers, they can mainly improve the mechanical performance of the original polymers, besides obtaining benefit in lowering the density; so it may be possible to obtain lighter, economical, and resistant products, as it is already known applications to the automobile industry where natural fibers are replacing the synthetic fibers in different parts of automobiles due to their light weight and low cost [8–13]. Cellulosic fibers such as sisal, fique, coir, jute, palm, bamboo, wood, and among others, in their natural condition, and several of cellulosic wastes such as shells, wood flour, and pulp are used as reinforcing agents or filled thermoplastic and thermosetting resins in different years.

In Colombia, researcher are working on the development of different biocomposites with natural resources that have already been prepared and cultivated for different uses, one of these resources is the fique. This natural fiber grows on the leaves of the plants and *furcraea* in Andes; it is native monocotiledón xerofítico of the Andean regions of Colombia, Ecuador, and Peru. These plants are grown from Venezuela to the east coast of Brazil. The common names of these plants are fique, cabuya, pita, penca, penco, maguey, cabui, chuchao, or cokes. Mainly in Colombia the fique has been used as an alternative to develop compounds with ceramic and polymeric matrices. Investigations have been carried out with the aim of finding alternatives to the use of short fiber waste fique [14]. They have evaluated the flexural properties and voltage matrix composite with high-density polyethylene (HDPE), and fique fiber reinforced percentages are found between 7 and 55% (v/v). Similarly, we have investigated the effect of composition on the mechanical properties by incorporating 20% of calcium carbonate, in order to stiffen the material for use in construction, especially for the manufacture of plates or rectangular profiles for manufacturing pallets. Because of the interest to include sisal in other manufacturing processes, we have studied the influence of different surface fibers of sisal treatments, in the case of alkalization, chemical modification with maleic anhydride, acrylic acid, and silane was carried out in order to improve the mechanical behavior of a compound of unsaturated polyester resin matrix. It was possible to analyze the mechanical behavior of the composite material through bending tests, where it was observed that the best properties are presented in both compounds with fibers subjected to alkalization, as those in which the alkali treatment was a preprocessing of other modification surface [15]. We also studied the behavior of the hydrolysis of compounds of epoxy matrix, in which two types of surface treatments were analyzed in which fique fibers used as reinforcement (alkalinization and silanization). The authors tested specimens by immersing in tap and distilled water for obtaining decreased flexural mechanical performance, and also reduction in weight due to the presence of water in the material [16, 17].

Now, it is possible to develop new alternatives for fique, especially to develop new composite materials, particularly fique arranged as blanket, which uses short fibers in two-dimensional random arrangement. This material is susceptible to be used in manufacturing of various products and various thermoplastic matrices, especially for structural applications or products such as pallets or similar products, which are typically subjected to withstand loads varying time intervals and temperature changes. This chapter presents, as an example, a study of the mechanical and viscoelastic performance biocomposite low-density polyethylene, filled with aluminum and reinforced with natural fibers sisal which is called LDPE-Al-Fique. It was possible to obtain a formulation of biocomposite, especially based on analysis of micromechanical interactions between the continuous phase and the dispersed phase, including study parameters such as surface treatments and the arrangement of the fibers in the composite. Also, a study of the effect of fibers on sisal treatments alkalization, silanization, and impregnation regarding the effect on the strain rate, and viscoelastic properties, such as the module TORAGE, loss modulus, and tangent delta was performed. The behavior of the compliance function of time, compared to other biocomposites reinforced or filled bagasse and wood, was analyzed [6, 7].

2. Fillers or natural fibers reinforced biocomposites

The biocomposites are composite materials consisting of one or more phases of biological origin. They could be made from natural fibers, or natural fillers such as wood flour, and combined with various common polymers such as polyolefins. Biopolymers can also be used for its formation, which identify different types of polymeric materials, in the case of common polymers such as polyethylene, but based on renewable raw materials, for example, from cultures of sugarcane, or biodegradable polymers such as the PLA or PHB. The design of a biocomposite material arises from the intention to optimize the mechanical performance and/or physical materials, or fill, to achieve the improvement of different properties, among which are: thermal, water absorption, tribological, viscoelastic behavior, stress relaxation, slowing flame, energy absorption, and among others, in summary seeks to improve physical and mechanical properties and/or thermochemical, studying various effects of mechanical, chemical and/or physical treatments specially made of fibers to improve the properties of biocomposites of these fibers or work as fillers. The formation of the phases of the biocomposites determines their properties, usually, the formed fibers or fillers, phase aims at strengthening properties such as increased stiffness, or increasing the breaking load and achieving a low density [7, 18–26]. In general, polymeric materials, especially thermoplastics, are transformed by injection molding, extrusion, and thermoforming; these materials allow a dispersion of fibers that can be used for obtaining new materials and products, which can be fiber reinforced or fillers. The function of the fibers in the compounds is directly related to the applied stress resistance, while the matrix is responsible for the transmission of efforts to the reinforcement; conjugation of the two functions results in a better response of the reinforcement, which in turn can lead to an increase in the rigidity and strength of the material. The fiber-reinforced thermoplastic materials should be considered important factors in the

theoretical study of the properties of the matrix, fiber characteristics, matrix content, fibers or fillers, relationship, and response of the interface between the matrix fibers and fillers, and reinforcing fiber content is presented in terms of volume or weight [18, 27–29]. Applications of biocomposites reinforced with natural fibers or fillers are being investigated as a result of the increasing demand for sustainable and environmentally friendly products, the most common applications are: construction, automotive industry, and of packaging. Applications for the production of housing roofs, structural panels, beams, and door frames have been investigated. There are other applications in the construction in which the NFCS could be an economic and ecological choice. Now, we can find several applications for the development of new packaging and interior automotive parts, which are mainly developed by extrusion, injection molding, and thermoforming [30–33]. The use of renewable for designing biocomposite materials obtained from sources such as palm, flax, sisal, sisal, jute, and among others, these cellulose fibers can be classified into bast fibers and seed fibers such as cotton, coir fibers cane, rice bran, and wheat, as well as all other types such as wood and roots [34]. A global approach of the annual production of these fibers can be seen in **Table 1**.

Fiber source	World production (10 ³ Ton)
Bamboo	30,000
Sugarcane bagasse	75,000
Jute	2300
Kenaf	970
Flax	830
Grass	700
Sisal	375
Hemp	214
Coir	100
Ramie	100
Abaca	70
Fique*	22

Table 1. A global approach of the annual production of natural fibers [35].

It is known today for automotive applications, such as the German automotive industry companies such as Volkswagen, BMW, Ford, Audi, Daimler Chrysler, Mercedes, and among others. The applications of biocomposites are also in the construction industry, packaging, sports, and others, applied to the design of various products [36], some physical and mechanical properties of these natural fibers currently used for production biocomposites as shown in **Table 2** [37, 38].

Logistics problems for the collection of agro-industrial waste, emissions of greenhouse gases generated by incineration and subsequent problematic waste volumes continue to motivate

the use of natural fibers from various sources for the development of biocomposites for various applications. These new composite materials using wastes of agricultural and industrial processes are a sustainable alternative, provided that the production volume of these residues is not greater than the volume of use in the development of biocomposites for various applications [39]. Currently, applications in the development of structural products are also sought, which require a more precise understanding as to their physical and mechanical behavior, especially when trying to develop products that claim to have a long shelf life of months or years, which required to have a comprehensive understanding of the behavior or performance biocomposite in time, under different stress conditions and temperature mainly. By the technique of dynamic mechanical analysis (DMA) plus a good mathematical approximation behavior viscoelásto-plastic of biocomposites, it is possible to predict the behavior, physical, and mechanical modified biocomposite or reinforced with natural fibers based on experiments using this technique assays laboratory short-term (hours, days, or weeks) and align them with mathematical models that can predict behavior for longer periods, months or years [7, 40]. For structural applications, where biocomposites are subjected to cyclic or constant long periods of time loads, natural fibers such as bamboo, jute, sisal, sisal, hemp, and among others, by its constitution at the macro-level, have better mechanical performance and viscoelasticity when supporting loads over time [6, 10]. In the case of south American sisal, especially in the Andean region (Colombia, Ecuador, and Peru), it promises be a fiber with an acceptable reinforcing materials for various applications and manufacturing processes, also nowadays cultivation is sustainable, and widely used in South America for the production of textiles blankets, bags for packing coffee mattresses, and among others.

Fiber	Density (g/cm ³)	Tensile strength (MPa)	Young's modulus (GPa)	Elongation (%)
Fique	1.47	132.4	8.2–9.1	9.8
Flax	1.4	88–1500	60–80	1.2–1.6
Hemp	1.48	550–900	70	1.6
Jute	1.46	400–800	10–30	1.8
Ramie	1.5	500	44	2
Coir	1.25	220	6	15–25
Sisal	1.33	600–700	38	2-3
Abaca	1.5	980	—	—
Cotton	1.51	400	12	3–10
Kenaf (bast)	1.2	295	295	—
Kenaf (core)	0.21	—	—	—
Bagasse	1.2	20–290	19.7–27.1	1.1
Henequen	1.4	430–580	—	3–4.7
pineapple	1.5	170–1672	82	1–3
Banana	1.35	355	33.8	53

Table 2. Physical and mechanical properties of natural fibers.

2.1. Biocomposites fillers or reinforced with fique fibers

Fique, commonly called Cabuya, Fique, Motua in the countries of the Andean region and its scientific name is *Furcraea bedinghausii*, is a large plant stem erect; its height varies from 2 to 7 m, with green leaves, long (1–3 m), narrow (10–20 cm), pointed, ribbed, and thorny; in some varieties, it has faint lines or stripes of about 3 mm long. Young plants consist of a rosette of thick fleshy leaves bluish-green; as the plant grows, it develops at the base of a short stem carrying 75–100 sheets whose length and width ranges from 150 to 200 cm and 15 to 20 cm, respectively, in the widest part near the middle, tapering to 10 cm near the base, having a thickness of 6–8 cm and can be seen in **Figure 1** [41].



Figure 1. Plant of fique in the Andean region.

Some characteristics and properties of fique fiber are shown in **Table 3**, the great variability of diameters can be obtained from fibers of the same batch, and even along the same fiber is highlighted, as is usual in the natural fibers [42].

Characteristic	Fique	Average
Equivalent diameter (mm)	0.16–0.42	0.24
Bulk density (g/cm ³)	0.72	–
Specific density (g/cm ³)	1.47	–
Water absorption (%)	60.00	
Water (%)	12.00	–
Effort last tension (MPa)	43.00–71.00	132.40
Last elongation (%)	9.80	
Modulus of elasticity (GPa)	8.20–9.10	–

Table 3. Characteristics of fique fiber [42].

Table 4 shows the chemical characterization of fique leaf, and composition of the fiber and bagasse juice leaf. They have been reported thermal analysis of fiber properties by thermogravimetry, which shows that the fiber supports fique at 220°C without degradation. The authors reported a bulk density of 0.87 g/cm³ density important in terms of specific properties [43].

Fiber		Juice	chaff	
Ashes	0.70%	Chlorophyll	Cenizas	12.20%
Cellulose	73.80%	Carotenoids	E.E.	3.64%
Resins, ceras and fats	1.90%	Saponins	Proteína	9.84%
Lignin	11.30%	Resins	Calcium	21.65%
Pentosan	10.50%	Flavonoids	Phosphorus	0.09%
Total	98.20%	Orgánic acids	Magnesium	0.2%
		Tras	Phosphorus	1.81%
		Water	Sodium	0.04%
		Lignin	Copper	14 ppm
		Calcium	Iron	647.00 ppm
		Lipoides	Manganese	33.00 ppm
		Phosphorus	Zinc	17.00 ppm

Table 4. Chemical composition of leaf sisal [41].

Position	Fiber	Country	Tons/year	Participation
1	Jute	India	1,900,000	57%
2	Jute	Bangladesh	800,000	24%
3	Fique	Brazil	191,103	6%
4	Abaca	Filipinas	70,356	2%
5	Jute	China	68,000	2%
6	Fique	México	41,856	1%
7	Abaca	Ecuador	27,194	1%
8	Jute	Myanmar	26,169	1%
9	Fique	Kenya	25,000	1%
10	Fique	Colombia	22,000	1%

Table 5. World production of natural fibers [45].

Table 5 shows some data are presented worldwide in the production of fibers, which leaves observe the position of women Colombia. It should be noted that in many countries have industrialized the use of compounds based on natural fibers that are available in their regions,

showing a very positive outlook for the industrial production of compounds based on fique fiber [14]. At present, there are very positive reports on an international level studies fique, where it has been used as reinforcement for polymer matrix composites with PE, PP, and among others [14, 17, 44].

The fibers of fique, regarding mechanical properties, have an approximate tensile strength of 237 MPa, a modulus of elasticity of 8.01 GPa resistance, and a strain of 6.02% at break [37, 42].

Fiber	Density (g/cm ³)	Strain (%)	Tensile strength(MPa)	Young's modulus(GPa)
Cotton	1.50–1.60	7.00–8.00	287.00–597.00	5.50–12.60
Jute	1.30	1.50–1.80	393.00–773.00	26.50
Linen	1.50	2.70–3.20	345.00–1035.00	27.60
Fique	1.47	9.80	43.00–571.00	8.20–9.10
Hemp	-	1.60	690.00	-
Ramie	-	3.60–3.80	400.00–938.00	61.40–128.00
Fique	1.50	2.00–2.50	511.00–635.00	9.40–22.0
Coconut	1.20	30.00	175.00	4.00–6.00
Soft wood	1.50	-	1000.00	40.00
E Glass	2.50	2.50	2000.00–3500.00	70.00
S Glass	2.50	2.80	4570.00	86.00
Aramid (normal)	1.40	3.30–3.70	3000.00–3150.00	63.00–67.00
Carbon (standard)	1.40	1.40–1.80	4000.00	230.00–240.00

Table 6. Comparison of natural and synthetic fiber properties [11, 37, 42, 47, 48].

This has facilitated fique understand that is a good alternative to reinforce a thermoplastic materials to develop different products and different manufacturing processes. Fique is a natural plant that is used in ancient as fiber in the manufacture of packaging and others, which led to its establishment as permanent cultivation in the Andean region countries. However, currently, it is recognized as a vegetable product with different craft and agro-industrial applications and with immense potential in generating environmental benefits, employment, and income. The cultivated area fique in Colombia is distributed along 13 national departments: 98% of the 21,445 tons of fique produced are concentrated in 4 Colombian departments (Cauca, Nariño, Santander, and Antioquia); about 60% of the total production is in Nariño and Cauca. Fique fiber is used in products like ropes and sacks of seeds, grains, and coffee [37, 45]. The presence of synthetic fibers such as polypropylene has gradually made inroads in these markets. To develop products based on natural fibers de-

manding structural rigor required mainly improving mechanical properties and viscoelastic biocomposites who wish to develop. Previous studies in the field show that the viscoelastic performance of biocomposites varies with the type of filler, fiber, coupling treatment, and types of polymer matrices [6, 7, 10, 46]. Several modeling techniques have also been applied to analyze the flow behavior (CREEP) [6, 10–13]. **Table 6** shows a comparison of the most important properties of some natural and synthetic fibers, including fique.

In **Table 6** it can be seen that the novel compounds manufactured from natural fibers have advantages over the weight of the end products compared to glass fibers with an average of 2.7 g/cm³ against 1.2–1.6 g/cm³ of natural fibers. Natural fibers like fique other natural fibers can be processed in different ways to produce reinforcing elements with different mechanical properties. Depending on the type of reinforcement produced and its method of production, the modulus of elasticity and resistance may vary. Among others, cellulose fibers are obtained from wood by a chemical pulping process, they could have a modulus of elasticity of 40 GPa. These fibers can be subdivided to obtain microfibers by the hydrolysis process, reaching moduli of 70 GPa. Finally, by theoretical calculations of modulus of elasticity they were obtained up to 250 GPa predictions for cellulose chains (crystallites). The properties and structure of fibers also are affected by conditions and growth parameters, such as growth area, climate, and plant age [34].

Fique shows that it is susceptible to develop new materials used for different magnifications, but have similar disadvantages of any natural fibers in the world. For example, the fiber quality is variable, depending on unpredictable influences such as weather, moisture absorption, which causes swelling of the fibers, the maximum processing temperature is restricted, there is uncertainty in the viscoelastic performance over time but treatments fiber can greatly improve the price of the fiber that may vary from the results of the crop or agricultural policy and natural fibers are less durable and less resistance than glass fibers. In the research context, the above disadvantages are considered as opportunities to deepen their study and facilitate disinherit its applicability, as well as motivating their uses. At the same time, they have advantages employ: thermal recycling, where the glass causes problems in combustion furnaces, low specific weight, which results in greater strength and specific stiffness than glass, a renewable resource is possible; production requires little energy, carbon dioxide is used as oxygen is returned to the environment, can be used with virgin polymer matrix, recycled, as fillers, producible at low cost, processing and handling are friendly; low tool wear, no skin irritation occurs, and having good thermal and acoustic insulation. The hydrophilic nature of fique for its high cellulose content is one of the most important problems when trying to reinforce polymer matrices, because the vast majority of polymer matrices in the market are hydrophobic thermoplastic; this difference in physicochemical properties occurs as a result of an incompatibility between the natural fiber and the thermoplastic matrix, and this is reflected in poor stress transfer and mechanical behavior depends on the micromechanical interfacial relationship matrix fiber, also it affected the viscoelastic performance and general structural products to be manufactured with materials using natural fibers Fique without any surface treatment that improves the performance micromechanical compound and therefore the product is designed.

3. Behavior of viscoelastic biocomposites

The biocomposites inherit the behavior of the matrix with which they were manufactured, making their mechanical properties strongly dependent on the ratio of applied strain; therefore the mechanical behavior and viscoelastic structural products that are designed as sustainable products, which can be applied to the construction industry and automotive, mainly be affected by the dependence of applied stress and temperature conditions at the time. When biocomposites are processed and take the desired shape, e.g., extruded beams, molded housings, or any product which may be subjected to a constant load, will be generated on these products efforts, bending or tension or combinations thereof, constants, the effect of a constant effort on a product manufactured in biocomposites can be seen reflected in unwanted time warps, inclusive could produce the product failure. In this context, the durability of biocomposites can limit their applications, and implement risk of all the efforts of previous research, in order to develop sustainable materials for sustainable products. Studying the behavior of NFPCs under constant load conditions, where the deformation increases in time, that is, the material flows under the load (effect of creep), can understand that in a system biocomposite load between redistributes the matrix and natural fibers during deformation, when these materials are subjected to constant loads, can be affected by various effects of creep, the matrix, fiber, and the interface. There are several applications that have achieved biocomposites for extrusion with an addition 40–60%, mixed with thermoplastics, such as HDPE, PP, PVC, and materials [6, 49]. Compounds where manufacturers use natural fibers from different sources, as one of the fillers or reinforcements. These thermoplastic biocomposites can be used as tables for decks, fences, railway sleepers, etc. When used under these requirements, the CREEP or viscoelastic deformation becomes a problem, because the application of the effort takes the material to work under load long periods of time (months and years). This has been studied extensively in the case of advanced thermoset composites, and nowadays the investigations on biocomposites observed that the viscoelastoplastic behavior can lead to failure sustainable product, when subjected to large deformations and long periods of time, under conditions of dynamic or static load and temperature variations. These materials progressively accumulate deformation, causing internal damage occurs due to creep and/or fatigue, both cause cumulative damage [7, 50, 51]. There have also been efforts to correlate effects at smaller scales, relating effort plastic flow [52–54], according to the nonlinear response which it is due to permanent deformation. Investigations of some thermoplastic compounds have focused on deformation patterns, and have shown the strain-fluence compounds with particulate wood plastic, with alteration of the compositions and components of compound [49, 55, 56]. It has also been observed that with increased fiber content, the effect of creep decreases. Agro compounds used to develop products for structural construction, often requiring improved mechanical properties, particularly creep performance. It has been shown that the fluence of biocomposites varies with the type of filler and content, coupling treatment, and types of polymer matrices [6, 10]. Several molding techniques have also been applied to analyze the behavior CREEP [7, 10–12, 57].

At present, it is of interest to develop new thermoplastic biocomposites for sustainable products, and it is about the future course of implementation and sustainability over time of

biocomposites. There are estimates based on theoretical predictions, especially validated parameters obtained from accelerated tests, using the technique of dynamic mechanical analysis, DMA; this is the case study of creep behavior of composite materials based on different fibers such as bagasse, bamboo, and wood flour as matrix polyvinyl virgin and recycled vinyl and high density polyethylene. They tried to develop and adjust different theoretical models during all stages of CREEP to help predict long-term behavior. And observing different treatments and source matrices, they observed that models fit well in the linear zone CREEP, difficulties in predicting the primary and tertiary CREEP, referring difficulties in predicting the adjustment parameters, on lacking. Experimental long-term break in the tertiary CREEP, for the limited number of experiments that can be done using only accelerated techniques with DMA, especially those of CREEP long term [6, 10]. At constant load level a biocomposite has better creep resistance than ordinary polymer systems at low temperatures. However, biocomposites usually show higher temperature dependence. Various models of creep (Burgers model, model Findley power law, and a model of simple power law two parameters) have been used to adjust the data flow. The principle of time-temperature superposition (TTS) is typically used for predicting long-term creep, where it is important to understand that this method is valid mainly in the linear viscoelastic region of the biocomposites, however this method suffers from a prediction of the aging of natural fibers, including an error in time, which has now become complex including models for developing sustainable biocomposites. It has been shown that the four elements of the model Burgers and the power law with two parameters, adjust flow curves of biocomposite [6, 7]. Other authors have shown that PP-agglomerate compounds show different behaviors yield according to the processing conditions, i.e., with increasing fiber content, fluence compounds for example with wood fibers decreases [11, 56], studies are not derived from expressions that clearly include the flow properties of the matrix and fiber in their models, nor aging, or other factors associated with the nature of natural fibers. Therefore, the constant creep of these mathematical models is fully specified biocomposites, and are only valid for those compounds in particular and the conditions imposed nowadays. There is no complete method that can predict with high accuracy the viscoelastic performance of biocomposites, however, estimates that they are possible to perform with the use of the DMA, achieving reasonably guide the industry to seek applications for the development of new sustainable products, using biocomposite.

3.1. Linear viscoelasticity

Biocomposites have a typical response to mechanical loads, and can be studied as materials in some cases behave as elastic solids, and other, as viscous fluids. It is known that the mechanical and viscoelastic properties depend on the application time of loading, the type of load, temperature, micromechanics relationship between the natural fiber and the matrix, the type of anchor prevailing for the transfer effort to micro- and nanolevels, and cannot be treated mathematically only by the laws of solids or fluids, as viscoelastic behavior of biocomposites has high temperature dependence, especially if the work environment exceeds the glass transition temperature of the biocomposite, from the foregoing, the biocomposites in working conditions at constant load can be considered as super cold fluids. The above findings were mooted at the time of Boltzmann and others, but it is now clear that the vision of Boltzmann

was the right approach. As the understanding of the physical nature of the biocomposites and matured techniques has increased they have been developed many biocomposites. Since these materials are motivating the development of sustainable products, it is essential to analyze and understand from an engineering perspective, the response of biocomposites when load is applied and other environmental variables such as temperature and humidity. The difference between an elastic solid biocomposite and a viscous liquid is not an absolute difference, the ability to detect the elastic or viscous responses biocomposite object of study often depends on the time scale of the experiment and the conditions required recreate. Thus, from a strict point of view, all biocomposites have a viscoelastic behavior, i.e., depends not only on the state of stress to which the material is subjected, but also the history of preloading the material and all condition biocomposite that may affect the macrolevel, micro and nanolevel. The biocomposites are complex viscoelastic systems for manufacturing and high dependence on renewable raw materials, such as natural fibers. Viscoelastic behavior can be investigated using various methods; the use of dynamic mechanical analysis (DMA) is the most common nowadays. For example, in an experiment fluence (CREEP) a constant σ_0 effort applied to a sample and the deformation ϵ is observed as a response function of time t . Normally effort increases with time and the flow curves (as a function of time) may exhibit three regions (**Figure 2**): primary creep in which the curve is concave downward; the secondary creep deformation in which it is proportional to time; and tertiary creep where the deformation is accelerated until the creep rupture occurs. Strain rate, which would be represented by the derivative of the deformation curve, also exhibits three regions.

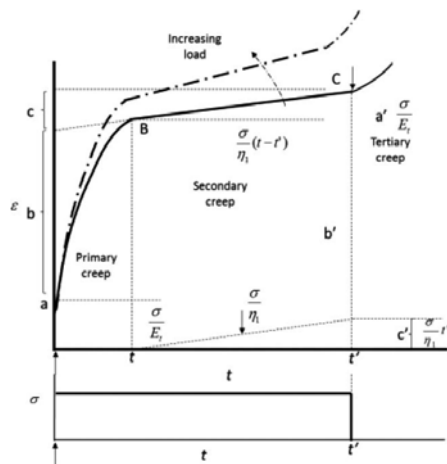


Figure 2. Schematic yield curve (CREEP).

In the yield curve (CREEP) high, the material has a linear viscoelastic behavior, so it is possible to apply the principle of superposition time TTSP temperature. However, nonlinearity presents high deformation speeds. In other words, the stress curves as a function of strain rate could show the transition from linear to nonlinear behavior in flow experiments (**Figure 2**).

A composite thermoplastic polymer matrix subjected to constant loads for periods of time and prolonged temperatures above the glass transition of the matrix work, regardless of the direction of load application, the material works to tension, bending, compression, or some combination of these efforts; its response to deformation over time is a combination of deformation, micromechanics, elastic, and viscous, which can be expressed in terms of compliance creep D , as:

$$\varepsilon_{(t)} = \sigma_o D(t, T, \sigma_o) \tag{1}$$

The creep compliance $D_{(t)}$ is the ratio of stress and strain generally as a function of time, as seen in Eq. (1). When considering the case of the response to creep as linear material, creep deformation is independent of the level of effort, which makes it look as a property of the material between different systems of composite materials, taken under similar environmental conditions. The total deformation at any instant of time $\varepsilon_{(t)}$ in a creep test of a biocomposite can be represented as the sum of the instantaneous elastic deformation ε_E (i.e., the initial deformation when the constant voltage is applied) and ε_V viscoelastic deformation. Similarly, compliance can be divided with elastic and viscous component. By submitting the biocomposites constant loads, regardless of your work address, the response of the material is creep or creeps. Where compliance depends on the deformation function in the time and effort that is subjected in Eq. (2) shows an expression for compliance:

$$D_{(t)} = \frac{E_{(t)}}{\sigma_o} \tag{2}$$

For the design and manufacture of products based on biocomposites require to define the CREEP as the change in function of time in the dimensions of a product polymer or composite when subjected to constant stress in different working conditions, which may include, temperature, environmental, cyclic loading, and among others. The biocomposites usually have CREEP behavior at room temperature; which is due mainly to its micromechanical relationship fiber-filler with the matrix, and the combined efforts to which the material may be subjected to some cases also the flow behavior may be generally negligible. Therefore, design procedures are simpler because the module can be considered constant (except at high temperatures). However, the modulus of a polymer or composite material is not constant (as shown in Eq.(2)), because the deformation is a function of time, and compliance is directly related to the stiffness of the material. Whenever variation is known, the behavior CREEP of biocomposites can be compensated by the precise use and well-established design procedures, or by modifying the composition of the biocomposite, using reinforcements and/or fillers to correct their mechanical performance and viscoelastic. For biocomposites, the aim of the design methods to determine the stress values does not cause permanent deformation intolerable products or fractures. Excessive deformation becomes a limiting factor in the selection of work effort, leading to the conclusion that it is essential to qualify and specifically quantify the

deformation behavior of the biocomposites, depending on time and temperature. A schematic diagram of flow behavior (creep) can be seen in **Figure 3**; given load shows a configuration of four point bending biocomposite. The weight or load, along with gravity, provides a constant effort in biocomposite. After 5 days in this condition no significant unfavorable deformation occurs. However, after 7 months deformation caused by the effort has increased, and deforms further after 2 years.

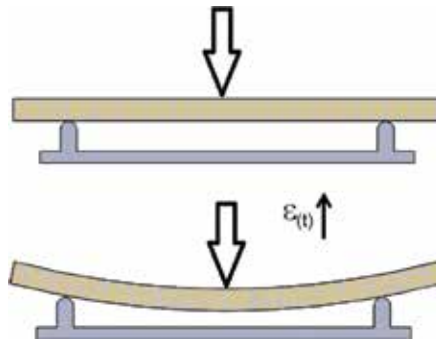


Figure 3. CREEP response of a biocomposite beam subjected to bending at four points, an illustrative estimate given by the author.

The biocomposites polymer matrix has significant sensitivity to use a function of time and temperature, resulting in a limited use of structural applications demanding applications or in dimensional stability value. When the biocomposite is subjected to high stresses, it can result in the material, and excessive deformations that may cause the product to lose its functionality, one could get the material to the tertiary region where creep occur until fracture. This is called the upper region and is also known as the acceleration phase of CREEP. The importance of the tertiary region for normal operation and design to CREEP is also important, since parts of polymer or compound should be designed to avoid this area; safety factors must ensure away from this region over the lifetime of the products developed with biocomposites.

3.2. Mathematical models

The experimental response of a dynamic test to tension, bending, or compression creep compliance of a biocomposite can be modeled with provisions of springs and dampers, where the springs represent the elastic solid behavior and cushion the behavior of a viscous liquid. It represents the Hooke spring deformation force that is proportional to the applied stress and the damper flow proportional to the strain rate Newtonian. To model mathematically one biocomposite, the stress, strain and time, you can relate to the constant characteristics of the mechanical elements [57]. The mechanical model mimics the actual behavior of biocomposites, although the elements themselves may not have direct analogies with real material. However, these models represent a mathematical understanding of the problems of viscoelastic performance of biocomposites, studied by accelerated tests in the laboratory, which can easily be articulate studies of continuum mechanics means to solve even more complex models with the

help of numerical methods and approach to more realistic models that include visco-elastic-plastic. It is emphasized that mathematical models presented in this chapter are classical performances already studied by several authors, that when applied to biocomposites, approximate their behavior and allow you to compare and study relationship deformation at short times and long-term predictions that might suggest designers, which are the most desirable when applying for the development of sustainable products made from biocomposite materials.

3.3. Maxwell, Kelvin, and four parameter models

Figure 4(a) shows the Maxwell model, which is represented by a spring connected in series with a damper and **Figure 4(b)** shows Kelvin model (or Voigt), which is represented by a spring connected in parallel with a damper; in both cases an approximation of a system characterized by time dependent and the ratio of η viscosity (damper) with the modulus of elasticity E represented by the spring is obtained, which they can be approximated to describe the viscoelastic behavior of a biocomposite. The parameter η leads to model a related response delay time for the Kelvin model, and the relaxation time for the Maxwell model.

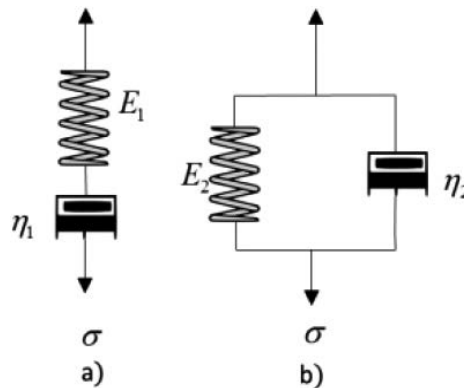


Figure 4. Models: (a) Maxwell, (b) Kelvin.

To analyze the flow behavior (CREEP) of biocomposites, it is possible to apply the model of four parameters successfully, which is derived from a series combination of the Maxwell model and Kelvin model, as shown in **Figure 5**.

The four-facing model fits the response obtained experimentally for the controlled creep test, based on the technique of dynamic mechanical analysis (DMA). **Figure 6** depicts a curve of biocomposite creep subjected to a three-point bending at a constant effort in the linear viscoelastic region. The fraction of O to A shows the rapid response of the initial deformation on the flow curve, i.e., it occurs an instantaneous elastic response. This behavior is followed by a region of creep from A to B, where the shear rate decreases at a constant rate introduced in Section B to C. Once the stress is removed, the instantaneous elastic O to A response is fully retrieved from C to D, i.e., the distance $a' = a$. Then the curve drops from D to E in a slower

recovery. However, this recovery is not complete due to the initial state by increasing $c' = c$. This response is completely unrecoverable, and is a measure of plastic flow [58].

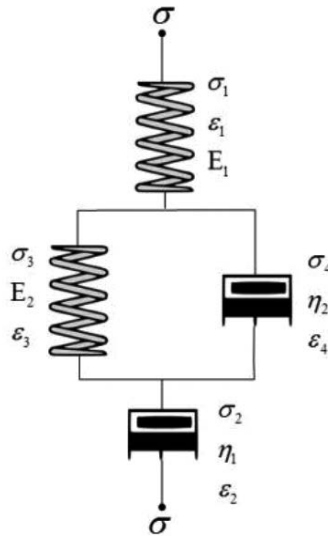


Figure 5. Four-parameter model.

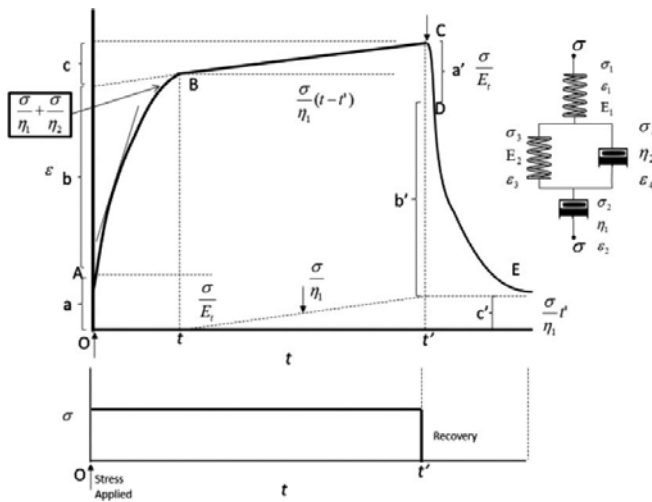


Figure 6. Four-parameter model and yield curve (CREEP).

Figure 5 represents the elastic response changes in A and A'. A convenient to model this response element is the Hooke law. The Kelvin-Voigt model corresponds to changes in b' (change symbol) in the region of creep; it represents a damping plastic flow c'. Figure 6 shows the mechanical models for the purpose of better illustrating the appearance of the flow curve.

The four-parameter model is an assembly of a Maxwell element and Kelvin-Voigt element, where the latter component is time dependent. **Figure 7** shows that (zone 1) the system is idle effortless. When it exposed to constant stress to three-point bending, in **Figure 7** (zone 2), the spring system with a constant amount of E_1 extends instantaneously to “a” $\sigma/E_1 = a$. Then, in **Figure 7** (zone 3), the fluence rate decreases with a gradual increase in load bearing spring E_2 , until fully extended and the damping η_2 no longer carry any load. As the spring is now E_2 fully extended, the creep ratio to a solid phase, corresponding to the plastic flow of the linear viscoelastic region represented by the constant η_1 damper. The damper deforms until the load is removed, as illustrated in **Figure 7** (zone 4), leaving permanent deformation. Now, the spring retracts quickly E_1 to a' and the recovery period is b' . During this time, the damper η_2 is forced to retreat to its initial position by spring E_2 representing a delayed or anelasticity elastic response. The damper position η_3 remains in the extended state, since the spring cannot influence its final position; this can be seen in **Figure 7** (zone 5). Thus, the nonrecoverable plastic flow is equal to $c' = \sigma t/\eta_3$. The model fully represents the elastic, inelastic, and viscous behaviors of biocomposites, indicating that if possible with fillers or natural fibers affecting the interfacial relationship, fiber matrix polymer or cross-linked polymer, the variable η_1 increase, which it is reflected in a decrease in permanent deformation c .

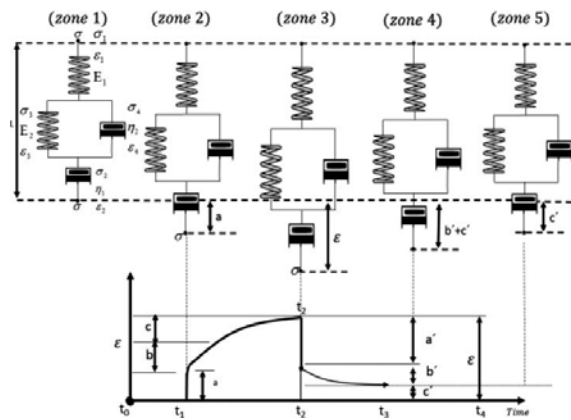


Figure 7. Response of four-parameter model adjusted to fit a creep curve.

Given the balance of forces occurring in the four-parameter model, we can write the following expression, with respect to the effort and deformation:

$$\sigma = \sigma_1 = \sigma_2 = \sigma_3 + \sigma_4 \tag{3}$$

$$\varepsilon = \varepsilon_1 + \varepsilon_2 + \varepsilon_{3,4} = \varepsilon_1 + \varepsilon_2 + \varepsilon_k \dots \dots \dots \varepsilon_3 = \varepsilon_4 \tag{4}$$

where ε_k is the strain response of the Kelvin-Voigt model, the equations representing different relationship stress-strain are:

$$\sigma_1 = E_1 \varepsilon_1, \sigma_2 = \eta_2 (d\varepsilon_2 / dt), \sigma_3 = E_3 \varepsilon_3, \sigma_4 = \eta_4 (d\varepsilon_4 / dt) \quad (5)$$

And the equation that relates and models the behavior of biocomposite visco-elastic-plastic holistically can be arranged as follows:

$$\frac{\eta_1 \eta_2}{E_1 E_2} \left[\frac{d^2 \sigma}{dt^2} \right] + \left[\frac{\eta_1}{E_1} + \frac{\eta_1 + \eta_2}{E_2} \right] \frac{d\sigma}{dt} + \sigma = \frac{\eta_1 \eta_2}{E_2} \frac{d^2 \varepsilon}{dt^2} + \eta_1 \frac{d\varepsilon}{dt} \quad (6)$$

Equation (7) can be solved for flow conditions and/or relaxation; response to deformation is:

$$\varepsilon(t) = \frac{\sigma_0}{E_1} + \frac{\sigma_0}{\eta_1} t + \frac{\sigma_0}{E_2} \left[1 - e^{-\frac{E_2 t}{\eta_2}} \right] \quad (7)$$

Response to creep recovery is:

$$\varepsilon(t) = \frac{\sigma_0}{\eta_1} t + \frac{\sigma_0}{E_2} \left[e^{-\frac{E_2 t_1}{\eta_2}} - 1 \right] e^{-\frac{E_2 t}{\eta_2}} \dots t > t_1 \quad (8)$$

where $\varepsilon_{(t)}$ is the yield strength, σ_0 is the initial applied stress, t is time, E_1 and E_2 are the elastic modulus of the springs of Maxwell and Kelvin, respectively, and η_1 and η_2 are the viscosities of the Maxwell and Kelvin dampers. η_2/E_2 is usually denoted as τ , the delay time required to generate 63.2% strain on the Kelvin unit [59].

In Equation (7), the first term is the instantaneous elastic strain. The second term is the early stage of creep deformation, and is due to mechanisms such as relaxation, extension of the molecular chain, and biocomposites closely related to the performance of the fiber matrix micromechanic relationship. The last term represents the long-term creep deformation, and is due to the overall performance of the biocomposite. The parameters E_1 , E_2 , η_1 , and η_2 can be obtained by adjusting the equation to the experimental data and can be used to describe the creep behavior. The strain rate of the linear viscoelastic region of the biocomposite is possible to calculate, if we derive Eq. (7), and obtain the strain rate:

$$\dot{\varepsilon} = \frac{\sigma_0}{\eta_1} + \frac{\sigma_0}{\eta_2} e^{-\frac{E_2 t}{\eta_2}} \quad (9)$$

For all models of linear viscoelasticity, it is important to note that the response of deformation creep is independent of the level of effort, giving the opportunity to study and compare with

other systems evaluated under the same environmental conditions, must obtain curves and models of creep. The equation for calculating the compliance $D_{(t)}$ is defined by:

$$D_{(t)} = \frac{1}{E_1} + \frac{t}{\eta_1} + \frac{1}{E_2} \left[1 - e^{-\frac{E_2 t}{\eta_2}} \right] \quad (10)$$

The viscoelastic behavior of a system biocomposite presents different delay times; therefore, it is possible to model more precisely repeating n Kelvin-Voigt models, which are particularly adjusted in the delayed elastic region or annalistic, which has default a typical nonlinear region. In **Figure 8**, you can see a diagram showing this behavior.

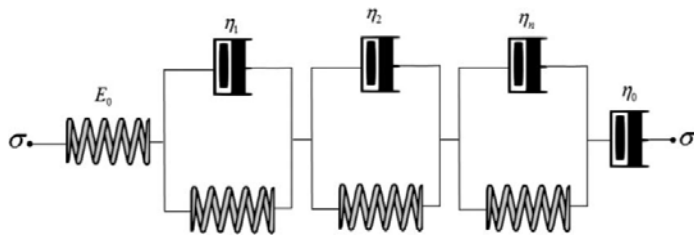


Figure 8. Multiple models for adjusting creep curves.

Fundamental viscoelastic properties such as creep compliance module or relaxation can be found by solving the differential equation that represents including for the appropriate load if necessary. For example, the compliance fluence can be determined using the conditions for a creep test and would be represented by:

$$D_{(t)} = \frac{1}{E_1} + \frac{t}{\eta_1} + \sum_{i=2}^n \frac{1}{E_i} \left[1 - e^{-\frac{t}{\tau_i}} \right] \tau_i = \frac{\eta_i}{E_i} \varepsilon_{(t)} = D_{(t)} \sigma \quad (11)$$

The determination of initial conditions is achieved by inspection of the physical model. Since the input force is constant for the creep test, the change in stress is zero. The solutions of differential equations for relaxation conditions, constant deformation, or changes in stress and other conditions can be obtained similarly.

3.4. Time-dependent deformation behavior of biocomposite

A way to study the effect of a reinforcement or filler natural fibers to manufacture biocomposites is to show the interdependence of the stress, strain, and time through curve creep and recovery creep performed in short tests using the DMA technique dynamic mechanical analysis. To perform the creep tests and recovery (creep and creep recovery), it is necessary to set a DMA with the force of flow required to maintain the constant effort during testing of

creep at a given time, and rezero when it reaches the estimated time then deformation is recorded by another equal time. For example, for a biocomposite made of polyethylene aluminum fiber fique, we can observe the response to creep and creep recovery in **Figure 9**, a maximum stress of 1.2 MPa was applied in a bending test at three points at 25°C, 1.2 MPa effort is an attempt that was obtained after identifying the linear viscoelastic region, a biocomposite test strain sweeps at 25°C in a DMA (RSAIII).

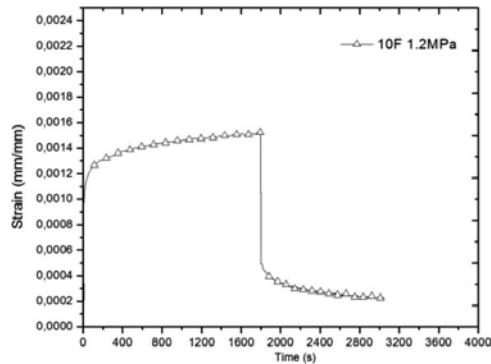


Figure 9. Creep curves and creep recovery for biocomposite LDPE-Al-Fique 10% reinforcement of natural fibers.

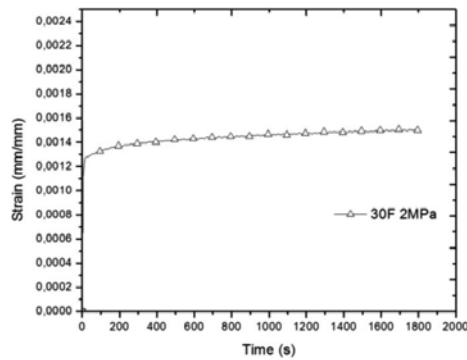


Figure 10. Creep curves for biocomposite LDPE-Al-Fique 30%.

As presented schematically in **Figure 6**. For an adjustment with a four-parameter interpretation is the same, it is important to note that the effect of reinforcement on a biocomposite can be studied by this method, especially when amending fiber volume, nanoreinforcements, fillers, filler, or some surface modification is made to the fibers or fillers in order to improve performance micromechanical, and default creep performance is used. In **Figure 10**, one can see a behavior of an LDPE manufactured biocomposite-Al-Fique 30% fiber volume. Being possible to observe the effect of increased volume is positive with respect to creep, decreasing the speed of decoration and to increase enforcement effort in the linear viscoelastic region by nearly 60%.

4. Strain rate of biocomposites

To calculate the strain rate of the biocomposites subjected to creep tests, one can be approximated using the four-parameter model represented by Eq. (6), or model parameters n represented by Eq. (11). By making adjustments mathematical models, is provided mainly for comparing quantitatively the effect of strain rate, and further study of the performance of the incorporation of fibers, surface treatment agents couplings for fibers or polymers, fillers, nanoreinforcements, and fillers to manufacture biocomposites, controlled conditions of temperature and constant effort. In **Figure 11**, one can observe an experimental curve creep, and the respective model adjustment four parameters and the model of n parameters, it is emphasized that in the two curves creep models over four parameters. It is better than the four-parameter fit, which facilitates the study of the incorporation of fillers, reinforcements, nanoreinforcements for biocomposites.

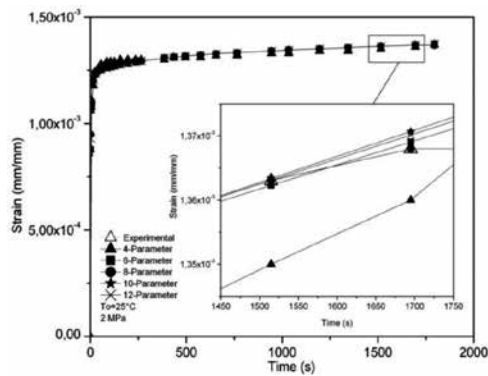


Figure 11. Adjustment of an experimental curve of a biocomposite creep, using the four-parameter model and model parameters n .

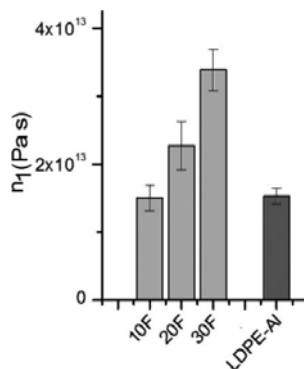


Figure 12. n_1 parameter for 10, 20, and 30% biocomposites reinforced with natural fiber sisal, and unreinforced LDPE-Al.

In **Figure 12**, we can see the response of viscous parameter n_1 , which allows the calculation of the strain rate for creep tests; this exercise was carried out, varying the volume of natural fibers fique biocomposite, corroborating the possibility of deepening the study of the effect of reinforcements or fillers to biocomposites.

Figure 13 shows the setting of the four-parameter model, two biocomposites, with different volumes of natural fiber reinforcement sisal. It is possible to corroborate and validate the model.

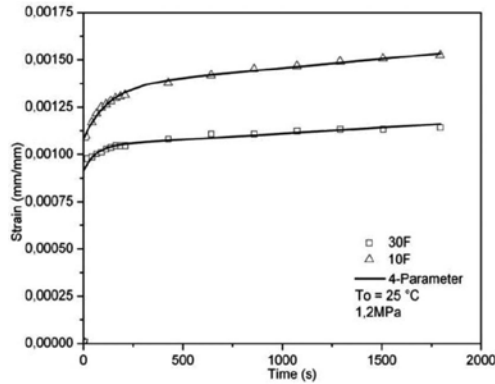


Figure 13. Setting the four -parameter model to LDPE-Al-Fique 10 and 30% incorporation biocomposites of fibers.

Table 7 shows the adjustment of the different parameters for a model of six parameters, including error, which is the estimate of least squares adjustment parameters can be obtained using the weighted sum of squares (weighted sum of squares, WSS), using Eq. (12):

Parameter	10%	30%
E1 (Pa)	1.10E + 09	1.50E + 09
E2 (Pa)	4.79E + 09	1.53E + 10
E3 (Pa)	7.91E + 09	8.39E + 07
N1 (Pa.s)	1.49E + 13	3.12E + 13
N2 (Pa.s)	6.48E + 11	9.32E + 11
N3 (Pa.s)	7.83E + 13	3.33E + 15
WSS	9.23E-08	6.43E-08

Table 7. Parameters of creep tests obtained by adjustment to a model of six parameter biocomposites LDPE-Al-Fique 10 and 30% incorporation biocomposites of fibers.

$$WSS = \sum_{i=1}^n w_i \left[\varepsilon(t_i) - \hat{\varepsilon}(t_i) \right]^2 \tag{12}$$

where $\varepsilon(t_i)$ represents the observed at time t_i experimental deformation (t_i), ε is estimated by the model, and w_i the difference between two samples of time deformation. A smaller value indicates a better fit WSS model to experimental data.

In **Figure 14**, we can see micrographs obtained by electronic scanning microscopy of an LDPE-Al-Fique biocomposite, where you can see that the fiber has a hydrophobic property, not adhere completely to the polymer, while aluminum has some adhesion but the manufacturing process of compression molding favors the adhesion between the faces, which can be reflected in a decrease of mechanical and viscoelastic performance of the biocomposites.

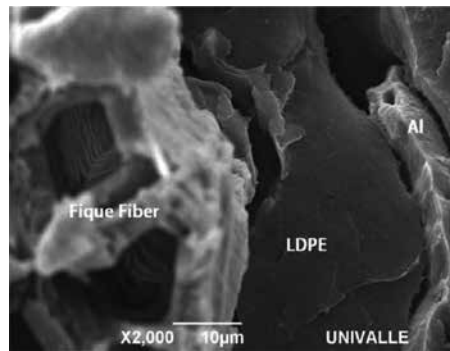


Figure 14. SEM micrographs of LDPE-Al-Fique biocomposite.

Currently, it is known that these defects can be corrected by surface treatments in the fibers, primarily using coupling agents or modifications to the polymers to achieve a greater adhesion and micromechanical relationship to reduce the strain rate.

5. Conclusions

Natural fibers as reinforcement of nonbiodegradable and biodegradable polymers have been used for decades for the development of various products, especially in the automotive, construction, and packaging industry. The importance of studying the viscoelastic behavior of biocomposites lies in understanding the impact of natural fibers or fillers on any scale, in the matrices that you want to use for different applications. Now, it is known that the structural rigor for automotive, construction, and/or packaging parts lies mainly in the relationship of the shape of the products with the stresses to which these materials are subjected, temperature changes, environmental and even other physicochemical factors that could alter the performance of the biocomposite in time. The articulation of theoretical models and experimental results using the technique of dynamic mechanical analysis (DMA) to predict the behavior over time, and the effect of filler or reinforcement, nanoreinforcements, micromechanics, surface treatments to the fibers, or modifications to polymer matrices facil-

itate a better understanding of its operation and its use at an industrial level for various applications. In South America, the natural fibers have recently become an attractive reinforcement or filler for researchers, engineers, and scientists as an alternative to develop biocomposites. Because of its low cost, sometimes good mechanical properties and good specific resistance generate a high environmental impact and additionally, it is biodegradable. It has been found that the use of natural fibers such as fique of South American Andean region can be used as reinforcement in composite materials and generate a lot of possibilities for industrial applications. It was found that the addition of fibers in different polymer matrices leads to produce new natural compounds with good physical properties for use in different sectors. The study revealed that biocomposites inherited effects relaxations attributed to transitions suffered by the polymer matrices used, whereby the relationship of fiber-matrix-filled showed evidence that the biocomposites always have a positive effect creep (creep), however, and while being exposed to constant loads over time and while working above the glass transition temperature, the biocomposite will behave predominantly as a super-cold fluid, and not likely as an elastic solid.

Acknowledgements

I express my gratitude to Universidad Autónoma de Occidente, Cali-Colombia, Wisconsin University and Universidad del Valle, Colciencias and packaging company from Medellín Colombia, for providing the fique, the sponsors of project.

Author details

Miguel Ángel Hidalgo Salazar

Address all correspondence to: mahidalgo@uao.edu.co

Universidad Autónoma de Occidente, Cali, Colombia

References

- [1] Väisänen T, Haapala A, Lappalainen R, Tomppo L. Utilization of agricultural and forest industry waste and residues in natural fiber-polymer composites: A review. *Waste Manag.* 2016; 54:62–73.
- [2] Thakur VK, Thakur MK, Gupta RK. Review: raw natural fiber-based polymer composites, *Int. J. Polym. Anal. Charact.* 2014; 19:256–271.

- [3] Rana A, Mitra B, Banerjee A. Short jute fiber-reinforced polypropylene composites: dynamic mechanical study. *J. Appl. Polym. Sci.* 1999; 71:531–539.
- [4] Puglia D, Biagiotti J, Kenny J. A review on natural fibre-based composites—Part II: application of natural reinforcements in composite materials for automotive industry. *J. Nat. Fibers.* 2005; 1:23–65.
- [5] Prithivirajan, R, Jayabal S, Bharathiraja G. Bio-based composites from waste agricultural residues: mechanical and morphological properties. *Cellulose Chem. Technol.* 2015; 49, 65–68.
- [6] Xu Y, Wu Q, Lei Y, Yao F. Creep behavior of bagasse fibre reinforced polymer composites. *Bioresour. Technol.* 2010; 101:3280–3286.
- [7] Suardana NPG, Piao Y, Lim JK. Mechanical properties of hemp fibers and hemp/PP composites: effects of chemical surface treatment. *Mater. Phys. Mech.* 2011; 11:1–8.
- [8] Omrani E, Menezes P L, Rohatgi P K. State of the art on tribological behavior of polymer matrix composites reinforced with natural fibers in the green materials world. *Int. J. Eng. Sci. Technol.* 2016; 19(2):717–736.
- [9] Ahmad F, Choi HS, Park MK. A review: natural fiber composites selection in view of mechanical, light weight, and economic properties. *Macromol. Mater. Eng.* 2015; 300:10–24.
- [10] Acha BA, Reboredo MM, Marcovich NE. Creep and dynamic mechanical behavior of PP–jute composites: effect of the interfacial adhesion. *Compos. Part A: Appl. Sci. Manuf.* 2007; 38:1507–1516.
- [11] Premalal HG, Ismail H, Baharin A. Comparison of the mechanical properties of rice husk powder filled polypropylene composites with talc filled polypropylene composites. *Polym. Test.* 2002; 21:833–839.
- [12] Nuñez AJ, Marcovich NE, Aranguren MI. Short-term and long-term creep of polypropylene–wood flour composites. *Polym. Eng. Sci.* 2004; 44(8):1594–1603.
- [13] Reddy N, Yang Y. Preparation and characterization of long natural cellulose fibers from wheat straw. *J. Agric. Food. Chem.* 2007; 55:8570–8575.
- [14] Delvasto S, Toro E, Perdomo F, Mejía R. An appropriate vacuum technology for manufacture of corrugated fique fibre reinforced cementitious sheets. *Constr. Build. Mater.* 2010; 24:187–192.
- [15] Gurunathan T, Mohanty S, Nayak SK. A review of the recent developments in biocomposites based on natural fibres and their application perspectives. *Compos. Part A.* 2015; 77:1e25.
- [16] Sood M, Dharmपाल D, Gupta VK. Effect of fiber chemical treatment on mechanical properties of sisal fiber/recycled HDPE composite. *Mater. Today: Proc.* 2015; 2(4–5): 3149–3155.

- [17] Gómez C, Vázquez A. Flexural properties loss of unidirectional epoxy/fique composites immersed in water and alkaline medium for construction application. *Compos. Part B: Eng.* 2012; 43(8):3120–3130.
- [18] Greco F, Leonetti L, Nevone Blasi P. Adaptive multiscale modeling of fiber reinforced composite materials subjected to transverse micro cracking. *Compos. Struct.* 2014; 113:249–63.
- [19] Ramesh M, Atreya TSA, Aswin US, Eashwar H, Deepa C. Processing and mechanical property evaluation of banana fiber reinforced polymer composites. *Procedia Eng.* 2014; 97:563–572.
- [20] N Uddin, *Developments in Fiber-Reinforced Polymer (FRP) Composites for Civil Engineering*, 1st ed. Woodhead Publishing; 2013. p. 18-26.
- [21] Venkateshwaran N, Elaya Perumal A, Arunsundaranayagam D. Fiber surface treatment and its effect on mechanical and visco-elastic behaviour of banana/epoxy composite. *Mater. Design.* 2013; 47:151–159.
- [22] Chin CW, Yousif BF. Potential of kenaf fibres as reinforcement for tribological applications. *Wear.* 2009; 267(9–10):1550–1557.
- [23] Zhan J, Song L, Nie S, Hu Y. Combustion properties and thermal degradation behavior of polylactide with an effective intumescent flame retardant. *Polym. Degrad. Stabil.* 2009; 94(3):291–296.
- [24] Kim SJ, Moon JB, Kim GH, Ha CS. Mechanical properties of polypropylene/natural fiber composites: comparison of wood fiber and cotton fiber. *Polym. Test.* 2008; 27:801–806.
- [25] Le Troedec M, Sedan D, Peyratout C et al., “Influence of various chemical treatments on the composition and structure of hemp fibres.” *Compos. Part A: Appl. Sci. Manuf.* 2008; 39(3):514–522.
- [26] John MJ, Francis B, Varughese KT, Thomas S. Effect of chemical modification on properties of hybrid fiber biocomposites. *Compos. Part A: Appl. Sci. Manuf.* 2008; 39(2): 352–363.
- [27] D. Dai, M. Fan. Wood fibres as reinforcements in natural fibre composites: structure, properties, processing and applications. In: A. Hodzic and R. Shanks, editors. *Natural Fibre Composites Materials, Processes and Applications*. Woodhead Publishing Limited: 2014. p.3–65. DOI:10.1533/9780857099228.1.3
- [28] May-Pat A, Valadez-González A, Herrera-Franco PJ. Effect of fiber surface treatments on the essential work of fracture of HDPE-continuous henequen fiber-reinforced composites.” *Polym. Test.* 2013; 32(3):1114–1122.

- [29] Kumari R, Ito H, Takatani M, Uchiyama M, Okamoto T. Fundamental studies on wood/cellulose-plastic composites: effects of composition and cellulose dimension on the properties of cellulose/PP composite. *J. Wood. Sci.* 2007; 53:470–80.
- [30] Bocz K, Szolnoki B, Marosi A, T'abi T, Wladyka-Przybylak M, Marosi G. Flax fibre reinforced PLA/TPS biocomposites flame retarded with multifunctional additive system. *Polym. Degrad. Stabil.* 2014; 106:63–73.
- [31] Tawakkal ISMA, Cran MJ, Bigger SW, Effect of kenaf fibre loading and thymol concentration on the mechanical and thermal properties of PLA/kenaf/thymol composites. *Ind. Crops Prod.* 2014; 61:74–83.
- [32] Graupner N, Herrmann AS, M'ussig J. Natural and man-made cellulose fibre-reinforced poly (lactic acid) (PLA) composites: an overview about mechanical characteristics and application areas. *Compos. Part A: Appl. Sci. Manuf.* 2009; 40(6–7):810–821.
- [33] Rong MZ, Zhang, MQ, Liu Y, Yang GC and Zeng HM. "The effect of fiber treatment on the mechanical properties of unidirectional sisal-reinforced epoxy composites." *Compos. Sci. Technol.* 2001; 61(10):1437–1447.
- [34] Faruk O, Bledzki AK, Fink HP, Sain M. Biocomposites reinforced with natural fibers: 2000–2010." *Prog. Polym. Sci.* 2012; 37(11):1552–1596.
- [35] Hidalgo Salazar MA, Munoz Velez MF, Quintana KJ. Mechanical analysis of polyethylene aluminum composite reinforced with short fique fibers available a in two-dimensional arrangement; *Revista Latinoamericana De Metalurgia Y Materiales.* 2012; 31(1): 89–95.
- [36] Shinoj S, Visvanathan R, Panigrahi S, Kochubabu M. Oil palm fiber (OPF) and its composites: a review. *Ind. Crops Prod.* 2011; 33(1):7–22.
- [37] Miguel A. Hidalgo-Salazar, Mario F. Muñoz, and José H. Mina. Influence of incorporation of natural fibers on the physical, mechanical, and thermal properties of composites LDPE-Al reinforced with fique fibers: *International Journal of Polymer Science.* Volume 2015 (2015), Article ID 386325, 8 pages. DOI:10.1155/2015/386325
- [38] Jawaid M. Abdul Khalil HPS. Cellulosic/synthetic fibre reinforced polymer hybrid composites: a review. *Carbohydr. Polym.* 2011; 86(1):1–18.
- [39] Väisänen T, Haapala A, Lappalainen R, Tomppo L. Utilization of agricultural and forest industry waste and residues in natural fiber-polymer composites. *Waste Manage.* 2016; 54:62–73.
- [40] Frédérique T, Vincent P, Violaine GR, Boubakar ML. Nonlinear tensile behaviour of elementary hemp fibres. Part II: Modelling using an anisotropic viscoelastic constitutive law in a material rotating frame. *Compos. Part A: Appl. Sci. Manuf.* 2015; 68:346–355.

- [41] Hidalgo MA, Muñoz MF, Quintana KJ. Mechanical behavior of polyethylene aluminum composite reinforced with continuous agro fique fibers. *Revista Latinoamericana de Metalurgia y Materiales*. 2011; 31(2):187–194.
- [42] Delvasto S, de Gutiérrez R, Váldez Y. Comparative study of the pull-out behavior of fique fibers in mortars of Portland cement. In: *Brazilian Conference on Non-conventional Materials and Technologies (NOCMAT): Affordable Housing and Infrastructure*; 2004; Brazil
- [43] Gañán P, Mondragon I. Fique fiber-reinforced polyester composites: effects of fiber surface treatments on mechanical behavior. *J. Mater. Sci*. 2004; 39(9):3121–3128.
- [44] Li Y, Shen YO. The use of sisal and henequen fibres as reinforcements in composites. In: Omar Faruk and Mohini Sain, editors. *Biofiber Reinforcements in Composite Materials*. Elsevier Ltd: 2015: p. 165–210. DOI:10.1533/9781782421276.2.165
- [45] Aziz SH, Ansell MP. The effect of alkalization and fibre alignment on the mechanical and thermal properties of kenaf and hemp bast fibre composites: Part 1 — Polyester resin matrix. *Compos. Sci. Technol*. 2004; 64:1219–30.
- [46] Saba N, Jawaid M, Alothman OY, Paridah MT. A review on dynamic mechanical properties of natural fibre reinforced polymer composites. *Constr. Build. Mater.* March 2016; 106(1):149–159.
- [47] Maurya HO, Gupta MK, Srivastava RK, Singh H. Study on the mechanical properties of epoxy composite using short sisal fibre. *Mater. Today: Proc*. 2015; 2(4–5):1347–1355.
- [48] Herrera-Franco PJ, Valadez-González A. A study of the mechanical properties of short natural-fiber reinforced composites. *Compos. Part B: Eng*. 2005; 36: 597–608.
- [49] Cheung HY, Ho MP, Lau KT, Cardona F, Hui D. Natural fibre-reinforced composites for bioengineering and environmental engineering applications. *Compos. Part B: Eng*. 2009; 40:655e63.
- [50] Martins C, Pinto V, Rui Guedes M, Marques AT. Creep and stress relaxation behaviour of pla-cl fibres — a linear modelling approach. *Procedia Eng*. 2015; 114:768–775.
- [51] Dobah Y, Bourchak M, Bezazi A, Belaadi A. Static and fatigue strength characterization of sisal fiber reinforced polyester composite material. In: *9th International Conference on Composite Science and Technology: 2020 - Scientific and Industrial Challenges (ICCST/9)*; 24–26 April 2013; Sorrento, Naples, Italy.
- [52] Jabbar A, Militky J, Madhukar Kale B, Rwwiire S, Nawabb Y, Baheti V. Modeling and analysis of the creep behavior of jute/green epoxy composites incorporated with chemically treated pulverized nano/micro jute fibers. *Ind. Crops Prod*. 2016; 84:230–240.

- [53] Kiguchi M. Latest market status of wood and wood plastic composites in North America and Europe. In: *The Second Wood and Wood Plastic Composites Seminar in the 23rd Wood Composite Symposium, Kyoto, Japan; 2007*. pp. 61–73.
- [54] Belaadi A, Bezazi A, Maache M, Scarpa F. Fatigue in sisal fiber reinforced polyester composites: hysteresis and energy dissipation. *Procedia Eng.* 2014; 74:325–328.
- [55] Haq S, Srivastava R. Measuring the influence of materials composition on nano scale roughness for wood plastic composites by AFM. *Measurement.* 2016; 91:541–547.
- [56] Fibre properties and crashworthiness parameters of natural fibre-reinforced composite structure: A literature review. *Compos. Struct.* 2016; 148:59–73.
- [57] Ascione L, Berardi V, D'Aponte A. Creep phenomena in FRP materials. *Mech. Res. Commun.* 2012; 43:15–21.
- [58] Miguel A, Hidalgo-Salazar, José H, Mina, Pedro J, Herrera-Franco: The effect of interfacial adhesion on the creep behaviour of LDPE–Al–Fique composite materials. *Composites Part B: Engineering.* 2013; 55: 345–351. DOI: 10.1016/j.compositesb.2013.06.032
- [59] Pothan LA, Oommen Z, Thomas S. Dynamic mechanical analysis of banana fiber reinforced polyester composites. *Compos. Sci. Technol.* 2003; 63:283–93.



Edited by Matheus Poletto

Composites from Renewable and Sustainable Materials consists of 16 chapters written by international subject matter experts investigating the characteristic and current application of materials from renewable and sustainable sources. The reader will develop a deeper understanding about the concepts related to renewable materials, biomaterials, natural fibers, biodegradable composites, starch, and recycled materials. This book will serve as the starting point for materials science researchers, engineers, and technologists from the diverse backgrounds in physics, chemistry, biology, materials science, and engineering who want to know and better understand the fundamental aspects and current applications of renewable and sustainable materials in several applications.

Photo by Mediengestalter / pixabay

IntechOpen

